VERSLAGEN EN VERHANDELINGEN

REPORTS AND TRANSACTIONS

NATIONAAL LUCHTVAARTLABORATORIUM

NATIONAL AERONAUTICAL RESEARCH INSTITUTE

AMSTERDAM

XIII — 1947

ERRATA

Preface, seventh line from bottom: resarch should read research.

Report A.1011, p.A 10, left-hand column, ninth line of section 3: n_1 should read n_1^3.

Report S. 319, p. S 43, left-hand column: the last term of eq. (4.4) should read $\frac{\varepsilon^*}{s} \Delta' \frac{\partial f'_b}{\partial z}$.

Report V. 1366, p. V 73, left-hand column: caption of section 6 should read: First approximation of the amplitude ratios of the varied system.

Report V. 1386, p. V 129, right-hand column: the notations s' and s'' should read s_1 and s_2.

Report V. 1386, p. V 130, left-hand column: the notations m', m'', I' and I'' should read m_1, m_2, I_1 and I_2.

PREFACE.

In introducing this first post-war volume of the „Verslagen en Verhandelingen", a brief review of the research organization and of the publication policy of the „Nationaal Luchtvaartlaboratorium" to date will be appropriate.

The four scientific departments existing at the end of the war were organized as largely self-contained units, each having its own personnel for all its activities. This separation of the departmental activities was hardly practicable in several cases. So, some more or less radical changes were made in 1945 and 1946, aiming at a better internal cooperation, prevention of duplication of work, and an improvement of the efficiency.

All academically-graded research personnel are now comprised in one Main Division, whereas the lower-grade technical personnel and other assistants are grouped over a number of Subdivisions, whose services are, in principle, at the disposition of all members of the Main Division.

The Main Division, being too extensive for one-head supervision, is split up in five Sections, each headed by a Chief of Section, viz. Aerodynamics (A), Flight (V), Flutter and Theoretical Aerodynamics (F), Materials (M) and Structures (S). The Scientific Director, the Chief Engineer in General Service, also acting as a deputy for the Scientific Director, and the Chiefs of Section form the „Scientific Staff".

The Subdivisions are partly of a general character (Calculating Bureau, Library, Electronics Lab., Shops and Services), partly for the special assistance of a particular Section (Windtunnel Dept., Exp. Flight Dept., Materials Lab., Structures Lab.). Each Subdivision, except the Shops and Services, is supervised by the most qualified Chief of Section. The Shops and Services, including a temporary Building Development Bureau and the Design and Drawing Office, are separated from the Main Division and headed by a chief of the same status as the chiefs of the sections.

The results of scientific investigations are usually issued in the form of reports. These reports are indicated by the letter A, F, M, S or V, corresponding to the section by which they were prepared, and a number. The reports concerning visits and study tours form an exception, being all indicated by the letters RB. Reports dealing with research work of a general character and with the development of basic testing and measuring apparatus and instruments are usually released for publication.

The publications are issued partly in printed form, partly in typescript. Until 1945, the printed reports were published collected in volumes of „Verslagen en Verhandelingen" (Reports and Transactions) and written in Dutch with English and German summaries. These volumes contained, in general, the more important reports prepared since the foregoing collection was published. Twelve have appeared at irregular intervals, Vol. I in 1921 and Vol. XII in 1943. After the volume was issued, separate copies of reports were available.

The reports in typescript were and will be issued separately as soon as completed. A list of such reports, covering the period from November 1942 to November 1947 is given on the following pages. A complete list of publications is available upon application.

In order to improve their accessibility, it was decided after the war to write all reports for the Verslagen en Verhandelingen entirely in English, with some exceptions during the period of transition, and apart from special issues such as theses. It was further decided to distribute preprints of reports prepared for a volume as soon as they are available, identical copies being later obtainable as reprints. The purpose of these preprints will be to present advance information to resarch workers who are actively engaged in the field of aeronautical science to which the report relates.

Unfortunately, the latter scheme could not yet be employed to full advantage during the preparation of the present volume, because considerable delay in printing was experienced due to the post-war difficulties. Many of the reports contained in this volume have, consequently, been prepared several years ago. Still, it is hoped that they have retained most of their utility and that they will give an impression on the nature of the research work carried out by this institute during the latter years.

Amsterdam, December 1947.

C. KONING

Scientific Director.

CONTENTS

LIST OF PUBLICATIONS IN TYPESCRIPT, ISSUED BETWEEN 1st NOVEMBER 1942 and 1st NOVEMBER 1947.

N.B. These reports are in Dutch, unless indicated otherwise.

A. 811	BOELEN, A.	The method of Lotz for the solution of Prandtl's equation for the circulation.	1941
A. 944	DE LATHOUDER, A.	*Divergence and convergence of the free-jet boundaries of windtunnels 3 and 4* of the Nationaal Luchtvaartlaboratorium.	1944
A 949	SLOTBOOM, J. G.	The correction for a propeller in a closed windtunnel. Comparison of the exact with the approximate method of calculation.	1943
A. 957	DE LATHOUDER, A.	*Some data on the flow in windtunnel 3 with enlarged working section*	1944
A. 962	DE LATHOUDER, A.	Nomogram for determining the influence of tunnel interference on drag and angle of attack of a wing.	1944
A. 978	DE LATHOUDER, A.	Wind-driven electric generators. I. A simple method to calculate a high-speed *twin arm windmill (so-called wind-charger.)*	1945
A. 990	GREIDANUS, J. H.	Principles and methods of the theory of non-stationary flow around a wing.	1945
A. 1024	ERDMANN, S. F.	Measuring methods in the supersonic tunnel at Peenemünde (Kochel). (in German)	1946
F. 2	ERDMANN, S. F.	Numerical treatment of the method of characteristics in the design of supersonic *nozzles. (in German)*	1946
F. 3	ERDMANN, S. F.	Calculation of the pressure distribution around a body of revolution at subsonic and supersonic velocities with the aid of the „Sources and Sinks" method. (in German.)	1946
F. 4	GREIDANUS, J. H.	*Mathematical structure of aerofoil theory.*	1947
F. 5	ERDMANN, S. F.	Design of supersonic nozzles with graphical discussion of the initial-value problem. (in German)	1947
M. 1022	DOBBELMANN, TH. A. H. M.	The hydrogen peroxide concentration in the D.V.L. corrosion testing method *(DIN 4853) Part II.*	1943
S. 94	PLANTEMA, F. J.	Allowable stresses in tubes of circular cross section.	1942
S. 266	VAN DER NEUT, A., FLOOR, W. K. G.	The effective width of flat plates with longitudinal stiffeners of open cross section.	1943
S. 269	VAN DER NEUT, A., BRINKHORST, I.	The magnitude and frequency of the loads on aeroplanes. (with English abstract)	1944
S. 274	PLANTEMA, F. J.	The allowable rate of roll of aeroplanes. I	1943
S. 282	PLANTEMA, F. J., VAN DER NEUT, A.	Qualitative pictures of the stress distribution in shells. I. Wings.	1943
S. 285	PLANTEMA, F. J.	The allowable rate of roll of aeroplanes. II.	1943
S. 287	KOITER, W. T.	The effective width of infinitely long, flat, rectangular plates under various conditions of edge restraint. (with English abstract)	1943
S. 288	VAN DER NEUT, A.	Some general comments on buckling phenomenae	1943
S. 289	—	Tail loads in pull-ups. I. (with abstract in English)	1943
S. 292	—	Tail loads in pull-ups. II. (with abstract in English)	1944
S. 293	PLANTEMA, F. J. VAN DER NEUT, A.	Qualitative pictures of the stress distribution in shells. II. Fuselages	1944
S. 295	KOITER, W. T.	Theoretical investigation of the diagonal tension field of flat plates. (with abstract in English)	1944
S. 296	VAN DER NEUT, A.	Influence of the elasticity of the frames on the stress distribution in stressed-skin fuselages	1945
S. 297	PLANTEMA, F. J., VAN DER NEUT, A.	Calculation of the deformation of two-spar wings. (with abstract in English).	1945
S. 300	VAN DER NEUT, A., FLOOR, W. K. G., BRINKHORST, I.	Experimental investigation of the post-buckling behaviour of stiffened, flat, rectangular plates under combined shear and compression. Part I. (in English)	1947
S. 301	BRINKHORST, I.	The strength of structural elements under alternating loads.(with abstract in English)	1945
S. 302	KOITER, W. T.	On the elementary theory of elasticity, with particular regard to the energy principles	1945
S. 304	PLANTEMA, F. J.,	The loads on tricycle landing gears in landings. III	1945
S. 307	VAN WIJNGAARDEN, A.	Large distortions of circular rings and straight rods. (in English), (published in Proc. Kon. Ned. Ak. van Wet., 49, 1946, pp. 648—656, 657—664)	1946
S. 312	FLOOR W. K. G.,	The stiffness of a wing against torsional oscillations at different static torsional loads.	1946
S. 313	VAN WIJNGAARDEN, A.	Large deflections of semi-oval rings.	1946
S. 315	PLANTEMA, F. J.	Rationalization of symmetrical gust load requirements. (in English)	1946
S. 316	—	Description of a slope recorder and an elliptic enlarger. (in English).	1946
S. 317	—	Impact loads on seaplanes during landing, with particular reference to the influence of the forward speed. (in English)	1947
S. 318	PLANTEMA, F. J.	Rolling manoeuvring loads of aeroplanes. (in English)	1946
V. 1088	VAN DER MAAS, H. J., WYNIA, S., MARX, A. J.	Reduction of aircraft performance in steady symmetrical flight to other conditions of atmosphere, weight and engine power. Revised edition	1946

REPORT A. 950

Drag and Pressure Measurements with Plaster Spheres in Windtunnel 3 and 4 of the National Aeronautical Research Institute

by

Ir. S. I. WISELIUS

Summary.

Drag and pressure measurements with two plaster spheres in the closed working section of windtunnel 3 and the open working section of windtunnel 4, carried out to determine the turbulence of airflow, are discussed in this report. A description of the plaster spheres and of the attention paid to the suspension of the spheres in the windtunnels is given. It is concluded that the turbulence of airflow in windtunnel 3 is rather low.

Contents.

1 Introduction.

The measurements described in this report form part of a series of experiments, carried out to determine a measure for the turbulence of the airflow in windtunnels. In the unpublished Reports A. 777, A. 813 and A. 814 results are given of drag and pressure measurements with two metal spheres (diameter 99 mm and 200 mm respectively) carried out in the windtunnels 1, 3 [1]) and 4 [2]) of the N.L.L. In this report the results of similar measurements with two lacquered and polished plaster spheres, diameter 150 mm (6″) and 200 mm (8″), are given. These measurements were carried out in the closed working section of windtunnel 3 and the open working section of windtunnel 4. Special attention was given to the vibrationless suspension of the spheres. Afterwards the influence of the thickness of the supporting spindle and the influence of the tension in the suspension wires (by varying the tightening loads) on the results were determined.

2 Purpose and extent of the investigation.

The purpose of the investigation, carried out with two lacquered and polished plaster spheres in windtunnel 3 and windtunnel 4 of the N.L.L., was:

a. determination of a measure for the turbulence of the airflow in windtunnel 3 and 4. Comparison with the results obtained from earlier investigations was of no use because of the inaccurate finish of the surface of the metal sphere (diameter 200 mm) which was used in those investigations.

b. determination of the influence of the sphere diameter on the critical Reynolds number.

c. determination of the influence of the supporting spindle diameter.

[1]) Report A. 795: The large windtunnel of the N.L.L. Verslagen en Verhandelingen van het N.L.L. Volume XI, (1942), p. A 1.

[2]) Report A. 802: The small windtunnel of the N.L.L. Verslagen en Verhandelingen van het N.L.L. Volume XI, (1942), p. A 19.

d. determination of the influence of the tension in the suspension wires on the results.

Drag- and pressure measurements have been carried out both in windtunnel 3 (closed jet) and 4 (open jet). The influence of the supporting spindle diameter and the wire tension was determined in windtunnel 4 (drag measurements).

3 Description of the spheres (fig. 1).

The spheres, which were made in the workshops of the N.L.L., had diameters of 150 mm and 200 mm respectively and were of similar construction. The frame of the spheres consisted of three circular plates of galvanized iron sheet which were (perpendicular to each other) fixed to a hollow shaft as shown in fig. 1*b*. The support for the plaster covering of the sphere was formed by spherical sectors of galvanized iron sheet attached to the frame.

The outer surface consisted of a layer of plaster of Paris, about 5 mm thick. By means of a circular mould a clean spherical surface was obtained. The required smooth finish was obtained by scraping, lacquering and polishing. The hollow shaft (fig. 1*a*) was attached to a short solid shaft containing a pressure hole, which ended at the front of the sphere. In this shaft the supporting spindle which contained two pressure holes, was screwed. One of these holes was in communication with the pressure hole in the solid shaft, the other one ended in the hollow shaft. Through grooves between the supporting spindle and the hollow shaft the pressure in the latter hole corresponded with the pressure at the back of the sphere. In this way the pressure of airflow at the front and at the back of the sphere could be measured.

The diameter of the supporting spindle was 12 mm ($\frac{1}{2}$″). To determine the influence of the spindle diameter on the drag measurements and so on the critical Reynolds number, it was possible to mount successively two cylinders with diameters 19 mm ($\frac{3}{4}$″) and 28,7 mm (~ $1\frac{1}{8}$″) around the supporting spindle.

4 Method of suspension and measurement; reduction of the test results.

4.1 *Suspension.*

In order to determine the critical Reynolds number drag and pressure measurements were

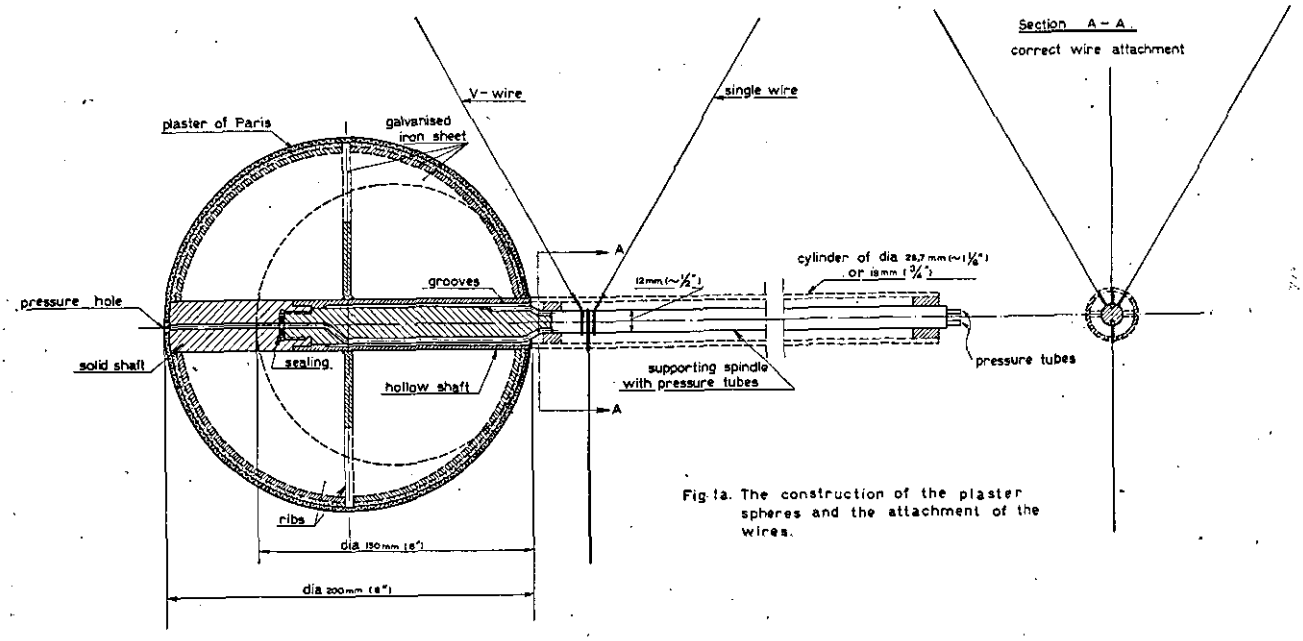

Fig. 1a. The construction of the plaster spheres and the attachment of the wires.

Fig. 1c. Incorrect wire attachment.

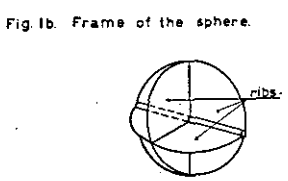

Fig. 1b. Frame of the sphere.

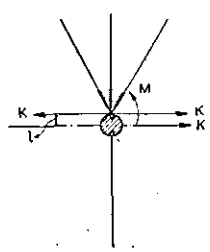

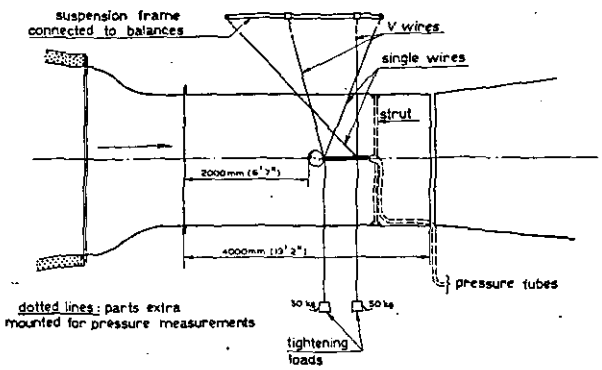

FIGURE 2a.
Arrangement in windtunnel 3 for drag and pressure measurements.

carried out with the spheres described in section 3 (see section 4.2 and 4.3). The spheres were mounted in the centre of the working section of the windtunnels. In windtunnel 3 the front of the spheres was about 2000 mm (6′ 7″) behind the inlet cone — total length of the closed jet 4000 mm (13′ 2″), fig. 2*a* —, in windtunnel 4 about 1000 mm (3′ 3½″) — total length of the open jet 2100 mm (6′ 11″), fig. 2*b*. With the suspension method described in section 3 it is possible to carry out both drag and pressure measurements in succession. It was desirable to get a vibrationless mounting of the spheres. For this reason it was necessary to attach the suspension wires to the supporting spindle in such a manner, that no free moments might occur. In fig. 1*c* the often used incorrect wire mounting is shown. As may be seen the force K, which acts in the case of unsymmetrical airflow around the sphere, gives a free moment $M = K \times l$ at the wire junction at distance l from the shaft centre. As the aerodynamic forces are variable both in magnitude and direction, the moment M is variable and causes undesirable vibrations. The correct wire attachment is shown in fig. 1*a*, Section A-A.

Another source of vibrations is the elasticity of the suspension wires. As these steel wires are rather long it appeared to be desirable to use a diameter of 1 mm (0,04″) and to apply large loads (10, 25 or 50 kg) to tighten the wires. The influence of these loads was determined in windtunnel 4 by reducing the loads in the front suspension point from 50 to 25 kg (see section 5.2).

To avoid vibrations, caused by the drag of the pressure tubes, special provisions were made with the pressure measurements. In the closed working section of windtunnel 3 (fig. 2*a*) a vertical strut was mounted behind the spindle to conduct the tubes downwards. In windtunnel 4 a support fixed by wire bracing was used for this purpose (fig. 2*b*). Special attention was paid to the rigidity of the whole arrangement.

4.2 *Drag measurements.*

During the drag measurements in the closed jet of windtunnel 3 the spheres were mounted to the balance-frame as shown in fig. 2*a* (full lines), in the open jet of windtunnel 4 as shown in fig. 2*b* (full lines). The measured values of the drag were corrected for the drag of the suspension wires. This drag was determined with the same arrangement, the sphere, however, being removed from the supporting spindle and mounted in front of the spindle on a separate shaft. The drag, corrected in this way, was reduced to a dimensionless coefficient as follows:

$$c_d = \frac{D}{qA},$$

where

c_d = drag coefficient,

D = drag in kg,

q = dynamic pressure in kg/m²,

$A = \frac{\pi}{4} d^2$, the projected area of the sphere in m².

Before the sphere measurements were carried out the dynamic pressure q was measured with a pitot-static tube mounted in the same position as the spheres.

4.3. *Pressure measurements.*

During the pressure measurements in the closed jet of windtunnel 3 the spheres were mounted as shown in fig. 2*a* with the extra strut for the

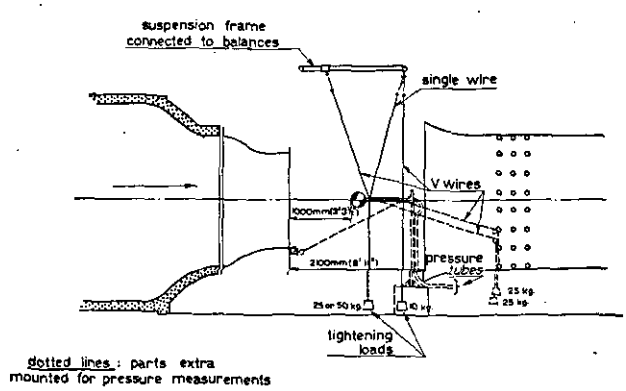

FIGURE 2b.
Arrangement in windtunnel 4 for drag and pressure measurements.

pressure tubes in position (dotted lines). In the open jet of windtunnel 4 the spheres were mounted as shown in fig. 2*b* with the extra support and wire-bracing (dotted lines).

The pressure difference p_f and p_b was reduced to a dimensionless coefficient as follows:

$$c_p = \frac{p_f - p_b}{q} = \frac{\Delta p}{q},$$

where:

c_p = pressure coefficient,

p_f = pressure in front of the sphere in kg/m^2,

p_b = pressure at the back of the sphere in kg/m^2,

q = dynamic pressure in kg/m^2.

Before the pressure measurements were carried out, the dynamic pressure was measured with a pitot-static tube mounted in the same position as the spheres.

5 Results.

5.1 *General.*

The results of the drag and pressure measurements, carried out in the closed jet of windtunnel 3, are plotted as a function of the Reynolds number *Re* in figs. 3 and 7.

The results of the corresponding measurements in the open jet of windtunnel 4 are given in figs. 4, 5, 6 and 8.

The Reynolds number is calculated from the formula:

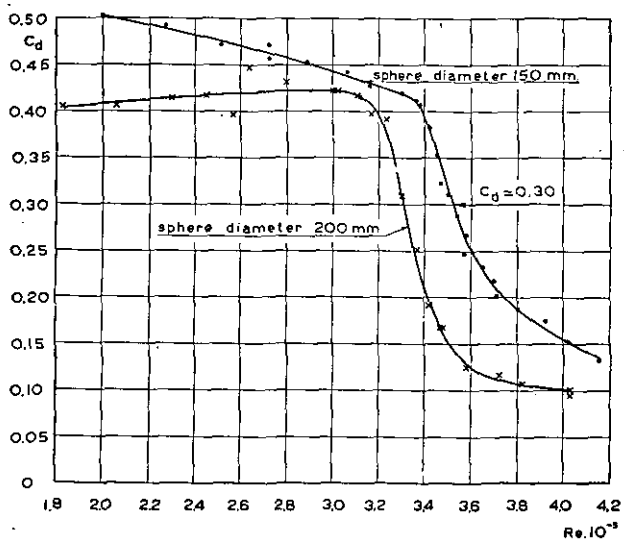

FIGURE 3.
Windtunnel 3
Drag coefficient of two spheres in terms of Reynolds number.

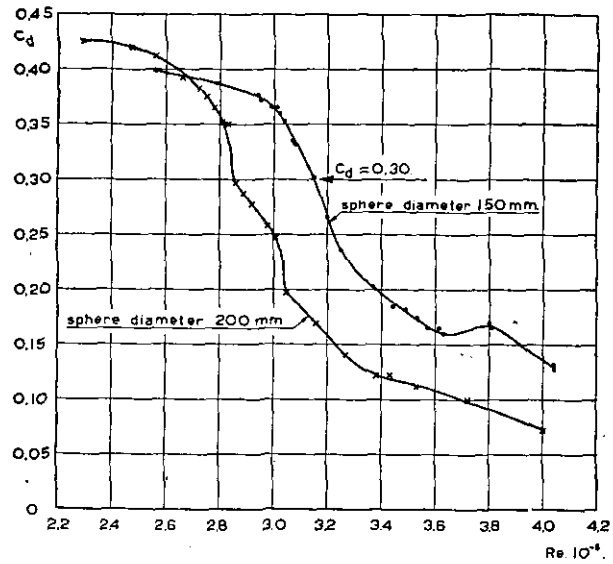

FIGURE 4.
Windtunnel 4
Drag coefficient of two spheres in terms of Reynolds number.

$$Re = \frac{Vd}{\vartheta}$$

where:

V = airspeed in m/sec,

d = sphere diameter in m,

ϑ = kinematic viscosity in m^2/sec,

The value of the critical Reynolds number Re_k, generally regarded as a convenient criterion of the turbulence of airflow, is taken to be the value of *Re* at which the dragcoefficient c_d is 0,30 (drag measurements) and the pressure coefficient c_p is 1,22 (pressure measurements). In table 1 these values are collected for the case of the most favourable conditions such as the smallest spindle diameter and the largest tightening loads. In table 2 similar values, obtained with different spindle diameters and tightening loads, are summarized.

5.2 *Drag measurements.*

The drag measurements in windtunnel 3 and 4 show that the curves obtained have no discontinuity, as often happens, but the transition is shown by a steep decline of the curve. Both fig. 3 (windtunnel 3) and 4 (windtunnel 4) show that Re_k decreases when the sphere diameter increases. The influence of the sphere diameter on Re_k is a well-known effect. Measurements carried out by DRYDEN [3]) showed that the intensity of the

[3]) DRYDEN, H. L., SCHUBAUER, G. B., MOCK, W. C. and SKRAMSTAD, H.K.: Measurements of intensity and scale of windtunnel turbulence and their relation to the critical REYNOLDS number of spheres, N.A.C.A. Rep. 581, 1937.

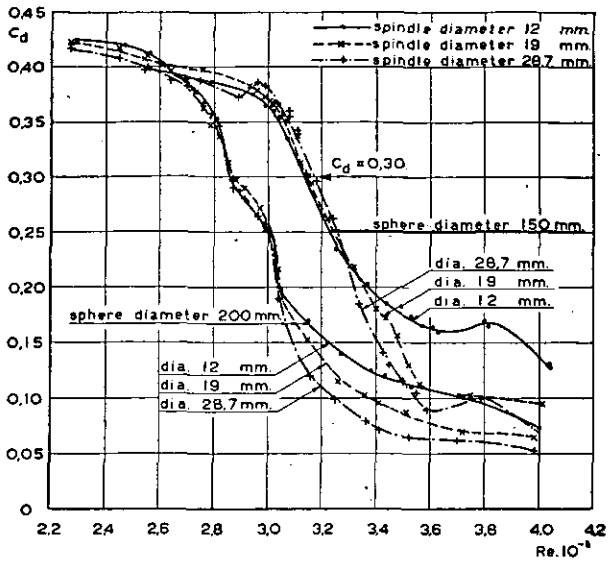

FIGURE 5.
Windtunnel 4
The influence of the spindle diameter on the drag coefficient of two spheres. (tightening loads in tunnel 4: 50 and 10 kg)

turbulence in the windtunnel concerned was not affected by changing the airvelocities. As however the value of Re_k decreases with increasing sphere diameter this effect is to be ascribed to the influence of the scale of the turbulence on Re_k. According to the above mentioned investigations, Re_k varies inversely proportional to $d^{0,20}$.

When the values of Re_k, obtained in windtunnel 3 are compared with those obtained in windtunnel 4, it is evident, that the turbulence in windtunnel 3 is lower than that in windtunnel 4. The value of Re_k of the smaller sphere in windtunnel 3 is $Re_k = 3{,}52 \times 10^5$, in windtunnel 4 $Re_k = 3{,}15 \times 10^5$. Corresponding values obtained with the larger sphere are $Re_k = 3{,}31 \times 10^5$ in windtunnel 3 and $Re_k = 2{,}86 \times 10^5$ in windtunnel 4.

The influence of the sphere diameter is derived by comparing the results of the 150 mm sphere with those of the 200 mm sphere, both in tunnel 3 and 4. In windtunnel 3 Re_k varies inversely proportional to $d^{0,21}$, in windtunnel 4 to $d^{0,34}$. The result of the measurements in tunnel 3 confirm the experiments of DRYDEN, for tunnel 4 the exponent is somewhat higher. It may be possible however, that this difference is caused by variation of turbulence in tunnel 4, due to the different airspeeds at which Re_k for both spheres occurs.

The influence of the diameter of the supporting spindle, determined in windtunnel 4 (fig. 5), gives no appreciable difference in the value of Re_k.

As described in section 4.1, the influence of the tightening loads on the values of c_d has been determined by decreasing the load in the front suspension point from 50 kg to 25 kg. The influence of decreasing the tightening loads determined from measurements with the two spheres

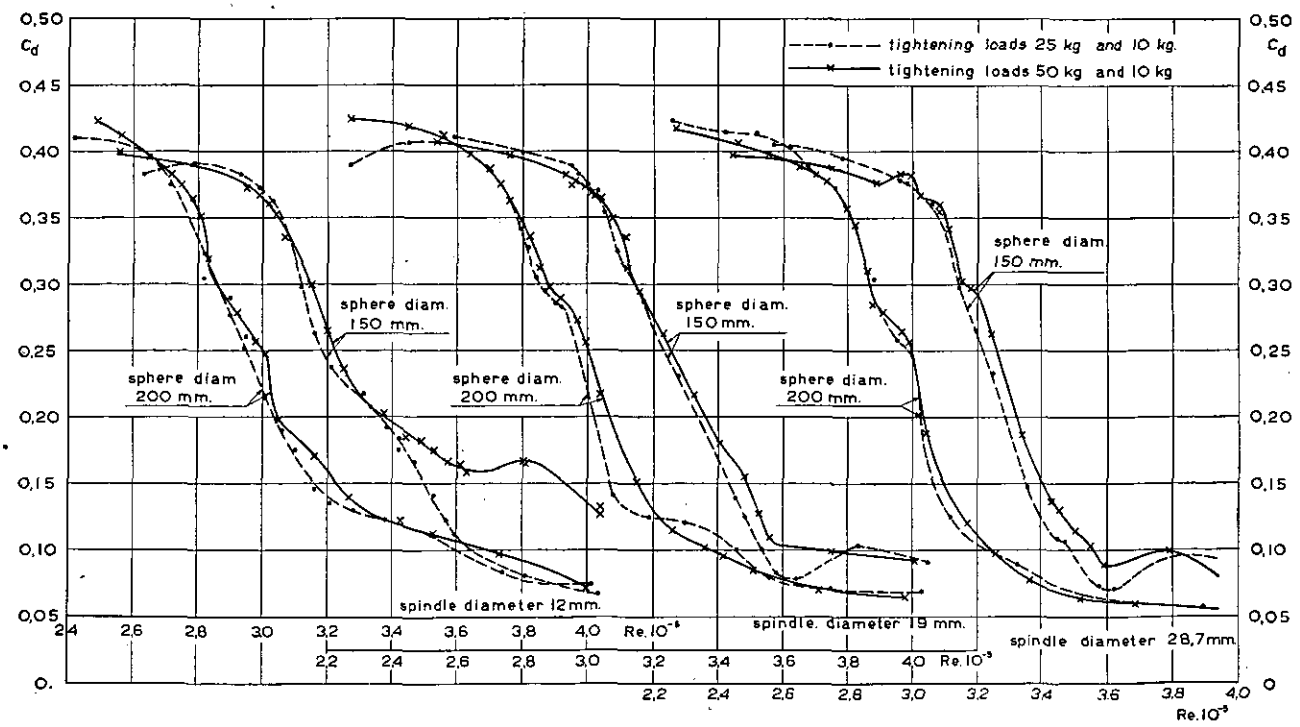

FIGURE 6.
Windtunnel 4
The influence of the tightening load on the drag coefficient of the spheres for spindle diameters 12 mm, 19 mm and 28,7 mm.

and different shaftdiameters, results in most cases in lower values of c_d (fig. 6). In the region of Re_k, however, the effect is almost negligible.

In table 2 the values of Re_k, obtained with various spindle diameters and tightening loads, are given. The maximum differences of Re_k from the values obtained in the standard conditions (spindle diameter 12 mm, tightening loads in front suspension point 50 kg) are $-0{,}03 \times 10^5$ and $+0{,}02 \times 10^5$.

5.3 *Pressure measurements.*

The curves obtained in windtunnel 3 and 4 show a steep decline which resembles that of the curves obtained from the drag measurements. The values of Re_k, obtained from the pressure measurements, differ only slightly from those obtained from the drag measurements. The value of Re_k for the smaller sphere in windtunnel 3 is $Re_k = 3{,}5 \times 10^5$, in windtunnel 4 $Re_k = 3{,}11 \times 10^5$. These values are for the larger sphere in windtunnel 3 $Re_k = 3{,}34 \times 10^5$, in windtunnel 4 $Re_k = 2{,}81 \times 10^5$. As shown in table 1 these values are a little lower than those obtained by drag measurements except the value obtained with the larger sphere in the closed jet of windtunnel 3, which is slightly higher.

6 Conclusions.

a. The critical Reynolds number, derived from the drag measurements with spheres, is nearly equal to that, derived from the pressure measurements.

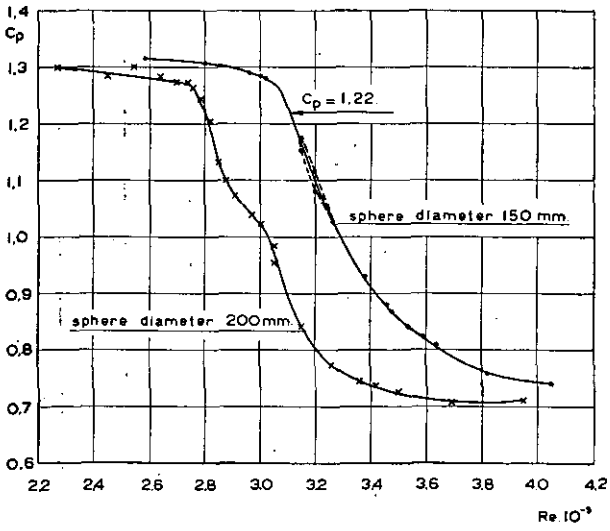

FIGURE 7.
Windtunnel 3
Pressure coefficient of two spheres in terms of Reynolds number.

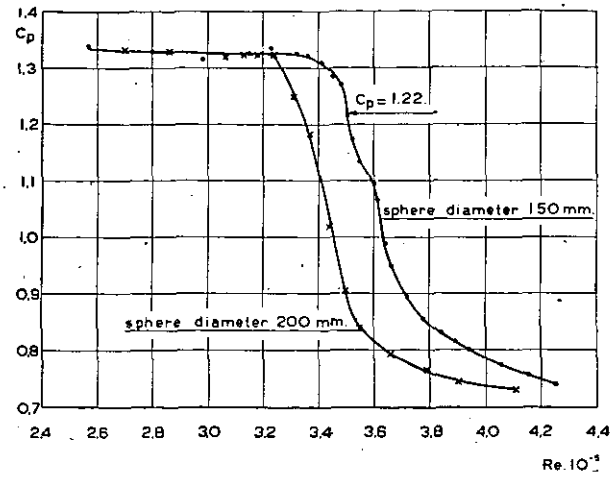

FIGURE 8.
Windtunnel 4
Pressure coefficient of two spheres in terms of Reynolds number.

b. The curves obtained from drag and pressure measurements show a steep decline in the region of Re_k. In general no discontinuity occurs in the curves.

c. The values of Re_k obtained with the smaller sphere (diameter 150 mm) are higher than those obtained with the larger sphere (diameter 200 mm). As DRYDEN has pointed out this phenomenon is due to the influence of the scale of turbulence. In windtunnel 3 Re_k determined from drag measurements varies inversely proportional to $d^{0{,}21}$, in windtunnel 4 to $d^{0{,}34}$. The result for tunnel 3 confirms the experiments of DRYDEN ($Re_k :: 1/d^{0{,}20}$), for tunnel 4 the somewhat higher exponent may be caused by a slight variation of turbulence at different airspeeds.

d. The airflow in the closed jet of windtunnel 3, as determined by drag and pressure measurements, has a critical Reynolds number of about:

$3{,}5 \times 10^5$ with sphere diameter 150 mm
$3{,}3 \times 10^5$ with sphere diameter 200 mm

e. The airflow in the open jet of windtunnel 4, as determined by drag and pressure measurements, has a critical Reynolds number of about:

$3{,}1 \times 10^5$ with sphere diameter 150 mm
$2{,}8 \times 10^5$ with sphere diameter 200 mm

f. The airflow in the closed jet of windtunnel 3 is less turbulent than the airflow in the open jet of windtunnel 4.

g. Although no qualitative data of the turbulence of airflow were determined, it may be concluded from a comparison with the results of sphere measurements in similar tunnels, that the turbulence in tunnel 3 is rather low.

h. The diameter of the supporting spindle affects the drag-curves somewhat, although the value of the critical Reynolds number is almost unaltered.

i. Decreasing the tightening loads has about the same effect as increasing the diameter of the supporting spindle.

Completed: May 1946.

TABLE 1.

The values of Re_k in windtunnel 3 and 4, determined from pressure and drag measurements with two spheres (supporting spindle 12 mm, tightening loads in tunnel 4, 50 kg and 10 kg).

Sphere diam.	Windtunnel 3		Windtunnel 4	
	Re. 10^{-5} ($c_p = 1{,}22$)	*Re.* 10^{-5} ($c_d = 0{,}30$)	*Re.* 10^{-5} ($c_p = 1{,}22$)	*Re.* 10^{-5} ($c_d = 0{,}30$)
150 mm	3.50	3.52	3.11	3.15
200 mm	3.34	3.31	2.81	2.86

TABLE 2.

Windtunnel 4.
The influence of the diameter of the supporting spindle and the tightening loads on the value of Re_k.

Diameter of supporting spindle	Tightening loads	Sphere diameter	
		150 mm	200 mm
		Re. 10^{-5} ($c_d = 0{,}30$)	*Re.* 10^{-5} ($c_d = 0{,}30$)
12 mm	25 kg and 10 kg	3.12	2.86
12 mm	50 kg and 10 kg	3.15	2.86
19 mm	25 kg and 10 kg	3.14	2.85
19 mm	50 kg and 10 kg	3.15	2.87
28.7 mm	25 kg and 10 kg	3.14	2.88
28.7 mm	50 kg and 10 kg	3.14	2.86

REPORT A. 1011

Some Remarks about High-Frequency Rotary-Current Electric Motors for Driving Model Propellers

by

Ir. J. G. SLOTBOOM

Summary.

The requirements to be met by electric motors for driving model propellers can be expressed in a simple condition. Starting from the formula giving the power required as a function of the propeller diameter, the number of revolutions and the torque coefficient, a relation is derived which represents the power for all motors as a function of the revolutions per min. only. This is evident after having been shown that the possibility of carrying out useful measurements at a reasonable wind speed — especially measurements concerning the stability at minimum speed — requires a value of $\frac{nD}{60}$ of about 100 m/sec. It is not necessary to choose higher values.

Furthermore, a few requirements about the dimensions of the motors and the number of poles (with regards to an economical use of the alternator) are given.

Contents.

1 Introduction.

As a consequence of the experience of the National Aeronautical Research Institute, obtained by the use of fast-running rotary-current electric motors for driving model propellers, the necessity of a clear formulation of the requirements to be met by those motors has been felt for some time.

Judged by their dimensions and maximum speeds the smaller ones especially appeared to be lacking in power and, therefore, to be less suited for carrying out useful measurements at reasonable airspeeds than the bigger ones, which seem to have better performances. For manufacturers of this type of high-speed electric motors as well as for laboratories using them it will be of great interest to know the maximum and minimum requirements concerning dimensions, power and speed, to be expected in the near future. They are given in this paper in graphical form.

2 Thrust and torque coefficients of the propeller. Dimensions of the nacelle.

For correctly estimating the behaviour of an aeroplane with operating engines from the results of measurements on a model in a wind channel, the velocity field around the model should be similar to that around the original aeroplane. At the same time the scale of the model propeller diameter must be the same as that of the model, while $\frac{V}{n_1 D}$, K_T and K_Q must have identical values for model and full-scale propeller.

K_T and K_Q are defined by

$$K_T = \frac{T}{\rho n_1^2 D^4} , \qquad (1)$$

$$\text{and } K_Q = \frac{Q}{\rho n_1^2 D^5} . \qquad (2)$$

Without scale effect, pure geometrical similarity and the same value $\frac{V}{n_1 D}$ for model and full-scale propeller are sufficient to obtain similar velocity fields. There will, however, always be some scale effect and in order to avoid its influence becoming excessive, it is necessary to carry out

the measurements at reasonable wind speeds. Neglecting the scale effect we can write:

$$K_Q \text{ (model)} = K_Q \text{ (full scale)}.$$

A mean value of K_Q for modern propellers is about 0,015. The calculation of the power required to drive model propellers is based on this value.

Of great importance is the requirement concerning the motor diameter. The diameter should be such that the entire motor can be placed inside the model nacelle. Therefore, the maximum diameter of the motor is not allowed to exceed $\frac{1}{4}$ of the propeller diameter. When in the future piston engines are replaced by gas turbines, it is likely that this maximum motor diameter should be decreased still further. The maximum length of the motor should not exceed 2 to $2\frac{1}{2}$ times its diameter.

3 Power and speed.

The power N, required to drive a propeller is equal to $2\ \pi n_1 Q$ or with formula (2) and using metric units:

$$N = \frac{2\ \pi \rho K_Q}{75}\ n_1^3 D^5 \quad \text{hp}. \qquad (3)$$

Now the problem is to find those combinations of n_1 and D, for which all conditions of flight can be simulated in the model tests. D being constant, the required power is proportional to n_1, as appears from formula (3). On the other hand, in the case of a rotary-current electric motor, the available power is roughly proportional to n_1. Hence, the requirements to be put to electric motors driving propellers, are to be based on the highest value of n_1, expected at a given D. In flight modern airscrews operate at tip speeds up to about 1,1 times the velocity of sound. At minimum flight velocity the tip speed of the propeller still is 310 to 320 m/sec. That minimum velocity is about the same as the wind speed at which the measurements in a windtunnel of medium size and speed can be carried out comfortably. The stability of an aeroplane at minimum flying speed being of great importance, it is necessary also to fulfil the corresponding conditions when testing the model in a wind channel. These considerations lead to the conclusion that the model propeller should be able to operate at tip speeds of about 310 m/sec or at $n_1 D = \frac{310}{\pi} = 100$. Normally a higher value of $n_1 D$ is not to be expected. A lower value may for instance give trouble with respect to the stability tests in the minimum speed condition.

Substituting $n_1 D = 100$; $K_Q = 0{,}015$ and $\rho = 0{,}125$ in (3) we obtain the required power as a function of the speed n_1 (revolutions/sec) or $n = 60\ n_1$ (rev/min). The heavy curve in fig. 1 represents this function. Figure 1 also shows a few N-n curves for some higher values of $n_1 D$, on which it is, however, not necessary to base requirements.

The dotted curves in fig. 1 represent N as a function of n for several values of the maximum motor diameter d_{max} $(= \frac{1}{4} D)$.

The requirements to be met by electric motors driving model propellers now can be formulated as follows:

The point given by N_{max} and n_{max} should be located on the N-n curve for $\frac{nD}{60} = 100$ in fig. 1. Combinations of N_{max} and n_{max} in the region above the given curve, in general are of no practical use. The motor diameter should not be greater than that belonging to the dotted curve going through the given point for N_{max} and n_{max} and the length should not exceed 2 or 2,5 times the diameter.

Fig. 1 is very useful for determining the required maximum motor power and speed for a given diameter D of the model propeller. The point where the dotted curve for $d_{max} = \frac{1}{4} D$ and the heavy curve intersect indicates the required values.

Obviously, the general requirements can be made independent of the wind channel in which the measurements are carried out.

For a large number of model motors used at present for wind tunnel research, the values of N_{max}, n and d_{max} do not correspond to the given curve. In some cases the number of revolutions is unnecessarily high and mostly the diameter is more or less excessive. Specially for the smaller motors, the demands concerning the dimensions seem to be rather exacting. It is possible, of course, to formulate other requirements than those given in this report, but it is believed that this closer examination of the problem will give a lead to the right requirements for this type of motors.

In applying the requirements to geared motors the curves mentioned above are valid only for motor and gear box together.

4 The number of poles.

The power available to drive the model propellers

will often be dependent on the power which can be delivered by the high-frequency alternator. In section 3 of this paper we learned, that the fast-running motors are the smallest. A fast-running motor means an alternator running at high speed and, in consequence, having much power available. The big motors run relatively slow and when they have two poles only, the high-frequency alternator also runs slow and has a small power output, under certain circumstances even too small. To get more power the use of a larger alternator is required, but it will be simpler to make use of a motor with four or six poles, in order to run the alternator at twice or three times the speed of the motor.

For alternators running at a maximum frequency of 500 cycles, the desirable number of poles is:

for motors with

n_{max}	= 15000—30000	rev/min,	two,
n_{max}	= 10000—15000	rev/min	four,
n_{max}	= 7500—10000	rev/min	six,
n_{max}	= 6000— 7500	rev/min	eight.

5 List of symbols.

D = diameter of the propeller (or model propeller)

n_1 = number of revolutions per sec.

Q = torque of the propeller (or model propeller)

T = thrust of the propeller (or model propeller)

V = airspeed

ρ = density of the air.

Completed: July 1946.

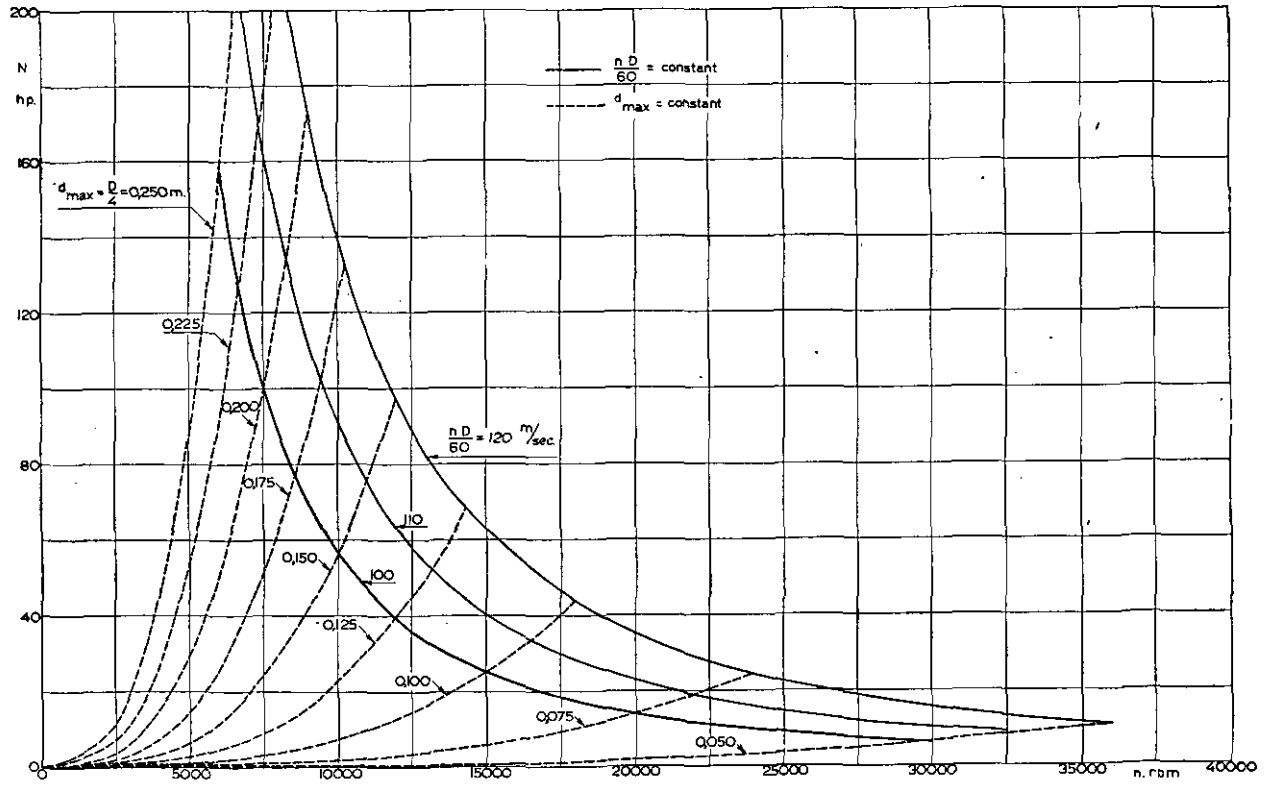

FIGURE 1.

N as a function of n for various values of $\frac{nD}{60}$ *and* d_{max} *or* D.

REPORT S. 311 [1])

Calculation of the Deformation of Two-Spar Wings with Shear-Resistant Skin

by

Ir. F. J. PLANTEMA and Prof. Dr. Ir. A. VAN DER NEUT

Summary.

The equations giving the relation between the internal loads and the deformations of two-spar wings with shear-resistant skin, are derived by applying a modified version of CASTIGLIANO's theorem, stating that the energy $F = A - A_r - A_q = \text{Min.}$, to an arbitrary part of the wing located between an arbitrary pair of consecutive ribs. The deformation of the wing can be completely described by five functions v_1, v_2, ψ, Θ_1 and Θ_2. The five equations of equilibrium (3.19) to (3.23) incl., which are necessary for the computation of the energy A_q, are derived in art. 3, whereupon the elastic energy A (4.15), the work of the boundary forces A_r (4.7) and the work of the virtual loads A_q (4.8, 14), are computed in art. 4. The solution of the variational problem $F = \text{Min.}$, given in art. 5, yields five differential equations which, together with the appropriate boundary conditions, determine the five deformation functions. These equations can yet be simplified by introducing new variables φ_1, φ_2 instead of Θ_1, Θ_2; thus, eqs. (5.12) to (5.15) incl., which do not contain the function ψ, are obtained. The boundary conditions at the ribs and in the plane of symmetry of the wing are derived in art. 6. Finally, a numerical method for solving the equations is indicated in art. 7.

Contents.

1 Introduction.

The computation of the stress distribution in two-spar wings with shear-resistant skin has been dealt with in two papers in Vol. XII of the Reports and Transactions of the National Aeronautical Research Institute (Nationaal Luchtvaartlaboratorium) (*ref.* 1 and 2). However, in several investigations it is necessary also to compute the deformations of the wing. The solution of the latter problem, assuming the internal loads to be known, is given in this report. [2])

It is to be expected, that the derivation of the formulae based solely on geometrical considerations, would be very complicated. Therefore, no attempt has been made to do so; instead the energy method, starting from CASTIGLIANO's theorem, has been used. With the rules of the calculus of variations the equations giving the relation between the internal loads and the deformations, can be derived very elegantly. Some relatively simple examples have been given by TREFFTZ (*ref.* 3) and MARGUERRE (*ref.* 4). In view of the complexity of the wing problem it appeared desirable to start from a modified statement of CASTIGLIANO's theorem, which can also appropriately be called the theorem of virtual loads. This modified statement and its application are being discussed in art. 2. The differential equations of the wing problem, holding for each part of the wing between two consecutive ribs, are derived in art. 3, 4 and 5. Their boundary conditions at the ribs, and at the plane of symmetry of the wing are given in art. 6 and the solution of the equations is discussed in art. 7.

The wing scheme is equal to that mentioned in *ref.* 1 and 2 and also the same notations have been used as far as possible (see art. 8).

[1]) This report is an abbreviated translation of N.L.L.-Report S. 297, March 1945 (written in Dutch with an English summary).

[2]) In principle it is possible to compute simultaneously the internal loads and the deformations, independent of *ref.* 1 and 2. This method has been developed for the relatively simple case of a wing with parallel spars; see *ref.* 8. However, pending the execution of the complete numerical calculations, it is expected that no important gain in time can be obtained, whereas the possibility of making errors would definitely increase.

2 CASTIGLIANO'S theorem and its application.

Usually the theorem is stated as follows (see a.o. *ref.* 5 and 6): Of all stress systems that satisfy the equations of equilibrium in a body and balance the specified loads at the boundary, but need not satisfy the specified boundary conditions for the displacements and rotations, the actually occurring system minimizes the expression $A—A_r$, where A is the elastic energy expressed in the stresses or loads and A_r is the work, done by the unknown boundary forces at the specified displacements.

In order to compute certain displacements (or rotations) these are formally considered to be given quantities. As the equations of equilibrium can then no longer be satisfied, this can only be done by introducing certain virtual loads q. If the equations of equilibrium in the body and at that part of its boundary where the loads are given are symbolically denoted by $E\ (\sigma, \tau) = 0$, the virtual loads must now satisfy the equations $E\ (\sigma, \tau) + q = 0$. The virtual forces may be considered as unknown boundary forces at points, where the displacements are specified. Denoting the work of the virtual forces at their corresponding displacements by A_q, the modified theorem may be expressed as

$$F = A - A_r - A_q = \text{Min.} \qquad (2.1)$$

The solution of this variational problem yields the equations, which enable the computation of the deformations. A very simple illustrative example may be given here, namely the calculation of the deflexions v of the beam in fig. 2.1. The elastic energy is

$$A = \int_0^l \left(\frac{M^2}{2 S_b} + \frac{D^2}{2 S_s} \right) dx.$$

The specified displacements are the deflections at both ends and the slope at the built-in end; as they are all zero the work $A_r = 0$.

The equations of equilibrium are

$$M' + D = 0, \qquad (2.2)$$
$$D' + p = 0, \qquad (2.3)$$
$$M_{x=l} = 0. \qquad (2.4)$$

Considering the deflexions v as given quantities means, that eq. (2.3) can not be satisfied; virtual forces q must be introduced such, that

$$D' + p + q = 0 \quad \text{or} \quad q = -(D' + p) = M'' - p.$$

The work A_q is therefore given by

$$A_q = \int_0^l v\ q\ dx = \int_0^l v\ (M'' - p)\ dx.$$

The variational problem (2.1) is expressed in this case by

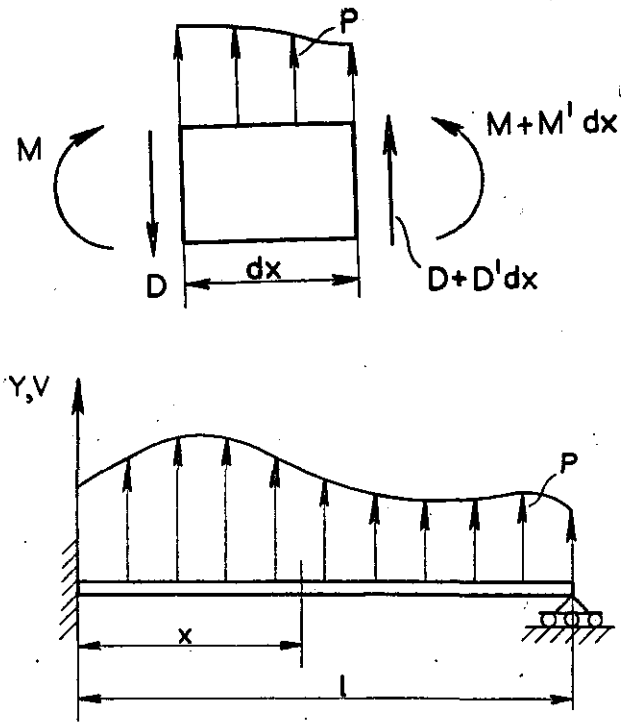

FIGURE 2.1.
Example.

$$F = A - A_r - A_q = \int_0^l \left\{ \frac{M^2}{2 S_b} + \frac{M'^2}{2 S_s} - v\ (M'' - p) \right\} dx = \text{Min.}$$

The variation δF at a variation of M must be zero

$$\delta F = \int_0^l \left(\frac{M}{S_b}\ \delta M + \frac{M'}{S_s}\ \delta M' - v\ \delta M'' \right) dx =$$

$$= \int_0^l \left(\frac{M}{S_b} - \frac{M''}{S_s} - v'' \right) \delta M\ dx +$$

$$+ \left[\left(\frac{M'}{S_s} + v' \right) \delta M \right]_0^l - \left[v\ \delta M' \right]_0^l = 0.$$

Bearing in mind that $v = 0$ at $x = 0$ and $x = l$, $\delta M = 0$ at $x = l$ and substituting eq. (2.2), the following differential equation and boundary condition at $x = 0$ follow from the requirement that $\delta F = 0$ at any arbitrary variation of the bending moments M:

$$v'' = \frac{M}{S_b} + \frac{D'}{S_s};\ v' = \frac{D}{S_s} \text{ at } x = 0.$$

For a complex problem, where the development of the final equations of equilibrium contains various eliminations and other operations, it is essential, in order to avoid errors, to introduce the virtual loads before the equations of equilibrium are derived and to eliminate them immediately before proceeding with the variational problem $\delta F = 0$.

3 The equations of equilibrium.

3.1 *Introduction of the virtual loads.*

A cross section of the schematized wing is given in fig. 4.1; the shaded portions are considered to be infinitely rigid. The deformation of the wing in the YZ-plane is completely determined by the displacements v_1 and v_2 of the shear centres of the spars and the rotation of

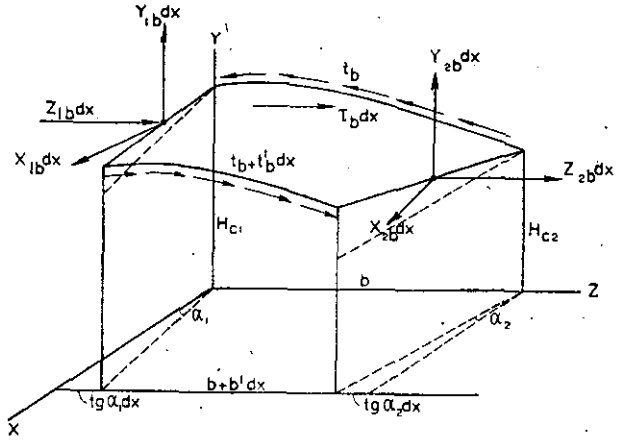

FIGURE 3.1.
The equilibrium of a strip of the top skin.

one spar, e.g. ψ_1 (see fig. 4.2). However, it appears to be more convenient to introduce the quantity $\psi = \dfrac{\psi_1 + \psi_2}{2\,(h_{c1} - h_{c2})}$ as the third „displacement" instead of ψ_1. The deformation in the XY-plane is determined by the displacements v_1 and v_2 and the rotations Θ_1 and Θ_2 of the cross sections of both spars in the XY-plane. The deformation of the wing can therefore be completely described (excepting the displacement in Z-direction) by the five functions v_1, v_2, ψ, Θ_1 and Θ_2. In order to enable the computation of these functions by means of the modified theorem of CASTIGLIANO the virtual running loads q_1, q_2, τ, m_1 and m_2 are introduced (see fig. 4.3).

3.2 *The equilibrium of the skin.*

We first consider the equilibrium of a strip of the top skin of a width dx (fig. 3.1). The running loads acting on this strip are indicated in fig. 3.1; the forces X, Y and Z are transferred from the skin (including the rigid formers) to the spars. Pending the formal proof, that the virtual loads on the top and bottom skins are equal, a suffix has been added to the symbol τ. The virtual load τ acts at a distance H, parallel to the wing plane (XZ-plane), where H is the distance to the wing plane of the intersection of the resultant of the shear loads t in the skin, indicated in fig. 3.1 or 3.3 in cross section x, with the plane $z = \frac{1}{2}\,b$. From the equation of equilibrium of the force components parallel to the X-axis together with that of the moments about the Y-axis, neglecting terms of higher order, follow the identities

$$-X_{1b} = X_{2b} = t_b. \tag{3.1}$$

The equilibrium of the force components parallel to the Y-axis and that of the force components parallel to the Z-axis yield

$$Y_{1b} + Y_{2b} - t_b \left[(H_{c1} - H_{c2}) \right]' = 0, \tag{3.2}$$

$$\tau_b + Z_{1b} + Z_{2b} + (t_b b)' = 0. \tag{3.3}$$

From the equilibrium of the moments about the X-axis follows

$$-\tau_b H_b - Z_{1b} H_{c1} - Z_{2b} H_{c2} + Y_{2b} b - 2\,(t_b \bar{O}_{b1})' - t_b\,(H_{c1} - H_{c2})\,\mathrm{tg}\,\alpha_1 = 0, \tag{3.4}$$

where $\bar{O}_{b1}$ is defined according to fig. 3.2.

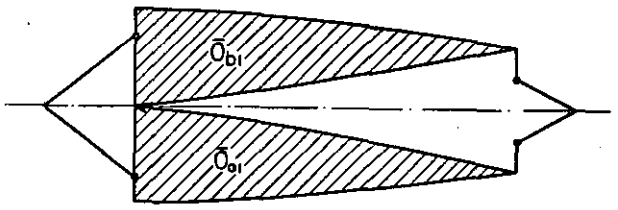

FIGURE 3.2.
The definition of $\bar{O}_{b1}$, $\bar{O}_{o1}$, $\bar{O}_{b2}$ and $\bar{O}_{o2}$.

The equilibrium of a strip of the bottom skin (fig. 3.3) yields, in precisely the same way, the equations

$$-X_{1o} = X_{2o} = t_o, \tag{3.5}$$

$$Y_{1o} + Y_{2o} + \left[t_o\,(\bar{H}_{c1} - \bar{H}_{c2}) \right]' = 0, \tag{3.6}$$

$$-\tau_o + Z_{1o} + Z_{2o} + (t_o\,b)' = 0, \tag{3.7}$$

$$-\tau_o H_o + Z_{1o} \bar{H}_{c1} + Z_{2o} \bar{H}_{c2} + Y_{2o}\,b + 2\,(t_o \bar{O}_{o1})' + t_o\,(\bar{H}_{c1} - \bar{H}_{c2})\,\mathrm{tg}\,\alpha_1 = 0. \tag{3.8}$$

3.3 *The equilibrium of the spars.*

An element of the front spar with the loads acting on it is given in fig. 3.4. q_1 is a virtual force acting in the shear centre of the front spar, m_1 a virtual moment in the XY-plane. From the equilibrium of the forces in X-direction we find

$$X_{1b} + X_{1o} = 0; \tag{3.9}$$

hence, from (3.1) and (3.5)

$$t_b = -t_o = t. \tag{3.10}$$

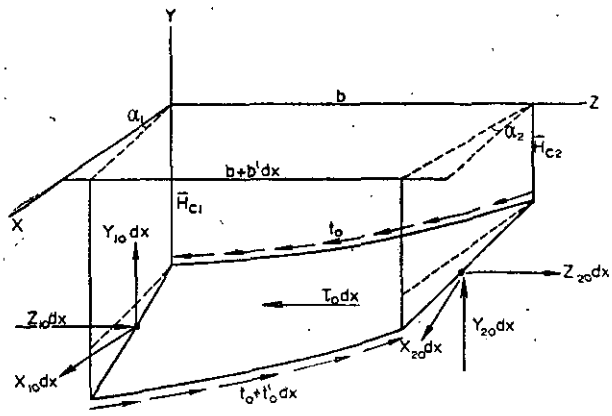

FIGURE 3.3.
The equilibrium of a strip of the bottom skin.

This equality has already been used in fig. 3.4. The equilibrium of the forces parallel to the Y- and Z-axes and of the moments about the X- and Z-axes gives, again neglecting terms of higher order, the following four equations

$$-Y_{1b} - Y_{1o} + D'_{s1} + D'_{g1} + p_1 + q_1 + [t\ (h_{c1} - h_1)]' = 0, \tag{3.11}$$

$$Z_{1b} + Z_{1o} = 0, \tag{3.12}$$

$$(D_{s1}\, e_1)' - \operatorname{tg}\alpha_1 \Big\{ M'_1 + D_{s1} + D_{g1} + t\,(h_{c1} - h_1) \Big\} + (p_1 + q_1)\, e_1 - Z_{1b}\, H_{c1} + Z_{1o}\, \bar{H}_{c1} = 0, \tag{3.13}$$

$$m_1 + D_{s1} + D_{g1} + t\ (h_{c1} - h_1) + M'_1 + X_{1b}\, H_{c1} - X_{1o}\, \bar{H}_{c1} = 0. \tag{3.14}$$

For an element of the rear spar we find in exactly the same way

$$X_{2b} + X_{2o} = 0,$$

$$-Y_{2b} - Y_{2o} + D'_{s2} + D'_{g2} + p_2 + q_2 - [t\ (h_{c2} - h_2)]' = 0, \tag{3.15}$$

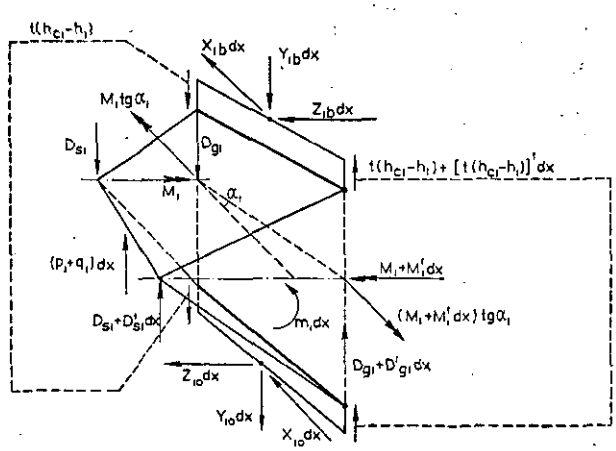

FIGURE 3.4.
The equilibrium of an element of the front spar.

$$Z_{2b} + Z_{2o} = 0, \tag{3.16}$$

$$(D_{s2}\, e_2)' - \operatorname{tg}\alpha_2 \Big\{ M'_2 + D_{s2} + D_{g2} - t\,(h_{c2} - h_2) \Big\} + (p_2 + q_2)\, e_2 + Z_{2b}\, H_{c2} - Z_{2o}\, \bar{H}_{c2} = 0, \tag{3.17}$$

$$m_2 + D_{s2} + D_{g2} - t\ (h_{c2} - h_2) + M'_2 + X_{2b}\, H_{c2} - X_{2o}\, \bar{H}_{c2} = 0. \tag{3.18}$$

The first of these equations is dependent upon (3.1, 5 and 9). Further, from (3.3 and 7), we find that $\tau_b = \tau_o = \tau$.

3.4 *The final equations.*

With the identities $-X_{1b} = X_{2b} = X_{1o} = -X_{2o} = t$ we obtain from (3.14 and 18)

$$m_1 + M'_1 + D_{s1} + D_{g1} - th_1 = 0, \tag{3.19}$$

$$m_2 + M'_2 + D_{s2} + D_{g2} + th_2 = 0. \tag{3.20}$$

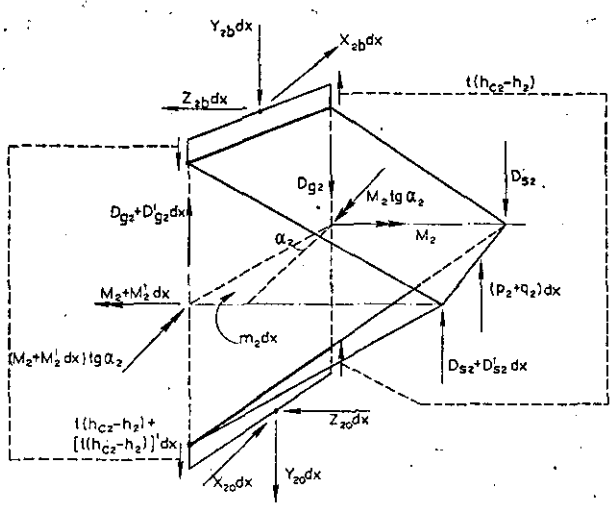

FIGURE 3.5.
The equilibrium of an element of the rear spar.

With $Z_{1b} = -Z_{1o} = Z_1$ and $Z_{2b} = -Z_{2o} = Z_2$ from (3.12) and (3.16) we obtain from (3.13) and (3.17), also substituting (3.19) and (3.20),

$$Z_1\, h_{c1} = (D_{s1}\, e_1)' + p_1\, e_1 - th_{c1} \operatorname{tg}\alpha_1 + m_1 \operatorname{tg}\alpha_1 + q_1\, e_1,$$

$$-Z_2\, h_{c2} = (D_{s2}\, e_2)' + p_2\, e_2 + th_{c2} \operatorname{tg}\alpha_2 + m_2 \operatorname{tg}\alpha_2 + q_2\, e_2.$$

Substituting these expressions in (3.3) or (3.7), as well as $\operatorname{tg}\alpha_1 + \operatorname{tg}\alpha_2 = -b'$, the following equation is found

$$\tau + m_1 \frac{\operatorname{tg}\alpha_1}{h_{c1}} - m_2 \frac{\operatorname{tg}\alpha_2}{h_{c2}} + q_1 \frac{e_1}{h_{c1}} - q_2 \frac{e_2}{h_{c2}} + \frac{1}{h_{c1}}\,(D_{s1}\, e_1)' - \frac{1}{h_{c2}}\,(D_{s2}\, e_2)' + \frac{p_1\, e_1}{h_{c1}} - \frac{p_2\, e_2}{h_{c2}} + \frac{1}{b}\,(tb^2)' = 0. \tag{3.21}$$

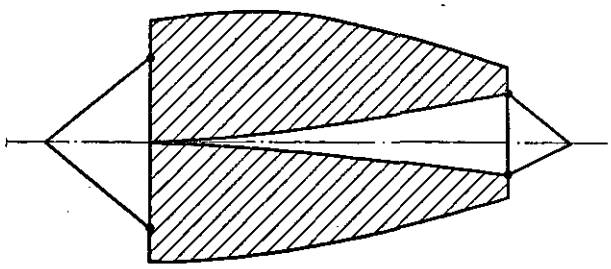

FIGURE 3.6.
The definition of O_1.

Substituting the expressions for Z_1 and Z_2 in (3.4) we get

$$b\,Y_{2b} = \frac{H_{c1}}{h_{c1}}\,(D_{s1}\,e_1)' - \frac{H_{c2}}{h_{c2}}\,(D_{s2}\,e_2)' +$$

$$+ \frac{H_{c1}}{h_{c1}}\,p_1\,e_1 - \frac{H_{c2}}{h_{c2}}\,p_2\,e_2 + t\,H_{c2}\,b' +$$

$$+ 2\,(t\,\bar{O}_{b1})' + \tau\,H_b + \frac{H_{c1}}{h_{c1}}\,m_1\,\mathrm{tg}\,\alpha_1 -$$

$$- \frac{H_{c2}}{h_{c2}}\,m_2\,\mathrm{tg}\,\alpha_2 + \frac{H_{c1}}{h_{c1}}\,q_1\,e_1 - \frac{H_{c2}}{h_{c2}}\,q_2\,e_2;$$

similarly from (3.8)

$$b\,Y_{2o} = \frac{\bar{H}_{c1}}{h_{c1}}\,(D_{s1}\,e_1)' - \frac{\bar{H}_{c2}}{h_{c2}}\,(D_{s2}\,e_2)' +$$

$$+ \frac{\bar{H}_{c1}}{h_{c1}}\,p_1\,e_1 - \frac{\bar{H}_{c2}}{h_{c2}}\,p_2\,e_2 + t\,\bar{H}_{c2}\,b' +$$

$$+ 2\,(\bar{O}_{o1})' + \tau\,H_o + \frac{\bar{H}_{c1}}{h_{c1}}\,m_1\,\mathrm{tg}\,\alpha_1 -$$

$$- \frac{\bar{H}_{c2}}{h_{c2}}\,m_2\,\mathrm{tg}\,\alpha_2 + \frac{\bar{H}_{c1}}{h_{c1}}\,q_1\,e_1 - \frac{\bar{H}_{c2}}{h_{c2}}\,q_2\,e_2$$

and by addition, with $h = H_b + H_o$,

$$Y_{2b} + Y_{2o} = \frac{1}{b}\left\{(D_{s1}\,e_1)' - (D_{s2}\,e_2)' + \right.$$

$$+ p_1\,e_1 - p_2\,e_2 + th_{c2}\,b' + 2\left[t\,(\bar{O}_{b1} + \right.$$

$$\left.\left. + \bar{O}_{o1})\right]' + \tau h + m_1\,\mathrm{tg}\,\alpha_1 - m_2\,\mathrm{tg}\,\alpha_2 + q_1\,e_1 - \right.$$

$$\left. - q_2\,e_2\right\}.$$

From (3.2) and (3.6)

$$Y_{1b} + Y_{1o} = \left[t\,(h_{c1} - h_{c2})\right]' - (Y_{2b} + Y_{2o}).$$

Substituting in the right side of this equation

$$\bar{O}_{b1} + \bar{O}_{o1} + \tfrac{1}{2}\,bh_{c2} = \bar{O}_{b2} + \bar{O}_{o2} + \tfrac{1}{2}\,bh_{c1},$$

we obtain

$$Y_{1b} + Y_{1o} = \frac{1}{b}\left\{-(D_{s1}\,e_1)' + (D_{s2}\,e_2)' - \right.$$

$$- p_1\,e_1 + p_2\,e_2 - th_{c1}b' - 2\left[t\,(\bar{O}_{b2} + \bar{O}_{o2})\right]' -$$

$$\left. - \tau\,h - m_1\,\mathrm{tg}\,\alpha_1 + m_2\,\mathrm{tg}\,\alpha_2 - q_1\,e_1 + q_2\,e_2\right\}.$$

The equations of equilibrium (3.11) and (3.15) of the spar can now be written

$$(b + e_1)\,q_1 - e_2\,q_2 + \tau\,h + m_1\,\mathrm{tg}\,\alpha_1 - m_2\,\mathrm{tg}\,\alpha_2 +$$

$$+ (b + e_1)\,D'_{s1} + e_1'\,D_{s1} - (e_2\,D_{s2})' +$$

$$+ b\,D'_{g1} + (b + e_1)\,p_1 - e_2\,p_2 + 2\,t'\,O_2 +$$

$$+ t\,(2\,O'_2 + b'\,h_1) = 0, \qquad (3.22)$$

$$- e_1\,q_1 + (b + e_2)\,q_2 - \tau\,h - m_1\,\mathrm{tg}\,\alpha_1 +$$

$$+ m_2\,\mathrm{tg}\,\alpha_2 - (e_1\,D_{s1})' + (b + e_2)\,D'_{s2} +$$

$$+ e'_2\,D_{s2} + b\,D'_{g2} - e_1\,p_1 + (b + e_2)\,p_2 -$$

$$- 2\,t'\,O_1 - t\,(2\,O'_1 + b'\,h_2) = 0, \qquad (3.23)$$

where O_1 is the shaded area in fig. 3.6 and O_2 is defined similarly.

Omitting the virtual loads, the equations (3.19, 20 and 21) are identical with equations (4 a, b) and (14) of *ref.* 1, that have been derived in a different way; equations (3.22 and 23) replace equations (3 a, b) of *ref.* 1.

From the definition of D_g (see *ref.* 1, art. 03.2) we further have the equations of equilibrium

$$D_{g1} + M_1\,h'_1/h_1 = 0,$$

$$D_{g2} + M_2\,h'_2/h_2 = 0.$$

Finally, for wings with torsionally rigid spars (*ref.* 2), we have

$$Y_1 = Y_{1i}, \quad Y_2 = Y_{2i} \qquad (3.26)$$

where Y_1 and Y_2 are the torsional moments in the torsion tubes, that occur in the wing scheme.

4 Computation of A_r, A_q and A.

The modified theorem of CASTIGLIANO will be applied to an arbitrary part of the wing located between an arbitrary pair of consecutive ribs.

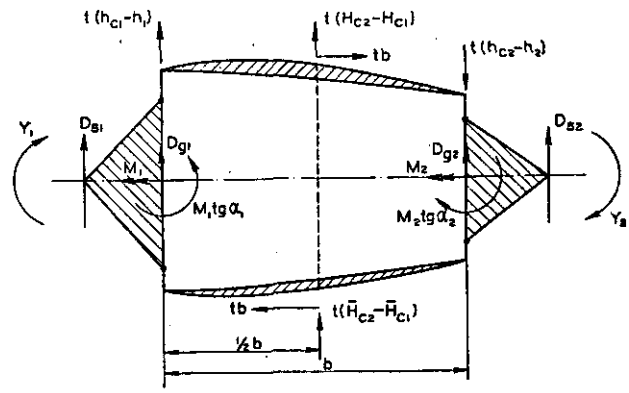

FIGURE 4.1.
The boundary loads.

The forces, acting on the boundaries of this part are given in fig. 4.1 and the specified displacements v_1, v_2, ψ, Θ_1 and Θ_2 in fig. 4.2 (see also art. 3.1). The work A_r, done by the boundary forces, is therefore expressed by

$$A_r = \Big[D_{s1}\, v_1 + D_{s2}\, v_2 + \Big\{ D_{g1} + t\,(h_{c1} - h_1) \Big\}\, y_1 + \Big\{ D_{g2} - t\,(h_{c2} - h_2) \Big\}\, y_2 + t\,(H_{c2} - H_{c1})\, y_b + t\,(\bar{H}_{c2} - \bar{H}_{c1})\, y_o + t\,b\,(u_b + u_o) + M_1\,\Theta_1 + M_2\,\Theta_2 + (M_1 \operatorname{tg}\alpha_1 - Y_1)\,\psi_1 + (M_2 \operatorname{tg}\alpha_2 + Y_2)\,\psi_2 \Big]_L^R .$$

The displacements v_1, v_2, y_1, y_2, y_b, y_o, u_b and u_o are interdependent due to the given kinematical assembly of the wing cross section (fig. 4.1). Their interrelation is expressed by the following equations, which will not be derived here,

$$\psi_1 = -\frac{v_1 - v_2}{a} + r_1\,\psi;\quad \psi_2 = \frac{v_1 - v_2}{a} + r_2\,\psi, \tag{4.1,2}$$

$$y_1 = v_1 + e_1\,\psi_1 = \Big(1 - \frac{e_1}{a}\Big)\, v_1 + \frac{e_1}{a}\, v_2 + e_1\, r_1\,\psi, \tag{4.3}$$

$$y_2 = v_2 + e_2\,\psi_2 = \frac{e_2}{a}\, v_1 + \Big(1 - \frac{e_2}{a}\Big)\, v_2 + e_2\, r_2\,\psi, \tag{4.4}$$

$$y_b = y_o = \tfrac{1}{2}\,(y_1 + y_2) = \tfrac{1}{2}\Big(1 - \frac{e_1 - e_2}{a}\Big)\, v_1 + \tfrac{1}{2}\Big(1 + \frac{e_1 - e_2}{a}\Big)\, v_2 + \tfrac{1}{2}\,(e_1\, r_1 + e_2\, r_2)\,\psi, \tag{4.5}$$

$$u = u_b + u_o = \frac{h}{a}\,(v_1 - v_2) + s\,\psi. \tag{4.6}$$

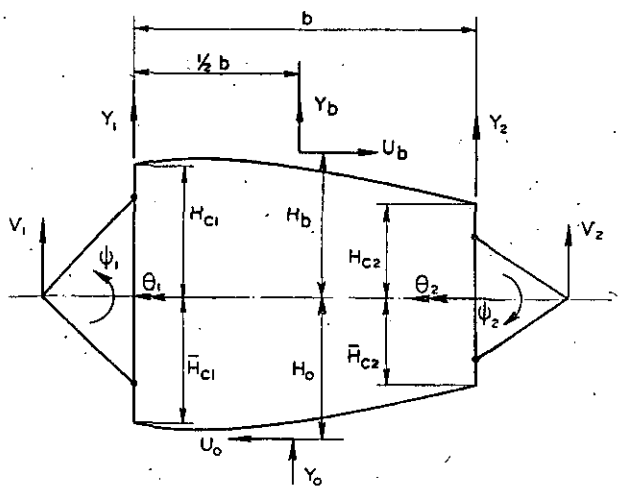

FIGURE 4.2.
The displacements and rotations.

Substitution of (4.1 to 6 incl.) in the expression for A_r and simultaneous elimination of D_{g1} and D_{g2} by means of (3.24,25) leads to [3])

$$A_r = \Big[M_1 \Big\{ \Theta_1 - v_1 \frac{h'_1}{h_1} + \psi_1 \Big(\operatorname{tg}\alpha_1 - e_1 \frac{h'_1}{h_1}\Big) \Big\} + M_2 \Big\{ \Theta_2 - v_2 \frac{h'_2}{h_2} + \psi_2 \Big(\operatorname{tg}\alpha_2 - e_2 \frac{h'_2}{h_2}\Big) \Big\} + D_{s1}\, v_1 + D_{s2}\, v_2 + t \Big\{ v_1 \Big[H_1 \Big(1 - \frac{e_1}{a}\Big) - H_2 \frac{e_2}{a} + h \frac{b}{a} \Big] + v_2 \Big[H_1 \frac{e_1}{a} - H_2 \Big(1 - \frac{e_2}{a}\Big) - h \frac{b}{a} \Big] + \psi\,(H_1\, e_1\, r_1 - H_2\, e_2\, r_2 + bs) \Big\} - Y_{1i}\,\psi_1 + Y_{2i}\,\psi_2 \Big]_L^R . \tag{4.7}$$

The virtual loads, that have been introduced in art. 3.1, are indicated in fig. 4.3. The work A_q can be written

$$A_q = \int_L^R A'_q\, dx, \text{ where} \qquad A'_q = q_1\, v_1 + q_2\, v_2 + m_1\,\Theta_1 + m_2\,\Theta_2 + \tau\, u. \tag{4.8}$$

The virtual loads will now be expressed in the internal loads M_1, M_2, D_{s1}, D_{s2} and t by means of (3.19 to 25 incl.). Thus

$$m_1 = -M'_1 + M_1 \frac{h'_1}{h_1} - D_{s1} + th_1, \tag{4.9}$$

$$m_2 = -M'_2 + M_2 \frac{h'_2}{h_2} - D_{s2} - th_2, \tag{4.10}$$

$$q_1 = \frac{2\,h_{c1}\,h_{c2}}{as} \Big[-m_1 \Big(1 - \frac{h}{h_{c1}}\Big) \operatorname{tg}\alpha_1 + m_2 \Big(1 - \frac{h}{h_{c2}}\Big) \operatorname{tg}\alpha_2 \Big] + q^\circ_1, \tag{4.11}$$

$$q_2 = \frac{2\,h_{c1}\,h_{c2}}{as} \Big[m_1 \Big(1 - \frac{h}{h_{c1}}\Big) \operatorname{tg}\alpha_1 - m_2 \Big(1 - \frac{h}{h_{c2}}\Big) \operatorname{tg}\alpha_2 \Big] + q^\circ_2, \tag{4.12}$$

$$\tau = -\frac{2\,m_1}{s} \operatorname{tg}\alpha_1 \Big[-h_{c1} \frac{e_2}{a} + h_{c2} \Big(1 - \frac{e_1}{a}\Big) \Big] + \frac{2\,m_2}{s} \operatorname{tg}\alpha_2 \Big[h_{c1} \Big(1 - \frac{e_2}{a}\Big) - h_{c2} \frac{e_1}{a} \Big] - \frac{e_1}{h_{c2}}\, q^\circ_1 + \frac{e_2}{h_{c2}}\, q^\circ_2 + \tau^\circ. \tag{4.13}$$

[3]) For reasons of compactness ψ_1 and ψ_2 have also been retained as separate functions.

The functions q°_1, q°_2 and τ° are defined in art. 8. Substituting (4.6, 11, 12 and 13) in (4.8) we obtain

$$A'_q = q^\circ_1 \left[\nu_1 \left(1 - \frac{e_1 h}{a h_{c1}}\right) + \nu_2 \frac{e_1 h}{a h_{c2}} - \frac{e_1 s}{h_{c1}} \psi \right] + q^\circ_2 \left[\nu_1 \frac{e_2 h}{a h_{c1}} + \nu_2 \left(1 - \frac{e_2 h}{a h_{c2}}\right) + \frac{e_2 s}{h_{c2}} \psi \right] + \tau^\circ \left[\frac{h}{a} (\nu_1 - \nu_2) + s \psi \right] + m_1 \left[\Theta_1 - \operatorname{tg} \alpha_1 \left\{ \frac{\nu_1 - \nu_2}{a} + 2 \left(- h_{c1} \frac{e_2}{a} + h_{c2} \left(1 - \frac{e_1}{a}\right) \right) \psi \right\} \right] + m_2 \left[\Theta_2 + \operatorname{tg} \alpha_2 \left\{ \frac{\nu_1 - \nu_2}{a} + 2 \left(h_{c1} \left(1 - \frac{e_2}{a}\right) - h_{c2} \frac{e_1}{a} \right) \psi \right\} \right]. \quad (4.14)$$

The elastic energy A is given in art. 05 of *ref.* 1 and art. 05 of *ref.* 2

$$A = \tfrac{1}{2} \int_L^R \left\{ \frac{M_1^2}{S_{b1} \cos^3 \alpha_1} + \frac{M_2^2}{S_{b2} \cos^3 \alpha_2} + \frac{D^2_{s1}}{S_{s1} \cos \alpha_1} + \frac{D^2_{s2}}{S_{s2} \cos \alpha_2} + t^2 b \left(\frac{1}{G_b d_b} + \frac{1}{G_o d_o} \right) + \frac{Y^2_{1i}}{S_{w1}} + \frac{Y^2_{2i}}{S_{w2}} \right\} dx. \quad (4.15)$$

5 The load-deformation equations.

The equations giving the relation between the deformation functions ν_1, ν_2, Θ_1, Θ_2, ψ and the internal loads result from the solution of the variatonal problem (2.1). Successively, the variation of F is determined at a variation of D_{s1}, D_{s2}, M_1, M_2 and t; thus, five differential equations are obtained which are necessary and sufficient for the computation of the five unknowns. The first variation of F at a variation of D_{s1} can be written in the form

$$\delta F = \delta A - \delta A_r - \delta A_q = - \left[\nu_1 \delta D_{s1} \right]_L^R + \int_L^R (A_1 \delta D'_{s1} + B_1 \delta D_{s1}) \, dx,$$

where A_1 and B_1 are certain expressions obtained directly from the variation of (4.14) and (4.15). By partial integration we obtain

$$\delta F = \left[(A_1 - \nu_1) \delta D_{s1} \right]_L^R + \int_L^R (- A'_1 + B_1) \delta D_{s1} \, dx.$$

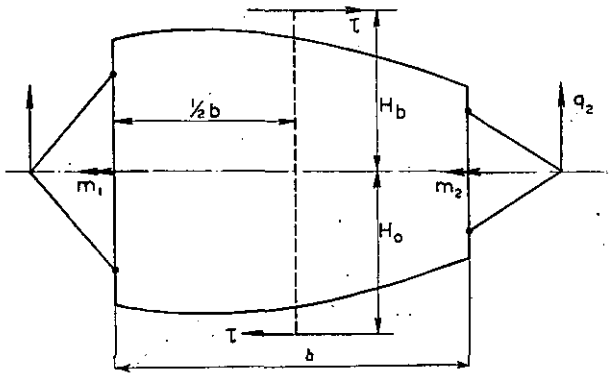

FIGURE 4.3.
The virtual loads.

The first variation δF can only be zero at any arbitrary variation of D_{s1} if $\nu_1 = A_1$ and $-A'_1 + B_1 = 0$. After some rearrangement of the expression A_1 it appears, that the first condition is an identity. The second condition can be reduced, after reduction of the expression B_1, to

$$\frac{D_{s1}}{S_{s1} \cos \alpha_1} + \Theta_1 - \nu'_1 - \psi_1 (e'_1 - \operatorname{tg} \alpha_1) = 0. \quad (5.1)$$

At a variation of D_{s2} we obtain in the same way

$$\frac{D_{s2}}{S_{s2} \cos \alpha_2} + \Theta_2 - \nu'_2 - \psi_2 (e'_2 - \operatorname{tg} \alpha_2) = 0. \quad (5.2)$$

At a variation of M_1, we find

$$\delta A = \int_L^R \frac{M_1}{S_{b1} \cos^3 \alpha_1} \delta M_1 \, dx,$$

$$\delta A_r = \left[\left\{ \Theta_1 - \nu_1 \frac{h'_1}{h_1} + \psi_1 \left(\operatorname{tg} \alpha_1 - e_1 \frac{h'_1}{h_1} \right) \right\} \delta M_1 \right]_L^R,$$

whereas δA_q can be given in the form

$$\delta A_q = \int_L^R (C_1 \delta M'_1 + D_1 \delta M_1) \, dx =$$

$$= \left[C_1 \delta M_1 \right]_L^R + \int_L^R (- C'_1 + D_1) \delta M_1 \, dx.$$

The first variation δF can only be zero at any variation of M_1 if

$$\Theta_1 - \nu_1 \frac{h'_1}{h_1} + \psi_1 \left(\operatorname{tg} \alpha_1 - e_1 \frac{h'_1}{h_1} \right) + C_1 = 0$$

and

$$\frac{M_1}{S_{b1}\cos^3\alpha_1} + C'_1 - D_1 = 0.$$

Again, it appears that the first condition is satisfied identically, whereas the second condition can be reduced to

$$\frac{M_1\,h_1}{S_{b1}\cos^3\alpha_1} + \left[h'_1\,v_1 - h_1\left\{\Theta_1 - \psi_1\left(e_1\frac{h'_1}{h_1} - \operatorname{tg}\alpha_1\right)\right\}\right]' = 0. \qquad (5.3)$$

At a variation of M_2 we obtain in the same way

$$\frac{M_2\,h_2}{S_{b2}\cos^3\alpha_2} + \left[h'_2\,v_2 - h_2\left\{\Theta_2 - \psi_2\left(e_2\frac{h'_2}{h_2} - \operatorname{tg}\alpha_2\right)\right\}\right]' = 0. \qquad (5.4)$$

At a variation of t we get

$$\delta A = \int_L^R tb\left(\frac{1}{G_b\,d_b} + \frac{1}{G_o\,d_o}\right)\delta t\,dx,$$

$$\delta A_r = \left[\left\{v_1\left(H_1\left(1 - \frac{e_1}{a}\right) - H_2\frac{e_2}{a} + \frac{bh}{a}\right) + v_2\left(H_1\frac{e_1}{a} - H_2\left(1 - \frac{e_2}{a}\right) - \frac{bh}{a}\right) + \psi\left(H_1\,e_1\,r_1 - H_2\,e_2\,r_2 + bs\right)\right\}\delta t\right]_L^R,$$

whereas δA_q can be given in the form

$$\delta A_q = \int_L^R (E_1\,\delta t' + E_2\,\delta t)\,dx = \left[E_1\,\delta t\right]_L^R + \int_L^R (-E'_1 + E_2)\,\delta t\,dx.$$

The first variation δF can only be zero at any variation of t if

$$v_1\left[H_1\left(1 - \frac{e_1}{a}\right) - H_2\frac{e_2}{a} + \frac{bh}{a}\right] + v_2\left[H_1\frac{e_1}{a} - H_2\left(1 - \frac{e_2}{a}\right) - \frac{bh}{a}\right] + \psi\left(H_1\,e_1\,r_1 - H_2\,e_2\,r_2 + bs\right) + E_1 = 0$$

and

$$tb\left(\frac{1}{G_b\,d_b} + \frac{1}{G_o\,d_o}\right) + E'_1 - E_2 = 0.$$

As before, the first condition can be shown to be an identity. By means of (4.3, 4, 6) E_1 can also be expressed as

$$E_1 = -H_1\,y_1 + H_2\,y_2 - bu.$$

By substitution of this expression and reduction of E_2 we obtain from the second condition

$$tb\left(\frac{1}{G_b\,d_b} + \frac{1}{G_o\,d_o}\right) - H_1\,y'_1 + H_2\,y'_2 - h_1\left(\Theta_1 + \psi_1\operatorname{tg}\alpha_1\right) + h_2\left(\Theta_2 + \psi_2\operatorname{tg}\alpha_2\right) - \frac{h_{c1}\,h_{c2}}{h}\left[\left(h_{c1} + h_{c2} - 2h\right)b' + 2bh'\right]\psi + \left(\frac{h_{c1} + h_{c2}}{2h}\,b' + \frac{bh'}{h}\right)u - bu' = 0. \qquad (5.5)$$

Note: It can be shown, that the abovementioned „first conditions" must necessarily be identities. Thus, they provide a check on the validity of the preceding work.

The five differential equations (5.1 to 5 incl), holding for any part of the wing between two successive ribs, together with the appropriate boundary conditions, determine the five deformation functions v_1, v_2 Θ_1, Θ_2 and ψ. For a wing with two parallel spars ($b' = \alpha_1 = \alpha_2 = 0$) and $e_1 = e_2 = 0$ the equations (5.1 to 4 incl.) reduce to

$$\frac{D_{s1}}{S_{s1}} + \Theta_1 - v'_1 = 0, \quad \frac{D_{s2}}{S_{s2}} + \Theta_2 - v'_2 = 0, \qquad (5.6,7)$$

$$\frac{M_1}{S_{b1}} + \frac{D_{s1}}{S_{s1}}\frac{h'_1}{h_1} - \Theta'_1 = 0, \qquad (5.8)$$

$$\frac{M_2}{S_{b2}} + \frac{D_{s2}}{S_{s2}}\frac{h'_2}{h_2} - \Theta'_2 = 0. \qquad (5.9)$$

The function ψ has disappeared and the displacements and rotations of the front and the rear spar can be computed from separate pairs of equations, respectively (5.6,8) and (5.7,9). These equations have formerly been derived from geometrical considerations (*ref.* 7).

Also for the general case, equations (5.1 to 5 incl.), it is possible to simplify the computation of the deformations by eliminating the function ψ from the first four equations. In order to attain this, new variables φ_1 and φ_2, being the rotations of a cross section of the front resp. rear spar in the plane through the shear centres parallel to the Y-axis, are introduced instead of Θ_1 and Θ_2. (The positive direction of φ is the same as that of y'). The angles β_1 and β_2 between these vertical planes through the shear centres and the X-axis (β has the same positive direction as e') are obtained from

$$\operatorname{tg}\beta_1 = e'_1 - \operatorname{tg}\alpha_1;\ \operatorname{tg}\beta_2 = e'_2 - \operatorname{tg}\alpha_2.$$

By means of the relations

$$\varphi_1 = \Theta_1\cos\beta_1 - \psi_1\sin\beta_1, \qquad (5.10)$$

$$\varphi_2 = \Theta_2\cos\beta_2 - \psi_2\sin\beta_2, \qquad (5.11)$$

and of equation (*a*) from the appendix to *ref.* 1 we obtain from (5.1 to 4 incl.), successively,

$$v'_1 = \frac{D_{s1}}{S_{s1} \cos \alpha_1} + \frac{\varphi_1}{\cos \beta_1}, \qquad (5.12)$$

$$v'_2 = \frac{D_{s2}}{S_{s2} \cos \alpha_2} + \frac{\varphi_2}{\cos \beta_2}, \qquad (5.13)$$

$$\left(\frac{\varphi_1 h_1}{\cos \beta_1}\right)' = \frac{M_1 h_1}{S_{b1} \cos^3 \alpha_1} + (h'_1 v_1)', \qquad (5.14)$$

$$\left(\frac{\varphi_2 h_2}{\cos \beta_2}\right)' = \frac{M_2 h_2}{S_{b2} \cos^3 \alpha_2} + (h'_2 v_2)'. \qquad (5.15)$$

From equation (5.5) Θ_1 and Θ_2 can be eliminated by replacing

$$- h_1 (\Theta_1 + \psi_1 \operatorname{tg} \alpha_1) + h_2 (\Theta_2 + \psi_2 \operatorname{tg} \alpha_2)$$

with

$$- \varphi_1 h_1/\cos \beta_1 + \varphi_2 h_2/\cos \beta_2 - e'_1 h_1 \psi_1 + e'_2 h_2 \psi_2.$$

Thus we have obtained a system of five equations of which only the last contains ψ; this last equation can be written as a differential equation of the first order in v_1, v_2, φ_1, φ_2 and ψ by means of (4.1 to 6 incl.).

6 The boundary conditions.

The *boundary conditions at the ribs* can most easily be derived geometrically. The continuity of the displacements of the spar booms at a rib requires

$$\Theta_1 = \Theta_1^-, \quad \Theta_2 = \Theta_2^-. \qquad (6.1, 2)$$

The quantities Θ, φ and ψ at a rib are interrelated as follows

$$\begin{aligned} \varphi_1 &= \Theta_1 \cos \beta_1 - \psi_1 \sin \beta_1; \\ \varphi_1^- &= \Theta_1 \cos \beta_1^- - \psi_1 \sin \beta_1^-, \end{aligned} \qquad (6.3)$$

$$\begin{aligned} \varphi_2 &= \Theta_2 \cos \beta_2 - \psi_2 \sin \beta_2; \\ \varphi_2^- &= \Theta_2 \cos \beta_2^- - \psi_2 \sin \beta_2^-, \end{aligned} \qquad (6.4)$$

$$\begin{aligned} \psi_1 &= \psi_1^- = - \triangle v_1/\triangle e_1; \\ \psi_2 &= \psi_2^- = - \triangle v_2/\triangle e_2. \end{aligned} \qquad (6.5, 6)$$

From (6.3 and 5) and (6.4 and 6) follow the boundary conditions

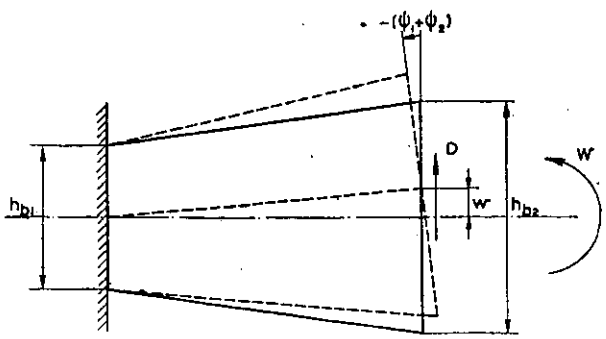

FIGURE 6.1.
Centre part of a rib.
——— undistorted, ----- distorted.

$$\Theta_1 = \frac{\varphi_1}{\cos \beta_1} + \psi_1 \operatorname{tg} \beta_1 = \left(\frac{\varphi_1}{\cos \beta_1}\right)^- + \psi_1 \operatorname{tg} \beta_1,$$

or

$$\triangle \left(\frac{\varphi_1}{\cos \beta_1}\right) = \frac{\triangle v_1}{\triangle e_1} \triangle \operatorname{tg} \beta_1; \qquad (6.7)$$

and similarly

$$\triangle \left(\frac{\varphi_2}{\cos \beta_2}\right) = \frac{\triangle v_2}{\triangle e_2} \triangle \operatorname{tg} \beta_2. \qquad (6.8)$$

If we assume rib i built in at the front spar, we obtain, keeping in mind that the rib caps are considered to be infinitely rigid (fig. 6.1)

$$\psi_1 + \psi_2 = - \frac{w}{b h_{b2}} (h_{b2} - h_{b1}), \qquad (6.9)$$

where w is the displacement of the rear spar relative to the front spar. The difference between the actual spar displacements y_1 and y_2 (fig. 4.2) is

$$y_2 - y_1 = \psi_1 b + w,$$

whereas, from (4.3) and (6.5),

$$y_1 = v_1 + e_1 \psi_1 = v_1 - e_1 \frac{\triangle v_1}{\triangle e_1}$$

and similarly

$$y_2 = v_2 - e_2 \frac{\triangle v_2}{\triangle e_2}.$$

Thus

$$(b + e_1) \frac{\triangle v_1}{\triangle e_1} - e_2 \frac{\triangle v_2}{\triangle e_2} = v_1 - v_2 + w.$$

By elimination of ψ_1, ψ_2 and $\triangle v_2/\triangle e_2$ resp. $\triangle v_1/\triangle e_1$ from these equations and (6.3,4,7) we obtain

$$\frac{\triangle v_1}{\triangle e_1} = \frac{v_1 - v_2}{a} + \left(1 + \frac{e_2}{h_{b2}} \frac{h_{b2} - h_{b1}}{b}\right) \cdot \frac{w}{a} \qquad (6.10)$$

resp.

$$\frac{\triangle v_2}{\triangle e_2} = - \frac{v_1 - v_2}{a} + \left(-1 + \frac{b + e_1}{h_{b2}} \frac{h_{b2} - h_{b1}}{b}\right) \frac{w}{a}. \qquad (6.11)$$

The magnitude of w is obtained considering the elastic energy stored in the centre part of the rib. If the shear force and the bending moment in the rib cross section immediately in front of the rear spar are denoted by D and W, this elastic energy is (fig. 6.1)

$$A_i = \left[\tfrac{1}{2} Dw - \tfrac{1}{2} W (\psi_1 + \psi_2)\right]_i =$$

$$= \tfrac{1}{2} \left[w \left(D + W \frac{h_{b2} - h_{b1}}{b h_{b2}}\right)\right]_i =$$

$$= \tfrac{1}{2} w_i D_{s\,i\,2},$$

where $D_{si\,2}$ is the part of the shear force resisted by shear stresses in the web, according to equation (9) of *ref.* 1. According to equations (10) and (17*d*) of *ref.* 1 we may also write

$$A_i = \tfrac{1}{2}\, k_i\, D^*{}_i{}^2 \text{ and } D_{si\,2} = \left[\frac{h_{a1}\, h_{a2}}{a h_{b2}}\, D^*\right]_i .$$

Therefore

$$w_i = \left[\, k\, D^*\, \frac{a h_{b2}}{h_{a1}\, h_{a2}}\, \right]_i . \qquad (6.12)$$

Substituting (6.12) in (6.10,11) we obtain the boundary conditions

$$\frac{\triangle v_1}{\triangle e_1} = \frac{v_1 - v_2}{a}\, \frac{k D^*}{h_{a1}} \text{ or}$$

$$\frac{a - \triangle e_1}{a\ \triangle e_1}\, v_1 + \frac{v_2}{a} = \frac{\bar{v_1}}{\triangle e_1} + \frac{k D^*}{h_{a1}}\,, \qquad (6.13)$$

$$\frac{\triangle v_2}{\triangle e_2} = -\,\frac{v_1 - v_2}{a} - \frac{k D^*}{h_{a2}} \text{ or}$$

$$\frac{v_1}{a} + \frac{a - \triangle e_2}{a\ \triangle e_2}\, v_2 = \frac{\bar{v_2}}{\triangle e_2} - \frac{k D^*}{h_{a2}}\,, \qquad (6.14)$$

from which v_1 and v_2 can be computed. If $\bar{\Theta_1}$, $\bar{\Theta_2}$, $\bar{v_1}$, $\bar{v_2}$ and $\bar{\psi}$ (immediately inside a rib) are known, Θ_1, Θ_2, v_1, v_2 and ψ can be computed successively from (6.1), (6.2), (6.13 and 14), and from $\psi = \bar{\psi}$; further φ_1 and φ_2 follow from (6.3, 4, 7 and 8). v_1 and v_2 are continuous at a rib if $\triangle e_1$ and $\triangle e_2$ are zero, φ_1 and φ_2 are continuous if $\triangle \beta_1$ and $\triangle \beta_2$ are zero.

Note: The boundary conditions at the ribs can also be derived from CASTIGLIANO's theorem, if this theorem is applied to half of the wing. In this case additional virtual forces are introduced at each rib at the front and rear spars. The variational problem $\delta F = 0$ (F for the half wing) then yields the boundary conditions as well as the load-deformation equations. Also some additional equations are supplied, such that the complete system of equations is sufficient for the simultaneous computation of the internal loads and the deformations (see footnote 2), art. 1). Only if this simultaneous calculation is desired, the energy method of deriving the boundary conditions is preferable to the geometrical method (see *ref.* 8).

The *boundary conditions in the plane of symmetry* of the wing still remain to be determined. As any loading can be divided into a symmetric and an antisymmetric loading, we can restrict the investigation to these two loading conditions.

With *symmetric loading* the boundary conditions for Θ_1 and Θ_2 are

$$\Theta_{10} = \Theta_{20} = 0. \qquad (6.15,\ 6.16)$$

Generally, the magnitudes of v_1 and v_2 are prescribed at the wing-fuselage fittings. However, without restriction to the generality of the solution, we can assume provisionally

$$v_{10} = v_{20} = 0. \qquad (6.17,\ 6.18)$$

These boundary conditions do not influence the curvatures and shearing deformations; they only define the position of the wing as a whole. Therefore, satisfying the actual boundary conditions means only, that a rigid body movement has to be added to the computed deflexions. The boundary condition for ψ is supplied by equation (6.9) for rib 1; substituting (6.12) we obtain

$$(\psi)_1 = \left[\frac{a\, k\, D^*}{2\, b h_{a1}\, h_{a2}}\, \frac{h_{b1} - h_{b2}}{h_{c1} - h_{c2}}\right]_1 . \qquad (6.19)$$

With *antisymmetric loading* equations (6.17 to 19 incl.) also hold. The antisymmetry further requires, that

$$(\psi)_0 = 0. \qquad (6.20)$$

To define the position of the wing as a whole we can provisionally, without restricting the generality of the solution, specify Θ_{10} or Θ_{20}, e.g. by means of (6.15).

7 The solution of the equations.

If we are satisfied with the knowledge of the most important displacements v_1 and v_2 we need not consider the complicated equation (5.5). We can restrict ourselves to the solution of equations (5.12 to 5.15 incl.), with the corresponding boundary conditions (6.7, 8, 13 and 14) at the ribs and (6.15 to 19 incl.), where Θ must be replaced with φ, in the plane of symmetry.

To find the numerical solution we divide the distance between two consecutive ribs into a certain number of intervals. Assuming v_{1k}, v_{2k}, φ_{1k} and φ_{2k} at the beginning of the k-th interval to be known we compute their first derivatives successively from (5.12, 13, 14 and 15). Then, we compute the values of the four functions at the centre of the k-th interval from

$$v_{1,\,k+\frac{1}{2}} = v_{1k} + \tfrac{1}{2}\, v'_{1k}\ \triangle k\ x, \text{ etc.}$$

and the first derivatives at this station again from (5.12) etc. At the end of the interval we then obtain

$$\bar{v_1}_{,\,k+1} = v_{1k} + v_1{}'_{,\,k+\frac{1}{2}}\ \triangle k\ x, \text{ etc.}$$

In the same way we deal with all successive intervals. If there is a rib between two intervals where e and/or β are discontinuous, we must use the boundary conditions to find the values outside the rib; if e and β are continuous v and φ are also continuous.

Both for symmetric and for antisymmetric loading we start the calculations at $x = 0$. With symmetric loading v_{10}, v_{20}, φ_{10} and φ_{20} are all prescribed by the boundary conditions. With antisymmetric loading φ_{20} is not prescribed. We can determine the deformations for the part $0 \leqq x \leqq x_1$ of the wing by combining the solution of the non-homogeneous equations, starting from an arbitrary value φ_{20}, with c times the solution of the homogeneous equations, also starting from an arbitrary value $\varphi_{20} \neq 0$, computing $(\psi)_1$ for both solutions from equations (6.5,6, 13 and 14), and determining the proper value of c such that equation (6.19) is satisfied.

From the solutions for ν and φ we can compute the values of Θ and ψ at the ribs by means of equations (6.3 to 6 incl.), (6.13) and (6.14). However, if we want to know all deformation functions completely we have also to solve equation (5.5). The solution of the complete set of equations does not present any difficulty; it is found completely similarly as has been described heretofore.

8 Notations.

a distance between the shear centres of the spars parallel to the Z-axis;

b distance between the spar planes parallel to the Z-axis;

$b^* = \frac{a}{h_{a1}\, h_{a2}} \left[h_{a1} \frac{2\, O}{a} - h_{b1}^2 - h_1 (h_{a1} - h_{b1}) \right] \approx b \left[1 - \frac{e_1}{b} \left(1 - \frac{h_1}{h_{b1}}\right) - \frac{e_2}{b} \left(1 - \frac{h_2}{h_{b2}}\right) \right]$;

d thickness of a spar web (d_1, d_2), a rib web (d_i) or the skin (d_b, d_o);

e_1, e_2 distance from the shear centre of the front resp. rear spar in front of resp. behind the spar plane, parallel to the Z-axis;

$h = H_b + H_o$;

h_1, h_2 distance between the centres of area of the front resp. rear spar booms;

h_{a1}, h_{a2} $h_{a1} = h_{b1} + e_1 (h_{b1} - h_{b2})/b$, $h_{a2} = h_{b2} - e_2 (h_{b1} - h_{b2})/b$;

h_{b1}, h_{b2} $h_{b1} = h_{c1} (2\, O_1 + bh_2)/b\,(h_{c1} + h_{c2})$, $h_{b2} = h_{c2} (2\, O_1 + bh_2)/b\,(h_{c1} + h_{c2})$;

h_{c1}, h_{c2} distance between the top and bottom skins at the front resp. rear spar booms;

$k_i = \left[\left(\frac{h_{a1}\, h_{a2}}{h_{b1}\, h_{b2}} \right)^2 \frac{b\,(h_{b1} + h_{b2})}{2\, a^2\, Gd} \right] i$;

m_1, m_2 virtual moments in the XY-plane, see art. 3.3;

n *number of ribs per half wing; also notation* of end rib;

o as a suffix denotes the bottom skin;

p_1, p_2 external running load on the front resp. rear spar per unit of length in X-direction, statically distributed between the shear centres of the spars;

q_1, q_2 virtual running loads in the shear centres of the spars (art. 3.3);

$$q^\circ_1 = \frac{2\, h_{c1}\, h_{c2}}{as} \left[-b \left\{ \left(D_{s1} - M_1 \frac{h'_1}{h_1} \right)' + p_1 \right\} - \left(1 - \frac{h}{h_{c1}}\right) \left\{ (D_{s1}\, e_1)' + p_1 e_1 \right\} + \left(1 - \frac{h}{h_{c2}}\right) \left\{ (D_{s2}\, e_2)' + p_2 e_2 \right\} - 2\,(t\, O_2)' + \frac{h}{b} (tb^2)' - tb' h_1 - e_2 \left(1 - \frac{h}{h_{c2}}\right) \left\{ \left[D_{s1} + D_{s2} - M_1 \frac{h'_1}{h_1} - M_2 \frac{h'_2}{h_2} - t\,(h_1 - h_2) \right]' + p_1 + p_2 \right\} \right];$$

$$q^\circ_2 = \frac{2\, h_{c1}\, h_{c2}}{as} \left[-b \left\{ \left(D_{s2} - M_2 \frac{h'_2}{h_2} \right)' + p_2 \right\} + \left(1 - \frac{h}{h_{c1}}\right) \left\{ (D_{s1}\, e_1)' + p_1 e_1 \right\} - \left(1 - \frac{h}{h_{c2}}\right) \left\{ (D_{s2}\, e_2)' + p_2 e_2 \right\} + 2\,(t\, O_1)' - \frac{h}{b} (tb^2)' + tb' h_2 - e_1 \left(1 - \frac{h}{h_{c1}}\right) \left\{ \left[D_{s1} + D_{s2} - M_1 \frac{h'_1}{h_1} - M_2 \frac{h'_2}{h_2} - t\,(h_1 - h_2) \right]' + p_1 + p_2 \right\} \right];$$

$r_1 = 2 \left[h_{c1} \frac{e_2}{a} - h_{c2} \left(1 - \frac{e_1}{a}\right) \right]$;

$r_2 = 2 \left[h_{c1} \left(1 - \frac{e_2}{a}\right) - h_{c2} \frac{e_1}{a} \right]$;

$s = 2\, h_{c1}\, h_{c2} \left(1 - \frac{he_1}{ah_{c1}} - \frac{he_2}{ah_{c2}} \right)$;

t shear flow in the skin;

$u = u_b + u_o$;

u_b, u_o see fig. 4.2;

v_1, v_2 displacement parallel to the Y-axis of the shear centre of the front resp. rear spar (fig. 4.2);

x coordinate in the direction normal to the plane of symmetry of the wing;

y coordinate normal to the wing plane (XZ-plane);

y_1, y_2 displacement parallel to the Y-axis of the centre of gravity of the front resp. rear spar (fig. 4.2);

y_b, y_o displacement parallel to the Y-axis of the centre of a skin former (fig. 4.2);

z coordinate normal to the XY-plane;

A elastic energy;

A_q work done by the virtual loads;

A_r work done by the boundary forces over the specified displacements;

D_{g1}, D_{g2} shear force resisted by the booms of the front resp. rear spar;

D_{s1}, D_{s2} shear force resisted by the web of the front resp. rear spar;

D^* $= -\frac{1}{h_{a1}}\left[W_1 + M_1\left(\triangle \mathrm{tg}\,\alpha_1 - e_1\frac{h'_1}{h_1}\right) - \bar{D}_{s1}\,\triangle e_1\right] + \frac{1}{h_{a2}}\left[W_2 + M_2\left(\triangle \mathrm{tg}\,\alpha_2 - e_2\,\frac{\triangle h'_2}{h_2}\right) - \bar{D}_{s2}\,\triangle e_2\right] + b^*\,\triangle t + \frac{\triangle Y_1}{h_{a1}} + \frac{\triangle Y_2}{h_{a2}}$;

E modulus of elasticity of the boom material;

F energy that is to be minimized;

G shear modulus of the web or skin material;

H_1 $= \frac{1}{2}\,(h_{c1} + h_{c2}) - h_1$;

H_2 $= \frac{1}{2}\,(h_{c1} + h_{c2}) - h_2$;

H_b, H_o defined in art. 3.2 (see also fig. 4.2);

H_{c1}, H_{c2} parts of h_{c1} and h_{c2} above the wing plane (fig. 3.1);

$\bar{H}_{c1}, \bar{H}_{c2}$ parts of h_{c1} and h_{c2} below the wing plane (fig. 3.3);

I_1, I_2 moment of inertia of a cross section of the front resp. rear spar normal to the spar plane;

M_1, M_2 Z-component of the bending moment in the front resp. rear spar;

O $= O_1 + \frac{1}{2}\,e_1\,h_1 + \frac{1}{2}\,(b + e_2)\,h_2$;

O_1 defined by fig. 3.6; $O_2 = O_1 - \frac{1}{2}\,b\,(h_1 - h_2)$;

$\bar{O}_{b1}, \bar{O}_{o1}, \bar{O}_{b2}, \bar{O}_{o2}$ defined by fig. 3.2;

$O_{b1} + O_{o1} = O_1 + \frac{1}{2}\,e_1\,(h_1 - h_2)$;

$O_{b2} + O_{o2} = O_2 - \frac{1}{2}\,e_2\,(h_1 - h_2)$;

S_{b1}, S_{b2} bending stiffness of the front resp. rear spar,

$$S_{b1} = EI_1 \Big/ \left(1 + \tfrac{1}{2}\,h'^2_1\right),$$

$$S_{b2} = EI_2 \Big/ \left(1 + \tfrac{1}{2}\,h'^2_2\right);$$

S_{s1}, S_{s2} shear stiffness of the front resp. rear spar

$S_{s1} = G_1\,d_1\,h_1$, $S_{s2} = G_2\,d_2\,h_2$;

S_{w1}, S_{w2} torsional stiffness of the front resp. rear spar;

Y_1, Y_2 torsional moment in the front resp. rear spar; see also art. 3 for other significance of Y;

α_1, α_2 angle between the front resp. rear spar plane and the XY-plane (fig. 3.1, 3);

β_1, β_2 angle between the XY-plane and the plane through the shear centres of the front resp. rear spars parallel to the Y-axis (art. 5);

$\delta\,(\text{- -})$ first variation of the function (- -);

φ_1, φ_2 rotation of a front resp. rear spar cross section in the plane through the shear centres of that spar parallel to the Y-axis;

ψ $= (\psi_1 + \psi_2)/2\,(h_{c1} - h_{c2})$;

ψ_1, ψ_2 rotation of a front resp. rear spar cross section in the XZ-plane (fig. 4.2);

τ virtual shear flow in the skin (art. 3.2);

τ° $= -\frac{1}{h_{c1}}\left[(D_{s1}\,e_1)' + p_1\,e_1\right] + \frac{1}{h_{c2}}\left[(D_{s2}\,e_2)' + p_2\,e_2\right] - \frac{1}{b}\,(tb^2)'$;

$\triangle i\,(\text{- - -}) = (\text{- - -})_i - (\text{- - -})_{\bar{i}}$;

Θ_1, Θ_2 rotation of a front resp. rear spar cross section in the XY-plane (fig. 4.2);

$(\text{- - -})_i$ value of the function (- - -) immediately outboard of rib i or at rib i;

$(\text{- - -})_{\bar{i}}$ value of the function (- - -) immediately inboard of rib i;

$(\text{- - -})' = \frac{d}{dx}\,(\text{- - -})$.

9 References. [4])

1. VAN DER NEUT, A. The stress distribution in cantilever wings with two non-parallel spars interconnected by elastically deformable ribs and skin. Report S. 251. Verslagen en Verhandelingen van het Nationaal Luchtvaartlaboratorium, Amsterdam, Vol. XII, p. S 15—32 (1943).
2. PLANTEMA, F. J. and VAN DER NEUT, A. The stress distribution in wings with two non-parallel torsionally rigid spars, interconnected by elastically deformable ribs and skin. Report S. 279. Verslagen en Verhandelingen van het Nationaal Luchtvaartlaboratorium, Amsterdam, Vol. XII p. S. 33—41 (1943).
3. TREFFTZ, E. Ableitung der Schalenbiegungsgleichungen mit dem CASTIGLIANO'schen Prinzip. Z.A.M.M. 15 (1935), S. 101—108.
4. MARGUERRE, K. Bestimmung der Verzerrungsgrößen eines räumlich gekrümmten Stabes mit Hilfe des Prinzips von CASTIGLIANO. Z.A.M.M. 21 (1941), S. 218—227.
5. BIEZENO, C. B. und GRAMMEL, R. Technische Dynamik, Kap. II, par. 3. Berlin 1939.
6. WEBER, C. Ueber die Minimalsätze der Elastizitätstheorie. Z.A.M.M. 21 (1941), S. 32—42.
7. VAN DER NEUT, A. The influence of the ribs and wing covering on the strength of aeroplane wings. II. Report S. 67. Verslagen en Verhandelingen van den Rijksstudiedienst voor de Luchtvaart, Amsterdam, Vol. VII, p. 55—65 (1934).
8. PLANTEMA, F. J. The stresses and deformations of wings with two parallel spars and shear-resistant skin. Report S. 299. Nationaal Luchtvaartlaboratorium; Amsterdam (unpublished).

Completed: July 1946.

[4]) *Ref.* 1, 2 and 7 are written in Dutch with an English summary; *ref.* 8 is written in Dutch.

REPORT S. 326

Supplement to the Method of Wing Analysis Developed in Reports S. 251 and S. 279 (Vol. XII)

Summary.

The particular case of a wing where the top or bottom skin is entirely absent between the two spars and two ribs is discussed in section 1. A revised method of solution of the moment equations is discussed in section 2.

Contents.

1 Wings with the skin partly absent.

The procedure for calculating the distribution of the stresses in two-spar wings with shear-resistant skin, developed in *refs.* 1, 2 and 3, can not be applied without some revision to wings, where the top and/or bottom skin is absent over part of the span between the spars. An attempt to apply the method as given in these reports fails due to the fact that the functions B, T, V, Λ and Γ become infinite or indefinite. This is caused by the presence of the quantities d_b and d_o, the thicknesses of the top and bottom skin between the spars, in the denominator of certain terms. In general, these terms become infinitely large; in the special case that $\lambda = 0$ most of them are indefinite, as λ occurs in their numerator.

Now, it is easy to show that in itself this difficulty is only apparent, because the absence of part of the top or bottom skin means that the corresponding terms in the strain energy, *ref.* 2 *eq.* (17c), must simply be omitted. It can be proved that the troublesome terms of B, T, V, Λ and Γ over the region where the skin is absent, must equally be omitted.

In this way, the difficulties in computing the coefficient u_{11} when the top or bottom skin is missing between $x = 0$ and rib 1, are disposed of. However, if the skin is missing elsewhere, e.g. between ribs j and $j+1$, an essential revision has still to be made. It is caused by the fact that if the skin between the spars at top or bottom is missing, there is a statically determinate relation between X_j and X_{j+1}. This relation is supplied by eq. (8a) of *ref.* 2, with $t = 0$ between x_j and x_{j+1}. In solving this equation it is satisfactory to use the approximation $\lambda = 0$, that is also the base of the fundamental equations (16a) of *ref.* 2. The solution is then simply

$$X_j = X_{j+1}.$$

Consequently, in the variational problem $\delta A = 0$, eq. (21) of *ref.* 2 or eq. (5.3) of *ref.* 3, $\delta X_j = \delta X_{j+1}$, and the coefficients of δX_j and δX_{j+1} do not vanish separately, but only their sum vanishes. This leads immediately to the conclusion that in the set of five-moment equations (33) of *ref.* 2 the equations for $i = j$ and $i = j+1$ are to be replaced by one equation, viz.

$$u_{j,\,j-2} X_{j-2} + (u_{j,\,j-1} + u_{j+1,\,j-1}) X_{j-1} + (u_{jj} + u_{j,\,j+1} + u_{j+1,\,j} + u_{j+1,\,j+1}) X_j + (u_{j,\,j+2} + u_{j+1,\,j+2}) X_{j+2} + u_{j+1,\,j+3} X_{j+3} = U_j + U_{j+1},$$

which results from the addition of the said two equations.

It is to be noted that the moment equation for $i = j-1$ now only contains four unknowns, as $X_j = X_{j+1}$; similarly, the moment equation for $i = j+2$ contains only four unknowns.

The consequence is that the method of solution, described in section 10 of *ref.* 2, can not be applied. When choosing arbitrary values for X_1

and X_2, the moment equations for $i = j - 2$ and $i = j - 1$ are in general incompatible and, moreover, the next equation contains the two new unknowns X_{j+2} and X_{j+3}. The solution of this complication is dealt with in section 2.

The revision to the equations (6.1) to (6.4) incl. of *ref.* 3 is obtained in the same way by simply adding the two equations (6.1) for $i = j$ and $i = j + 1$. Also, similar difficulties occur when applying the method of solution after section 08 of *ref.* 3.

2 Revised method of solution.

The calculations after the manual (*ref.* 1) have been carried out for a numerical example, which did not contain the peculiarity, discussed in sec. 1.[1]) In principle, the method of solution of the moment equations after section 10.1 of *ref.* 2 should therefore be applicable. However, when the solutions of the non-homogeneous equations and of two sets of homogeneous equations had been calculated, the two equations for determining r_1 and r_2 proved to be so nearly dependent that it was impossible to compute r_1 and r_2 with anything like the required accuracy by means of a normal calculating machine. This difficulty is caused o.a. by u_{ii} and $u_{i,\,i+1}$ being large compared to $u_{i,\,i+2}$.

It may well be that it also resulted from an unfortunate choice of the stiffness and the load distributions, but it is desirable to use a standard method of solution which does not lead to such difficulties. Several other procedures were tried and it was concluded that the GAUSSIAN method of solving a set of simultaneous linear equations seems to be most adequate. It is also applicable to the set of equations discussed in the foregoing section. The equations derived in *ref.* 2 are restated in table 1, where absence of the top or bottom skin between the spars from rib 4 to rib 5 is assumed, so that

$$a_{34} = u_{34} + u_{35} \quad ; \; A_4 = U_4 + U_5 ;$$
$$a_{44} = u_{44} + 2u_{45} + u_{55} ; \; a_{46} = u_{46} + u_{56} .$$

It may be noted that the set of equations remains symmetrical with respect to the principal diagonal. The method of solution is then as follows.

We multiply the first equation by $-\frac{u_{12}}{u_{11}}$ and add the result to the second equation, thus obtaining eq. (7) which does not contain X_1.

Next, we add the equations $(3) - \frac{u_{13}}{u_{11}}(1) - \frac{b_{23}}{b_{22}}(7) = (8)$, which does not contain X_1 and X_2.

The following step leads to the elimination of X_3 by the summation:

$$(4) - \frac{u_{14}}{u_{11}}(1) - \frac{u_{24}}{b_{22}}(7) - \frac{c_{34}}{c_{33}}(8) = (9),$$

and proceeding in exactly the same way we finally have eliminated X_1 to X_{n-2} incl. and obtain X_{n-1} (X_n and X_{n+1} in the last two equations are equal to zero).

The application of this method of solution [2]) in the above-mentioned case did not lead to computational difficulties and was also advantageous because it cost less time than the method after *ref.* 2. The application to the set of equations after *ref.* 3 will of course be more involved, but presents no inherent difficulties.

If the stress analysis of a wing has to be carried through for several loading conditions, it is doubtful whether the method after GAUSZ will retain the advantage of a saving of time as compared with the method after *ref.* 2, because in the latter case only the non-homogeneous equations need be solved anew.

For the case discussed in section 1, the latter method can be modified by assuming arbitrary values for X_j and X_{j+2}, instead of for X_1 and X_2. X_1 to X_{j+3} incl. can then be solved from the first j equations, e.g. after GAUSZ, and X_{j+4} to X_{n+1} incl. follow from the remaining equations. However, the risk remains that the equations for solving r_1 and r_2 will not permit a sufficiently accurate solution.

3 References.

1. VAN DER NEUT, A. Handleiding voor de uitvoering der sterkteberekening van vrijdragende vleugels van het tweeligger type (Manual for the stress analysis of two-spar wings with shear-resistant skin). N.L.L.-report S. 250 (1941) Dutch.
2. VAN DER NEUT, A. De spanningsverdeeling in vleugels met twee niet-evenwijdige liggers, verbonden door elastisch vervormbare ribben en bekleeding. (The stress distribution in cantilever wings with two non-parallel spars interconnected by elastically deformable ribs and skin), Dutch, with English and German summary.
N.L.L.-report S. 251. Verslagen en Verhandelingen N.L.L. Vol. XII p. S. 15—32 (1943).

[1]) A report on this numerical example is being prepared.

[2]) Acknowledgement for drawing our attention to this method is made to mr. H. F. MICHIELSEN, of the Fokker Aeroplane Comp.

3. PLANTEMA, F. J. and VAN DER NEUT, A. De spanningsverdeeling *in vleugels met twee niet-evenwijdige*, torsie-stijve liggers, verbonden door elastisch-vervormbare ribben en bekleeding. (The stress distribution in wings with two non-parallel torsionally rigid spars, interconnected by elastically deformable ribs and skin). *Dutch, with English and German summary.* N.L.L.-report S. 279. Verslagen en Verhandelingen N.L.L. Vol. XII, p. S. 33—41 (1943).

Completed: December 1947.

TABLE 1.

Method of solution after GAUSZ.

(1)	$u_{11}\ X_1 + u_{12}\ X_2 + u_{13}\ X_3$	$= U_1,$
(2)	$u_{12}\ X_1 + u_{22}\ X_2 + u_{23}\ X_3 + u_{24}\ X_4$	$= U_2,$
(3)	$u_{13}\ X_1 + u_{23}\ X_2 + u_{33}\ X_3 + a_{34}\ X_4$	$= U_3,$
(4)	$u_{24}\ X_2 + a_{34}\ X_3 + a_{44}\ X_4 + a_{46}\ X_6 + u_{57}\ X_7$	$= A_4,$
(5)	$a_{46}\ X_4 + u_{66}\ X_6 + u_{67}\ X_7 + u_{68}\ X_8$	$= U_6,$
(6)	$u_{57}\ X_4 + u_{67}\ X_6 + u_{77}\ X_7 + \text{- - - -}$	
(2)	$u_{12}\ X_1 + u_{22}\ X_2 + u_{23}\ X_3 + u_{24}\ X_4$	$= U_2$
(1′)	$-(u_{11}\ X_1 + u_{12}\ X_2 + u_{13}\ X_3)\ \frac{u_{12}}{u_{11}}$	$= -\frac{u_{12}}{u_{11}}\ U_1$
(7)	$b_{22}\ X_2 + b_{23}\ X_3 + u_{24}\ X_4$	$= B_2$
(3)	$u_{13}\ X_1 + u_{23}\ X_2 + u_{33}\ X_3 + a_{34}\ X_4$	$= U_3$
(1″)	$-(u_{11}\ X_1 + u_{12}\ X_2 + u_{13}\ X_3)\ \frac{u_{13}}{u_{11}}$	$= -\frac{u_{13}}{u_{11}}\ U_1$
(7′)	$-(b_{22}\ X_2 + b_{23}\ X_3 + u_{24}\ X_4)\ \frac{b_{23}}{b_{22}}$	$= -\frac{b_{23}}{b_{22}}\ B_2$
(8)	$c_{33}\ X_3 + c_{34}\ X_4$	$= C_3$
(4)	$u_{24}\ X_2 + a_{34}\ X_3 + a_{44}\ X_4 + a_{46}\ X_6 + u_{57}\ X_7$	$= A_4$
(7″)	$-(b_{22}\ X_2 + b_{23}\ X_3 + u_{24}\ X_4)\ \frac{u_{24}}{b_{22}}$	$= -\frac{u_{24}}{b_{22}}\ B_2$
(8′)	$-(c_{33}\ X_3 + c_{34}\ X_4)\ \frac{c_{34}}{c_{33}}$	$= -\frac{c_{34}}{c_{33}}\ C_3$
(9)	$d_{44}\ X_4 + d_{46}\ X_6 + u_{57}\ X_7$	$= D_4$

etc.

REPORT S. 280

Collapsing Stresses of Circular Cylinders and Round Tubes

by

Ir. F. J. PLANTEMA

Summary.

Based on a critical investigation of the data, given in the literature, and on some supplementary considerations, proposals are made for determining the collapsing stresses of circular thin-walled cylinders and round tubes *under compression, bending, torsion or shear, or under a combination of two or more of these loads.*
The proposals are given in the form of non-dimensional diagrams or formulae. The coordinates of the diagrams follow from theoretical considerations; the diagrams themselves are then determined from experimental data.

Contents.

1 Introduction.

In three earlier reports of the National Aeronautical Research Institute (N.L.L.) [1]) the results of a critical study of the available literature on the collapsing stresses of circular or elliptical thin-walled cylinders and of thick-walled round tubes are given. Thin-walled cylinders are defined as cylinders, collapsing by elastic local instability. Of these, only cylinders stiffened by frames, spaced at a distance of the order of the diameter of the cylinder, have been considered, whereas the problem of general instability has been excluded.

Thick-walled tubes are defined as tubes in which local instability will only occur in the plastic region. The buckling stress will depend largely on the shape of the stress-strain curve beyond the proportional limit.

In this report the results obtained for thin-walled cylinders and thick-walled tubes of circular cross section are summarized.

Formulae and curves are given for the computation of the buckling stresses with com-

[1]) Reports S. 94, S. 176 and S. 261.

pression, bending, torsion, shear or a combination of these loads.

The proposed values are to be considered as the minimum values occurring with properly fabricated tubes. However, the proposals made for thin-walled cylinders under compressive and bending loads may be too conservative. They are mainly based on test results of small sized specimens (*ref.* 8, 10 and 30) for which the initial deviations from the true cylindrical shape, which have a large influence on the buckling stress, may be relatively larger than in actual aeroplane structures.

Furthermore, the results given in this report have been based entirely on the reduced-modulus theory, as originally developed by VON KARMAN. Recently, the somewhat simpler tangent-modulus theory, due to ENGESSER, has been widely adopted for compressive loads, as it is considered to agree better with test results. No theoretical explanation, supporting the tangent-modulus theory, has as yet been published. It is only pointed out here that adoption of the tangent-modulus theory instead of the reduced-modulus theory would not affect the results obtained in this report.

2 Pure compression.

2.1 *The non-dimensional diagram for flexural buckling.*

The buckling stress of a thick-walled tube in the elastic range is given by the well-known EULER formula. In the plastic range we can use the same formula, if YOUNG's modulus E is replaced with the reduced modulus E_r (*ref.* 1, art. 29), so that

$$F_c = \frac{\pi^2 E_r}{\lambda^2}, \qquad (2.1a)$$

where F_c is the critical compressive stress and λ the effective slenderness ratio.

For round tubes the reduced modulus is only slightly affected by the ratio $\frac{d}{t}$. A satisfactory approximation is obtained from

$$\frac{E_r}{E} = \frac{4}{\left(1 + \sqrt{\frac{E}{d\sigma/d\varepsilon}}\right)^2}, \qquad (2.2)$$

where $\frac{d\sigma}{d\varepsilon}$ is the tangent modulus, i.e. the slope of the tangent to the stress-strain curve at the stress F_c.

When the σ—ε diagram is known, we can plot the F_c—λ diagram from (2.1a) and (2.2). In the elastic range this is the EULER curve. In the plastic range different σ—ε curves will give different F_c—λ curves. However, a special case exists if we consider materials having affinely related σ—ε curves, where affine relationship is defined as the relationship between the curves $\psi(\sigma, \varepsilon) = 0$ and $\psi(p\sigma, q\varepsilon) = 0$, p and q being constants. If a material property is defined (fig. 2.1)

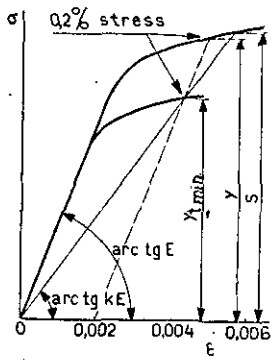

FIGURE 2.1.
The σ—ε diagram and the definition of S.

as the intersection $\sigma = S$ of the σ—ε curve with a straight line through the origin having a slope kE $(0 < k < 1)$, all $\frac{\sigma}{S} - \frac{\varepsilon E}{S}$ curves coincide, provided that k has the same value for all materials.

Consequently, the $\frac{\sigma}{S} - \frac{E_r}{E}$ curves also coincide and, writing (2.1a) in the form

$$\frac{F_c}{S} = \frac{E_r}{E}\left(\frac{\pi}{\lambda}\sqrt{\frac{E}{S}}\right)^2, \qquad (2.1b)$$

it appears that the $\frac{F_c}{S} - \frac{\lambda}{\pi}\sqrt{\frac{S}{E}}$ curves, *i.e.* the non-dimensional buckling-stress diagrams, are identical for materials with affinely related σ—ε curves.

2.2 *Application of non-dimensional diagrams.*

It will be shown that also in other loading conditions non-dimensional diagrams can be plotted which coincide for materials with affinely related σ—ε curves. The main significance of these non-dimensional diagrams is that scatter of test results due to scatter of the material properties is largely eliminated. The explanation is that the σ—ε curves of test specimens of the same material, though not being identical, will be very nearly affinely related if the scatter is not too large.

The material property S should preferably be chosen so as to represent an already well-known stress. OSGOOD (*ref.* 2 and 6) has chosen k such that in a tensile test S_t is equal to the 0,2 %

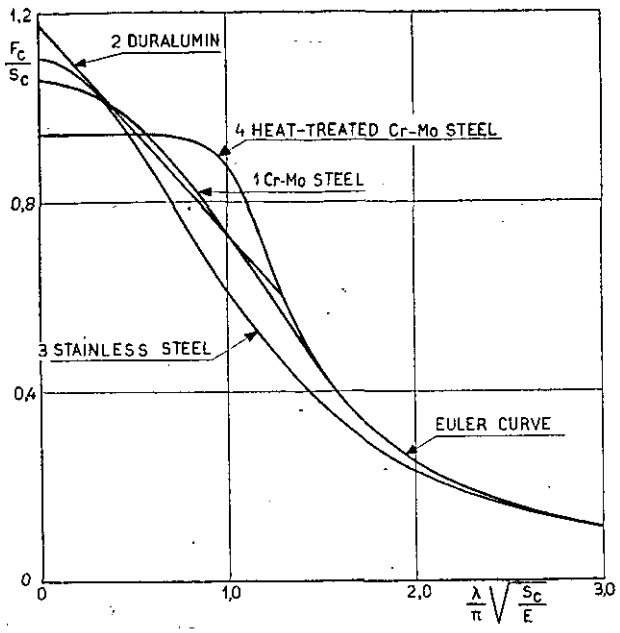

FIGURE 2.2.

Critical compressive stresses with flexural buckling according to tests of ref. 2. For the material properties see table 2.1 and fig. 2.3.

yield stress Y_t, if the material complies with the minimum specified values of the material properties; thus

$$k = \frac{Y_{t\ \min.}}{Y_{t\ \min.} + 0{,}002\,E} \quad . \qquad (2.3)$$

Usually, the material actually used will have a higher 0,2 % stress Y. The stress S, determined from (2.3), will then exceed Y; the deviation will increase with the difference between Y and $Y_{\min}$ and with the slope of the σ—ε curve at the stress Y (fig. 2.1).

Therefore, to determine S accurately, we must know the complete σ—ε curve for every test specimen. However, these curves are only given in *ref.* 2 and 6. With all other tests only Y was determined. Therefore, evaluating these tests, it has been assumed that $S = Y$. The error made in doing so probably is less than the test scatter if all tests relate to one particular material. (See *ref.* 19, tables V and VI, which show that the difference between S and Y is very small).

2.3 *Experiments with flexural buckling.*

In *ref.* 2 it has been assumed that all σ—ε curves of a particular material are affinely related and

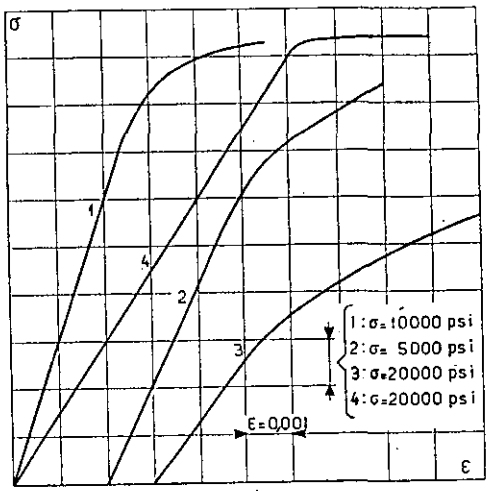

FIGURE 2.3.

Typical σ—ε curves from compression tests. For no. 1—4 see table 2.1.

the k-method has been applied in order to correct for scatter in material properties.

It actually appeared that the $\frac{F_c}{S} - \frac{\lambda}{\pi}\sqrt{\frac{S}{E}}$ diagrams showed considerably less scatter than

TABLE 2.1

Material properties, belonging to fig. 2.2 and 2.3

MATERIAL	Y_t min p. s. i.	S_c/S_t [1]	E. 10^{-6} p. s. i.	k	F_t min
1. Chromium-molybdenum steel .	75000	1,000	29,8	5/9	95000 [5]
2. duralumin	40000	0,908 [2]	10,59 [2]	2/3	55000 [5]
3. stainless steel.....	135000	0,827	26,3	5/8 [4]	—
4. heat-treated Cr-Mo steel	150000	1,120 [3]	30,0	5/7	175000

[1]) Mean values from tests.
[2]) From *ref.* 6 $S_c/S_t = 0{,}864$ and $E = 10{,}61 \times 10^6$ p. s. i.
[3]) In *ref.* 2 it is recommended to use the minimum value 0,99.
[4]) From (2.3) follows $k = 0{,}72$. Working out the tests of *ref.* 2, however, $k = 5/8$ was used. Though this value is smaller than the one from (2.3), S_c yet agrees fairly well with the 0,2 % stress, as S_c/S_t is considerably less then 1,0.
[5]) From *ref.* 26.

the F_c — λ diagrams. The plastic regions of the $\frac{F_c}{S}$ — $\frac{\lambda}{\pi}\sqrt{\frac{S}{E}}$ diagrams of the four materials investigated (three steels and duralumin) differed very much. The empirical non-dimensional diagrams, proposed by OSGOOD, and corresponding typical σ—ε curves in compression are given in figs. 2.2 and 2.3. Table 2.1 summarizes the properties of the materials investigated.

With the tests of *ref.* 2 the tubes were loaded as centrically as possible. It clearly appears that under these circumstances the character of the σ—ε curve beyond the proportional limit has a systematical influence on the shape of the non-dimensional diagram. If the material has a pronounced yield stress (curve 4) the values of $\frac{F_c}{S_c}$ in the plastic range are large at large slenderness ratios and small at small slenderness ratios; the reverse is true if the σ—ε curve has a gradual transition from the elastic to the plastic range (compare curves 3 and 4).

Computing the non-dimensional diagrams from the σ—ε curves by means of (2.1b) and (2.2), their shapes are predicted fairly well; however, the computed buckling stresses exceed the experimental buckling stresses by 10 to 30 %, for medium slenderness ratios approximately by 15 %.

For a material, the σ—ε curve of which is affinely related with one of those given in fig. 2.3, the corresponding diagram from fig. 2.2 can be used, provided that S_c is determined as the intersection of the σ—ε curve with a line through the origin having a slope kE, where k has the appropiate value from table 2.1. In general it is not permissible, as in the case of correcting for scatter in the material properties, to assume $S_c = Y_c$, except for materials having a pronounced yield stress, where the choice of k does not influence the value found for S_c.

2.4 *Local buckling.*

2.4.1 *Thin-walled cylinders.*

From the classical theory of instability the buckling stress of cylinders with moderate ratios of frame spacing to diameter follows from

$$\frac{F_c}{E} = \left\{3\ (1-\nu^2)\right\}^{-0,5}\ \frac{2\,t}{d} \doteqdot 1,21\ \frac{t}{d} \qquad (2.4)$$

as a good approximation (see a.o. *ref.*, 1 and 3).

By a large number of experiments (*ref.* 3, 5 and 7 to 12 incl.), where $180 \leqq \frac{d}{t} \leqq 8000$ and $0,015 \leqq \frac{L}{d} \leqq 16$, it has been confirmed that F_c is independent of $\frac{L}{d}$, except for very short cylinders ($\frac{L}{d} < 0,35$; see *ref.* 12). However, the actual buckling stress is much smaller than the theoretical value according to (2.4); it is only 0,12 to 0,7 times the theoretical value. This fact has been ascribed by several authors to the influence of initial eccentricities from the true cylindrical shape and a satisfactory explanation has been given by COX (*ref.* 10), VON KARMAN (*ref.* 11) and in particular by KOITER (*ref.* 34). Notwithstanding large experimental scatter it clearly appears that the ratio of the experimental to the theoretical stress decreases if $\frac{d}{t}$ increases. This may be explained by observing that the eccentricity as a fraction of t will increase with increasing $\frac{d}{t}$.

The following proposed formulae approximately correspond to the minimum values of F_c from the tests of *ref.* 8 and 9; they hold for $0,35 \leqq \frac{L}{d} \leqq 16$. As most of those tests were made on small-sized specimens some reserve must be made. It is not improbable that the initial eccentricities, as a fraction of t, will necessarily increase with decreasing size of the specimens, so that the proposals made here might be too conservative for actual factory-made constructions. However, only very few results of tests with such constructions are available. For the time being, therefore, more favourable proposals are unwarranted and the following formulae are recommended

$$\frac{F_c}{E} = 0,34\,\frac{t}{d} - 0,00006 \quad \text{when } 500 < \frac{d}{t} < 2330, \qquad (2.5a)$$

$$\frac{F_c}{E} = 0,2\,\frac{t}{d} \quad \text{when } 2330 < \frac{d}{t} < 8000. \qquad (2.5b)$$

When $\frac{d}{t} < 500$ the value of $\frac{F_c}{E}\,\frac{d}{t}$ increases fairly rapidly, as long as elastic buckling occurs.

2.4.2 *Thick-walled tubes.*

A theoretical determination of the buckling stress in the plastic range has been given by TIMOSHENKO (*ref.* 1, art. 81) and by GECKELER (*ref.* 4), assuming that the buckled cylinder is

a body of revolution and that during buckling the bending stiffness of the wall in axial direction is computed with E_r, whereas in tangential direction it is computed with E. The latter assumption is disputable, as the addition of an infinitesimal tangential tensile stress causes an increase of the first order in both the maximum shear stress (GUEST) and the energy of deformation (HUBER—HENCKY). This addition will therefore also be accompanied by plastic deformation. However, data on the plastic behaviour of materials, on which a satisfactory theory should be based, are missing. The results, obtained by both authors, can be written as

$$\frac{F_c}{S} = 2\,\frac{t}{d}\,\frac{E}{S}\left\{\frac{1}{3\,(1-\nu^2)}\,\frac{E_r}{E}\right\}^{0,5}. \qquad (2.6)$$

Assuming all σ—ε diagrams of a particular material to be affinely related and ν to be a material constant, it can be shown that the non-dimensional $\frac{F_c}{S}$ — $\frac{E}{S}\,\frac{t}{d}$ diagram is not affected by scatter of the material properties (sec. 2.1.)

Experiments are mentioned in *ref.* 5, 6, 7 and 13. The experiments of *ref.* 6 have been made with tubes of chromium-molybdenum steel ($15{,}5 < \frac{D}{t} < 100$) and 17 ST aluminium alloy ($13{,}5 < \frac{D}{t} < 100$); $\frac{L}{D}$ varied between 4 and 5. The above-mentioned non-dimensional diagrams have been determined and it appeared that the experimental results showed little scatter. For the steel tubes S has been taken equal to Y_t, as it was impossible to determine S_c with the k-method on account of local buckling. For the duralumin tubes S_c has been determined according to the k-method with $k = \frac{2}{3}$. The proposals made in *ref.* 6 for duralumin, which hold for $\frac{E}{S_c}\,\frac{t}{d} > 2{,}5$, and for chromium-molybdenum steel [2]), holding for $\frac{E}{S}\,\frac{t}{d} > 5$, are represented in fig. 2.4. In the region of thin-walled cylinders, $\frac{d}{t} > 500$, F_c follows from (2.5). In drawing the diagrams of fig. 2.4 it has been assumed, that $\frac{E}{S_c} = 300$. Little is known about the parts of the curves between the elastic buckling region and the region covered by the tests of *ref.* 6. For duralumin

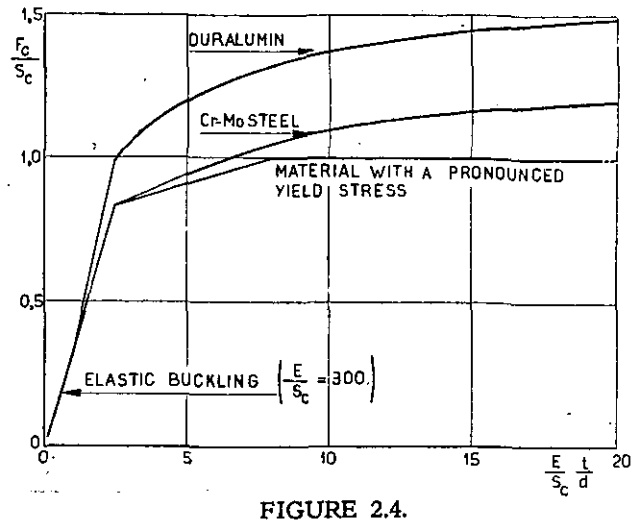

FIGURE 2.4.

Non-dimensional diagrams for local buckling under compression. For material properties see table 2.1 and fig. 2.3.

(2.5a) is retained up to $\frac{E}{S_c}\,\frac{t}{d} = 1$ and a straight transition line has been drawn for $1 \leqq \frac{E}{S_c}\,\frac{t}{d} \leqq 2{,}5$. Referring to the results of the tests mentioned in art. 2.4.1, this procedure may be assumed to be conservative. For Cr—Mo steel the proposed transition line is a broken line consisting of an extension of the elastic buckling line and the tangent to the curve from *ref.* 6.

The non-dimensional diagram for 17 ST may also be used for other aluminium alloys which do not differ much from 17 ST in their material properties (Y and $\frac{F_t}{Y}$; the latter ratio determines the general shape of the stress-strain diagram). [3])

Tests with mild steel, Cr—Ni steel and alloy steel tubing are reported in *ref.* 5, 7 and 13. These materials all have a pronounced yield stress. The evaluation of the tests, assuming $S_c = Y$, yielded minimum values of $\frac{F_c}{S}$ as represented in fig. 2.4. The maximum values of $\frac{F_c}{S}$ for $2{,}5 < \frac{E}{S}\,\frac{t}{d} < 20$ are approximately 20 % larger, so the scatter is not large. Considerably larger values of $\frac{F_c}{S}$ occurred with $\frac{E}{S}\,\frac{t}{d} > 20$, namely between 1,0 and 1,94. However, in this region, where $\frac{d}{t} < 45$, flexural buckling will almost always be critical; these results may therefore be ignored. The magnitude of $\frac{E}{Y}$, varying

[2]) As for this material $S_t = S_c$ (table 2.1), no distinction between S_t and S_c need be made.

[3]) The diagram does not hold for a material such as 51 ST aluminium alloy; see section 4.2.2.2.

between 160 and 474, appears to have no influence on the plastic region of the non-dimensional diagram. As the choice of k in this case is unimportant (c.f. the last sentence of sec. 2.3), this phenomenon could have been expected beforehand. Consequently, the diagrams given in fig. 2.4 may be applied to every isotropic material having a pronounced yield stress, taking $S_c = Y_c$.

As far as the buckled configuration of the tubes has been reported, it is the same as has been assumed in the theory, except with 4 tests reported in *ref.* 5. Here, also in tangential direction a fairly large number of waves occurred; otherwise the results of these tests do not show special features.

2.5 *The critical buckling stress.*

Tubes with a moderate ratio $\frac{d}{t}$ can be critical either in flexural or in local buckling, dependent upon their length. No indication exists that these two modes of buckling interact upon each other. Therefore, in every particular case, the critical buckling stress can be determined as the smallest of the stresses following from fig. 2.2 and fig. 2.4.

3 Pure bending.

3.1 *Thin-walled cylinders.*

The buckling stress of thin-walled cylinders under combined axial and bending loads has been determined formally by FLÜGGE (*ref.* 3). It appears that it differs from the buckling stress under pure compression only by a constant factor. A numerical example for the case of pure bending yields a factor of about 1,3. The buckling pattern shows several waves, both in axial and tangential direction, at the compression side of the tube.

The buckling of infinitely long tubes under bending has been investigated by BRAZIER (*ref.* 14) and CHWALLA (*ref.* 15). In this case the tube cross section gradually flattens to an oval shape, until it suddenly flattens totally when the buckling stress is reached. The virtual buckling stress (i.e. the maximum bending stress computed from the formula for the unflattened tube) is given by

$$\frac{F_b}{E} = C_b \frac{t}{d} . \qquad (3.1)$$

BRAZIER obtains $C_b = 0{,}66$ and CHWALLA [4]) $C_b = 0{,}756$ for $\nu = 0{,}3$. This mode of buckling, however, never occurs with cylinders of finite lengths. Formula (3.1) also holds for the buckling pattern investigated by FLÜGGE; then C_b is much larger; about $1{,}3 \times 1{,}21 = 1{,}57$ in the example evaluated by FLÜGGE.

Experiments have been reported in *ref.* 8, 14, 16, 17 and 30. Here, $\frac{L}{d}$ ranged from 0,125 to 22,5 and $\frac{d}{t}$ from 150 to 3000. The experiments mentioned in *ref.* 33 can approximately be regarded as pure bending tests too, though here a small transverse load was applied as well. The experimental results show the same characteristic features as those of the compression tests (sec. 2.4.1); C_b ranges from 0,22 to 1,11. Under the same reserve as mentioned in sec. 2.4.1, the following formula is proposed for thin-walled cylinders, where L and d are of the same order of magnitude.

$$\frac{F_b}{E} = 0{,}4 \frac{t}{d} - 5.10^{-5} \quad \text{when } 350 < \frac{d}{t} < 3000. \qquad (3.2)$$

This formula approximately represents the minimum values from *ref.* 8 and 30. The values from *ref.* 17 mostly are still lower, however, the tubes with which these tests were made, probably were not fabricated as accurately as is common in aircraft manufacturing.

3.2 *Thick-walled tubes.*

Theoretical treatises on buckling of tubes in the plastic region are not known. According to TIMOSHENKO (*ref.* 1, art. 86) the buckling mode investigated by BRAZIER and CHWALLA occurs with thick-walled tubes, loaded above the yield stress.

On account of the close similarity to buckling under compressive loads, which also appears from the results given in sec. 3.1 for the elastic region, it is reasonable to assume, for bending in the plastic region, a formula analogous to (2.6). Then, the $\frac{F_b}{S} - \frac{E}{S}\frac{t}{d}$ diagram will be identical for materials with affinely related σ—ε curves; for a particular material it will only be slightly affected by scatter of the material properties.

Based on this assumption the four-point bending tests with 17 ST-duralumin and chromium-molybdenum steel tubing ($15{,}5 < \frac{D}{t} < 100$ and $\frac{L}{D} > 5$) have been worked out in *ref.* 6 (for further particulars see sec. 2.4.2). Fig. 3.1 contains

[4]) The actual maximum bending stress follows from (3.1) with $C_b = 1{,}02$. For an infinitely long tube under axial compression (3.1) holds with $C_c = 0{,}726$ (*ref.* 1, art. 85).

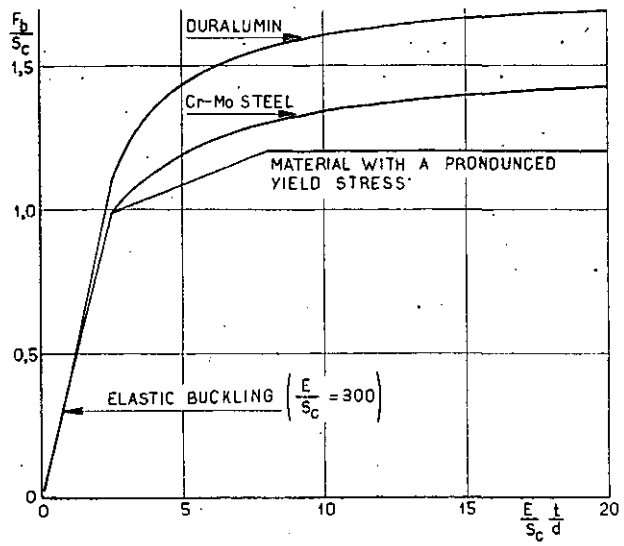

FIGURE 3.1.
Non-dimensional diagrams for bending. For material properties see table 2.1 and fig. 2.3.

OSGOOD's proposals for duralumin tubing with $\frac{E}{S_c}\frac{t}{d} > 2.5$ and for chromium-molybdenum steel tubing with $\frac{E}{S}\frac{t}{d} > 5$. For the elastic region (3.2) holds and for the transition region the proposals of fig. 3.1 are analogous to those for compression (fig. 2.4). *Ref.* 16 gives the results of tests of IMPERIAL and BERGSTROM with duralumin tubing; however, only F_b is communicated but not E and S_c. Assuming typical values, $\frac{E}{S_c} = 300$ and $S_c = 36000$ p.s.i. these tests $(0{,}47 < \frac{E}{S_c}\frac{t}{d} < 13{,}3)$ agree very satisfactorily with the curve for duralumin of fig. 3.1.

Tests with materials having a pronounced yield stress are mentioned in *ref.* 17 and 18. In *ref.* 17 the yield stress is not communicated; *ref.* 18 only reveals that F_b = (1,2 to 1,3) F_c and that $\frac{D}{t}$ varied from 60 to 120. Besides, experiments (*ref.* 13 and unpublished reports) are known with steel tubing loaded partly in pure bending and for the other part in bending with a small transverse load (bending moment = $9D$ to $12D$ times shear force). However, on account of the considerable scatter it is impossible to draw conclusions from these tests. As both for thin-walled and for thick-walled duralumin and Cr-Mo steel tubing $F_b \simeq 1{,}2\ F_c$, and *ref.* 18 also mentions this ratio, the curve proposed in fig. 3.1 for materials with a pronounced yield stress will be a reasonable proposal.

4 Pure torsion.

4.4 *Thin-walled cylinders.*

4.1.1 *Theory.*

The buckling of circular cylinders has been investigated theoretically by several authors. The shear stress at which buckling occurs, appears to depend upon the parameters $\frac{d}{t}$, $\frac{l}{d}$ and $\frac{L^2t}{d^3}$. If $\frac{L^2t}{d^3}$ is large, two possible modes of buckling exist. With the first mode the cross section remains undistorted and the tube axis distorts into a helical line; the buckling stress is obtained from (see a.o. *ref.* 1, arts. 31 and 90)

$$F_T = \frac{\pi}{2}\ E\ \frac{d}{l}\ . \qquad (4.1)$$

This mode will hereafter be called helical buckling. With the second mode the tube axis remains straight and the distortion of every cross section consists of two complete waves around its circumference, the nodal lines being helical lines on the surface of the cylinder. The corresponding buckling stress is (see a.o. *ref.* 1, art. 90)

$$F_T = \tfrac{2}{3}\ E\ (1-\nu^2)^{-0{,}75}\ \left(\frac{t}{d}\right)^{1{,}5} \simeq$$
$$\simeq 0{,}715\ E\ \left(\frac{t}{d}\right)^{1{,}5}\ . \qquad (4.2)$$

From (4.1) and (4.2) the second mode appears to be critical if

$$\frac{l}{d} < 0{,}75\ \pi\ (1-\nu^2)^{0{,}75}\ \left(\frac{d}{t}\right)^{1.5} \simeq$$
$$\simeq 2{,}2\ \left(\frac{d}{t}\right)^{1.5}\ . \qquad (4.3)$$

With thin-walled cylinders this condition will always be satisfied.

With small or moderate values of $\frac{L^2t}{d^3}$ helical buckling can also be disregarded. For the remaining case, where the axis of the buckled cylinder is straight, DONNELL has, after introducing several simplifications, derived the relation between the quantities A and H (*ref.* 20). This relation can be approximated by the following formulae

$$A = 4{,}6 + 1{,}292\ (4{,}67 + H^{1{,}5})^{0{,}5} \qquad (4.4)$$

for clamped edges and

$$\frac{L^2t}{d^3} < 7{,}8\ (1-\nu^2)^{0{,}5} \simeq 7{,}45;$$

$$A = 2{,}8 + 1{,}183\ (1{,}86 + H^{1{,}5})^{0{,}5} \qquad (4.5)$$

for hinged edges and

$$\frac{L^2t}{d^3} < 5{,}5\ (1 - \nu^2)^{0{,}5} \doteq 5{,}25.$$

For larger values of $\frac{L^2t}{d^3}$ DONNELL obtains a formula analogous to (4.2) but with a factor 0,77 instead of $\frac{2}{3}$, thus yielding values of F_T that are 15 % too large. The error probably is a consequence of the simplications made. It is possible that (4.4) and (4.5) contain errors of the same order.

4.1.2 *Experiments.*

Many test data can be found in *ref.* 9, 19, 20, 21 and 24. All tested cylinders had no intermediate frames ($l = L$) and the edges can be considered clamped. All cylinders where $\frac{L^2t}{d^3} > 7{,}45$ had moderate ratios $\frac{d}{t}$, viz. $49{,}5 \leqq \frac{d}{t} \leqq 168$. For these cylinders F_T ranges from 1,00 to 1,35 times the theoretical stress from (4.2), with three exceptions which can be considered abnormal. No explanation has been given of this rather surprising phenomenon; it may be that collaps of the cylinder does not occur simultaneously with buckling. The theoretical buckling stress will be a conservative estimate of the collapsing stress in this range of $\frac{d}{t}$ values, as long as elastic instability occurs. This conclusion will also hold

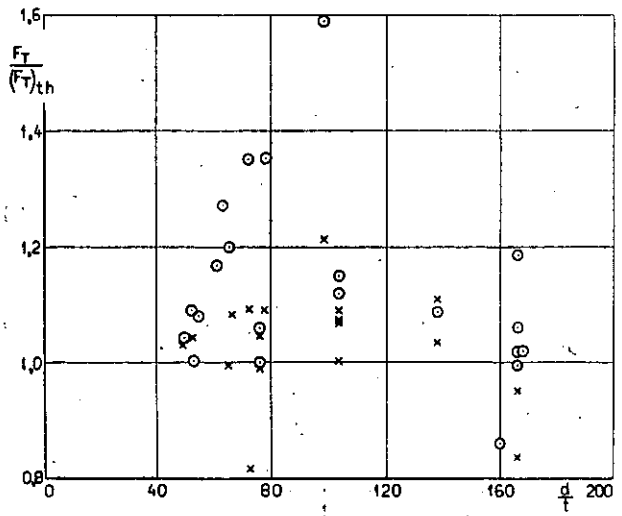

FIGURE 4.1.

Verification of the proposed formula (4.6.).
× *tests with* $L^2t/d^3 < 9$, $(F_T)_{th}$ *from* (4.6).
⊙ *Tests with* $L^2t/d^3 > 9$, $(F_T)_{th}$ *from* (4.2.)

for cylinders having smaller values of $\frac{L^2t}{d^3}$. Assuming that (4.4) is correct but for a multiplying factor, this factor can be determined either from the condition that the minimum test results agree with the theoretical values, or from an empirical limiting value of $\frac{L^2t}{d^3}$ below which this parameter influences the magnitude of F_T. In the latter case the values of F_T from (4.2) and from the corrected equation (4.4) must be equal at the limiting value of $\frac{L^2t}{d^3}$.

Experimental evidence on elastic buckling is too limited to yield a conclusive result. From the tests with thick-walled tubes (sec. 4.2.2) it may be concluded that the said limiting value there is about 9. Retaining the same value for the elastic buckling region, the multiplying factor is 0,903 [5]); (4.4) is then replaced with

$$A = 4{,}15 + 1{,}167\ (4{,}67 + H^{1{,}5})^{0{,}5} \qquad (4.6)$$

for clamped edges and $\frac{L^2t}{d^3} < 9$.

Computing the theoretical values $(F_T)_{th}$ from (4.2) or (4.6), as appropiate, the ratios of the experimental and the theoretical stresses in the range of $\frac{d}{t}$ values between 49 and 168 are as represented in fig. 4.1. The test results of the category $\frac{L^2t}{d^3} < 9$ scatter in the same region as those of the category $\frac{L^2t}{d^3} > 9$, equation (4.6) is therefore acceptable. This formula has also been used in the evaluation of the tests with $\frac{d}{t} > 200$, where $\frac{L^2t}{d^3} < 9$ without exception. The test results [6]) scatter within the region bounded by the dotted lines in fig. 4.2. The drawn line represents the proposed values of $\frac{F_T}{(F_T)_{th}}$ which, in combination with (4.2) or (4.6), as appropiate, will yield a conservative estimate of the collapsing stress. For the case of hinged edges it is proposed

[5]) When $\frac{L^2t}{d^3} = 9$ the only significant term is $1{,}292\ H^{0{,}75}$; then we obtain from (4.4): $F_T = 1{,}372\ E \left(\frac{t}{d}\right)^{1{,}5} \left(\frac{d^3}{L^2t}\right)^{0{,}25}$ if $\nu = 0{,}3$.

[6]) Three abnormal results have been omitted.

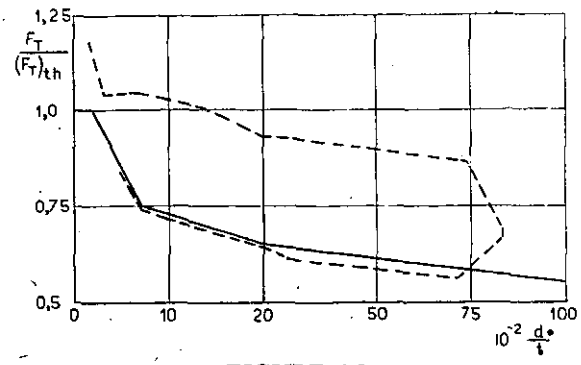

FIGURE 4.2.

Ratio of the experimental and theoretical values of F_T for elastic buckling. $(F_T)_{th}$ from (4.2) or from (4.6, 7).
- - - - scatter region of the tests.
—— proposal for the computation of F_T.

to use the same values of $\frac{F_T}{(F_T)_{th}}$ and to compute $(F_T)_{th}$ from (4.5) multiplied by the correction factor 0,903, obtained with clamped edges,

$$A = 2{,}5 + 1{,}068\ (1{,}86 + H^{1{,}5})^{0{,}5}\ , \quad (4.7)$$

for hinged edges and $\frac{L^2t}{d^3} < 6{,}3$,

or from (4.2) if $\frac{L^2t}{d^3} \geqq 6{,}3$.

4.2 *Thick-walled tubes.*

4.2.1 *Theoretical considerations.*

According to TIMOSHENKO it is reasonable to assume that the mechanical properties of a plate, loaded in shear beyond the proportional limit, will be reduced in the same ratio regardless of the direction considered, i.e. that the plate remains isotropic. Consequently, in the formulae for elastic instability YOUNG's modulus must be replaced with the reduced modulus E_r.

The same will be true for twisted tubes (*ref.* 1, art. 71, p. 390. However, this assumption probably underestimates the buckling stress, as the addition of an infinitesimal normal stress only causes a change of the second order of the equivalent principal stress from GUEST's and HUBER-HENCKY's formulae. Therefore, TIMOSHENKO's assumption will underestimate the bending stiffness of the wall).

The relation between the stress-strain diagrams in tension ($\sigma - \varepsilon$ diagram) and torsion ($\tau - \gamma$ diagram) is discussed in *ref.* 19 for Cr-Mo steel and duralumin. [7]) It is shown, that these diagrams are affinely related with good approximation. Consequently, the non-dimensional $\frac{\sigma}{S_t} - \frac{E\varepsilon}{S_t}$ and $\frac{\tau}{S_T} - \frac{G\gamma}{S_T}$ diagrams will coincide, and it may be assumed that in a torsion test the value of $\frac{E_r}{E}$ is determined exclusively by the magnitude of $\frac{\tau}{S_T}$ and that in different tests equal values of $\frac{\tau}{S_T}$ correspond to equal values of $\frac{E_r}{E}$, provided that all $\sigma - \varepsilon$ diagrams are affinely related. Again assuming that all $\sigma - \varepsilon$ diagrams of a particular material are affinely related and also that $\frac{S_T}{S_t}$ is a material constant, we conclude from the generalized formula (4.2) for plastic buckling,

$$\frac{F_T}{S_t} = 0{,}715\,\frac{E_r}{E}\,\frac{E}{S_t}\left(\frac{t}{d}\right)^{1{,}5} = 0{,}715\ \alpha_T\,\frac{E_r}{E}\ , \quad (4.8)$$

that the $\frac{F_T}{S_t} - \alpha_T$ diagram is not affected by scatter of the material properties. [8]) Thus, this diagram will be used in evaluating the tests on long tubes complying with (4.3), which condition is nearly always satisfied in practice.

For short or moderately long tubes we obtain an analogous diagram from the formulae obtained from (4.4) to (4.7) incl. by replacing E with E_r. We can assume $H = \infty$ in these formulae for all practical purposes. [9]) Then, they all have the form

$$F_T = c_T\,\frac{E_r}{E}\,\frac{E}{S_t}\left(\frac{t}{d}\right)^{1{,}5}\left(\frac{d^3}{L^2t}\right)^{0{,}25} = c_T\,\beta_T\,\frac{E_r}{E}\ , \quad (4.9)$$

where the magnitude of c_T (resp. 1,372; 1,256; 1,238 and 1,133) depends upon the limiting value of $\frac{L^2t}{d^3}$, at which the formula yields the same result as (4.8). From (4.9) we conclude that for this category of tubes we must plot the test results *in an* $\frac{F_T}{S_t} - \beta_T$ *diagram.*

4.2.2 *Experiments.*

4.2.2.1 Tests with duralumin tubes have been reported in *ref.* 19, 23 and 24; tests with steel

[7]) Only torsion tests have been considered where no buckling occurred.

[8]) S_t has been chosen instead of S_T because the latter will in general be unknown; it has only been given in *ref.* 19.

[9]) Doing this, the error is only 5 % when $H = 300$ (e. g. $\frac{L}{d} = 5$ and $\frac{d}{t} = 12$).

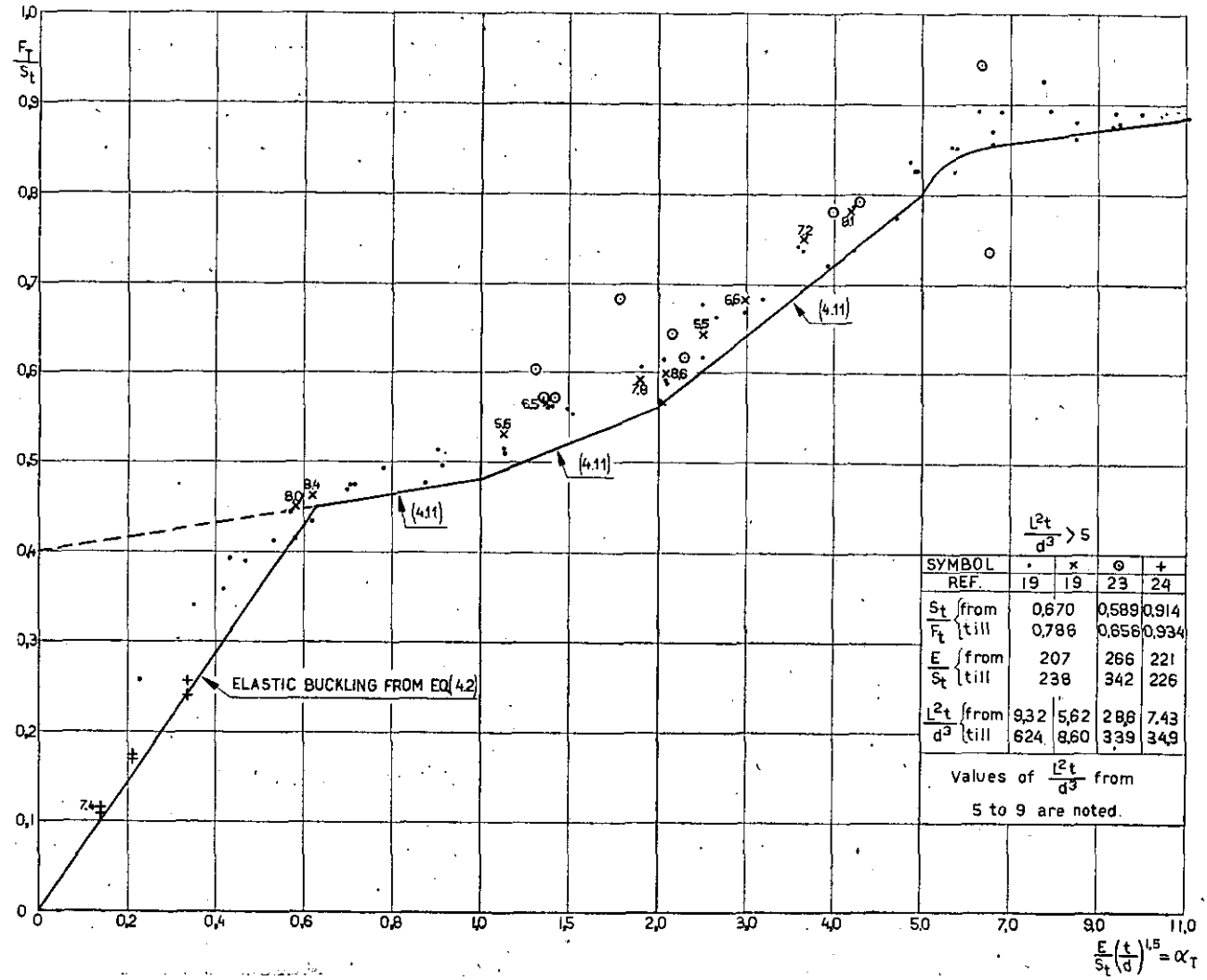

FIGURE 4.3.
Torsion tests of duralumin tubes; $d/t < 200$, $L^2t/d^3 > 5$.

tubes in *ref.* 19, 22 and 23. With all tubes $l = L$ and the edges can be considered clamped. *Evaluating the tests* F_T has been defined as the average shear stress at failure

$$F_T = \frac{M_T d}{2 I_p} = \frac{2 M_T}{\pi D^2 t} \frac{1 - \frac{t}{D}}{1 - 2\frac{t}{D} + 2\left(\frac{t}{D}\right)^2}. \quad (4.10)$$

With the tests of *ref.* 19 S_t has been determined with the values of k from table 2.1; from table VI of *ref.* 19 $S_t \simeq Y_t$. With all other tests S_t has been assumed equal to Y_t. The results obtained from *ref.* 24 are averages of two or three identical tests; the same applies to part of the results from *ref.* 19. Further, the tests mentioned in *ref.* 19 have been made on pairs of tubes differing only in length. If both tubes had $\frac{L^2t}{d^3} > 9$ no systematical influence of L can be established; as a rule only the average of both results is given here.

4.2.2.2 The results of the tests with *duralumin tubes* ($7{,}4 < \frac{d}{t} < 138$) are summarized in figs. 4.3 and 4.4.

In order to determine the limiting value of $\frac{L^2t}{d^3}$ (sec. 4.1.1) the tests have been divided into three groups, viz. (1) $\frac{L^2t}{d^3} > 9$, (2) $\frac{L^2t}{d^3} < 5$ and (3) $5 < \frac{L^2t}{d^3} < 9$. In accordance with sec. 4.2.1 fig. 4.3 represents $\frac{F_T}{S_t}$ as a function of α_T for groups (1) and (3) and fig. 4.4 $\frac{F_T}{S_t}$ as a function of β_T for groups (2) and (3). Fig. 4.3 shows that elastic buckling occurs up to $\alpha_T \simeq 0{,}6$; the tests in this region have already been discussed in sec. 4.1.2 (fig. 4.1). In the region $\alpha_T > 0{,}6$ the scatter is not large, excepting the tests from *ref.* 23 which, dating from before 1924, may

probably be considered obsolete. The collapsing stresses may be computed from the proposal, represented by the uninterrupted line in fig. 4.3, which corresponds to (4.2) up to $\alpha_T = 0{,}63$ and to

$$\frac{F_T}{S_t} = 0{,}4 + 0{,}08\ \alpha_T \text{ when } 0{,}63 \leqq \alpha_T < 5\,. \quad (4.11)$$

In general the results of group (3) lie at the upper boundary of the region of scatter of group (1), thus indicating a small influence of $\frac{L}{d}$ for the tests of group (3). It may be concluded that the limiting value of $\frac{L^2t}{d^3}$, beyond which L does not influence F_T, will be approximately 9 for tubes with clamped edges. Accepting this value, the proposals (4.2) and (4.11), holding for $\frac{L^2t}{d^3} \geqq 9$ yield the following formulae for the region $\frac{L^2t}{d^3} < 9$:

$$\frac{F_T}{S_t} = 1{,}24\ \beta_T \text{ when } \beta_T \leqq 0{,}363\,, \quad (4.12)$$

$$\frac{F_T}{S_t} = 0{,}4 + 0{,}1386\ \beta_T \text{ when } 0{,}363 \leqq \beta_T \leqq 2{,}9. \quad (4.13)$$

Fig. 4.4 shows that the test results agree well with these proposals, excepting the failures in the plastic region from *ref.* 24, where eq. (4.13) is unconservative. The explanation of this discrepancy is that with the material of these tubes

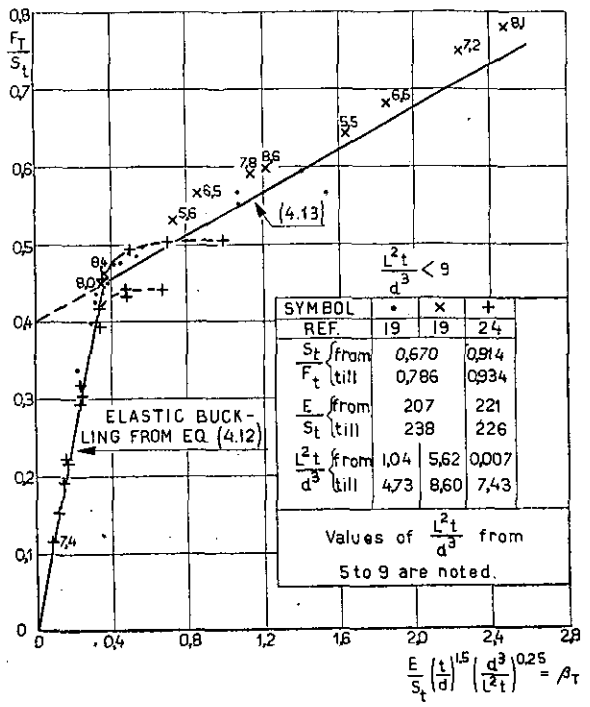

FIGURE 4.4.
Torsion tests of duralumin tubes; $d/t < 200$, $L^2t/d^3 < 9$.

TABLE 4.1

Torsion tests on steel tubes

reference material		22 carbon steel			23 Nickel steel	19 Cr-Mo steel			
$\frac{d}{t}$	from	3			6,8	10,9			
	till	61,5			33,6	73,5			
group		1	2	3	—	1	2	3	4
$\frac{S_t}{T_t}$	from	0,59	0,75	0,87	0,84	0,60		0,86	
	till	0,79	0,90	0,97	0,98	0,78		0,98	
$\frac{E}{S_t}$	from	501	386	336	205	207		261	
	till	1200	832	518	276	423		359	
$\frac{L^2t}{d^3}$	from	23	9,6	16	11,1	0,80	10,7	1,71	11,9
	till	2140	4500	2500	151	8,27	65,5	8,77	289
$\frac{F_T}{S_t}$	from	see fig. 4.5		0,51 [2]	0,49	0,55	0,52	0,55	0,53
	till			0,70	0,62	0,66	0,64	0,61	0,64
	mean	—	—	0,61 [2]	0,54	0,59	0,58	0,59	0,585
α_T [1]	from	2,42	1,01	2,45	1,36	0,70	1,37	0,60	0,99
β_T	till	70,1	25,0	78,5	12,0	2,59	4,90	1,58	8,12

[1]) For group 1 and 3 of *ref.* 19 the limits of β_T, for all other tests the limits of α_T are mentioned.
[2]) The abnormal result $F_T/S_t = 0{,}221$ for $\alpha_T = 7{,}48$ is omitted.

(51 ST aluminium alloy) $\frac{S_t}{F_t}$ is considerably larger than with the material of the tubes according to *ref.* 19. Therefore, the σ—ε curve will possess a much more pronounced knee and so will the $\frac{F_T}{S_t}$ — β_T diagram (c.f. the dotted curves in fig. 4.4). The proposals (4.11) and (4.13) will only hold for duralumin having approximately the same material properties as in *ref.* 19 (c.f. fig. 4.4). It should be noted that the curves of figs. 4.3 and 4.4 will coincide if $\frac{L^2t}{d^3} = 9$; for design purposes they may be combined to one curve in a diagram with two different horizontal scales.

4.2.2.3 The important results of the tests on *steel tubes*, collapsing by plastic buckling, are collected in table 4.1. For the tests of *ref.* 22 and 23 $E = 30 \times 10^6$ p.s.i. has been assumed. On account of the large scatter of the material properties the tests of *ref.* 22 have been divided into three, more or less arbitrarily chosen, groups. The tests of *ref.* 19 have first been arranged in order of the magnitude of $\frac{S_t}{F_t}$ and then subdivided into groups $\frac{L^2t}{d^3} < 9$ and $\frac{L^2t}{d^3} > 10$. The results of the tests of *ref.* 19 and 23 and of group 3 from *ref.* 22 do not indicate an influence of either $\frac{d}{t}$ or $\frac{L^2t}{d^3}$ on F_T; the scatter is fairly large (c.f. table 4.1) [10]) The average of all test results [11]) is $\frac{F_T}{S_t} = 0{,}585$. Excepting two obviously abnormally small values, the test results of groups 1 and 2 from *ref.* 22 ($\alpha_T < 21$) cover the area indicated by the dotted lines in fig. 4.5; besides, 7 tests with $\alpha_T > 21$ yield $0{,}655 \leqq \frac{F_T}{S_t} \leqq 1{,}14$. No separation of the results of these two groups can be made.

From a survey of the test results no definite conclusion appears to be possible. No indication exists that with equal E and decreasing $\frac{S_t}{F_t}$ the transition from the elastic to the plastic range of the $\frac{F_T}{S_t}$ — (α_T or β_T) diagram is becoming more gradual, as could have been expected. The tendency of $\frac{F_T}{S_t}$ to decrease with increasing S_t (E and $\frac{S_t}{F_t}$ remaining unchanged) which is established by a comparison of the results from *ref.* 22 with those from *ref.* 19 and 23, is even contrary to the theoretical conclusion, assuming affinely related σ—ε curves. [12]) The following provisional proposals, therefore, should be verified by further tests.

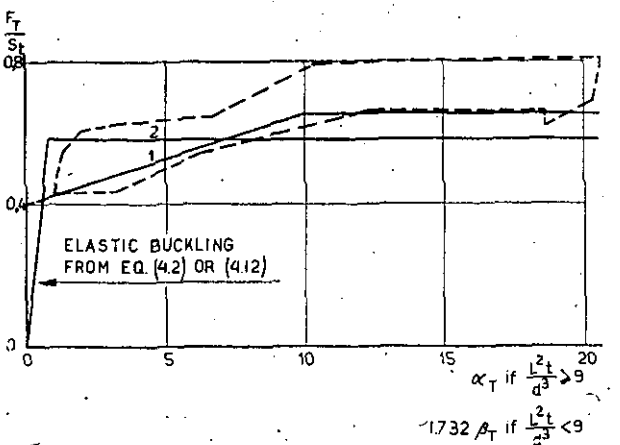

FIGURE 4.5.

Proposals for the determination of F_T for steel tubes with clamped edges:

1 *proposal for* $0{,}6 \leqq S_t/F_t \leqq 0{,}75$.

2 *proposal for* $S_t/F_t \geqq 0{,}85$.

- - - - *region of scatter for groups* 1 *and* 2 *of ref.* 22.

For $0{,}6 \leqq \frac{S_t}{F_t} \leqq 0{,}75$ it is recommended to use curve 1 of fig. 4.5, based on the tests from groups 1 and 2 of *ref.* 22. If $\frac{S_t}{F_t} \geqq 0{,}85$ curve 2 of fig. 4.5 may be used; this proposal is based on the tests from group 3 of *ref.* 9 and from *ref.* 19 and 23. For intermediate values of $\frac{S_t}{F_t}$ a linear interpolation with this variable is reasonable.

---

[10]) *Ref.* 19 shows that the scatter is not due to scatter of $\frac{S_T}{S_t}$.

[11]) With the tests of *ref.* 19 the average values $\frac{F_T}{S_t} = 0{,}586$, $\frac{F_T}{S_T} = 1{,}0$ and $\frac{S_t}{S_T} = 1{,}73$ show a good mutual agreement.

[12]) The theoretical conclusion follows from the considerations that $\frac{F_T}{S_t}$ would not change if S_t had been determined from the k-method, and that actually S_t has been assumed equal to Y_t.

4.2.2.4 In the case of *hinged edges* the limiting value of $\frac{L^2t}{d^3}$ can be assumed to be 6,3 as in sec. 4.1.2. Then curves 1 and 2 of fig. 4.5 remain valid, provided that α_T is taken as abscissa for $\frac{L^2t}{d^3} > 6{,}3$ and $\beta_T \sqrt[4]{6{,}3} = 1{,}584\ \beta_T$ is taken as abscissa for $\frac{L^2t}{d^3} < 6{,}3$. The curve of fig. 4.3 remains valid for $\frac{L^2t}{d^3} > 6{,}3$; that of fig. 4.4 for $\frac{L^2t}{d^3} < 6{,}3$, provided that the abscissa represents $0{,}915\ \beta_T$ instead of β_T.

4.2.2.5 As far as *the mode of buckling* is communicated the tubes with $\frac{d}{t} > 12{,}5$ collapsed by local buckling while the axis of the tube remained straight. Of the tubes with $\frac{d}{t} < 12{,}5$ some collapsed in the same way, some without noticeable buckling distortions, but most of these tubes showed the helical buckling described in sec. 4.1.1 or a combination of local and helical buckling. Plotting the results of these latter tests in the non-dimensional diagram for helical buckling ($\frac{F_T}{S_t} - \gamma_T$ diagram), it appears that the test results of the duralumin tubes ($3{,}3 \leqq \gamma_T \leqq 20$) scatter around $\frac{F_T}{S_t} = 0{,}875$ with deviations less than 7 %. For the steel tubes there are only two measurements; for these tubes the least value of $\gamma_T \simeq 3$ and the corresponding value of $\frac{F_T}{S_t} = 0{,}715$. Comparing these results with figs. 4.3 to 4.5 incl., we may conclude that helical buckling will not be critical if $\gamma_T > 3$.

4.2.3 *Comparison with other proposals.* [13])

Ref. 26 gives diagrams of F_T as a function of $\frac{D}{t}$ for 17 ST and 24 ST duralumin. Als $\frac{L}{D}$ does not occur, these diagrams obviously apply to long tubes, they can be compared with fig. 4.3. This comparison is illustrated in fig. 4.6. Curve 2, applying to the material of *ref.* 19 is in good

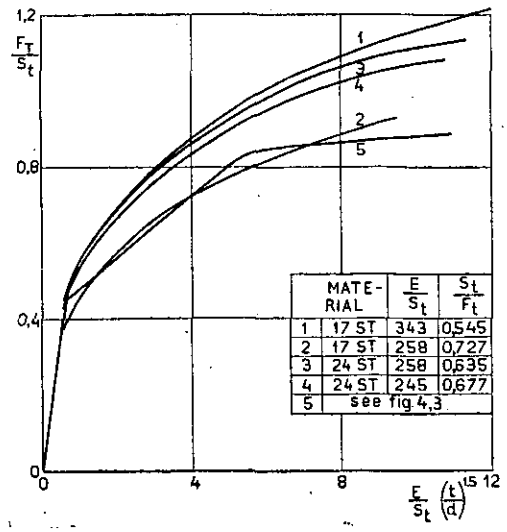

FIGURE 4.6.

Comparison of the proposal of fig. 4.3 with the curves of ANC-5 (ref. 26), fig. 5—7.

agreement with fig. 4.3. From the values of $\frac{E}{S_t}$ and $\frac{S_t}{F_t}$ it might be expected, that curves 1, 3 and 4 slightly exceed 2 or 5, but the actual difference is unreasonably large, the more so, because the values of $\frac{E}{S_t}$ and $\frac{S_t}{F_t}$ for 2, 3 and 4 are between the limits noted on fig. 4.3. It is recommended to use figs. 4.3,4 for all these materials, except for 51 ST duralumin (see sec. 4.2.2.2).

In *ref.* 26 a proposal is made for 1025 steel ($\frac{E}{S_t} = 778$; $\frac{S_t}{F_t} = 0{,}655$). From $\alpha_T = 4$ on, this proposal yields values for $\frac{F_T}{S_t}$ which considerably exceed the maxima of the test results, discussed in sec. 4.2.2.3; therefore, this proposal is not acceptable. For alloy steel ($\frac{E}{S_t} = 176$ to 645; $\frac{S_t}{F_t} = 0{,}69$ to $0{,}92$) *ref.* 26 gives a diagram of $\frac{F_T}{F_t}$ as a function of $\frac{D}{t}$ with $\frac{L}{D}$ as a parameter. For heat-treated chromium-molybdenum steel ($\frac{E}{S_t} = 160$ to 320; $\frac{S_t}{F_t} \simeq 0{,}9$) *ref.* 25 gives a diagram of $\frac{F_T}{F_t}$ as a function of $\frac{L}{D}$ with $\frac{D}{t}$ as a parameter. Taking $\frac{L^2t}{d^3} = 9$ as a limiting value, the theory and experiments discussed in this section indicate that these diagrams should be similar to figs. 4.7a

[13]) For compression and bending the comparison with the proposals of *ref.* 26 is omitted. The latter are conservative.

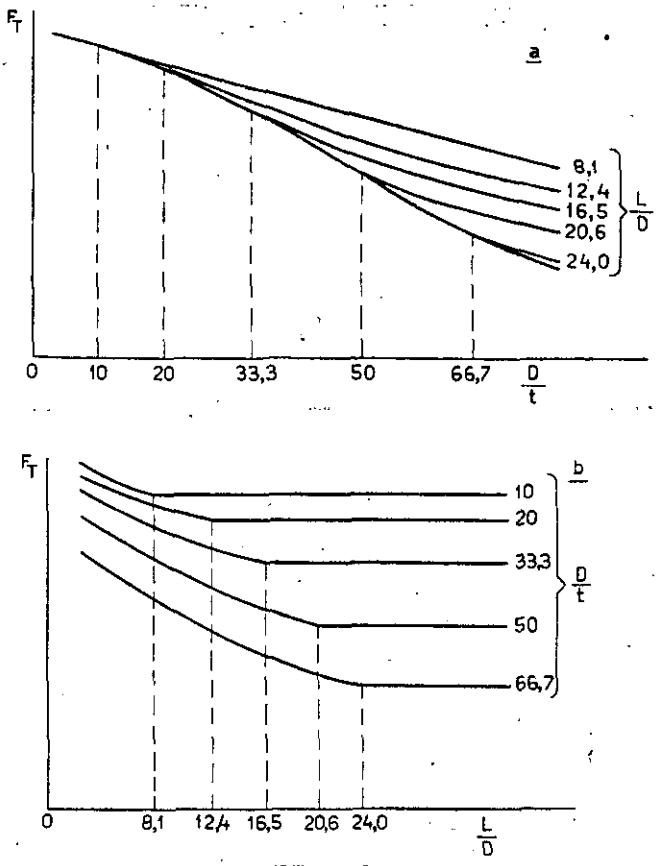

FIGURE 4.7.
Schematical diagrams for F_T.

and b. Yet, the deviations are so large, that these diagrams have presumably been established without a sufficiently critical investigation of the data available.

5 Pure shear.

Ref. 32 recommends to use $F_s = 1{,}25\ F_T$ for thin-walled cylinders. This result is based on tests with short cylinders, whose ends were rigidly clamped; thus preventing at the ends the displacements normal to the plane of the cross section (warping) corresponding to the assumed SAINT VENANT stress distribution. Consequently, the shear stress distribution will have been more uniform and the maximum shear stress will have been reduced. The actual shear stress causing buckling, therefore, will be smaller then $1{,}25\ F_T$. A conservative recommendation will be

$$F_s = F_T. \qquad (5.1)$$

No data at all are available on the critical shear stress of thick-walled tubes. For the time being (5.1) is recommended as a probably conservative approximation.

6 Combined loadings.

6.1 *Compression and bending.*

In this article only tubes which show flexural buckling under compressive loads alone, are considered; i.e. rather thick-walled tubes. The graphs given in the U.S. Civil Strength Requirements for Aircraft of 1929 and 1935 (see e.g. *Ref.* 28 figs. 71 and 72, and *Ref.* 31, fig. 4) are unsatisfactory, as they give combinations of compressive stress and 'primary' bending stress. [14]) They are only valid for the type of bending load obtained in a four point bending test.

Experiments are mentioned in *ref.* 13, 27, 28 and 29. *Ref.* 27 and *ref.* 28 refer to the same experiments and the data given are complementary to each other.

In *ref.* 13 several assumptions are made in evaluating the experiments, which do not conform to the actual conditions. Therefore, the unreasonable conclusion, that $f_b + f_c = S$ except that for $f_c = 0$, $f_b = F_b$ and for $f_b = 0$ $f_c = F_c$, can readily be ignored. The experiments mentioned in *ref.* 29 must be ignored because neither the material properties nor F_b and F_c are communicated. So, only the experiments with duralumin and chromium-molybdenum steel tubes given in *ref.* 27 and 28 are useful. In evaluating these experiments the assumption has been made that the critical combination of compression stress and actual bending stress does not depend on the variation of the bending loads along the tube.

From the data in *ref.* 27 and 28 the maximum bending moments, and from these the fictitious bending stresses, have been computed, using the formulae for the elastic range. The stress f_b is not the actual stress, for the distribution of the bending stresses no longer is linear beyond the proportional limit and the actual moment is not equal to the moment following from the formulae. Therefore, when applying the graphs, obtained for the critical combinations of f_b and f_c, one must use the same method of analysis.

Even then the fact, that the actual moment differs from the computed moment is accounted for only in a rough approximation. The way in which the moment at the critical section increases due to plastic deformation, not only depends on the plastic deformation at this section, but also on the plastic deformation at other points of the tube. The latter deformations depend to a large extent upon the shape of the bending moment diagram of the tube.

[14]) This is the bending stress which would occur in the absence of the compressive load.

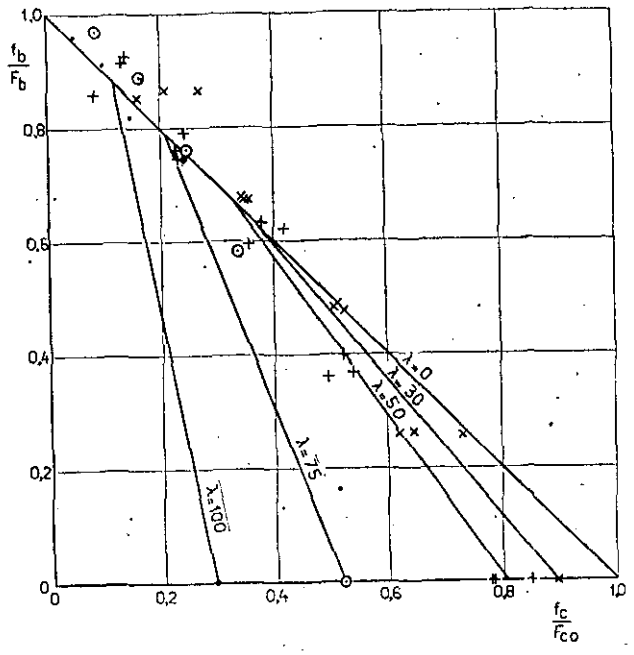

FIGURE 6.1.
Results of the tests on duralumin tubes, from ref. 27 and 28.

With the chromium-molybdenum steel tubes [15]) with $\lambda = 75$ and $\lambda = 100$ and the duralumin tubes the computations have been based on the mean values of f_c and F_b from *ref.* 27 and 28 for all tubes with the same λ. For the shorter steel tubes it has been assumed that tubes with the same dimensions also had the same material properties. The values of E have been computed from the EULER range of the F_c — λ curves. In figs. 6.1 and 6.2 the computed values of $\frac{f_b}{F_b}$ are plotted as a function of $\frac{f_c}{F_{co}}$, F_{co} being the value of F_c at $\lambda = 0$. By means of the curves on fig. 2.2 F_{co} has been computed from the experimental values of F_c at $\lambda = 30$ (or $\lambda = 50$). It appears that the test points coincide fairly well with the broken lines, the right parts of which connect the point $f_c = 0{,}4\ F_c$ on the line $\lambda = 0$ with the point $f_c = F_c$ on the horizontal axis. In some cases the deviations are fairly large, but this was to be expected in view of the assumptions made in evaluating the tests. The critical combinations of f_c and f_b represented by the broken lines can be accepted as long as more reliable data are not available. As they agree reasonably well with the test results both of the duralumin and of the chromium molybdenum steel tubes it is proposed to use the same criteria also for other materials. The proposals made, expressed in formulae are:

$$\left.\begin{aligned} &\frac{f_b}{F_b} + \frac{f_c}{F_{co}} = 1 \text{ for } \frac{f_c}{F_c} \leqq 0{,}4\ , \\ &0{,}6\,\frac{f_b}{F_b} = \left(1 - 0{,}4\,\frac{F_c}{F_{co}}\right)\left(1 - \frac{f_c}{F_c}\right) \\ &\text{for } \frac{f_c}{F_c} > 0{,}4\ . \end{aligned}\right\} \quad (6.1)$$

6.2 *Compression (local buckling), bending and torsion.*

6.2.1 *Thin-walled cylinders.*

Only the combination of compression or tension with torsion has been investigated experimentally, the experiments are discussed in *ref.* 9 and 30. In both publications it is recommended to use the following formula for compression and torsion

$$\frac{f_c}{F_c} + \left(\frac{f_T}{F_T}\right)^n = 1\ , \qquad (6.2)$$

with $n = 2$ (*ref.* 9) or $n = 3$ (*ref.* 30). The value $n = 3$ agrees with the average results of *ref.* 30; for the minimum values $n =$ (1 to 1,5). An additional uncertainty is caused by the large scatter, especially in the neighbourhood of $f_c = F_c$. Therefore, it is recommended to take $n = 1{,}5$. F_c is to be computed from (2.5) and F_T from fig. 7.

The average results of the experiments with

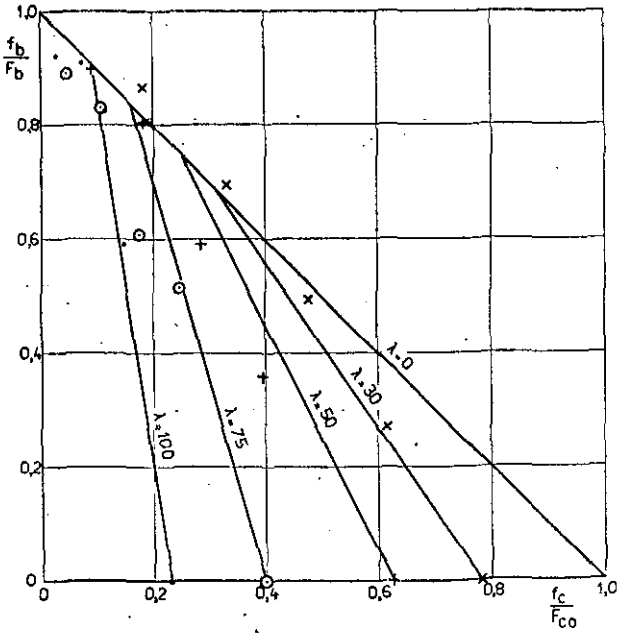

FIGURE 6.2.
Results of the tests on chromium-molybdenum steel tubes, from ref. 27 and 28.

[15]) Only the experiments with 2″ tubes have been evaluated, because only for these tubes F_b is given.

tension and torsion are, according to *ref.* 9, represented by

$$\frac{f_T}{F_T} + m\frac{f_c}{F_c} = 1, \qquad (6.3)$$

with $m = 0{,}5$. In *ref.* 30 it is recommended to use formula (6.2) with $n = 3$. Here f_c is negative and thus $\frac{f_T}{F_T} > 1$. The results from *ref.* 30 can also be approximated satisfactorily by a linear relation; the minimum values in *ref.* 9 yield $m = 1/3$, those in *ref.* 30 $m = 1/6$. For the present it is recommended to take $m = 0{,}2$.

Because of the similarity between compression and bending it seems reasonable to use a formula analogous to (6.2) in the case of bending and torsion

$$\frac{f_b}{F_b} + \left(\frac{f_T}{F_T}\right)^{1,5} = 1, \qquad (6.4)$$

whereas for bending and compression we may assume

$$\frac{f_c}{F_c} + \frac{f_b}{F_b} = 1, \qquad (6.5)$$

where F_b is computed from (3.2). The critical combinations of f_c, f_b and f_T will follow from

$$\frac{f_c}{F_c} + \frac{f_b}{F_b} + \left(\frac{f_T}{F_T}\right)^{1,5} = 1. \qquad (6.6)$$

6.2.2 *Thick-walled tubes.*

Only the combination of bending and torsion has been experimentally investigated. The results of experiments with steel tubes are given in *ref.* 31, fig. 2. From this graph it follows that the critical combinations are obtained from

$$\left(\frac{f_b}{F_b}\right)^2 + \left(\frac{f_T}{F_T}\right)^2 = 1. \qquad (6.7)$$

This formula is confirmed by unpublished experiments with steel tubes ($15 < \frac{d}{t} < 30$) and duralumin tubes ($\frac{d}{t} = 110$), which collapsed in the plastic range when loaded in pure torsion or pure bending.

Formula (6.7) thus applies to steel as well as to duralumin tubes; F_b follows from fig. 3.1 and F_T from fig. 4.3, 4.4 or 4.5 (see sec. 4.2.2).

The case of compression and bending is represented by (6.5); then F_c is taken from fig. 2.4. When compression, bending and torsion occur, we may compute the critical combinations from

$$\left(\frac{f_c}{F_c} + \frac{f_b}{F_b}\right)^2 + \left(\frac{f_T}{F_T}\right)^2 = 1. \qquad (6.8)$$

6.3 *Bending with transverse load.*

6.3.1 *Thin-walled cylinders.*

LUNDQUIST (*ref.* 32) assumes that at the critical point of the cross section $\frac{\sigma}{F_b} + \frac{\tau}{F_s} = 1$. The critical point is defined as the point in which this sum is a maximum. The result can be written as:

$$\left(\frac{f_b}{F_b}\right)^2 + \left(\frac{f_s}{F_s}\right)^2 = 1. \qquad (6.9)$$

A number of experiments (*ref.* 32) with $0{,}25 < \frac{L}{d} < 1$ and $646 < \frac{d}{t} < 2910$ showed satisfactory agreement with (6.9); f_b is taken as the largest bending stress, occurring in the part of the cylinder considered.

6.3.2 *Thick-walled tubes.*

It is impossible to draw a conclusion from the available experiments (*ref.* 17 and unpublished data). It may be deemed reasonable to take formula (6.9). But we could just as well define the critical point as the point in which $\left(\frac{\sigma}{F_b}\right)^2 + \left(\frac{\tau}{F_s}\right)^2$ is maximal, based on (6.7), and then compute the critical combination of f_b and f_s from the condition that this sum is unity. In this way it appears that the transverse load and the bending moment do not interact. In *ref.* 31 the actual situation is presumed to lie between these two possibilities and it is proposed to use

$$\left(\frac{f_b}{F_b}\right)^3 + \left(\frac{f_s}{F_s}\right)^3 = 1. \qquad (6.10)$$

For the present this proposal is taken over.

6.4 *Bending with transverse load and torsion.*

No experiments are known. At the point where the shear stress is maximum, the bending stress is zero; one condition to be satisfied is therefore

$$\frac{f_T}{F_T} + \frac{f_s}{F_s} \leqq 1. \qquad (6.11)$$

From (6.9) or (6.10) the critical bending stress f_{bs} in the absence of torsion can be found. As a second condition it is proposed to apply the criteria.

$$\frac{f_b}{f_{bs}} + \left(\frac{f_T}{F_T}\right)^{1,5} \leqq 1,$$

analogous to (6.4), for thin-walled cylinders;

$$\left(\frac{f_b}{f_{bs}}\right)^2 + \left(\frac{f_T}{F_T}\right)^2 \leqq 1,$$

analogous to (6.7), for thick-walled tubes.

After substitution of f_{bs} we obtain for thin-walled cylinders

$$\frac{f_b}{F_b}\left\{1 - \left(\frac{f_s}{F_s}\right)^2\right\}^{-0,5} + \left(\frac{f_T}{F_T}\right)^{1,5} \leqq 1, \quad (6.12)$$

and for thick-walled tubes

$$\left(\frac{f_b}{F_b}\right)^2\left\{1 - \left(\frac{f_s}{F_s}\right)^3\right\}^{-2/3} + \left(\frac{f_T}{F_T}\right)^2 \leqq 1. \quad (6.13)$$

6.5 *Formulae for the transition region.*

The formulae proposed in sec. 6.2 to 6.4 were, as far as they were checked experimentally, deduced from experiments where, under each of the separate components of the loading, the tube would have failed either in the elastic or in the plastic region. The formulae obtained for these two cases appear to be different. The available experimental evidence does not allow to make proposals for intermediate cases, where under one or more separate components elastic failure and under the remaining separate components plastic failure would occur. For the time being it is recommended to use the formulae for thin-walled cylinders, when none of the separate components would cause failure in the plastic region, i.e. when $\frac{E}{S_c}\frac{t}{d} < 2,5$ and when F_T follows from (4.2) or from (4.6), (4.7) resp. (4.12). In all other cases it is recommended to use the formulae for thick-walled tubes, unless it is to be expected that these formulae would give too optimistic results. For instance in the case of a duralumin tube with $\frac{d}{t} = 110$, $\frac{L}{D} = 35$, $\frac{E}{S} = 280$ and $\frac{S_c}{S_t} = 0,9$, and therefore $\frac{E}{S_c}\frac{t}{d} = 2,55$ and $\alpha_T = 0,22$, the use of (6.7) will not be permitted, so that (6.4) must be preferred.

7 Recapitulation.

Based on a study and further elaboration of the data, given in the literature, proposals are made, giving the minimum collapsing stresses of accurately manufactured round tubes under different types of loading.

For thin-walled cylinders, [16]) which are defined as cylinders, collapsing by elastic local instability, the buckling stresses are dependent upon the elastic material properties (E, ν) and upon the dimensions of the cylinder ($\frac{d}{t}$, $\frac{L}{d}$). The proposals for compression and for bending are only valid for cylinders, having a ratio $\frac{L}{d}$ between 0,3 and approximately 15. They are based mainly on experiments with small-sized test pieces and may be unreasonably conservative for actual structures, due to scale effects, caused by the large influence of initial deviations from the true cylindrical shape, which are probably relatively larger with decreasing dimensions of the test piece.

For thick-walled tubes, [16]) which are defined as tubes, collapsing locally in the plastic region, non-dimensional diagrams are given from which the collapsing stresses can be determined.

The coordinates of these diagrams follow from theoretical considerations; the diagram itself is then determined from available experimental data. The quantity S, occurring in the coordinates, is defined as the intersection of the stress-strain curve with a straight line through the origin having a slope kE (fig. 2.1). As a rule k is defined by eq. (2.3), sec. 2.2 (c.f. table 2.1), in which case S is approximately equal to the 0,2 %-yield stress (*ref.* 19, table V, VI). In the same loading case different non-dimensional diagrams are found for different materials, depending upon the shape of the stress-strain curve of the material. However, for materials with affinely related σ—ε curves, the diagrams are identical if for all these materials k has the same value. As a rule, S can then for one of these materials only be chosen equal to the 0,2 %-yield stress.

For cases of combined loading the critical stress combinations are expressed in the collapsing stresses with a single type of loading by means of non-dimensional equations.

7.1 *Pure compression.*

For thin-walled cylinders (sec. 2.4.1) F_c is given by (2.5). For thick-walled tubes (sec. 2.3, 2.4.2, 2.5) F_c is the smallest of both values, following from figs. 2.2 and 2.4. Typical σ — ε curves for the materials are given in fig. 2.3; further material properties (E, k) in table 2.1.

[16]) It may be pointed out that the same tube can be either thin-walled or thick-walled, depending upon the type of loading.

7.2 *Pure bending.*

For thin-walled cylinders (sec. 3.1) F_b is given by (3.2) and for thick-walled tubes (sec. 3.2) by fig. 3.1.

7.3 *Pure torsion.*

Long and shorter tubes must be considered separately. Long tubes are defined as tubes, where $\frac{L^2t}{d^3}$ exceeds a certain limiting value; for these tubes F_T is not influenced by the distance L between the bulkheads. With the shorter tubes, where $\frac{L^2t}{d^3}$ is smaller than the limiting value mentioned above, F_T depends also upon L. The experimental evidence shows, that for tubes, whose edges are clamped at the bulkheads, the limiting value may be put equal to $\frac{L^2t}{d^3} = 9$; for tubes, whose edges are hinged at the bulkheads, the limiting value is chosen at $\frac{L^2t}{d^3} = 6{,}3$. The proposals for thick-walled tubes apply to the case, that $\frac{d}{t} < 200$ and $\gamma_T > 3$.

7.3.1 *Long tubes.*

For thin-walled cylinders F_T follows from the uninterrupted line, drawn in fig. 4.2, if the theoretical value $(F_T)_{th}$ is computed from (4.2), sec. 4.1. For thick-walled duralumin tubes F_T follows from the line drawn in fig. 4.3 and for steel tubes from lines 1 or 2 in fig. 4.5 if α_T is taken as abscissa. In the latter case linear interpolation is recommended if $0{,}75 < \frac{S_t}{F_t} < 0{,}85$.

7.3.2 *Shorter tubes.*

For thin-walled cylinders F_T follows from the uninterrupted line in fig. 4.2 if the theoretical value $(F_T)_{th}$ is computed from (4.6) (clamped edges) resp. (4.7) (hinged edges). For thick-walled tubes with clamped edges F_T follows from fig. 4.4 if the material is duralumin; for steel tubes from fig. 4.5 if 1,732 β_T is taken as abscissa. With hinged edges β_T in fig. 4.4 must be replaced with 0,915 β_T and in fig. 4.5, 1,584 β_T should be taken as abscissa ($\frac{L^2t}{d^3} < 6{,}3$).

7.4 *Pure shear.*

Both for thin-walled cylinders and for thick-walled tubes it is conservatively recommended to take $F_s = F_T$.

7.5 *Combined loading.*

The following proposals apply to tubes, which collaps under each of the component types of loading either by elastic or by plastic instability. For intermediate cases the proposals, made for the second class of tubes, will usually be sufficiently accurate. (c.f. sec. 6.5).

7.5.1 *Thin-walled cylinders.*

The critical stress combinations with a combination of compression, bending and torsion follow from (6.6); with a combination of bending and shear from (6.9) and with bending, shear and torsion they must satisfy both (6.11) and (6.12).

7.5.2 *Thick-walled tubes.*

The strength of a strut with bending load may be computed from (6.1) if F_c and F_{co} are taken from fig. 2.2. The critical stress combinations with compression (causing local instability, when acting alone), bending and torsion follow from (6.8) if F_c is taken from fig. 2.4; with bending and shear from (6.10) and with bending, shear and torsion they must satisfy both (6.11) and (6.13).

8 **Notations.**

d = $D - t$ mean diameter of the tube;

f_b maximum bending stress at critical combined loading;

f_c compression stress at critical combined loading;

f_T mean torsional shear stress at critical combined loading;

f_s maximum shear stress by transverse load at critical combined loading;

k constant, used to determine the yield stress (sec. 2.2, fig. 2.1);

l length of the tube;

t wall thickness of the tube;

A = $(1 - \nu^2) \frac{F_T}{E} \frac{L^2}{t^2}$;

D outer diameter of tube;

E YOUNG's modulus;

E_r reduced modulus in the plastic range, sec. 2.2;

F_b ultimate stress in pure bending;

F_c ultimate stress in pure compression;

F_{co} value of F_c when $\lambda = 0$ (see fig. 2.2);

F_s ultimate stress in pure shear;

F_t ultimate tensile stress;

$F_{t\ min}$ specified minimum ultimate tensile stress;

F_T ultimate mean shear stress in pure torsion, see eq. (4.10);

$(F_T)_{th}$ theoretical value of F_T in the case of *elastic instability;*

G modulus of rigidity;

$H = (1 - \nu^2)^{0,5} \frac{L^2}{td}$;

I_p polar moment of inertia of tube cross section;

L distance between frames;

M_T moment causing failure in pure torsion;

S_c yield stress from k-method (sec. 2.2) in compression, may as a rule be assumed equal to the 0,2 % stress (exception sec. 2.3);

S_t ditto in tension;

S_T ditto in torsion;

Y 0,2 % yield stress;

$Y_{t\ min}$ specified minimum 0,2 % stress in tension;

$\alpha_t = \frac{E}{S_t} \left(\frac{t}{d}\right)^{1,5}$;

$\beta_T = \frac{E}{S_t} \left(\frac{t}{d}\right)^{1,5} \left(\frac{d^3}{L^2 t}\right)^{0,25}$;

$\gamma_T = \frac{E}{S_t} \frac{d}{l}$;

γ angle of shear;

ε axial strain;

$\nu = 0.3$ POISSON's ratio;

σ normal stress;

τ shear stress.

9 References.

1. TIMOSHENKO, S. Theory of elastic stability. Mc.Graw-Hill, New York and London, 1936.
2. OSGOOD, W. R. Column strength of tubes elastically restrained against rotation at the ends. NACA-Report 615 (1938).
3. FLÜGGE, W. Die Stabilität der Kreiszylinderschale. Ingenieur-Archiv 1932, S. 463.
4. GECKELER, J. W. Plastisches Knicken der Wandung von Hohlzylindern und einige andere Faltungserscheinungen an Schalen und Blechen. Z.A.M.M. 1925, S. 341.
5. ROBERTSON, A. The strength of tubular struts. R. and M. 1185 (1927).
6. OSGOOD, W. R., *The crinkling strength and the bending* strength of round aircraft tubing. NACA-Report 632 (1938).
7. LUNDQUIST, E. E. Strength tests of thin-walled duralumin cylinders in compression. NACA-Report 473. (1933).
8. DONNELL, L. H. A new theory for the buckling of thin cylinders under axial compression and bending. Transactions of the A.S.M.E. Nov. 1934 p. 795.
9. BALLERSTEDT, W. und WAGNER, H. Versuche über die Festigkeit dünner unversteifter Zylinder unter Schub und Längskräften. Luftfahrtforschung XIII (1936), S. 309.
10. COX, H. L. Stress analysis of thin metal construction. J.R. Aer. Soc. 1940, p. 231.
11. General instability criteria for stiffened metal cylinders. Galcit Quarterly Report No. 1, November 1938.
12. VON KÁRMÁN, TH., DUNN, L. G. and HSUE SHEN TSIEN. The influence of curvature on the buckling characteristics of structures. J. Aer. Sc. Vol. 7 (1940), p. 276.
13. GREENE, T. W. Strength of steel tubing under combined column and transverse loading, including tests of columns and beams. Technologic papers of the Bureau of Standards No. 258 (1924).
14. BRAZIER, L. G. The flexure of thin cylindrical shells and other „thin" sections. R. and M. 1081 (1926).
15. CHWALLA, E. Reine Biegung schlanker, dünnwandiger Rohre mit gerader Achse. Z.A.M.M., Band 13 (1933). S. 48.
16. LUNDQUIST, E. E. Strength tests on thin-walled duralumin cylinders in pure bending. NACA Techn. Note 479 (1933).
17. HANSEN, K. E. Bending strength of thin-walled cylindrical tubes. Structural Research Lab. Roy. Techn. Coll. Rep. No. 9, Kopenhagen 1937, Lab for Bygningsstatik.
18. EBNER, H. *Zur Festigkeit von Schalen-* und Rohrholmflügeln, part IV. Luftfahrtforschung XIV (1937), p. 179.
19. STANG, A. H., RAMBERG, W. and BACK, G. Torsion tests of tubes. NACA-Report 601 (1937).
20. DONNELL, L. H. Stability of thin-walled tubes under torsion. NACA-Report 479 (1933).

21. LUNDQUIST, E. E. Strength tests on thin-walled duralumin cylinders in torsion. NACA-Techn. Note 427 (1932).

22. Investigation of the effect of the ratio of diameter to gage thickness upon the torsional strength of steel tubing. Air Service Information Circular No. 263 (1921).

23. OTEY, N. S. Torsional strength of nickel steel and duralumin tubing as affected by the ratio of diameter to gage thickness. NACA-Techn. Note 189 (1924).

24. MOORE, R. L. and PAUL, D. A. Torsional strength of aluminum alloy seamless tubing. NACA-Techn. Note 696 (1939).

25. FULLER, F. B. The torsional strength of solid and hollow cylindrical sections of heat-treated alloy steel. Journal of the Aeronautical Sciences Vol. 3 (1935—1936), p. 248.

26. Strength of aircraft elements. A.N.C.-5. Issued by the Army-Navy-Commerce Committee on aircraft requirements. Washington, January 1938.

27. TUCKERMAN, L. B., PETRENKO, S. H. and JOHNSON, C. D. Strength of tubing under combined axial and transverse loading. NACA-Techn.-Note 307 (1929).

28. YOUNGER, J. E. Structural design of metal airplanes. Mac.Graw-Hill, New York and London, 1935.

29. CASSENS, J. Knickbiegeversuche. Luftfahrtforschung XVII (1940), S. 306.

30. BRIDGET, F. J., JEROME, C. C. and VOSSELER, A. B. Some new experiments on buckling of thin wall construction. Transactions of the A.S.M.E. Nov. 1934, p. 569.

31. SHANLEY, F. R. and RYDER, E. I. Stress ratios. Aviation, June 1937, p. 28.

32. LUNDQUIST, E. E. Strength tests of thin-walled duralumin cylinders in combined transverse shear and bending. NACA-Techn. Note 523 (1935).

33. MOSMAN, R. W. and ROBINSON, R. G. Bending tests of metal monocoque fuselage construction. NACA-Techn. Note 357 (1930).

34. KOITER, W. T. On the stability of elastic equilibrium, Doctor Thesis, Delft; printed Paris, Amsterdam (1945). (Dutch with English summary).

Completed: Sept. 1946.

REPORT S. 319

The Elastic Stability of Flat Sandwich Plates [1)]

by

Dr. Ir. A. VAN WIJNGAARDEN

Summary.

The investigation is concerned with the elastic stability of flat sandwich plates, having an isotropic core, under a combination of compressive and shear loads. In contrast to earlier work (*refs. 1 and 2*), where the core was replaced by a simplified mechanical structure, the core is treated as a three-dimensional elastic body, thus leaving open the possibility of investigating cases of symmetrical buckling (not yet dealt with in this report). The conditions of stability of the faces, derived in chapter 2, contain boundary stresses which can be related to the properties of the core (chapter 3); the final equations of stability and their boundary conditions are given in chapter 4.

In principle, exact solutions for the case of antisymmetrical buckling, both without and with shear load (in the latter case only for infinitely long plates), are given (sections 5.1 and 6.1). The numerical solutions have been confined to infinitely long plates. For the numerical solution of the case of shear-free loading only minor simplifications are introduced (sections 5.2 and 6.5). For the cases of loading with shear, however, the numerical solutions have so far only been computed for a greatly simplified wave pattern (sections 6.2 to 6.4 incl.). Consequently, the results for the case of pure shear loading are not yet satisfactory (chapter 7). The numerical results of the calculations are presented in figs. 6.2 to 6.4 incl. and figs. 6.7 to 6.12 incl.; an example of their use is given in appendix 2.

Contents.

1 Introduction.

We shall develop a theory concerning the stability of a flat plate, loaded in its plane, that is built up according to the so-called sandwich principle, which means that the plate consists of two thin but stiff faces connected by a relatively thick but light and weak core. The faces, for instance, can be made from metal, plywood or plastic sheets. The core can be more or less continuous if it is made from balsa wood or an artificial spongy material, or it can be a structure itself, e.g. a corrugated sheet, a number of thin strips, a honeycomb structure, etc. The function of the core consists of keeping the faces at the proper distance and, moreover, to connect them in such a way that they behave more or less as

[1)] This investigation was carried out by order of the Nederlands Instituut voor Vliegtuigontwikkeling (Netherlands Aircraft Development Board).

if they were the extreme layers of a single thick plate. More especially in bending, the core must prevent the faces from bending separately, and it must be able to exert such shearing forces on the faces as to keep one sheet in compression and the other in tension. It is obvious that under this condition the stiffness of the plate is considerably higher than that of the two faces working separately. Accordingly, the stress at which buckling occurs if the plate is loaded in its own plane by compressive and shearing forces, is high as compared with that of the single faces, a most useful property for application to aircraft structures.

Several authors have already paid attention to the underlying problem. Mostly they confine themselves, however, to the buckling of struts instead of plates which are also supported at the lateral edges. The problem is then a two-dimensional stability problem and is already a rather complicated one; the work done on this problem at the N.L.L. is summarized in report S. 284 (*ref.* 1). The three-dimensional plate problem has also been dealt with by VAN DER NEUT in *ref.* 2. Although the equations were set up in a general form they were only solved for the case of shear-free loading. Moreover, to avoid the difficulties connected with the three-dimensional deformation of the core, the latter was replaced by a mechanical structure which is equivalent to a core with infinite stiffness in the direction normal to the surface of the plate. Although this assumption rather well accounts for the 'antisymmetric' type of buckling, i.e. a type of buckling in which the plate buckles as a whole in a series of waves with appreciably constant distance between the faces, it 'fails completely to describe the 'symmetric' type of buckling, which is a type of buckling in which the middle surface of the plate remains plane whereas the distance between the faces varies in a series of waves.

Early in 1946, an extension of the investigation reported in S. 286 to the case of a combination of normal and shear loads in the plane of the plate was started, retaining the basic assumption with regard to the core structure. In the course of the investigation it proved to be possible to develop a theory, in which the three-dimensional deformation of the core is exactly accounted for. This theory will be presented hereafter. For the sake of simplicity it has so far been restricted to the case of an isotropic core, but that of an aeolotropic core could be dealt with by means of the same methods as used here, without many fundamental changes, except a considerable increase in complexity.

2 The equilibrium of the faces.

2.1 *The stresses in the faces.* (fig. 2.1).

As to the deformation of the faces we shall make the two ordinary assumptions of the theory of bending of thin plates, viz. that points situated in the undistorted state on a straight line normal to the middle surface, lie in the distorted state

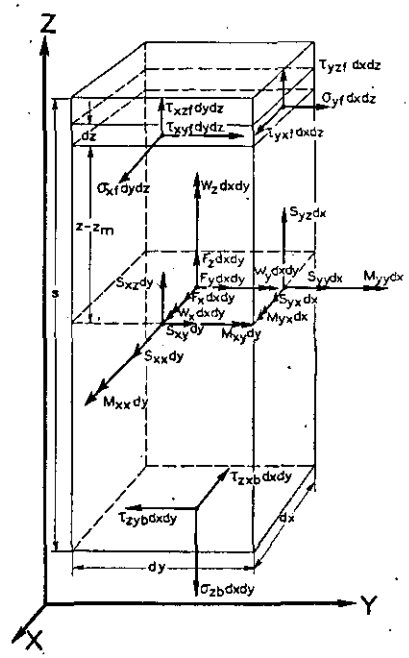

FIGURE 2.1.
Forces and stresses at an element of the face.

on a straight line normal to the deflected middle surface, and that the normal stresses on planes that are parallel to the middle surface are negligible.

The second assumption infers:

$$\sigma_{zf} = \frac{E_f}{1+\nu_f}\left(\frac{\partial w_f}{\partial z} + \frac{\nu_f}{1-2\,\nu_f}\,e_f\right) = 0. \quad (2.1)$$

From this it follows that

$$\frac{\partial w_f}{\partial z} = -\frac{\nu_f}{1-\nu_f}\left(\frac{\partial u_f}{\partial x} + \frac{\partial v_f}{\partial y}\right), \quad (2.2)$$

and, therefore,

$$e_f = \frac{1-2\,\nu_f}{1-\nu_f}\,.\,e'_f\,. \quad (2.3)$$

So, we find for the stresses normal to the Z-axis the expressions

$$\sigma_{xf} = \frac{E_f}{1-\nu^2_f}\left(\frac{\partial u_f}{\partial x} + \nu_f\,\frac{\partial v_f}{\partial y}\right), \quad (2.4)$$

$$\sigma_{yf} = \frac{E_f}{1-\nu^2_f}\left(\nu_f\,\frac{\partial u_f}{\partial x} + \frac{\partial v_f}{\partial y}\right), \quad (2.5)$$

$$\tau_{xyf} = \tfrac{1}{2} \frac{E_f}{1+\nu_f} \left(\frac{\delta u_f}{\delta y} + \frac{\delta v_f}{\delta x} \right) + \tau^*{}_f, \quad (2.6)$$

$$\tau_{yxf} = \tfrac{1}{2} \frac{E_f}{1+\nu_f} \left(\frac{\delta u_f}{\delta y} + \frac{\delta v_f}{\delta x} \right) - \tau^*{}_f. \quad (2.7)$$

Formulae (2.6) and (2.7) might cause some surprise as different values are given for τ_{xyf} and τ_{yxf}. They consist of a common part that is responsible for the shear deformation of the element $dxdy$, and of a second part $\pm \tau^*$ that causes no deformation but is not, like the first part, in equilibrium, and has to be opposed by a 'body couple', as will be introduced afterwards. As we shall introduce the resultant of these couples acting on a normal to the middle surface as a single twisting couple in the middle surface, it follows that τ^* is distributed symmetrically with respect to the middle surface and will, therefore, not result in couples around lines in the middle surface.

The shearing stresses τ_{xz} and τ_{yz} are not found in this way, but this does not matter as their resultant forces S_{xz} and S_{yz} can be eliminated afterwards.

From the first assumption, mentioned in the beginning of this section, we derive

$$u_f = u_m - (z_f - z_m) \frac{\delta w_m}{\delta x}, \quad (2.8)$$

$$v_f = v_m - (z_f - z_m) \frac{\delta w_m}{\delta y}. \quad (2.9)$$

By substituting this in eqs. (2.4) — (2.7) we obtain the stresses, expressed in the deformations of the middle surface:

$$\sigma_{xf} = \frac{E_f}{1-\nu_f^2} \left\{ \frac{\delta u_m}{\delta x} + \nu_f \frac{\delta v_m}{\delta y} - (z_f - z_m) \left(\frac{\delta^2 w_m}{\delta x^2} + \nu_f \frac{\delta^2 w_m}{\delta y^2} \right) \right\}, \quad (2.10)$$

$$\sigma_{yf} = \frac{E_f}{1-\nu_f^2} \left\{ \nu_f \frac{\delta u_m}{\delta x} + \frac{\delta v_m}{\delta y} - (z_f - z_m) \left(\nu_f \frac{\delta^2 w_m}{\delta x^2} + \frac{\delta^2 w_m}{\delta y^2} \right) \right\}, \quad (2.11)$$

$$\tau_{xyf} + \tau_{yxf} = \frac{E_f}{1+\nu_f} \left\{ \frac{\delta u_m}{\delta y} + \frac{\delta v_m}{\delta x} - 2 (z_f - z_m) \frac{\delta^2 w_m}{\delta x \, \delta y} \right\}. \quad (2.12)$$

By integrating these stresses over the thickness s of the faces, we find the resultant forces and couples (cf. fig. 2.1)

$$S_{xx} = \frac{12}{s^2} D \left(\frac{\delta u_m}{\delta x} + \nu_f \frac{\delta v_m}{\delta y} \right), \quad (2.13)$$

$$S_{yy} = \frac{12}{s^2} D \left(\nu_f \frac{\delta u_m}{\delta x} + \frac{\delta v_m}{\delta y} \right), \quad (2.14)$$

$$S_{xy} + S_{yx} = \frac{12}{s^2} D (1-\nu_f) \left(\frac{\delta u_m}{\delta y} + \frac{\delta v_m}{\delta x} \right), \quad (2.15)$$

$$M_{xx} = - M_{yy} = D (1-\nu_f) \frac{\delta^2 w_m}{\delta x \, \delta y}, \quad (2.16)$$

$$M_{xy} = - D \left(\frac{\delta^2 w_m}{\delta x^2} + \nu_f \frac{\delta^2 w_m}{\delta y^2} \right), \quad (2.17)$$

$$M_{yx} = D \left(\nu_f \frac{\delta^2 w_m}{\delta x^2} + \frac{\delta^2 w_m}{\delta y^2} \right). \quad (2.18)$$

2.2 *The external loads, due to buckling.*

As it was assumed that the loads in the faces act in the plane of the faces, they cannot exert bending or twisting couples if the faces remain plane. In general, the core will exert some forces on the faces even if they remain plane. If e.g. a compressive load is lead into the plate by compression of the faces, shear stresses at the boundary plane between the face and the core must act to transfer a small part of the compressive force into the core, as, of course, the strains of face and core must be equal. These shearing stresses, however, are small, and only restricted to the neighbourhood of the loaded edges, and finally, they act tangentially to the face, so that their influence can be neglected. Also, normal stresses at the boundary plane will arise if the distance between the faces is kept constant at the edges, as the core, being in longitudinal compression, is hampered in its lateral expansion. We shall also neglect this phenomenon, if need be by assuming that the distance between the faces is left free at the edges of the plate, but point out that under actual conditions it might give rise to bulging of the faces symmetrically with respect to the middle surface of the plate, so that under certain circumstances the symmetrical buckling of the plate might be favoured above the anti-symmetrical type of buckling.

According to this, the stresses σ_{zb}, τ_{zxb} and τ_{zyb} that the core exerts on the faces will only begin to act as soon as buckling occurs and are, therefore, of the first order of the buckling amplitude. The same holds for the bending and twisting moments that result from the loads in the plate. Those loads are not altered in the first instance but are no longer in equilibrium after buckling has occurred. The loads acting

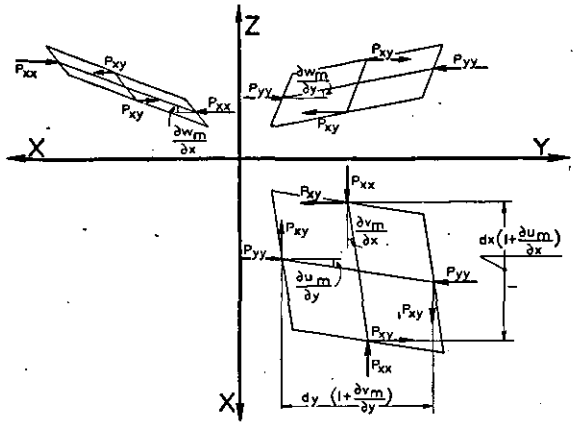

FIGURE 2.2.
The origin of the buckling moments.

on the element $dx\ dy$ when the plate buckles are denoted by P_{xx}, P_{xy} and P_{yy} (cf. fig. 2.2), which are for convenience taken positive as compressive forces or shearing forces of the opposite direction than usually. After buckling they give rise to body forces and couples in the middle surface as indicated in fig. 2.1. From fig. 2.2, where the middle surface element $dxdy$ is considered, the values of these forces and couples immediately follow:

$$F_x = F_y = F_z = 0, \tag{2.19}$$

$$W_x = P_{yy}\frac{\delta w_m}{\delta y} + P_{xy}\frac{\delta w_m}{\delta x}, \tag{2.20}$$

$$W_y = -P_{xx}\frac{\delta w_m}{\delta x} - P_{xy}\frac{\delta w_m}{\delta y}, \tag{2.21}$$

$$W_z = P_{xx}\frac{\delta v_m}{\delta x} - P_{yy}\frac{\delta u_m}{\delta y} - P_{xy}\left(\frac{\delta u_m}{\delta x} - \frac{\delta v_m}{\delta y}\right). \tag{2.22}$$

2.3 *Equations of equilibrium.*

By equating to zero the resultants of the forces and moments acting at the element of the face in fig. 2.1 in the three directions of the axes, we obtain the equations of equilibrium:

$$\frac{\delta S_{xx}}{\delta x} + \frac{\delta S_{yx}}{\delta y} + F_x - \tau_{zxb} = 0, \tag{2.23}$$

$$\frac{\delta S_{xy}}{\delta x} + \frac{\delta S_{yy}}{\delta y} + F_y - \tau_{zyb} = 0, \tag{2.24}$$

$$\frac{\delta S_{xz}}{\delta x} + \frac{\delta S_{yz}}{\delta y} + F_z - \sigma_{zb} = 0, \tag{2.25}$$

$$\frac{\delta M_{xx}}{\delta x} + \frac{\delta M_{yx}}{\delta y} + S_{yz} + W_x - \frac{s}{2}\tau_{zyb} = 0, \tag{2.26}$$

$$\frac{\delta M_{xy}}{\delta x} + \frac{\delta M_{yy}}{\delta y} - S_{xz} + W_y + \frac{s}{2}\tau_{zxb} = 0, \tag{2.27}$$

$$S_{xy} - S_{yx} + W_z = 0. \tag{2.28}$$

With the aid of eqs. (2.13) — (2.22) and (2.26) — (2.28) we can calculate the boundary stresses from eqs. (2.23) — (2.25).

$$\frac{s^2}{6D}\tau_{zxb} = 2\frac{\delta^2 u_m}{\delta x^2} + p_{xy}\frac{\delta^2 u_m}{\delta x \delta y} + (1 - \nu_f - p_{yy})\frac{\delta^2 u_m}{\delta y^2} + (1 + \nu_f + p_{xx})\frac{\delta^2 v_m}{\delta x \delta y} - p_{xy}\frac{\delta^2 v_m}{\delta y^2}, \tag{2.29}$$

$$\frac{s^2}{6D}\tau_{zyb} = -p_{xy}\frac{\delta^2 u_m}{\delta x^2} + (1 + \nu_f + p_{yy})\frac{\delta^2 u_m}{\delta x \delta y} + (1 - \nu_f - p_{xx})\frac{\delta^2 v_m}{\delta x^2} + p_{xy}\frac{\delta^2 v_m}{\delta x \delta y} + 2\frac{\delta^2 v_m}{\delta y^2}, \tag{2.30}$$

$$\frac{s^2}{12D}\left\{\sigma_{zb} - \frac{s}{2}\left(\frac{\delta \tau_{zxb}}{\delta x} + \frac{\delta \tau_{zyb}}{\delta y}\right)\right\} = -\frac{s^2}{12}\Delta'\Delta' w_m - p_{xx}\frac{\delta^2 w_m}{\delta x^2} - 2p_{xy}\frac{\delta^2 w_m}{\delta x \delta y} - p_{yy}\frac{\delta^2 w_m}{\delta y^2}. \tag{2.31}$$

In the important case of constant p_{xx}, p_{xy} and p_{yy} we can simplify these expressions by passing from the horizontal displacements u_m and v_m to the equivalent dilatation $e'_m = \frac{\delta u_m}{\delta x} + \frac{\delta v_m}{\delta y}$ and the (minus double) rotation $f'_m = \frac{\delta u_m}{\delta y} - \frac{\delta v_m}{\delta x}$ of the middle surface. Actually we find:

$$\frac{s^2}{6D}\left(\frac{\delta \tau_{zxb}}{\delta y} - \frac{\delta \tau_{zyb}}{\delta x}\right) = \left\{p_{xy}\frac{\delta^2}{\delta x^2} + (p_{xx} - p_{yy})\frac{\delta^2}{\delta x \delta y} - p_{xy}\frac{\delta^2}{\delta y^2}\right\} e'_m + \left\{(1 - \nu_f - p_{xx})\frac{\delta^2}{\delta x^2} + 2p_{xy}\frac{\delta^2}{\delta x \delta y} +\right.$$

$$+ (1 - \nu_f - p_{yy}) \frac{\delta^2}{\delta y^2} \Big\} f'_m , \qquad (2.32)$$

$$\frac{s^2}{6D} \left(\frac{\delta \tau_{zxb}}{\delta x} + \frac{\delta \tau_{zyb}}{\delta y} \right) = 2 \Delta' e'_m , \qquad (2.33)$$

$$\frac{s^2}{12D} \left\{ \sigma_{zb} - \frac{s}{2} \left(\frac{\delta \tau_{zxb}}{\delta x} + \frac{\delta \tau_{zyb}}{\delta y} \right) \right\} =$$

$$= - \left(\frac{s^2}{12} \Delta' \Delta' + p_{xx} \frac{\delta^2}{\delta x^2} + \right.$$

$$\left. + 2 p_{xy} \frac{\delta^2}{\delta x \delta y} + p_{yy} \frac{\delta^2}{\delta y^2} \right) w_m . \qquad (2.34)$$

As the stresses exerted by the core depend rather on the displacements of the boundary plane than on those of the middle surface of the faces, we shall replace e'_m, f'_m and w_m by the corresponding quantities of the boundary plane e'_b, f'_b and w_b. By means of (2.2), (2.8) and (2.9) we find, keeping in mind that for the boundary plane $z_b - z_m = -\frac{s}{2}$:

$$u_b = u_m + \frac{s}{2} \frac{\delta w_m}{\delta x} , \qquad (2.35)$$

$$v_b = v_m + \frac{s}{2} \frac{\delta w_m}{\delta y} , \qquad (2.36)$$

$$w_b = w_m - \int_{z_b}^{z_m} \frac{\delta w_f}{\delta z} \, dz = w_m +$$

$$+ \frac{\nu_f}{1 - \nu_f} \left(\frac{s}{2} e'_m + \frac{s^2}{8} \Delta' w_m \right) , \qquad (2.37)$$

and hence

$$e'_b = e'_m + \frac{s}{2} \Delta' w_m , \qquad (2.38)$$

$$f'_b = f'_m . \qquad (2.39)$$

As both w_m and $\Delta' w_m$ appear in these relations, the introduction of the quantities e'_b, f'_b and w_b instead of e'_m, f'_m and w_m requires also some differential operations. The result is:

$$\frac{s^2}{12D} \left[2 \Delta' \left(\frac{\delta \tau_{zxb}}{\delta y} - \frac{\delta \tau_{zyb}}{\delta x} \right) - \right.$$

$$- \left\{ p_{xy} \frac{\delta^2}{\delta x^2} + (p_{xx} - p_{yy}) \frac{\delta^2}{\delta x \delta y} - \right.$$

$$\left. \left. - p_{xy} \frac{\delta^2}{\delta y^2} \right\} \left(\frac{\delta \tau_{zxb}}{\delta x} + \frac{\delta \tau_{zyb}}{\delta y} \right) \right] =$$

$$= \left\{ (1 - \nu_f - p_{xx}) \frac{\delta^2}{\delta x^2} + 2 p_{xy} \frac{\delta^2}{\delta x \delta y} + \right.$$

$$\left. + (1 - \nu_f - p_{yy}) \frac{\delta^2}{\delta y^2} \right\} \Delta' f'_b , \qquad (2.40)$$

$$\frac{s^2}{12D} \left(1 - \frac{\nu_f}{1 - \nu_f} \cdot \frac{s^2}{8} \Delta' \right) \left(\frac{\delta \tau_{zxb}}{\delta x} + \frac{\delta \tau_{zyb}}{\delta y} \right) =$$

$$= \left(1 + \frac{\nu_f}{1 - \nu_f} \cdot \frac{s^2}{8} \Delta' \right) \Delta' e'_b -$$

$$- \frac{s}{2} \Delta' \Delta' w_b , \qquad (2.41)$$

$$\frac{s^2}{12D} \left(1 - \frac{\nu_f}{1 - \nu_f} \cdot \frac{s^2}{8} \Delta' \right) \left\{ \sigma_z - \frac{s}{2} \left(\frac{\delta \tau_{zxb}}{\delta x} + \right. \right.$$

$$\left. \left. + \frac{\delta \tau_{zyb}}{\delta y} \right) \right\} = - \left(\frac{s^2}{12} \Delta' \Delta' + p_{xx} \frac{\delta^2}{\delta x^2} + \right.$$

$$+ 2 p_{xy} \frac{\delta^2}{\delta x \delta y} + p_{yy} \frac{\delta^2}{\delta y^2} \Big) \left(w_b - \right.$$

$$\left. - \frac{\nu_f}{1 - \nu_f} \cdot \frac{s}{2} \cdot e'_b \right) . \qquad (2.42)$$

These three equations represent the conditions under which the face is in equilibrium in a buckled state. It remains to express the stresses that the core exerts on the face in terms of the displacements of the boundary surface.

3 The elastic reactions of the core.

3.1 *The stresses at the boundary surface.*

We assume that the core is rigidly connected to the faces. Then the displacements of the face at the boundary surface will be the same as those of the core at that surface. As the core material is assumed to be isotropic we can express the stresses in terms of the displacements as follows:

$$\frac{s^2}{12D} \cdot \tau_{zx} = \frac{\varepsilon^*}{2s} \left(\frac{\delta u}{\delta z} + \frac{\delta w}{\delta x} \right) , \qquad (3.1)$$

$$\frac{s^2}{12D} \cdot \tau_{zy} = \frac{\varepsilon^*}{2s} \left(\frac{\delta v}{\delta z} + \frac{\delta w}{\delta y} \right) , \qquad (3.2)$$

$$\frac{s^2}{12D} \cdot \sigma_z = \frac{\varepsilon^*}{s} \left(\frac{\nu}{1 - 2\nu} e' + \right.$$

$$\left. + \frac{1 - \nu}{1 - 2\nu} \frac{\delta w}{\delta z} \right) . \qquad (3.3)$$

From this it follows that

$$\frac{s^2}{12D} \left(\frac{\delta \tau_{zx}}{\delta x} + \frac{\delta \tau_{zy}}{\delta y} \right) = \frac{\varepsilon^*}{2s} \left(\frac{\delta e'}{\delta z} + \Delta' w \right) , \qquad (3.4)$$

$$\frac{s^2}{12D} \left(\frac{\delta \tau_{zx}}{\delta y} - \frac{\delta \tau_{zy}}{\delta x} \right) = \frac{\varepsilon^*}{2s} \cdot \frac{\delta f'}{\delta z} . \qquad (3.5)$$

3.2 *The equilibrium of the core.*

The terms in eqs. (3.3), (3.4) and (3.5) that involve differentiations with respect to z are brought into relation with the other ones by the equations of equilibrium. These conditions of

equilibrium, expressed in terms of the displacements, are as follows

$$(1-2\nu)\,\Delta u + \frac{\delta e}{\delta x} = 0\,, \tag{3.6}$$

$$(1-2\nu)\,\Delta v + \frac{\delta e}{\delta y} = 0\,, \tag{3.7}$$

$$(1-2\nu)\,\Delta w + \frac{\delta e}{\delta z} = 0\,. \tag{3.8}$$

By differentiating (3.6) with respect to x, (3.7) with respect to y, (3.8) with respect to z, and adding, it appears that e is harmonic, $\Delta e = 0$, or

$$\Delta e' + \frac{\delta}{\delta z}\,\Delta w = 0\,. \tag{3.9}$$

Furthermore, (3.8) may be written as follows

$$(1-2\nu)\,\Delta w + \frac{\delta^2 w}{\delta z^2} + \frac{\delta e'}{\delta z} = 0\,. \tag{3.10}$$

Equations (3.9) and (3.10) can be used to eliminate e'_b from the equations (2.41) and (2.42). Therefore we rewrite (3.10) as

$$\frac{\delta e'}{\delta z} = -(1-2\nu)\,\Delta w - \frac{\delta^2 w}{\delta z^2}\,. \tag{3.11}$$

From this it follows that

$$\frac{\delta^2 e'}{\delta z^2} = -(1-2\nu)\,.\,\frac{\delta}{\delta z}\,\Delta w - \frac{\delta^3 w}{\delta z^3} \tag{3.12}$$

and again from (3.9)

$$\Delta' e' = \Delta e' - \frac{\delta^2 e'}{\delta z^2} = \frac{\delta^3 w}{\delta z^3} - 2\nu\,\frac{\delta}{\delta z}\,\Delta w\,. \tag{3.13}$$

The term e' itself may be written according to (3.11) as

$$e' = \left(e' + \frac{\delta w}{\delta z}\right)_{z=z_0} - \frac{\delta w}{\delta z} - (1-2\nu)\int_{z_0}^{z} \Delta w.dz, \tag{3.14}$$

where z_0 is some value of z for which e' should be known.

By differentiating (3.6) with respect to y and (3.7) with respect to x and subtracting we find

$$\Delta f' = 0\,. \tag{3.15}$$

By the fact that e is harmonic it follows from (3.8) that w is biharmonic:

$$\Delta\Delta w = 0\,. \tag{3.16}$$

4 The equations of stability.

4.1 *The equations of stability when the faces do not remain plane.*

If we insert in (2.41) and (2.42) the expressions (3.3) and (3.4) for the boundary stresses and, moreover, eliminate the terms involving e'_b by means of (3.11), (3.13) and (3.14) we obtain the following two equations of stability:

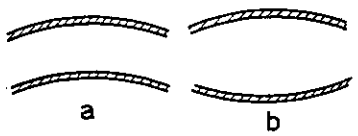

FIGURE 4.1.
Antisymmetric (a) and symmetric (b) type of buckling.

$$\frac{\varepsilon^*}{s}\left(1 - \frac{\nu_f}{1-\nu_f}\,.\,\frac{s^2}{8}\,\Delta'\right)\left(\nu\Delta w - \frac{\delta^2 w}{\delta z^2}\right) = -\left(1 + \frac{\nu_f}{1-\nu_f}\,\frac{s^2}{8}\,\Delta'\right)\frac{\delta}{\delta z}\left(2\nu\Delta w - \frac{\delta^2 w}{\delta z^2}\right) - \frac{s}{2}\,\Delta'\Delta' w\;;\; z = z_b\,, \tag{4.1}$$

$$\frac{\varepsilon^*}{s}\left(1 - \frac{\nu_f}{1-\nu_f}\,.\,\frac{s^2}{8}\,\Delta'\right)\left\{\nu\int_{z_0}^{z}\Delta w.dz - \frac{\delta w}{\delta z} - \frac{\nu}{1-2\nu}\left(e' + \frac{\delta w}{\delta z}\right)_{z=z_0} + \frac{s}{2}\left(\nu\Delta w - \frac{\delta^2 w}{\delta z^2}\right)\right\} = \left(\frac{s^2}{12}\,\Delta'\Delta' + p_{xx}\,\frac{\delta^2}{\delta x^2} + 2\,p_{xy}\,\frac{\delta^2}{\delta x\,\delta y} + p_{yy}\,\frac{\delta^2}{\delta y^2}\right)\left[w + \frac{\nu_f}{1-\nu_f}\,.\,\frac{s}{2}\left\{(1-2\nu)\int_{z_0}^{z}\Delta w.dz + \frac{\delta w}{\delta z} - \left(e' + \frac{\delta w}{\delta z}\right)_{z=z_0}\right\}\right]\;;\; z = z_b\,. \tag{4.2}$$

The displacement w that appears in both equations has to fulfil the condition (3.16), and, moreover, some boundary conditions to be specified later on. These boundary conditions will be such that they are certainly satisfied by $w \equiv 0$. As (3.16), (4.1) and (4.2) are also satisfied then (if, at least, $e'_{z=z_0}$ vanishes) $w \equiv 0$ is always a solution. Other solutions are only possible if p_{xx}, p_{xy} and p_{yy}, appearing in (4.2), have

certain values that are, of course, just the values we are looking for. For all solutions $w \neq 0$ we find the buckling forces from the above-mentioned equations, where no use is made of the first of the three equations of equilibrium, viz. eq. (2.40). The reason why this equation can be suppressed will be explained in the next section.

4.2 *The equation of stability when the faces remain plane.*

We now turn to equation (2.40). Again, we eliminate the boundary stresses, by means of eqs. (3.4) and (3.5), and, moreover, e' by means of (3.11). Then we obtain

$$\frac{\varepsilon^*}{s}\left[\Delta' \frac{\delta f'}{\delta z} - \left\{p_{xy}\frac{\delta^2}{\delta x^2} + (p_{xx}-p_{yy})\frac{\delta^2}{\delta x \delta y} - p_{xy}\frac{\delta^2}{\delta y^2}\right\}\left(\nu\Delta w - \frac{\delta^2 w}{\delta z^2}\right)\right] = \left\{(1-\nu_f-p_{xx})\frac{\delta^2}{\delta x^2} + 2\,p_{xy}\frac{\delta^2}{\delta x \delta y} + (1-\nu_f-p_{yy})\frac{\delta^2}{\delta y^2}\right\}\Delta' f';\ z=z_b\ . \qquad (4.3)$$

If buckling occurs with $w \neq 0$, then equation (4.3) only supplies the corresponding f'_b, and is therefore not very interesting. It might, however, have importance, in the case of $w \equiv 0$, in so far as another type of buckling might be revealed, where the faces remain plane but rotations in that plane occur. In that case (4.3) apparently reduces to

$$\left\{(1-\nu_f-p_{xx})\frac{\delta^2}{\delta x^2} + 2\,p_{xy}\frac{\delta^2}{\delta x \delta y} + (1-\nu_f-p_{yy})\frac{\delta^2}{\delta y^2}\right\}\Delta' f'_b - \frac{\varepsilon^*}{s}\frac{\delta f'_b}{\delta z} = 0\ . \qquad (4.4)$$

We can easily verify that non-vanishing solutions of this equation can only occur if at least one of the quantities p_{xx}, p_{xy}, p_{yy} is of the order unity. This means stresses of the order of YOUNG's modulus, and is therefore completely beyond the scope of our theory. It is, therefore, no use to pay any attention at all to equation (4.3), and we can restrict ourselves to the equations (4.1) and (4.2).

4.3 *The boundary conditions.*

The problems that are, from a technical point of view, by far the most important ones, are those in relation to rectangular panels. The edges of the panels, that can be chosen parallel to the X- and Y-axes respectively, are, in general, elastically supported, which means that the supports undergo linear and angular deflections and exert restoring forces and moments on the plate. From a theoretical point of view, some limiting cases are important, for instance that of the simply supported plate, and that of the clamped one. In both cases we have the boundary condition

$$w = 0 \text{ along all edges.} \qquad (4.5)$$

In the case of the simply supported plate, the supports are supposed to be unable to exert any bending moments along the edges. In view of (2.17), (2.18) and (4.5) this requires:

$$\frac{\delta^2 w}{\delta x^2} = 0 \text{ along the edges parallel to the Y-axis,} \qquad (4.6)$$

$$\frac{\delta^2 w}{\delta y^2} = 0 \text{ along the edges parallel to the X-axis.} \qquad (4.7)$$

As to the core, it might be interesting, from a geophysical point of view, to consider the semi-infinite core. For our investigation of the sandwich construction, we shall restrict ourselves to the core of finite thickness c with two equal faces at both sides with thickness s.

Two typical forms of buckling are that of antisymmetric buckling, where both faces buckle in the same direction, and that of symmetric buckling, where the faces buckle in opposite directions (cf. fig. 4.1). It is convenient to take the middle surface of the core as the X-Y plane. Then, in the case of antisymmetric buckling, w is an even function of z, whereas in the case of symmetric buckling w is an odd function of z.

5 Antisymmetric buckling of a simply supported panel, compressed in two perpendicular directions.

5.1 *The complete expression for the buckling stress.*

We consider a panel, having a length a in the X-direction and a width b in the Y-direction (cf. fig. 5.1). We introduce nondimensional

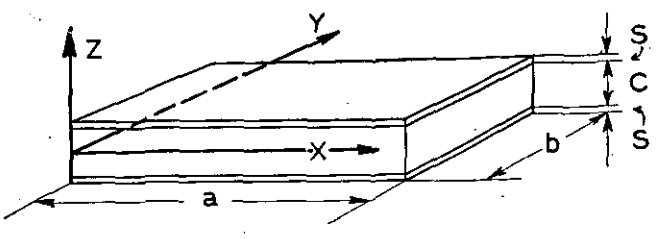

FIGURE 5.1.
The rectangular panel under consideration.

coordinates by putting $\xi = \alpha \frac{x}{c}$; $\eta = \beta \frac{y}{c}$; $\zeta = 2\gamma \frac{z}{c}$, where $\alpha = m \cdot \pi \frac{c}{a}$ and $\beta = n \cdot \pi \frac{c}{b}$ (m and n integer) and $4\gamma^2 = \alpha^2 + \beta^2$. For the boundary plane between core and face $\zeta_b = \gamma$.

The displacement w must satisfy (3.16), (4.6) and (4.7) (simply supported panel) and must be an even function of z (antisymmetric buckling). These requirements can be satisfied by taking:

$$w = (w^* \cosh \zeta + w^{**} \zeta \sinh \zeta) \sin \xi \sin \eta \quad (5.1)$$

Before substituting this in eqs. (4.1) and (4.2) we must consider the term $\left(e' + \frac{\delta w}{\delta z}\right)_{z=z_0}$ in (4.2). Conveniently we take $z_0 = 0$ so that the treatment of both faces becomes identical. For $z_0 = 0$ evidently $\frac{\delta w}{\delta z} = 0$. At first sight also the term e' appears to vanish, because the antisymmetrical character of the buckling infers that u and v, and therefore e' are odd functions of z. But this is only true if we neglect the fact that, due to the compressive stresses in the core, a pattern of constant compressive strain is to be superimposed over this odd pattern. Therefore, e' does not vanish at $z = 0$, but has a constant value there (that means, independent of x and y), which can easily be expressed in p_{xx} and p_{yy}. However, we can add to w as defined by (5.1) a third term $w^{***}\zeta$ which corresponds to a uniform thickening of the panel. This term gives only a contribution to the left hand side of (4.2), and by choosing the correct value of w^{***}, it just cancels the term with e' there. At the right hand side the presence of e' is of no consequence because of the differential operator that is in front of the square brackets. Therefore the whole question of e' can be left out and then we can use equation (5.1) for w.

If we substitute (5.1) in (4.1) and (4.2) we get two homogeneous linear equations in the two unknowns w* and w^{**}. Introducing

$$\varepsilon = \frac{E}{E_f} \cdot \frac{1-\nu_f^2}{1+\nu} \cdot \frac{c}{2s}; \quad \bar{\varepsilon} = \varepsilon \left(1 + \frac{\nu_f}{1-\nu_f} \cdot \frac{\delta^2\gamma^2}{2}\right); \quad \omega = 1 - \frac{\nu_f}{1-\nu_f} \cdot \frac{\delta^2\gamma^2}{2}$$

we have: $w^* \left[\bar{\varepsilon} + \omega\gamma \tanh \gamma - \delta\gamma^2\right] + w^{**} \left[\bar{\varepsilon}(2 - 2\nu + \gamma \tanh \gamma) + \omega\left\{(3-4\nu)\gamma \tanh \gamma + \gamma^2\right\} - \delta\gamma^3 \tanh \gamma\right] = 0$, (5.2)

$$w^* \left[4\bar{\varepsilon}\gamma(\tanh \gamma + \delta\gamma) + \left(\frac{4}{3}\delta^2\gamma^4 - p_{xx}\alpha^2 - p_{yy}\beta^2\right)\left(1 + \frac{\nu_f}{1-\nu_f}\delta\gamma \tanh \gamma\right)\right] + w^{**}\left[4\bar{\varepsilon}\gamma\left\{(1-2\nu)\tanh \gamma + \gamma + \delta\gamma(2-2\nu+\gamma \tanh \gamma)\right\} + \gamma\left(\frac{4}{3}\delta^2\gamma^4 - p_{xx}\alpha^2 - p_{yy}\beta^2\right)\left\{\tanh \gamma + \frac{\nu_f}{1-\nu_f}\delta\left[(3-4\nu)\tanh \gamma + \gamma\right]\right\}\right] = 0. \quad (5.3)$$

These equations yield only non-vanishing values for w^* and w^{**} if the determinant vanishes. We introduce the function χ

$$2(1-\nu)\chi = (1-2\nu)\tanh \gamma + \gamma - \gamma \tanh^2 \gamma \quad (5.4)$$

and the function P

$$P = \gamma \frac{\bar{\varepsilon}(\tanh \gamma - \chi) + \omega\gamma(\tanh^2 \gamma + \delta\gamma\chi) + \frac{\delta\gamma^2(\delta\gamma + \chi)}{\bar{\varepsilon}\left(1 - \frac{\nu_f}{1-\nu_f}\delta\gamma\chi\right) + \omega\gamma(\tanh \gamma + \chi) + \frac{\nu_f}{1-\nu_f}\delta^2\gamma^3(\tanh \gamma + \chi)}}. \quad (5.5)$$

Then we find by evaluating the determinant, the value of the buckling stress p, where $p_{xx} = \pi_{xx} \cdot p$ and $p_{yy} = \pi_{yy} p$:

$$p = \frac{4}{\pi_{xx}\alpha^2 + \pi_{yy}\beta^2}\left\{\frac{1}{3}\delta^2\gamma^4 + \bar{\varepsilon} P\right\}. \quad (5.6)$$

5.2 *Approximate expressions for the buckling stress.*

The function P that appears in eq. (5.6) is, according to (5.4) and (5.5), a rather complicated one. Fortunately, γ, δ and $\bar{\varepsilon}$ are all small quantities. Of these three δ is the most simple one. To have an idea, for the moment, of the order of magnitude it may be assumed to be something like 0,05. The quantity $\bar{\varepsilon}$ can vary considerably, but a reasonable value is 0,01. For γ it is very difficult to state beforehand a certain value, as here the wave length of the buckles comes in. For the moment, we shall simply assume that γ is small and afterwards we shall prove that γ is small indeed. Replacing $\tanh \gamma$ by $\gamma - \frac{1}{3}\gamma^3$

in (5.4) and (5.5) and neglecting terms of higher order we find the following approximate expression for P:

$$P = \gamma^4 \cdot \frac{(1+\delta)^2 - \frac{2}{3}\gamma^2 + \frac{\varepsilon}{3(1-\nu)}}{\varepsilon + 2\gamma^2} . \qquad (5.7)$$

The value of the critical stress is therefore

$$p = \frac{4\gamma^4}{\pi_{xx}\alpha^2 + \pi_{yy}\beta^2} \left\{ \frac{\delta^2}{3} + \right.$$
$$\left. + \varepsilon \frac{(1+\delta)^2 - \frac{2}{3}\gamma^2 + \frac{\varepsilon}{3(1-\nu)}}{\varepsilon + 2\gamma^2} \right\} . \qquad (5.8)$$

To find the minimum value of p we must determine the value γ^* of γ for which $\frac{dp}{d\gamma} = 0$. As, of course, the value of p in the neighbourhood of the minimum does not vary appreciably with γ, we can, at least for the determination of γ^*, neglect the small terms δ, γ^2 and ε against 1. The value of γ^*, which is found in this way, is generally not such that the number of half waves is integer over the length and width of the plate, but in a given case, we must take the nearest integer numbers of half waves and take that for which the critical stress is the lowest. For a panel with infinite length a, our value of γ^* is directly the correct one.

A difficulty is still that both α and β play a role in (5.8). To keep the results surveyable, we shall first confine ourselves to the case of a panel only compressed in the X-direction. Then $\pi_{yy} = 0$ and without loss of generality we can take $\pi_{xx} = 1$. The lowest critical stress is then obtained with one half wave in the Y-direction, and β is therefore known beforehand, viz. $\beta = \pi \frac{c}{b}$.

Carrying out the differentiation, we obtain the condition:

$$8\delta^2 \left(\frac{\gamma^*}{\beta}\right)^6 + 4\delta^2 \left\{ 2\frac{\varepsilon}{\beta^2} - 1 \right\} \left(\frac{\gamma^*}{\beta}\right)^4 +$$
$$+ 3\frac{\varepsilon}{\beta^2} \left(2\frac{\varepsilon}{\beta^2} - 1\right) \left(\frac{\gamma^*}{\beta}\right)^2 -$$
$$- 3\left(\frac{\varepsilon}{\beta^2}\right)^2 = 0 . \qquad (5.9)$$

If $\frac{\varepsilon}{\beta^2} \gg 1$, the first two terms are of no importance and we find immediately $\frac{\gamma^*}{\beta} = \frac{1}{\sqrt{2}}$, that means $\alpha = \beta$. This result can easily be understood. For if ε is high enough, that means the core is stiff enough, then the panel buckles as a whole (without appreciable shear deformation of the core), and it is a well-known result of the theory of the buckling of plates that the square wave requires the lowest buckling stress.

If $\frac{\varepsilon}{\beta^2}$ is not so large but still preponderating over 1 the first two terms of (5.9) are still of minor importance, and we see that $\frac{\gamma^*}{\beta} = \sqrt{\frac{\varepsilon/\beta^2}{2\,\varepsilon/\beta^2 - 1}} > \frac{1}{\sqrt{2}}$. Apparently γ increases with decreasing ε, which means that the wave length in the X-direction decreases. The core begins to act as an elastic support of the faces. This phenomenon becomes still more important with still smaller ε. If $\frac{\varepsilon}{\beta^2}$ decreases toward $\frac{1}{2}$ the relative importance of the first term increases sharply and if $\frac{\varepsilon}{\beta^2} = \frac{1}{2}$ only the first and the last terms are present. Then $\frac{\gamma^*}{\beta} = \sqrt[6]{\frac{3}{32\,\delta^2}}$. For $\frac{b}{c} = \frac{c}{s} = 20$ we find $\gamma^* = 0{,}288$, which is still small. If ε decreases still further the core begins to lose its grip on the faces, and the wave length in the X-direction reaches a minimum, and accordingly γ^* a maximum. This maximum value γ^{**} is found easily enough by considering (5.9) as a quadratic equation in the unknown $\frac{\varepsilon}{\beta^2}$. From this, $\frac{\varepsilon}{\beta^2}$ can be calculated for given δ and $\frac{\gamma^*}{\beta}$, if, of course, γ^* does not exceed γ^{**}. Therefore, by equating to zero the discriminant of (5.9) in its new form, we can calculate γ^{**}, which appears to be $\frac{\gamma^{**}}{\beta} = \sqrt{\frac{\sqrt{3}}{8\,\delta} + \frac{3}{8}}$. The maximum of γ^* appears at $\frac{\varepsilon}{\beta^2} \sim \frac{1}{4}$. For the same values of β and δ as used before, we find $\gamma^{**} = 0{,}340$.

If ε decreases still further the faces begin more and more to buckle each for themselves, and in the limiting case of vanishing ε, we see from equation (5.9) that again $\frac{\gamma^*}{\beta} = \frac{1}{\sqrt{2}}$, which is obvious, as now again the theory of the simple plate holds.

We see that γ is actually small throughout the whole range of possible ε; and the simplication of (5.5) to (5.7) is quite satisfactory.

If some compression in the Y-direction is also present ($\pi_{yy} > 0$), things are even better. For, if only one half wave in the Y-direction appears, we have only to replace β from the foregoing analysis by $\beta \sqrt{1 - \frac{\pi_{yy}}{\pi_{xx}}}$. So all the critical values of γ decrease with increasing π_{yy}.

Finally, comparing eq. (5.8) with the result obtained by VAN DER NEUT in *ref.* 2, eq. (27), it appears that the latter equation differs from (5.8) in that the numerator of the last fraction is $(1+\delta)^2 + \varepsilon\,(1+\delta)^3\,/3\,(1-\nu)$ and the denominator is $\varepsilon + 2\gamma^2\,(1+\delta)$.

Observing that δ and γ^2 are of the same order of magnitude, we find that the differences between the results obtained from the two equations will also be of the order δ. We may conclude that the mechanical structure of the core, assumed in *ref.* 2, is indeed quite satisfactory for calculating antisymmetrical buckling loads. The stiffness of the core in a direction normal to the surface of the plate will not influence these loads to any appreciable extent.

6 Antisymmetric buckling of a simply supported, infinitely long panel, compressed in two perpendicular directions and loaded, moreover, by shearing forces.

6.1 *The rigorous treatment.*

We shall now introduce also the external shearing load π_{xy}. To prevent, however, great difficulties we shall only consider the case of an infinitely long panel ($a = \infty$). We choose the X-axis, this time, halfway between the two infinitely long edges.

A solution of (3.16) that is suited for our purpose is:

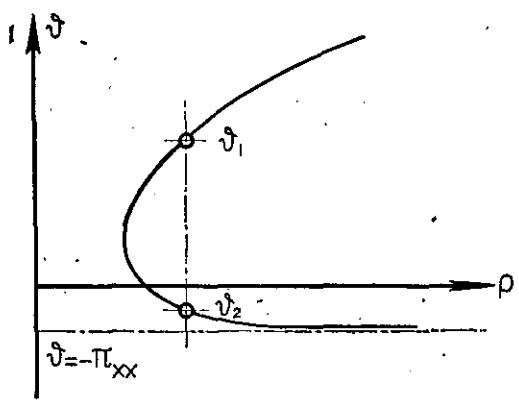

FIGURE 6.1.
The $\rho - \vartheta$ *curve, if* $\pi_{yy} = 0$.

$$w = \sum_{j=1}^{4} (w^*_j \cosh \zeta_j + w^{**}_j \zeta_j \sinh \zeta_j) \cos(\xi + \eta_j) , \quad (6.1)$$

where again $\xi = \alpha \frac{x}{c}$; $\eta_j = \beta_j \frac{y}{c}$ and $\zeta_j = 2\,\gamma_j \frac{z}{c}$, whereas $4\,\gamma^2_j = \alpha^2 + \beta^2_j$. For the middle surface of the plate, therefore,

$$w_0 = \sum_{j=1}^{4} w^*_j \cos(\xi + \eta_j) . \quad (6.2)$$

For this middle surface we can satisfy the boundary conditions (4.5) and (4.7) for $y = \pm \frac{b}{2}$. After substituting (6.2) in (4.5) and (4.7) we find the following set of conditions ($\lambda = \frac{c}{b}$):

$$\sum_{j=1}^{4} w^*_j \cos \frac{\beta_j}{2\lambda} = 0 , \quad (6.3)$$

$$\sum_{j=1}^{4} w^*_j \sin \frac{\beta_j}{2\lambda} = 0 , \quad (6.4)$$

$$\sum_{j=1}^{4} w^*_j \beta^2_j \cos \frac{\beta_j}{2\lambda} = 0 , \quad (6.5)$$

$$\sum_{j=1}^{4} w^*_j \beta^2_j \sin \frac{\beta_j}{2\lambda} = 0 . \quad (6.6)$$

Obviously, non-vanishing values of w^* can only satisfy these four equations, if their determinant vanishes. Therefore

$$\begin{vmatrix} \cos\frac{\beta_1}{2\lambda} & \cos\frac{\beta_2}{2\lambda} & \cos\frac{\beta_3}{2\lambda} & \cos\frac{\beta_4}{2\lambda} \\ \sin\frac{\beta_1}{2\lambda} & \sin\frac{\beta_2}{2\lambda} & \sin\frac{\beta_3}{2\lambda} & \sin\frac{\beta_4}{2\lambda} \\ \beta_1^2\cos\frac{\beta_1}{2\lambda} & \beta_2^2\cos\frac{\beta_2}{2\lambda} & \beta_3^2\cos\frac{\beta_3}{2\lambda} & \beta_4^2\cos\frac{\beta_4}{2\lambda} \\ \beta_1^2\sin\frac{\beta_1}{2\lambda} & \beta_2^2\sin\frac{\beta_2}{2\lambda} & \beta_3^2\sin\frac{\beta_3}{2\lambda} & \beta_4^2\sin\frac{\beta_4}{2\lambda} \end{vmatrix} = 0 . \quad (6.7)$$

Evaluating the determinant, we find that (6.7) can be rewritten as

$$T_{1234} + T_{1342} + T_{1423} = 0 , \quad (6.8)$$

where

$$T_{pqrs} = (\beta^2_p - \beta^2_q)(\beta^2_r - \beta^2_s)\left(\tan\frac{\beta_p}{2\lambda}\tan\frac{\beta_q}{2\lambda} -\right.$$

$$- \tan \frac{\beta_r}{2\lambda} \tan \frac{\beta_s}{2\lambda} \Big) \ . \qquad (6.9)$$

Next, we insert (6.1) into the conditions of stability (4.1) and (4.2). Because of the linear character both equations have to be satisfied by the four components of w separately. The result is four pairs of equations analogous to (5.2) and (5.3), and the same way of reasoning as applied there, gives the conditions:

$$p = \frac{4}{\pi_{xx}\alpha^2 + 2\ \pi_{xy}\alpha\beta_j + \pi_{yy}\beta^2_j} \left\{ \frac{1}{3}\ \delta^2\gamma^4_j + \right.$$
$$\left. + \ \bar{\varepsilon}_j P_j \right\} ; \ (j = 1,\ 2,\ 3,\ 4.) , \qquad (6.10)$$

where the suffix j at $\bar{\varepsilon}$ and P means that for γ should be read γ_j. For P either the rigorous formula (5.5) or the approximate one (5.7) can be used.

In a given case the problem is to determine the lowest value of p for which (6.8) and (6.10) yield a set of values for α and β_j. (one should keep in mind that γ_j is known when α and β_j are known). As for α, there is still the condition that it is real, as the buckling pattern should be periodical with respect to x. For β_j this does not hold. As a matter of fact, complex roots β_j have to be taken into account.

It is, however, practically impossible to carry out the calculations required for a single case. Another way of solving a whole program of cases is to start from fixed values of δ and ε (defining the properties of the sandwich as a material) and then to choose values for both p and α. Then (6.10) can be solved for β_j, and when these have been found, (6.8) can be solved for λ. By repeating this process for a number of other values of p and α we can by interpolation find corresponding values of p and α for given values of λ. The minimum value of p for a given λ is the critical stress belonging to the specified values of δ, ε and λ.

6.2 *An approximate treatment.*

Even if we use the approximate expression (5.7) for P, the rigorous solution of the foregoing section requires a considerable amount of calculating. Therefore, we make a, though rather crude, approximation by confining ourselves to the first two components of the sum in formula (6.1), and moreover we take $w^*_2 = - w^*_1$. Therefore, for the middle surface of the plate we assume

$$w_0 = w^*_1 \{\cos(\xi + \eta_1) - \cos(\xi + \eta_2)\} . \qquad (6.11)$$

We choose the X-axis again, as in section 5, along one of the edges of the plate.

The geometrical meaning of these approximations becomes evident, if we rewrite (6.11) in the form

$$w_0 = 2\ w^*_1 . \sin\left(\xi + \frac{\eta_2 + \eta_1}{2}\right) . \sin \frac{\eta_2 - \eta_1}{2} . \qquad (6.12)$$

Now we see clearly that the nodal lines of the buckling pattern consist of two sets of straight lines, viz. $\eta_2 - \eta_1 = 2\,n\pi$, and $2\xi + \eta_1 + \eta_2 = 2\,n'\pi$ (n and n' integer). The first set consists of lines parallel to the X-axis, and two of them must coincide with the edges of the plate. As due to the absence of edges parallel to the Y-axis, the buckling always occurs with one half wave in the Y-direction, we immediately find the boundary condition:

$$\beta_1 - \beta_2 = 2\ \lambda\pi \ . \qquad (6.13)$$

This is, therefore, the analogue of eq. (6.7) or (6.8). Attention is drawn to the fact that we can no longer ensure freedom of bending moments along the edges of the plate.

The second set of nodal lines consists of straight lines at a certain angle with the X-axis, whereas in the exact treatment they appear as curved lines.

The stability conditions are again eqs. (6.10), now, of course, only for $j = 1$ and 2.

It is, of course, wholly meaningless to use the rigorous expression (5.5) for P, after having already made such far more drastic simplifications. Therefore, we use the expression (5.7), which is further simplified by retaining only the term $(1 + \delta)^2$ in the numerator of the fraction. The error, thus introduced, does not exceed a few per cent. We shall follow a somewhat different line of attack than used in the foregoing number. Therefore, we introduce $\alpha^* = \frac{\alpha^2}{2\varepsilon}$; $\delta^* = \frac{\delta^2}{3(1+\delta)^2}$, $\rho = \frac{4p}{(1+\delta)^2\alpha^2}$, and $\vartheta_j = \frac{\beta_j}{\alpha}$. Then, the condition of stability (6.10) can be written as

$$\rho = \frac{(1 + \vartheta^2_j)^2}{\pi_{xx} + 2\ \pi_{xy}\vartheta_j + \pi_{yy}\vartheta^2_j} \left\{ \delta^* + \right.$$
$$\left. + \frac{1}{1 + \alpha^*\ (1 + \vartheta^2_j)} \right\} ; \ (j = 1,2) . \qquad (6.14)$$

From the discussion of the buckling pattern it appears that only real values of ϑ_j come into consideration. They have, of course, to satisfy (6.13), which can be rewritten as

$$\vartheta_1 - \vartheta_2 = 2\ \lambda\pi/\alpha . \qquad (6.15)$$

The course of the calculation is as follows.

We start from given values of δ and ε/λ^2; then, δ^* is known. We now assume a value for α^*. Using the boundary condition (6.15) we easily derive the relation

$$(\vartheta_1 - \vartheta_2)^2 = \frac{2\,\pi^2}{\alpha^*}\,\frac{\lambda^2}{\varepsilon}\,. \qquad (6.16)$$

Therefore $\vartheta_1 - \vartheta_2$ is known. Solving eq. (6.14) for ϑ as a function of ρ we can then determine the value of ρ corresponding to the known value of $\vartheta_1 - \vartheta_2$ (see also sections 6.3 to 6.5 incl.). The buckling load parameter p follows, according to the definition of ρ and eq. (6.15), from

$$\frac{p}{\pi^2\lambda^2\,(1+\delta)^2} = \frac{\rho}{(\vartheta_1 - \vartheta_2)^2}\,. \qquad (6.17)$$

In order to solve the buckling problem we have only to repeat this procedure for several values of α^* and to determine the minimum value of $\rho/(\vartheta_1 - \vartheta_2)^2$ as a function of α^*.

We see that this method of solution enables us to keep λ out of the given data, and we need only give beforehand the two parameters δ and ε/λ^2. This is only possible, because of the considerable simplification in the boundary conditions that are reduced from the transcendental relation (6.7) or (6.8) to the simple relation (6.13) or (6.15).

This simplification is urgently needed, as we have already a number of parameters in the problem from the external load system, viz. π_{xx}, π_{xy} and π_{yy}.

We shall investigate in detail the following three cases of loading. The first is that of shear and longitudinal compression ($\pi_{yy} = 0$), the second that of shear and lateral compression ($\pi_{xx} = 0$), and the third that of longitudinal and lateral compression without shear ($\pi_{xy} = 0$).

6.3 *Shear and longitudinal compression.*

In this case $\pi_{yy} = 0$ and we shall take $\pi_{xy} = \frac{1}{2}$. Then equation (6.14) becomes:

$$\rho = \frac{(1+\vartheta^2 j)^2}{\pi_{xx} + \vartheta_j}\left\{\delta^* + \frac{1}{1+\alpha^*\,(1+\vartheta^2 j)}\right\}\,;\ (j = 1,2)\,. \qquad (6.18)$$

If we plot a curve of ϑ against ρ, we get something as illustrated in fig. 6.1. For large values of ϑ_j we have approximately $\rho = \frac{\delta^*}{\pi_{xx}}\,\vartheta^3$. For $\vartheta = -\pi_{xx}$ the curve shows a horizontal asymptote. For values of $\vartheta < -\pi_{xx}$, ρ becomes negative, and is, therefore, of no interest. For convenience, we take ϑ_1 to be the largest of the two roots of ϑ for a given ρ. Then $\vartheta_1 - \vartheta_2$ is a one-valued increasing (from 0 to ∞) monotonic function of ρ, and there is no difficulty in determining ρ at given $\vartheta_1 - \vartheta_2$ to any desired accuracy.

For $\pi_{xx} \gg 1$ nothing particular happens. As now a large compressive force acts on the panel, this will chiefly determine the buckling process and the magnitude of the buckling force will be essentially the same as if no shear was present. In the limiting case of large π_{xx} we can therefore immediately take the value for a panel that is under longitudinal compression only, which will be dealt with in section 6.5 as a special case.

If $\pi_{xx} \ll -1$, however, the panel is under a large tension, which is a stabilizing factor and the shear cannot be neglected, but is, on the contrary, the only thing that causes the panel to buckle. As calculations with decreasing $\pi_{xx} < -1$ show that ϑ_1 increases almost linearly with $|\pi_{xx}|$, we shall try to find an asymptotic solution, valid for $\pi_{xx} \ll -1$, by assuming $\vartheta_1 = \pi_{xx}\,\mu$, where μ is some negative fixed quantity (that does not depend on π_{xx}). When $\vartheta_1 \gg 1$, ρ is large and therefore ϑ_2 must be close to its asymptotic value. Therefore $\vartheta_2 = -\pi_{xx}$. From (6.16) the (variable) value of α^* follows, and after inserting these results in (6.18) we find the quantity $\rho/(\vartheta_1 - \vartheta_2)^2$, that governs the magnitude of the buckling load, from

$$\frac{\rho}{(\vartheta_1 - \vartheta_2)^2} = \pi_{xx}\,\frac{\mu^4}{\mu+1}\left\{\frac{\delta^*}{(\mu+1)^2} + \frac{1}{(\mu+1)^2 + \frac{2\,\pi^2\lambda^2}{\varepsilon}\,\mu^2}\right\}. \qquad (6.19)$$

Now μ has to be determined in such a way that the expression takes its minimum value. It is obvious that this value does not depend on π_{xx}, and therefore it is the correct asymptotic value of ϑ_1 that we have chosen. Equating to zero the derivative of (6.19) with respect to μ we find the condition for μ:

$$C_1C_3\,.\,\mu^5 + (4\,C_1C_3 + 4\,C_1)\,\mu^4 + (13\,C_1 + 4\,C_2 + 5\,C_2C_3)\,\mu^3 + (6\,C_1 + 20\,C_2 + 2\,C_2C_3)\,\mu^2 + 17\,C_2\,\mu + 4\,C_2 = 0, \qquad (6.20)$$

where we have written for abbreviation:

$$C_1 = 1 + \delta^*C_3\ ;\ C_2 = 1 + \delta^*\ ;\ C_3 = 1 + \frac{2\,\pi^2\lambda^2}{\varepsilon}\,.$$

Equation (6.20) is an algebraic equation of the

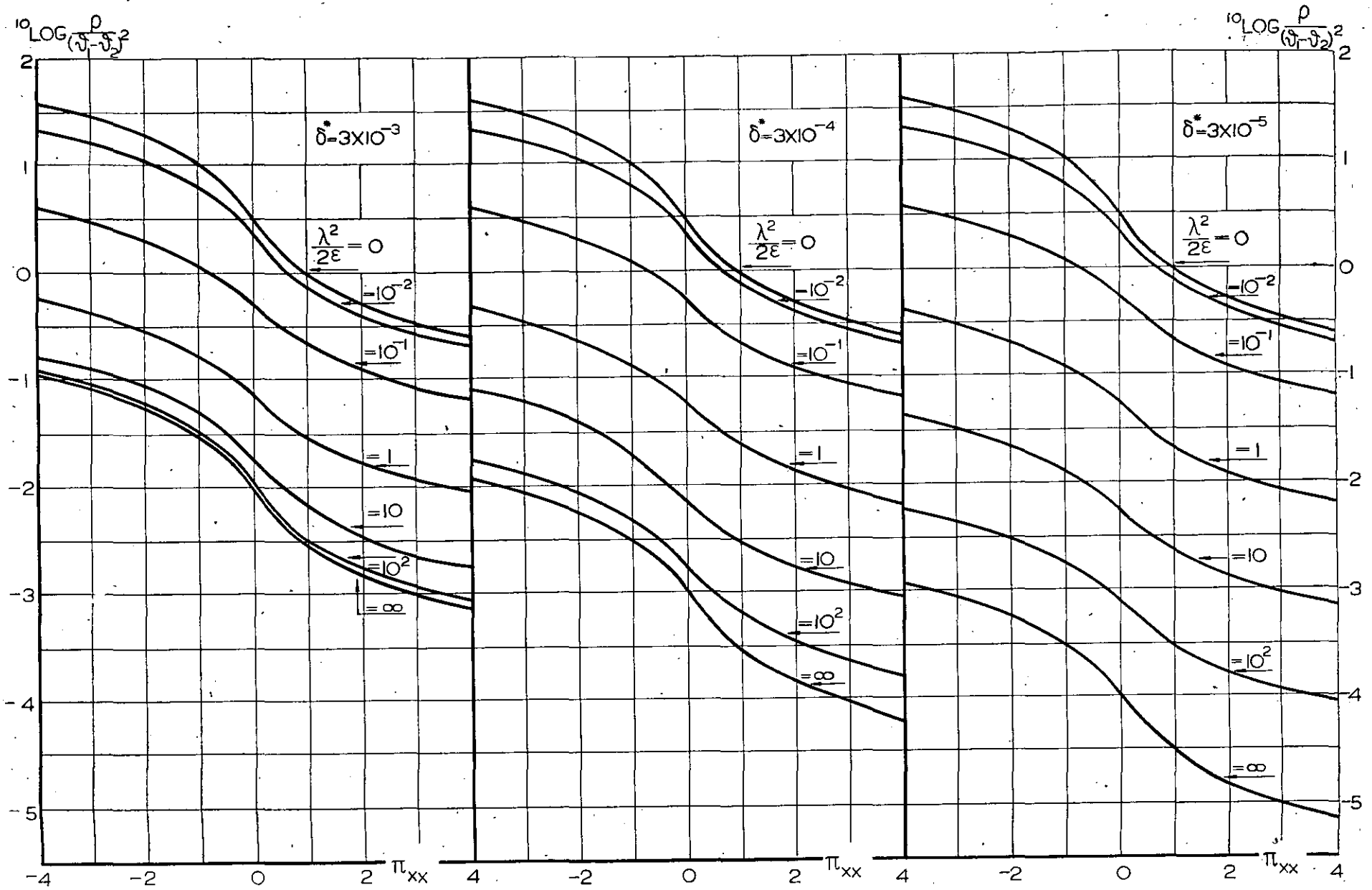

FIGURES 6.2, 6.3, 6.4.

Buckling of an infinitely long plate under shear and longitudinal compression; $\pi_{xy} = 0{,}5$.

fifth degree with one real root that can be calculated without difficulty.

We have actually calculated the minima of the buckling force for three values of δ^*, viz. 3.10^{-3}; 3.10^{-4} and 3.10^{-5}, and for seven values of $\frac{\lambda^2}{2\varepsilon}$, viz. 0, 10^{-2}, 10^{-1}, 1, 10, 10^2 and ∞, for a number of values of π_{xx}. The results are plotted in figs. 6.2, 6.3 en 6.4.

6.4 *Shear and lateral compression.*

In this case $\pi_{xx} = 0$ and we shall again take $\pi_{xy} = \frac{1}{2}$. Equation (6.14) becomes:

$$\rho = \frac{(1+\vartheta^2 j)^2}{\vartheta_j\ (1+\pi_{yy}\ \vartheta_j)} \left\{ \delta^* + \right.$$
$$\left. + \frac{1}{1+\alpha^*\ (1+\vartheta^2 j)} \right\};\ (j = 1,2) \qquad (6.21)$$

If we again plot a curve of ϑ against ρ (cf. figs. 6.5 and 6.6), we must distinguish between the case of positive π_{yy} and that of negative π_{yy}. In the case of positive π_{yy} (lateral compression) the curve consists (for positive ρ) of two separate branches, one above the horizontal asymptote $\vartheta = 0$ and one below the horizontal asymptote $\vartheta = -1/\pi_{yy}$. If, however, π_{yy} is negative (lateral tension) for positive ρ only one branch is present between the upper horizontal asymptote $\vartheta = -1/\pi_{yy}$ and the lower one $\vartheta = 0$.

If $\pi_{yy} > 0$ there are, for values of ρ above a certain value, four roots of ϑ instead of two. Therefore, it is not obvious which two roots should be taken, but from (6.17) it follows that always two roots should be combined such that, with given $\vartheta_1 - \vartheta_2$ (and α^*), the corresponding ρ has the lowest value. If π_{yy} is small, the asymptotes are far from another and we have only to

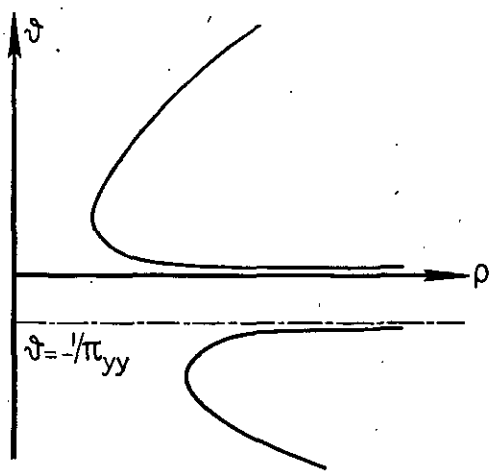

FIGURE 6.5.
The $\rho - \vartheta$ curve, if $\pi_{xx} = 0$ and $\pi_{yy} > 0$.

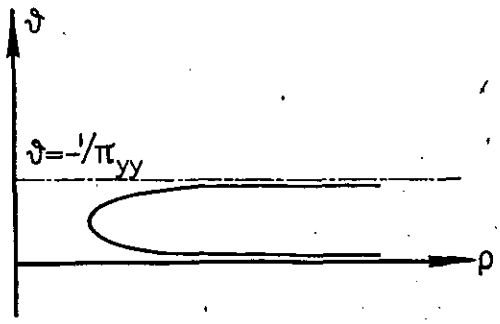

FIGURE 6.6.
The $\rho - \vartheta$ curve, if $\pi_{xx} = 0$ and $\pi_{yy} < 0$.

deal with the left part of the upper half of the curve, therefore with a situation that is essentially the same as in the case of fig. 6.1 with $\pi_{xx} = 0$ (pure shear). If, however, π_{yy} increases above a critical value $\pi_{yy\ \mathrm{crit}}$ a situation arises in which it is necessary to combine roots from the two branches, and, of course, one from the upper half of the upper branch and another from the lower half of the lower branch, as in this way ρ is minimum. Then, however, it appears that we must take $\alpha^* = 0$ and consequently ρ and $\vartheta_1 - \vartheta_2$ infinite to obtain the minimum of $\rho/(\vartheta_1 - \vartheta_2)^2$. This minimum follows to be:

$$\left[\frac{\rho}{(\vartheta_1 - \vartheta_2)^2}\right]_{\min} = \frac{1}{\pi_{yy}} \left\{ \delta^* + \right.$$
$$\left. + \frac{1}{1+\pi^2\lambda^2/2\varepsilon} \right\};\ (\pi_{yy} > \pi_{yy\ \mathrm{crit}}) \qquad (6.22)$$

We must, therefore, calculate the quantity $\rho/(\vartheta_1 - \vartheta_2)^2$, as derived from the upper branch of the curve only, for increasing values of π_{yy}, and as soon as this quantity exceeds the value given by (6.22), we must then use that value. From (6.15) it appears that above $\pi_{yy\ \mathrm{crit}}$ we have $\alpha = 0$, which means that the wave length of the buckles in the X-direction is infinite. The plate therefore buckles in the shape of a cylindrical surface, just as it would do if no shear was present. This phenomenon was already known for the simple plate and it appears also to exist for the sandwich panel. Only the value of $\pi_{yy\ \mathrm{crit}}$ cannot be given beforehand, but must result from the calculations.

If $\pi_{yy} < 0$ (lateral tension) there are always two roots of ϑ for each value of ρ.

As in the foregoing section, the lateral tension acts as a stabilizing factor, and the force needed for buckling is high. For large negative values of π_{yy}, we can again make an asymptotic calculation. As ϑ_1 and ϑ_2 are intermediate between the asymptotes $\vartheta = 0$ and $\vartheta = -1/\pi_{yy}$, and

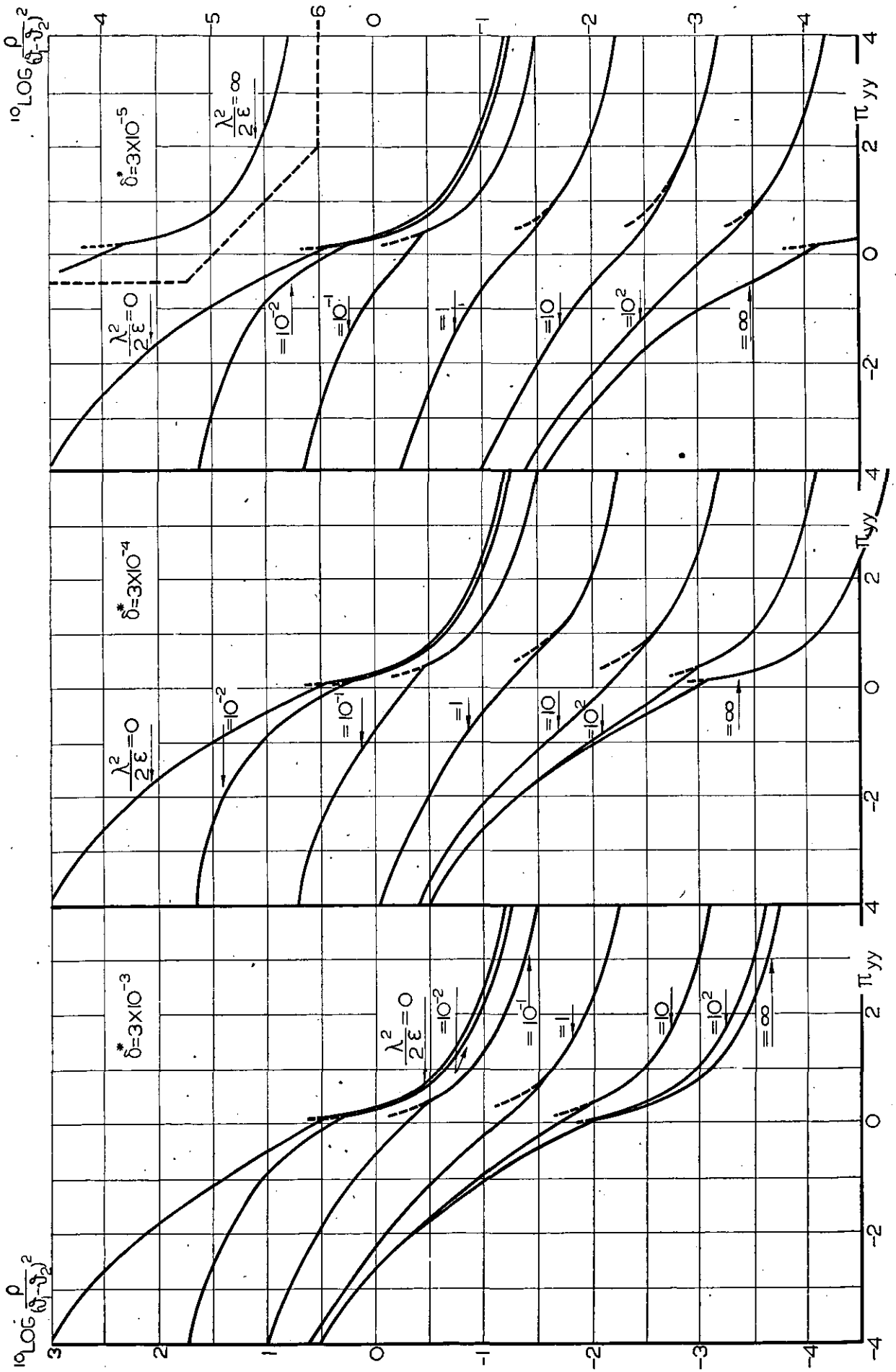

FIGURES 6.7, 6.8, 6.9.
Buckling of an infinitely long plate under shear and lateral compression;
$\pi_{xy} = 0{,}5$.

$\pi_{yy} \ll -1$, ϑ_1 and ϑ_2 are both small, and therefore

$$\rho = \frac{1+\delta^*+\alpha^*\delta^*}{1+\alpha^*} \cdot \frac{1}{\vartheta_j\,(1+\pi_{yy}\,.\,\vartheta_j)}; \; (j=1,2)\,. \tag{6.23}$$

Apparently

$$\vartheta_1\,(1+\pi_{yy}\,\vartheta_1) = \vartheta_2\,(1+\pi_{yy}\,\vartheta_2). \tag{6.24}$$

From this we may infer that

$$\vartheta_{1,2} = \frac{-1 \pm 2\,\mu}{2\,\pi_{yy}}\,, \tag{6.25}$$

and from (6.16) we obtain

$$\alpha^* = \frac{\pi^2\lambda^2}{2\,\varepsilon} \cdot \frac{\pi^2 yy}{\mu^2}\,. \tag{6.26}$$

If we insert these values in (6.23), we find

$$\frac{\rho}{(\vartheta_1-\vartheta_2)^2} = \pi^3 yy\;\frac{\delta^*\,\varphi+(1+\delta^*)\,\mu^2}{\mu^2\,(4\,\mu^2-1)\,(\mu^2+\varphi)}\,, \tag{6.27}$$

where $\varphi = \pi^2\lambda^2\pi^2 yy/2\,\varepsilon$. Now μ^2 has still to be varied so as to minimize the expression (6.27). By equating to zero the derivative with respect to μ^2, we find the condition for μ^2:

$$C_4\,\mu^6 + C_5\,\mu^4 + C_6\,\mu^2 + C_7 = 0\,, \tag{6.28}$$

where $C_4 = -8\;(1+\delta^*)$; $C_5 = 1+\delta^*-4\,\varphi.\,(1+4\;\delta^*)$; $C_6 = -2\;\delta^*\;\varphi\;(4\;\varphi-1)$ and $C_7 = \delta^*\;\varphi^2$. Equation (6.28) is an algebraic equation of the third degree, which yields one positive root for μ^2. This time, this value depends also on π_{yy}, as φ depends on π_{yy}.

If $\lambda^2/\varepsilon = 0$, also $\varphi = 0$, and the root of (6.28) is easily calculated to be $\mu^2 = \frac{1}{8}$. The corresponding value of $\rho/(\vartheta_1-\vartheta_2)^2 = -16\;\pi^3 yy\;(1+\delta^*)$. If $\varphi \gg 1$ which is the case if $\lambda^2/\varepsilon \gg 1$, and also for every other value of λ^2/ε if only $|\,\pi_{yy}\,|$ is large enough, the root of (6.28) is also $\mu^2 = \frac{1}{8}$, but now the corresponding value $\rho/(\vartheta_1-\vartheta_2)^2 = -16\;\pi^3 yy\;.\;\delta^*$.

Therefore, with decreasing π_{yy} ($\ll -1$), the value of $\rho/(\vartheta_1-\vartheta_2)^2$ tends to $-16\;\pi^3 yy.\;\delta^*$ for every value of λ^2/ε, except for $\lambda^2/\varepsilon = 0$, when it is $-16\;\pi^3 yy\;(1+\delta^*)$. It is obvious that the limiting value of $\rho/(\vartheta_1-\vartheta_2)^2$ is much quicker reached (i.e. with smaller $|\,\pi_{yy}\,|$) if λ^2/ε is large than if it is small.

We have again calculated the minima of the buckling force for the same values of δ^* and $\lambda^2/2\,\varepsilon$ as mentioned before, for a number of values of π_{yy}. The results have been plotted in figs. 6.7, 6.8 and 6.9.

6.5 *Longitudinal and lateral compression without shear.*

If no shear is present, the buckling formula (6.11) or (6.12) is exact, as the panel buckles in rectangular waves. Obviously $\beta_1 = -\beta_2$, and therefore also $\vartheta_1 = -\vartheta_2$. This is also evident from (6.14), for this is an equation in $\vartheta^2 j$ if the term $\pi_{xy}\vartheta_j$ vanishes. In chapter 5 we already gave a discussion of some features of the problem, but we now give a more fully detailed description in our new formulas.

We shall take $\pi_{xx} = 1$, which is, of course, no restriction.

As now $\vartheta_1 = -\vartheta_2$, the awkward term $\vartheta_1 - \vartheta_2$ can be replaced by 2ϑ simply.

After some intermediate calculations, we therefore find

$$\frac{\rho}{(\vartheta_1-\vartheta_2)^2} = \frac{(1+\vartheta^2)^2}{4\;\vartheta^2}\;\frac{\delta^*\,(\psi-1)+(1+\delta^*\psi)\,\vartheta^2}{\psi-1+\{\pi_{yy}\,(\psi-1)+\psi\}\,\vartheta^2+\pi_{yy}\,\psi\vartheta^4}\,, \tag{6.29}$$

where $\psi = 1 + \pi^2\lambda^2/2\,\varepsilon$.

Now, ϑ^2 has still to be chosen so as to make this expression minimum. Equating to zero the derivative with respect to ϑ^2, we obtain for ϑ^2 an algebraic equation of the third degree (the coefficient of ϑ^8 vanishes)

$$C_8\vartheta^6 + C_9\vartheta^4 + C_{10}\vartheta^2 + C_{11} = 0\,, \tag{6.30}$$

where $C_8 = \psi + \delta^*\psi^2 - \pi_{yy}\;(1+\psi+2\delta^*\;\psi^2)$; $C_9 = -2 + (1-2\;\delta^*)\;\psi + \delta^*\psi^2 + \pi_{yy}\,\{1 - (1-4\;\delta^*)\;\psi - 4\;\delta^{*2}\psi^2\}$; $C_{10} = \delta^*\;(1-\psi^2) - \pi_{yy}\;2\;\delta^*\;(1-\psi)^2$ and $C_{11} = -\delta^*\;(1-\psi)^2$.

Apart from the values of ϑ^2, given by (6.30), there is still, from the vanishing of the coefficient of ϑ^8, a minimum for infinite value of ϑ^2. This follows to be:

$$\frac{\rho\,\infty}{(\vartheta_1-\vartheta_2)^2} = \frac{1}{4\,\pi_{yy}}\;(\delta^* + \frac{1}{\psi})\,. \tag{6.31}$$

For all π_{yy} above a critical value $\pi_{yy\;\mathrm{crit}}$ this is indeed the minimum value. This time the value of $\pi_{yy\;\mathrm{crit}}$ can be easily calculated beforehand, as the transition requires that for $\pi_{yy} = \pi_{yy\;\mathrm{crit}}$, equation (6.30) also has an infinite root, and therefore that C_8 should vanish. Therefore

$$\pi_{yy\;\mathrm{crit}} = \frac{\psi+\delta^*\,\psi^2}{1+\psi+2\;\delta^*\psi^2}\,. \tag{6.32}$$

Above the critical value of π_{yy}, the plate again buckles in a cylindrical shape.

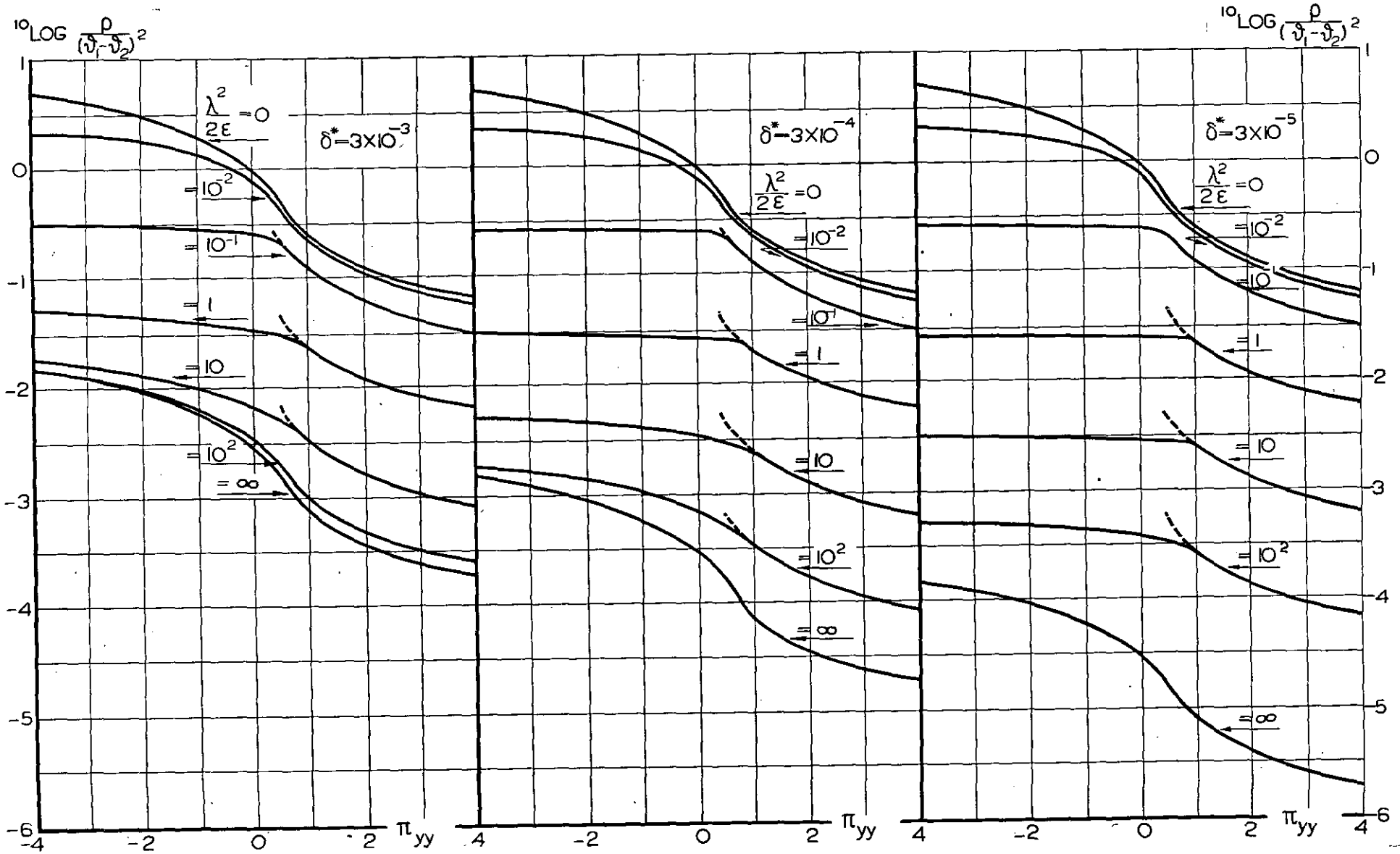

FIGURES 6.10, 6.11, 6.12.

Buckling of an infinitely long plate under biaxial compression;
$\pi_{xx} = 1$.

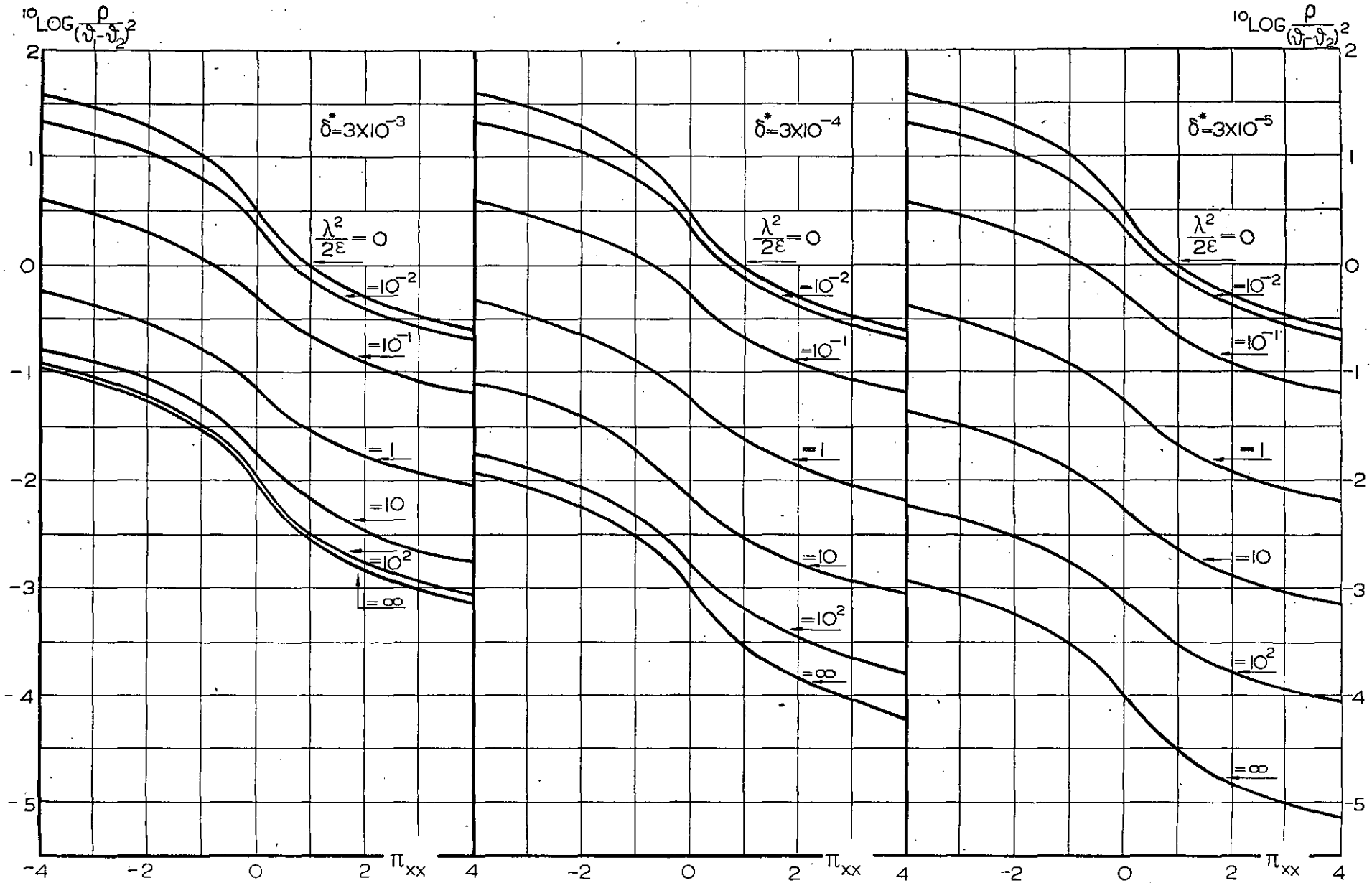

FIGURES 6.10, 6.11, 6.12.
Buckling of an infinitely long plate under biaxial compression;
$\pi_{xx}=1$.

For the same values of δ^* and of $\frac{\lambda^2}{2\varepsilon}$ as mentioned before, the minimum values of the buckling force have been calculated for a number of values of π_{yy}. The results have been plotted in figs. 6.10, 6.11 and 6.12; an example of the use of these graphs is given in appendix 2.

7 Discussion of the results.

As has already been stated before, the results obtained for the cases of shear-free loading are exact, apart from the simplifications introduced in deriving the formulas (5.8) or (6.14) or (6.29). This can easily be checked by applying these formulas to the case $\varepsilon = 0$, which corresponds to the buckling of a simple plate.

In this case (5.6) or (5.8) reduces to

$$p = \frac{\delta^2}{12} \frac{(\alpha^2 + \beta^2)^2}{\pi_{xx}\alpha^2 + \pi_{yy}\beta^2} . \qquad (7.1)$$

With $\pi_{xx} = 1$ and $\pi_{yy} = 0$ we obtain for the minimum value $p_{min} = \frac{\pi^2 s^2}{3b^2}$ or $P_{xx} = 4\frac{\pi^2 D}{b^2}$ at $\alpha = \beta$, i.e. square waves. The same result is obtained from (6.29) with $\varepsilon = 0$ and $\pi_{yy} = 0$.

With $\pi_{xx} = 0$ and $\pi_{yy} = 1$ we obtain $p_{min} = \frac{\pi^2 s^2}{12\ b^2}$ or $P_{yy} = \frac{\pi^2 D}{b^2}$ at $\alpha = 0$, i.e. cylindrical buckling.

Both results are, indeed, the well-known exact solutions of the simple plate. Unfortunately, the result obtained for the case of pure shear is far from exact. With $\varepsilon = 0$ and $\pi_{xx} = 0$ we obtain from figs. 6.2 to 6.4 incl. $\rho/(\vartheta_1 - \vartheta_2)^2 = 3{,}39\ \delta^*$, which can be rewritten as $p = 1{,}13\frac{\pi^2 s^2}{b^2}$ or $P_{xy} = 6{,}78\frac{\pi^2 D}{b^2}$. The exact solution for the simple plate is $P_{xy} = 5{,}35\frac{\pi^2 D}{b^2}$ (*ref.* 3) so that the buckling load obtained from wave form (6.12) is 27 % too large. An independent check on the validity of the numerical computations (see Appendix 1) confirmed this result. This unsatisfactory feature was not anticipated because the energy method, starting from the same wave form, leads to a buckling load which is only 6 % too large.

The most urgent extension of this investigation will, therefore, be an attempt to obtain a satisfactory solution for the case of pure shear. If this attempt is successful, a satisfactory correction of the interaction curves for combined loadings will present no difficulties.

8 Notations.

The suffix b means boundary plane between face and core

f means face

m means middle surface of the face

o means middle surface of the plate

No suffix is used for quantities related to the core.

a Length of panel in X-direction

b Width of panel in Y-direction

c Thickness of the core

$C_1, C_2 \ldots$ Several constants defined in the text

$e = \frac{\delta u}{\delta x} + \frac{\delta v}{\delta y} + \frac{\delta w}{\delta z}$

$e' = \frac{\delta u}{\delta x} + \frac{\delta v}{\delta y}$

$f' = \frac{\delta u}{\delta y} - \frac{\delta v}{\delta x}$

m, n integers

p Quantity defining the magnitude of the buckling load; $p = \frac{p_{xx}}{\pi_{xx}} = \frac{p_{xy}}{\pi_{xy}} = \frac{p_{yy}}{\pi_{yy}}$

$p_{xx}, p_{xy}, p_{yy} = \frac{s^2}{12D}\cdot (P_{xx}, P_{xy}, P_{yy})$

s thickness of the face

u, v, w displacements in X, Y, Z-direction

x, y, z Cartesian coordinates

$D = \frac{E_f . s^3}{12\ (1 - \nu_f^2)}$

E YOUNG's modulus

$M_{xx}, \ldots$ Elastic bending moments in the faces, defined in fig. 2.1

P Function defined by (5.5) or (5.7).

P_{xx}, P_{xy}, P_{yy} External normal and shearing forces on one face per unit of width

$S_{xx}, \ldots$ Elastic forces in the faces, defined in fig. 2.1

α, β Parameters defining the wave length of the buckles in X- and Y-direction:

$\alpha = m\pi\frac{c}{a}, \quad \beta = n\pi\frac{c}{b}$

$\alpha^* = \alpha^2/2\,\varepsilon$

$\gamma = \frac{1}{2}\sqrt{\alpha^2+\beta^2}$

$\delta = s/c$

$\delta^* = \frac{\delta^2}{3\,(1+\delta)^2}$

$\varepsilon = \frac{E\,(1-\nu^2_f)}{E_f\,(1+\nu)}\,\frac{c}{2\,s}$

$\varepsilon^* = 2\,\delta\varepsilon$

$\bar{\varepsilon} = \varepsilon\left(1+\frac{\nu_f}{1-\nu_f}\,\frac{\delta^2\gamma^2}{2}\right)$

$\zeta = 2\,\gamma z/c$

$\eta = \beta y/c$

$\vartheta = \beta/\alpha$

$\lambda = c/b$

ν POISSON'S ratio

$\xi = \alpha x/c$

$\pi_{xx},\ \pi_{xy},\ \pi_{yy} = p_{xx}/p,\ p_{xy}/p,\ p_{yy}/p$

$\rho = \frac{4\,p}{(1+\delta)^2\,\alpha^2}$

$\sigma,\ \tau$ normal and shear stresses

$\varphi = \pi^2\lambda^2\pi^2 y y/2\,\varepsilon$

$\psi = 1+\pi^2\lambda^2/2\varepsilon$

$\omega = 1-\frac{\nu_f}{1-\nu_f}\,\frac{\delta^2\gamma^2}{2}$

χ function, defined by (5.4)

$\Delta = \frac{\delta^2}{\delta x^2}+\frac{\delta^2}{\delta y^2}+\frac{\delta^2}{\delta z^2}$

$\Delta' = \frac{\delta^2}{\delta x^2}+\frac{\delta^2}{\delta y^2}$

9 References.

1. VAN DER NEUT, A., Die Stabilität geschichteter Streifen (The stability of sandwich strips). Report S. 284 of the Nationaal Luchtvaartlaboratorium (National Aeronautical Research Institute), Amsterdam, 1943.

2. VAN DER NEUT, A., Die Stabilität geschichteter Platten (The stability of sandwich plates) Report S. 286 of the Nationaal Luchtvaartlaboratorium (National Aeronautical Research Institute), Amsterdam, 1943.

3. TIMOSHENKO, S., Theory of elastic stability. McGraw-Hill, 1936.

Acknowledgement.

The original issue of this report in the form of preprints contained a slight error in the derivation of eq. (5.2), the correction of which also necessitated some changes in subsequent formulae and definitions. The author is indebted to messrs F. J. PLANTEMA and A. C. DE KOCK for pointing out this error and making the necessary revisions, as well as for preparing the appendices to the report.

Completed: February 1947.
Revised : August 1948.

Appendix 1.

Approximate calculation of the buckling load of a simply supported infinitely long plate under pure shear.

In order to verify the results obtained in section 6 the buckling load of a simple plate was independently computed, assuming the wave form (6.12), which can be rewritten as

$$w = w_1 \sin\frac{\pi y}{b}\,\sin\frac{\pi}{l}\,(x+\bar{n}y)\ , \qquad (1)$$

where l is the wave length in X-direction and account has been taken of the boundary condition (6.13).

Substituting (1) into the differential equation

$$\Delta'\Delta' w + 2\,\frac{P_{xy}}{D}\,\frac{\delta^2 w}{\delta x\delta y} = 0 \qquad (2)$$

we obtain an expression of the form

$$Aw + Bw_1 \cos\frac{\pi y}{b}\,\cos\frac{\pi}{l}\,(x+\bar{n}y) = 0\ . \qquad (3)$$

This condition can only be satisfied for every arbitrary combination of x and y if $A=0$ and $B=0$. Thus, we obtain two equations

$$\frac{\pi^4}{l^4} + 2\,\frac{\pi^4}{b^2l^4}\,(l^2+\bar{n}^2b^2) + \frac{\pi^4}{b^4l^4}\left\{(l^2+\bar{n}^2b^2)^2 + 4\,\bar{n}^2b^2l^2\right\} = \frac{2\,P_{xy}}{D}\,\frac{\pi^2\,\bar{n}}{l^2}\ , \qquad (4)$$

$$4\,\frac{\pi^4\,\bar{n}}{l^3b} + 4\,\frac{\pi^4\,\bar{n}}{l^3b^3}\,(l^2+\bar{n}^2b^2) = \frac{2\,P_{xy}}{D}\,\frac{\pi^2}{lb}\ . \qquad (5)$$

Elimination of P_{xy} from (4) and (5) leads to a quadratic equation in $\frac{l^2}{b^2}$ and $\bar{n}^2$, giving

$$\frac{l^2}{b^2} = -\,(\bar{n}^2+1) + 2\sqrt{\bar{n}^2\,(\bar{n}^2+1)}\ . \qquad (6)$$

Eliminating l/b from (5) with the aid of (6) and

minimizing the resulting expression for P_{xy} with respect to n^2 we obtain the final solution

$$\bar{n}^2 = 1{,}154 \; ; \; \frac{l}{b} = 0{,}999 \; ; \; P_{xy} = 6{,}78 \; \frac{\pi^2 D}{b^2}. \quad (7)$$

Starting from the same wave form, the energy method (*ref.* 3) yields the much better results

$$\bar{n}^2 = 0{,}5 \; ; \; \frac{l}{b} = 1{;}12 \; ; \; P_{xy} = 5{,}66 \; \frac{\pi^2 D}{b^2} \; . \quad (8)$$

This may be explained by the fact that the energy method leaves us free to minimize P_{xy} both with respect to l/b and to $\bar{n}$.

Appendix 2.

Numerical example of the use of the graphs.

We consider a plate loaded only by compressive forces in the X-direction. Therefore $\pi_{xy} = \pi_{yy} = 0$ and we may take $\pi_{xx} = 1$.
We take $b = 30$ cm, $c = 1$ cm, $s = 0{,}05$ cm, $E = 700$ kg/cm², $E_f = 700\,000$ kg/cm², $\nu = \nu_f = 0{,}3$.

From these data we compute

$$\delta = \frac{s}{c} = 0{,}05, \; \delta^* = \frac{\delta^2}{3\,(1+\delta)^2} = 7{,}55.\; 10^{-4}, \; \lambda = \frac{c}{b} = \frac{1}{30} \; ,$$

$$\varepsilon = \frac{E\,(1-\nu^2 f)}{E_f\,(1+\nu)} \; \frac{1}{2\delta} = 0{,}00700, \; \frac{\lambda^2}{2\varepsilon} = 0{,}0794 = 10^{-1{,}100} \; .$$

From the appropriate graphs, figs. 6.10, 6.11 and 6.12 we read that for $\pi_{yy} = 0$ and $\log \lambda^2/2\varepsilon = -1{,}100$

$\log \frac{\rho}{(\vartheta_1 - \vartheta_2)^2} = -0{,}50$ for $\delta^* = 3.10^{-3}$; $-0{,}50$ for $\delta^* = 3.10^{-4}$, and $-0{,}50$ for $\delta^* = 3.10^{-5}$. This is most accurately done by cross-plotting in each figure $\log \frac{\rho}{(\vartheta_1 - \vartheta_2)^2}$ against $\log \frac{\lambda^2}{2\varepsilon}$ for the required value of π_{yy}.

By interpolation we obtain $\log \frac{\rho}{(\vartheta_1 - \vartheta_2)^2} = -0{,}50$ for $\delta^* = 7{,}55.\,10^{-4}$, so that $\frac{\rho}{(\vartheta_1 - \vartheta_2)^2} = 0{,}316$. From (6.17) $p = \pi^2 \lambda^2 (1+\delta)^2 \frac{\rho}{(\vartheta_1 - \vartheta_2)^2} = 0{,}00382$, and from the definitions of P_{xx} and p_{xx}: $P_{xx} = \frac{12D}{s^2} \pi_{xx} p = \frac{12D}{s^2} p = \frac{E_f s}{1-\nu_f^2} p =$ = 147 kg/cm. The buckling load on the plate is therefore $2 \times 147 \times 30 = 8820$ kg.

REPORT S. 314.

The General Instability of Stiffened Cylindrical Shells under Axial Compression

by

Prof. Dr. Ir. A. VAN DER NEUT.

Summary.

This paper is mainly concerned with the bending strength of large fuselage shells, stiffened by stringers and frames. Apart from the usual type of failure, due to instability of the stringers between the frames at the compression side of the fuselage, the structure may fail due to "general instability". In this type of failure the whole structure, including the frames, is being distorted. Obviously, this type of failure is not critical with structures having very stiff frames. With smaller aircraft the relative stiffnesses of stringers and frames are usually such that column failure or local failure of the stringers will prevail. However, it appears that with larger aircraft bodies the frames are becoming more flexible and the buckling load from general instability may be critical.

This paper considers instability by axial compression, whereas it aims at giving information on instability in bending. This has been done in order to reduce mathematical difficulties, since it is known that even with the ordinary cylindrical shell bending is more difficult to deal with than compression.

From the fact that the circumferential half wave length comprises only something like half a radian it is apparent that the critical stress in bending will not be so much in excess of the critical stress in compression; the latter is giving a somewhat conservative estimate of the former.

Literature known to the author is almost entirely confined to theoretical attacks upon the problem; all of them replacing the shell with stringers and frames by an orthotropic shell having constant stiffnesses per unit of length. Flügge (ref. 1) incorporates all stiffnesses that may occur in stiffened shells; however, his results need further evaluation. Dschou's (ref. 2) considerations are far form clear and presumably they are not correct. Dschou and Taylor (ref. 3, 4) are dealing with a simplified system in neglecting the eccentricity of stringers and frames with respect to the skin, which this paper proves to be a circumstance of primary importance.

Like all former investigations part I of this paper is dealing with the orthotropic shell, a system allowing for straightforward methods to solve the problem. This simplification is obviously justified, if one half wave length of the buckled shell comprises several (3 or more) stringers and frames. It appears that there are no cases of buckling in which the circumferential waves are so short, that there can be any doubt on the allowability of distributing the stiffness of the stringers uniformly over the contour of the shell with shells having the usual narrow stringer spacing. With respect to the action of the frames conditions are different; longitudinal half wave length and frame spacing may be almost equal. So part II of this paper is dealing with shells having uniformly distributed stringers but equally spaced frames.

Further details of the elastic systems are: the skin is assumed to carry shear stresses only, as far as it is capable of carrying longitudinal and circumferential stresses the aequivalent stiffness has been included in the stiffness of the stringers and frames. As far as the orthotropic shell is concerned this is all right. However, this assumption may affect the results of part II in those cases, where the longitudinal half wave length is below 1.5 times the frame spacing. An extension of the theory in this respect has to meet considerable mathematical difficulties. The stringers and frames are allowed to have torsional stiffness as well as bending and extensional stiffness; they are connected to the skin and they are intereonnected such that the elements of the material situated upon the common normal to the neutral axes of stringers and frames will stay upon this normal after distortion. The neutral axes have some distance to the skin.

Part I. Uniformly distributed frames.

All strains and stresses can be expressed as usual in 3 displacement functions u, ψ and v (sec. 3,4). The derivation of the equations of equilibrium of the buckled shell is preceded by a general discussion of what terms containing the initial stresses are negligible in the equations of equilibrium for problems of stability (sec. 5). Proceeding in the usual way the buckling load is obtained as a function of the longitudinal and circumferential wave length and as a matter of fact of the structural parameters too. This formal result (eq. 7.4) is too complicated to be conclusive. A discussion of the parameters (sec. 7.2) reveals what terms have the same order of magnitude as those terms of the equations of equilibrium which are being neglected in general. Introducing new structural and load parameters, all of which are of the order of unity, the negligible terms are being separated and the expression for the buckling load is greatly simplified (eq. 7.7). These parameters are: structural parameters A, B, C, F, the load parameter P and the wave form parameters N and Y (see notations sec. 9). These latter parameters have no definite order of magnitude. Depending upon the order of magnitude of Y several classes of buckling cases have been considered (sec. 8), for each of which the buckling load formula is simplified further by neglecting the small order quantities.

There prove to be three main groups of buckling cases (see table I):

1°. Short longitudinal waves and long circumferential waves. This group comprises axially symmetrical buckling (sec. 8.1) and axially non-symmetrical buckling with a small (up to about 3) number of waves over the entire circumference (table I, class I and II). The load parameter is $P=2$ and decreasing with increasing number of circumferential waves (n). The longitudinal wave length is small compared to the radius of the cylinder.

2°. Long waves in both directions and especially longitudinally (table I, class IV and V). This group comprises as a particular case the classical column failure of the cylinder as a whole ($n=1$). In this case the cross section is not distorted. The case $n=2$ yields the minimal buckling load in this group: $P={}^6/_5\,C^{1/2}$; the longitudinal half wave length is larger than the radius. With increasing n the critical load increases and the wave length decreases, remaining however in the order of magnitude of the radius.

3°. Short waves in both directions (table I, class III). All structural parameters prove to be important for the critical load, so the minimal buckling load cannot be expressed explicitly in a formula. In a given numerical case, however, the critical load can be determined quite rapidly from the equations (8.14, 15) by successive approximations (see Appendix).

Part II. Equally spaced frames.

The shell between successive frames is a particular case of the orthotropic shell, dealt with in part I, by the fact that this is a shell without frames. So the equations of equilibrium are less complicated. Advantage is taken of the circumstance that this particular investigation is confined to buckling with short longitudinal waves. From part I it appears that cases to be considered are: axially symmetrical buckling and buckling in cases I, II and III. The preliminary knowledge of these types of buckling, obtained from the system with distributed frames serves to give a judgement of what terms in the differential equations may be neglected. Thus it proves to be possible to simplify these equations so much that they can readily be integrated, leaving to be determined 8 integration constants for each bay ν (shell between 2 successive frames ν and $\nu+1$) of the cylinder (sec. 10 and 12.1). The integration constants of two successive bays are linked up by 8 conditions of compatibility of the distorted shell to each side of the frame and of the distorted frame itself (sec. 11). These equations (12.6 to 12.13) are difference equations in the integration constants. With a cylinder having m frames there are $m-1$ bays, 8 $(m-1)$ integration constants and 8 $(m-2)$ difference equations resulting from the compatibility of the distortions at the intermediate frames. The compatibility of the distortions or the stresses at the end frames yields 8 boundary conditions, making the system of linear equations complete. The coefficients of the difference equations contain the structural parameters introduced in part I: A, B_x, B_φ, C, F and in addition the parameter Q, characterizing the frame spacing; the buckling form parameter R, determined by the number of circumferential waves, therefore replacing N; the load parameter X, replacing P.

The solution of the system of 8 $(m-2)$ difference equations is assumed to be given by eq. (12.15). In this way the system of difference equations is being replaced by 8 homogeneous linear equations in the coefficients w_i (eq. 12.16). Equating its determinant to zero the expression (12.17) is obtained, linking up the parameters R, X and the buckling form parameter ρ. Due to the fact that (12.17) is of the 8th degree in ρ there are 8 solutions of the type (12.15) to each set of parameters R, X. So each set of boundary conditions can be satisfied by summing these 8 solutions. This means that (12.15) gives the general solution of the system of difference equations.

The critical load of cylinders having some length will not be affected very much by the conditions at the end frames, provided that the end frames are not weaker than the intermediate frames: A good approximation will be obtained by assuming the cylinder to be infinitely long. The infinitely long cylinder is analyzed further (sec. 12.3). From the condition that the displacements along the whole length of the cylinder are of equal order of magnitude, it follows that the parameter ϑ, replacing ρ and defined by eq. (12.18), is between the limits 0 and -4, and that the displacements of the frames are harmonic functions of the axial coordinate. Thus the buckling form can be characterized again by a longitudinal half-wave length, defined by eq. (12.27). The relation between the parameter ϑ and the average number of frames (ν_l) comprised in a half wave length has been plotted in fig. 14.

From equation (12.17) the value of ϑ, giving the minimal buckling load, should be determined. This equation is being discussed in sec. 13. The case $\vartheta = -4$, $\nu_l = 1$ corresponds to column failure of the stringers with the frames behaving as if they were rigid supports, hence the critical stress equals the column strength of the stringers.

In the case of axially symmetrical buckling ($R = 0$) the only structural parameter affecting the buckling load is Q. Fig. 15 shows what relation exists between Q, the critical load parameter P and the number of frames in a half-wave length ν_l. With increasing Q ν_l decreases. Increasing the extensional stiffness of the frames till it corresponds to $Q = 2\pi$ the half-wave length decreases till it is equal to the frame spacing. Thus, by making the frames so stiff, that Q exceeds 2π (condition 13.8) axially symmetrical general instability will not occur; the strength of the shell equals the column strength of the stringers.

For $Q < 2.5$ the load parameter P is less than 1 pct smaller than the value $P_{\min} = 2$, obtained from the orthotropic shell of part I. Over this range of Q, $\nu_l > 2$. Therefore, 2 frames on the half-wave length should be mechanically appreciated to be "many" frames. Only for $\nu_l < 1.5$ the critical load is affected more than 5 pct by the finiteness of frame spacing.

The critical load for axially non-symmetrical buckling can be determined by means of fig. 16. In order to have some idea of the critical wave form N_0 and Y_0 are determined assuming the uniformly distributed frame system. From eq. (13.10) the circumferential wave number n, being the nearest integer to n_0, is calculated, then R is known. The longitudinal wave length parameter γ_0 is computed from eq. (13.11); the corresponding parameter ϑ_0 is taken from fig. 14. Then K, being the left side of equation (12.17), is computed for the said value of R and three values of ϑ mentioned in fig. 16 and in the vicinity of ϑ_0. Thus, we find 3 numbers $K(\vartheta)$ and taking from the curves of fig. 16 the corresponding X we can plot X against ϑ. $P_{\min}$ is calculated from (13.12). This solution is correct only for structures having torsionally weak frames. For $B_\varphi \neq 0$ this method gives an approximation, that usually will be less than 1 pct in error. However, it is possible to calculate the correct value of the critical load; the method how to do it has been given in sec. 13.3.2.

Comparing the results obtained with distributed and with spaced frames it is concluded, that cases, having $\nu_l > 2$ ($\gamma_0 < \pi/2$), may be appreciated to be cases having "many" frames in one halfwave length; the approximation given by the distributed frame system being only a few percents in error.

The appendix to this paper illustrates by a numerical example how to calculate the critical load from given structural parameters.

Contents.

1 Introduction.

In order to provide sufficient bending strength the thin skin of fuselage shells is usually reinforced by a large number of equally spaced longitudinal stiffeners (stringers). A second system of stiffeners is given by the frames, the spacing of which is uniform as well. By these frames the correct shape of the cross section is maintained; local loads will be transmitted by them to the skin and last not least the frames provide support to the stringers in such a way that the stringers under compressive loads will fail as columns rigidly supported at the frames. It is not self-evident that this latter purpose will be realized by any system of frames. It may be that the structure will fail by "general instability", a type of instability in which the buckling of the stringers is accompanied by distortions of the frames. Obviously this type of failure is more likely to occur with frames that are more flexible in their plane. Therefore, the flexural rigidity of the frames should be such that general instability will occur at stresses that are equal to or larger than the stresses that will induce "column failure". Usually, the frames of smaller aircraft satisfy this requirement; with increasing body sizes, however, the frames tend to be relatively weaker and general instability may be the critical condition.

General instability of stiffened shells corresponds to local buckling in the case of the unstiffened shell; the wave length is circumferentially and longitudinally small compared to the diameter of the shell. On the other hand the longitudinal half-wave length will be larger than the frame spacing, since smaller wave lengths would raise the critical load over the buckling load corresponding to column failure. The circumferential wave length will be of the same order of magnitude. The stringer spacing being much more close than the frame spacing, each circumferential half-wave will comprise several stringers e.g. more than 3. This means that the system of stringers may be represented by a uniformly distributed system. This scheme is adopted in this report giving a theoretical investigation of the problem of general elastic instability. The first approach to the solution (part I) assumes the frames to be uniformly distributed as well. This solution will be reliable provided that the longitudinal half-wave length comprises several frames. In order to cover conditions in which the ratio of half-wave length and frame spacing approaches unity part II of this report deals with the system, in which the frames are equally spaced.

Though the phenomenon of general instability of fuselages will be due to bending of the fuselage, this report considers uniform axial compression, since this load system is mathematically easier to deal with, as known from the problem of the unstiffened cylindrical shell. The allowable compressive stress is of course somewhat smaller than the allowable bending stress.

2 The elastic scheme [1]).

2.1 *The skin.*

General instability should occur only at high stresses in the stringer. The thin skin (thickness t, radius a) will be loaded far beyond its buckling stress and the ability of the skin to carry additional loads due to additional strain will be greatly reduced. As far as the stiffness with respect to longitudinal and circumferential strain is concerned, the action of the skin may be represented by an "effective width" of skin, acting together with the stringer, resp. the frame. This width of skin is considered to be included in the stringer or the frame section. Thus, the skin panel between two successive stringers and frames will act as a "shear panel", carrying shear only. The skin being buckled by primary loads, the shear rigidity is assumed to be ηG, η being a number smaller than unity, depending upon the strain ratio $\frac{\bar{\varepsilon}}{\varepsilon_b}$, ε_b being the strain at which the panel will buckle. The stiffness of the skin against inextensional distortions is small compared to the corresponding stiffnesses of stringers and frames; therefore, this stiffness is assumed to be negligible.

The way in which the "effective width" is to be defined needs some further consideration. At the critical load the average stress in the skin panel is σ_{av}, whereas the stringer stress is $\bar{\sigma}$. The effective width of skin *carrying the load* is

$$w_e = w \frac{\sigma_{av}}{\bar{\sigma}}. \qquad (2.1)$$

The distortions connected with general instability will induce a change of strain at the edge of the skin panel; the edge stress changes with the amount $\Delta\bar{\sigma}$. The average stress in the skin panel changes with $\Delta\sigma_{av}$ and the increment of load carried by the panel $w\,\Delta\sigma_{av}$ can be represented by the effective width

$$w_e^* = w \frac{\Delta\sigma_{av}}{\Delta\bar{\sigma}}. \qquad (2.2)$$

This effective width represents the *stiffness of the panel* in compression at the critical load. w_e^* is smaller than w_e; the former can be expressed in the latter by

$$w_e^* = w_e \left[1 + \frac{1}{w_e} \frac{d w_e}{d \bar{\varepsilon}}\right]. \qquad (2.3)$$

[1]) Notations, not explained in the text, are being defined in sec. 9.

The effective width of skin operating with the frames (w_f) is assumed to be small compared to the frame spacing (b). Deflection of the stringers will cause extensional deformation of the skin. Small deflections, however, may be taken by the skin without extensional deformation since the curved skin panel can be flattened by bending moments allowing for a radial displacement $w^2/24a$ at the edges. Therefore, small deflections of the stringers are resisted by the skin only due to its bending stiffness which is very small indeed compared to the other stiffnesses.

The classical theory of elastic stability considers the possibility of infinitesimal unstable deformations, so, investigating this type of instability it seemed to be sound to neglect the stresses in the skin by radial deflections for those positions of the skin which are situated at some distance from the frames. The active portion near the frame is included in w_f.

Larger deflections are counteracted by extensional strains of the skin. In order to get some idea of the magnitude of the deflections at which the extensional strains will be important we take the example $a = 200$ cm, $w = 15$ cm. The radial displacement at which the skin between the stringers is completely flat is $\frac{-15^2}{24 \times 200} = 0.05$ cm. Actual failure will occur at larger deflections, so the extensional strains must be considered to be of practical importance. The correct consideration of the extensional strains is thwarted by 1° the fact, that inward deflections may occur without extensional strain; 2° the fact, that the skin is not cylindrical, but by local buckling of the skin the distortions due to instability of the structure apply to a corrugated skin. These circumstances need further investigation.

As far as part I is concerned the assumption of a small effective width w_f is of no basic importance. Just by assuming the correct numerical value of w_f the theory yields the correct critical load. Part II however would be affected more by a different behaviour of the skin. Since all lateral support by the skin is assumed to be confined to a narrow region near the frames, the stringers between the frames are free to deflect, the forces exerted by the skin and transmitted to the stringers being shear stresses only. Introduction of the tangential stresses of the skin would result in a serious increase of mathematical difficulties, which is avoided here. These difficulties have to be met if there would be experimental evidence that this effect of the skin cannot be expressed by an effective width.

2.2 *The grid of stringers and frames.*

Stringers and frames both are assumed to be connected to the skin. After distortion their cross sections remain plane and they are normal to the respective neutral axes. Stringers and frames are interconnected such that the elements, situated on the common normal to both neutral axes, stay upon this normal after distortion.

Stringers and frames have finite stiffnesses against extension, bending and torque. The latter stiffness is being introduced in order to account for closed stringer and frame sections.

The load p is applied to a cylinder with radius a_{xp}, this radius being defined by the centre of gravity of the stringer section together with the effective width of skin w_e. The neutral axis for buckling lies in the centre of gravity of the stringer section together with the effective width w_e^*; its radius is a_x. The load (p) and the cross

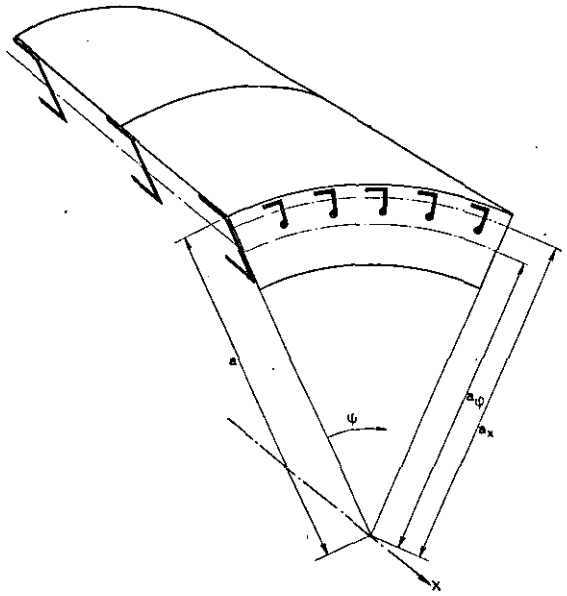

Fig. 1.
Main dimensions of the shell and coordinates.

section of stringers plus effective width (t_{xp}, t_x) is given per unit of length of the circle with radius a_x by

$$t_{xp} = \frac{a}{a_x} \frac{Q_s + w_e t}{w}, \tag{2.4}$$

$$t_x = \frac{a}{a_x} \frac{Q_s + w_e^* t}{w}, \tag{2.5}$$

$$p = \bar{\sigma} t_{xp}. \tag{2.6}$$

The neutral axis of the frame plus effective width w_f lies on a cylinder with radius a_φ, and its cross section (t_φ) is given per unit of length of the axis of x by

$$t_\varphi = \frac{1}{b} (Q_f + w_f t). \tag{2.7}$$

Part I. Uniformly distributed frames.

3 The distortions.

For the elastic scheme described in sec. 2 the displacement of any point can be calculated from the following displacements:

1, the axial displacement u_0 of the point with equal x and φ upon the cylinder a_x;

2, the angular displacement ψ_0 in the direction of φ of the point with equal x and φ upon the cylinder a_φ;

3, the radial displacement v, that is equal for all points with equal x and φ.

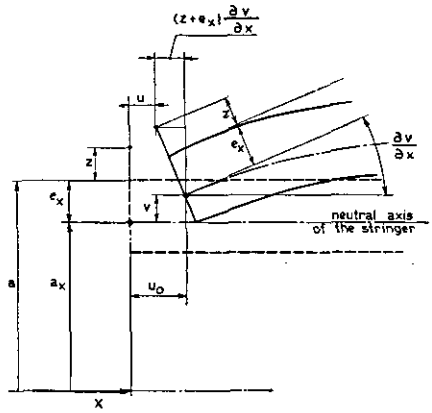

Fig. 2.
Determination of the axial displacement u.

$$\varepsilon_\varphi = \frac{\partial\,(a+z)\,\psi}{\partial\,(a+z)\,\varphi} + \frac{v}{a+z} = \frac{\partial\psi_0}{\partial\varphi} - \frac{z+e_\varphi}{a+z}\,\frac{\partial^2 v}{a_\varphi\,\partial\varphi^2} + \frac{v}{a+z}. \qquad (3.4)$$

The shear strain of the skin ($z=0$) is

$$\varepsilon_{x\varphi} = \left(\frac{\partial u}{a\partial\varphi} + \frac{\partial a\psi}{\partial x}\right)_{z=0} = \frac{\partial u_0}{a\partial\varphi} + \frac{a\partial\psi_0}{\partial x} - \left(\frac{e_x}{a} + \frac{e_\varphi}{a_\varphi}\right)\frac{\partial^2 v}{\partial x\partial\varphi}. \qquad (3.5)$$

The slope ω_x of the neutral axis of the frame in x, φ is (see fig. 3)

$$\omega_x = \varphi + \psi_0 - \frac{\partial v}{a_\varphi\,\partial\varphi}.$$

The specific twist of the stringer is (see fig. 4)

$$\kappa_{x\varphi} = -\frac{\partial\omega_x}{\partial x} = -\frac{\partial\psi_0}{\partial x} + \frac{\partial^2 v}{a_\varphi\,\partial x\partial\varphi}. \qquad (3.6)$$

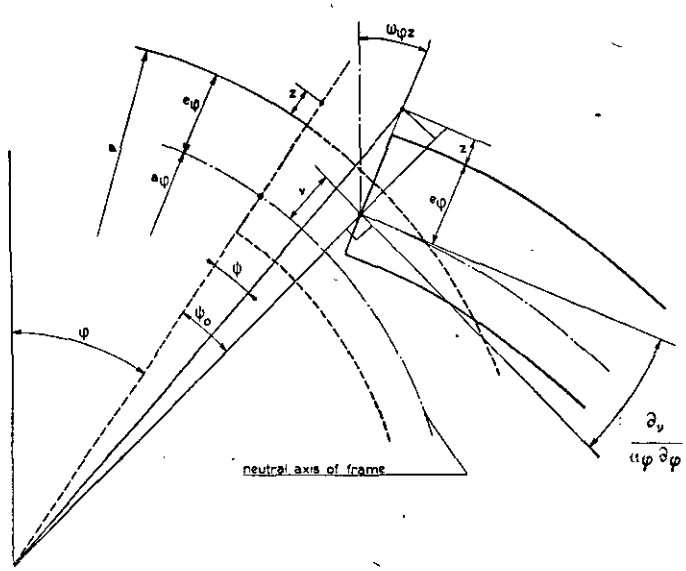

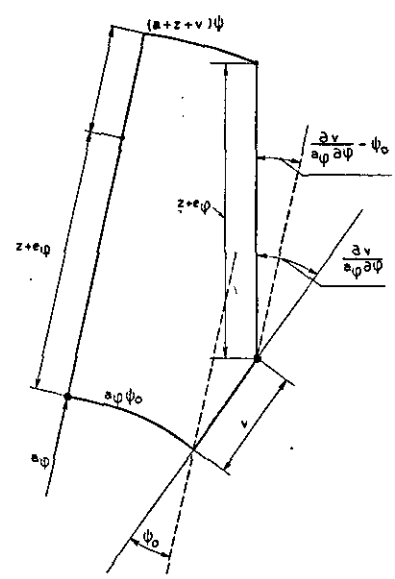

Fig. 3.
Determination of the angular displacement ψ.

$$a_\varphi\psi_0 + v\psi_0 - (z+e_\varphi)\left(\frac{\partial v}{a_\varphi\,\partial\varphi} - \psi_0\right) - (a+z+v)\,\psi = 0.$$

The displacements u and ψ of an arbitrary point x, φ, z (z = distance to the skin) are (see fig. 2 and 3):

$$u = u_0 - (z+e_x)\,\frac{\partial v}{\partial x}, \qquad (3.1)$$

$$\psi = \psi_0 - \frac{z+e_\varphi}{a+z}\cdot\frac{\partial v}{a_\varphi\,\partial\varphi}. \qquad (3.2)$$

The direct strains in the point z of the stringer, resp. the frame are

$$\varepsilon_x = \frac{\partial u}{\partial x} = \frac{\partial u_0}{\partial x} - (z+e_x)\,\frac{\partial^2 v}{\partial x^2}. \qquad (3.3)$$

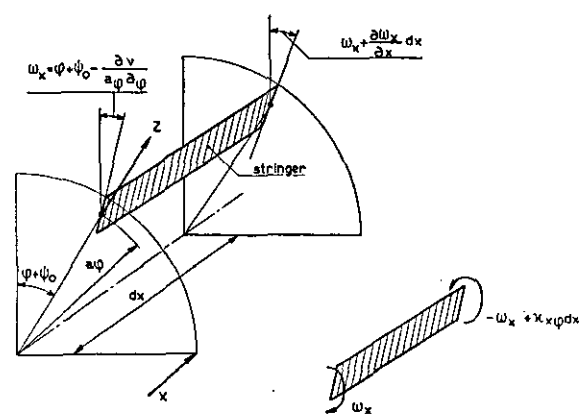

Fig. 4.
Determination of the specific twist of the stringers.

The slope ω_φ of the neutral axis of the stringer being (see fig. 2)

$$\omega_\varphi = -\frac{\partial v}{\partial x},$$

the specific twist of the frame is (see fig. 5)

$$\varkappa_{\varphi x} = -\frac{\partial \omega_\varphi}{a_\varphi \partial \varphi} = \frac{\partial^2 v}{a_\varphi \partial x \partial \varphi}. \tag{3.7}$$

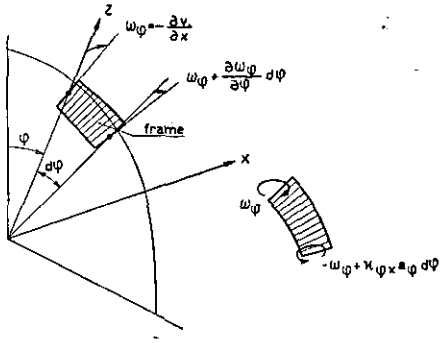

Fig. 5.

Determination of the specific twist of the frames.

4 The stresses upon an element of the shell.

Fig. 6 gives the stress resultants on the faces of the element dx, $d\varphi$ of the shell; induced by buckling. We will give them the name: additional

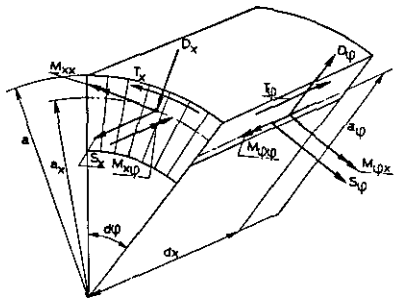

Fig. 6.

The stress resultants upon an element over the entire thickness of the shell.

stresses. The initial load p has not been reproduced. The forces S_x and D_x and the moments M_{xx} and $M_{x\varphi}$ refer to the unit of length along the circle with radius a_x; the shear load T_x refers to the unit of length of the circle a; the forces S_φ, T_φ and D_φ and the moments $M_{\varphi\varphi}$ and $M_{\varphi x}$ refer to the unit of length along the axis of x.

The additional stresses S, T, M_{xx} and $M_{\varphi\varphi}$ can be computed from the stress-strain relations

$$\left.\begin{aligned} \sigma_x &= E\,\varepsilon_x, \\ \sigma_\varphi &= E\,\varepsilon_\varphi, \\ \tau_{x\varphi} &= \eta\, G\, \varepsilon_{x\varphi} \end{aligned}\right\} \tag{4.1}$$

by means of

$$S_x\, a_x\, d\varphi = \int \sigma_x\, dt_x,$$

$$M_{xx}\, a_x\, d\varphi = -\int \sigma_x\, (z + e_x)\, dt_x,$$

$$T_x\, a\, d\varphi = \tau_x\, t a\, d\varphi,$$

$$S_\varphi\, dx = \int \sigma_\varphi\, dt_\varphi,$$

$$M_{\varphi\varphi}\, dx = -\int \sigma_\varphi\, (z + e_\varphi)\, dt_\varphi,$$

$$T_\varphi\, dx = \tau_\varphi\, t\, dx.$$

The centre of gravity of the cross section of the frame is being defined by

$$a_\varphi \int \frac{z + e_\varphi}{a + z}\, dt_\varphi = 0. \tag{4.2}$$

In this way it represents the centre of gravity of the elementary areas multiplied by $a_\varphi/a + z$. Nevertheless,

$$a_\varphi \int \frac{dt_\varphi}{a + z} = \int dt_\varphi = t_\varphi\, dx.$$

Defining I_{xx} and $I_{\varphi\varphi}$ by

$$\int (z + e_x)^2 dt_x = I_{xx} t_x d\varphi, \tag{4.3}$$

$$a_\varphi \int \frac{(z + e_\varphi)^2}{a + z}\, dt_\varphi = I_{\varphi\varphi}\, dx, \tag{4.4}$$

it follows from the formulas given above that

$$S_x = E\, t_x \frac{\partial u_0}{\partial x}, \tag{4.5}$$

$$M_{xx} = E I_{xx} \frac{\partial^2 v}{\partial x^2}, \tag{4.6}$$

$$S_\varphi = E t_\varphi \left(\frac{\partial \psi_0}{\partial \varphi} + \frac{v}{a_\varphi}\right), \tag{4.7}$$

$$M_{\varphi\varphi} = E I_{\varphi\varphi} \left(-\frac{\partial \psi_0}{a_\varphi\, \partial \varphi} + \frac{\partial^2 v}{a_\varphi^2\, \partial \varphi^2}\right) \tag{4.8}$$

The shear stresses τ_x and τ_φ are unequal (see sec. 5); their difference, however, is of the order $\overline{\varepsilon\, \tau}$. Terms of this order may be neglected in the relations between buckling stresses and buckling deformation (see sec. 5); therefore it is arbitrary which of these stresses is assumed to be equal to $\tau_{x\varphi}$. We assume

$$\tau_\varphi = \tau_{x\varphi},$$

from which it follows that

$$T_\varphi = \eta G t \left[\frac{\partial u_0}{a \partial \varphi} + a \frac{\partial \psi_0}{\partial x} - \left(\frac{e_x}{a} + \frac{e_\varphi}{a_\varphi}\right) \frac{\partial^2 v}{\partial x \partial \varphi}\right]. \tag{4.9}$$

Indicating the torsional rigidities of stringers and frames, with respect to the unit of length along the circle a_x and the axis of x resp. with $G\, I_{x\varphi}$ and $G\, I_{\varphi x}$, it follows

$$M_{x\varphi} = G\, I_{x\varphi}\, \varkappa_{x\varphi} = G\, I_{x\varphi} \left(-\frac{\partial \psi_0}{\partial x} + \frac{\partial^2 v}{a_\varphi\, \partial x \partial \varphi}\right), \tag{4.10}$$

$$M_{\varphi x} = G\, I_{\varphi x}\, \varkappa_{\varphi x} = G\, I_{\varphi x} \frac{\partial^2 v}{a_\varphi \partial x \partial \varphi}. \tag{4.11}$$

The forces T_x, D_x and D_φ cannot be expressed in the displacements u_0, ψ_0, v by direct stress-strain relations.

5 The equilibrium.

5.1 *A general remark on problems of stability.*

The equations of equilibrium for an element dx, $d\varphi$ of the shell at the critical load may be written as

$$\Sigma \text{ additional stresses} = -\text{external load.}$$

The terms forming the left side of this equation are identical to those occurring in the linear equations of equilibrium of the common problem of elasticity, formally written: S. The right side is characteristic for stability problems; it is composed of terms of the shape: critical load times linear function of the additional displacements, formally written pu. If the right side vanishes the homogeneous equations allow for the solution $u = 0$ only. The possibility of buckling, therefore of additional stresses, requires $p \neq 0$.

If the right side contains terms of the shape p times strain (ε or κ) its order of magnitude is $p\,\varepsilon = \bar{\varepsilon}\,S$. In this case the right side would be of the order $\bar{\varepsilon}$ small compared to each term of the left hand side. This implies that the initial load p will be able to distort the structure only if $\bar{\varepsilon}$ approaches unity. This case however is of no technical importance; we are interested only in instabilities with small $\bar{\varepsilon}$. The latter instabilities will occur only if the right side contains terms pu, in which the functions of u are of a larger order of magnitude than the strains. The other terms, of the order $p\,\varepsilon$, may be neglected; they are not essential. These larger functions of u are represented by the rotations ω. Though these rotations originate from the strains, they can have a higher order of magnitude by the fact, that they are being built up by integrating strains along the length of the structure. This is the basic reason for the fact that instability at strains in the technically important region will occur only with slender structures, in which the length is much larger than one of the cross sizes.

We have found that the essential terms of the right side have the shape $p\,\omega$, whereas the terms $p\,\varepsilon = \bar{\varepsilon}\,S$ are negligible. This conclusions implies:

1. that the relations (4.1) for additional stress and strain are correct. (It is not essential to compute the additional stresses from the strains that according to Hooke's law refer to the sizes of the unloaded structure. E. g. the strain ε_x had to be replaced by $\varepsilon_x(1-\bar{\varepsilon})$ in the expression $\sigma_x = E\,\varepsilon_x$.);
2. that for the stability of shells the pu-terms referring to the rotations in planes normal to the shell are essential;
3. that for the stability of shells the pu-terms referring to the rotation parallel to the shell are essential only, if the wave length of the buckled shell is much larger than the circumferential size of the shell.

5.2 *The equations of equilibrium.*

According to sec. 5.1 we may determine separately:

1. The terms constituted by the additional stresses, which refer to the unbuckled element of the shell;
2. the terms depending upon the initial load p, which represent the external load of the element and refer to the element distorted by buckling.

In determining the first group of terms we must introduce the second group by assuming external loads R_x, R_φ, R_z in the direction of x, φ and z and external moments J_x, J_φ, J_z. The additional forces and the additional moments are given in

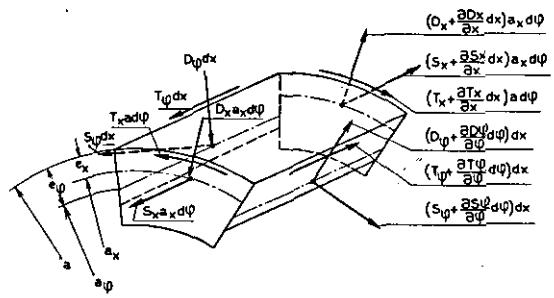

Fig. 7a.

The additional forces applied to the element of the shell.

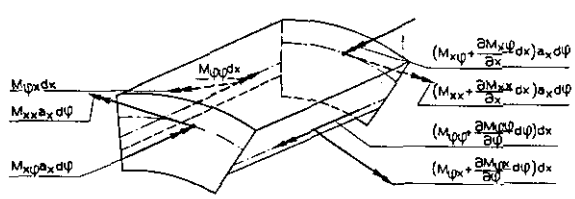

Fig. 7b.

The external load of the distorted element of the shell.

fig. 7a, b respectively. The equations of equilibrium are

$$a_x \frac{\partial S_x}{\partial x} + \frac{\partial T_\varphi}{\partial \varphi} + R_x = 0, \tag{5.1}$$

$$\frac{\partial S_\varphi}{\partial \varphi} + a\frac{\partial T_x}{\partial z} + D_\varphi + R_\varphi = 0, \tag{5.2}$$

$$a_x \frac{\partial D_x}{\partial x} + \frac{\partial D_\varphi}{\partial \varphi} - S_\varphi + R_z = 0, \tag{5.3}$$

$$-a_x \frac{\partial M_{x\varphi}}{\partial x} - \frac{\partial M_{\varphi\varphi}}{\partial \varphi} - a\,D_\varphi - e_\varphi \frac{\partial S_\varphi}{\partial \varphi} + J_z = 0, \tag{5.4}$$

$$a_x \frac{\partial M_{xx}}{\partial x} + \frac{\partial M_{\varphi x}}{\partial \varphi} + a_z D_x + e_x a_z \frac{\partial S_x}{\partial_x} + J_\varphi = 0, \tag{5.5}$$

$$-M_{\varphi x} - aT_x + aT_\varphi + J_z = 0. \tag{5.6}$$

The external load is given in fig. 8; it consists of the pair of forces $p\, a_x d\varphi$ acting upon the radial faces x and $x + dx$ of the cylinder with radius a_{xp}. These two forces are equal and parallel to the axis of x; their points of application are shifted normal to the axis of x. Therefore, the external loads of

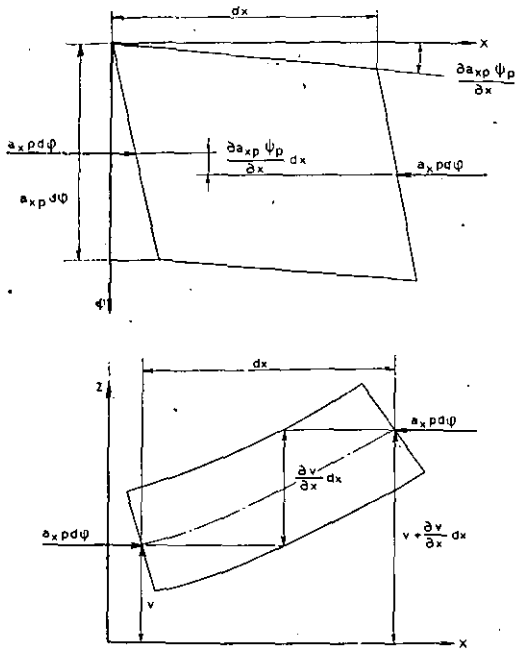

Fig. 8.

The external load of the distorted element of the shell.

the elements consist of moments about the axis of φ and z.

$$J_\varphi = p\,\frac{\partial v}{\partial x}, \tag{5.7}$$

$$J_z = -\,p\,\frac{\partial a_{xp}\psi_p}{\partial x}. \tag{5.8}$$

ψ_p is the tangential displacement upon the cylinder with radius a_{xp}

$$\psi_p = \psi_0 + \frac{e_{xp} - e_\varphi}{a_{xp}}\;\frac{\partial v}{a_\varphi\,\partial\varphi}. \tag{5.9}$$

The other components of the external load are equal to zero.

$$R_x = R_\varphi = R_z = J_x = 0. \tag{5.10}$$

6 The differential equations in the displacements.

Substituting from (4.5/11) into (5.1/6) the equations of equilibrium will be expressed in the displacement functions u_0, ψ_0, v, except for the additional stresses D_x, D_φ and T_x. Eliminating these latter quantities by

$$(5.2) + \frac{1}{a}\,(5.4) + \frac{\partial}{\partial x}\,(5.6) = 0, \tag{6.1}$$

$$-\,(5.3) - \frac{1}{a}\,\frac{\partial}{\partial\varphi}\,(5.4) + \frac{\partial}{\partial x}\,(5.5) = 0, \tag{6.2}$$

we will obtain 3 differential equations in u_0, ψ_0, v. We do not give these equations explicitly, since we want to give them in a simplified and non-dimensional form. We introduce the non-dimensional coordinate ξ instead of x, the quantity λ and the non-dimensional parameters c, f_x, f_φ, f, f_p, r, s, K_{xx}, $K_{\varphi\varphi}$, $K_{x\varphi}$, $K_{\varphi x}$, K, which describe the elastic system, and the non-dimensional displacement functions U, Ψ, V (see notations, sec. 9). The way in which U and Ψ have been defined is somewhat artificial; however, in this way the differential equations will have a more regular structure since all partial differential quotients of the same equation will be simultaneously of odd or even order. Finally we introduce the symbols

$$(\;)' = \frac{\partial(\;)}{\partial\xi} \quad\text{and}\quad (\;)^{\cdot} = \frac{\partial(\;)}{\partial\varphi}.$$

With these symbols the additional stress resultants given in (4.5/11) are

$$S_x = \frac{a_x}{a\lambda}\,U'', \quad S_\varphi = \frac{s}{\lambda}\,(\Psi^{\cdot\cdot} + V),$$

$$T_\varphi = \frac{a_x}{(a\;a_\varphi)^{1/2}}\;\frac{r}{\lambda}\,(U + \Psi - fV)'^{\cdot} \tag{6.3}$$

$$M_{xx} = \frac{aa_x}{a_\varphi}\;\frac{K_{xx}}{\lambda}\,V'', \quad M_{\varphi\varphi} = a\,\frac{K_{\varphi\varphi}}{\lambda}\,(-\Psi + V)^{\cdot\cdot},$$

$$M_{x\varphi} = \left(\frac{a^3}{a_\varphi}\right)^{1/2}\frac{K_{x\varphi}}{\lambda}\,(-\Psi + V)'^{\cdot},$$

$$M_{\varphi x} = a_x\left(\frac{a}{a_\varphi}\right)^{1/2}\frac{K_{\varphi x}}{\lambda}\,V'^{\cdot}.$$

Then the equations of equilibrium (5.1) (6.1, 2) can be written

$$X' \equiv \left\{\frac{1}{r}\,(1 - f_\varphi)\,U'' + \dot{U}^{\cdot} + \dot{\Psi}^{\cdot} - fV^{\cdot\cdot}\right\}' = 0, \tag{6.4}$$

$$\Phi^{\cdot} \equiv \{rU'' + [r + K_{x\varphi} - (1 + f_p)c]\,\Psi'' + [s(1 - f_\varphi) + K_{\varphi\varphi}]\,\Psi^{\cdot\cdot} + s(1 - f_\varphi)\,V - (rf + K - f_p c)\,V'' - K_{\varphi\varphi}\,V^{\cdot\cdot}\}^{\cdot} = 0, \tag{6.5}$$

$$-Z \equiv f_x U''''' + s\,\Psi^{\cdot\cdot} - K_{x\varphi}\,\Psi''^{\cdot\cdot} + (sf_\varphi - K_{\varphi\varphi})\,\Psi^{\cdot\cdot\cdot\cdot} + sV + cV'' + sf_\varphi\,V^{\cdot\cdot} + K_{xx}V''''' + KV''^{\cdot\cdot} + K_{\varphi\varphi}\,V^{\cdot\cdot\cdot\cdot} = 0. \tag{6.6}$$

Integrating (6.4) over ξ and (6.5) over φ we get

$$X = C_1(\varphi) \quad\text{and}\quad \Phi = C_2(\xi).$$

Due to the way in which U and Ψ have been defined, these functions themselves have no physical sense, only their derivatives U' and $\Psi^{\cdot\cdot}$ Therefore, if U and Ψ satisfy, the functions $U_1 = U + \overline{U}(\varphi)$ and $\Psi_1 = \Psi + \overline{\Psi}(\xi)$ will satisfy as well.

Choosing $\overline{U}$ and $\overline{\Psi}$ such that

$$-\,\overline{U}^{\cdot\cdot} = C_1(\varphi),$$

$$-\,[r + K_{x\varphi} - (1 + f_p)c]\,\overline{\Psi}'' = C_2(\xi),$$

U_1 and Ψ_1 will satisfy the equation $X = \Phi = 0$. Therefore without restriction of the physical sense of U and Ψ we may replace the equations (6.4, 5) by

$$X \equiv \frac{1}{r}\,(1-f_\varphi)\,U'' + U^{\cdot\cdot} + \Psi^{\cdot\cdot} - fV^{\cdot\cdot} = 0, \qquad (6.7)$$

$$\Phi \equiv r\,U'' + [r + K_{x\varphi} - (1+f_p)c]\,\Psi'' + [s(1-f_p) + K_{\varphi\varphi}]\,\Psi^{\cdot\cdot} + s(1-f_\varphi)\,V - (rf + K - f_p c)V'' - K_{\varphi\varphi}\,V^{\cdot\cdot} = 0. \qquad (6.8)$$

7 The solution of the equations.

7.2 *The determinant.*

For suitable boundary conditions, as are present with the infinitely long cylinder, the solution will be

$$\frac{U}{-U_0} = \frac{\Psi}{-\Psi_0} = \frac{V}{-V_0} = \cos m\,\xi \cos n\,\varphi. \qquad (7.1)$$

So the differential equations (6.6, 7, 8) yield 3 linear homogeneous equations in U_0, Ψ_0, V_0. Buckling occurs if the determinant of this system of equations is equal to zero. Thus, we obtain the following condition for calculating the critical load parameter c from the structural parameters and the buckling parameters m and n:

$$\begin{vmatrix} \frac{1}{r}(1-f_\varphi)m^2 + n^2 & n^2 & fn^2 \\ r\,m^2 & [r + K_{x\varphi} - (1+f_p)c]m^2 + [s(1-f_\varphi) + K_{\varphi\varphi}]n^2 & s(1-f_\varphi) + K_{\varphi\varphi}\,n^2 + (rf + K - f_p c)m^2 \\ -f_x m^4 & n^2[s + K_{x\varphi}m^2 - (sf_\varphi - K_{\varphi\varphi})n^2] & s - cm^2 - sf_\varphi n^2 + K_{xx}m^4 + Km^2n^2 + K_{\varphi\varphi}\,n^4 \end{vmatrix} = 0$$

For $n = 0$ this equation yields

$$[r + K_{x\varphi} - (1+f_p)c]\left(\frac{s}{m^2} - c + K_{xx}m^2\right) = 0. \qquad (7.3)$$

For $n \neq 0$, introducing the parameter $y = \frac{m^2}{n^2}$, (7.2) yields

$$\begin{vmatrix} \frac{1}{r}(1-f_\varphi)\,y + 1 & 1 & f \\ ry & [r + K_{x\varphi} - (1+f_p)c]\,y + s(1-f_\varphi) + K_{\varphi\varphi} & \frac{s}{n^2}(1-f_\varphi) + (rf + K - f_p c)y + K_{\varphi\varphi} \\ -f_x y^2 & \frac{s}{n^2} + K_{x\varphi}y - sf_\varphi + K_{\varphi\varphi} & \frac{s}{n^4} - \frac{c}{n^2}y - \frac{s}{n^2}f_\varphi + K_{xx}y^2 + Ky + K_{\varphi\varphi} \end{vmatrix} = 0 \qquad (7.4)$$

The evaluation of this determinant will be simplified after a discussion of the order of magnitude of the parameters involved, which will reveal the terms that may be neglected.

7.2 *Discussion of the parameters.*

t, t_x and t_φ represent areas of cross sections per unit of length; therefore r and s are of the order of unity.

I_{xx}, $I_{\varphi\varphi}$, $I_{x\varphi}$ and $I_{\varphi x}$ are of the order $i^2 t$, where i is the radius of gyration of the stringer or the frame section. Therefore K_{xx}, $K_{\varphi\varphi}$, $K_{x\varphi}$, $K_{\varphi x}$ and K are of the order $\left(\frac{i}{a}\right)^2$. The strain $\bar{\varepsilon}$ at which general instability will occur is of the order $\frac{i}{a}$, as will appear later in this report. Therefore the K's will be of the order $\bar{\varepsilon}^2$.

The parameters f and g are of the order $\frac{e}{a}$ and as e and i are of the same order of magnitude the f's and g are of the order $\bar{\varepsilon}$. The load parameter c is of the order $\bar{\varepsilon}$.

The parameter n gives the number of waves over the circumference of the cylinder; therefore it can be any integer.

The parameter y is equal to the square of the wave length ratio longitudinally and circumferentially. With infinitely long cylinders it can have any positive value; there are 3 classes to be considered: $y \ll 1$; $y \approx 1$; $y \gg 1$.

We now introduce new structural parameters A, B_x, B_φ, B, C, F_x, F_φ, F, F_p and the new load parameter P, all of them being of the order of unity. The buckling parameters n and y are replaced by N and Y, which can have various

orders of magnitude. Quantities of the order $\bar{\varepsilon}$ are represented by the number k, which served to transform our original parameters into the parameters of the order of unity. The determinant (7.4) written in the new parameters is

$$\begin{vmatrix} 1+AY-(AF_\varphi\, Y)k & 1 & F \\ Y/A & 1+Y/A-(F_\varphi+PY)k+(C+B_xY-F_pPY)k^2 & N+FY/A+ \\ & & +(-NF_\varphi+ \\ & & +C+BY- \\ & & -F_pPY)k \\ -F_xY^2 & N-F_\varphi+(C+B_xY)k & N^2-NF_\varphi+C+ \\ & & +BY+Y^2-NPY \end{vmatrix} = 0 \qquad (7.5)$$

7.3 *Evaluation of the determinant.*

Evaluating the determinant (7.5) simultaneously taking together terms with equal powers of k, N and Y, we find:

$$\sum_{i=1}^{3}\sum_{j=0}^{2}\sum_{l=0}^{4}\gamma_{i,j,l}\,k^iN^jY^l=0\,. \qquad (7.6)$$

Owing to the way in which the structural parameters have been chosen $\gamma_{i,j,l}$ is of the order of unity. Therefore $\gamma_{i+1,j,l}\,k^{i+1}N^jY^l$ will be small of the order k (or $\bar{\varepsilon}$) compared to $\gamma_{i,j,l}\,k^i\,N^j\,Y^l$. Neglecting $\bar{\varepsilon}$ to unity, as we have done before in deducing the equations of equilibrium, we may neglect all terms $\gamma_{i,j,l}\,k^iN^jY^l$ of higher order in k than k^i, provided that $\gamma_{i,j,l}$ is unequal to zero. So the evaluation of (7.5) results in:

$$\begin{gathered}(\gamma_{000}+\gamma_{001}Y+\gamma_{002}Y^2+\gamma_{003}Y^3+\gamma_{004}Y^4)+\\ +N(\gamma_{011}Y+\gamma_{012}Y^2+\gamma_{013}Y^3)+\\ +\gamma_{022}N^2Y^2+k[\gamma_{110}N+\gamma_{121}N^2Y]+k^2\gamma_{220}N^2=0,\end{gathered}$$

or expressed in the parameters

$$\begin{gathered}(N-F)^2Y^2+(Y^2+AY+1)(Y^2+BY+C)-\\ -PNY(Y^2+AY+1)-k(PN^2Y+2CN)+\\ +k^2CN^2=0\,.\end{gathered}$$

Solving for the load parameter P we obtain, replacing kN by $\frac{1}{n^2}$,

$$\begin{aligned}P=\Big[&\frac{(N-F)^2}{N(Y+A+1/Y)}+\frac{Y+B+C/Y}{N}-\\ &-(2-1/n^2)\frac{C}{NY}\;\frac{1}{n^2(Y^2+AY+1)}\Big]:\Big(1+\\ &+\frac{1}{n^2(Y^2+AY+1)}\Big)\,. \qquad (7.7)\end{aligned}$$

We conclude from (7.7) that the critical load depends upon the structural parameters A, B, C, F and k and upon the wave form parameters N and Y.

8 Discussion of the various cases of buckling.

8.1 *Axially symmetrical buckling.*

According to (7.3) the critical load is

$$\left.\begin{aligned}&c=\frac{r+K_{x\varphi}}{1+f_p}\\ \text{and}\qquad&\\ &c=\frac{s}{m^2}+K_{xx}m^2.\end{aligned}\right\} \qquad (8.1)$$

The first solution corresponds to critical strains of the order of unity, therefore it is of no real significance.

The second solution is of the order of k for $m^2\sim 1/k$.

The critical load is

$$c_{\min}=2\,s^{1/2}k \quad\text{or}\quad P_{\min}=2 \quad\text{at}\quad m_0=s^{1/4}k^{-1/2}. \qquad (8.2a)$$

The half-wave length l_0 is, neglecting terms of the order k to unity,

$$l_0=\pi\,s^{-1/4}k^{1/2}\,a_x\,, \qquad (8.2b)$$

therefore, it is of the order $k^{1/2}$ small in comparison to a_x.

8.2 *Axially non-symmetrical buckling.*

Equation (7.7) yields ∞^2 buckling loads: one buckling load for each pair of N and Y-values that is consistent with the boundary conditions.

The series of possible values of N and Y are

$$\left.\begin{aligned}N&=\frac{1}{n^2k}\,,\\ Y&=\left(\frac{\pi\,\mu}{n}\;\frac{a_x}{L}\right)^2\frac{a}{a_\varphi s^{1/2}}\,,\end{aligned}\right\} \qquad (8.3)$$

where

$n=1,\ 2,\ 3,\ \ldots\ldots\ldots,$

$\mu=$ the number of half waves over the length L of the cylinder, which is supported in some particular way at its edges.

The minimum buckling load, the critical load, is determined by assuming that N and Y are continuous. Those values of N and Y which yield the critical load will correspond in general to values of n and μ (n_0, μ_0) that are not integer. To get a more accurate value of the critical load the buckling load is to be calculated for the adjacent integers n_1, n_2, μ_1, μ_2. Therefore the calculation *starts with determining the minimum of P as a* continuous function of N and Y. We will not do

that from (7.7) directly, but in order to simplify the analysis we will split up the whole range of possible values of Y in 5 partial ranges, for each of which the formula (7.7) reduces to a less complicated shape owing to the fact that quantities of the order k should be neglected to unity.

The various classes of Y are: Y of the order k^{-1}, $k^{-1/2}$, 1, $k^{1/2}$, k respectively. Table I gives a survey of the results obtained for these classes except for class $Y \sim 1$ and the way in which they are obtained. In order to give a more detailed description of the method we will deal with the *class* $Y \sim k^{-1}$.

According to the limit of exactness of our solutions k is negligible to 1, and 1 is negligible to Y. Hence, (7.7)reduces to

$$P = \frac{(N-F)^2}{NY} + \frac{Y}{N}. \qquad (8.4)$$

In order to quarantee that the buckling stress is in the elastic range, P should not be larger than the order of unity; therefore $\frac{(N-F)^2}{NY}$ and $\frac{Y}{N}$ both should not be larger than the order of unity. $\frac{(N-F)^2}{NY} = \frac{N}{Y} - \frac{2F}{Y} + \frac{F^2}{NY} \lesssim 1$ implies $\frac{N}{Y} \lesssim 1$. Together with $\frac{Y}{N} \lesssim 1$ the former result yields $\frac{N}{Y} \sim 1$; therefore $N \sim k^{-1}$ and from (8.1) $n^2 \sim 1$.

Neglecting now F to N (8.4) reduces to

$$P = \frac{N}{Y} + \frac{Y}{N}, \qquad (8.5)$$

which is minimum for $N/Y = 1$.

In basically the same manner all results listed in table I have been obtained.

The class $Y \sim 1$.

With $Y \sim 1$ P can be of the order of unity only if $N \sim 1$, therefore (7.7) reduces to

$$P = \frac{(N-F)^2}{N(Y+A+1/Y)} + \frac{1}{N}(Y+B+C/Y). \qquad (8.6)$$

P is minimum with $\frac{\partial P}{\partial N} = \frac{\partial P}{\partial Y} = 0$.

$\frac{\partial P}{\partial N} = 0$ at $N = N_0$, satisfying:

$$N_0^2 - F^2 = (Y+A+1/Y)\,(Y+B+C/Y). \qquad (8.7)$$

$\frac{\partial P}{\partial Y} = 0$ at $Y = Y_0$, satisfying

$$N - F = (Y_0+A+1/Y_0)\left(\frac{Y_0^2-C}{Y_0^2-1}\right)^{1/2}. \qquad (8.8)$$

We have to determine N_0, Y_0, satisfying both equations.

(8.7) : (8.8) yields

$$N_0 + F = (Y_0+B+C/Y_0)\left(\frac{Y_0^2-1}{Y_0^2-C}\right)^{1/2} \qquad (8.9)$$

(8.8) + (8.9) yields

$$N_0 = \frac{1}{2}\left(\frac{Y_0^2-1}{Y_0^2-C}\right)^{1/2}\left[(Y_0+A+1/Y_0)\,\frac{Y_0^2-C}{Y_0^2-1} + Y_0+B+C/Y_0\right], \qquad (8.10)$$

and (8.8) — (8.9) yields the equation of the 4th degree in Y_0

$$(A-B)\,Y_0^2 + 2\,(1-C)\,Y_0 + (B-AC) + 2F\,[\,(Y_0^2-1)\,(Y_0^2-C)\,]^{1/2} = 0, \qquad (8.11)$$

the positive real roots of which in the range $k^{1/2} \ll Y \ll k^{-1/2}$ give the solution to our problem. Substituting $N_0 - F$ from (8.8) and N_0 from (8.10) into (8.6) we find the critical load

$$P_{\min} = 2\left(\frac{Y_0^2-C}{Y_0^2-1}\right)^{1/2}. \qquad (8.12)$$

(8.12) gives $P_{\min}$ provided that $\frac{\partial^2 P}{\partial N^2}$ and $\frac{\partial^2 P}{\partial Y^2}$ are positive. Obviously this is true as far as $\frac{\partial^2 P}{\partial N^2}$ is concerned, since

$$\frac{\partial^2 P}{\partial N^2} = \frac{2}{N\,(Y + A + 1/Y)}.$$

However, it seems that

$$\frac{\partial^2 P}{\partial Y^2} = \frac{2}{NY^3}\,\frac{(Y^2-C)\,(Y^2-1)}{Y^2+AY+1} + \frac{(C-1)\,Y^2}{Y^2-1}$$

may be negative. $P_{\min}$ being a real positive number between 0 and 2 it follows from (8.12) that

$$\text{for } C < 1\text{: } Y_0^2 < C, \qquad \text{and} \quad \text{for } C > 1\text{: } Y_0^2 > C. \qquad (8.13)$$

Hence we conclude that $(Y_0^2-C)\,(Y_0^2-1)$ and $\frac{C-1}{Y_0^2-1}$ are positive, and $\frac{\partial^2 P}{\partial Y^2}$ will be positive as well.

An objection against applying (8.11, 12) is that (8.11) is rather tedious to solve. We therefore prefer a graphical method of dealing with the condition $\partial P/\partial Y = 0$.

Substituting N_0 from (8.7) into (8.6) we find

$$P = \frac{2}{Y+A+1/Y}\left\{\left[(Y+A+1/Y)\,(Y+B+C/Y)+F^2\right]^{1/2} - F\right\}, \qquad (8.14)$$

which is to be calculated for a few values of Y. Plotting P against Y we will find $P_{\min}$. A more accurate calculation of $P_{\min}$ is obtained in the following way. Taking the smallest of the calculated values of P as a first approximation P_1 of $P_{\min}$, we determine Y_0 from (8.12)

$$Y_0 = \left(\frac{C - {}^1/_4\,P_1^2}{1 - {}^1/_4\,P_1^2}\right)^{1/2}. \qquad (8.15)$$

Substituting this approximation of Y_0 into (8.14) we find $P_{\min}$. In determining P_1 it is useful to have a guide in choosing the range of Y such that it comprises Y_0.

class	$\underset{\sim}{Y}$	P	$P \sim 1$ yields	simplified formula for P	P_{min}	P is minimal at	$\boxed{\frac{l_0}{a_x}}$
I	k^{-1}	$\frac{(N-F)^2}{NY} + \frac{Y}{N}$	1° $\frac{N}{Y} \lesssim 1$ } $N/Y \sim 1$ 2° $\frac{Y}{N} \lesssim 1$ } $N \sim k^{-1}$ $\boxed{n^2 \sim 1}$	$\frac{N}{Y} + \frac{Y}{N}$	from $\frac{dP}{d\,(N/Y)} = 0$: $\boxed{2}$	$Y_0 = N$	$\pi\, s^{-1/4}\, k^{1/2}$ (order of $k^{1/2}$)
II	$k^{-1/2}$	$\frac{(N-F)^2}{N(Y+A)} + \frac{Y+B}{N}$	$\frac{Y}{N} \sim 1 \rightarrow N \sim k^{-1/2}$ $\boxed{n^2 \sim k^{-1/2}}$	no simplification	from $\frac{\partial P}{\partial Y} = 0$: $\boxed{2 - n^2 k (A - B + 2F)}$	$Y_0 + A = N - F$	$\frac{\pi\, s^{-1/4}\, k^{1/2}}{1 - \frac{n^2}{2} - k(A+F)}$ order of $k^{1/2}$
III	1	no simplification	$N \sim 1$ $\boxed{n^2 \sim k^{-1}}$	$\frac{(N-F)^2}{N(Y+A+1/Y)} +$ $+ (Y + B + C/Y)/N$	see sec. 8.2		$\pi\, s^{-1/4}\, k^{1/2} \left(\frac{N}{Y}\right)_0^{1/2}$ order of $k^{1/2}$
IV	$k^{1/2}$	$(N-F)^2 Y + B + A C + \frac{\left(1-\frac{1}{n^2}\right)^2 \frac{C}{Y}}{N\left(A Y + 1 + \frac{1}{n^2}\right)}$	1°, $\frac{(N-F)^2\, Y}{N} \lesssim 1 \rightarrow$ $\rightarrow N Y \lesssim 1$ 2°, $\frac{C}{NY} \lesssim 1 \rightarrow$ $\rightarrow N Y \gtrsim 1$ $\rightarrow N Y \sim 1$ $N \sim k^{-1/2}$ $\boxed{n^2 \sim k^{-1/2}}$	$NY\left(1 - \frac{1}{n^2} - A Y\right) +$ $+ \frac{C}{NY}\left(1 - \frac{3}{n^2}\right) +$ $+ \frac{B}{N} - 2 F Y$	from $\frac{\partial P}{\partial Y} = 0$: $\boxed{(1 - 2/n^2)\, 2\, C^{1/2} - n^2 k\,(A C + 2 F C^{1/2} - B)}$	$Y_0 = \frac{C^{1/2}}{N}\left[1 - \frac{1}{n^2} + n^2 k\,(A C^{1/2} + 2F)\right]$	$\frac{\pi\,(Cs)^{-1/4}\, k^{-1/2}\, n^{-2}}{1 - \frac{1}{2n^2} + \frac{n^2}{2} k\left(A C^{1/2} + 2F\right)}$ (order of unity)
V	k	$\frac{NY + (1 - 1/n^2)^2 \frac{C}{NY}}{1 + 1/n^2}$	1°, $NY \lesssim 1$ 2°, $NY \gtrsim 1$ $N Y \sim 1$ ↓ $N \sim k^{-1}$ $\boxed{n^2 \sim 1}$	1°, $n \neq 1$; no simplification	from $\frac{\partial P}{\partial NY} 0$; $\boxed{\frac{n^2 - 1}{n^2 + 1}\, 2\, C^{1/2}}$	$Y_0 = \left(1 - \frac{1}{n^2}\right) \frac{C^{1/2}}{N}$	$\frac{\pi\,(Cs)^{-1/4}\, k^{-1/2}\, n^{-2}}{(1 - 1/n^2)^{1/2}}$ (order of $k^{-1/2}$)
				2°, $n = 1$: $\frac{1}{2} NY$, from wich $c = \frac{1}{2} m^2$ and bucking load $\frac{\pi^2 EI}{l^2}$ (column failure)			

It can be shown, that

$$\left.\begin{array}{l}\text{for } C<1\text{: } (Y_0)_{F>0} > (Y_0)_{F=0} > (Y_0)_{F<0};\\ \text{and}\\ \text{for } C>1\text{: } (Y_0)_{F>0} < (Y_0)_{F=0} < (Y_0)_{F<0}.\end{array}\right\} \quad (8.16)$$

These relations together with the relations (8.13) have been plotted in fig. 9. As in aircraft struc-

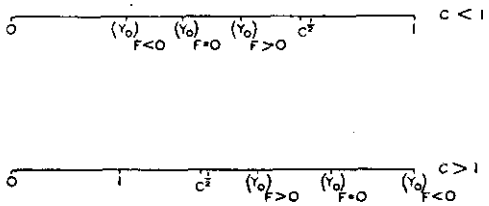

Fig. 9.

Succession of the buckling form parameter Y_0 for the critical loads of stiffened shells without ($F=0$), with internal ($F>0$) and with external ($F<0$) eccentricity of the stiffeners (stringers and frames).

tures usually $F>0$, the range of Y_0 is limited by $C^{1/2}$ en $(Y_0)_{F=0}$. This latter limit can easily be calculated from (8.11), which is quadratic for $F=0$. Usually, Y_0 is very close to the limit $C^{1/2}$; therefore, substituting $Y=C^{1/2}$ into (8.14) we will find a close approximation to P_{min}, which can be improved by calculating Y_0 from (8.15) and substituting it into (8.14).

Comparing now the results obtained for all classes we observe that the classes I and II yield approximately the same critical load at approximately the same wave length, though the number of circumferential waves is different. The reason is that the circumferential half-wave length l_n is large compared to l_0, since

$$\frac{l_n}{l_0} = s^{1/4}\, Y^{1/2}. \quad (8.17)$$

With this type of buckling the energy required for bending the frames is negligible and the relative bending stiffness C of the frames does not affect the critical load.

Increasing n from 0 to $\sim k^{-1/4}$ (about 3 or 4) we arrive at class II, were P_{min} slightly decreases below 2 by the fact that $A-B+2F$ usually will be positive. This decrease is more distinct for larger relative shear weakness of skin (A), larger relative eccentricity of stiffeners (F) and smaller relative torsional rigidity of the stiffeners (B).

The classes IV and V give approximately the same critical load. They are characterized by a small value Y, which according to (8.17) means that the longitudinal wave length l_0 is large compared to the circumferential half-wave length l_n. With this type of buckling the energy required for bending the stringers is negligible. The magnitude of the critical load depends primarily upon the relative bending stiffness of the frames (C). With increasing n from 2 to $k^{-1/4}$ (about 3 or 4) the critical load increases.

Buckling according to class IV or V will occur only if the corresponding critical load is smaller than that for class I or II. This implies that for $C>$ about unity buckling according to class IV or V usually will not be critical.

The factor $\frac{n^2-1}{n^2+1}$ in class V reminds of the case of buckling of an isotropic shell. Its minimal value with $n=2$ usually will not be realized since the corresponding half-wave length is very large, $\frac{l_0}{a_x}$ being of the order $k^{-1/2}$. In class IV l_0 decreases, $\frac{l_0}{a_x}$ being of the order of unity. With these long waves the actual boundary conditions may increase the critical load since the actual Y differs from Y_0.

Class III, closing the gap between the classes II and IV, will be affected by the stiffnesses of primary importance for the classes I and V: the bending stiffnesses of stringers and frames. The wave length ratio l_n/l_0 is of the order of unity. The half-wave length l_0 is of the same order as in class I; the number of circumferential waves is larger than in any of the other classes (4 or more). In this type of buckling the waves in both directions are short, the shell is corrugated as much as possible; thus all stiffnesses will affect the critical load. Even the relative eccentricity proves to be of primary importance. Comparing the critical load with and without eccentricity it may be that it is reduced up to $^1/_3$ of the critical load for $F=0$.

Discussing class V we left the case $n=1$ out of consideration. In this case the cross section of the tube is not distorted, it moves as a whole in just the same way as a solid section. The critical load proves to be equal to the critical column load of a tube supported at its end.

9 Notations.

a radius of skin

a_x, a_{xp}, a_φ distance of the centre to the centre of gravity of the composite section out of the stringer (index x) resp. the frame (index φ) together with the effective width w_e^*, w_e and w_f resp.

b frame spacing

$c = p\,\lambda\,\frac{a_\varphi}{a_x}$

e_x, e_{xp}, $e_\varphi = a - a_x$, $a - a_{xp}$, $a - a_\varphi$ resp.

$f = f_x + f_\varphi$

$f_p = (e_\varphi - e_{xp})\,a_\varphi^{-1}$

$f_x = e_x a_\varphi\, a^{-2}$

$f_\varphi = e_\varphi\, a^{-1}$

i radius of gyration of the composite section of stringers or frames

$k = K_{xx}^{1/2}$

l, l_n half longitudinal, resp. circumferential wave length

m, n parameter of buckling form defined by (7.1)

p buckling load per unit of length along the circle a_x

$r = \eta\, G\, t\, \lambda \left(\frac{a}{a_x}\right)^2$

$s = E\, t_\varphi\, \lambda\, \frac{a}{a_\varphi}$

t skin thickness

t_x, t_φ active cross section with respect to additional stresses per unit of length along the circle a_x, resp. a_φ in the longitudinal plane

t_{xp} active cross section with respect to the buckling load p

u, u_0 axial displacement of an arbitrary point x, φ, z, resp. a point $x, \varphi, -e_x$

v radial displacement in an arbitrary point x, φ

w_e, w_f effective width of skin at buckling load for stringer and frame resp.

w_e^* effective width of skin with respect to additional strain

x coordinate in axial direction

$y = m^2/n^2$

z coordinate in radial direction, distance from skin

$A = r^{-1}s^{1/2}$, relative shear weakness of the skin

$B = B_x + B_\varphi$, relative torsional rigidity of stringers and frames together

$B_x = K_{x\varphi}\, k^{-2} s^{-1/2}$

$B_\varphi = K_{\varphi x}\, k^{-2} s^{-1/2}$

$C = K_{\varphi\varphi}\, k^{-2} s^{-1}$, relative bending stiffness of frames

D_x, D_φ shear load per unit of length of $a_x\varphi$ and x resp.

E Young's modulus

$F = F_x + F_\varphi$, relative eccentricity of stringers and frames

$F_p = f_p k^{-1}$

$F_x = f_x k^{-1}$

$F_\varphi = f_\varphi\, k^{-1}$

G modulus of rigidity

I moment of inertia of the cross section of the whole cylinder

I_{xx}, $I_{\varphi\varphi}$ moments of inertia of stringers and frames together with the effective width w_e, w_f resp., per unit of length of $a_x\varphi$ and x resp.

$I_{x\varphi}$, $I_{\varphi x}$ $1/G$ times torsional rigidity of stringers and frames per unit of length of $a_x\varphi$ and x resp.

J_x, J_φ, J_z load terms in the equations of equilibrium

$K_{xx} = EI_{xx}\lambda a_\varphi{}^2 a^{-1} a_x^{-3}$

$K_{\varphi\varphi} = EI_{\varphi\varphi}\,\lambda a_\varphi{}^{-2}$

$K_{x\varphi} = GI_{x\varphi}\,\lambda a^{-1} a_x^{-1}$

$K_{\varphi x} = GI_{\varphi x}\lambda a_x^{-2}$

L length of shell between its supported edges

M_{xx}, $M_{x\varphi}$ bending, resp. torsional moment in the stringers per unit of length of $a_x\varphi$

$M_{\varphi\varphi}$, $M_{\varphi x}$ bending, resp. torsional moment in the frames per unit of length of x

$N = n^{-2}k^{-1}$, buckling form parameter

$P = c\, k^{-1} s^{-1/2}$, buckling load parameter

Q_s, Q_f area of the cross section of a stringer resp. a frame

R_x, R_φ, R_z load terms in the equations of equilibrium

$S_x, S_\varphi, T_x, T_\varphi$ additional normal forces and shear forces due to buckling on the radial resp. the axial plane per unit of length of $a_x\varphi$, resp. x

U defined by $u_0 = \frac{a^3}{a_\varphi}\,\frac{\partial U}{\partial x}$

U_0 amplitude of U

$V = v/a$

V_0 amplitude of V

X symbol for the equation of equilibrium in axial direction

$Y = y\, s^{-1/2}$, buckling form parameter

Y_0 value of Y at the minimal buckling load, the critical load

Z symbol for the equation of equilibrium in radial direction

$\bar{\varepsilon}$ stringer strain at buckling load

ε_x, ε_φ direct axial and circumferential strain by buckling

$\varepsilon_{x\varphi}$ shear strain of the skin

η reduction factor to the modulus of rigidity of the skin, allowing for tension field in skin

$\kappa_{x\varphi}$, $\kappa_{\varphi x}$ specific twist of stringers and frames

$\lambda = a_x^3 E^{-1} t_x^{-1} a^{-3}$

μ number of half waves over the length of the shell

$\xi = x\, a_x^{-1} (a_\varphi / a)^{1/2}$

$\bar{\sigma} = p/t_{xp}$, buckling stress

σ_x, σ_φ, τ_x, τ_φ additional normal stress and shear stress due to buckling on the radial resp. the axial plane

$\tau_{x\varphi}$ shear stress from strain $\varepsilon_{x\varphi}$

φ coordinate in the radial plane

ψ, ψ_0, ψ_p circumferential displacement of an arbitrary point x, φ, z; x, φ, $-e_\varphi$; x, φ, $-e_{xp}$ resp.,

ω_φ, ω_x slope of the element of the shell in the axial resp. the radial plane

Φ symbol for the equation of equilibrium in circumferential direction

Ψ defined by $\psi_0 = \frac{a}{a_\varphi} \frac{\partial \Psi}{\partial \varphi}$

Ψ_0 amplitude of Ψ

$( )' = \frac{\partial ( )}{\partial \xi}$

$( )^{\cdot} = \frac{\partial ( )}{\partial \varphi}$

$\sim$ "equal order of magnitude as"

Part II. Equally spaced frames.

10 The shell between successive frames.

The shell between successive frames is an orthotropic structure; it constitutes a particular case of the shell considered in part I by the fact that the stiffnesses of the circumferential structural elements are equal to zero

$$t_\varphi = I_{\varphi\varphi} = I_{\varphi x} = 0. \tag{10.1}$$

The neutral axis of the infinitely weak frames can be assumed to lie in the plane of the skin; therefore,

$$e_\varphi = 0. \tag{10.2}$$

From (10.1, 2) it follows that

$$s = K_{\varphi\varphi} = K_{\varphi x} = f_\varphi = 0$$

and the differential equations (6.7, 8 and 6) simplify to

$$X \equiv \frac{1}{r}\, U'' + U\cdot\cdot + \Psi\cdot\cdot - f_x V\cdot\cdot = 0, \tag{10.3}$$

$$\Phi \equiv rU'' + [r + K_{x\varphi} - (1+f_p)c]\,\Psi'' - (rf_x + K_{x\varphi} - f_p c)V'' = 0, \tag{10.4}$$

$$-Z \equiv f_x U''\,'' - K_{x\varphi}\Psi''\cdot\cdot + cV'' + K_{xx}V''\,'' + K_{x\varphi}V''\cdot\cdot = 0. \tag{10.5}$$

Integrating (10.4, 5) twice over ξ (using the symbol $''(\ )$ for this integration) yields

$$''\Phi \equiv rU + [r + K_{x\varphi} - (1+f_p)c]\,\Psi - (rf_x + K_{x\varphi} - f_p c)V + \xi F_1(\varphi) + F_2(\varphi) = 0, \tag{10.6}$$

$$-''Z = f_x U'' - K_{x\varphi}\Psi\cdot\cdot + cV + K_{xx}V'' + K_{x\varphi}V\cdot\cdot + \xi G_1(\varphi) + G_2(\varphi) = 0. \tag{10.7}$$

We eliminate U and Ψ from (10.3, 6, 7) by the operation

$$-\left\{\left(\frac{K_{x\varphi}}{r} + f_x\right)(\ )'' + K_{x\varphi}(\ )\cdot\cdot\right\}\{[r + K_{x\varphi} - (1+f_p)c]\,X - ''\Phi\cdot\cdot\} + \left\{\left[1 + \frac{K_{x\varphi}}{r} - \frac{(1+f_p)c}{r}\right](\ )'' + [K_{x\varphi} - (1+f_p)c](\ )\cdot\cdot\right\}\{K_{x\varphi}X - ''Z\} \equiv$$

$$\equiv \left[1 + \frac{K_{x\varphi}}{r} - \frac{(1+f_p)c}{r}\right]cV'' - [K_{x\varphi} - (1+f_p)c]\,cV\cdot\cdot + \left[1 + \frac{K_{x\varphi}}{r} - \frac{(1+f_p)c}{r}\right]K_{xx}V''\,'' + \left\{K_{x\varphi}(1-f_x)^2 + [K_{x\varphi} - (1+f_p)c]\,K_{xx} - \left[\frac{K_{x\varphi}}{r} + f_x{}^2 - f_x f_p(1-f_x)\right]c\right\}V''\cdot\cdot - K_{x\varphi}\,cV\cdot\cdot\cdot\cdot + K_{x\varphi}\,[\xi F_1(\varphi) + F_2(\varphi)]\cdot\cdot\cdot\cdot + [K_{x\varphi} - (1+f_p)c]\,[\xi G_1(\varphi) + G_2(\varphi)]\cdot\cdot = 0. \tag{10.8}$$

Since c, $K_{xx}{}^{1/2}$, $K_{x\varphi}{}^{1/2}$, f_x, f_p are of the same order of magnitude which is negligible to unity, (10.8) simplifies to

$$c(V'' - cV\cdot\cdot) + K_{xx}V''\,'' + K_{x\varphi}(V'' - cV\cdot\cdot)\cdot\cdot + K_{x\varphi}[\xi F_1(\varphi) + F_2(\varphi)]\cdot\cdot\cdot\cdot - c[\xi G_1(\varphi) + G_2(\varphi)]\cdot\cdot = 0. \tag{10.9}$$

A further simplification is obtained by considering the wave pattern. This particular investigation is concerned with buckling cases having short longitudinal waves; therefore it may be confined to the case of axially symmetrical buckling and to the classes I, II and III (sec. 8, table I) in which the circumferential wave length is much larger than the longitudinal one (clas I, II) or of the same order of magnitude (class III). Therefore, $V\cdot\cdot$ is smaller than or of the same order of magnitude as V'' and (10.9) may be simplified to:

$$cV'' + K_{xx}V''\,'' + K_{x\varphi}V''\cdot\cdot + K_{x\varphi}[\xi F_1(\varphi) + F_2(\varphi)]\cdot\cdot\cdot\cdot - c[\xi G_1(\varphi) + G_2(\varphi)]\cdot\cdot = 0, \tag{10.10}$$

Neglecting small order quantities in (10.4) we get

$$''\Phi \equiv r(U + \Psi - f_x V) + \xi F_1(\varphi) + F_2(\varphi) = 0, \tag{10.11}$$

and substituting it in (10.3):

$$rX - ''\Phi\cdot\cdot \equiv U'' - \{\xi F_1(\varphi) + F_2(\varphi)\}\cdot\cdot = 0. \tag{10.12}$$

Integrating twice over ξ we obtain

$$U = {}^1/_2\,\xi^2[{}^1/_3\,\xi F_1(\varphi) + F_2(\varphi)]\cdot\cdot + \xi F_3(\varphi) + F_4(\varphi) \tag{10.13}$$

and from (10.11)

$$\Psi = f_x V - U - [\xi F_3(\varphi) + F_4(\varphi)]. \tag{10.14}$$

It appears from part I that the displacements in the plane of the shell are small quantities of the order $k^{1/2}$ compared to the radial displacement. The wave length ratio l_0/a being of the order $k^{1/2}$ in the buckling cases considered here, the displacement functions U and Ψ are of the order kV. Then it follows from (10.12) that $[\xi F_1(\varphi) + F_2(\varphi)]\cdot\cdot\cdot\cdot$ is of the order $kV''\cdot\cdot$. Therefore, the corresponding term in (10.10) is negligible. From (10.7) it appears that $[\xi G_1(\varphi) + G_2(\varphi)]\cdot\cdot$ is of the order $kV\cdot\cdot$. Then integrating (10.10) twice over ξ it simplifies to

$$cV + K_{xx}V'' + K_{x\varphi}V\cdot\cdot + \xi F_5(\varphi) + F_6(\varphi) = 0. \tag{10.15}$$

The equations (10.13, 14, 15) apply to the shell between 2 successive frames. Their solution requires the knowledge of the functions $F_1 \ldots F_6$ and of the boundary conditions for V for each bay of the shell. $F_1 \ldots F_6$ have to be determined from boundary conditions as well, which apply to the equilibrium of the frames and to the compatibility of the distortions of the frames and the shell.

11 The frames.

11.1 *The continuity of the shell.*

The slopes of the stringers at both sides of the frame ν are equal

$$\Delta_\nu V' = 0. \tag{11.1}$$

The displacements at both sides are equal as well:

$$\Delta_\nu U' = 0, \tag{11.2}$$

$$\Delta_\nu \Psi' = 0, \tag{11.3}$$

$$\Delta_\nu V = 0. \tag{11.4}$$

11.2 *The loads upon the frames.*

The loads upon the frame originate from the stresses in the shell at both sides of the frame. The stress resultants in the plane $x =$ constant have been indicated in fig. 10. They can be ex-

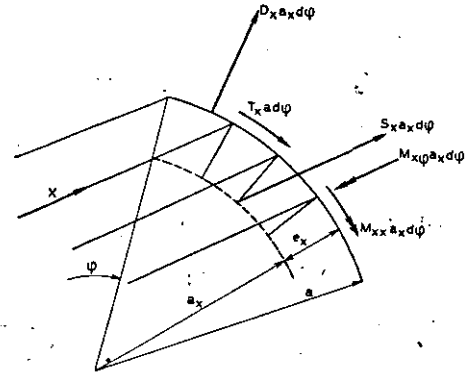

Fig. 10.

Stress resultants upon the element $d\varphi$ of the cross section $\nu-$ just in front of frame ν.

pressed in the displacement functions by the equations (6.3), (5.5, 6, 7, 8, 9), replacing a_φ by a and putting $K_{\varphi x} = 0$.

The loads upon the frames are given by fig. 10 as well, provided that D_x is replaced by $\Delta_\nu D_x$, etc. Thus we obtain

$$\left.\begin{aligned}
\Delta_\nu S_x &= \frac{a_x}{\lambda a}\,\Delta_\nu U'',\\
\Delta_\nu T_x &= \frac{a_x}{\lambda a}\,[r(\Delta_\nu U + \Delta_\nu \Psi - f_x \Delta_\nu V) - \\
&\qquad - c(1+f_p)\Delta_\nu \Psi + c\, f_p \Delta_\nu V]'\,,\\
\Delta_\nu D_x &= -\frac{1}{\lambda}\,[f_x \Delta_\nu U''' + c\Delta_\nu V' + \\
&\qquad + K_{xx}\Delta_\nu V'''],\\
\Delta_\nu M_{xx} &= \frac{a_x}{\lambda}\,K_{xx}\Delta_\nu V'',\\
\Delta_\nu M_{x\varphi} &= \frac{a}{\lambda}\,K_{x\varphi}(-\Delta_\nu \Psi + \Delta_\nu V)'\cdot
\end{aligned}\right\} \tag{11.5}$$

(11.1, 2) holding for any point φ, we have $\Delta_\nu V'' = \Delta_\nu U'' = 0$; therefore,

$$\Delta_\nu T_x = \frac{a_x}{\lambda a}\,[r - c(1+f_p)]\,\Delta_\nu \Psi''\cdot,$$

$$\Delta_\nu D_x = -\frac{1}{\lambda}\,[f_x \Delta_\nu U''' + K_{xx}\Delta_\nu V'''],$$

$$\Delta_\nu M_{x\varphi} = -\frac{a}{\lambda}\,K_{x\varphi}\Delta_\nu \Psi''\cdot.$$

These stress resultants are composed to give forces and moments with respect to the neutral axis of the frame (fig. 11)

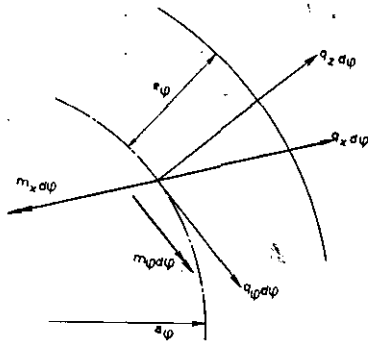

Fig. 11.

The frame loads acting in the plane of the frame.

$$q_x = \Delta_\nu S_x a_x = \frac{1}{\lambda}\,\frac{a_x^2}{a}\,\Delta_\nu U'',$$

$$q_\varphi = \Delta_\nu T_x a = \frac{1}{\lambda}\,a_x\,[r - c\,(1+f_p)]\,\Delta_\nu \Psi''\cdot,$$

$$q_z = \Delta_\nu D_x a_x = -\frac{1}{\lambda}\,a_x\,[f_x \Delta_\nu U''' + K_{xx}\Delta_\nu V'''],$$

$$m_x = \Delta_\nu M_{x\varphi} a_x - \Delta_\nu T_x a e_\varphi = - \tag{11.6}$$

$$-\frac{1}{\lambda_\varphi}\,a\,a_x\,[f_\varphi\, r + K_{x\varphi} - f_\varphi\, c\,(1+g)]\,\Delta_\nu \Psi'\cdot,$$

$$m_\varphi = \Delta_\nu M_{xx} a_x - \Delta_\nu S_x a_x\,(e_\varphi - e_x) =$$

$$= \frac{1}{\lambda}\,a_x^2\,[(f_x - f_\varphi)\,\Delta_\nu U'' + K_{xx}\Delta_\nu V''].$$

11.3 *The distortions of the frames.*

The loads q_φ, q_z and m_x distort the frame in its plane; we call them *symmetrical* loads. The loads q_x and m_φ give rise to distortions normal to the plane of the frame; we will call them *anti-symmetrical* loads. These two groups of loads will be considered separately.

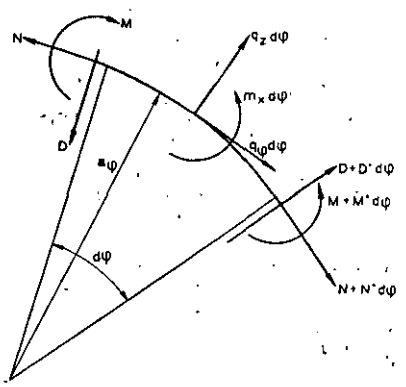

Fig. 12.

The symmetrical external and internal frame loads.

Fig. 12 gives an element of the frame with its *symmetrical* external and internal loads.

Eliminating the shear load D from the equations of equilibrium we find

$$\left.\begin{aligned} a_\varphi q_\varphi - m_x + a_\varphi N' - M' &= 0, \\ -a_\varphi q_z + m_x' + a_\varphi N + M'' &= 0. \end{aligned}\right\} \quad (11.7)$$

The relations between the internal loads N, M and the deformations ψ_0 and v follow from (4.7, 8) after replacing S_φ, $M_{\varphi\varphi}$, t_φ, $I_{\varphi\varphi}$ resp. by N, M, bt_φ, $bI_{\varphi\varphi}$. The displacement ψ_0 in the neutral axis of the frame is expressed in the displacement functions Ψ, V by

$$\psi_0 = \Psi' + \frac{e_\varphi}{a_\varphi} V'. \quad (11.8)$$

Substituting from (4.7, 8), (11.8) and (11.6) into (11.7) we obtain the conditions of compatibility, as far as the symmetrical distortions are concerned,

$$\begin{aligned} &\beta s\,[(1-f_\varphi)\,\Psi'' + f_\varphi V'' + V'] + \\ &+ \beta k_{\varphi\varphi}(\Psi - V)'' + \frac{1}{1-f_\varphi}[r - c\,(1+f_p) + \\ &+ K_{x\varphi}]\,\Delta_\nu \Psi' = 0 \end{aligned} \quad (11.9)$$

$$\begin{aligned} &\beta s\,[(1-f_\varphi)\,\Psi'' + f_\varphi V'' + V] + \\ &+ \beta K_{\varphi\varphi}(-\Psi + V)'' + f_x \Delta_\nu U''' + K_{xx}\Delta_\nu V''' - \\ &- \frac{1}{1-f_\varphi}[f_\varphi\,(r - c\,(1+f_p)) + K_{x\varphi}]\,\Delta_\nu \Psi'' = 0. \end{aligned}$$

Recalling sec. 10 we know

$$U \sim \Psi \sim kV,$$

$$(\,)'' \lesssim \frac{1}{k}\,(\,).$$

The frame spacing is assumed to be of the same order of magnitude as the longitudinal half wave length; therefore,

$$\beta\,(\,)' \lesssim (\,).$$

Neglecting again quantities of the order k to unity the equations (11.9) simplify to

$$\{\beta s\,(\Psi'' + f_\varphi V'' + V) + r\,\Delta_\nu \Psi'\} = 0, \quad (11.10)$$

$$\begin{aligned} &\beta s\,(\Psi'' + f_\varphi V'' + V) + \beta K_{\varphi\varphi} V'' + f_x \Delta_\nu U''' - \\ &- f_\varphi r\,\Delta_\nu \Psi'' + K_{xx}\Delta_\nu V''' = 0. \end{aligned} \quad (11.11)$$

Fig. 13 shows an element of the frame with its *antisymmetrical* external and internal loads.

Eliminating the shear load D from the equations of equilibrium we get

$$\begin{aligned} m_\varphi + M_\varphi' - M_z &= 0, \\ a_\varphi q_x + M_\varphi' + M_z'' &= 0. \end{aligned} \quad (11.12)$$

The bending stiffness of the stringers in the plane of the shell is assumed to be zero, since it is negligible compared to the bending stiffness of the beam formed by two successive stringers and the skin in between. In the same way the bending stiffness of the frames in the plane of the shell

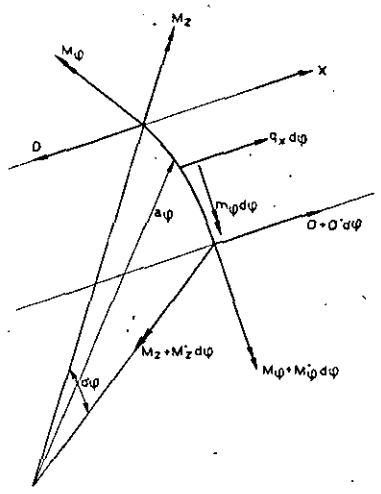

Fig. 13.
The antisymmetrical external and internal frame loads.

is negligible, therefore $M_z = 0$. Now (11.12) becomes

$$\begin{aligned} m_\varphi + M_\varphi' &= 0, \\ a_\varphi q_x - m_\varphi &= 0. \end{aligned} \quad (11.13)$$

The equation of elasticity follows from (4.11) after replacing $M_{\varphi x}$, $I_{\varphi x}$ resp. by M_φ, $bI_{\varphi x}$. Substituting from (4.11) and (11.6) into (11.13) we find the conditions of compatibility, as far as the antisymmetrical deformations are concerned,

$$\begin{aligned} &(f_x - f_\varphi)\,\Delta_\nu U'' + K_{xx}\Delta_\nu V'' + \\ &+ \beta \frac{K_{\varphi x}}{1-f_\varphi} V'' = 0, \end{aligned} \quad (11.14)$$

$$-(1-f_x)\Delta_\nu U'' + K_{xx}\Delta_\nu V'' = 0. \quad (11.15)$$

Eliminating U from (11.14) by means of (11.15) and neglecting small order quantities we find:

$$\beta K_{\varphi x} V'' + K_{xx}\Delta_\nu V'' = 0, \quad (11.16)$$

$$-\Delta_\nu U'' + K_{xx}\Delta_\nu V'' = 0. \quad (11.17)$$

Recalling that U'' is of the order kV'' it follows from (11.17) that $\Delta_\nu U''$ is of the order kU''. Therefore $\Delta_\nu U''$ is a negligible quantity compared to U'' and (11.17) may be written

$$\Delta_\nu U'' = 0. \quad (11.18)$$

11.4 *The boundary conditions.*

Integrating (11.3) and (11.10) over φ we find

$$\begin{aligned} \Delta_\nu \Psi &= K_{1\nu}, \\ \beta s\,(\Psi'' + f_\varphi V'' + V) + r\Delta_\nu \Psi' &= K_{2\nu}. \end{aligned}$$

Recalling sec. 6 we may replace Ψ by $\Psi_1 = \Psi + \overline{\Psi}\,(\xi)$, choosing $\overline{\Psi}$ such that it satisfies the differential equation

$$-[r + K_{x\varphi} - (1+f_p)c]\,\overline{\Psi}'' = C_2(\xi).$$

Assuming now the boundary conditions of $\overline{\Psi}$ to be

$$\Delta_\nu \overline{\Psi} = K_{1\nu},$$
$$r\Delta_\nu \overline{\Psi}' = K_{2\nu},$$

Ψ_1 will satisfy

$$\Delta_\nu \Psi = 0, \qquad (11.19)$$
$$\beta s\,(\Psi'' + f_\varphi V'' + V) + r\,\Delta_\nu \Psi' = 0. \qquad (11.20)$$

Therefore we replace (11.3, 10) by (11.19, 20), and thereafter (11.11) by

$$\beta K_{\varphi\varphi} V \cdots + f_x \Delta_\nu U''' - r\,\Delta_\nu \Psi' - f_\varphi\, r\,\Delta_\nu \Psi'' + K_{xx}\Delta_\nu V''' = 0. \qquad (11.21)$$

The complete set of boundary conditions to the equations (10.13, 14, 15) is (11.1, 2, 4, 16, 18, 19, 20, 21). We have to consider that each bay of the shell has its own functions $F_1 \ldots F_6$; so we have to introduce a suffix ν to F, indicating the bay between the frames ν and $\nu+1$.

Eliminating now U and Ψ by the use of (10.13, 14) and considering that $\Delta_\nu(\xi F) = 0\,.\,F_\nu - \beta F_{\nu-1}$ we get:

from (11.21) and (11.2) $-K_{xx}\Delta_\nu V''' = \beta K_{\varphi\varphi} V_\nu \cdots + f\Delta_\nu F_1'' + \Delta_\nu F_1$, (11.22)

from (11.20) and (11.2) $\Delta_\nu F_1 = \beta s\,(fV'' + V - \frac{1}{r}F_2'' - F_4'')_\nu$, (11.23)

from (11.18) $\Delta_\nu F_2'' = \beta F_{1\nu-1}''$, (11.24)

from (11.2) $\Delta_\nu F_3 = \beta\left(\frac{1}{2}\beta F_1'' + F_2''\right)_{\nu-1}$, (11.25)

from (11.19) $\Delta_\nu F_4 = \frac{1}{2}\beta^2\left(\frac{1}{3}\beta F_1'' + F_2''\right)_{\nu-1} + \beta\left(\frac{1}{r}F_1 + F_3\right)_{\nu-1} - \frac{1}{r}\Delta_\nu F_2$. (11.26)

The variable V can not be solved from the differential equation (10.15) and the boundary conditions (11.1, 4) alone, since (10.15) contains F_5 and F_6. The six equations (11.16, 22 to 26) are sufficient for solving F_5 and F_6, since they contain apart from F_5, F_6 the four unknown quantities F_1 to F_4.

There are m frames along the length of the cylinder; so there are $m-1$ bays and $m-2$ intermediate frames and, consequently, the determination of V and F in all bays requires $8\,(m-1)$ boundary conditions. The boundary conditions considered thus far refer to the intermediate frames. So there are $8\,(m-2)$ of them. 8 boundary conditions more are required; they are obtained by examining the conditions at the end frames $\nu=1$ and $\nu=m$. The stresses in the shell at the end frames will distort these frames such that the frames and the shell fit together. In this way each end will provide 4 boundary conditions, similar to (11.10, 11, 16, 17).

We will not give these conditions explicitly, since we intend to deal with the cylinder of infinite length. It is to be expected that the correct end conditions will not appreciably affect the buckling load, since the wave length is short and by that fact the total length of the cylinder will comprise a fairly large number of waves.

12 The solution of the equations.

12.1 *The difference equations.*

The functions V and F should be periodical with $\varphi = 2\pi$; therefore V and F are goniometric functions with the argument $n\varphi$, n being integer. In each separate equation the derivatives to φ are all of odd or even order; therefore,

$$V(\xi, \varphi) = W(\xi)\sin n\varphi \qquad (12.1a)$$

is accompanied by

$$F_j(\varphi) = F_j \sin n\varphi \qquad j = 1, 2 \ldots 6 \qquad (12.1b)$$

and

$$V(\xi, \varphi) = W(\xi)\cos n\varphi \quad \text{by} \quad F_j(\varphi) = F_j \cos n\varphi. \qquad (12.2)$$

Changing the origin of φ we can transform the solution (12.2) into (12.1); therefore, we may take the general solution to be (12.1). Substituting (12.1) into the partial differential equation (10.15) it yields the differential equation of the 2nd order

$$(c - K_{x\varphi}n^2)W + K_{xx}W'' + \xi F_5 + F_6 = 0,$$

the general solution of which is

$$W(\xi) = \frac{1}{\beta}\xi W_5 + W_6 + W_7 \sin\alpha\xi + W_8\cos\alpha\xi, \qquad (12.3)$$

where

$$\alpha^2 = \frac{c - K_{x\varphi}n^2}{K_{xx}} \qquad (12.4)$$

$$W_5 = -\frac{\beta}{c - K_{x\varphi}n^2}F_5,$$

$$W_6 = -\frac{1}{c - K_{x\varphi}n^2}F_6. \qquad (12.4)$$

The formulas are simplified if the constants $F_1, \ldots F_4$ are replaced by $W_1, \ldots W_4$, defined by

$$F_1 = \frac{1}{\beta}(K_{xx}s)^{1/2}W_1, \quad F_2 = (K_{xx}s)^{1/2}W_2,$$

$$F_3 = \frac{1}{\beta}K_{xx}^{1/2}W_3, \quad F_4 = K_{xx}^{1/2}W_4.$$

Substituting (12.1, 3) in the boundary conditions, using the known symbols A, B_φ, C, F, P and the new symbols

$$Q = \beta^2 K_{xx}^{-1/2}s^{1/2}, \quad R = (\beta n)^2 s^{1/2}, \quad X = \alpha\beta = (PQ - B_x R)^{1/2}, \qquad (12.5)$$

we get

from (11.1) $(W_7X' + W_5)_\nu - (W_7X\cos X - W_8X\sin X + W_5)_{\nu-1} = 0$, (12.6)

from (11.4) $(W_8 + W_6)_\nu - (W_7\sin X + W_8\cos X + W_5 + W_6)_{\nu-1} = 0$, (12.7)

from (11.6)

$$W_{8\nu} - (W_7 \sin X + W_8 \cos X)_{\nu-1} + \frac{B_\varphi R}{x^2} (W_7 X + W_5)_\nu = 0, \qquad (12.8)$$

from (11.22)

$$-W_{7\nu} + (W_7 \cos X - W_8 \sin X)_{\nu-1} + \frac{CR^2}{X^3} (W_8 + W_6)_\nu + \frac{Q - FR}{X^3} \Delta_\nu W_1 = 0, \qquad (12.9)$$

from (11.23)

$$\Delta_\nu W_1 = (Q - FR)(W_8 + W_6)_\nu + R(AW_2 + W_4)_\nu, \qquad (12.10)$$

from (11.24)

$$\Delta_\nu W_2 = W_{1\nu-1}, \qquad (12.11)$$

from (11.25)

$$\Delta_\nu W_3 = -R\,(1/2\, W_1 + W_2)_{\nu-1}, \qquad (12.12)$$

from (11.26)

$$\Delta_\nu W_4 = \left[-\frac{R}{2} (1/3\, W_1 + W_2) + AW_1 + W_3 \right]_{\nu-1} - A\Delta_\nu W_2. \qquad (12.13)$$

In these equations the structural parameters, A, B_x, B_φ, C, F and Q are given, R is a buckling parameter depending upon the number of circumferential waves, X is the load parameter and the stability problem is to determine those values of X for which the 8 homogeneous linear equations in $W_1 \ldots W_8$ will yield a solution different from zero. The equations enable to calculate the $W_{j\nu}$ if the $W_{j,\nu-1}$ are given; they are difference equations.

The structural parameters have been chosen such that they all are of the order of unity. The buckling parameter R is of the order of unity as well in the buckling case with short circumferential waves (class III) and so is the load parameter X. All coefficients of (12.6 to 13) being of the order of unity the W_j will be of equal order of magnitude.

In the buckling cases with long circumferential waves ($n^2 \sim 1$, class I, and $n = 0$, axial symmetrical buckling) R is of the order k and X is of the order of unity.

Examining our difference equations we conclude from (12.6 to 9, and 11) that W_1, W_2, W_5 to W_8 have the same order of magnitude. Substituting $\Delta_\nu W_2$ from (12.11) into (12.13) we find

$$\Delta_\nu W_4 = \left[-\frac{R}{2} (1/3\, W_1 + W_2) + W_3 \right]_{\nu-1}, \qquad (12.14)$$

so we conclude from (12.11) and (12.14) that W_3 and W_4 are of the order RW_1, which is negligible.

The system of difference equations is simplified now by neglecting all terms containing R. Eliminating W_1 the system reduces to

$$\begin{aligned}
&(W_7 X + W_5)_\nu - (W_7 X \cos X - W_8 X \sin X + W_5)_{\nu-1} = 0,\\
&W_{8\nu} - (W_7 \sin X + W_8 \cos X)_{\nu-1} = 0,\\
&\Delta_\nu W_5 + \frac{Q^2}{X^2} (W_8 + W_6)_\nu = 0,\\
&\Delta_\nu W_6 - W_{5\nu-1} = 0,\\
&X^2 = PQ.
\end{aligned}$$

In these equations the only structural parameter is Q, depending upon the flexural rigidity of the stringers and the extensional stiffness of the frames. This preliminary result corresponds to what we found in part I for axially symmetrical buckling and for class I.

12.2 *The general solution of the difference equations.*

The difference equation with constant coefficients is the algebraïc analogue to the differential equation with constant coefficients. The general solution of the former will correspond to that of the latter, so we put

$$W_{j\nu} = \omega_j \rho^\nu \qquad j = 1, 2 \ldots 8. \qquad (12.15)$$

Substituting it in (12.6 to 13) we obtain

$$\left.\begin{aligned}
&\rho(\omega_7 X + \omega_5) - (\omega_7 X \cos X - \omega_8 X \sin X + \omega_5) = 0,\\
&\rho(\omega_8 + \omega_6) - (\omega_7 \sin X + \omega_8 \cos X + \omega_5 + \omega_6) = 0,\\
&\rho\,\omega_8 - (\omega_7 \sin X + \omega_8 \cos X) + \frac{B_\varphi R}{X^2} \rho(\omega_7 X + \omega_5) = 0,\\
&-\rho\,\omega_7 + (\omega_7 \cos X - \omega_8 \sin X) + \frac{CR^2}{X^3} \rho(\omega_8 + \omega_6) + \frac{Q - FR}{X^3} (\rho - 1)\,\omega_1 = 0,\\
&(\rho - 1)\omega_1 = (Q - FR)\,\rho(\omega_8 + \omega_6) + R\rho(A\omega_2 + \omega_4),\\
&(\rho - 1)\omega_2 = \omega_1,\\
&(\rho - 1)\omega_3 = -R\,(1/2\,\omega_1 + \omega_2),\\
&(\rho - 1)\omega_4 = -\frac{R}{2}(1/3\,\omega_1 + \omega_2) + A\omega_1 + \omega_3 - A(\rho - 1)\omega_2.
\end{aligned}\right\} \qquad (12.16)$$

At a given value of the load parameter X buckling will occur, or in mathematical terms: the equations (12.16) will yield $\omega_j \neq 0$, provided that the determinant of the system is zero.

Equating the determinant to zero we obtain

$$K \equiv CR^2 + \frac{(Q - FR)^2}{1 - \frac{R}{\vartheta}\left(A - \frac{R}{6}\right) + \frac{R^2}{\vartheta^2}} = \frac{-\vartheta X^2}{1 - \dfrac{\vartheta \sin X - 2\frac{B_\varphi R}{X}(1 - \cos X)}{X\left[\vartheta + 2(1 - \cos X) - \frac{B_\varphi R}{X} \sin X\right]}}, \qquad (12.17)$$

where

$$\vartheta = \frac{(\rho - 1)^2}{\rho}$$

or

$$\rho^2 - (2 + \vartheta)\,\rho + 1 = 0. \qquad (12.18)$$

(12.17) gives the relation between X and ϑ (or ρ). It is in ϑ an algebraïc equation of the 4th degree, so to any pair of values X and R

there are in general 4 different roots ϑ satisfying (12.17). According to (12.18) 2 roots ρ correspond to each root ϑ; so there are in general 8 different roots ρ_k. Substituting ρ_k in (12.16) we can solve these equations for the ratios $\frac{\omega_{jk}}{\omega_{1k}}$ and we can calculate the displacement functions $(W_{j\nu})_k$ corresponding to this root ρ_k

$$(W_{j\nu})_k = \frac{\omega_{jk}}{\omega_{1k}} \rho_k{}^\nu \, \omega_{1k} .$$

The general expression for these displacement functions is:

$$W_{i\nu} = \sum_{k=1}^{8} \left(\frac{\omega_{jk}}{\omega_{1k}} \rho_k{}^\nu \right) \omega_{1k} . \qquad (12.19)$$

In (12.19) the coefficient of ω_{1k} is a known function of X and R. Now the 8 quantities ω_{1k} have to be given such values that the 8 conditions at the ends of the cylinder are satisfied. The 8 boundary conditions being homogeneous equations in the ω_{1k}, instability will only occur if the determinant Δ, that can be formed out of the coefficients of these 8 linear equations by means of (12.19), is equal to zero. At a given value of R the condition $\Delta = 0$ will only be satisfied at particular values of X, which are the buckling load parameters at these particular boundary conditions.

Assuming the formula (12.15) for the displacement functions we are able to take account of any type of boundary conditions, so the assumption (12.15) indeed gives the general solution of our problem.

12.3 *The infinitely long cylinder.*

The buckling load of a cylinder of finite length and arbitrary end conditions can be computed with the method described in sec. 12.2. However, its practical application requires lengthy calculations. Usually, actual cylinders will have a length that is a multiple of the diameter. In this case the effect of the particular end conditions upon the wave formation in the centre part of the cylinder will be very small, provided that the end frames are not weaker than the intermediate frames. Then a good approximation of the buckling load will be obtained by assuming the cylinder to be infinitely long. Usually, the end frames will be stiffer than the normal frames, so the approximation will have the merit to be conservative.

In general ρ_k will be complex. We may put it in the form

$$\rho_k = \Gamma_k (\cos \gamma_k + i \sin \gamma_k).$$

It appears from (12.18) that to each root ρ there will be a conjugated root $\bar{\rho} = 1/\rho$; therefore,

$$\bar{\rho}_k = \Gamma_k{}^{-1} (\cos \gamma_k - i \sin \gamma_k)$$

and the general solution of (12.16) can be written in the form

$$W_{j\nu} = \sum_{k=1}^{4} [(\Gamma_k{}^\nu \omega_{jk} + \Gamma_k{}^{-\nu} \bar{\omega}_{jk}) \cos \nu\gamma_k + i (\Gamma^\nu{}_k \omega_{jk} - \Gamma_k{}^{-\nu} \bar{\omega}_{jk}) \sin \nu\gamma_k]. \qquad (12.20)$$

With the infinitely long cylinder $W_{j\infty}$ should be of the same order of magnitude as W_{j1}, therefore Γ_k should be equal to unity and

$$\vartheta_k = \rho_k + \frac{1}{\rho_k} - 2 = \rho_k + \bar{\rho}_k - 2 = = -2 (1 - \cos \gamma_k) \qquad (12.21)$$

will be a negative number between 0 and -4.

$$0 > \vartheta > -4. \qquad (12.22)$$

Then from (12.18) we conclude that ρ_k and $\bar{\rho}_k$ are conjugated complex numbers and thereupon from (12.16) that ω_{jk}/ω_{1k} and $\bar{\omega}_{jk}/\bar{\omega}_{1k}$ are conjugated complex numbers as well.

Hence we may write

$$\frac{\omega_{jk}}{\omega_{1k}} = A_{jk} (1 + a_{jk} i), \quad \frac{\bar{\omega}_{jk}}{\bar{\omega}_{1k}} = A_{jk} (1 - a_{jk} i), \qquad (12.23)$$

A_{jk} and a_{jk} being real numbers, following from the equations (12.16). Substituting these expressions in (12.20) and using $\Gamma_k = 1$ we obtain

$$W_{j\nu} = \sum_{k=1}^{4} A_{jk} [(\omega_{1k} + \bar{\omega}_{1k}) (\cos \nu\gamma_k - a_{jk} \sin \nu\gamma_k) + i (\omega_{1k} - \bar{\omega}_{1k}) (a_{jk} \cos \nu\gamma_k + \sin \nu\gamma_k)] . \qquad (12.24)$$

In this expression ω_{1k} and $\bar{\omega}_{1k}$ can be chosen arbitrarily. $W_{j\nu}$ should be real, therefore ω_{1k} and $\bar{\omega}_{1k}$ should be conjugated complex numbers and substituting this result in (12.23) ω_{jk} and $\bar{\omega}_{jk}$ prove to be conjugated complex numbers as well. Thus, we obtain from (12.24), putting $\omega_{1k} + \bar{\omega}_{1k} = \lambda_k$ and $\omega_{1k} - \bar{\omega}_{1k} = \mu_k i$,

$$W_{j\nu} = \sum_{k=1}^{4} A_{jk} [(\lambda_k - a_{jk}\mu_k) \cos \nu\gamma_k - (a_{jk}\lambda_k + \mu_k) \sin \nu\gamma_k] . \qquad (12.25)$$

The boundary conditions of the infinitely long cylinder do not impose additional requirements upon the $W_{j\nu}$, therefore the λ_k and μ_k can be chosen arbitrarily. Taking all λ_k and μ_k equal to zero except one λ we obtain one elementary case of buckling

$$W_{j\nu} = A_{jk}\lambda_k (\cos \nu\gamma_k - a_{jk} \sin \nu\gamma_k). \qquad (12.26)$$

The displacements are repeated after ν_0 frame spacings, $\nu_0 = \frac{2\pi}{\gamma_k} \zeta$, where ζ is the smallest integer making ν_0 integer. The length $\nu_0 b$ could be considered to be the wave length of the buckled cylinder; this would be sound from the mathematical point of view. Mechanically, and with the aim to give a general picture of the way in which the cylinder buckles, it is of more interest to define the half-wave length by

$$l = \nu_l b = \frac{\pi}{\gamma_k} b. \qquad (12.27)$$

This length is something like an average half-wave length and ν_l is the average number of frames

comprised in this half-wave length. The relation between ϑ, γ and ν_l as given by (12.21) and (12.27) has been plotted in fig. 14.

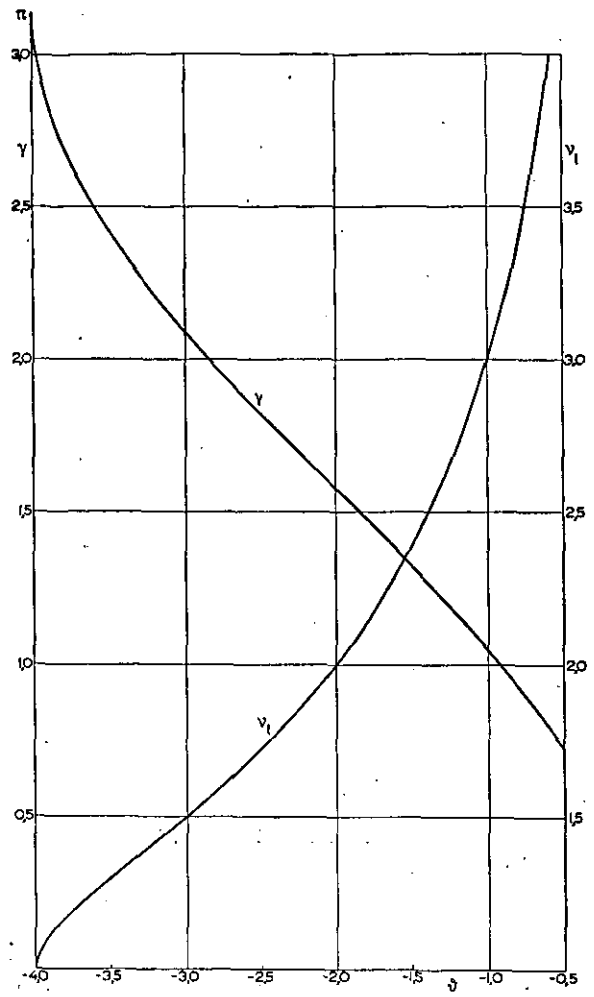

Fig. 14.

The relation between the buckling form parameters ϑ, γ, and the number of frames in one half-wave length ν_l.

13 The critical load.

13.1 *Column failure of stringers.*

The left side of (12.17) gives the magnitude of K required for a given ϑ and X. The magnitude of K is undetermined if

$$\vartheta \sin X - 2\,\frac{B_\varphi R}{X}\,(1-\cos X)=0,$$

$$\vartheta + 2\,(1-\cos X) - \frac{B_\varphi R}{X}\sin X = 0.$$

Solving these equations for X and ϑ we find:

$$\cot \tfrac{1}{2} X = -\frac{B_\varphi R}{2X},$$

$$\vartheta = -4. \qquad (13.1)$$

From (12.21, 27) we conclude $\nu_l = 1$; the half-wave length equals the frame spacing. The critical load corresponds to the smallest value of X satisfying (13.1). The relative torsional stiffness of the frames proving to be the only stiffness affecting the critical load, the nodal lines of the waves coincide with the frames; the stringers fail as columns between the frames, restrained by the torsional stiffness of the frames only.

From (13.1) it follows that $X > \pi$. With B_φ or R approaching zero X reaches its minimum

$$X_{\min} = \pi, \qquad (13.2)$$

hence by the use of

$$p = Et_x\,\frac{k^2}{\beta^2}\,(X^2 + B_x R)$$

follows

$$p = \pi^2\,\frac{EI_{xx}}{b^2} + n^2\,\frac{GI_{x\varphi}}{a^2}. \qquad (13.3)$$

The smallest column load is obtained from $R = n = 0$

$$p_{\min} = \frac{\pi^2 EI_{xx}}{b^2},$$

being the well-known formula for column failure.

13.2 *Axially symmetrical buckling.*

Since $n = R = 0$ (12.17) simplifies to

$$\frac{X^2}{Q^2} = -\frac{1}{\vartheta} + \frac{\sin X}{X\,[\,\vartheta + 2\,(1-\cos X)\,]}. \qquad (13.4)$$

The only structural parameter to be of importance proves to be Q. We want to determine $X_{\min}$ for a given value of Q. Equation (13.4), $f(\vartheta, X) = 0$, holding for any ϑ, we have

$$\frac{df}{d\vartheta} = \frac{\partial f}{\partial \vartheta} + \frac{\partial f}{\partial X}\,\frac{dX}{d\vartheta} = 0.$$

Therefore we may replace the condition $\frac{dX}{d\vartheta} = 0$ by $\frac{\partial f}{\partial \vartheta} = 0$. Thus we find

$$\vartheta = -\frac{2\,(1-\cos X)}{1 \pm \sqrt{\frac{\sin X}{X}}} \qquad (13.5)$$

The root, having the negative sign in the denominator, is real only for $\vartheta < -4$, so it falls outside the range (12.22), holding for the infinitely long cylinder. The other root yields

$$Q = X\,\frac{\sqrt{2\,(1-\cos X)}}{1 + \sqrt{\frac{\sin X}{X}}} \qquad (13.6)$$

$$P = \frac{X + \sqrt{X \sin X}}{\sqrt{2\,(1-\cos X)}}. \qquad (13.7)$$

In fig. 15 P, Q, ϑ and ν_l have been plotted as functions of X. For a given magnitude of Q we can determine P and ν_l immediately. With increasing Q, ν_l decreases. $\nu_l = 1$, corresponding to column failure of stiffeners, occurs at $Q = 2\pi$. The maximum effect the frames can have is that they allow for column failure of the stringers only, the frames behaving as if they were completely

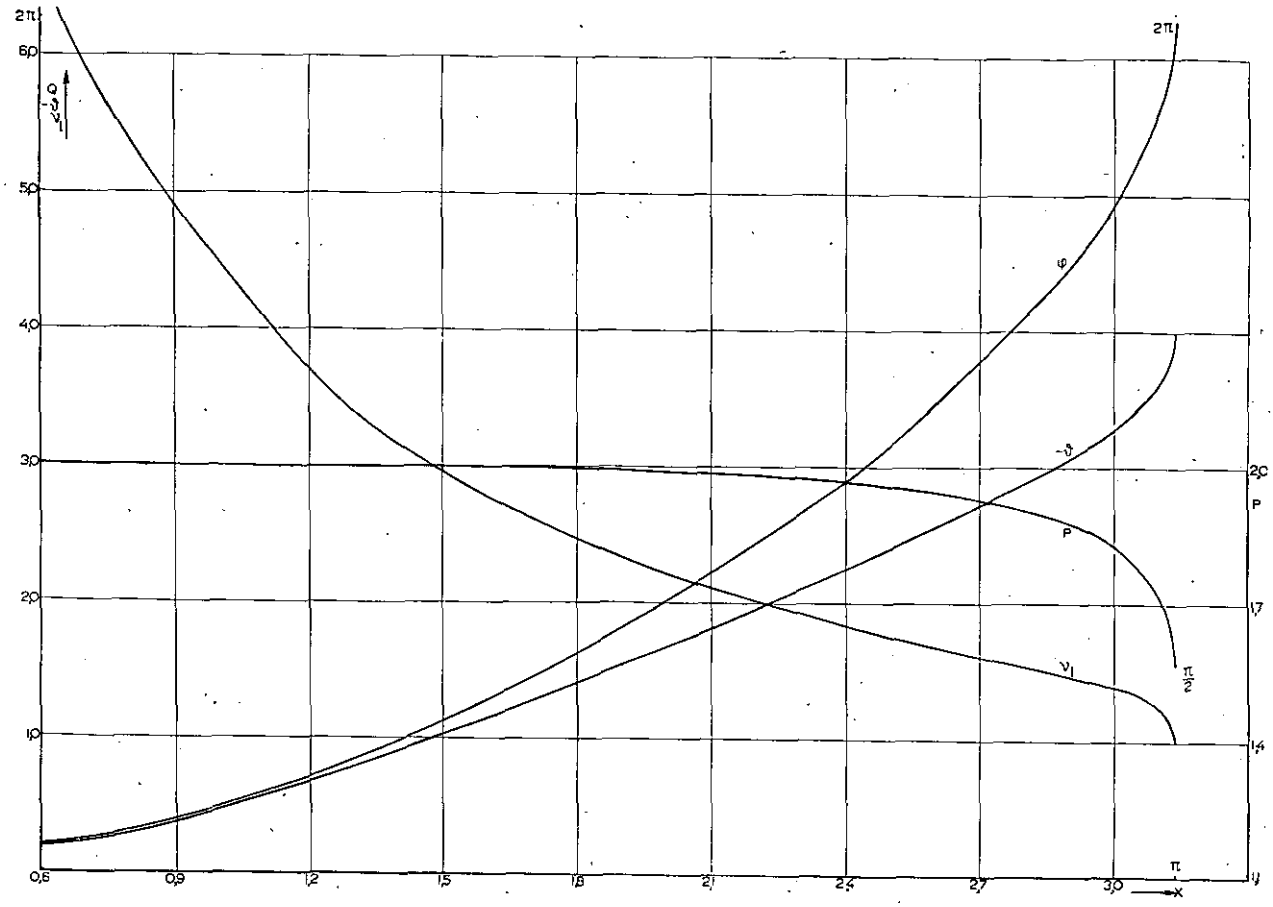

Fig. 15.

Axially symmetrical buckling. Curves for the computation of the minimal buckling load P and the number of frames in one half-wave length ν_l.

rigid. This effect is attained with $Q = 2\pi$. Therefore, it is of no use, as far as axially symmetrical buckling is concerned, to increase the stiffness of the frames over $Q = 2\pi$. This means that in order to prevent general axially symmetrical instability the extensional stiffness of the frames should satisfy

$$t_\varphi \geqq 4\pi^2 \frac{a^2}{b^4} I_{xx}. \qquad (13.8)$$

From fig. 15 we conclude that the approximation of the critical load ($P_{\min} = 2$), given by the system with uniformly distributed frames (sec. 8.1), is less than 1 % in error for $\nu_l > 2$. Therefore, two frames on the half-wave length is mechanically aequivalent to many frames. Only for $\nu_l < 1.5$ the critical load is affected appreciably (more than 5 %) by the frame spacing.

13.3 *Axially non-symmetrical buckling.*

13.3.1 *Frames without torsional stiffness.*

Putting $B_\varphi = 0$ (12.17) simplifies to:

$$K \equiv CR^2 + \frac{(Q - FR)^2}{1 - \frac{R}{\vartheta}\left(A - \frac{R}{6}\right) + \frac{R^2}{\vartheta^2}} =$$

$$= \frac{-\vartheta X^2}{1 - \frac{\vartheta \sin X}{X\,[\vartheta + 2\,(1 - \cos X)]}} \qquad (13.9)$$

The right side of this equation does not contain the structural parameters. Calling it $f(\vartheta, X)$ this function has been plotted in fig. 16 for various values of ϑ between -1.0 and -4.0.

The envelope of this family of curves, following from $\frac{\partial f}{\partial \vartheta} = 0$, yields equation (13.6); therefore, it represents axially symmetrical buckling.

With a given structure A, C, F and Q are known quantities, let us suppose R to be known as well. Then we are able to compute the left side K of equation (13.9) for the value of ϑ used in plotting fig. 16. From fig. 16 we take X as a function of ϑ satisfying (13.9). Plotting X against ϑ we can determine $X_{\min}$ graphically.

We supposed R to be known. In fact, R is unknown and the computations should be repeated for several values of R in order to determine the critical condition. Fortunately, it is not necessary to consider several values of R and the whole range of values of ϑ, since the system with uniformly distributed frames will give a reliable picture of the mode of buckling in the critical condition. Determining N_0, Y_0 by the method developed in sec. 8.2 we find the circumferential wave number from

$$n_0^2 = \frac{1}{k N_0}. \qquad (13.10)$$

With a tube n should be integer, so the mode of

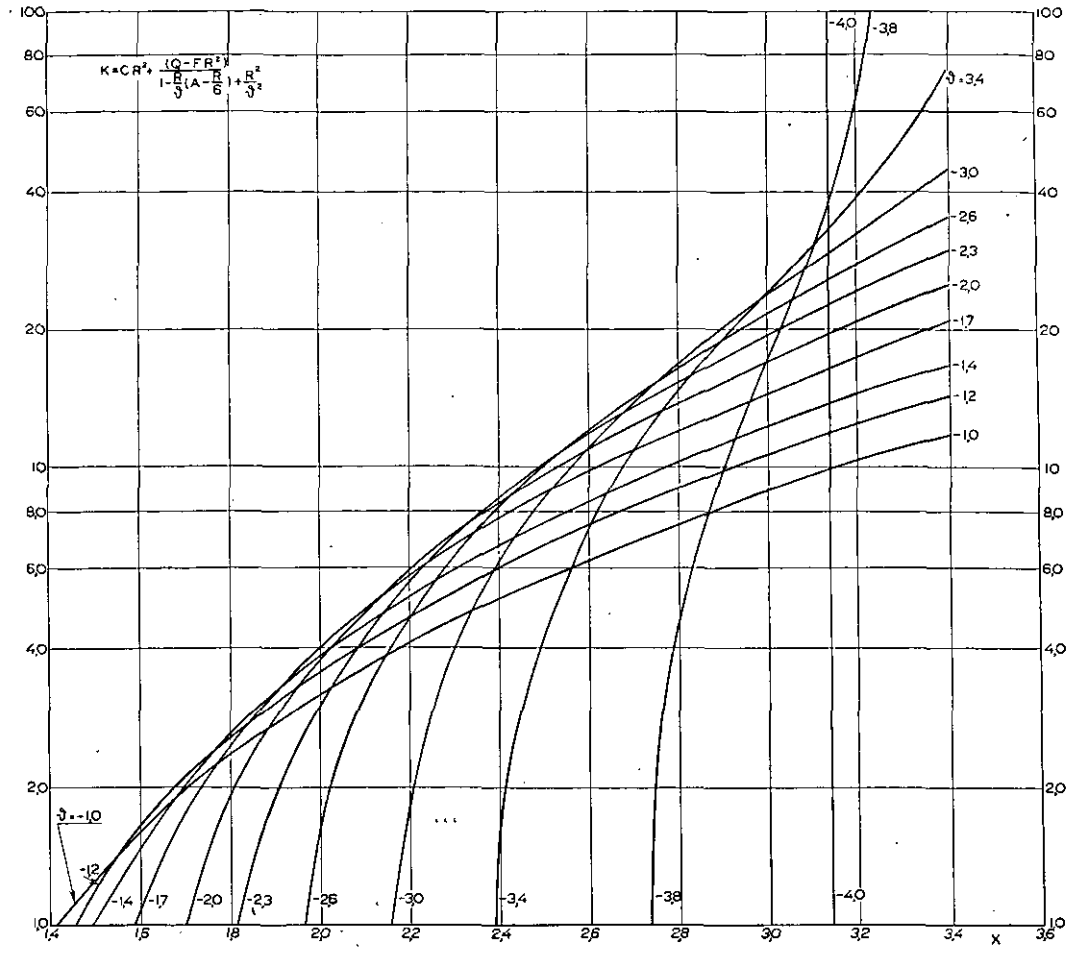

Fig. 16.

Axially non-symmetrical buckling. Diagram for computing the buckling load parameter X.

buckling will be such that n is the integer most adjacent to n_0. Thus we obtain R.

Equating the half-wave length (12.27) to the half-wave length with uniformly distributed frames we find

$$\gamma_0^2 = \frac{Y_0}{N_0}\, Q. \qquad (13.11)$$

Then we take from fig. 14 ϑ_0 which will be a good approximation of ϑ. Choosing 3 values of ϑ near to ϑ_0 we will cover the range in which $X_{\min}$ lies.

13.3.2 *Torsionally rigid frames.*

A direct method to consider the effect of B_φ would involve very cumbersome calculations, since equation (12.17) cannot be split up in a left side not including X and a right side containing X and ϑ only. The following method which is very straightforward indeed, proves to give an accurate approximation.

According to (12.5)

$$P = \frac{X^2}{Q} + \frac{B_x R}{Q} = \frac{X^2}{Q} + \frac{B_x}{N}.$$

The term $\frac{B_x}{N}$ occurs in the same way in the expression (8.6) for the buckling load with distributed frames. From (8.6) it appears that B_x and B_φ affect the buckling load in the same way; so the torsional rigidity of the frames may be added to that of the stringers. This knowledge will be our starting point in dealing with the critical load of the cylinder with equally spaced torsionally stiff frames. Adding the torsional stiffness of the frames to that of the stringers and assuming the frames to have no torsional stiffness, we find $X_{\min}$ by the method developed in sec. 13.3.1; thereupon $P_{\min}$ is determined from

$$P_{\min} = \frac{X^2{}_{\min}}{Q} + (B_x + B_\varphi)\frac{R}{Q}. \qquad (13.12)$$

This approximation, though generally less than 1 % in error, may be used to find the correct result in the following way.

Indicating the first approximation by the suffix $(\ )_1$ we have

$$P_{\min} = \frac{X^2{}_{\min}}{Q} + B_x \frac{R}{Q} \approx (P_{\min})_1 = \frac{(X^2{}_{\min})_1}{Q} + (B_x + B_\varphi)\frac{R}{Q},$$

from which

$$X^2{}_{\min} \approx (X^2{}_{\min})_2 = (X^2{}_{\min})_1 + B_\varphi R. \qquad (13.13)$$

We may expect that X_{min} is quite close to $(X_{min})_2$; 3 values of X in this region are used to compute the correct value.

We can represent equation (12.17) in the form

$$f(\vartheta, X) \equiv \vartheta^4 + x_3\vartheta^3 + x_2\vartheta^2 + x_1\vartheta + x_0 = 0, \qquad (13.14)$$

where

$$x_0 = C R^4 \delta_2,$$
$$x_1 = R^2 [\delta_1 - CR(A - {}^1/_6 R)\,\delta_2 + CR^2\delta_3],$$
$$x_2 = R^2 - R(A - {}^1/_6 R)\,\delta_1 + [CR^2 + (Q - FR)^2]\,\delta_2 - CR^3(A - {}^1/_6 R)\,\delta_3,$$
$$x_3 = -R(A - {}^1/_6 R) + \delta_1 + [CR^2 - (Q - FR)^2]\,\delta_3,$$

and

$$\delta_1 = 2(1 - \cos X) - B_\varphi R \frac{\sin X}{X},$$
$$\delta_2 = \frac{1}{X^2}\left(\delta_1 + B_\varphi R \frac{2(1-\cos X)}{X^2}\right),$$
$$\delta_3 = \frac{1}{X^2}\left(1 - \frac{\sin X}{X}\right).$$

X_{min} and the corresponding value of ϑ should satisfy the equation (13.14) and the condition

$$\frac{dX}{d\vartheta} = 0,$$

or (compare sec. 13.2)

$$\frac{\partial f}{\partial \vartheta} \equiv 4\vartheta^3 + 3x_3\vartheta^2 + 2x_2\vartheta + x_1 = 0. \qquad (13.15)$$

From these two equations ϑ can be eliminated. We can replace (13.14) by an equation of the third degree in ϑ by the operation

$$4\,(13.14) - \vartheta\,(13.15) \equiv x_3\vartheta^3 + 2x_2\vartheta^2 + 3x_1\vartheta + 4x_0 = 0. \qquad (13.16)$$

From (13.15) and (13.16) we come down in a similar way to two quadratic equations,

$$g(X) \equiv x_4\vartheta^2 + x_5\vartheta + x_6 = 0, \qquad (13.17)$$

where

$$x_4 = 8x_2 - 3x_3^2, \quad x_5 = 12x_1 - 2x_2x_3, \quad x_6 = 16x_0 - x_1x_3,$$

and

$$(4x_5 - 3x_3x_4)\vartheta^2 + (4x_6 - 2x_2x_4)\vartheta - x_1x_4 = 0. \qquad (13.18)$$

From (13.17, 18) we derive

$$\vartheta = \frac{x_1x_4^2 + x_6(4x_5 - 3x_3x_4)}{2x_4(x_6 - x_2x_4) - x_5(4x_5 - 3x_3x_4)}. \qquad (13.19)$$

For an assumed value of X we compute x_1, $x_2 \ldots x_6$ and thereafter ϑ from (13.19). These values of X and ϑ do not satisfy (13.14, 15) since in general the assumed value of X will not be equal to X_{min}. Therefore, substituting these X and ϑ in one of the equations (13.15 to 18))they will not satisfy them. Computing now $g(X)$ from (13.17) for 3 values of X and plotting $g(X)$ against X we determine $X = X_{min}$ from $g(X) = 0$ by interpolation.

14 Notations.

To the notations listed in sec. 9 are added the following, apart of a few of local importance,

$g(X) = x_4\vartheta^2 + x_5\vartheta + x_6$
m moment, frame load per radian
q force, " " " "
$x_0, \ldots x_3$ functions of X defined by (13.14)
$x_4, \ldots x_6$ " " " " " (13.17)
$F_1, \ldots F_6$, G_1, G_2 functions of φ
$K = CR^2 + \dfrac{(Q - FR)^2}{1 - \dfrac{R}{\vartheta}(A - {}^1/_6 R) + \dfrac{R^2}{\vartheta^2}}$
$Q = \beta^2 k^{-1} s^{1/2}$, structural parameter characterizing frame spacing
$R = \beta^2 n^2 s^{1/2}$, buckling form parameter
$W_{1\nu} \ldots W_{8\nu}$ $(W_{j\nu})$ integration constants belonging to the bay ν of the cylinder
$X = PQ - B_xR$, load parameter
$\alpha = (c - K_{x\varphi} n^2)^{1/2} k^{-1}$
$\beta = b\, a_x^{-1}$
γ argument of ρ, buckling form parameter, defined by (12.21)
δ defined by (13.14)
ϑ buckling form parameter, defined by (12.18)
ν suffix, indicating frame number, or bay between the frames ν and $\nu + 1$
ν_l average number of frames per half-wave length
ρ buckling form parameter, defined by (12.15)
ω_j coefficient, defined by (12.15)
Γ modulus of ρ, buckling form parameter
$\Delta_\nu = (\,)_{\nu+} - (\,)_{\nu-}$

15 References.

1 Flügge, W.: Die Stabilität der Kreiszylinderschale — Ingenieur-Archiv, Bd. 3 (1932), S. 497—501.

2 Dschou, Dji-Djüän: Die Druckfestigkeit versteifter zylindrischen Schalen — Luftfahrtforschung, Bd. 11 (1934), S. 223—234.

3 Taylor, J. L.: The stability of a monocoque in compression — Aer. Res. Comm. Reports and Memoranda Nr. 1679 (1935).

4 Taylor, J. L.: Monocoque stability in compression-Aircraft Engineering, Vol. 11 (1939), pg. 349, 350.

Completed: October 1946.

Appendix.

Numerical example.

A cylinder, radius $a = 150$ cm, frame spacing $b = 40$ cm, is stiffened by stringers with open section and by frames with closed section. The structural parameters are

$$A = 2.43, \quad B_x = 0, \quad B_\varphi = 0.79, \quad C = 4.76,$$
$$F_x = 0.90, \quad F_\varphi = 2.24, \quad Q = 5.72,$$
$$K_{xx} = 0.370 \times 10^{-4}, \quad s = 0.235.$$

Uniformly distributed frames.

Class I (see table I) $P_{min} = 2$, $l_0 = 53$ cm. This half-wave length being little more than the frame spacing, this case of buckling has to be reconsidered.

Class V (see table I) $P_{min} = 2.62$, $l_0 = 1705$ cm.

Class III As a first approximation of Y_0 we take $Y_1 = C^{1/3} = 2.18$. Substituting it in (8.14) we obtain $P_1 = 1.125$. The second approximation of Y_0 follows from (8.15): $Y_2 = 2.55$, thereafter (8.14) is yielding $P_2 = 1.120$.

The third approximation of Y_0 from (8.15) is again 2.55, so no further calculation is required $P_{min} = 1.12$. We calculate N_0 from (8.7): $N_0 = 6.15$; therefore, $n_0 \doteq 5.2$.

However, n should be integer; the nearest integer being 5, n will be 5 and $N = 6.57$. The circumferential wave length being increased, the longitudinal wave length will decrease, so we conclude from (8.17) that Y will increase. We can determine Y_0 for the given value of N from (8.8), so we would find $Y_0 = 2.67$ and from (8.6) $P = 1.125$. It is easier however to calculate P from (8.6) for a few adjacent values of Y. In this way we find:

Y	2.55	2.75	2.95
P	1.126	1.125	1.128

and we conclude that $Y_0 = 2.7$, yielding $P_{min} = 1.125$.

From (8.17) we calculate the half-wave length $l_0 = 82$ cm.

Equally spaced frames.

Axially symmetrical buckling. For the given value of Q we take from fig. 15 $X = 3.11$, $P = 1.70$, $\nu_l = 1.225$. So the half-wave length, $l \doteq 49$ cm, is somewhat smaller than the half-wave length for uniformly distributed frames and the critical load is 15 % smaller.

Axially non-symmetrical buckling.

The number of circumferential waves is known from the system with distributed frames, $n = 5$ and $N = 6.57$, so $R = \frac{Q}{N} = 0.87$ and the left side of (12.17 is)

$$K = 3.63 + \frac{8.88}{1 - \frac{1.996}{\vartheta} + \frac{0.762}{\vartheta^2}}.$$

Approximating γ by means of (13.11) and taking $Y_0 = 2.7$

$$\gamma = \sqrt{Y_0 R} = 1.53;$$

hence, using fig. 14 $\vartheta = -1.92$.

Then we determine X for the adjacent values of ϑ, $\vartheta = -1.7$; -2.0; -2.3, from fig. 16.

ϑ	-1.7	-2.0	-2.3
K	7.28	7.69	8.04
X	2.36	2.345	2.373

Plotting X against ϑ we find $(X_{\min})_1 = 2.345$ at $\vartheta = -1.96$.

Calculating P_{min} from (13.12) we get

$$(P_{min})_1 = 1.083.$$

The half-wave length, following from $\vartheta = -1.96$ by means of fig. 14 and (12.27), is $l_1 = 81$ cm ($\nu_l = 2.025$).

We shall show now how to determine the exact solution of our problem with the method developed in sec. 13.3.2.

From (13.13) we find $(X_{\min})_2 = 2.49$, so we make our calculations for $X = 2.45$; 2.50; 2.55. Computing then δ_1, δ_2, δ_3, x_0, $x_1 \ldots x_6$ we find, from (13.19), ϑ and thereafter, from (13.17), $g(X)$.

X	2.45	2.50	2.55
δ_1	3.359	3.437	3.508
δ_2	0.628	0.614	0.5985
δ_3	0.1230	0.1218	0.1201
x_0	1.737	1.697	1.654
x_1	-1.642	-1.485	-1.326
x_2	1.030	0.714	0.376
x_3	2.902	2.964	3.014
x_4	-1.065	-1.293	-1.514
x_5	-1.605	-1.378	-1.136
x_6	2.035	1.972	1.904
ϑ	-0.623	-2.09	-5.00
$g(X)$	2.62	-0.82	-30.3

Interpolating graphically we find $g(X) = 0$ for $X = 2.495$, yielding

$$\frac{P_{\min}}{\vartheta} = \frac{X^2}{Q} = 1.085$$

$\vartheta = -1.91$ and $l = 82.2$ cm.

Our first approximation proves to be quite satisfactory.

Comparing these results with those obtained from the system with uniformly distributed frames we conclude that this latter system yields approximately the correct wave length and a critical load that is about 4 % too large.

In this case ν_l is about 2 and the approximation given by the system with distributed frames is surprisingly good. We will consider a different case, characterized by a smaller value ν_l. Let us assume the frame spacing to be 50 cm instead of 40 cm, the structural parameters being the same except Q which is now 8.95. The system with distributed frames is not affected by this change; it will yield the same results as before.

The critical load for column failure is, according to (13.2),

$$P = \frac{\pi^2}{Q} = 1.103.$$

Axially symmetrical buckling will not occur since $Q > 2\pi$. Now in the case of axially non-symmetrical buckling $R = 1.36$ and the approximate critical value of $\gamma = 1.92$, yielding $\vartheta = -2.69$. So we determine X from the values of $\vartheta = -2.3$; -2.6; -3.0; -3.4, giving $X = 2.90$; 2.87; 2.865, 2.92.

The first approximation is $(X_{\min})_1 = 2.86$; $(P_{\min})_1 = 1.035$; $\vartheta_1 = -2.90$, $l_1 = 77$ cm. From (13.13) we find $(X_{\min})_2 = 3.04$ and making the calculations for 3 values of X near to $(X_{\min})_2$ we find $X_{\min} = 3.076$; $P_{\min} = 1.054$; $\vartheta = -2.71$; $\nu_l = 1.625$, $l = 81.1$ cm.

The difference between the first approximation of the critical load and its correct magnitude is about 2 %; the difference between the critical loads for uniformly distributed and equally spaced frames is even in this case only 6 %.

REPORT V. 1297.

Diagrams of critical flutter speed for wings of a certain standard type

by

Ir. A. I. VAN DE VOOREN and Drs. J. H. GREIDANUS

Summary.

In order to obtain a more complete knowledge of the influence of some structural parameters as wing density, positions of flexural and inertia axes, aerodynamic aileron balance, stiffness-ratio, etc., on the critical flutter speed of wing-aileron systems, calculations were made for a large number of cases in which these parameters were varied systematically. This report gives a short review of the applied method, together with diagrams, containing the results of the calculations. In these graphs the critical flutter speed is plotted against the stiffness ratio. A comparison of the diagrams reveals the influence of the parameters. The principal conclusions are listed in section 4. Some of the most important are that, generally, the critical speed increases with increasing wing-density (if resonance frequencies are assumed to be constant), with increasing aerodynamic aileron balance (see section 22), with increasing torsional stiffness and with increasing chord. For the wing without aileron no flutter occurs when the flexural axis lies aft of the inertia axis, but for a wing with a statically balanced aileron, which can be deflected freely (antisymmetrical flutter), the critical speed nearly always decreases when the flexural axis is shifted backwards.

Contents.

1 Introduction.

The calculation of the critical flutter speed of a wing-aileron system, as it can be performed on the basis of the aerodynamic theory of the oscillating aerofoil, is extremely laborious. Therefore it would be of the greatest importance if it were possible to give the results of these calculations once for all in such a systematical form, that the flutter speed of any wing of conventional construction could immediately be taken from these results. This is, however, impossible because the flutter speed depends on too many variables, which in each case have their special values. Such a catalogue would show an almost unlimited extent; the compiling of it would require an immense program of calculations.

Nevertheless it is widely known that some characteristics of the wing structure have a strong influence on flutter speed and that in many cases it is possible to qualify a construction as "good" or "bad" with regard to the occurrence of flutter.

Such a qualitative judgment, which in favourable cases may even quantitatively not be quite unsatisfactory, could be sharpened considerably if the results of systematic calculations of a not too confined extent were available for simplified wing-aileron models, which show a reasonable analogy with real systems. To obtain these results a program of investigation was composed, leading to diagrams for the flutter speed, which will be published in three reports.

This first report deals with the calculated flutter characteristics of some wing and wing-aileron models, of which the aileron can be deflected freely (antisymmetrical oscillations). For the complete range of investigation the reader is referred to section 23. The second report will give the change of the flutter speed in consequence of certain small variations in the aileron construction, while the third report will contain diagrams referring to a wing-aileron system of which the deflection of the aileron is influenced by a spring between wing and

aileron (symmetrical oscillations). To simplify the calculations the flexural stiffness of the wing will be neglected in the last report.

In what degree and with what numerical accuracy this material will be useful for the examination of a real wing is difficult to predict, because too many influences play a part. In particular one has to await how far these results, calculated for a wing, which is built in at the root, will agree with the symmetrical resp. antisymmetrical oscillations of a real aeroplane. It may, however be expected that the influence of certain structural changes in the flutter speed can be deduced wih reasonable accuracy from the diagrams.

The flutter speed has been calculated chiefly according to the methods described in the N.L.L. reports V. 1252 and V. 1304 [1]). Only a first approximation was worked out, which means that the modes of displacement were not improved by an iterative process. The aerodynamic forces were introduced in accordance with the theory of Küssner and Schwarz [2]).

2 The wing-aileron model.

21 General shape.

The calculations were performed for a tapered wing, which is rigidly fixed at the root. The tip chord amounts to $^1/_3$ of the root chord. All characteristic lines, i.e. the leading and trailing edges of the wing, the flexural and inertia axes, the leading edge of the aileron and the aileron hinge axis, are straight and have the same point of intersection. Thus ε, σ, η and ε_1 are constant along the span (s. fig. 1 and list of symbols, section 4). Likewise μ, $\varkappa$, μ_1 and $\varkappa_1$ are constant.

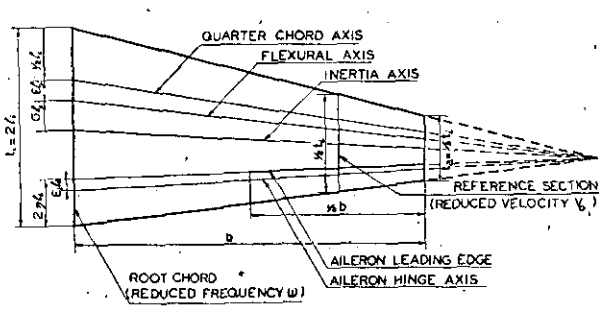

Fig. 1. Plan of tapered wing-aileron model.

Both flexural and torsional wing stiffness have been supposed to be directly proportional to the third power of the chord. The aileron torsional stiffness is taken as infinitely large, while the bending of the aileron is determined by the fact, that the hinge axis has been considered as part of the wing.

The aileron, which is completely statically balanced, extends from the section at $y = {}^1/_2\, b$ to the wing tip and can be deflected freely without interference of any spring. The critical speed has been calculated also for a wing of the same shape but without aileron (the wing completed with the area of the removed aileron).

22 Aerodynamic assumptions.

The aerodynamic forces are assumed to be in agreement with the limiting case when there is no airflow through the gap between wing and aileron (see Küssner and Schwarz, loc. cit.). As it is known, the limiting value $\eta_s \longrightarrow 0$ cannot be introduced consequently, owing to a term which would give a logarithmic infinity. Therefore it is necessary to assume a certain width of the gap, which must be substituted in the term mentioned, while in all other terms the width of the gap is neglected. It can be shown that the value of the aerodynamic aileron balance at $\omega = 0$ depends on the supposed gap width (see section 33). To investigate the influence of the assumed value of the gap width, calculations were performed for two different values of the gap width, corresponding with two different values of the aerodynamic aileron balance. Attention must be paid to the fact that in this report a change in aerodynamic aileron balance always means that another value has been given to the width of the gap, but that the position of the hinge axis remains unaltered.

The value of the air density corresponds to the standard value at sea level

$$\varrho = \frac{1}{8}\,\mathrm{kg\ m^{-4}\ sec^2}.$$

23 Values of the varied parameters.

As basic variations the following values were given to the parameters ε, $\varepsilon+\sigma$ and μ:

ε =	−0,1	0,1	0,3
$\varepsilon+\sigma$ =	0,1	0,3	0,5
μ =	5	15	30

These values were combined in all possible ways, so 27 different cases were investigated. The other, not varied parameters had the values:

$\varkappa = 0{,}6$, $\eta = 0{,}25$, $\varepsilon_1 = 0{,}10$ and $\mu_1 \varkappa_1^2 = 0{,}05$.

Calculations were made for two values (80 % and 62,4 %) of the aerodynamic aileron balance. Because ε_1 is kept constant, this means that the width of the gap between wing and aileron has been fixed on two different values (viz. $\eta_s = 3{,}048.10^{-4}$ and $\eta_s = 7{,}881.10^{-3}$).

The critical flutter speed has been plotted as a function of the stiffness ratio $\lambda = \left(\frac{\nu_A}{\nu_B}\right)^2$. For the completeness of the diagrams, negative values of λ, which result from the calculations simultaneously with the positive values, but which have no physical meaning, have also been included.

24 Modes of displacement.

These were put equal to the modes of displacement of the uncoupled fundamental oscillations of the wing in still air. They are illustrated in figs.

---

[1]) Published in Vol X, resp. Vol. XII of the „Verslagen en verhandelingen van het Nationaal Luchtvaartlaboratorium", Amsterdam.

[2]) Luftfahrtforschung Vol. 17 (1940), p. 337.

2a and 2b and take the following values along the span:

y	0	$\frac{1}{8}b$	$\frac{2}{8}b$	$\frac{3}{8}b$	$\frac{4}{8}b$
z_1	0	0,0169	0,0682	0,1547	0,2752
φ_1	0	0,1490	0,3170	0,4890	0,6511

y	$\frac{5}{8}b$	$\frac{6}{8}b$	$\frac{7}{8}b$	b
z_1	0.4268	0,6039	0,7983	1
φ_1	0,7921	0,9029	0,9745	1

No chordwise oscillating motion is supposed to occur and each fore and aft section is assumed to move as a rigid body.

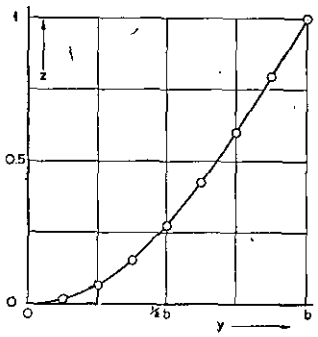

Fig. 2a. Fundamental flexural mode

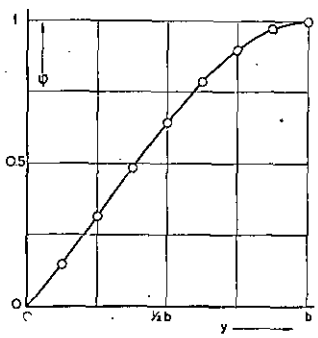

Fig. 2b. Fundamental torsional mode

25 Structural damping.

The structural damping was represented by giving a phase lead to the elastic restoring force in regard to the displacement. The phase leads were assumed to be equally large for flexure and torsion and thus damping could be introduced in the calculations by the multiplication of all elastic terms with the same factor $1 + ih$, where h is the angle of lead (in radians). Besides the values 0 and 0,1 there were also given negative values to h ($-0{,}1$ and $-0{,}05$), which, especially in cases that are still stable for large reduced velocities V_0, can give valuable information about the influence of the parameters on the flutter speed. For the significance of negative values of the damping the reader is referred to report V.1304.

It should be born in mind that, owing to the fact that the aileron deflection is not influenced by a spring and that it cannot be twisted, the motion of the aileron is not restricted by any direct damping.

3 General method of solution.

31 The equations of motion.

For the wing these equations are obtained immediately, when the two conditions of equilibrium, mentioned hereunder, are applied to an infinitely narrow wing strip.

1° The total of all forces, perpendicular to the wing plane, is zero.

2° The total of all moments about the flexural axis is zero.

With the usual symbols (see report V. 1304 and list of symbols, section 4 of this paper) the equations become

$$\left.\begin{aligned} m_{11}\ddot{z}+m_{12}\ddot{\varphi}+(Bz'')''&=K\\ m_{12}\ddot{z}+m_{22}\ddot{\varphi}-(T\varphi')'&=M+\varepsilon lK-N-\varepsilon_1 lR \end{aligned}\right\} \quad (1)$$

The aileron being torsionally rigid, the equation which determines the aileron deflection is obtained by equating to zero the total moment of the complete aileron about its hinge axis. Hence

$$\ddot{\gamma}\int_{\frac{1}{2}b}^{b} m_{33}\,dy=\int_{\frac{1}{2}b}^{b}(N+\varepsilon_1 lR)\,dy \quad (2)$$

Introducing the ratio:

$$\frac{l}{l_i}=f \quad (3)$$

all chords can be referred to the root chord ($=2l_i$), thus giving:

$$\left.\begin{aligned} m_{11}&=\mu f^2\pi\varrho l_i^2\\ m_{12}&=-\mu\sigma f^3\pi\varrho l_i^3\\ m_{22}&=\{\mu(\varkappa^2+\sigma^2)-\mu_1\varkappa_1^2\}f^4\pi\varrho l_i^4\\ m_{33}&=\mu_1\varkappa_1^2 f^4\pi\varrho l_i^4\\ B&=B_0 f^3\\ T&=T_0 f^3 \end{aligned}\right\} \quad (4)$$

According to report V. 1304 for a sinusoïdal oscillation the aerodynamic forces (resp. moments) can be written in the following form:

$$\left.\begin{aligned} K&=m_L\nu^2\{a_{11}z+2a_{12}f l_i\varphi+2a_{13}f l_i\gamma\}\\ M+\varepsilon lK-N-\varepsilon_1 lR&=m_L\nu^2\{2a_{21}f l_i z+\\ &\qquad+4a_{22}f^2 l_i^2\varphi+4a_{23}f^2 l_i^2\gamma\}\\ N+\varepsilon_1 lR&=m_L\nu^2\{2a_{31}f l_i z+\\ &\qquad+4a_{32}f^2 l_i^2\varphi+4a_{33}f^2 l_i^2\gamma\} \end{aligned}\right\} \quad (5)$$

with $m_L=\pi\varrho f^2 l_i^2$

The a_{ik} are dimensionless, complex coefficients of the aerodynamic forces, which depend on ω, η, ε and ε_1. Their values can be taken from the tables 1 and 2 of report V. 1304.

As it is impossible to solve the equations (1) and (2) exactly, the usual procedure is to derive from them approximate algebraic equations. This is done by substituting:

$$z=l_i q_1 e^{i\nu\tau}z_1(y),\quad \varphi=q_2 e^{i\nu\tau}\varphi_1(y),\quad \gamma=q_3 e^{i\nu\tau} \quad (7)$$

where q_1, q_2, q_3 are coefficients, which are beforehand unknown, while $z_1(y)$ and $\varphi_1(y)$ are the assumed modes of displacement of the wing. This causes the appearance of errors $\varepsilon_K(y)$, $\varepsilon_M(y)$ and ε_N in the equations (1) and (2). The errors $\varepsilon_K(y)$ and $\varepsilon_M(y)$, which depend on the values, given to q_1, q_2 and q_3, can vanish only when the functions z_1 and φ_1 allow the construction of an exact solution.

Two of the approximate algebraic equations are now obtained by multiplying ε_K and ε_M with suitable weightfunctions and putting the integral (along the span) of the resulting product equal

to zero. The introduced weightfunctions are respectively

$$\frac{3w^2-w^3}{6} \text{ and } w, \text{ where } w=\frac{y}{b} \qquad (8)$$

The third equation for q_1, q_2 and q_3 is obtained by putting $\varepsilon_N=0$.

Thus the reduction from the equations of motion into algebraic equations is not carried out according to the Galerkin method, in which z_1 and φ_1 themselves are chosen as weightfunctions. The introduction of the weightfunctions (8) has, however, certain advantages, as it gives not only the exact solution (ν, q_1 q_2 and q_3) when the real modes of displacement are the same as the assumed ones, but also when the real modes are equal to the weightfunctions. Therefore, when the real modes do not quite agree with z_1 and φ_1 and the weightfunctions show some resemblance to the real modes, (and this is the case for the choice (8) of the weightfunctions) the method used here may give a better approximation than the Galerkin method.

The terms in the algebraic equations, resulting from the aerodynamic forces, were evaluated by means of a development in Taylor-series to the reduced frequency, which varies along the span in accordance with the variation of the chord. Only the constant, linear and quadratic terms of these series are considered. For reference section was taken the fore and aft section at the middle of the aileron $\left(y=\frac{3}{4}b \text{ and } l=\frac{1}{2}l_i\right)$.

The set of homogeneous, algebraic equations has a solution only when its determinant is equal to zero. As the determinant is formed by complex elements, this conditions leads to two equations, giving the stiffness-ratio, for which the system will produce a critical oscillation at the given value of V_0, as well as the frequency of this oscillation. Introducing the uncoupled resonance frequencies in still air, ν_A and ν_B, a solution is found in which $\frac{\nu_A}{\nu_B}$ is a measure for the stiffness-ratio and $\frac{\nu}{\nu_B}$ for the frequency. The determinant equation being quadratic in ν, two values for $\frac{\nu_A}{\nu_B}$ and for $\frac{\nu}{\nu_B}$ are calculated, which may be complex indicating that the system is stable. By

$$\frac{v_{crit.}}{\nu_B . l_i}=V_0\frac{\nu}{\nu_B} \qquad (9)$$

the critical speed, also dimensionless, was calculated.

32 Divergence speed.

The divergence speed can be found easily by replacing the instationary aerodynamic forces by the stationary forces, which is carried out with the aid of the following limits:

$$\nu \longrightarrow 0,\ V_0 \longrightarrow \infty,\ \nu V_0 \longrightarrow \frac{v}{l_i},\ \nu^2 \sum_0^2 P_{1n}\xi^n \longrightarrow 0$$

$$\nu^2 \sum_0^2 P_{2n}\xi^n \longrightarrow 4\frac{v^2}{l_i^2},\ \nu^2 V_0^2(1+\xi)^2 \longrightarrow \frac{v^2}{l_i^2}; \qquad (10)$$

the last three of which appear in the series of the aerodynamic forces.

For the wing without aileron the divergence speed becomes infinite, when the flexural axis lies before the quarter chord axis.

33 The aerodynamic balance.

Definition. When the aerodynamic balance for $\omega=0$ amounts to n %, this means that the moment of the aerodynamic forces, which is caused by a stationary aileron deflection, is (100—n) % of the aerodynamic moment obtained for an equally large deflection when the aileron hinge axis is shifted to the aileron nose. In both cases the wing is assumed to show no distortion, i.e. $z=0$ and $\varphi=0$.

Thus the aerodynamic balance n is determined by the equation (for the aileron considered here is $\varepsilon_1=0{,}10$ and $\eta=0{,}25$):

$$\left|(N+\varepsilon_1 lR)_{\substack{\varepsilon_1=0{,}10\\ \eta=0.25}}=\left(1-\frac{100}{n}\right)(N)_{\substack{\varepsilon_1=0\\ \eta=0{,}25}}\right| \text{ stat.}$$

or, with the aid of equation (5):

$$\left|(a_{33})_{\substack{\varepsilon_1=0{,}10\\ \eta=0{,}25}}=\left(1-\frac{n}{100}\right)(a_{33})_{\substack{\varepsilon_1=0\\ \eta=0{,}25}}\right| \text{ stat,} \qquad (11)$$

When the aerodynamic balance is given, it is possible to calculate from equation (11) the width of the gap between wing and aileron, which has to be substituted in that term of the aerodynamic forces, showing the logarithmic singularity for $\eta_s=0$. If η_s represents the ratio of this gap to the whole chord, then it appears that:

Aerodynamic balance 80 % : $\eta_s=3{,}048.10^{-4}$

" " 62,4 % : $\eta_s=7{,}881.10^{-3}$

4 Results.

41 General.

In the diagrams the critical flutter speed, reduced to a dimensionless form, is plotted against the stiffness-ratio λ. Calculated points are specially marked. Points which refer to the same damping are connected by drawn lines, while points obtained by the same values of reduced velocity V_0 are connected by dotted lines. The numbers near the dotted lines denote the reduced frequency ω at the wing root. For negative values of the damping h, both oscillations are unstable for small values of the velocity v. This is indicated by double-shading of the boundary of the area. Single-shading means that one oscillation is unstable. Thus the flutter speed is given by a line, which is single-shaded at the upper side and not shaded at the lower side.

In other diagrams the flutter speed is plotted as a function of ε, $\varepsilon+\sigma$ and μ.

42 Influence of wing density.

When the wing density increases and the resonance frequencies in still air are unvaried, the critical speed rises in most cases (fig. 11, 18, 19).

For small values of the wing density there exists a minimum of critical speed. When the wing density is decreased still more, the critical speed increases very quickly.

When instead of the resonance frequencies the stiffnesses are kept constant, the minimum critical speed is shifted towards very large values of the wing density.

43 Influence of position of flexural axis.

When the flexural axis is shifted backwards, the critical speed of the wing without aileron falls until this axis closely approaches the inertia axis (fig. 13). Then the critical speed increases quickly, which ultimately leads to the complete vanishing of the instability. When the flexural axis lies aft of the inertia axis, no flutter occurs. An exception of this general rule, however, was found, namely for large wing density, very backward position of both axes and small stiffness-ratio (fig. 8).

44 Influence of position of inertia axis.

For the wing without aileron the critical speed decreases when the inertia axis is located more backward (fig. 12). For the wing with aileron the position of the inertia axis has no pronounced influence on flutter speed, though a small separation of the flexural and inertia axes may cause an increase of the critical speed (fig. 18, 20).

45 Influence of aerodynamic aileron balance.

The flutter speed falls with decreasing aerodynamic balance (compare fig. 14, 15 with fig. 16, 17). For large values of the aerodynamic balance, the critical speed for the wing-aileron-system (aileron completely statically balanced) is higher than for the wing without aileron, except in those cases, in which the flexural and inertia axes are almost coïnciding or in which the flexural axis lies aft of the inertia axis.

46 Influence of flexural stiffness.

Usually the flexural resonance frequency ν_A is considerably lower than the torsional resonance frequency ν_B. Therefore an increase in flexural stiffness gives a diminution of the difference between these frequencies. For the simple system of a wing without aileron the lowest value of the critical speed occurs when both frequencies are nearly equal (fig. 3/10). Thus an increase of the flexural stiffness of a conventional wing tends to diminish the critical speed.

For wing-aileron systems with high aerodynamic balance the minimum in flutter speed occurs at

$$\nu_A \approx 0{,}7\,\nu_B \text{ (fig. 14, 15).}$$

This minimum is more pronounced for larger values of the wing density. For flexural stiffnesses higher than the one for which the minimum occurs, the critical speed increases rapidly. For $\nu_A = \nu_B$ the instability has vanished.

For wing-aileron systems with low aerodynamic balance, the influence of the flexural stiffness depends very much on the wing density (fig. 16, 17). For small values of the wing density, an increase in flexural stiffness (when $\nu_A < \nu_B$) tends to raise the critical speed. For large values of the wing density there is on the contrary a considerable fall in the flutter speed for increasing flexural stiffness, which brings the minimum again near to $\nu_A = \nu_B$.

47 Influence of torsional stiffness.

It is nearly always favourable to increase the torsional stiffness as this results in an important rise of the flutter speed (fig. 3/10, 14/17). Though very low values of the torsional stiffness ($\nu_B < \nu_A$) remove also the instability for a wing with aileron this possibility cannot be realized in practice, unless ν_A, i.e. the flexural stiffness is very large.

48 Influence of structural damping.

The structural damping always raises the critical speed because it absorbs energy from the oscillation. It is not possible to give general indications when the influence of the damping will be large and when small. But for the wing-aileron system with small aerodynamic balance (fig. 16, 17), there are large ranges of the stiffness-ratio for which the flutter speed raises considerably or may even become infinite, when there is some damping (so-called undangerous flutter). This is favoured by a large distance between the flexural and the inertia axis and by a large wing density.

49 Influence of wing chord.

When all other variables (wing density, resonance frequencies etc.) are kept constant, the critical speed increases linearly with the chord.

5 List of symbols.

y	coordinate along the span, measured from and perpendicular to the root chord.
z	displacement of point of flexural axis normal to the wing (upwards positive)
φ	angle of twist of the wing (positive when trailing edge moves downwards)
γ	aileron deflection (downward deflection positive)
$2\,l$	chord
$2\,l_i$	root chord
f	$= \frac{l}{l_i}$
$\varepsilon\,l$	distance of flexural axis aft of quarter chord axis
$\sigma\,l$	distance of inertia axis (wing+aileron) aft of flexural axis
$\varepsilon_1\,l$	distance of aileron hinge axis aft of aileron leading edge
$\varkappa\,l$	radius of gyration (wing+aileron) about inertia axis
$\varkappa_1\,l$	radius of gyration (aileron) about aileron hinge axis
η	ratio of aileron chord to total chord

η_s	ratio of gap between wing and aileron to total chord
ϱ	air density
$\mu \pi \varrho l^2$	mass of wing + aileron per unit span
$\mu_1 \pi \varrho l^2$	mass of aileron per unit span
$m_L = \pi \varrho l^2$	mass of the air per unit span in the cylinder round wing + aileron
b	semi-span
w	$= \frac{y}{b}$
B	flexural stiffness of the wing
B_0	flexural stiffness of the wing at the root
T	torsional stiffness of the wing
T_0	torsional stiffness of the wing at the root
ν_A	uncoupled flexural resonance frequency in still air
ν_B	uncoupled torsional resonance frequency in still air
ν	frequency of critical oscillation
$\lambda = \left(\frac{\nu_A}{\nu_B}\right)^2$	stiffness-ratio
v	airspeed
v_{crit}	critical flutter speed
V	reduced velocity $\left(V = \frac{v}{2 \nu l}\right)$
V_0	reduced velocity at the reference section $y = \frac{3}{4} b$
ω	reduced frequency at the wing root $\left(\omega = \frac{1}{V_0}\right)$
τ	time
n	aerodynamic balance of aileron (in %)
h	structural damping (angle by which the elastic flexural or torsional moments lead the displacements)
q_i	amplitude of flexural, resp. torsional, resp. aileron oscillation
K	total aerodynamic force of wing + aileron per unit span (positive upwards)
M	total aerodynamic moment of wing + aileron per unit span about the quarted chord axis (positive if it tends to increase the angle of incidence)
R	aerodynamic force of aileron per unit span (positive upwards)
N	aerodynamic moment of aileron per unit span about the aileron nose (positive if it tends to increase the aileron deflection)
ε_K, ε_M, ε_N	errors of the equations of motion, when the assumed modes of displacements z_1 and φ_1 are substituted
a_{ik}	complex aerodynamic coefficients

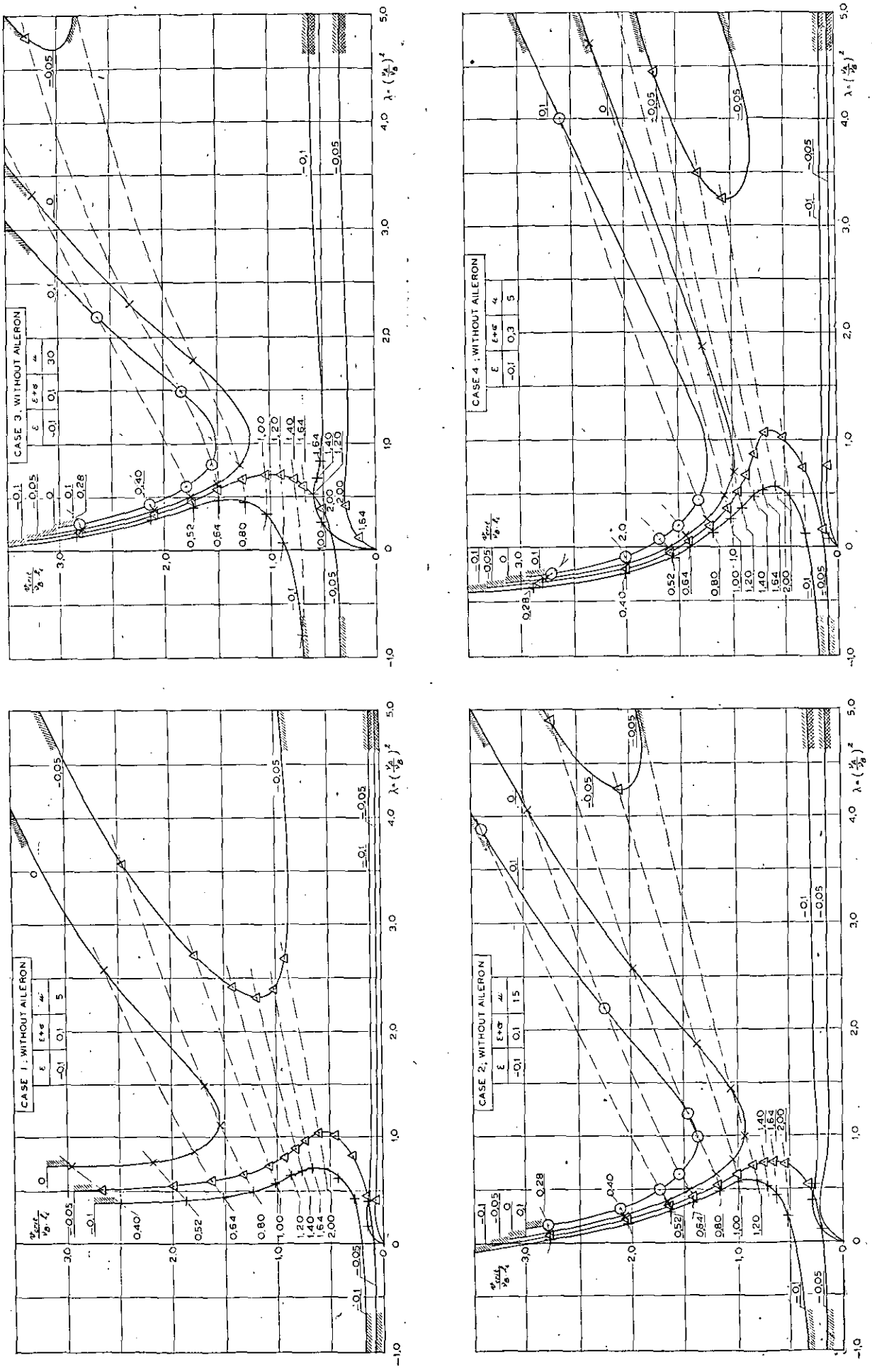

Fig. 3. *Critical flutter speed as function of the stiffness ratio.*

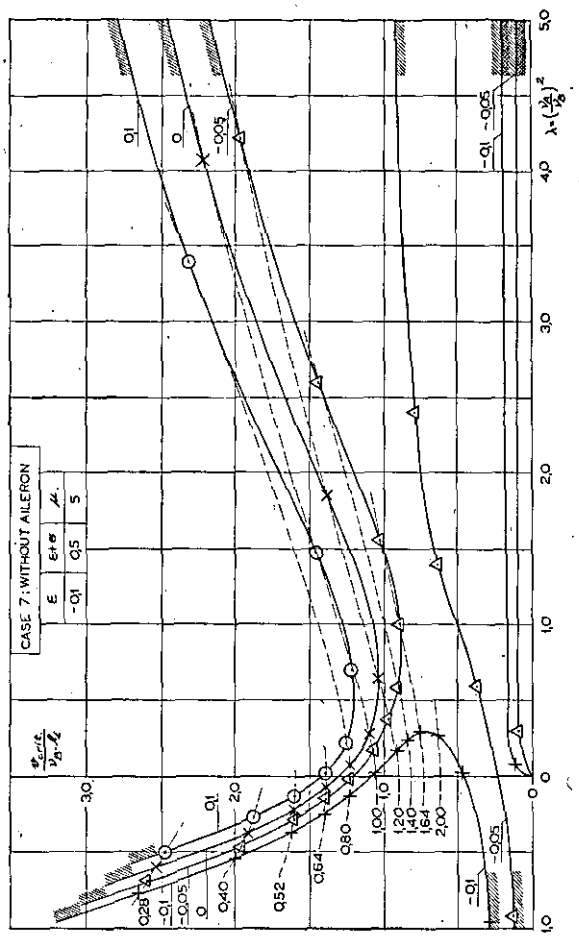

Fig. 4. Critical flutter speed as function of the stiffness ratio.

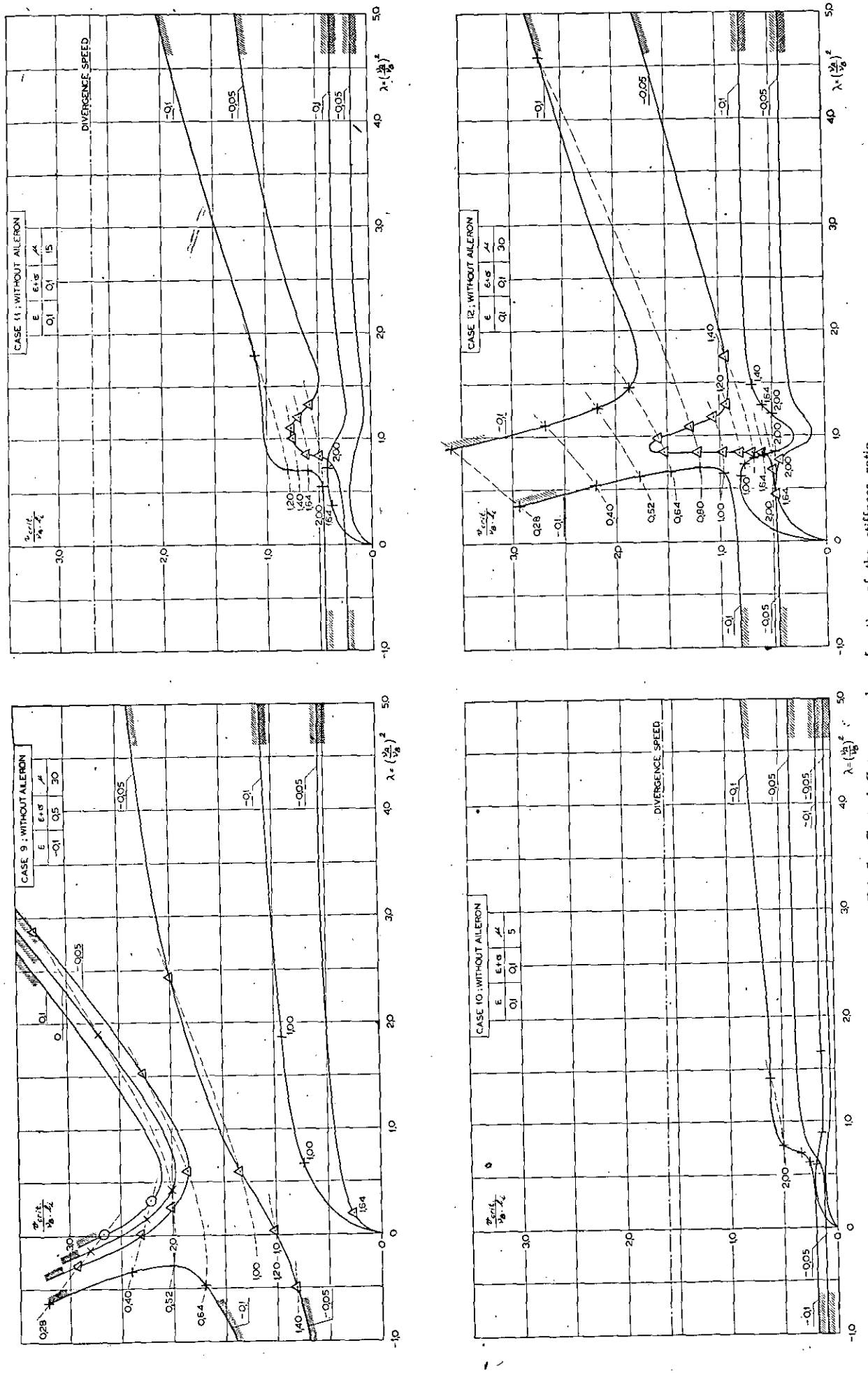

Fif. 5. Critical flutter speed as function of the stiffness ratio.

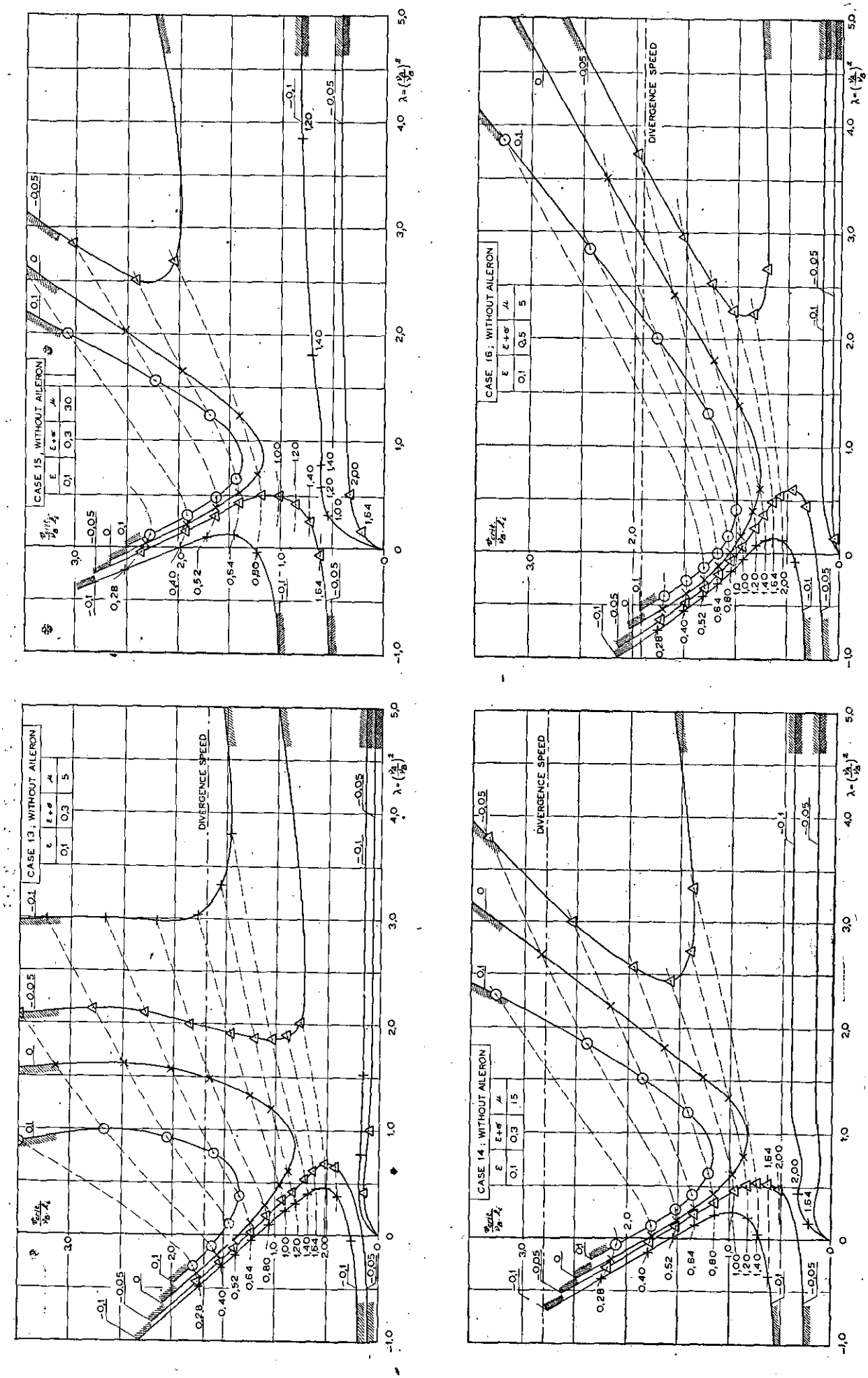

Fig. 6. Critical flutter speed as function of the stiffness ratio.

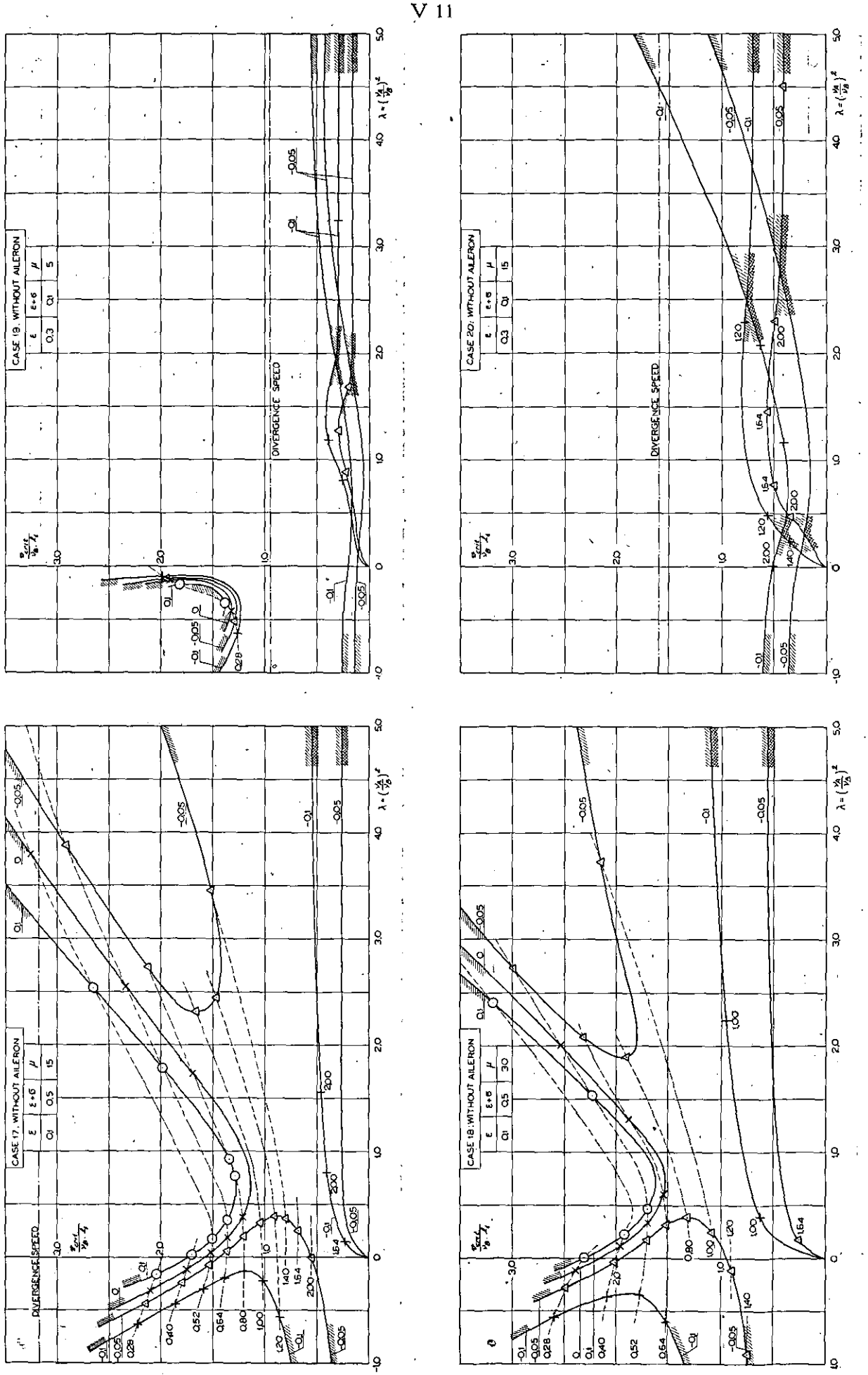

Fig. 7. Critical flutter speed as function of the stiffness ratio.

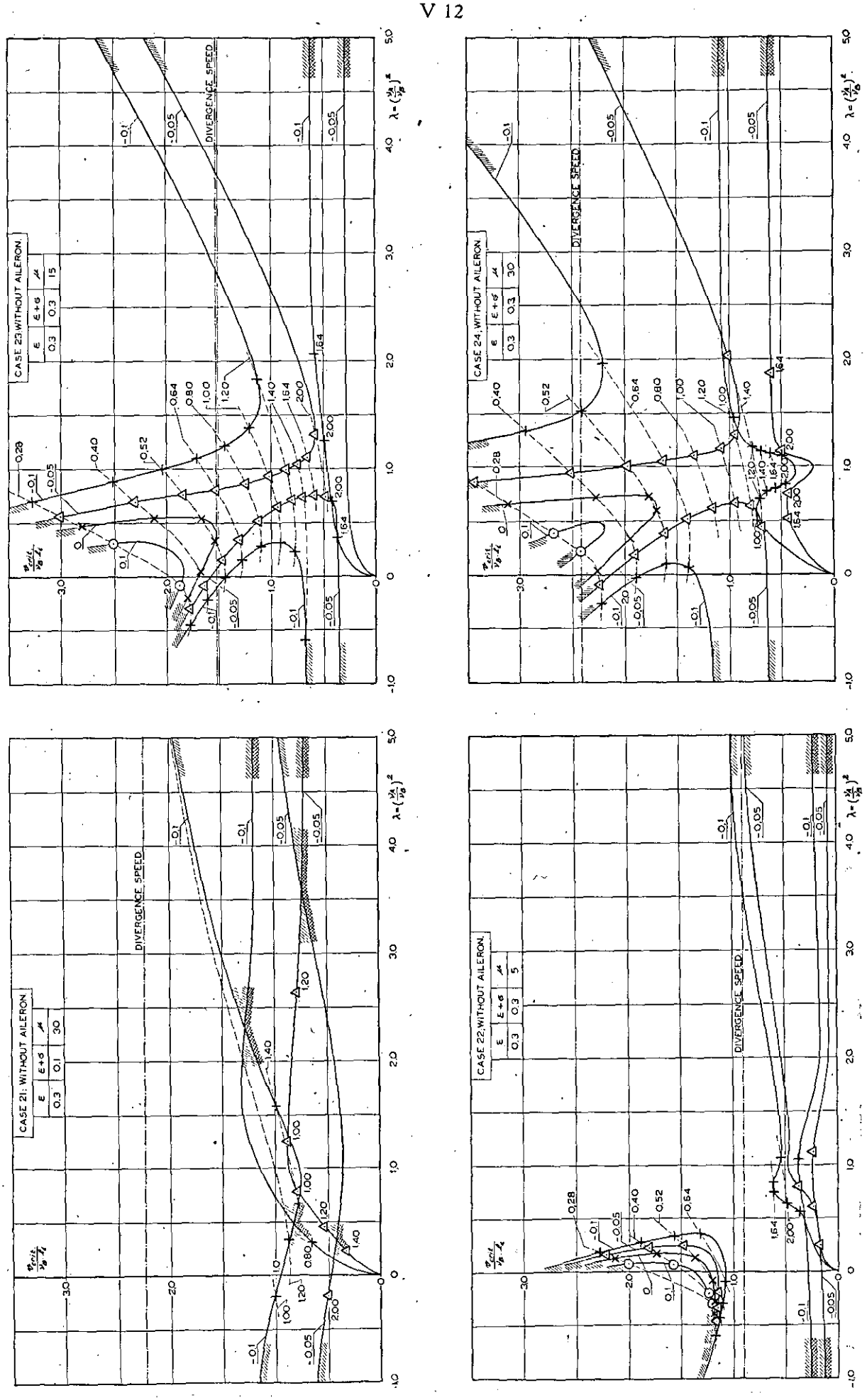

Fig. 8. Critical flutter speed as function of the stiffness ratio.

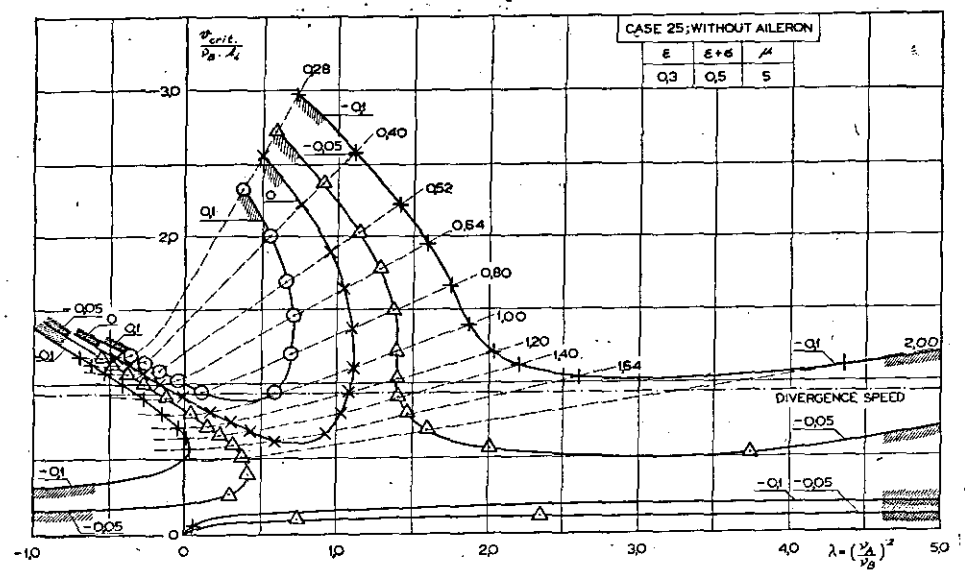

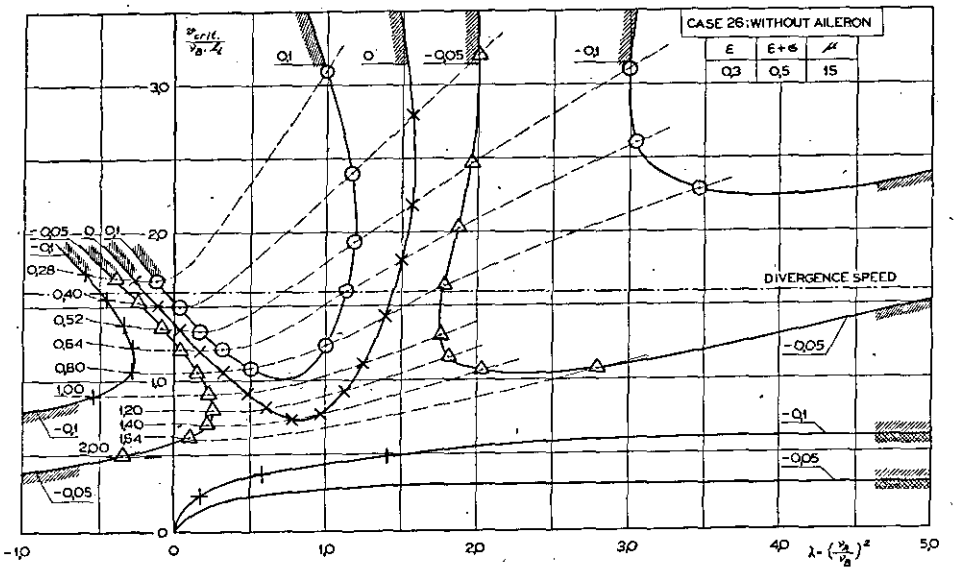

Fig. 9. Critical flutter speed as function of the stiffness ratio.

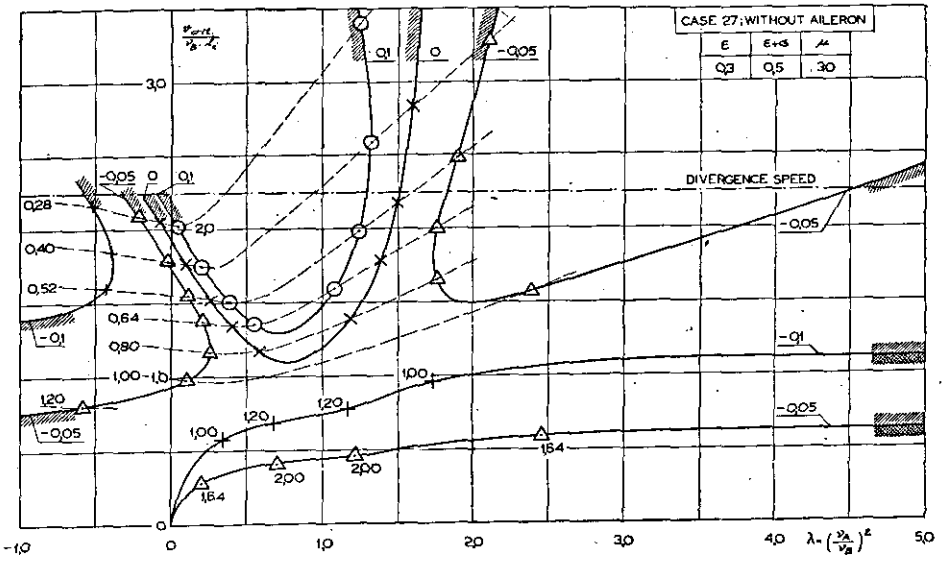

Fig. 10. Critical flutter speed as function of the stiffness ratio.

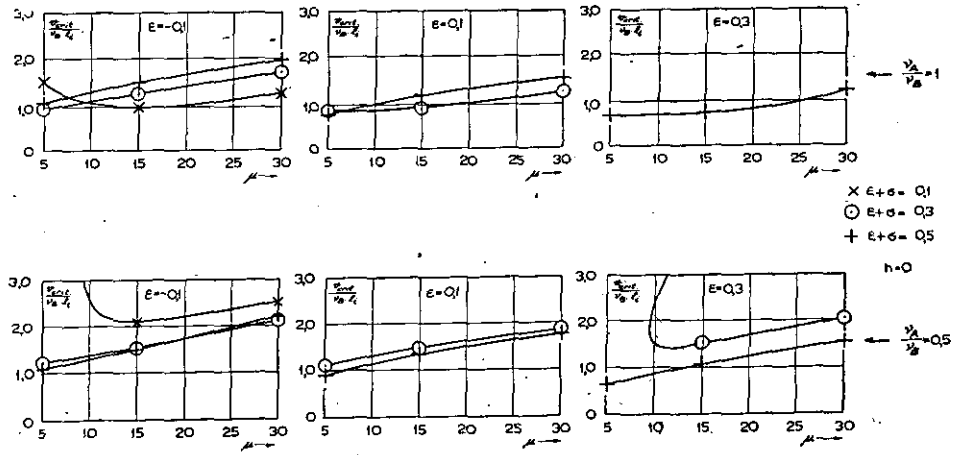

Fig. 11. Critical flutter speed as function of the wing density (wing without aileron).

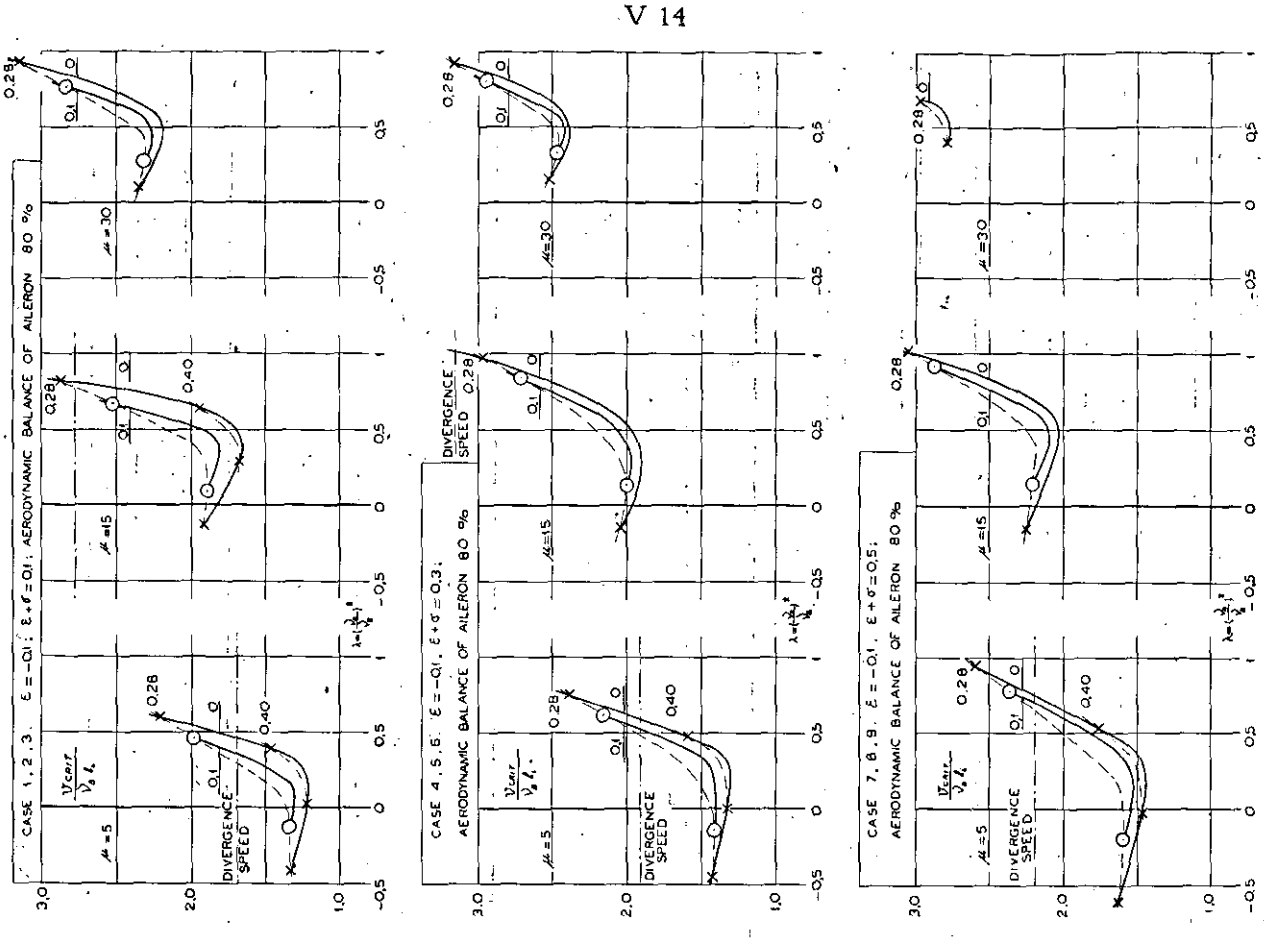

Fig. 14. Critical flutter speed as function of the stiffness ratio.

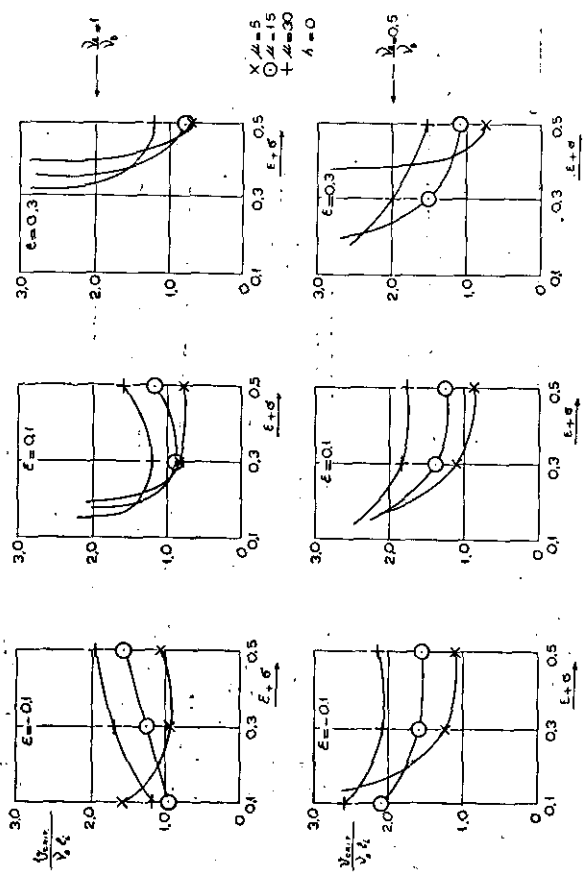

Fig. 12. Critical flutter speed as function of the position of the inertia axis (wing without aileron).

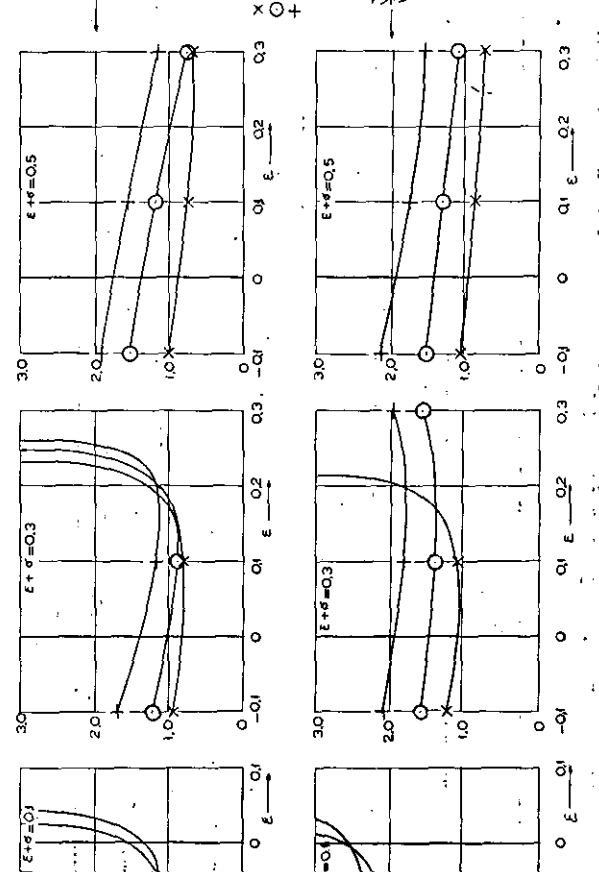

Fig. 13. Critical flutter speed as function of the position of the flexural axis (wing without aileron).

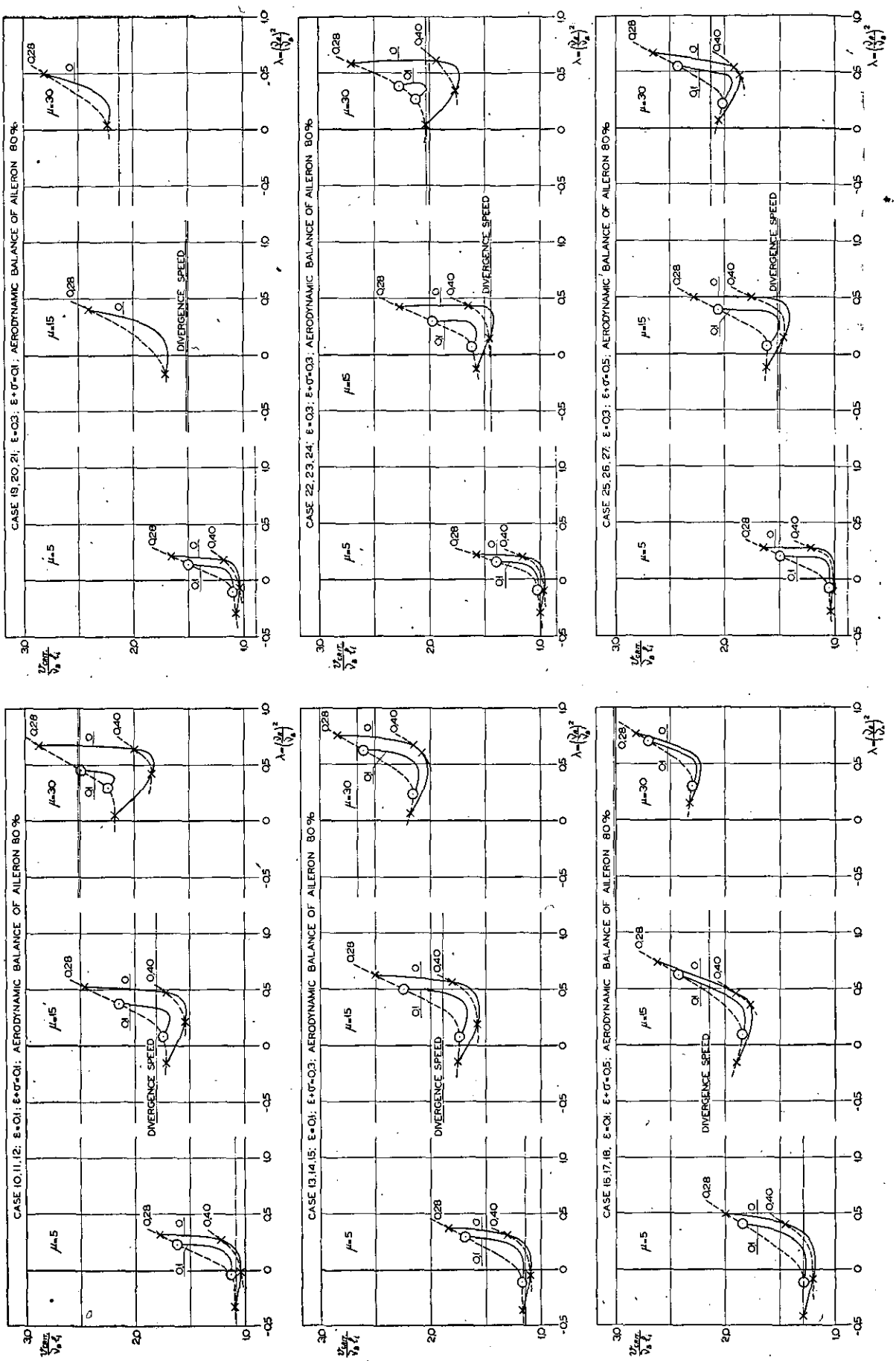

Fig. 15. Critical flutter speed as function of the stiffness ratio.

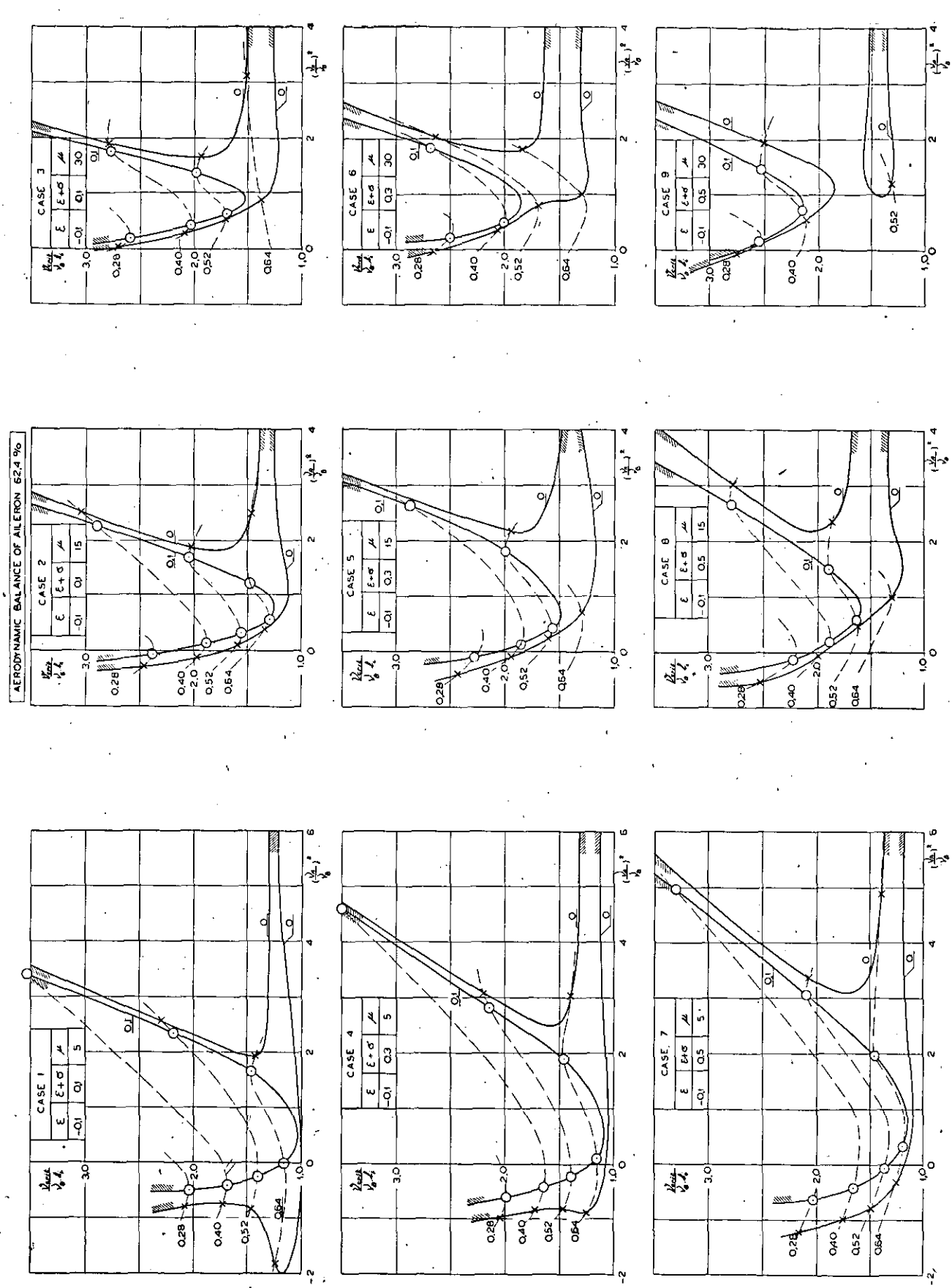

Fig. 16. Critical flutter speed as function of the stiffness ratio.

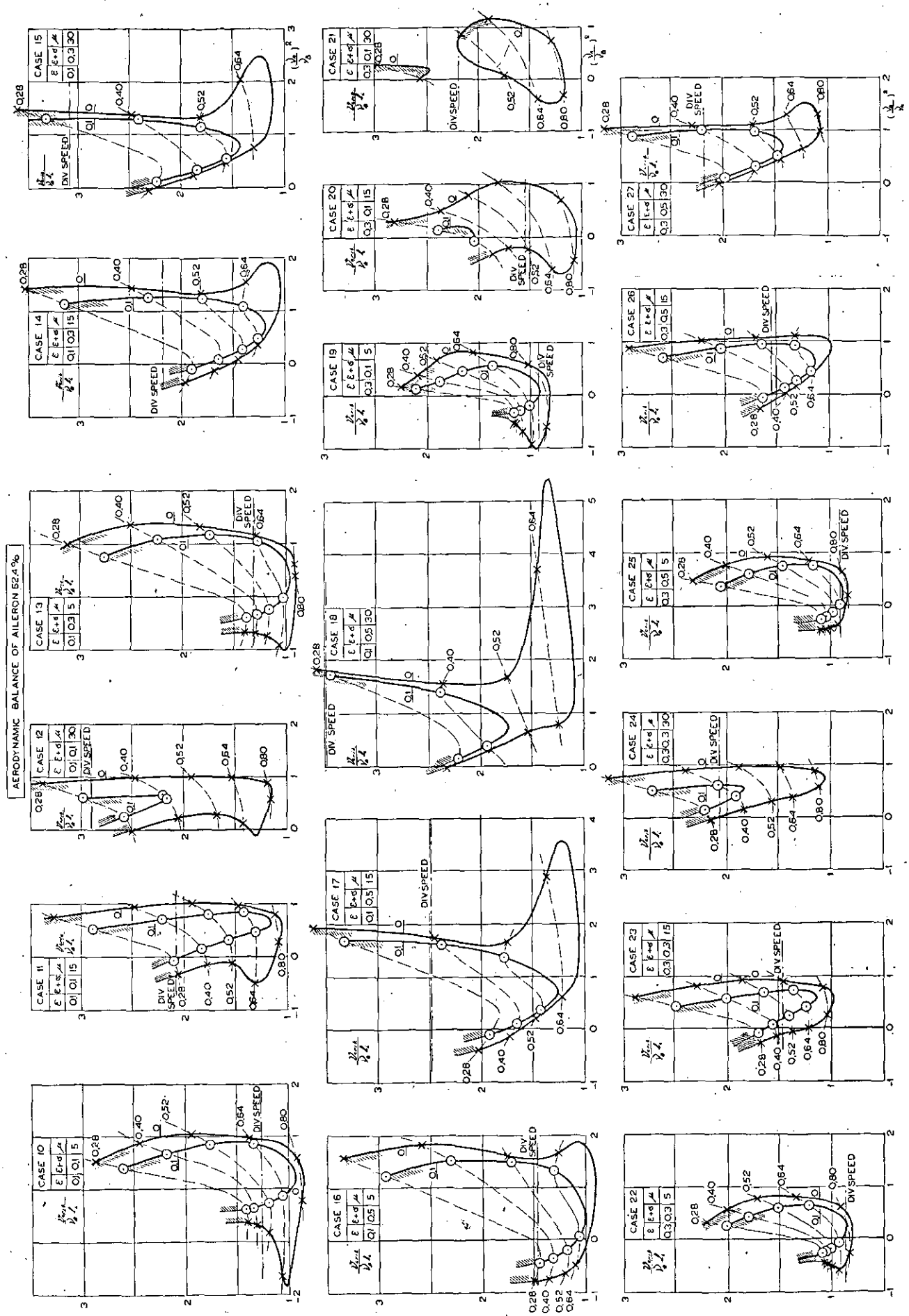

Fig. 17. Critical flutter speed as function of the stiffness ratio.

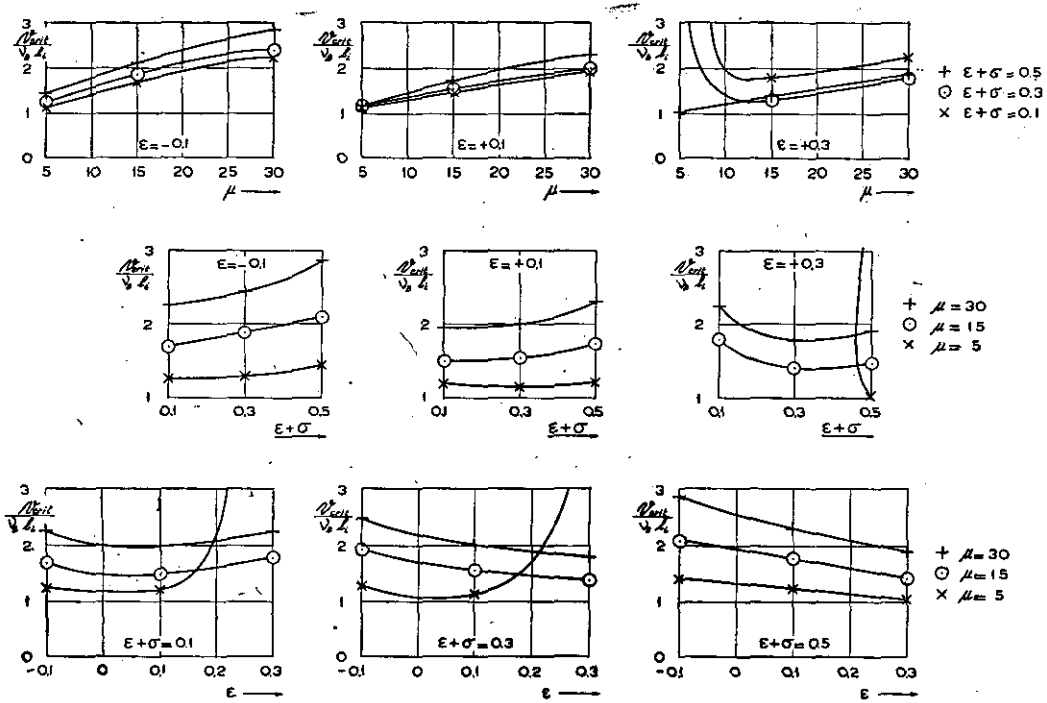

Fig. 18. Critical flutter speed as function of wing density and of the position of inertia and flexural axes (wing with aileron; aerodynamic balance of aileron 80 %; $\frac{\nu_A}{\nu_B}=0{,}5$).

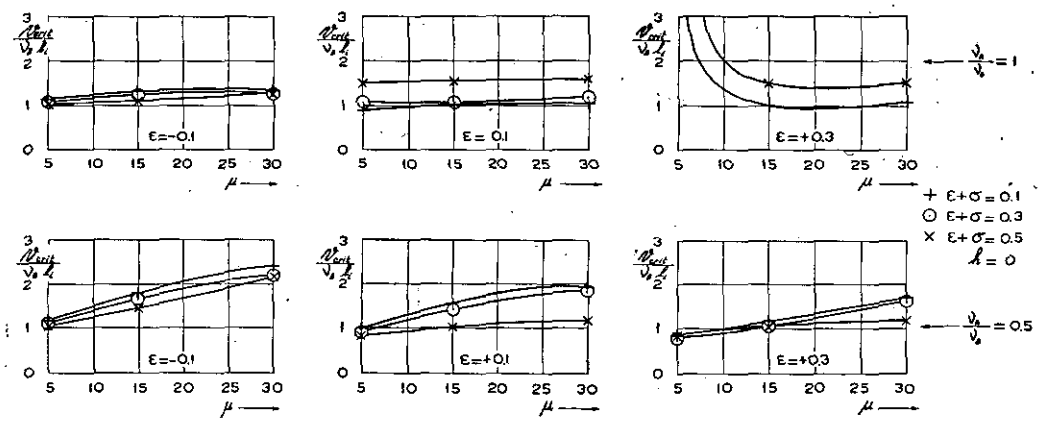

Fig. 19. Critical flutter speed as function of wing density (wing with aileron; aerodynamic balance of aileron 62.4 %).

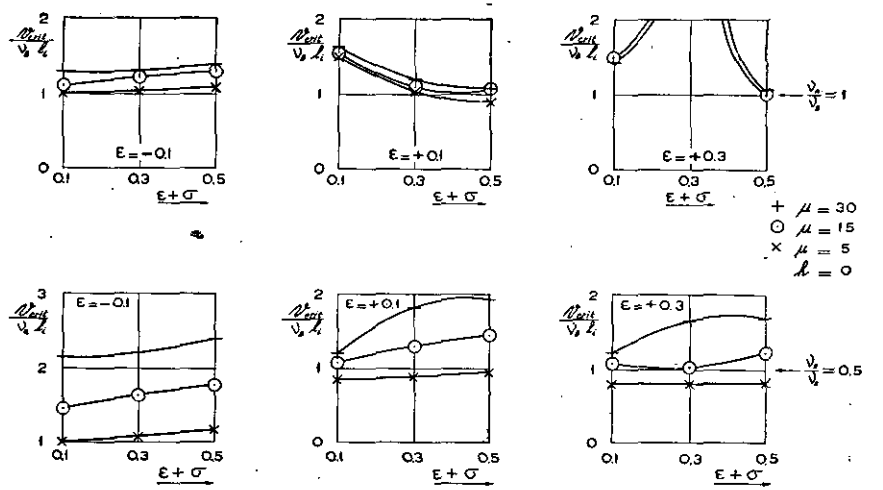

Fig. 20. Critical flutter speed as function of the position of the inertia axis (wing with aileron; aerodynamic balance of aileron 62.4 %).

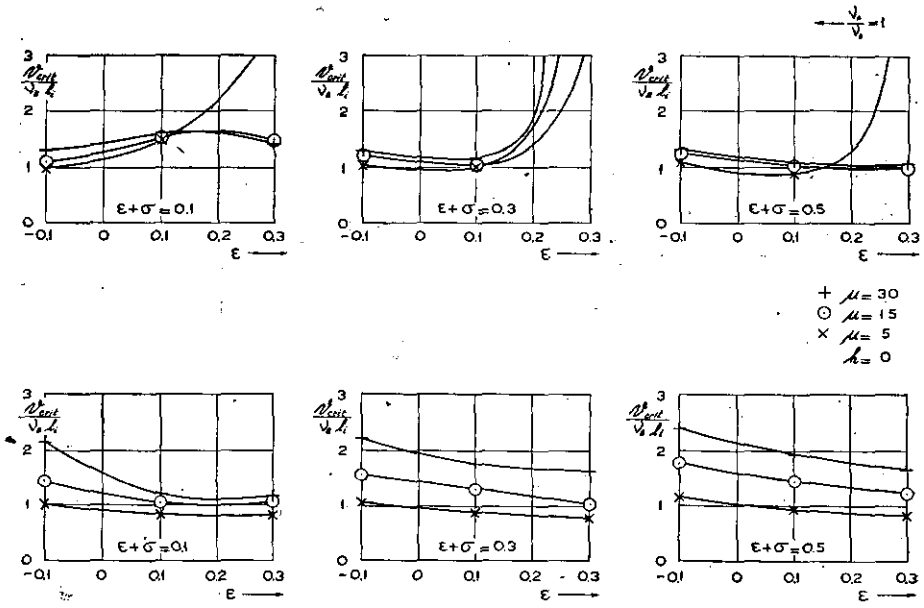

Fig. 21. Critical flutter speed as function of the position of the flexural axis (wing with aileron; aerodynamic balance of aileron 62.4 %

RAPPORT V. 1286.

Benaderende methode voor het berekenen van de voor het landen van een vliegtuig vereischte hoogteroeruitslagen en van de meest voorlijke ligging van het zwaartepunt, welke met het oog op het landen toelaatbaar is.

door

Ir. A. J. MARX.

Overzicht.

Er wordt een benaderingsmethode ontwikkeld voor het berekenen van de roeruitslagen, die noodig zijn om een vliegtuig tijdens de landing af te vangen. De landing wordt daarbij uitgevoerd gedacht na een stationnaire zweefvlucht. Uitgegaan wordt van een bepaald verloop van den invalshoek tijdens het afvangen, zooals dit bij een normale landing verwacht mag worden. Dit invalshoekverloop wordt weergegeven door het verband tusschen den invalshoek en den „relatieven" tijd, d.w.z. de tijd uitgedrukt in den duur van de geheele afvangsmanoeuvre t_a als eenheid. Aan de hand van een aantal bekende — uit de eischen voor een normale landing voortspruitende — beginvoorwaarden wordt een bundel krommen aangenomen, die een verband tusschen baanhoek en relatieven tijd weergeven. Uit dezen bundel wordt op grond van de twee vereenvoudigde vergelijkingen voor de beweging van het zwaartepunt die kromme gekozen, die het werkelijke baanhoekverloop, dat bij het vastgestelde invalshoekverloop behoort, het beste benadert. Tevens wordt daarbij de duur van de afvangmanoeuvre in seconden bepaald. Op grond van het vastgelegde invalshoekverloop, het bij benadering bepaalde baanhoekverloop en den duur van de afvangperiode t_a worden met de derde bewegingsvergelijking (voor de beweging om het zwaartepunt) de voor het afvangen noodige roeruitslagen als functie van den tijd of van den invalshoek berekend. Deze roeruitslag wordt bij iedere waarde van den invalshoek bepaald als de „extra"-roeruitslag, die voor het afvangen noodig is, boven den in stationnaire zweefvlucht bij denzelfden invalshoek behoorenden roerhoek. Kent men derhalve voor eenige zwaartepuntsliggingen de stuurstandslijnen voor stationnaire zweefvlucht, dan kan met de gegeven benaderingsmethode de absolute waarde van den voor het afvangen vereischten roerhoek bij verschillende zwaartepuntsliggingen worden berekend.

De berekeningsmethode geeft verder de mogelijkheid bij benadering te bepalen wat de, met het oog op het landen, uiterst toelaatbare voorlijke zwaartepuntsligging is, wanneer de maximale roeruitslag of beter nog de maximaal bereikbare normaalkrachtcoëfficiënt van de horizontale staartvlakken gegeven is.

Een en ander wordt aan eenige uitgewerkte voorbeelden toegelicht; tevens wordt daarbij een beperkt onderzoek ingesteld naar de wijze waarop de grootte van de noodige roeruitslagen wordt beïnvloed door de keuze van den stationnairen begintoestand (snelheid bij binnenkomen), en door de aerodynamische eigenschappen van een vleugel met verschillende typen van inrichtingen voor het verhoogen van de draagkracht en den weerstand tijdens het landen.

Indeeling.

01 Inleiding.

Dit rapport werd opgesteld naar aanleiding van een desbetreffende opdracht van de Kon. Luchtvaart Maatschappij. Voor de toestemming tot publicatie ervan zij haar te dezer plaatse dank gebracht. Er wordt hierin beschreven een benaderingsmethode, die werd ontwikkeld voor het berekenen van de voor het uitvoeren van een landing noodige hoogteroeruitslagen, teneinde op grond daarvan te kunnen aangeven wat de meest voorlijke zwaartepuntsligging is, welke met het oog op het landen nog toelaatbaar mag worden geacht.

Opgemerkt zij, dat slechts beschouwd wordt het gedeelte van de landing vóór het punt waar het vliegtuig den grond raakt, dus het „afvangen", en wel in het bijzonder de roeruitslagen, die voor het uitvoeren van deze beweging noodig zijn, terwijl verder verondersteld wordt, dat de landing wordt uitgevoerd van een gegeven stationnairen vliegtoestand in zweefvlucht uit.

De gegeven benaderingsmethode is opgebouwd op de veronderstelling, dat van het vliegtuig, behalve de belangrijkste constructiegegevens bekend zijn: het verloop van c_a en c_w met den invalshoek en de stuurstandslijnen voor zweefvlucht, voor de vliegtuigtoestanden (met name t.a.v. klepstanden en zwaartepuntsliggingen), waarvoor men de berekeningen omtrent de landing wenscht uit te voeren. Ook wordt als gegeven beschouwd de normaalkrachtcoëfficiënt van de horizontale staartvlakken als functie van den invalshoek van het staartvlak en den roerhoek. Aangezien het afvangen, vooral wat het laatste gedeelte van deze manoeuvre betreft, zich afspeelt op zeer geringen afstand van den grond, is er bij het opstellen van deze methode rekening mee gehouden, dat men den invloed daarvan op de bovengenoemde grootheden, die als gegeven worden beschouwd, kan invoeren.

02 De bewegingsvergelijkingen.

02.1 *Algemeen.*

De vergelijkingen, die de symmetrische beweging van een vliegtuig in zweefvlucht beschrijven, kunnen, wanneer de schroeftrek wordt verwaarloosd, in den volgenden vorm worden geschreven:

$$\frac{G}{g} v \dot{\varphi} = \tfrac{1}{2} \varrho v^2 c_a F - G \cos \varphi \qquad (1)$$

$$\frac{G}{g} \dot{v} = - G \sin \varphi - \tfrac{1}{2} \varrho v^2 c_w F \qquad (2)$$

$$B \ddot{\Theta} = M. \qquad (3)$$

Hierin stellen, naast de algemeen bekende notaties (zie **10**), voor:

B het traagheidsmoment van het vliegtuig om de dwarsas,

Θ de standhoek van het vliegtuig (betrokken op de vleugelkoorde) en

M het moment van alle luchtkrachten om de dwarsas, positief gerekend in staartlastigen zin.

Voor de richting waarin de verschillende hoeken positief worden gerekend, wordt verwezen naar fig. 1. Het moment M in de 3e bewegingsvergelijking kan men zich voorstellen te zijn opgebouwd uit het moment van de luchtkrachten op het geheele vliegtuig, echter zonder horizontale staartvlakken, en het moment van de luchtkrachten op de horizontale staartvlakken.

Het eerstgenoemde moment wordt voorgesteld door:

$$M_v = \tfrac{1}{2} \varrho v^2 F t_v c_m(\alpha), \qquad (4)$$

waarin t_v de grootste of de gemiddelde vleugelkoorde voorstelt en $c_m(\alpha)$ den momentencoëfficiënt van het vliegtuig zonder horizontale staartvlakken. Het laatstgenoemde moment wordt met goede benadering voorgesteld door:

$$M_h = \tfrac{1}{2} \varrho v_h^2 f l c_n(\alpha_h, \beta). \qquad (5)$$

Hierin is v_h de snelheid en α_h de invalshoek van de strooming ter plaatse van de staartvlakken.

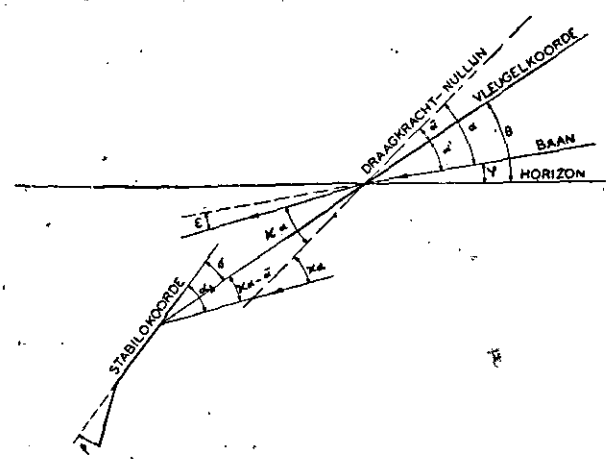

Fig. 1. Richtingen en hoeken t.o.v. het vliegtuig.

De normaalkrachtcoëfficiënt van de staartvlakken c_n kan in het algemeen weergegeven worden als functie van den invalshoek aan het stabilo α_h en van den roerhoek β (t.o.v. het stabilo) door:

$$c_n = c_1 \alpha_h + c_2 \beta, \qquad (6)$$

waarin c_1 en c_2 binnen ruime grenzen van α_h en β constanten zijn [1]). Opgemerkt wordt, dat, gezien de keuze van de positieve richtingen voor M, α en β, de waarden van c_1 en c_2 negatief zullen zijn.

De invalshoek α van den vleugel wordt gerekend t.o.v. de lijn voor draagkracht nul, welke een hoek $\bar{\alpha}$ maakt met de vleugelkoorde. De invalshoek α_h aan het stabilo wordt, wanneer de vliegtoestand stationnair is, bepaald door den instelhoek σ van het stabilo t.o.v. de vleugelkoorde, door den invalshoek van den vleugel α, door den bovengenoemden hoek $\bar{\alpha}$ en door den neerstroomingshoek ε, welke kan worden ingevoerd door middel van den neerstroomfactor

$$\varkappa = 1 - \frac{d\varepsilon}{d\alpha}. \qquad (7)$$

$\frac{d\varepsilon}{d\alpha}$ en dus ook $\varkappa$ kunnen met goede benadering voor een bepaald vliegtuig en bij een bepaalden klepstand als constant worden beschouwd.

De invalshoek α_h in stationnaire vlucht kan dan weergegeven worden door (zie fig. 1):

$$\alpha_h = \varkappa \alpha + \sigma - \bar{\alpha}. \qquad (8)$$

De snelheid van de lucht t.o.v. de staartvlakken, v_h, zal tengevolge van beïnvloeding door vleugel en romp kleiner zijn dan de snelheid v van het vlieg-

[1]) Hierop wordt onder 05.4 nader teruggekomen.

tuig t.o.v. de ongestoorde lucht; v_h wordt daarom uitgedrukt als

$$v_h = \eta v. \qquad (9)$$

Wanneer, zooals bij het uitvoeren van de landing het geval is, de vliegtoestand niet stationnair is, treedt een rotatiesnelheid $\dot{\Theta}$ om de dwarsas op, waarmede ook een verandering van den invalshoek α met snelheid $\dot{\alpha}$ gepaard gaat. Hierdoor ontstaat een dempend moment. Verreweg het grootste gedeelte van dit dempend moment zal opgewekt worden door de staartvlakken. Zooals b.v. uit *lit.* 1 blijkt mag men met voor het hier gestelde doel voldoende benadering, den invloed van vleugel en romp in het dempend moment invoeren als een procentueele toeslag op het dempend moment van de staartvlakken. Op grond van laatstgenoemde literatuur, waar voor het aandeel van den vleugel in het totale dempend moment circa 10% van het dempend moment der staartvlakken wordt opgegeven, wordt hier om het totale dempend moment van vleugel en romp in te voeren, een toeslag van 20% gelegd op het dempend moment van de staartvlakken alléén.

Laatstgenoemd moment nu kan als volgt worden berekend.

Het dempend moment ontstaat door de vergrooting van den invalshoek aan de staartvlakken t.g.v. de rotatie. Deze invalshoekvergrooting kan worden weergegeven door:

$$\Delta\alpha_h = \frac{l}{v_h}\dot{\Theta} + \frac{d\varepsilon}{d\alpha}\dot{\alpha}\frac{l}{v} = \frac{l}{v}\left(\frac{\dot{\Theta}}{\eta} + \frac{d\varepsilon}{d\alpha}\dot{\alpha}\right) \qquad (10)$$

waarin l de afstand van het zwaartepunt tot het drukpunt van de staartvlakken voorstelt.

De eerste term van (10) $\frac{l\dot{\Theta}}{\eta v}$ ontstaat, zooals direct is in te zien, rechtstreeks door de rotatiesnelheid $\dot{\Theta}$ om de dwarsas.

De tweede term is een gevolg van de verandering van de neerstrooming door de verandering van den invalshoek. De neerstroomingshoek ter plaatse van de staartvlakken verandert evenwel niet onmiddellijk met den invalshoek; er is een soort traagheid in het spel. De verandering t.g.v. een invalshoekverandering kan nu in eerste benadering (zie *lit* 1) worden bepaald door te veronderstellen, dat de neerstrooming ter plaatse van de staartvlakken op een bepaald oogenblik wordt bepaald door den invalshoek van den vleugel toen deze zich t.o.v. de ongestoorde lucht op de plaats van de staartvlakken bevond, d.w.z. een tijd l/v vóór het oogenblik, waarop men de neerstrooming wil berekenen.

De invalshoek van den vleugel was op dien tijd een bedrag $\frac{l}{v}\dot{\alpha}$ kleiner; de neerstroomingshoek ε is dus op het oogenblik waarvoor men den neerstroomingshoek aan de staartvlakken berekent een bedrag $\frac{d\varepsilon}{d\alpha}\dot{\alpha}\frac{l}{v}$ kleiner dan de hoek, die bij de waarde van α op het oogenblik van berekening behoort. De invalshoek aan de staartvlakken is dus op een bepaald oogenblik in totaal een bedrag $\frac{l}{v}\left(\frac{\dot{\Theta}}{\eta} + \frac{d\varepsilon}{d\alpha}\dot{\alpha}\right)$ grooter dan die, welke behoort bij den invalshoek α op dat oogenblik wanneer geen rotatie zou optreden.

De totale waarde van den invalshoek aan de staartvlakken tijdens de niet-stationnaire beweging wordt dus gegeven door

$$\alpha_h = \varkappa\alpha + \sigma - \bar{\alpha} + \frac{l}{v}\left(\frac{\dot{\Theta}}{\eta} + \frac{d\varepsilon}{d\alpha}\dot{\alpha}\right). \qquad (11)$$

Het totale moment van de staartvlakken tijdens de niet-stationnaire beweging kan, volgens (5), (6') en (11) nu geschreven worden als

$$M_h = \tfrac{1}{2}\varrho\eta^2 v^2 f l\,[c_1(\varkappa\alpha + \sigma - \bar{\alpha}) + c_2\beta] + \\ + \tfrac{1}{2}\varrho\eta^2 v^2 f l c_1 \frac{l}{v}\left(\frac{\dot{\Theta}}{\eta} + \frac{d\varepsilon}{d\alpha}\dot{\alpha}\right). \qquad (12)$$

De laatste term in deze uitdrukking stelt het dempend moment der staartvlakken voor.

Zooals reeds eerder is uiteengezet, wordt nu in het vervolg voor het dempend moment van het geheele vliegtuig ingevoerd de waarde van het dempend moment der staartvlakken vermeerderd met 20%. Men kan dan voor het totale moment M van de luchtkrachten tijdens de niet-stationnaire beweging volgens (4), (5) en (12) schrijven

$$M = \tfrac{1}{2}\varrho v^2 F t_v\left[c_m(\alpha) + \eta^2\frac{fl}{Ft_v}\left\{c_1(\varkappa\alpha + \sigma - \bar{\alpha}) + \right.\right. \\ \left.\left. + 1{,}2\,c_1\frac{l}{v}\left(\frac{\dot{\Theta}}{\eta} + \frac{d\varepsilon}{d\alpha}\dot{\alpha}\right) + c_2\beta\right\}\right]. \qquad (13)$$

Beschouwt men nu een *stationnaire* vlucht met invalshoek $\alpha^x = \alpha$ dan behoort daarbij een roerhoek β^x, welke bepaald wordt door

$$0 = c_m(\alpha) + \eta^2\frac{fl}{Ft_v}\left\{c_1(\varkappa\alpha + \sigma - \bar{\alpha}) + c_2\beta^x\right\}. \qquad (14)$$

zoodat hiermede $c_m(\alpha)$ uitgedrukt kan worden als functie van α en den daarbij in *stationnaire* vlucht behoorenden roerhoek β^x.

Vergelijking (13) geeft met (14)

$$M = \tfrac{1}{2}\varrho\eta^2 v^2 f l\left\{1{,}2\,c_1\frac{l}{v}\left(\frac{\dot{\Theta}}{\eta} + \frac{d\varepsilon}{d\alpha}\dot{\alpha}\right) + \right. \\ \left. + c_2(\beta - \beta^x)\right\}. \qquad (15)$$

zoodat bewegingsvergelijking (3) geschreven kan worden:

$$\frac{2B}{\varrho\eta^2 v^2 f l}\ddot{\Theta} = 1{,}2\,c_1\frac{l}{v}\left(\frac{\dot{\Theta}}{\eta} + \frac{d\varepsilon}{d\alpha}\dot{\alpha}\right) + \\ + c_2(\beta - \beta^x). \qquad (16)$$

$(\beta - \beta^x)$ stelt dus voor den „extra"-roeruitslag, die men tijdens de *niet-stationnaire* beweging (i.c. het afvangen) op een bepaald oogenblik noodig heeft *boven* den roeruitslag, die in *stationnaire* vlucht behoort bij eenzelfden invalshoek als die, welke op dat bepaalde oogenblik tijdens het afvangen optreedt.

Om dus den grootsten roeruitslag te vinden, dien men voor het landen noodig heeft, moet men het verschil $(\beta - \beta^x)$ als functie van α bepalen; kent men nu het verband $\beta^x(\alpha)$ dan kan hieruit de groot-

ste absolute waarde van het verband $\beta(\alpha)$ tijdens het landen, d.w.z. de grootste benoodigde roeruitslag, worden bepaald.

02.2 *Vereenvoudiging van de bewegingsvergelijkingen.*

De in het vorengaande aangegeven bewegingsvergelijkingen luiden

$$\frac{G}{g} v \dot{\varphi} = \tfrac{1}{2} \varrho v^2 c_a F - G \cos \varphi , \qquad (1)$$

$$\frac{G}{g} \dot{v} = - G \sin \varphi - \tfrac{1}{2} \varrho v^2 c_w F , \qquad (2)$$

en

$$\frac{2B}{\varrho \eta^2 v^2 f l} \ddot{\Theta} = 1{,}2\, c_1 \frac{l}{v} \left(\frac{\dot{\Theta}}{\eta} + \frac{d\varepsilon}{d\alpha} \dot{\alpha} \right) + c_2 (\beta - \beta^x) . \qquad (16)$$

Voor het vervolg zal het noodig zijn de bewegingsvergelijkingen (1) en (2) te vereenvoudigen en wel als volgt:

1° Bij het landen treden betrekkelijk kleine waarden van φ op; de baanhoek is het grootst bij het begin van het afvangen, doch heeft dan in de meeste gevallen nog een zoodanige waarde, dat cos φ circa 0,99 of meer bedraagt. In de vergelijkingen (1) en (2) wordt daarom cos $\varphi = 1$ en sin $\varphi = \varphi$ gesteld.

2° Er wordt verondersteld, dat met goede benadering mag worden geschreven

$$c_a = \frac{d c_a}{d \alpha} \alpha = c_a' \alpha . \qquad (17)$$

Weliswaar vertoont de c_a-α-kromme veela een afwijking van het lineaire verband in het gebied van de groote invalshoeken, maar de berekeningen, die in dit rapport over het landen gegeven zullen worden, strekken zich uit over een beperkt gebied van invalshoeken, n.l. van den invalshoek α_o in de stationnaire zweefvlucht, voorafgaande aan de landing, welke reeds betrekkelijk groot is, tot ten hoogste de kritische waarde α_{kr}. In dit gebied kan men het verloop van c_a met α benaderen door een rechte, welke dan niet behoeft samen te vallen met de rechte, welke $c_a(\alpha)$ bij de kleinere invalshoeken weergeeft. Op deze wijze kan in het gebied $\alpha_0 < \alpha < \alpha_{kr}$ in vrijwel alle gevallen met voor het hier gestelde doel voldoende benadering c_a worden weergegeven als een lineaire functie van α. De invalshoek α t.o.v. de „draagkracht-nullijn" moet dan ook gemeten worden t.o.v. de „fictieve" draagkracht-nullijn, die gevonden wordt door extrapolatie van het lineaire verband tot $c_a = 0$. Een en ander wordt in fig. 2 nader toegelicht.
Indien men beschikt over gegevens omtrent den grondinvloed op de c_a-waarde kan men dezen invloed bij benadering in rekening brengen door de c_a-waarde bij den invalshoek op het oogenblik van landen te bepalen en dan een lineair verloop van c_a met α aan te nemen tusschen deze laatste c_a-waarde en de c_a-waarde (zonder grondinvloed) bij den invalshoek α_0 (toestand waarbij de afvangmanoeuvre wordt begonnen). Een betere benadering kan men verkrijgen door eerst de berekening uit te voeren met de op de hierboven beschreven wijze bepaalde gegevens. Met het hiermede verkregen baanverloop t.o.v. den grond, kan daarna door in rekening brengen van den op ieder punt van die baan te verwachten grondinvloed, de c_a-kromme gecorrigeerd worden en hiermede een 2e benadering worden uitgevoerd. Het is nog van belang te vermelden, dat men, zooals uit het vervolg van de berekeningen blijkt, door verwaarloozing van den grondinvloed op c_a in het algemeen iets te groote waarden voor de noodige roeruitslagen zal vinden; men rekent dus aan den veiligen kant.

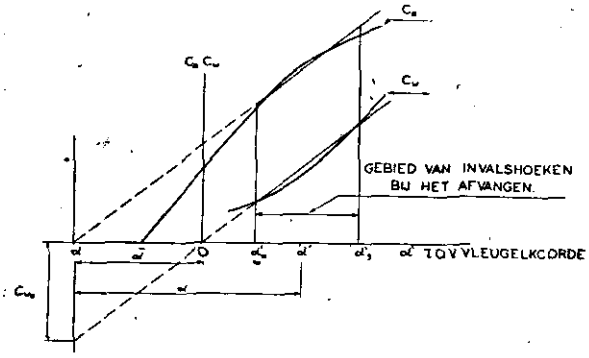

Fig. 2. Vereenvoudiging van het verband $c_a(\alpha)$ en $c_w(\alpha)$.

3° Voorts wordt ter vereenvoudiging van de vergelijkingen gesteld

$$c_w = \frac{d c_w}{d \alpha} \alpha + c_{w_u} = c_w' \alpha + c_{w_u} . \qquad (18)$$

Hiervoor gelden dezelfde overwegingen als hierboven voor $c_a(\alpha)$ gegeven. In het gebied $\alpha_0 < \alpha < \alpha_{kr}$ kan $c_w(\alpha)$ met voor het hier gestelde doel voldoende benadering door een lineair verband worden voorgesteld. De waarde c_{w_u} is dan de waarde, die gevonden wordt door extrapolatie van dit lineaire verband tot den invalshoek, waarvoor bij extrapolatie van het lineaire verband $c_a(\alpha)$, $c_a = 0$ is (zie fig. 2).

Uit het hierna onder **07** te geven uitgewerkte voorbeeld blijkt, dat voor het gebied $\alpha_0 < \alpha < \alpha_{kr}$ de lineaire benaderingen voor c_a en c_w procentueel slechts kleine verschillen van de werkelijke c_a- en c_w-waarden opleveren, mede omdat in het beschouwde gebied c_a en c_w (de laatste met name voor het geval van geopende landingskleppen) groot zijn. Het verdient, teneinde de benadering beter te maken, aanbeveling voor c_w waarden in te voeren, die berekend zijn met inachtname van de negatieve trekkracht van de, bij gesloten gasklep in stationnaire vlucht werkende, schroeven. De invloed van de nabijheid van den grond op de c_w-waarden, kan op dezelfde wijze als hierboven voor de c_a-waarden is aangegeven, in

rekening worden gebracht. Zooals uit het vervolg van de berekening zal blijken, heeft het verwaarloozen van den grondinvloed op de c_w-waarden ten gevolge, dat de berekende roeruitslagen iets te groot zullen zijn; men rekent dus aan den veiligen kant.

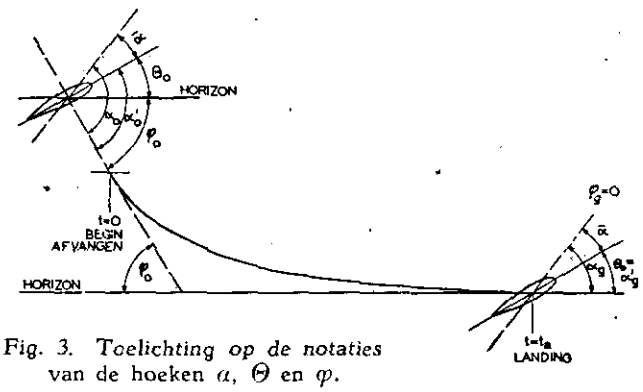

Fig. 3. *Toelichting op de notaties* van de hoeken α, Θ en φ.

Beschrijft men nu den stationnairen vliegtoestand vóór het „afvangen" door de kenmerkende grootheden α, φ, v van een index 0 te voorzien (zie fig. 3), dan kan men op grond van bovengenoemde 3 veronderstellingen de bewegingsvergelijkingen (1) en (2) als volgt vereenvoudigen.

De eerste bewegingsvergelijking

$$\frac{G}{g} v \dot{\varphi} = \tfrac{1}{2} \varrho v^2 c_a F - G \cos \varphi \qquad (1)$$

wordt

$$\frac{G}{g} v \dot{\varphi} = \tfrac{1}{2} \varrho F c_a' v^2 \alpha - G .$$

Wanneer men in het 2de lid voor G invoert

$$G = \tfrac{1}{2} \varrho v_0^2 F c_a' \alpha_0 , \qquad (19)$$

dan ontstaat

$$v \dot{\varphi} = \tfrac{1}{2} \varrho g \frac{F}{G} c_a' (v^2 \alpha - v_0^2 \alpha_0) . \qquad (20)$$

Verder kan uit deze vierkantsvergelijking v worden opgelost:

$$v = \frac{\dot{\varphi}}{\varrho g \frac{F}{G} c_a' \alpha} + \frac{1}{\varrho g \frac{F}{G} c_a' \alpha} \sqrt{\dot{\varphi}^2 + \left(\varrho g \frac{F}{G} c_a'\right)^2 v_0^2 \alpha_0 \alpha} . \qquad (21)$$

De wortel met het negatieve teeken levert, zooals een beschouwing voor het tijdstip $t = 0$ waarvoor $\dot{\varphi} = 0$ en $\alpha = \alpha_0$ leert, een negatieve waarde voor de snelheid v, zoodat deze wortel buiten beschouwing kan blijven.

Een eenvoudige schatting, welke ook door het uitgewerkte voorbeeld onder **07** wordt bevestigd, toont aan dat tijdens de geheele landingsmanoeuvre $\dot{\varphi}^2$ *zeer klein* is t.o.v. $\left(\varrho g \frac{F}{G} c_a'\right)^2 v_0^2 \alpha_0 \alpha$, zoodat (21) met goede benadering vervangen mag worden door

$$v = \frac{\dot{\varphi}}{\varrho g \frac{F}{G} c_a' \alpha} + v_0 \sqrt{\frac{\alpha_0}{\alpha}} . \qquad (22)$$

De tweede bewegingsvergelijking

$$\frac{G}{g} \dot{v} = - G \sin \varphi - \tfrac{1}{2} \varrho v^2 c_w F \qquad (2)$$

kan op grond van de ingevoerde vereenvoudigingen geschreven worden:

$$\dot{v} = - g \varphi - \tfrac{1}{2} \varrho g \frac{F}{G} (c_w' \alpha + c_{w_u}) v^2 . \qquad (23)$$

In deze vergelijking wordt voor v de waarde ingevoerd, volgens (22). Daar echter $\frac{\dot{\varphi}}{\varrho g \frac{F}{G} c_a' \alpha}$ klein is t.o.v. $v_0 \sqrt{\frac{\alpha_0}{\alpha}}$ wordt in de uitdrukking voor v^2 de term $\left(\frac{\dot{\varphi}}{\varrho g \frac{F}{G} c_a' \alpha}\right)^2$ verwaarloosd.

Aldus verkrijgt men voor (23)

$$\dot{v} = - g \varphi - \tfrac{1}{2} \varrho g \frac{F}{G} c_w' v_0^2 \alpha_0 - \tfrac{1}{2} \varrho g \frac{F}{G} c_{w_u} v_0^2 \frac{\alpha_0}{\alpha} - \frac{c_w'}{c_a'} v_0 \dot{\varphi} \sqrt{\frac{\alpha_0}{\alpha}} - \frac{c_{w_u}}{c_a'} v_0 \dot{\varphi} \frac{1}{\alpha} \sqrt{\frac{\alpha_0}{\alpha}} . \qquad (24)$$

Recapituleerende zijn in het bovenstaande de bewegingsvergelijkingen (1) en (2) door de besproken vereenvoudigingen gebracht in den vorm, welke men, wanneer gesteld wordt

$$\varrho g \frac{F}{G} = \mu , \qquad (25)$$

waarin μ de dimensie m^{-1} heeft, kan schrijven:

$$v = \frac{\dot{\varphi}}{\mu c_a'} \alpha^{-1} + v_0 \sqrt{\frac{\alpha_0}{\alpha}} , \qquad (26)$$

$$\dot{v} = - g \varphi - \tfrac{1}{2} \mu c_w' v_0^2 \alpha_0 - \tfrac{1}{2} \mu c_{w_u} v_0^2 \alpha_0 \alpha^{-1} - \frac{c_w'}{c_a'} v_0 \dot{\varphi} \sqrt{\frac{\alpha_0}{\alpha}} - \frac{c_{w_u}}{c_a'} v_0 \dot{\varphi} \frac{1}{\alpha} \sqrt{\frac{\alpha_0}{\alpha}} . \qquad (27)$$

Als derde bewegingsvergelijking komt hierbij (16), terwijl de in deze drie vergelijkingen voorkomende grootheden Θ, α en φ verbonden zijn door de betrekking (zie fig. 1)

$$\Theta = \alpha' + \varphi , \qquad (28)$$

waaruit ook een overeenkomstige betrekking voor de eerste en tweede afgeleiden van deze grootheden naar den tijd volgt.

03 De benaderingsmethode voor de berekening van de vereischte roeruitslagen.

03.1 *Bespreking van de methode.*

In principe geven de bewegingsvergelijkingen of de daaruit door vereenvoudiging afgeleide betrekkingen de mogelijkheid den benoodigden extra roeruitslag $(\beta - \beta^x)$ te berekenen, waaruit, wanneer de stuurstandslijnen in stationnaire vlucht voor het betreffende vliegtuigtype bekend zijn, de

voor het afvangen benoodigde roeruitslag β kan worden bepaald.

De bewegingsvergelijkingen bevatten 5 veranderlijken α, φ, Θ, β en v als functie van den tijd t, welke door de 4 betrekkingen (26), (27), (28) en (16) verbonden zijn.

In het algemeen wordt bij het berekenen van vliegtuigbewegingen uitgegaan van een bepaald verband $\beta(t)$, dat door de stuurbeweging van den vlieger wordt vastgelegd, zoodat dan de 4 veranderlijken α, φ, Θ en v als functie van t met behulp van de 4 vergelijkingen kunnen worden bepaald.

In het nu beschouwde geval, waar gevraagd wordt het verband $\beta(t)$ voor het afvangen te bepalen, moet een der andere veranderlijken als functie van den tijd gegeven zijn, en wel zoo, dat deze functie uitdrukt, dat „geland" wordt.

Men zou hiervoor b.v. het verband $\varphi(t)$ kunnen kiezen, d.w.z. vastleggen hoe de baanhoek tijdens het afvangen met den tijd zou moeten veranderen. In principe zou dan het verband $\beta(t)$ bepaald kunnen worden.

Een dergelijke wijze van werken stuit echter op verschillende bezwaren.

Het is in de eerste plaats moeilijk het verband tusschen een der grootheden α, φ of Θ met den tijd voor het *landen* van een bepaald vliegtuigtype aan te geven, omdat men den totalen duur van de afvangmanoeuvre tevoren niet kan vastleggen. Deze duur wordt n.l. in eerste instantie bepaald door de voorwaarde dat de snelheid, welke bij het begin van het afvangen gelijk is aan de snelheid in stationnaire zweefvlucht, aan het einde van de afvangmanoeuvre nagenoeg gelijk moet zijn aan de minimale snelheid.

Men kan derhalve dezen tijd niet zonder meer voorschrijven; hij moet uit het probleem zelf volgen.

Een tweede bezwaar, dat zich bij deze wijze van behandelen voordoet, wordt veroorzaakt door de moeilijkheden, waarop men bij het geven van een oplossing, in algemeenen en voor de praktijk bruikbaren vorm, stuit, wanneer men uitgaat van een tevoren vastgelegde functie $\alpha(t)$, $\varphi(t)$ of $\Theta(t)$.

Deze bezwaren hebben er toe geleid, dat een methode ontwikkeld is, die de gevraagde roerhoeken met voldoende benadering geeft en de genoemde bezwaren vermijdt; de gedachtengang, die hieraan ten grondslag ligt, is in het volgende weergegeven.

Noemt men den totalen duur van de afvangmanoeuvre t_a ($t=0$ is het oogenblik, waarop tijdens de stationnaire zweefvlucht met afvangen wordt begonnen en $t=t_a$ het oogenblik, waarop het vliegtuig den grond raakt (zie fig. 3)) dan kan men voor verschillende grootheden tevoren aangeven, welke waarden zij op het oogenblik $t=0$ en $t=t_a$ zullen moeten hebben. Zoo zullen b.v. ten tijde $t=0$ de grootheden α, φ en Θ de waarden α_0, φ_0 en Θ_0 hebben, behoorende bij de stationnaire zweefvlucht. Ten tijde $t=t_a$ zal voor een goede landing $\varphi=0$ of nagenoeg nul zijn, terwijl α afhankelijk van het type landing (staartlanding of wiellanding), dat men beschouwt, b.v. ten naasten bij de waarde α_{krit} zal hebben of de waarde van α overeenkomende met den horizontalen stand op hoofdwielen en neuswiel. Men kan nu het verband tusschen een der grootheden α, φ of Θ en den relatieven tijd $\gamma=\frac{t}{t_a}$ voorschrijven, zoodanig dat aan de bekende begin- en eindvoorwaarden is voldaan.

Men legt op deze wijze niet den duur van de afvangmanoeuvre vast, maar kan wel een voor de landing redelijk verloop van de grootheid gedurende het afvangen voorschrijven. Legt men op de bovenbeschreven wijze nu voor twee grootheden het verband met γ vast, dus b.v. $\alpha\equiv\alpha(\gamma)$ en $\varphi\equiv\varphi(\gamma)$, waarin $\gamma=\frac{t}{t_a}$, dan heeft men eigenlijk, aangezien het geheele probleem slechts 1 onafhankelijk veranderlijke bevat, 1 veranderlijke te veel vastgelegd, zij het dan op een constante t_a na. Men mag dan ook niet verwachten, dat bij invoering van de functies $\alpha(\gamma)$ en $\varphi(\gamma)$ (en een bepaalde waarde van t_a) in de bewegingsvergelijkingen of in de daaruit afgeleide vergelijkingen (26) en (27), deze voor *ieder punt* van de baan in een identiteit zullen overgaan.

Men kan nu echter de waarde van t_a zoodanig bepalen, dat bij benadering aan de bewegingsvergelijkingen wordt voldaan en wel als volgt.

Vergelijking (27) stelt bij gegeven $\alpha(\gamma)$ en $\varphi(\gamma)$ in staat in een bepaald punt van de baan (γ_1) de snelheid v_{γ_1} te bepalen op een constante t_a na. Vergelijking (26) levert echter, bij gegeven $\alpha(\gamma)$ en $\varphi(\gamma)$ — eveneens op de constante t_a na — de waarde van de snelheid v_{γ_1} in datzelfde punt. Gelijkstelling van beide uitdrukkingen voor v_{γ_1} levert een betrekking, waaruit t_a kan worden opgelost. Kiest men voor het punt γ_1 het einde van de baan, dus $\gamma=1$, dan beteekent de gelijkstelling van de beide uitdrukkingen voor v_{γ_1}, dat t_a zoo wordt bepaald, dat de waarde van de snelheid aan het einde van de afvangmanoeuvre, berekend volgens de eerste bewegingsvergelijking (26), gelijk is aan de waarde van de snelheid aan het einde van de afvangmanoeuvre berekend volgens de tweede bewegingsvergelijking (27). Weliswaar is nu niet in ieder punt van de baan aan de bewegingsvergelijkingen voldaan, zoodat b.v. de snelheid $v(t)$, volgende uit de eerste bewegingsvergelijking (26), bij invoering in de tweede (27), deze niet tot een identiteit doet overgaan. Dit zou, bij de tevoren vastgestelde functies $\alpha(\gamma)$ en $\varphi(\gamma)$ slechts mogelijk zijn, wanneer een denkbeeldige trekkracht K (positief of negatief) in de tweede bewegingsvergelijking wordt ingevoerd, die van punt tot punt varieert. Echter is, t.g.v. de boven beschreven wijze van bepaling van t_a, $\int_0^{t_a} K dt$, dus de in totaal door deze kracht aan het vliegtuig meegedeelde hoeveelheid van beweging over de geheele baan gerekend, gelijk nul.

Wanneer de snelheid tijdens de beweging con-

stant zou zijn, zou dit beteekenen dat ook de door deze fictieve trekkracht verrichte arbeid, over de geheele baan gerekend, nul zou zijn. Aangezien de snelheid slechts betrekkelijk weinig varieert (ca. 20%) is dit dus bij benadering het geval. Een en ander toont aan dat men op de beschreven wijze reeds een eerste, grove benadering van de beweging tijdens de landing kan verkrijgen.

Men kan nu met de op bovenbeschreven wijze berekende waarde van t_a en de aangenomen functies $\alpha(\gamma)$ en $\varphi(\gamma)$, de waarden van $\ddot{\Theta}$, $\dot{\Theta}$ en $\dot{\alpha}$ tijdens het afvangen in eerste benadering berekenen en daarmede met behulp van (16), $\beta(t)$ bepalen.

Er bestaat echter nog de mogelijkheid op betrekkelijk eenvoudige wijze de werkelijke baan beter te benaderen en wel als volgt. Men legt, geheel overeenkomstig het bovenstaande, een der grootheden, b.v. α, als functie van γ vast; de andere grootheid, b.v. φ, schrijft men nu echter voor als functie van γ en een parameter p, dus $\varphi(\gamma, p)$. Men kan nu weer t_a bepalen, door voor het tijdstip $\gamma = 1$ de snelheid volgens de vergelijkingen (26) en (27) aan elkaar gelijk te stellen. Men vindt dan t_a als functie van p. Men kan nu nog een andere voorwaarde stellen, waardoor de parameter p wordt vastgelegd. Deze voorwaarde kan b.v. zijn, dat ook op de helft van de afvangmanoeuvre b.v. voor $\gamma = 0{,}5$ de waarden van de snelheid, die men volgens de eerste en de tweede bewegingsvergelijking bepaalt, aan elkaar gelijk moeten zijn. Zoodoende verkrijgt men de functies $\alpha(\gamma)$ en $\varphi(p, \gamma)$ alsmede de waarde van t_a zoodanig, dat zoowel aan het einde van de afvangmanoeuvre als ook voor een bepaald oogenblik tijdens het afvangen (b.v. op de helft) de in totaal over die baangedeelten door de genoemde fictieve trekkracht aan het vliegtuig meegedeelde hoeveelheid van beweging nul is. Doordat de variatie van de snelheid over ieder van deze baangedeelten geringer is dan over de geheele baan gerekend, is dus ook de door die fictieve trekkracht verrichte arbeid over de beide baangedeelten, *met aanzienlijk betere benadering* dan in het eerste geval, gelijk aan nul. Men verkrijgt derhalve een belangrijk betere benadering van de werkelijke baan bij het gekozen invalshoekverloop, zoodat men mag verwachten, dat hiermede de waarden van $\ddot{\Theta}$, $\dot{\Theta}$ en $\dot{\alpha}$ met voldoende benadering kunnen worden vastgesteld om hiermede een behoorlijke benadering van $\beta(t)$ te verkrijgen.

03.2 *Uitwerking van de methode.*

Wanneer y een functie van γ en p is waarin

$$\gamma = \frac{t}{t_a}$$

en p een parameter voorstelt, dan volgt hieruit

$$\dot{y}(\gamma, p) = \frac{d}{dt} y(\gamma, p) = \frac{1}{t_a} \frac{d}{d\gamma} y(\gamma, p) \qquad (29)$$

en

$$\int_0^{t_1} y(\gamma)\, dt = t_a \int_0^{\gamma_1} y(\gamma)\, d\gamma . \qquad (30)$$

Denkt men zich nu de functies $\alpha(\gamma)$ en $\varphi(\gamma, p)$ gegeven, dan volgt uit (26) op grond van het bovenstaande

$$v = \frac{1}{t_a} \frac{1}{\mu c_{a'}} \alpha(\gamma)^{-1} \frac{d}{d\gamma} \varphi(\gamma, p) + v_0 \sqrt{\frac{\alpha_0}{\alpha(\gamma)}} , \qquad (31)$$

terwijl (27) wordt:

$$\dot{v} = -g\,\varphi(\gamma, p) - \tfrac{1}{2} \mu c_{w'} v_0^2 \alpha_0 - \tfrac{1}{2} \mu c_{w_u} v_0^2 \frac{\alpha_0}{\alpha(\gamma)} +$$
$$- \frac{1}{t_a} \frac{c_{w'}}{c_{a'}} v_0 \sqrt{\frac{\alpha_0}{\alpha(\gamma)}} \frac{d\varphi(\gamma, p)}{d\gamma} -$$
$$- \frac{1}{t_a} \frac{c_{w_u}}{c_{a'}} v_0 \frac{1}{\alpha(\gamma)} \sqrt{\frac{\alpha_0}{\alpha(\gamma)}} \frac{d\varphi(\gamma, p)}{d\gamma} . \qquad (32)$$

De snelheid v_{γ_1} op het tijdstip t_1 (overeenkomende met γ_1) kan geschreven worden als (zie ook (30)):

$$v_{\gamma_1} = v_0 + \int_0^{t_1} \dot{v}\, dt = v_0 + t_a \int_0^{\gamma_1} \dot{v}\, d\gamma , \qquad (33)$$

waarin voor $\dot{v}$ de uitdrukking (32) kan worden ingevuld. Men krijgt dan:

$$v_{\gamma_1} = v_0 - t_a . g \int_0^{\gamma_1} \varphi(\gamma, p)\, d\gamma - t_a \tfrac{1}{2} \mu c_{w'} v_0^2 \alpha_0 \gamma_1 -$$
$$- t_a \tfrac{1}{2} \mu c_{w_u} v_0^2 \alpha_0 \int_0^{\gamma_1} \frac{d\gamma}{\alpha(\gamma)} +$$
$$- \frac{c_{w'}}{c_{a'}} v_0 \sqrt{\alpha_0} \int_0^{\gamma_1} \frac{d\varphi(\gamma, p)}{d\gamma} \frac{d\gamma}{\sqrt{\alpha(\gamma)}} -$$
$$- \frac{c_{w_u}}{c_{a'}} v_0 \sqrt{\alpha_0} \int_0^{\gamma_1} \frac{d\varphi(\gamma, p)}{d\gamma} \frac{d\gamma}{\alpha(\gamma)\sqrt{\alpha(\gamma)}} . \qquad (34)$$

Noemt men nu

$$L_{\gamma_1} = \int_0^{\gamma_1} \varphi(\gamma, p)\, d\gamma , \qquad (35)$$

$$M_{\gamma_1} = \int_0^{\gamma_1} \alpha(\gamma)^{-1}\, d\gamma , \qquad (36)$$

$$N_{\gamma_1} = \int_0^{\gamma_1} \frac{d\varphi(\gamma, p)}{d\gamma} \frac{d\gamma}{\sqrt{\alpha(\gamma)}} , \qquad (37)$$

en

$$O_{\gamma_1} = \int_0^{\gamma_1} \frac{d\varphi(\gamma, p)}{d\gamma} \frac{d\gamma}{\alpha(\gamma)\sqrt{\alpha(\gamma)}} , \qquad (38)$$

dan luidt (34):

$$v_{\gamma_1} = v_0 + t_a \Big\{ - g L_{\gamma_1} - \tfrac{1}{2} \mu v_0^2 \alpha_0 (c_{w'} \gamma_1 + c_{w_u} M_{\gamma_1}) \Big\} -$$
$$- v_0 \sqrt{\alpha_0} \left(\frac{c_{w'}}{c_{a'}} N_{\gamma_1} + \frac{c_{w_u}}{c_{a'}} O_{\gamma_1} \right) , \qquad (39)$$

of

$$v_{\gamma_1} = v_0 + T_{\gamma_1} t_a - U_{\gamma_1} , \qquad (40)$$

waarin

$$T_{\gamma_1} = - g L_{\gamma_1} - \tfrac{1}{2} \mu v_0^2 \alpha_0 (c_{w'} \gamma_1 + c_{w_u} M_{\gamma_1}) , \qquad (41)$$

en

$$U_{\gamma_1} = v_0 \sqrt{\alpha_0} \left(\frac{c_{w'}}{c_{a'}} N_{\gamma_1} + \frac{c_{w_u}}{c_{a'}} O_{\gamma_1} \right) \qquad (42)$$

Volgens (31) is op het tijdstip t_1 (overeenkomende met γ_1)

$$v_{\gamma_1} = v_0 + v_0 \left\{ \sqrt{\frac{a_0}{a(\gamma_1)}} - 1 \right\} + \\ + \frac{1}{t_a} \frac{1}{\mu c_a'} \frac{1}{a(\gamma_1)} \left(\frac{d\varphi(\gamma,p)}{d\gamma} \right)_{\gamma=\gamma_1}, \quad (43)$$

of

$$v_{\gamma_1} = v_0 + V_{\gamma_1} + \frac{1}{t_a} W_{\gamma_1}, \quad (44)$$

waarin

$$V_{\gamma_1} = v_0 \left\{ \sqrt{\frac{a_0}{a(\gamma_1)}} - 1 \right\}, \quad (45)$$

en

$$W_{\gamma_1} = \frac{1}{\mu c_a'} \frac{1}{a(\gamma_1)} \left(\frac{d\varphi(\gamma,p)}{d\gamma} \right)_{\gamma=\gamma_1}. \quad (46)$$

Zooals onder 03.1 is beschreven, wordt nu t_a bepaald door gelijkstelling van (40) en (44) voor het tijdstip $\gamma = 1$, waardoor ontstaat:

$$T_{\gamma=1} t_a - U_{\gamma=1} = V_{\gamma=1} + \frac{1}{t_a} W_{\gamma=1}, \quad (47)$$

of

$$T_{\gamma=1} t_a^2 - (U_{\gamma=1} + V_{\gamma=1}) t_a - W_{\gamma=1} = 0 \quad (48)$$

Men vindt in het algemeen voor het geval van een normale landing twee reëele waarden voor t_a, waarvan er echter maar één een voor de landing practische beteekenis heeft; hierop wordt later teruggekomen.

In T, U en W komt nu de parameter p voor, zoodat met (48) t_a als functie van p is bepaald. Deze parameter wordt nu, zooals onder 03.1 is aangegeven, zoo gekozen, dat op het tijdstip $t_1 = 0{,}5\, t_a$ ($\gamma = 0{,}5$) de snelheden v_{γ_1} volgens (40) en (44) aan elkaar gelijk zijn, zoodat de, volgens (48) bepaalde, bij elkaar behoorende waarden van p en t_a, moeten voldoen aan de betrekking:

$$T_{\gamma=0,5} t_a^2 - (U_{\gamma=0,5} + V_{\gamma=0,5}) t_a - W_{\gamma=0,5} = 0 \quad (50)$$

De beide vierkantsvergelijkingen (48) en (50) moeten dus den, voor de landing van practische beteekenis zijnde, wortel $t_a = t_{a_1}$ gemeen hebben.

Dit levert in principe een voorwaarde voor de grootheden

$$T_{\gamma=1}, \quad T_{\gamma=0,5}, \quad (U+V)_{\gamma=1}, \\ (U+V)_{\gamma=0,5}, \quad W_{\gamma=1} \text{ en } W_{\gamma=0,5},$$

waaruit p kan worden bepaald.

Bij de hierna te behandelen keuze van de functies $a(\gamma)$ en $\varphi(\gamma, p)$ leidt dit echter tot een hoogeremachtsvergelijking in p, waarvan het oplossen groote moeilijkheden biedt.

Eenvoudiger kan men als volgt te werk gaan. Noemt men δv het verschil tusschen de waarden van de snelheid op het tijdstip $\gamma_1 = 0{,}5$ volgens vergelijking (40) en volgens (44), dan is

$$\delta v = T_{\gamma=0,5} t_a - (U_{\gamma=0,5} + V_{\gamma=0,5}) - \frac{1}{t_a} W_{\gamma=0,5} \quad (51)$$

Men kan nu de uit (48) volgende, voor de landing van practische beteekenis zijnde en bij elkaar behoorende waarden van t_a en p invoeren in (51) en δv grafisch weergeven als functie van p. Door interpolatie vindt men dan de waarde van p, waarvoor $\delta v = 0$ en daarmede de gezochte waarde van t_a.

04 Keuze van de functies $a(\gamma)$ en $\varphi(\gamma, p)$.

04.1 *Algemeen.*

Men kan een aantal voorwaarden aangeven waaraan de bovengenoemde functies moeten voldoen. Daarbij wordt, in overeenstemming met de praktijk bij het uitvoeren van een goede landing, uitgegaan van de veronderstelling, dat de afvangmanoeuvre zeer geleidelijk van de stationnaire zweefvlucht uit wordt begonnen en uitgevoerd, d.w.z. dat plotselinge stuurbewegingen ofwel knikken in het verloop van de grootheden a, φ en Θ met den tijd bij het begin of tijdens de afvangmanoeuvre niet mogen optreden.

Wanneer op het tijdstip $t = 0$ geen knikken in de $(a;t)$ en $(\varphi;t)$ krommen mogen optreden, beteekent dit, dat op dat tijdstip $\dot{a}$ en $\dot{\varphi}$ nul moeten zijn, dus ook $\frac{da}{d\gamma}$ en $\frac{d\varphi}{d\gamma}$ gelijk nul. In verband met (28) is dan ook $\dot{\Theta}$ gelijk nul.

Volgens (16) wordt de roerhoekverandering t.o.v. den roerhoek in stationnaire vlucht bepaald door $\ddot{\Theta}$, $\dot{\Theta}$ en $\dot{a}$.

Zijn nu ten tijde $t = 0$, $\dot{\Theta}$ en $\dot{a}$ gelijk nul, dan moet, om geen plotselinge stuurbewegingen op dit tijdstip te verkrijgen, ook $\ddot{\Theta} = 0$ zijn. Om te verkrijgen, dat voor $t = 0$ aan de voorwaarde $\ddot{\Theta} = 0$ voldaan wordt, zullen op dit tijdstip dus, mede in verband met $\dot{a} = 0$ en $\dot{\varphi} = 0$, $\ddot{a}$ en $\ddot{\varphi}$ gelijk nul moeten zijn.

Uit het bovenstaande volgt, dat voor het tijdstip $t = 0$ moet gelden $\ddot{a} = 0$ en $\ddot{\varphi} = 0$ of dat voor $\gamma = 0$ moet gelden

$$\frac{d^2a}{d\gamma^2} = 0 \text{ en } \frac{d^2\varphi}{d\gamma^2} = 0.$$

De te kiezen functies $a(\gamma)$ en $\varphi(p,\gamma)$ moeten derhalve aan de volgende voorwaarden voldoen (zie ook fig. 3):

1° voor $\gamma = 0$ moet $a = a_0$; a_0 is de invalshoek in stationnaire zweefvlucht,

2° voor $\gamma = 1$ moet $a = a_g$; a_g is de invalshoek bij het aan den grond komen; verondersteld wordt, dat deze bekend is,

3° voor $\gamma = 0$ moet $\frac{da}{d\gamma} = 0$,

4° voor $\gamma = 0$ moet $\frac{d^2a}{d\gamma^2} = 0$,

5° voor $\gamma = 0$ moet $\varphi = \varphi_0$; φ_0 is de baanhoek in de stationnaire zweefvlucht,

6° voor $\gamma = 1$ moet $\varphi = 0$; bij een goede landing moet het vliegtuig zich op het oogenblik van landen evenwijdig aan den grond bewegen,

7° voor $\gamma = 0$ moet $\frac{d\varphi}{d\gamma} = 0$,

8° voor $\gamma=0$ moet $\frac{d^2\varphi}{d\gamma^2}=0$.

Ten slotte moet in de functie $\varphi(\gamma)$ nog een parameter worden ingevoerd. Hiervoor is gekozen de helling van de $(\varphi;\gamma)$ kromme bij $\gamma=1$ en wel zoo, dat deze helling wordt weergegeven door $p\varphi_0$.

De laatste voorwaarde luidt dus:

9° voor $\gamma=1$ moet $\frac{d\varphi}{d\gamma}=p\varphi_0$.

De te kiezen functies moeten verder vanzelfsprekend zoodanig zijn, dat zij in overeenstemming zijn met het bij een normale landing te verwachten verloop van α en φ met den tijd. Aangezien, teneinde de berekeningen zoo eenvoudig mogelijk te houden, $\alpha(\gamma)$ wordt voorgeschreven en $\varphi(\gamma)$ door invoering van een uit de berekening volgenden parameter p zoo goed mogelijk aan dit α-verloop wordt aangepast, is bovenstaande overweging voor de keuze van $\alpha(\gamma)$ het meest van beteekenis.

De hierboven aangegeven begin- en eindvoorwaarden, waaraan bij een normale landing moet worden voldaan, leggen het invalshoekverloop reeds voor een belangrijk deel vast. Voldoende betrouwbare metingsresultaten omtrent het invalshoekverloop bij een normale landing, om hierop de keuze van de voor te schrijven functie $\alpha(\gamma)$ te baseeren, staan thans niet ter beschikking. Daar bij de ontwikkeling van de behandelde benaderingsmethode steeds wordt uitgegaan van de veronderstelling, dat bij een goede landing de geheele beweging zeer geleidelijk zal verloopen, zal men, naar verwacht kan worden, het invalshoekverloop voor een normale landing zeker voldoende goed benaderen, wanneer men daarvoor een functie invoert, die tusschen de aangegeven begin- en eindvoorwaarden een regelmatig toenemen van den invalshoek weergeeft zonder snelle veranderingen van de eerste en tweede afgeleiden met den tijd.

Het ligt voor de hand voor de functies $\alpha(\gamma)$ en $\varphi(\gamma,p)$ rationale hoogeremachtsfuncties in te voeren; in verband met het aantal voorwaarden, dat gesteld wordt, zou dan $\alpha(\gamma)$ een functie van den 3den en $\varphi(\gamma,p)$ een functie van den 4den graad moeten zijn. Om echter de integralen (37) en (38) te kunnen oplossen, is voor $\alpha(\gamma)$ gekozen een functie van den algemeenen vorm

$$\alpha(\gamma)=(a\gamma^3+b\gamma^2+c\gamma+d)^2. \qquad (51)$$

Voor $\varphi(\gamma,p)$ is ingevoerd een functie van den 4den graad, dus van den algemeenen vorm

$$\varphi(\gamma,p)=e\gamma^4+f\gamma^3+g\gamma^2+h\gamma+k. \qquad (52)$$

04.2 *Uitwerking van de gekozen functies.*

Wanneer een functie $\alpha(\gamma)$ van den algemeenen vorm (51) moet voldoen aan de voorwaarden 1° t/m 4°, zal zij, zooals gemakkelijk is in te zien, luiden

$$\alpha(\gamma)=\{(\sqrt{\alpha_g}-\sqrt{\alpha_0})\gamma^3+\sqrt{\alpha_0}\}^2. \qquad (53)$$

Stelt men, zooals later gewenscht zal blijken:

$$z=\sqrt[3]{\frac{\sqrt{\alpha_0}}{\sqrt{\alpha_g}-\sqrt{\alpha_0}}}, \qquad (54)$$

dan kan (53) geschreven worden:

$$\alpha(\gamma)=\frac{\alpha_0}{z^6}(\gamma^3+z^3)^2. \qquad (55)$$

De functie $\varphi(\gamma,p)$ van den algemeenen vorm (52) zal in verband met de voorwaarden 5° t/m 9°, luiden

$$\varphi(\gamma,p)=\varphi_0\{(p+3)\gamma^4-(p+4)\gamma^3+1\}. \qquad (56)$$

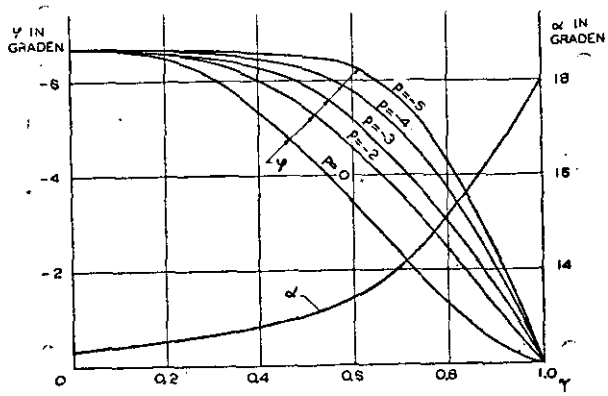

Fig. 4. Verloop van de functie $\alpha(\gamma)$ en $\varphi(\gamma,p)$.

In fig. 4 zijn voor bepaalde waarden van α_0, α_g en φ_0 de krommen volgens (55) en (56) weergegeven; de laatste voor een aantal waarden van den parameter p. Positieve waarden van p komen niet in aanmerking, omdat dit zou leiden tot positieve waarden van φ aan het einde van het afvangen, hetgeen zou beteekenen dat het vliegtuig eenige oogenblikken vóór het aan den grond komen op geringere hoogte zou zijn geweest dan op het oogenblik van landen zelf, hetgeen onmogelijk is. Waarden van p kleiner dan ca. —5 zullen ook praktisch niet bruikbaar zijn, omdat hierbij een steiler worden van den baanhoek bij het begin van het afvangen optreedt, hetgeen bij een normale landing niet het geval zal zijn.

Zooals uit beschouwing van fig. 4 volgt, is het waarschijnlijk, dat het verloop van den werkelijken invalshoek en baanhoek bij een normale landing met goede benadering door de beide functies wordt weergegeven. Later zal blijken, dat het vliegtuig, wanneer invalshoeken in de buurt van de maximale bereikt worden, nog slechts een zeer geringe hoogte boven den grond heeft, zoodat eventueele loslating of onaangename dwarsbesturingseigenschappen, wanneer deze b.v. tengevolge van remous reeds voor het aan den grond komen bij de zeer groote invalshoeken zouden optreden, geen ernstig bezwaar voor de veiligheid meer kunnen opleveren. Wanneer de waarde van $p<0$ is, beteekent dit, dat het vliegtuig na het punt $\gamma=1$ weer zou gaan stijgen, echter alléén, wanneer, zooals in de berekening is verondersteld, c_a met goede benadering lineair met α blijft aangroeien. De invalshoek bij het aan den grond komen (tijdstip $\gamma=1$) zal echter in het algemeen zóó gekozen worden, dat zij ongeveer overeenkomt met

de kritische, zoodat bij overschrijding daarvan in belangrijke mate loslating begint op te treden. Na het tijdstip $\gamma = 1$ zal het vliegtuig dan geen neiging meer vertoonen te gaan stijgen; het voert dus een goede driepuntslanding uit. Mocht men den invalshoek bij $\gamma = 1$ zoo wenschen te kiezen, dat de waarde er van nog belangrijk beneden de kritische ligt, dan moet, om aan den grond te blijven, de invalshoek worden verkleind, hetgeen overeenkomt met het uitvoeren van een wiellanding.

Uit (55) volgt nog:

$$\frac{d\,a}{d\,\gamma} = \dot{a}\,t_a = \frac{6\,a_0}{z^6}\,\gamma^2(\gamma^3 + z^3) \qquad (57)$$

en

$$\frac{d^2\,a}{d\,\gamma^2} = \ddot{a}\,t_a^2 = \frac{6\,a_0}{z^6}\,\gamma(5\,\gamma^3 + 2\,z^3). \qquad (58)$$

terwijl uit (56) volgt

$$\frac{d\,\varphi}{d\,\gamma} = \dot{\varphi}\,t_a = \varphi_0\{4(p+3)\gamma^3 - 3(p+4)\gamma^2\} \qquad (59)$$

en

$$\frac{d^2\varphi}{d\,\gamma^2} = \ddot{\varphi}\,t_a^2 = \varphi_0\{12(p+3)\gamma^2 - 6(p+4)\gamma\} \qquad (60)$$

05 Uitwerking van de benaderingsmethode met de gekozen functies $a(\gamma)$ en $\varphi(\gamma, p)$.

05.1 *Invoering van de gekozen functies.*

Onder 03.2 is in algemeenen vorm de benaderingsmethode uitgewerkt. Hierin kunnen nu de functies $a(\gamma)$ en $\varphi(\gamma, p)$ worden ingevoerd.

Daartoe worden eerst de integralen (35) t/m (38) uitgewerkt. Aangezien dit tot vrij omslachtige bewerkingen leidt, zal hier alleen het resultaat worden weergegeven; de uitwerking van de integralen is uitvoerig in de appendix onder **09** behandeld.

Er blijkt, dat de intergralen, waarin de parameter p voorkomt, nl. L_{γ_1} (35), N_{γ_1} (37) en O_{γ_1} (38) lineaire functies van p zijn en dat alle 4 integralen ten slotte geschreven kunnen worden in den volgenden vorm:

$$L_{\gamma_1} = \varphi_0'\,[p\,f_1(\gamma_1) + f_2(\gamma_1)], \qquad (61)$$

$$M_{\gamma_1} = \frac{1}{9\,a_0}\,f_3(z, \gamma_1), \qquad (62)$$

$$N_{\gamma_1} = \frac{\varphi_0}{a_0}\sqrt{a_0}\,[p\,f_4(z, \gamma_1) + f_5(z, \gamma_1)], \qquad (63)$$

en

$$O_{\gamma_1} = \frac{\varphi_0}{a_0^2}\sqrt{a^0}\,[p\,f_6(z, \gamma_1) + f_7(z, \gamma_1)]. \qquad (64)$$

f_1 t/m f_7 zijn nu functies van γ_1 en z of van γ alléén.

De uitwerking van deze functies is onder **09** gegeven. In de figuren 13 en 14 zijn zij voor een aantal in de praktijk voorkomende waarden van z weergegeven en wel voor de waarden $\gamma_1 = 1$ en $\gamma_1 = 0{,}5$, welke, zooals onder **03** is uiteengezet, in de berekening verder zullen worden gebruikt. Door gebruik van deze grafieken worden de berekeningen zeer vereenvoudigd. Men kan nu (61) t/m (64) invoeren in de uitdrukkingen (41) en (42) en verkrijgt dan:

$$T_{\gamma_1} = -\,g\,\varphi_0 f_1\,p - \{g\,\varphi_0 f_2 + \tfrac{1}{2}\mu\,v_0^2\,a_0(c_w'\,\gamma_1 + \frac{c_{w_u}}{9\,a_0}\,f_3)\} \qquad (65)$$

en

$$U_{\gamma_1} = v_0\,\varphi_0\left(\frac{c_w'}{c_a'}\,f_4 + \frac{c_{w_u}}{c_a'\,a_0}\,f_6\right)p + v_0\,\varphi_0\left(\frac{c_w'}{c_a'}\,f_5 + \frac{c_{w_u}}{c_a'\,a_0}\,f_7\right). \qquad (66)$$

Verder ontstaan, door invoering van (55) en (59) in (45) en (46)

$$V_{\gamma_1} = -\,v_0\frac{\gamma_1^3}{\gamma_1^3 + z^3}, \qquad (67a)$$

of

$$V_{\gamma_1} = -\,v_0 f_8 \qquad (67)$$

en

$$W_{\gamma_1} = \frac{1}{\mu\,c_a'}\frac{\varphi_0}{a_0}\left[\frac{\gamma_1^2(4\gamma_1 - 3)z^6}{(\gamma_1^3 + z^3)^2}\,p + 12\,\frac{\gamma_1^2(\gamma_1 - 1)z^6}{(\gamma_1^3 + z^3)^2}\right], \qquad (68a)$$

of

$$W_{\gamma_1} = \frac{1}{\mu\,c_a'}\frac{\varphi_0}{a_0}\,[p\,f_9(z, \gamma_1) + f_{10}(z, \gamma_1)] \qquad (68)$$

Ook de functies f_8 t/m f_{10} zijn voor $\gamma_1 = 1$ en $\gamma_1 = 0{,}5$ en voor een aantal in de praktijk voorkomende waarden van z berekend en in de figuren 13 en 14 weergegeven.

05.2 *Bepaling van p en t_a.*

Zooals onder 03.2 is behandeld, bepaalt men $t_a(p)$ als een der wortels van de vergelijking

$$T_{\gamma=1}\,t_a^2 - (U_{\gamma=1} + V_{\gamma=1})\,t_a - W_{\gamma=1} = 0. \qquad (48)$$

Deze heeft in het algemeen 2 wortels nl.

$$t_a = \frac{U_{\gamma=1} + V_{\gamma=1}}{2\,T_{\gamma=1}} \pm \frac{1}{2\,T_{\gamma=1}}\sqrt{(U_{\gamma=1} + V_{\gamma=1})^2 + 4\,W_{\gamma=1}\,T_{\gamma=1}}.$$

Eén dezer wortels is echter slechts voor de landing van practische beteekenis, hetgeen men als volgt kan inzien.

In het bijzondere geval, dat $p = 0$, is $W_{\gamma=1} = 0$. Een der wortels van (48) wordt dan

$$t_{a_2} = 0,$$

terwijl

$$t_{a_1} = \frac{U_{\gamma=1} + V_{\gamma=1}}{T_{\gamma=1}}.$$

Gaat men echter uit van de vergelijking (47), waaruit (48) is afgeleid, dán verkrijgt men voor dit bijzondere geval $p = W_{\gamma=1} = 0$ slechts één oplossing voor t_a nl.

$$t_{a_1} = \frac{U_{\gamma=1} + V_{\gamma=1}}{T_{\gamma=1}}.$$

De wortel $t_{a_2} = 0$ is dus ingevoerd en is voor het probleem niet van beteekenis.

Is nu $p \neq 0$ en dus $W_{\gamma=1} \neq 0$ dán zijn er inderdaad twee waarden van t_a mogelijk, die

(48) bevredigen en voor het probleem van reëele beteekenis zijn.

Een dezer wortels (t_{a_2}) echter is voor de waarden van p, die voor het probleem in aanmerking komen ($0 > p >$ ca. -5) belangrijk kleiner dan de andere; deze wortel is kleiner naarmate p grooter wordt en wordt nul voor het bijzondere geval, dat $p=0$. Deze wortel nu heeft voor de landing geen practische beteekenis; hij beschrijft het geval, dat het vliegtuig snel wordt opgetrokken uit de stationnaire zweefvlucht tot de invalshoek α_g is bereikt op het oogenblik, dat de baanhoek 0 is. De snelheid is daarbij dan echter niet of zeer weinig afgenomen t.o.v. de snelheid v_0. Vanzelfsprekend gaan hiermede groote roeruitslagen gepaard. Dit geval komt dus voor de landing niet in aanmerking.

De andere wortel t_{a_1}, welke belangrijk grooter is dan t_{a_2}, geeft op het oogenblik, dat $\varphi=0$ en $\alpha=\alpha_g$ is geworden, een waarde van de snelheid, die zeer weinig verschilt van die welke in stationnaire vlucht bij den invalshoek α_g behoort. Uit de berekeningen blijkt (zie b.v. onder **07**), dat deze wortel, welke dus voor de landing van practische beteekenis is, bepaald wordt uit

$$t_{a_1}(p)=\frac{U_{\gamma=1}+V_{\gamma=1}}{2\,T_{\gamma=1}}-\frac{1}{2\,T_{\gamma=1}}\sqrt{(U_{\gamma=1}+V_{\gamma=1})^2+4\,W_{\gamma=1}\,T_{\gamma=1}}. \quad (69)$$

T, U, V en W worden gegeven door (65) t/m (68), waarin de waarden van f_1 t/m f_{10} voor $\gamma_1=1$ zijn ingevoerd (zie fig. 14). Met (69) wordt voor een aantal waarden van p ($0>p>-5$) t_a berekend; t_a wordt dan uitgezet als functie van p.

Met behulp van

$$\delta v = T_{\gamma=0,5}\,t_a-(U_{\gamma=0,5}+V_{\gamma=0,5})-\frac{1}{t_a}\,W_{\gamma=0,5}, \quad (51)$$

waarin T, U, V en W wederom worden gegeven door (65) t/m (68) met dien verstande, dat nu de waarden van f_1 t/m f_{10} voor $\gamma_1=0{,}5$ worden ingevoerd (zie fig. 15), wordt δv als functie van t_a of p berekend en grafisch weergegeven. Door interpolatie worden de waarden van p en t_a bepaald, waarvoor $\delta v=0$. De gezochte waarde van t_a is hiermede verkregen.

De vraag zal kunnen rijzen, hoe de hoogte boven den grond tijdens de afvangmanoeuvre zal verloopen.

In een tijd dt is de hoogteverandering, wanneer men, zooals hier toelaatbaar is, sin $\varphi=\varphi$ stelt.

$$dh=\varphi\,v\,dt.$$

Men kan inzien, dat hieruit de hoogte op het tijdstip t_1 wordt bepaald als

$$h_{\gamma_1}=\int_0^{t_1}\varphi\,v\,dt-\int_0^{t_a}\varphi\,v\,dt=-\int_{t_1}^{t_a}\varphi\,v\,dt,$$

of

$$h_{\gamma_1}=-t_a\int_{\gamma_1}^{1}\varphi\,v\,d\gamma.$$

Vult men hierin de waarde van v volgens (26) in, dan verkrijgt men

$$h_{\gamma_1}=-t_a\,v_0\sqrt{a_0}\int_{\gamma_1}^{1}\frac{\varphi}{\sqrt{a}}\,d\gamma-\frac{1}{\mu\,c_a'}\int_{\gamma_1}^{1}\frac{\varphi}{a}\frac{d\varphi}{d\gamma}\,d\gamma. \quad (70a)$$

In het algemeen is de tweede term klein t.o.v. den eersten, zoodat men met goede benadering h_{γ_1} kan berekenen met

$$h_{\gamma_1}=-t_a\,v_0\sqrt{a_0}\int_{\gamma_1}^{1}\frac{\varphi}{\sqrt{a}}\,d\gamma, \quad (70b)$$

of

$$h_{\gamma_1}=-t_a\,v_0\sqrt{a_0}\,P_{\gamma_1}.$$

Hierin kan dan P_{γ_1} worden voorgesteld door

$$P_{\gamma_1}=\frac{\varphi_0\sqrt{a_0}}{a_0}\,[p\,f_{11}(z,\gamma_1)+f_{12}(z,\gamma_1)],$$

zoodat

$$h_{\gamma_1}=-t_a\,v_0\,\varphi_0\,[p\,f_{11}(z,\gamma_1)+f_{12}(z,\gamma_1)]. \quad (70)$$

De uitwerking van $f_{11}(z,\gamma_1)$ en $f_{12}(z,\gamma_1)$ is onder **09** gegeven. In fig. 15 zijn zij voor een aantal in de praktijk voorkomende waarden van z weergegeven en wel voor waarden van $\gamma=0$; 0,4 en 0,7. Met behulp hiervan kan het verloop van de hoogte tijdens de landing met voldoende benadering worden aangegeven.

Opmerking.

Niet voor alle mogelijke begintoestanden (a_0, φ_0) en eindtoestanden ($a_g, \varphi_g=0$) zal op de in het voorgaande beschreven wijze een benaderingsoplossing kunnen worden bepaald. Het kan nl. voorkomen, dat of de wortels van (48) voor de bruikbare waarden van p nl. $0>p>-5$ complex worden, of de met behulp van (51) berekende p-waarde voor $\delta v=0$ buiten het bruikbare gebied ($0>p>$ ca. -5) komt. Het eerste zal in hoofdzaak het geval zijn, wanneer een stationnaire begintoestand is gekozen met te grooten invalshoek en dus te lage snelheid, het laatstgenoemde daarentegen, wanneer de stationnaire beginsnelheid te hoog is gekozen. Een en ander wordt door het uitgewerkte voorbeeld onder **07** toegelicht.

Wanneer zich het eerstgenoemde verschijnsel (complexe waarde van t_a) voordoet, beteekent dit, dat het onmogelijk is een landing uit te voeren, waarbij voor het gekozen invalshoekverloop een baanhoekverloop optreedt, dat met goede benadering overeenstemt met het gekozen baanhoekverloop; men zal dan moeten verwachten, dat het vliegtuig niet meer bij een baanhoek $\varphi=0$ aan den grond gebracht kan worden. Dit verschijnsel treedt ook inderdaad in de praktijk op, wanneer met een te lage snelheid wordt binnengekomen.

Wanneer de berekende p-waarde buiten het bruikbare gebied valt b.v. $p>0$, dan wordt, zooals reeds vroeger is opgemerkt, het met deze benaderingsmethode bepaalde baanhoekverloop zoodanig, dat het niet meer voor een normale landing geschikt is. Dit verschijnsel doet zich in het algemeen echter voor wanneer de snelheid bij binnenkomen groot is.

In het gebied van normale snelheden voor het binnenkomen (v_0 tusschen circa 1,2 en 1,3 maal de minimale snelheid) zullen in het algemeen de genoemde verschijnselen niet optreden.

05.3 *Bepaling van de voor het landen vereischte roerhoeken.*

Met de, op de in 05.2 beschreven wijze, bepaalde waarden van t_a en p kan men $\ddot{\Theta}$, $\dot{\Theta}$ en $\dot{\alpha}$ als functie van γ bepalen en daarmede met behulp van (16) den roerhoek $\beta(\gamma)$ berekenen.

(16) kan men daartoe schrijven:

$$\beta(\gamma)=\frac{2B}{\varrho\eta^2 c_2 f l v(\gamma)^2}\ddot{\Theta}(\gamma)- -1{,}2\frac{c_1}{c_2}\frac{l}{v(\gamma)}\left(\frac{\dot{\Theta}(\gamma)}{\eta}+\frac{d\varepsilon}{d\alpha}\dot{\alpha}(\gamma)\right)+\beta^x(\alpha). \quad (71)$$

Hierin is

$$\ddot{\Theta}=\ddot{\alpha}+\ddot{\varphi} \quad \text{en} \quad \dot{\Theta}=\dot{\alpha}+\dot{\varphi} \quad (28)$$

Zooals reeds onder 04.2 is afgeleid, is

$$\ddot{\alpha}(\gamma)=\frac{1}{t_a^2}\frac{6a_0}{z^6}\gamma(5\gamma^3+2z^3) \quad (58)$$

en

$$\ddot{\varphi}(\gamma)=\frac{1}{t_a^2}\varphi_0\gamma\{12(p+3)\gamma-6(p+4)\}, \quad (60)$$

terwijl

$$\dot{\alpha}(\gamma)=\frac{1}{t_a}\frac{6a_0}{z^6}\gamma^2(\gamma^3+z^3) \quad (57)$$

en

$$\dot{\varphi}(\gamma)=\frac{1}{t_a}\varphi_0\gamma^2\{4(p+3)\gamma-3(p+4)\}. \quad (59)$$

Verder is, volgens (26)

$$v(\gamma)=\frac{\dot{\varphi}(\gamma)}{\mu c_a a(\gamma)}+v_0\sqrt{\frac{a_0}{a(\gamma)}}, \quad (72)$$

of met (55) en (59)

$$v(\gamma)=\frac{\varphi_0\{4(p+3)\gamma^3-3(p+4)\gamma^2\}}{t_a\mu c_a' a_0}\cdot\frac{z^6}{(\gamma^3+z^3)^2}+ +v_0\frac{z^3}{(\gamma^3+z^3)}. \quad (73)$$

β^x is, zooals onder 02.1 is uiteengezet, de waarde van β, die in stationnaire zweefvlucht behoort bij den invalshoek $\alpha(\gamma)$ (bij de zwaartepuntsligging en den klepstand, waarvoor men den voor het landen noodigen roeruitslag wil berekenen).

De grootste (wegens het teeken van β liever „kleinste") waarde van de zoo berekende roeruitslagen $\beta(\gamma)$ is de gezochte, voor het landen noodige roeruitslag, bij den vliegtuigtoestand, waarvoor men de berekeningen heeft uitgevoerd (bepaald door gewicht, zwaartepuntsligging, traagheidsmoment, klepstand, enz.).

Men kan de voor het landen vereischte roerhoeken ook weergeven in het voor de stationnaire zweefvlucht geldende $\beta^x-\alpha$-diagram door boven den bij iedere α-waarde behoorenden „stationnairen" roerhoek β^x, uit te zetten den „extra" roeruitslag $\beta-\beta^x$, die voor het landen bij iedere waarde van α noodig is. Dit is in fig. 12 geschied.

In het algemeen zal de grootste (absolute) waarde van den roerhoek bereikt worden op het tijdstip $\gamma=1$ (oogenblik van landen) en meestal zal daarbij ook de voor het landen noodige extra roeruitslag $\beta-\beta^x$ het grootst zijn of zeker weinig afwijken van de grootste waarde, die op eenig oogenblik tijdens het afvangen optreedt. Deze roeruitslagen (ten tijde $\gamma=1$) kunnen als volgt berekend worden.

De waarden $\ddot{\Theta}_{\gamma=1}$, $\dot{\Theta}_{\gamma=1}$ en $\dot{\alpha}_{\gamma=1}$ kunnen met (57) t/m (60) worden berekend.

Men verkrijgt

$$\ddot{\Theta}_{\gamma=1}=\frac{1}{t_a^2}\left\{\frac{6a_0}{z^6}(2z^6+5)+\varphi_0(6p+12)\right\}, \quad (74)$$

$$\dot{\Theta}_{\gamma=1}=\frac{1}{t_a}\left\{\frac{6a_0}{z^6}(z^3+1)+p\varphi_0\right\}, \quad (75)$$

en

$$\dot{\alpha}_{\gamma=1}=\frac{1}{t_a}\frac{6a_0}{z^6}(z^3+1) \quad (76)$$

en volgens (26), wanneer men voor $\gamma=1$ den index g gebruikt,

$$v_g=\frac{p}{t_a\mu c_a'}\frac{\varphi_0}{a_g}+v_0\sqrt{\frac{a_0}{a_g}}. \quad (77)$$

Met behulp van (71) kan hieruit de hoogteroerhoek op het oogenblik $\gamma=1$ berekend worden.

$$\beta_g=\frac{2B}{\varrho v_g^2 f l\eta^2 c_a}\ddot{\Theta}_g-1{,}2\frac{c_1}{c_2}\frac{l}{v_g}\left(\frac{\dot{\Theta}_g}{\eta}+\frac{d\varepsilon}{d\alpha}\dot{a}_g\right)+ +\beta^x(a_g). \quad (78)$$

Evenals op c_a en c_w, zal de nabijheid van den grond een invloed op c_m en op de neerstrooming uitoefenen en daardoor de waarden van β^x wijzigen.

Wanneer men over gegevens omtrent deze beinvloeding beschikt, doet men goed deze in rekening te brengen. Dit is mogelijk, omdat men op de onder 05.2 beschreven wijze de hoogte boven den grond kent. Zou de nabijheid van den grond ook $\frac{d\varepsilon}{d\alpha}$ doen veranderen, dan zal het waarschijnlijk niet noodig zijn deze verandering in rekening te brengen, aangezien de term, waarin deze waarde optreedt toch slechts een geringe rol speelt t.o.v. den term met $\dot{\Theta}$. De invloed van de nabijheid van den grond op den extra-roeruitslag zal dus hoofdzakelijk veroorzaakt worden door de veranderingen van c_a en c_w.

Daar verder de grootste roeruitslagen zullen optreden bij invalshoeken, welke ongeveer gelijk zijn aan den kritischen invalshoek, en de staartvlakken zich t.g.v. de nabijheid van den grond zeker in de van den vleugel (bij grooten invalshoek en uitgeslagen kleppen) afkomende gestoorde strooming zullen bevinden, zal men hiermede bij de keuze van η rekening dienen te houden. Terwijl men in normale zweefvlucht bij niet te groote invalshoeken op waarden voor η tusschen 0,8 en 0,9 kan rekenen, mag men aan het einde van de afvangmanoeuvre, bij zeer grooten invalshoek, in het algemeen

geen hoogere waarden voor η dan 0,70 verwachten, misschien zelfs nog lager.

Gegevens omtrent η voor invalshoeken van 3 à 4° beneden de kritische waarde en voor uitgeslagen kleppen vindt men b.v. in *lit.* 2.

05.4. *Beschouwing over het geval dat c_1 en c_2 niet als constanten mogen worden opgevat.*

Zooals volgt uit (6) is vergelijking (71) afgeleid in de veronderstelling, dat het verband tusschen den normaalkrachtcoëfficiënt op de staartvlakken en β en α_h lineair is. Dit is voor een staartvlak van het gebruikelijke type voor een groot gebied van roer- en invalshoeken zeker het geval. Bij zeer groote waarden van β en/of α_h, wanneer loslating begint op te treden, vertoonen de c_n-β en c_n-α_h krommen echter een afwijking van het lineaire verband.

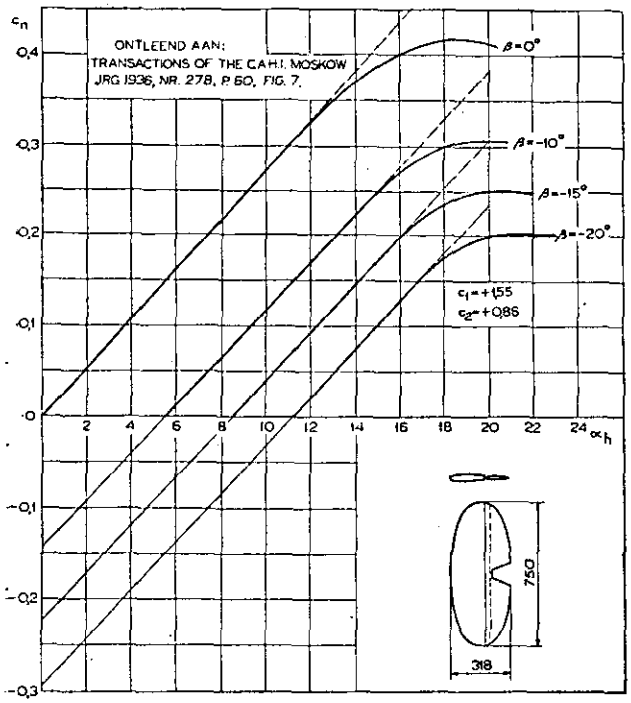

Fig. 5. Staartvlakgegevens.

Uit fig. 5 kan men, voor het model van een bepaald staartvlak, afleiden dat voor de bij de landing in aanmerking komende toestanden ($\beta<0$, $\alpha_h>0$) het lineaire verband tusschen c_n en β met voldoende benadering geldt voor roerhoeken tot meer dan 20° en het lineaire verband tusschen c_n en α_h bij groote negatieve roeruitslagen tot invalshoeken van ca. 18°. In de meeste gevallen zal dan ook bij de landing nog met goede benadering met constante waarden van c_1 en c_2 kunnen worden gerekend. (De tijdens het afvangen optredende waarden van α_h kunnen met (11) worden berekend).

Het zal ook veelal niet raadzaam zijn met hoeken α_h en β te rekenen, waarbij c_1 en c_2 niet meer constant zijn, aangezien men over het gedrag van de staartvlakken op ware-grootte bij hoeken, waarbij een niet onbelangrijke loslating begint op te treden, op grond van modelmetingen aan staartvlakken geen betrouwbare conclusies kan trekken. Het is echter wel mogelijk, ook wanneer c_1 en c_2 niet als constanten mogen worden beschouwd, dus in het algemeen voor een willekeurig verband $c_n(\alpha_h,\beta)$, den roerhoek β te berekenen, wanneer men over het $c_n(\alpha_h,\beta)$-diagram van het staartvlak beschikt en wel als volgt.

Volgens (5) is

$$M_h=\tfrac{1}{2}\varrho v(\gamma)^2\eta^2 f l c_n(\alpha_h,\beta). \qquad (5)$$

Hierin is, in de niet-stationnaire vlucht,

$$\alpha_h=\varkappa\alpha+\dot{\sigma}-\bar{\alpha}+\frac{l}{v(\gamma)}\left(\frac{\dot{\Theta}}{\eta}+\frac{d\varepsilon}{d\alpha}\dot{\alpha}\right). \qquad (11)$$

Het moment van de staartvlakken in stationnaire vlucht bij invalshoek α, dat gelijk is aan en tegengesteld gericht aan het moment van vleugel en romp tezamen (zie (14)), kan geschreven worden

$$M_h{}^x=\tfrac{1}{2}\varrho v(\gamma)^2\eta^2 f l.c_n(\alpha_h{}^x,\beta^x)=-\tfrac{1}{2}\varrho v^2 F t_v c_m(\alpha),$$

waarin

$$\alpha_h{}^x=\varkappa\alpha+\sigma-\bar{\alpha} \qquad (8)$$

en β^x bekend is uit de stuurstandslijn. De demping M_{ds}, geleverd door de staartvlakken bij de niet-stationnaire beweging, kan berekend worden als het verschil van de momenten der staartvlakken bij de invalshoeken α_h en $\alpha_h{}^x$, bij de, in de niet-stationnaire vlucht optredende, waarde van β.

Dus

$$M_{ds}=\tfrac{1}{2}\varrho v(\gamma)^2\eta^2 f l\{c_n(\alpha_h,\beta)-c_n(\alpha_h{}^x,\beta)\}.$$

Zooals onder 02,1 is uiteengezet, wordt voor de demping M_{vs} van vleugel en romp tezamen, 20% van de demping der staartvlakken alléén ingevoerd, zoodat

$$M_{vs}=0{,}2\,\tfrac{1}{2}\varrho v(\gamma)^2\eta^2 f l\{c_n(\alpha_h,\beta)-c_n(\alpha_h{}^x,\beta)\}.$$

Men kan dus voor het totale moment om het zwaartepunt, tijdens de niet-stationnaire beweging schrijven (analoog (15))

$$M=\tfrac{1}{2}\varrho v(\gamma)^2\eta^2 f l\{c_n(\alpha_h,\beta)-c_n(\alpha_h{}^x,\beta^x)+ +0{,}2\,c_n(\alpha_h,\beta)-0{,}2\,c_n(\alpha_h{}^x,\beta)\}, \qquad (15a)$$

zoodat nu uit (3) volgt:

$$1{,}2\,c_n(\alpha_h,\beta)-0{,}2\,c_n(\alpha_h{}^x,\beta)= =\frac{2B\ddot{\Theta}}{\varrho\eta^2 v(\gamma)^2 f l}+c_n(\alpha_h{}^x,\beta^x), \qquad (71a)$$

waarin α_h gegeven is door (11), $\alpha_h{}^x$ door (8) en β^x volgt uit de stuurstandslijn.

Deze vergelijking treedt dus in de plaats van (71): De waarde van β kan het eenvoudigst worden bepaald door in een grafiek uit te zetten de waarden van $[1{,}2\,c_n(\alpha_h,\beta)-0{,}2\,c_n(\alpha_h{}^x,\beta)]$ (bij de waarden van α_h en $\alpha_h{}^x$ volgens (8) en (11)) tegen β. De waarde van β, waarvoor deze functie gelijk is aan het rechterlid van (71a), is de gezochte roerhoek β.

Bovenbeschreven werkwijze moet worden gevolgd voor iedere waarde van γ, waarvoor men β wenscht te berekenen. Wanneer men dus alleen β_g wenscht te berekenen behoeft dit alleen voor de waarde $\gamma=1$ te geschieden. α_h en $\alpha_h{}^x$ worden berekend met (11) en (8), waarin de bij een bepaalde waarde γ behoorende waarden van α, $\dot{\Theta}$,

α en v volgens (55), (57), (59), (28) en (73) worden ingevoerd, terwijl $\ddot{\Theta}$ wordt bepaald met (28), (58) en (60). $c_n(\alpha_h,\beta)$, $c_n(\alpha_h{}^x,\beta)$ en $c_n(\alpha_h{}^x,\beta)$ worden afgelezen uit het gegeven $c_n(\alpha_h,\beta)$-diagram van de staartvlakken.

06 Bepaling van de meest voorlijke ligging van het zwaartepunt, welke met het oog op het landen toelaatbaar is.

Wanneer met (71) voor een bepaalde ligging van het zwaartepunt, waarmede een bepaald verband $\beta^x(\alpha)$ overeenkomt, de grootste (absolute) waarde van den voor het landen noodigen roeruitslag is bepaald, kan de vraag gesteld worden, wat nu bij een gegeven totaal beschikbaren roeruitslag (of — rekening houdende met het loslaten van de strooming bij groote roeruitslagen — bij de grootste bereikbare c_n-waarde) de meest voorlijke ligging van het zwaartepunt is, waarbij nog juist kan worden geland.

Het berekenen van deze zwaartepuntsligging kan bij benadering als volgt geschieden.

Bij een zwaartepuntsligging x_a (b.v. gemeten van den neus van de grootste vleugelkoorde af) is volgens (71) voor het landen een roeruitslag noodig, die bij een invalshoek α_1 haar grootste waarde β_a bereikt. Indien de totaal beschikbare roeruitslag β_{max} is, heeft men dus een overschot aan roeruitslag van $\beta_{max}-\beta_a$.

Wanneer men nu aanneemt, dat bij andere zwaartepuntsliggingen de grootste (absolute) waarde van β voor het landen eveneens bij dienzelfden invalshoek α_1 bereikt wordt (hetgeen niet altijd geheel juist behoeft te zijn, t.g.v. de verandering van de helling van het verband $\beta^x-\alpha$ bij verandering van de zwaartepuntsligging), zal, daar de extra-roeruitslag voor het landen onafhankelijk is van de zwaartepuntsligging, bij benadering het zwaartepunt nog zoodanig naar voren mogen worden verplaatst, dat bij den invalshoek α_1 in stationnaire vlucht een roeruitslag optreedt, welke $\beta_{max}-\beta_a$ grooter is dan de roerhoek $\beta_a{}^x$ in stationnaire vlucht bij den invalshoek α_1 en bij de zwaartepuntsligging x_a. De roeruitslag bij den invalshoek α_1 in stationnaire vlucht bij de zwaartepuntsligging x_a wordt gegeven door (14)

$$\beta_a{}^x=-\frac{1}{c_2}\frac{Ft_v}{fl}\frac{1}{\eta^2}c_{m_a}(\alpha_1)-c_1(\varkappa\alpha_1+\sigma-\bar{\alpha}), \qquad (79)$$

waarin c_{m_a} voorstelt den momentencoëfficiënt van het vliegtuig zonder staartvlakken bij de zwaartepuntsligging x_a.

Bij een zwaartepuntsligging x_b (zwaartepuntsverplaatsing Δx positief naar achteren) is

$$c_{m_b}(\alpha_1)=c_{m_a}(\alpha_1)+c_a(\alpha_1)\frac{\Delta x}{t_v} \qquad (80)$$

en dus

$$\beta_b{}^x=-\frac{1}{c_2}\frac{Ft_v}{fl}\frac{1}{\eta^2}\left\{c_{m_a}(\alpha_1)+c_a(\alpha_1)\frac{\Delta x}{t_v}\right\}- -c_1(\varkappa\alpha_1+\sigma-\bar{\alpha}). \qquad (81)$$

Hieruit volgt

$$\beta_b{}^x-\beta_a{}^x=-\frac{1}{c_2}\frac{Ft_v}{fl}\frac{1}{\eta^2}c_a(\alpha_1)\frac{\Delta x}{t_v}. \qquad (82)$$

Wanneer x_b de zwaartepuntsligging voorstelt, waarbij nog juist voldoende roeruitslag voor het landen beschikbaar is, moet

$$\beta_b{}^x-\beta_a{}^x=\beta_{max}-\beta_a.$$

De zwaartepuntsverplaatsing Δx, die, van de zwaartepuntsligging x_a uit, nog juist toelaatbaar is met het oog op het landen, volgt dan uit

$$\frac{\Delta x}{t_v}=-\eta^2\frac{fl}{Ft_v}\frac{1}{c_a(\alpha_1)}c_2(\beta_{max}-\beta_a). \qquad (83)$$

Wanneer de grootste roeruitslag bij het landen, zooals in het algemeen het geval zal zijn, bereikt wordt op het tijdstip $\gamma=1$, dan wordt β_a in (83) gegeven door (78).

Zooals reeds onder 05.4 is besproken, gelden de gegeven formules voor β (71) en (78) slechts voor zoover de functie $c_n(\alpha_h,\beta)$ als lineair mag worden beschouwd. Hetzelfde geldt vanzelfsprekend voor (83). Men moet dus β_{max} daarbij niet grooter kiezen dan de waarde tot welke de functie $c_n(\alpha_h,\beta)$ nog met goede benadering door een rechte lijn kan worden weergegeven; in het algemeen zal dit $-20°$ tot $-25°$ zijn.

07 Uitgewerkt voorbeeld.

07.1 *Gegevens van het vliegtuig.*

Ter toelichting van de berekeningsmethode en tevens ter toetsing van de resultaten zijn voor een vliegtuig, waarvan gegevens uit ware-grootteproeven ter beschikking stonden, de in het voorgaande behandelde berekeningen uitgevoerd, zoowel voor den toestand met geheel uitgeslagen kleppen als voor den toestand met gesoten kleppen.

De gegevens van het vliegtuig, voor zoover die voor de berekeningen van belang zijn, vindt men verzameld in tabel 1 (achterin) en in de figuur 6. Deze figuur geeft het verband tusschen c_a, c_w en α', zooals dit bij ware-grootte-proeven met het vliegtuig werd bepaald, alsmede de benadering door lineaire functies, welke voor de berekening noodzakelijk is.

Men ziet, dat, in het bij de afvangmanoeuvre voorkomende gebied van invalshoeken, de onnauwkeurigheid in de c_a en c_w waarden, die door deze benadering ontstaat, slechts gering is.

Opgemerkt moet nog worden, dat de c_a en c_w waarden direct zijn ontleend aan metingen in stationnaire zweefvlucht met gesloten gasklep zonder correctie voor den schroeftrek, zoodat in de c_w waarden is begrepen een correctie voor den invloed van de negatieve trekkracht van de schroef, welke ook bij de landing optreedt.

In fig 6 is verder uitgezet het uit dezelfde ware-grootteproeven afgeleide verband tusschen de stuwsnelheid v, de roerhoek β en α' in stationnaire zweefvlucht. Het verband $\beta-v$ is bepaald voor de klephoeken 0 en 40° en voor 2 zwaartepuntsliggingen nl. op ca. 27% en 24% van de gemiddelde koorde, doch is slechts voor de meest achterlijke ligging weergegeven.

Tenslotte is nog uitgezet het verband tusschen φ en α' in standaardatmosfeer (met invloed negatieve schroeftrek) voor een gewicht van 1000 kg, afgeleid uit de c_a-c_w-krommen.

De gegevens uit tabel 1 zijn onder meer aan fig. 6 ontleend.

De coëfficiënt c_2 is bepaald uit de bekende waarde van den hoogteroercoëfficiënt k_β, weergegeven in fig. 6, die uit de stuurstandslijnen voor verschillende zwaartepuntsliggingen kon worden afgeleid. Uit de definitie van k_β nl.

$$k_\beta = \frac{\Delta M}{q f l \Delta \beta},$$

waarin q de stuwdruk van de ongestoorde stroming voorstelt, en $\Delta\beta$ (in graden) het roerhoekverschil bij denzelfden vliegtoestand en verschillende zwaartepuntsliggingen, volgt, dat

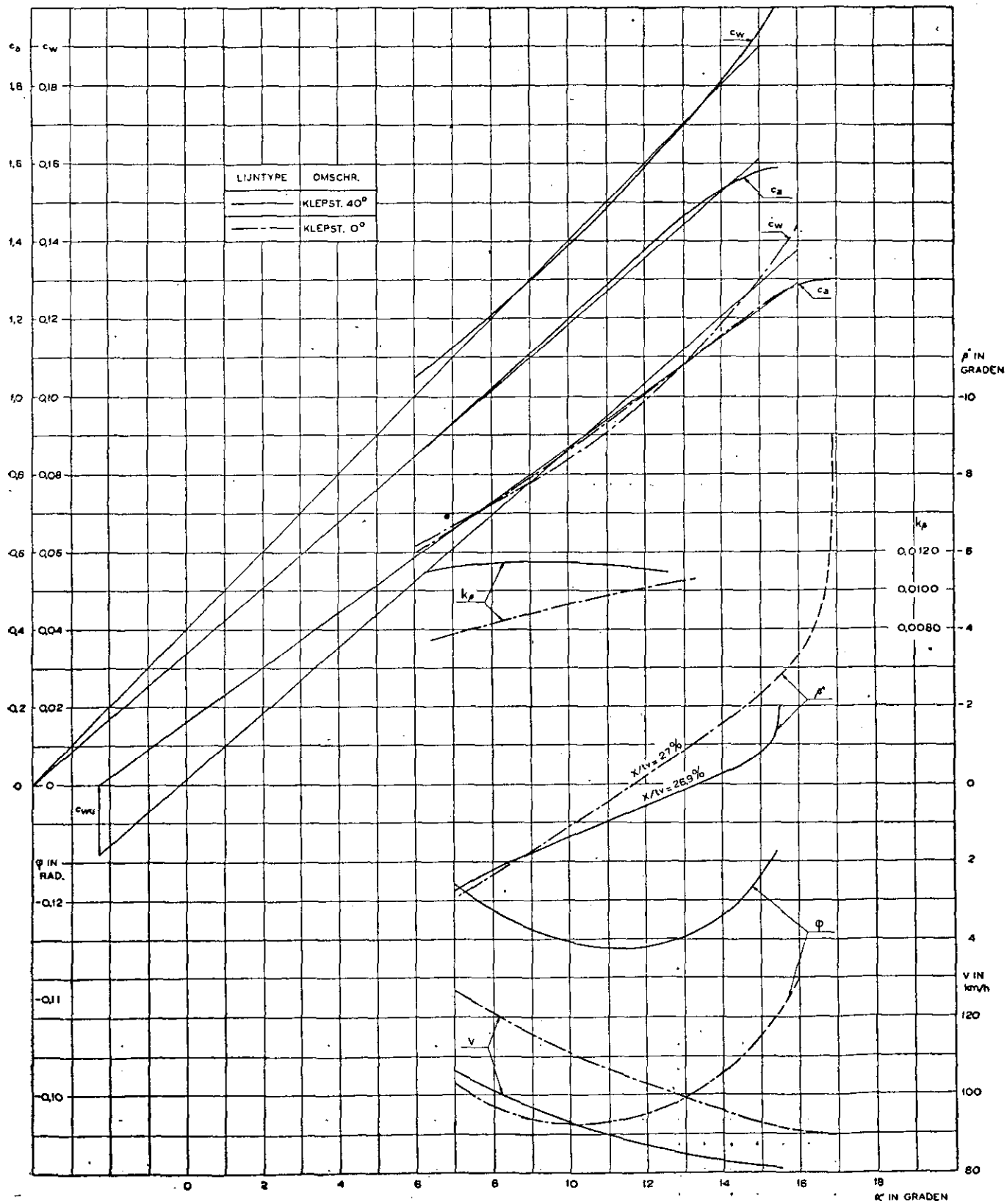

Fig. 6. Aerodynamische gegevens van het als voorbeeld beschouwde vliegtuig bij verschillende vliegtoestanden.

$$k_\beta = -\eta^2 c_2 .$$

Bij de niet-extreme invalshoeken ($\alpha' =$ ca. 10°) volgt uit de metingen bij 0 en 40° klephoek $k_\beta =$ ca. 0,010 per graad. Stelt men hierbij, zooals uit *lit.* 2 volgt, dat $\eta = 0{,}85$, dan is

$$c_2 = -0{,}79 \text{ per rad.}$$

Voor de zeer groote invalshoeken aan het einde van de afvangmanoeuvre wordt, eveneens aan de hand van *lit.* 2, voor den klephoek van 40° η gesteld op 0,70 en voor den klephoek van 0° op 0,80. De waarde van c_1/c_2 is bepaald op grond van theoretische overwegingen en modelmetingen aan staartvlakken met dezelfde slankheid en dezelfde verhouding tusschen stabilo- en roeroppervlak.

De waarde van het traagheidsmoment B is gevonden op grond van gegevens van vliegtuigen van overeenkomstig type, in den vorm van dimensielooze coëfficiënten voor het traagheidsmoment (zie b.v. *lit.* 5).

Voor de waarde van $\frac{d\varepsilon}{d\alpha}$ is 0,30 aangenomen; een meer nauwkeurige bepaling is, gezien den betrekkelijk geringen invloed van deze grootheid, niet noodzakelijk.

Teneinde de berekeningen eenvoudig te houden, werd de grondinvloed niet in rekening gebracht.

07.2 *Omvang en uitvoering van de berekeningen.*

De berekenigen zijn in twee groepen gesplitst; de eerste groep heeft betrekking op het bewuste vliegtuig, de tweede op eenige denkbeeldige veranderingen van de aerodynamische eigenschappen van den vleugel met klep van dit vliegtuig, teneinde den invloed van dergelijke veranderingen op de extra-roeruitslagen te onderzoeken.

De eerste groep berekeningen over de vereischte roeruitslagen werden uitgevoerd voor de meest achterlijke zwaartepuntsligging bij twee klephoeken, nl. $\delta = 0$ en $\delta = 40°$. Teneinde den invloed van de keuze van den stationnairen begintoestand vóór de afvangmanoeuvre te onderzoeken, werden voor beide klepstanden 0 en 40° de berekeningen uitgevoerd voor 3 begintoestanden a, *b* en *c*. Deze werden zóó gekozen, dat de snelheid bij één dezer drie toestanden voor elk geval gelijk was aan 1,2 maal de minimale snelheid behoorende bij den betreffenden klephoek. In het algemeen mag men wel zeggen, dat een snelheid van 1,2 v_{min} bij het binnenkomen als normale waarde mag gelden. De twee andere waarden werden in de nabijheid daarvan gekozen en wel voor de hoogste ca. 1,3 v_{min} en voor de laagste, voor zoover dit in verband met het complex worden van t_a mogelijk was, kleiner dan 1,2 v_{min}.

Uit fig. 6 en de gemeten waarden voor de minimale snelheid volgt, dat de kritische waarde van den invalshoek voor $\delta = 0°$ gelegen is bij $\alpha' =$ ca. 16,5° en voor $\delta = 40°$ bij $\alpha' =$ ca. 16°. Uit het verloop van de stuurstandslijnen ($\beta - \alpha$) in fig. 6 ziet men, dat bij α' ca. 15° voor $\delta = 40°$ en bij α' ca. 16° voor $\delta = 0°$ de stuurstandslijnen sterk beginnen af te buigen. Men mag dus verwachten, dat bij deze invalshoeken reeds in belangrijke mate loslating begint op te treden. Daarom is, voor den invalshoek, die bij het aan den grond komen wordt bereikt, voor $\delta = 0°$, $\alpha_g' = 16°$ en voor $\delta = 40°$ $\alpha_g' = 15°$ gekozen.

De standhoek bij het aan den grond komen bedraagt dan eveneens ca. 15° resp. 16°, terwijl stilstaande aan den grond de standhoek van dit vliegtuig ca. 12° bedroeg. Men mag dus concludeeren, dat bij bovengenoemde keuze van α_g' zeker een goede driepuntslanding zal worden uitgevoerd.

In tabel 2 zijn nu de gegevens (afgelezen uit fig. 6), waarvan bij de eerste groep berekeningen is uitgegaan, verzameld.

De tweede groep berekeningen betreffen als gezegd een tweetal denkbeeldige gevallen. Hieraan ligt de volgende gedachtengang ten grondslag.

Wanneer men, zooals in fig. 6 is geschied, de c_a- en c_w-waarden van het als voorbeeld gekozen vliegtuig uitzet op α', dan ziet men dat de kleppen een matige c_a-verhooging en een c_w-verhooging opleveren. Vergelijking van de berekende waarden van $(\beta - \beta^x)$ voor $\delta = 0$ en $\delta = 40°$ geeft een inzicht in den invloed van de klepwerking op de vereischte extraroeruitslagen. Teneinde nog iets dui-

TABEL 2

δ in graden v_{min} in km/h Begintoestand	0° ca. 90			40° ca. 80		
	a	*b*	*c*	*a*	*b*	*c*
v_0 in km/h	108	112	117	94	96	104
v_0 in m/sec	30,0	31,1	32,5	26,1	26,6	28,9
α_0' in graden (zie 09)	+ 10,74	+ 9,80	+ 8,76	+ 9,88	+ 9,35	+ 7,48
$\bar{\alpha}$ in graden (zie fig. 6)	+ 2,30	+ 2,30	+ 2,30	+ 4,00	+ 4,00	+ 4,00
α_0 in rad. (zie 09)	+ 0,228	+ 0,211	+ 0,193	+ 0,242	+ 0,233	+ 0,200
φ_0 in graden	− 5,55	− 5,55	− 5,62	− 6,65	− 6,6	− 6,88
φ_0 in rad.	− 0,097	− 0,097	− 0,098	− 0,1160	− 0,1165	− 0,120
α_g' in graden	16,00	16,00	16,00	15,00	15,00	15,00
α_g in rad.	+ 0,320	+ 0,320	+ 0,320	+ 0,332	+ 0,332	+ 0,332
z	1,76	1,63	1,52	1,803	1,727	1,51

delijker kwalitatieve gegevens omtrent den invloed van de aerodynamische eigenschappen van inrichtingen ter verhooging van draagkracht en weerstand op de voor het landen noodige extra-roeruitslagen te verkrijgen, zij nu nog voor een drietal denkbeeldige gevallen van dergelijke inrichtingen, toegepast op het als voorbeeld gekozen vliegtuig (tabel 1), de vereischte extra-roeruitslagen uitgerekend.

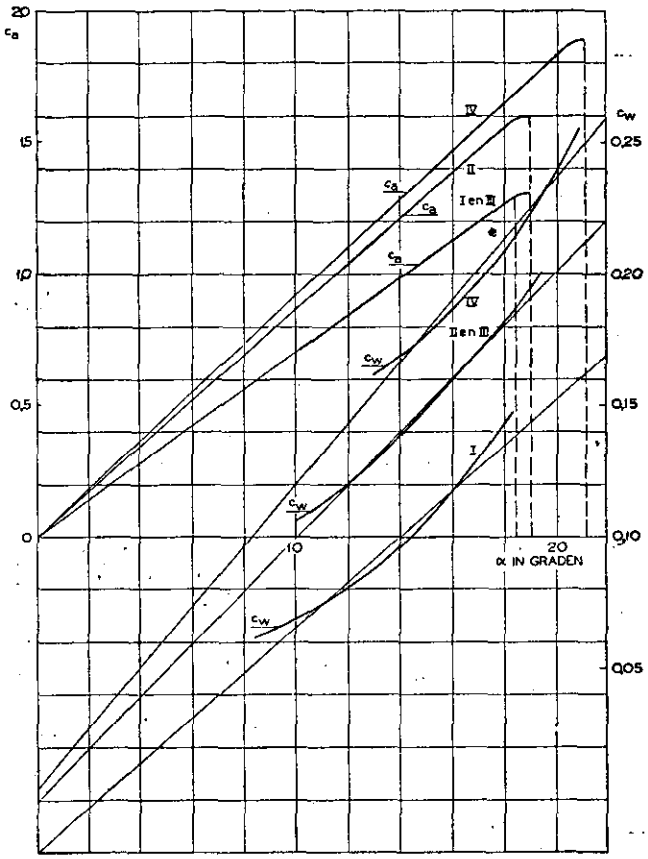

Fig. 7. $C_a(\alpha)$ en $c_w(\alpha)$ voor verschillende uitvoeringen van het vliegtuig.

Fig. 7 geeft hiervan een beeld. Hierin zijn uitgezet de c_a-α en c_w-α krommen (invalshoek t.o.v. de draagkracht-nullijn), waarop de berekeningen zijn gebaseerd. Hierin is geval I het gekozen voorbeeld zonder klepuitslag, geval II het voorbeeld met klepuitslag 40°, geval III de denkbeeldige klepvorm, (b.v. een remklep) die geen c_a-verhooging geeft en wel een verhooging van c_w, welke in dit geval gelijk wordt gesteld aan die voor het gekozen voorbeeld bij klepuitslag 40°. Geval IV stelt voor een goede landingsklep, die een aanzienlijke c_a-verhooging en daarbij een flinke weerstandsvermeerdering geeft.

Voor de gevallen III en IV wordt nu de extra-roeruitslag voor het afvangen berekend, uitgaande van de veronderstelling, dat het afvangen geschiedt van een stationnaire vlucht met een stuwsnelheid 1,2 v_{min} uit.

In tabel 3 zijn nu de voor de berekening noodige gegevens verzameld. Opgemerkt wordt nog, dat $(\beta - \beta^x)$ alleen is berekend voor het tijdstip $\gamma = 1$, omdat hierbij de grootste waarde optreedt.

TABEL 3.

Geval	III	IV
v_{min} in m/sec . . .	25,35	20,80
v_0 (1,2 v_{min}) in m/sec	30,4	25,0
$c_{a_{max}}$ . .	1,284	1,895
c_{a_0} $\left(=\frac{c_{a_{max}}}{1,44}\right)$ . .	0,892	1,315
α_0 in graden . . .	12,6	14,4
c_{w_0}	0,126	0,172
φ_0 in rad.	− 0,141	− 0,131
α_g in graden . . .	18,4	21,2
z	1,687	1,675
c_a'	4,06	5,21
c_w'	0,579	0,665
c_{w_u}	− 0,001	+ 0,005
η	0,70	0,70

De overige in de berekening voorkomende waarden volgen uit tabel 1.

07.3 *Resultaten.*

In tabel 4 (aan het einde van dit rapport) vindt men de berekening van den vereischten roeruitslag voor het afvangen op het oogenblik van landen, voor de klephoeken 0 en 40° en ieder voor 3 verschillende begintoestanden (zie 07.2).

In tabel 5 zijn de resultaten samengevat.

TABEL 5.

	Zwaartepuntsligging $x/t_v = 27\%$					
Klephoek δ in graden	0			40		
Stationnaire beginsnelheid v_0 in km/h	(1,2 v_{min}) 108	112	(1,3 v_{min}) 117	94	(1,2 v_{min}) 96	(1,3 v_{min}) 104
α_g' in graden	16	16	16	15	15	15
β_g in graden	− 6,0	− 5,0	− 4,6	− 5,6	− 4,5	− 3,2
$\beta_g - \beta^x$ in graden	− 2,6	− 1,7	− 1,2	− 4,8	− 3,8	− 2,4
h_0 in m	29,5	34,7	34,9	19,1	23,1	30,5

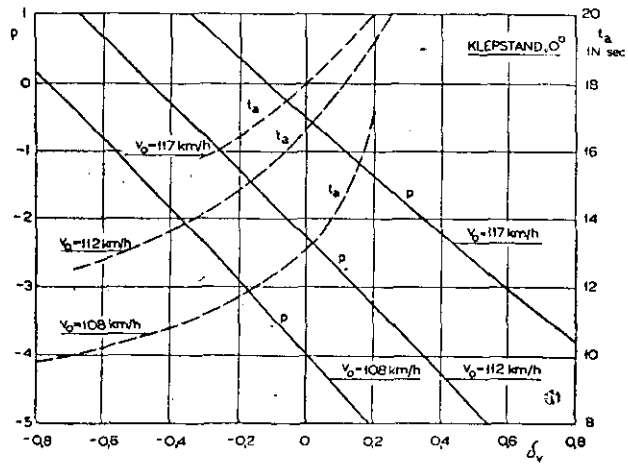

Fig. 8. Grafiek voor het bepalen van t_a en p (klepstand 0°).

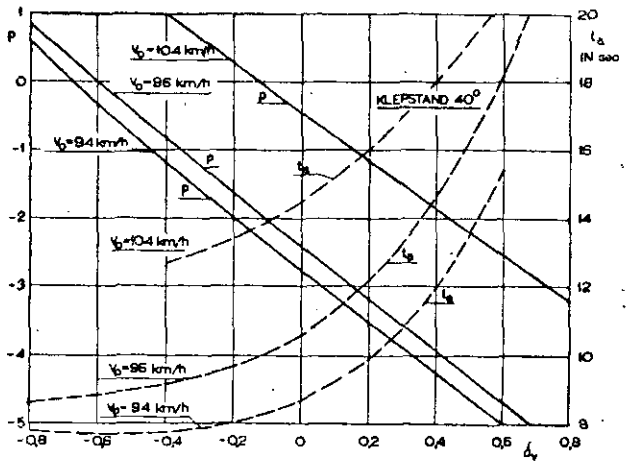

Fig. 9. Grafiek voor het bepalen van t_a en p (klepstand 40°).

De fig. 8 en 9 zijn hulpgrafieken voor de bepaling van p en t_a (zie tabel 4).

Bij het vliegtuig, waarop deze resultaten betrekking hebben en waarvan de stuurstandslijnen in fig. 6 zijn afgebeeld, moest met het oog op de overtrekbaarheid een roerbeperking worden aangebracht, waarvan echter de juiste waarde niet bekend is. Deze beperking zou echter, gezien den in stationnaire vlucht bereikten uitersten roeruitslag bij klephoek 40° en meest achterlijke zwaartepuntsligging ($x/t_v = 27\%$) bij ongeveer $-2°$ hebben moeten liggen.

Bij proefvluchten met de werkelijk aangebrachte roerbeperking bleek, dat het vliegtuig bij den bovengenoemden stationnairen vliegtoestand nog juist overtrekbaar was, bij andere klephoeken of bij de meer voorlijke zwaartepuntsligging (24%) echter niet meer. Men kan hieruit concludeeren, dat de werkelijk aangebrachte roerbeperking waarschijnlijk bij —4 à —5° gelegen zal zijn geweest.

Bij dezelfde proefvluchten bleek, dat met deze roerbeperking het vliegtuig alléén bij de meest achterlijke ligging van het zwaartepunt nog behoorlijk op drie punten kon worden geland.

De bovenstaande tabel toont, dat volgens de berekeningen een roerhoek van —4 à —5° voldoende is om het vliegtuig bij de meest achterlijke zwaartepuntsligging te landen, zeker bij klephoek 40° en bij niet te lage beginsnelheid ook bij klephoek 0°. Gezien de ligging van de stuurstandslijnen bij meer voorlijke zwaartepuntsliggingen zou echter voor de landing bij die liggingen volgens de berekeningen, een belangrijk grootere roeruitslag beschikbaar moeten zijn. De resultaten van de berekeningen zijn derhalve in dit geval in bevredigende overeenstemming met de bij proefvluchten geconstateerde feiten.

De resultaten van bovenstaande berekening zijn in fig. 10 weergegeven, waar zoowel voor klephoek 0° als voor klephoek 40°, als functie van de

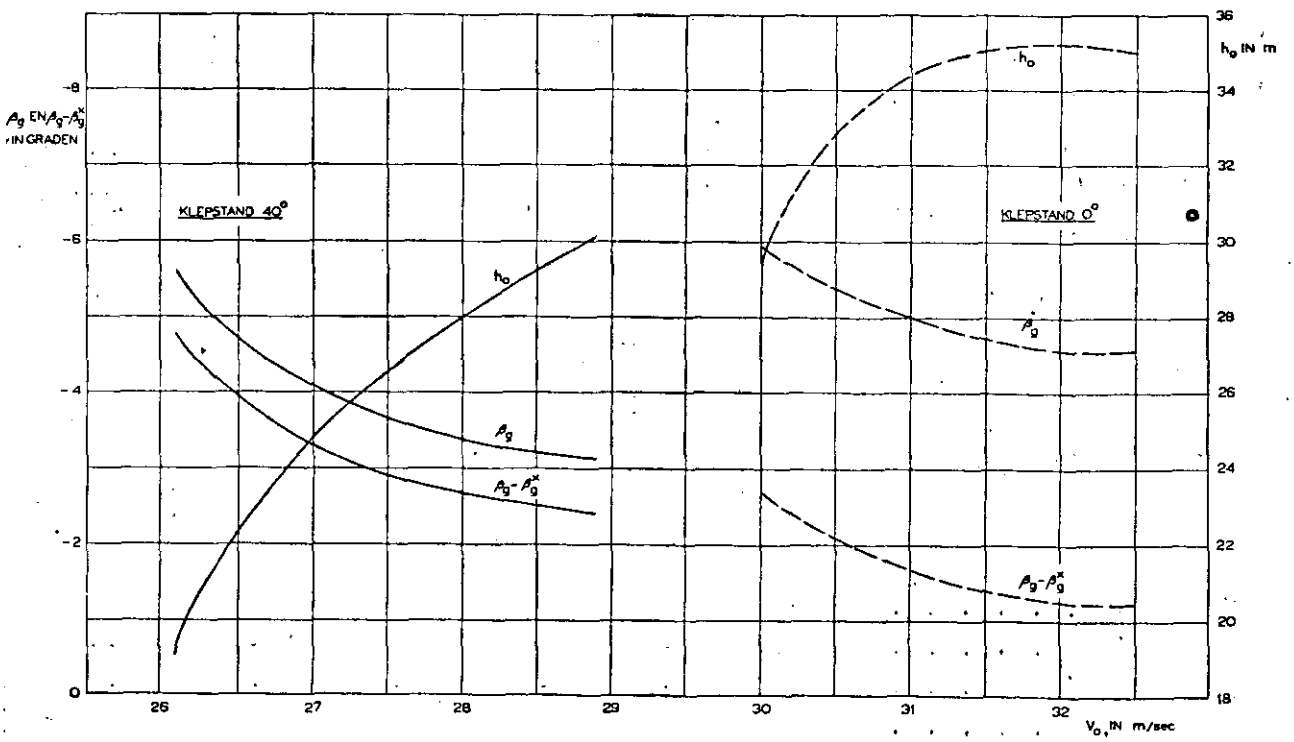

Fig. 10. De extra hoogteroeruitslag en de beginhoogte voor het afvangen als functie van de snelheid.

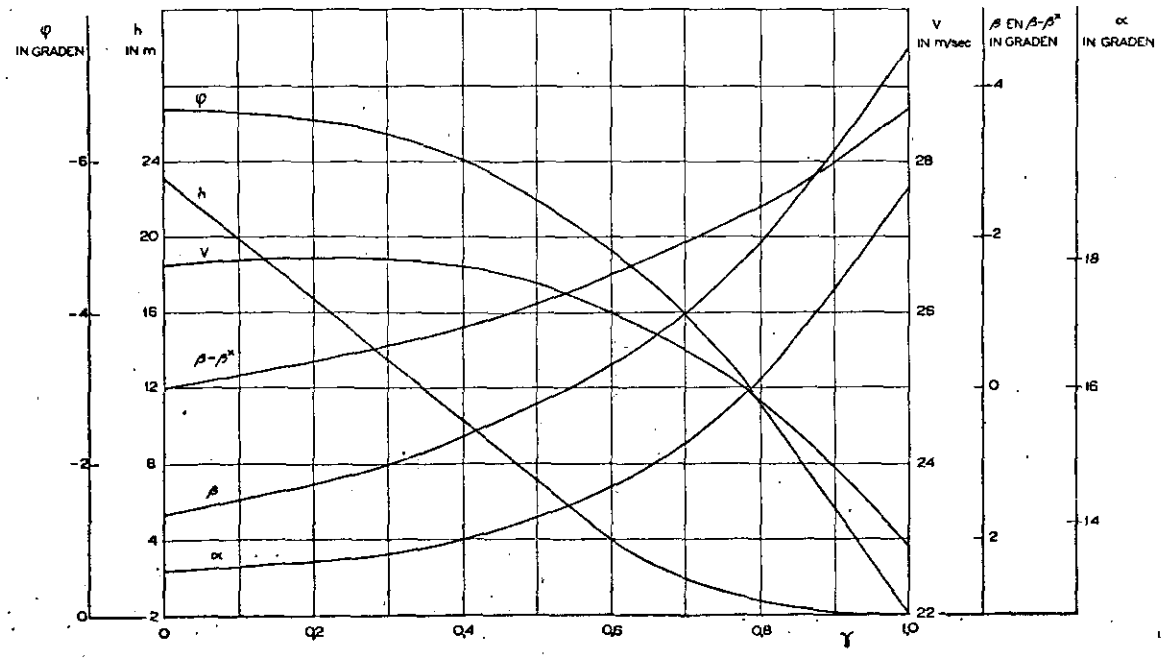

Fig. 11. Het verloop van eenige karakteristieke grootheden tijdens de landing.

stationnaire beginsnelheid zijn uitgezet, de vereischte extra-roeruitslag bij het einde van het afvangen ($\beta - \beta^x$) (d.w.z. de roeruitslag die, bij den invalshoek a_g aan het einde van de afvangmanoeuvre noodig is *boven* den in stationnaire vlucht bij dien invalshoek behoorenden roerhoek), de hoogte waarop met afvangen moet worden begonnen, alsmede de vereischte roeruitslag β bij het einde van het afvangen, voor de zwaartepuntsligging van 27%.

Bij de berekeningen bleek, dat in beide gevallen ($\delta = 0^0$ en $\delta = 40^0$) bij beginsnelheden van 1,1 v_{min} complexe waarden van t_a optreden voor $p < 0$. Dit wijst er dus op, dat een snelheid bij binnenkomen van 1,1 v_{min} te laag is om hierbij een landing uit te voeren volgens het gekozen invalshoek- en baanhoekverloop.

Een werkelijke landing met een dergelijke kleine beginsnelheid zal dus met dit vliegtype vermoedelijk niet meer op normale wijze kunnen worden uitgevoerd.

Ter illustratie van het verloop van verschillende grootheden tijdens de afvangmanoeuvre zijn in tabel 6 (achterin) berekend en in fig. 11 uitgezet, als functie van $\gamma (= t/t_a)$: de invalshoek α, de baanhoek φ, de snelheid v, de hoogte h, de extra-roeruitslag ($\beta - \beta^x$) en de roeruitslag β voor $x/t_v = 27\%$, alles voor het geval $\delta = 40^0$ en stationnaire beginsnelheid 96 km/h (1,2 v_{min}).

Men kan ook in het diagram van stuurstandslijnen $\beta(\alpha)$ voor de stationnaire zweefvlucht de vereischte roeruitslagen voor het afvangen weergeven. Daarbij wordt de extra-roeruitslag voor het afvangen ($\beta - \beta^x$) uitgezet boven den stationnairen roerhoek β^x bij de bijbehoorende waarde van α' tijdens het afvangen; fig 12 geeft hiervan voor het geval $\delta = 40^0$, $v_0 = 96$ km/h een voorbeeld.

Ten slotte zijn, op dezelfde wijze als in tabel 4 is gevolgd, de extra-roeruitslagen $\beta_g - \beta^x$ berekend, welke in de gevallen III en IV, waarvoor de aerodynamische gegevens in fig. 7 zijn weergegeven (uitvoerig besproken onder 07.2) noodig zijn voor het afvangen. Met de gevallen I en II waarvoor de berekenigen reeds in het voorgaande behandeld zijn, zijn de resultaten in tabel 7 vereenigd.

Men ziet door beschouwing van de gevallen I t/m IV, die allen geacht kunnen worden betrekking te hebben op landings- of remkleppen van het gebruikelijke type, dat de verhooging van c_w een belangrijke vergrooting van den vereischten extra-roeruitslag (vergel. I en III) met zich meebrengt, terwijl verhooging van $c_{a_{max}}$ een vermindering daarvan (vergelijk II en III) veroorzaakt. Hoe de vereischte extra-roeruitslag bij een bepaald type klep t.o.v. den toestand zonder klep zal zijn, hangt dus geheel af van de $c_{a_{max}}$- en c_w-verhooging. Men

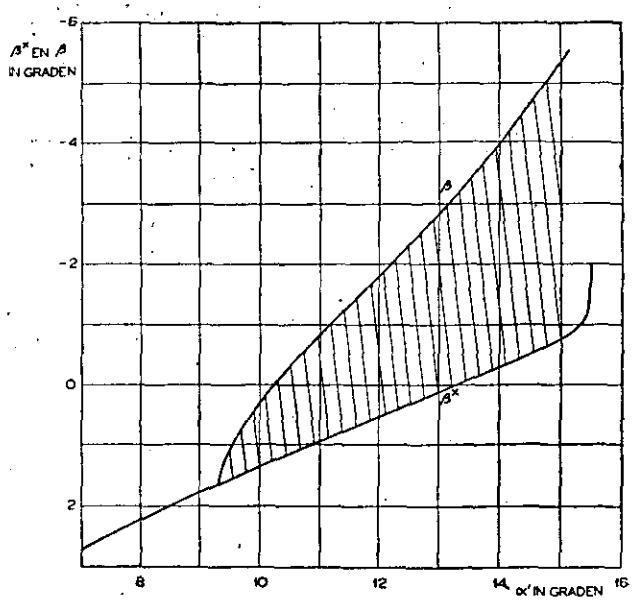

Fig. 12. De voor het afvangen benoodigde extra roeruitsla als functie van den invalshoek.

krijgt den indruk, dat de c_w-verhooging wel een zeer belangrijken invloed heeft.

De absolute grootte van den vereischten roerhoek voor het landen in de beschouwde gevallen, hangt mede af van de verplaatsing, die de stuurstandslijn ondergaat bij geopend zijn van de kleppen. Is deze verplaatsing zoodanig dat het vliegtuig bij openen van de klep koplastig wordt, dan wordt het verschil tusschen de totaal voor afvangen noodige roeruitslagen zonder en met klep grooter dan het verschil tusschen de extra-roeruitslagen in die gevallen; wordt het vliegtuig staartlastig dan wordt het verschil tusschen de absolute roeruitslagen kleiner dan het verschil tusschen de extra-roeruitslagen. In ieder geval volgt uit een en ander, dat de invloed van de verhooging van $c_{a_{max}}$ en c_w op de voor het landen vereischte roeruitslagen van dien aard is, dat hiermede bij het ontwerp van een vliegtuig rekening moet worden gehouden.

08 Eenige beschouwingen en conclusies.

De bovenbeschreven benaderingsmethode opent in de eerste plaats de mogelijkheid aan te geven, welke roeruitslag vereischt is om een bepaald vliegtuig van een te voren aan te geven stationnaire zweefvlucht uit, op normale wijze te landen.

De resulaten van de berekeningen onder **07** toonen, dat de vereischte roeruitslag grooter is naarmate de snelheid in de stationnaire zweefvlucht voorafgaande aan de landing, dus de „snelheid bij het binnenkomen" kleiner is.

Wil men dus voor een bepaald vliegtuigtype bij de meest voorlijke zwaartepuntsligging den maximaal benoodigden roeruitslag berekenen, of, bij een bekenden maximaal beschikbaren roeruitslag, de uiterst toelaatbare voorlijke zwaartepuntsligging, dan moet men een keuze doen omtrent de laagste waarde van de snelheid bij binnenkomen, waarmede nog juist een goede landing zal moeten kunnen worden uitgevoerd.

In het algemeen zal een snelheid bij binnenkomen van 1,2 à 1,3 maal de minimale snelheid (in stationnaire zweefvlucht bij den vliegtuigtoestand waarmede geland wordt) een normaal voorkomende waarde zijn. Voor belangrijk lagere waarden van de snelheid bij binnenkomen b.v. 1,1 v_{min} zal dikwijls een landing volgens het hier gekozen, als normaal te beschouwen, invalshoek- en baanhoekverloop niet meer mogelijk zijn. Voor het vaststellen van den bij een bepaald vliegtuigtype noodigen roeruitslag is het echter verstandig, in verband met het benaderende karakter van de berekeningsmethode en het ontbreken van voldoende ervaringsmateriaal, een reserve op den door berekening gevonden roerhoek te leggen.

Bovendien zal het gewenscht zijn een reserve in den beschikbaren roeruitslag te hebben met het oog op het uitvoeren van landingen van een vliegtoestand uit, die van den normalen stationnairen vliegtoestand afwijkt, zooals b.v. bij binnenkomen met lagere snelheid dan 1,2 maal de minimale.

Volgens de beschreven berekeningsmethode behoort verder bij iederen stationnairen begintoestand een bepaalde hoogte waarop met afvangen moet worden begonnen om op de in de berekeningsmethode aangenomen wijze te kunnen landen. Wordt nu bij een bepaalden stationnairen toestand te laat met afvangen begonnen, dan zal een landing met het ingevoerde baanhoek- en invalshoekverloop niet meer mogelijk zijn en zullen baanhoek en invalshoek sneller moeten veranderen dan bij afvangen op de juiste hoogte het geval zou zijn geweest. In vele gevallen zal dan met den voor een normale landing beschikbaren roeruitslag nog wel een wiellanding kunnen worden uitgevoerd.

Het zou naar aanleiding van het bovenstaande aanbeveling verdienen de hier beschreven berekeningen voor een aantal bekende vliegtuigtypen met bekende landingseigenschappen uit te voeren, teneinde de volgens deze methode berekende roeruitslagen te vergelijken met de inderdaad bij die vliegtuigen beschikbare roeruitslagen en daaruit de roerreserve te leeren kennen, die bij toepassing van de beschreven berekeningsmethode voor de praktijk gewenscht is.

Zoolang dergelijk ervaringsmateriaal nog niet ter beschikking staat, wordt aanbevolen bij gebruik van deze benaderingsmethode uit te gaan van een snelheid bij binnenkomen van 1,2 maal de minimale snelheid in stationnaire zweefvlucht bij den vliegtuigtoestand waarbij geland wordt en op de hiervoor berekende waarde van den extra-roeruitslag ($\beta - \beta^x$) een toeslag van ca. 25% te leggen. Mocht in zeer bijzondere gevallen blijken, dat een landing volgens het aangenomen baan- en invalshoekverloop bij een beginsnelheid van 1,2 v_{min} niet mogelijk is (complexe waarden van t_a voor

TABEL 7.

Geval	Omschrijving invloed klep (of andere inrichting) t.o.v. toestand zonder klepuitslag			Beginsnelheid in km/h	Vereischte extra-roeruitslag $\beta_g - \beta(\alpha_g)^x$ in graden
	$c_{a_{max}}$ verhooging	c_w verhooging bij $c_{a_{max}}$	α_{krit} verhooging		
I	geen klepuitslag			108	— 2,6
II	matig (0,3)	matig (0,05)	ca. 1°	96	— 3,8
III	geen	matig (0,05)	geen	108	— 5,3
IV	groot (0,6)	groot (0,11)	ca. 3°.	90	— 6,1

$0 > p >$ ca. -5) dan moet men de laagste beginsnelheid bepalen, waarvoor dit wel het geval is en hiervoor op de bovenbeschreven wijze den vereischten roeruitslag berekenen. Men dient dan echter in het oog te houden, dat in het optreden van complexe waarden mogelijk een aanwijzing schuilt, dat het vliegtuig onder de desbetreffende omstandigheden bij een snelheid bij binnenkomen van $1{,}2\ v_{min}$ reeds geen goede landing meer zal kunnen uitvoeren.

De beschreven methode geeft de mogelijkheid binnen zekere grenzen iedere willekeurige waarde van invalshoek (en dus ook standhoek) op het moment van landen in te voeren.

Wanneer de berekeningen op een vliegtuig met staartwielonderstel betrekking hebben, zal men voor het berekenen van de noodige roeruitslagen zonder meer een invalshoek aan den grond invoeren, die overeenkomt met den standhoek aan den grond en die dus slechts weinig verschilt van de kritische waarde, zoodat een goede driepuntslanding kan worden verwacht.

Voor het geval een vliegtuig met neuswiel wordt beschouwd, zou men de berekeningen kunnen uitvoeren voor een invalshoek aan den grond, welke ongeveer gelijk is aan den standhoek bij stilstaand vliegtuig, dus voor een wiellanding met groote landingssnelheid. Men zal echter ook wenschen, dat het vliegtuig geland kan worden met een zoo klein mogelijke landingssnelheid (staartlanding). Het zal daarom aanbeveling verdienen voor een neuswielvliegtuig de berekeningen toch uit te voeren voor een invalshoek aan den grond, die weinig verschilt van de kritische waarde; te meer daar in het algemeen de vereischte roeruitslagen voor de staartlanding grooter zullen zijn dan die voor de wiellanding.

De vraag kan nog rijzen, hoe het met de noodige roeruitslagen staat, wanneer niet in zweefvlucht, maar in motorvlucht wordt binnengekomen en de motoren worden afgezet op het oogenblik dat met afvangen wordt begonnen. Hierover kan het volgende gezegd worden. Wanneer men twee stationnaire vliegtoestanden beschouwt, waarbij de snelheid gelijk is, doch de eene in zweefvlucht, de andere in motorvlucht, dan zal de invalshoek in beide gevallen slechts weinig verschillen (enkele graden), de baanhoek echter in motorvlucht grooter zijn dan die in zweefvlucht. Zou men achtereenvolgens uitgaande van beide toestanden, een landing willen maken met denzelfden toestand aan het einde van de afvangmanoeuvre (b.v. driepuntslanding met dezelfde landingssnelheid), dan zal de standhoekverandering tijdens het afvangen in het geval van de motorvlucht kleiner zijn dan die in het geval van de zweefvlucht. De duur van de afvangperiode zal voor de twee gevallen, aangezien de snelheden gelijk zijn, weinig verschil vertoonen, zoodat de hoeksnelheden en -versnellingen in het geval van binnenkomen in motorvlucht kleiner zullen zijn dan bij binnenkomen in zweefvlucht. Men mag dus verwachten, dat de vereischte roeruitslagen in het geval van landing uit motorvlucht dan ook kleiner zullen zijn dan die bij landing uit zweefvlucht, zoodat dus, wanneer de roeruitslagen berekend worden voor het binnenkomen in zweefvlucht met de normale snelheid daarvoor, in het algemeen voldoende roeruitslag ter beschikking zal zijn om te landen, wanneer met werkende motoren wordt binnengekomen.

Ten slotte moet nog even de aandacht gevestigd worden op den eventueelen invloed van den wind. In de berekeningsmethode wordt geen rekening gehouden met een eventueele windsnelheid t.o.v. den grond. De baanhoek, die ingevoerd wordt, is dan ook alleen in het geval van windstilte de werkelijke baanhoek t.o.v. den grond. Wanneer een bepaalde constante windsterkte heerscht, geldt de geheele berekeningsmethode echter zonder meer, alleen moet dan onder den baanhoek φ niet verstaan worden de baanhoek t.o.v. den grond, maar de hoek t.o.v. de ongestoorde lucht. De berekeningsresultaten zijn echter allen onverminderd geldig; het afvangen zal zich alleen over een korteren horizontalen afstand afspelen. Slechts een tijdens het afvangen varieerende wind zal invloed hebben op de grootte van de noodige roeruitslagen; deze invloed zal echter in het algemeen klein zijn. Bovendien zal bij sterk varieerenden wind (zware remous) veelal met een grootere snelheid dan de normale worden binnengekomen en geland, zoodat daardoor de bij een bepaalden beschikbaren roeruitslag aanwezige roerreserve vanzelf wordt vergroot.

De berekeningen waarvan onder 07.2 een overzicht is gegeven en waarvan de resultaten onder 07.3 zijn samengevat leeren het volgende.

1° De voor het landen vereischte „extra"-roeruitslag bij een bepaalden vliegtuigtoestand (klepstand en zwaartepuntsligging) en dus ook de totaal vereischte roeruitslag, is grooter naarmate de snelheid in de stationnaire zweefvlucht, voorafgaande aan de landing, kleiner is.

2° Wanneer de stationnaire beginsnelheid kleiner is dan een bepaalde waarde, is het onmogelijk volgens de gegeven methode een voor een normale landing geschikt baanhoekverloop aan te geven, dat bij benadering aangepast is aan het aan deze berekeningsmethode ten grondslag gelegde invalshoekverloop. Daar dit invalshoekverloop vermoedelijk weinig van het bij een normale landing optredende invalshoekverloop zal afwijken, moet men in het genoemde geval verwachten, dat het dan ook in het algemeen niet meer mogelijk zal zijn bij een dergelijke waarde van de beginsnelheid een normale landing uit te voeren. Onder normale landing wordt hierbij verstaan, een landing waarbij op het oogenblik van aan den grond komen tegelijkertijd de invalshoek nagenoeg de kritische waarde heeft, de snelheid ongeveer gelijk is aan de minimale en de baan horizontaal is en waarbij tijdens het afvangen geen plotselinge standsveranderingen of stuurbewegingen plaats vinden.

3° Bij toepassing van landings- of remkleppen

zal de voor het landen vereischte extra-roeruitslag zoowel door de $c_{a_{max}}$- als door de c_w-verhooging beïnvloed worden en wel in het algemeen zoo, dat door de c_w-verhooging de vereischte extra-roeruitslag grooter wordt, en door de $c_{a_{max}}$-verhooging kleiner. Welke invloed zal overheerschen, hangt af van de aerodynamische eigenschappen van de klep. Bij de gebruikelijke typen van landingskleppen zal vermoedelijk steeds de invloed van de c_w-verhooging overheerschen en een grootere extra-roeruitslag noodig zijn voor het landen met klepuitslag dan voor het landen zonder klepuitslag. De invloed van de $c_{a_{max}}$- en c_w-verhooging t.g.v. landingskleppen e.d. is in ieder geval van dien aard, dat hiermede bij het ontwerp van een vliegtuig m.n. met het oog op de staartvlakken, rekening moet worden gehouden.

4° Beschouwing van de vergelijkingen voor de berekening van den duur van de afvangmanoeuvre t_a en voor den vereischten extra-roeruitslag $(\beta - \beta^x)$ leert nog het volgende. Beschouwt men twee vliegtuigen A en B met dezelfde uitwendige afmetingen en dezelfde aerodynamische eigenschappen, doch met verschillend gewicht, zoodanig dat het gewicht van B gelijk is aan n-maal het gewicht van A (dus ook n-maal zoo groote vleugelbelasting), dan is de duur van de afvangmanoeuvre voor B $\sqrt{n}$-maal die voor A (wanneer beide vliegtuigen geland worden van een stationnaire zweefvlucht uit met snelheid $1{,}2\, v_{min}$). De snelheid zal bij vliegtuig B $\sqrt{n}$-maal zoo groot zijn als bij A. De vereischte extra-roeruitslag $(\beta - \beta^x)$ ontstaat volgens (71) uit twee termen. De term, die afhankelijk is van $\dot{\Theta}$ en $\dot{\alpha}$ (invloed van de demping) zal voor het vliegtuig B $1/n$-maal zoo groot zijn als die voor vliegtuig A; de term, die afhankelijk is van $\ddot{\Theta}$ (invloed van de hoekversnelling) zal, wanneer wordt aangenomen, dat het traagheidsmoment om de dwarsas van B eveneens n-maal dat van A is, eveneens $1/n$-maal zoo groot zijn als die voor A. De totale vereischte extra-roeruitslag zal dus voor vliegtuig B bij benadering $1/n$-maal zoo groot zijn als voor vliegtuig A. Samenvattend volgt dus hieruit:

Wanneer bij gelijkblijvende uitwendige afmetingen en aerodynamische eigenschappen de vleugelbelasting n-maal zoo groot wordt gemaakt, zal de voor het landen vereischte extra-roeruitslag bij benadering $1/n$-maal zoo groot zijn.

Een bepaald vliegtuig zal dus, wanneer het licht beladen is, voor het uitvoeren van een normale landing een grooteren „extra" roeruitslag noodig hebben dan bij zware belading.

5° Het is noodzakelijk, teneinde de bruikbaarheid van de gegeven benaderingsmethode beter te onderzoeken, voor een aantal bekende vliegtuigtypen met bekende landingseigenschappen de voor het landen vereischte roeruitslagen voor verschillende vliegtuigtoestanden en stationnaire begintoestanden te berekenen.

Hieruit kan dan tevens een inzicht worden verkregen in de roerreserves die, bij toepassing van de gegeven methode, in de praktijk noodig zullen blijken.

6° Het is gewenscht, zoodra de omstandigheden dit toelaten, door middel van vliegproeven meer materiaal te verzamelen omtrent het werkelijk optredende invalshoek- en baanhoekverloop bij de landing, teneinde in de eerste plaats het aan deze methode ten grondslag gelegde verloop hiermede te vergelijken en in de tweede plaats een verdere studie van het landen, in het bijzonder met het oog op de eischen, die hieruit voor het ontwerp voortvloeien, mogelijk te maken.

Afgesloten Juli 1942.

Naschrift.

Ruim drie jaren na het afsluiten van dit rapport, doch vóór het ter perse gaan, kwam den schrijver *lit.* 3 in handen.

Hieruit blijkt in de eerste plaats dat de nabijheid van den grond een aanzienlijken invloed op c_a, c_w en c_m (met staartvlakken) uitoefent. Deze laatste invloed is voor het grootste deel afkomstig van de beïnvloeding van de neerstrooming door den grond.

Voor zoover het de twee eerstgenoemde grootheden betreft, wordt aangetoond, dat deze invloed met vrij goede benadering door eenige bestaande theorieën wordt weergegeven. Genoemd worden een theorie van Hutchinson (niet gepubliceerd) en *lit.* 4.

De invloed op c_m (met staartvlakken) echter kan, m.n. voor het geval van geopende kleppen nog niet voldoende door de theorie worden beschreven. De werkzaamheid van de staartvlakken wordt door de nabijheid van den grond niet verminderd, soms zelfs verbeterd.

Hieruit kan men t.a.v. de in het voorgaande gegeven berekeningsmethode het volgende concludeeren.

1° Het is in het algemeen noodzakelijk den invloed van den grond op c_a en c_w in rekening te brengen, waarvoor in dit rapport aanwijzingen zijn gegeven.

2° Het is noodzakelijk de stuurstandlijnen voor de stationnaire vlucht, welke bekend moeten zijn voor de berekening van de roeruitslagen voor het landen, te corrigeeren voor den invloed van den grond. Ook hiervoor zijn de mogelijkheden door de beschreven berekeningsmethode geopend. Gegevens over de grootte van den invloed kunnen voorloopig vermoedelijk alleen door windtunnelmetingen, zooals beschreven in R. and M. 1847, worden verkregen. Deze kunnen echter op eenvoudige wijze worden uitgevoerd.

3° De coëfficiënten c_1 en c_2 voor de staartvlakken ondergaan door de nabijheid van den grond geen veranderingen van beteekenis. De waarde van $\frac{d\varepsilon}{d\alpha}$ kan, aangezien zij toch een betrekkelijk kleine rol in de berekening van den roerhoek speelt, op grond van de resultaten van het beschreven modelonderzoek, nul gesteld worden. Het is echter mogelijk uit het onder 2° bedoelde modelonderzoek tevens een inzicht te krijgen in de waarden van $\frac{d\varepsilon}{d\alpha}$ wanneer het vliegtuig zich in de nabijheid van den grond bevindt.

09 Appendix.

Uitwerking van eenige in de berekening optredende bepaalde integralen.

Bij de uitwerking der benaderingsmethode onder 51 zijn een aantal bepaalde integralen, L_{γ_1}, M_{γ_1}, N_{γ_1} en O_{γ_1} naar voren gekomen, waarvan de nadere uitwerking hier wordt gegeven.

09.1 *Uitwerking van* L_{γ_1}.

$$L_{\gamma_1} = \int_0^{\gamma_1} \varphi(p,\gamma)\,d\gamma\,, \qquad (35)$$

Substitutie van (56) levert

$$L_{\gamma_1} = \varphi_0 \left\{ (p+3) \int_0^{\gamma_1} \gamma^4 d\gamma - (p+4) \int_0^{\gamma_1} \gamma^3 d\gamma + \gamma \Big|_0^{\gamma_1} \right\} =$$

$$= \varphi_0 \left[p \left(\frac{\gamma_1^5}{5} - \frac{\gamma_1^4}{4} \right) + \frac{3}{5}\gamma_1^5 - \gamma_1^4 + \gamma_1 \right].$$

Stelt men

$$L_{\gamma_1} = \varphi_0 [p f_1(\gamma_1) + f_2(\gamma_1)]\,, \qquad (61)$$

dan is

$$f_1(\gamma_1) = \frac{\gamma_1^5}{5} - \frac{\gamma_1^4}{4}$$

en

$$f_2(\gamma_1) = \frac{3\gamma_1^5}{5} - \gamma_1^4 + \gamma_1\,.$$

09.2 *Uitwerking van* M_{γ_1}.

$$M_{\gamma_1} = \int_0^{\gamma_1} \frac{d\gamma}{a(\gamma)}\,, \qquad (36)$$

Substitutie van (55) hierin levert

$$M_{\gamma_1} = \frac{z^6}{a_0} \int_0^{\gamma_1} \frac{d\gamma}{(\gamma^3+z^3)^2}.$$

Ter oplossing hiervan stelt men:

$$\frac{1}{(\gamma^3+z^3)^2} = \frac{A\gamma+B}{(\gamma+z)^2} + \frac{C\gamma^3+D\gamma^2+E\gamma+F}{(\gamma^2-z\gamma+z^2)^2}\,.$$

Oplossing van A t/m F levert

$$\frac{1}{(\gamma^3+z^3)^2} = \frac{\frac{2}{9z^5}\gamma + \frac{3}{9z^5}}{(\gamma+z)^2} + \frac{-\frac{2}{9z^3}\gamma^3 + \frac{5}{9z^4}\gamma^2 - \frac{8}{9z^3}\gamma + \frac{6}{9z^2}}{(\gamma^2-z\gamma+z^2)^2} =$$

$$= \frac{1}{9z^5}\left\{ \frac{2\gamma+3z}{(\gamma+z)^2} + \frac{-2\gamma+3z}{\gamma^2-z\gamma+z^2} + \frac{-3z^2\gamma+3z^3}{(\gamma^2-z\gamma+z^2)^2} \right\}.$$

Nu is

$$\int_0^{\gamma_1} \frac{d\gamma}{(\gamma^3+z^3)^2} = \frac{1}{9z^5}\left\{ \int_0^{\gamma_1} \frac{2\gamma+3z}{(\gamma+z)^2}\,d\gamma + \right.$$

$$+ \int_0^{\gamma_1} \frac{-2\gamma+3z}{\gamma^2-z\gamma+z^2}\,d\gamma + \int_0^{\gamma_1} \frac{-3z^2\gamma+3z^3}{(\gamma^2-z\gamma+z^2)^2}\,d\gamma =$$

$$= \frac{1}{9z^5}\left\{ ln(\gamma+z)^2 \Big|_0^{\gamma_1} - \frac{z}{\gamma+z}\Big|_0^{\gamma_1} - \right.$$

$$- ln(\gamma^2-z\gamma+z^2)\Big|_0^{\gamma_1} + \frac{4}{3}\sqrt{3}\; bg\; tg\; \frac{2\gamma-z}{z\sqrt{3}}\Big|_0^{\gamma_1} +$$

$$\left. + \int_0^{\gamma_1} \frac{-3z^2\gamma+3z^3}{(\gamma^2-z\gamma+z^2)^2}\,d\gamma \right\}.$$

Voor deze laatste integraal kan men stellen [1])

$$\int_0^{\gamma_1} \frac{-3z^2\gamma+3z^3}{(\gamma^2-z\gamma+z^2)^2}\,d\gamma = \frac{Q}{\gamma^2-z\gamma+z^2}\Big|_0^{\gamma_1} + \int_0^{\gamma_1} \frac{R\,d\gamma}{\gamma^2-z\gamma+z^2}\,.$$

Men verkrijgt dan $Q = z\gamma + z^2$ en $R = z$, zodat

$$\int_0^{\gamma_1} \frac{-3z^2\gamma+3z^3}{(\gamma^2-z\gamma+z^2)^2}\,d\gamma = \frac{z\gamma+z^2}{\gamma^2-z\gamma+z^2}\Big|_0^{\gamma_1} + z\int_0^{\gamma_1} \frac{d\gamma}{\gamma^2-z\gamma+z^2}\,.$$

of

$$\int_0^{\gamma_1} \frac{-3z^2\gamma+3z^3}{(\gamma^2-z\gamma+z^2)^2}\,d\gamma = \frac{z\gamma+z^2}{\gamma^2-z\gamma+z^2}\Big|_0^{\gamma_1} + \frac{2}{3}\sqrt{3}\; bg\; tg\; \frac{2\gamma-z}{z\sqrt{3}}\Big|_0^{\gamma_1}\,.$$

Derhalve is

$$\int_0^{\gamma_1} \frac{d\gamma}{(\gamma^3+z^3)^2} = \frac{1}{9z^5}\left\{ ln(\gamma+z)^2\Big|_0^{\gamma_1} - \frac{z}{\gamma+z}\Big|_0^{\gamma_1} - \right.$$

$$- ln(\gamma^2-z\gamma+z^2)\Big|_0^{\gamma_1} + \frac{z\gamma+z^2}{\gamma^2-z\gamma+z^2}\Big|_0^{\gamma_1} +$$

$$\left. + 2\sqrt{3}\; bg\; tg\; \frac{2\gamma-z}{z\sqrt{3}}\Big|_0^{\gamma_1} \right\}.$$

zoodat

$$M_{\gamma_1} = \frac{1}{9a_0} f_3(z,\gamma_1)\,, \qquad (62)$$

waarin

$$f_3(z,\gamma_1) = z\left\{ -1 + \frac{\gamma_1}{\gamma_1+z} + \frac{z\gamma_1+z^2}{\gamma_1^2-z\gamma_1+z^2} + \right.$$

$$+ ln\frac{\gamma_1^2+2z\gamma_1+z^2}{\gamma_1^2-z\gamma_1+z^2} +$$

$$\left. + 2\sqrt{3}\left(bg\; tg\; \frac{2\gamma_1-z}{z\sqrt{3}} - bg\; tg\; \frac{-1}{\sqrt{3}} \right) \right\}.$$

[1]) Zie Czuber: Vorlesungen über Differential- und Integralrechnung. Teil II, blz. 47 e.v.

09.3 *Uitwerking van* N_{γ_1}.

$$N_{\gamma_1}=\int_0^{\gamma_1}\frac{d\varphi(p,\gamma)}{d\gamma}\frac{d\gamma}{\sqrt{a(\gamma)}}.$$

Substitutie van (55) en (59) levert

$$N_{\gamma_1}=\frac{\varphi_0}{\sqrt{a_0}}z^3\int_0^{\gamma_1}\frac{4(p+3)\gamma^3-3(p+4)\gamma^2}{\gamma^3+z^3}d\gamma.$$

Stelt men $a=4(p+3)$ en $b=-3(p+4)$, dan is

$$\int_0^{\gamma_1}\frac{4(p+3)\gamma^3-3(p+4)\gamma^2}{\gamma^3+z^3}d\gamma=a\int_0^{\gamma_1}d\gamma+$$

$$+\int_0^{\gamma_1}\frac{b\gamma^2-az^3}{\gamma^3+z^3}d\gamma=a\gamma_1+\int_0^{\gamma_1}\frac{b\gamma^2-az^3}{\gamma^3+z^3}d\gamma=$$

$$=a\gamma_1+\frac{b}{3}ln(\gamma^3+z^3)\Big|_0^{\gamma_1}-az^3\int_0^{\gamma_1}\frac{d\gamma}{\gamma^3+z^3}=$$

$$=a\gamma_1+\frac{b}{3}ln\frac{\gamma_1^3+z^3}{z^3}-\frac{a}{3}z\int_0^{\gamma_1}\frac{d\gamma}{\gamma+z}+$$

$$+\frac{a}{3}z\int_0^{\gamma_1}\frac{\gamma-2z}{\gamma^2-z\gamma+z^2}d\gamma=$$

$$=a\gamma_1+\frac{b}{3}ln\frac{\gamma_1^3+z^3}{z^3}-\frac{a}{3}zln\frac{\gamma_1+z}{z}+$$

$$+\frac{a}{b}ln\frac{\gamma_1^2-z\gamma+z^2}{z^2}-$$

$$-\frac{a}{3}z\sqrt{3}\left(bg\,tg\frac{2\gamma_1-z}{z\sqrt{3}}-bg\,tg\frac{-1}{\sqrt{3}}\right).$$

Substitutie van a en b hierin levert ten slotte

$$N_{\gamma_1}=\frac{\varphi_0\sqrt{a_0}}{a_0}z^3\Big[4(p+3)\gamma_1-$$

$$-\left\{\left(\frac{4}{3}z+1\right)p+4z+4\right\}ln\frac{\gamma_1+z}{z}+$$

$$+\left\{\left(\frac{2}{3}z-1\right)p+2z-4\right\}ln\frac{\gamma_1^2-z\gamma_1+z^2}{z^2}-$$

$$-\left(\frac{4}{3}\sqrt{3}\,zp+4\sqrt{3}\,z\right)\left(bg\,tg\frac{2\gamma_1-z}{z\sqrt{3}}-bg\,tg\frac{-1}{\sqrt{3}}\right)\Big].$$

Schrijft men

$$N_{\gamma_1}=\frac{\varphi_0\sqrt{a_0}}{a_0}[pf_4(z,\gamma_1)+f_5(z,\gamma_1)],\quad(63)$$

dan is

$$f_4(z,\gamma_1)=z^3\Big[4\gamma_1-\left(\frac{4}{3}z+1\right)ln\frac{\gamma_1+z}{z}+$$

$$+\left(\frac{2}{3}z-1\right)ln\frac{\gamma_1^2-z\gamma_1+z^2}{z^2}-$$

$$-\frac{4}{3}\sqrt{3}\,z\left(bg\,tg\frac{2\gamma_1-z}{z\sqrt{3}}-bg\,tg\frac{-1}{\sqrt{3}}\right)\Big]$$

en

$$f_5(z,\gamma_1)=z^3\Big[12\gamma_1-4(z+1)ln\frac{\gamma_1+z}{z}+$$

$$+2(z-2)ln\frac{\gamma_1^2-z\gamma_1+z^2}{z^2}-$$

$$-4\sqrt{3}\,z\left(bg\,tg\frac{2\gamma_1-z}{z\sqrt{3}}-bg\,tg\frac{-1}{\sqrt{3}}\right)\Big].$$

09.4 *Uitwerking van* O_{γ_1}.

Volgens (38) is

$$O_{\gamma_1}=\int_0^{\gamma_1}\frac{d\varphi(\gamma,p)}{d\gamma}\frac{d\gamma}{a(\gamma)\sqrt{a(\gamma)}}.\quad(38)$$

Substitutie van (55) en (59) hierin levert

$$O_{\gamma_1}=\frac{\varphi_0\sqrt{a_0}}{a_0^2}z^9\int_0^{\gamma_1}\frac{4(p+3)\gamma^3-3(p+4)\gamma^2}{(\gamma^3+z^3)^3}d\gamma=$$

$$=\frac{\varphi_0\sqrt{a_0}}{a_0^2}z^9\left[\int_0^{\gamma_1}\frac{-3(p+4)\gamma^2}{(\gamma^3+z^3)^3}d\gamma+\right.$$

$$\left.+\int_0^{\gamma_1}\frac{4(p+3)\gamma^3}{(\gamma^3+z^3)^3}d\gamma\right]=$$

$$=\frac{\varphi_0\sqrt{a_0}}{a_0^2}z^9\left[-(p+4)\int_0^{\gamma_1}\frac{3\gamma^2}{(\gamma^3+z^3)^3}d\gamma+\right.$$

$$\left.+4(p+3)\int_0^{\gamma_1}\frac{\gamma^3}{(\gamma^3+z^3)^3}d\gamma\right]=$$

$$=\frac{\varphi_0\sqrt{a_0}}{a_0^2}z^9\left[\frac{p+4}{2}(\gamma^3+z^3)^{-2}\Big|_0^{\gamma_1}+\right.$$

$$\left.+4(p+3)\int_0^{\gamma_1}\frac{d\gamma}{(\gamma^3+z^3)^3}-4(p+3)z^3\int_0^{\gamma_1}\frac{d\gamma}{(\gamma^3+z^3)^3}\right]=$$

$$=\frac{\varphi_0\sqrt{a_0}}{a_0^2}z^9\left[-\frac{p+4}{2}\frac{\gamma_1^3(\gamma_1^3+2z^3)}{z^6(\gamma_1^3+z^3)^2}+\right.$$

$$\left.+\frac{4(p+3)}{9z^6}f_3(z,\gamma_1)-4(p+3)z^3\int_0^{\gamma_1}\frac{d\gamma}{(\gamma^3+z^3)^3}\right].$$

Laatstgenoemde integraal kan als volgt berekend worden.

Stel $\frac{1}{(\gamma^3+z^3)^3}=\frac{A\gamma^2+B\gamma+C}{(\gamma+z)^3}+$

$$+\frac{D\gamma^5+E\gamma^4+F\gamma^3+G\gamma^2+H\gamma+I}{(\gamma^2-z\gamma+z^2)^3}.$$

Men verkrijgt dan na oplossing van A t/m I

$$\frac{1}{(\gamma^3+z^3)^3}=\frac{1}{27z^9}\left\{\frac{5\gamma^2+13z\gamma+9z^2}{(\gamma+z)^3}+\right.$$

$$\left.+\frac{-5\gamma^5+17z\gamma^4-36z^2\gamma^3+46z^3\gamma^2-40z^4\gamma+18z^5}{(\gamma^2-z\gamma+z^2)^3}\right\}.$$

Nu is

$$\frac{5\gamma^2+13z\gamma+9z^2}{(\gamma+z)^3}=\frac{5}{\gamma+z}+\frac{3z}{(\gamma+z)^2}+\frac{z^2}{(\gamma+z)^3},$$

dus is

$$\int_0^{\gamma_1}\frac{d\gamma}{(\gamma^3+z^3)^3}=$$

$$=\frac{1}{27z^9}\left[5ln\frac{\gamma_1+z}{z}+\frac{3\gamma_1}{\gamma_1+z}+\frac{\gamma_1(\gamma_1+2z)}{2(\gamma_1+z)^2}+\right.$$

$$\left.+\int_0^{\gamma_1}\frac{-5\gamma^5+17z\gamma^4-36z^2\gamma^3+46z^3\gamma^2-40z^4\gamma+18z^5}{(\gamma^2-z\gamma+z^2)^3}d\gamma\right];$$

Ter oplossing van deze laatste integraal stelt men weer [1])

$$I=\int_0^{\gamma_1}\frac{-5\gamma^5+17z\gamma^4-36z^2\gamma^3+46z^3\gamma^2-40z^4\gamma+18z^5}{(\gamma^2-z\gamma+z^2)^3}d\gamma=$$

$$=\frac{Q}{(\gamma^2-z\gamma+z^2)^2}\Big|_0^{\gamma_1}+\int_0^{\gamma_1}\frac{R}{\gamma^3-z\gamma+z^2}d\gamma.$$

Dit leidt tot:

$$Q=3z\gamma^3-z^2\gamma^2+z^3\gamma+\frac{7}{2}z^4 \text{ en } R=-5\gamma+10z,$$

zoodat

$$I=\frac{6z\gamma_1^3-2z^2\gamma_1^2+2z^3\gamma_1+7z^4}{2(\gamma_1^2-z\gamma_1+z^2)^2}-$$

$$-\frac{7}{2}-\frac{5}{2}ln\frac{\gamma_1^2-z\gamma_1+z^2}{z^2}+\frac{15z}{2}\int_0^{\gamma_1}\frac{d\gamma}{\gamma^2-z\gamma+z^2}.$$

Nu is

$$\frac{15z}{2}\int_0^{\gamma_1}\frac{d\gamma}{\gamma^2-z\gamma+z^2}=$$

$$=5\sqrt{3}\left(bg\,tg\frac{2\gamma_1-z}{z\sqrt{3}}-bg\,tg\frac{-1}{\sqrt{3}}\right),$$

zoodat

$$\int_0^{\gamma_1}\frac{d\gamma}{(\gamma^3+z^3)^3}=\frac{1}{27z^8}\Big[5ln\frac{\gamma_1+z}{z}+\frac{3\gamma_1}{\gamma_1+z}+$$

$$+\frac{\gamma_1(\gamma_1+2z)}{2(\gamma_1+z)^2}+\frac{6z\gamma_1^3-2z^2\gamma_1^2+2z^3\gamma_1+7z^4}{2(\gamma_1^2-z\gamma_1+z^2)^2}-$$

$$-\frac{7}{2}-\frac{5}{2}ln\frac{\gamma_1^2-z\gamma_1+z^2}{z^2}+$$

$$+5\sqrt{3}\left(bg\,tg\frac{2\gamma_1-z}{z\sqrt{3}}-bg\,tg\frac{-1}{\sqrt{3}}\right)\Big].$$

Men verkrijgt dus

$$O_{\gamma_1}=\frac{\varphi_0\sqrt{a_0}}{a_0^2}z^3\Big[-\frac{p+4}{2}\frac{\gamma_1^3(\gamma_1^3+2z^3)}{(\gamma_1^3+z^3)^2}+$$

$$+\frac{4(p+3)}{9}f_3(z,\gamma_1)-\frac{4(p+3)}{27}z\Big\{-\frac{7}{2}+\frac{3\gamma_1}{\gamma_1+z}+$$

$$+\frac{\gamma_1(\gamma_1+2z)}{2(\gamma_1+z)^2}+\frac{6z\gamma_1^3-2z^2\gamma_1^2+2z^3\gamma_1+7z^4}{2(\gamma_1^2-z\gamma_1+z^2)^2}+$$

$$+5ln\frac{\gamma_1+z}{z}-\frac{5}{2}ln\frac{\gamma_1^2-z\gamma_1+z^2}{z^2}+$$

$$+5\sqrt{3}\left(bg\,tg\frac{2\gamma_1-z}{z\sqrt{3}}-bg\,tg\frac{-1}{\sqrt{3}}\right)\Big\}\Big].$$

Schrijft men

$$O_{\gamma_1}=\frac{\varphi_0}{a_0^2}\sqrt{a_0}\,[pf_6(z,\gamma_1)+f_7(z,\gamma_1)], \quad (64)$$

dan ontstaat

$$f_6(z,\gamma_1)=z^3\Big[-\frac{\gamma_1^3(\gamma_1^3+2z^3)}{2(\gamma_1^3+z^3)^2}+$$

$$+\frac{4}{9}f_3(z,\gamma_1)-\frac{4}{27}z\Big\{-\frac{7}{2}+\frac{3\gamma_1}{\gamma_1+z}+$$

$$+\frac{\gamma_1(\gamma_1+2z)}{2(\gamma_1+z)^2}+\frac{6z\gamma_1^3-2z^2\gamma_1^2+2z^3\gamma_1+7z^4}{2(\gamma_1^2-z\gamma_1+z^2)^2}+$$

$$+5ln\frac{\gamma_1+z}{z}-\frac{5}{2}ln\frac{\gamma_1^2-z\gamma_1+z^2}{z^2}+$$

$$+5\sqrt{3}\left(bg\,tg\frac{2\gamma_1-z}{z\sqrt{3}}-bg\,tg\frac{-1}{\sqrt{3}}\right)\Big\}\Big)$$

en

$$f_7(z,\gamma_1)=z^3\Big[-\frac{2\gamma_1^3(\gamma_1^3+2z^3)}{(\gamma_1^3+z^3)^2}+\frac{4}{3}f_3(z,\gamma_1)-$$

$$-\frac{4}{9}z\Big\{-\frac{7}{2}+\frac{3\gamma_1}{\gamma_1+z}+\frac{\gamma_1(\gamma_1+2z)}{2(\gamma_1+z)^2}+$$

$$+\frac{6z\gamma_1^3-2z^2\gamma_1^2+2z^3\gamma_1+7z^4}{2(\gamma_1^2-z\gamma_1+z^2)^2}+$$

$$+5ln\frac{\gamma_1+z}{z}-\frac{5}{2}ln\frac{\gamma_1^2-z\gamma_1+z^2}{z^2}+$$

$$+5\sqrt{3}\left(bg\,tg\frac{2\gamma_1-z}{z\sqrt{3}}-bg\,tg\frac{-1}{\sqrt{3}}\right)\Big\}\Big].$$

09.5 *Uitwerking van* P_{γ_1}.

Volgens (70a) is

$$P_{\gamma_1}=\int_{\gamma_1}^1\varphi(\gamma,p)\frac{d\gamma}{\sqrt{a(\gamma)}}.$$

Substitutie van (55) en (56) levert

$$P_{\gamma_1}=\frac{\varphi_0\sqrt{a_0}}{a_0}z^3\int_{\gamma_1}^1\frac{(p+3)\gamma^4-(p+4)\gamma^3+1}{\gamma^3+z^3}d\gamma=$$

$$=\frac{\varphi_0\sqrt{a_0}}{a_0}z^3\Big[\int_{\gamma_1}^1\{(p+3)\gamma-(p+4)\}d\gamma+$$

$$+\int_{\gamma_1}^1\frac{-(p+3)z^3\gamma+(p+4)z^3+1}{\gamma^3+z^3}d\gamma\Big]=$$

$$=\frac{\varphi_0\sqrt{a_0}}{a_0}z^3\Big\{\frac{p+3}{2}(1-\gamma_1^2)-(p+4)(1-\gamma_1)+I\Big\}.$$

$$I=\int_{\gamma_1}^1\frac{A}{\gamma+z}d\gamma+\int_{\gamma_1}^1\frac{B\gamma+C}{\gamma^2-z\gamma+z^2}d\gamma.$$

Daaruit volgt

$$A=\frac{1}{3}\Big\{(p+3)z^2+(p+4)z+\frac{1}{z^2}\Big\},$$

$$B=-\frac{1}{3}\Big\{(p+3)z^2+(p+4)z+\frac{1}{z^2}\Big\} \text{ en}$$

$$C=-\frac{1}{3}\Big\{(p+3)z^3-2(p+4)z^2-\frac{2}{z}\Big\},$$

zoodat

$$I=\frac{1}{3}\Big\{(p+3)z^2+(p+4)z+\frac{1}{z^2}\Big\}ln\frac{z+1}{\gamma_1+z}-$$

$$-\frac{1}{6}\Big\{(p+3)z^2+(p+4)z+\frac{1}{z^2}\Big\}\int_{\gamma_1}^1\frac{(2\gamma-z)d\gamma}{\gamma^2-z\gamma+z^2}-$$

$$-\Big[\frac{1}{6}\Big\{(p+3)z^3+(p+4)z^2+\frac{1}{z}\Big\}+$$

$$+\frac{1}{3}\Big\{(p+3)z^3-2(p+4)z^2-\frac{2}{z}\Big\}\Big]\int_{\gamma_1}^1\frac{d\gamma}{\gamma^2-z\gamma+z^2}$$

[1]) Zie noot onder 09.2.

$$I=\left(\frac{p+3}{3}z^2+\frac{p+4}{3}z+\frac{1}{3z^2}\right)ln\frac{z+1}{\gamma_1+z}-$$
$$-\left(\frac{p+3}{6}z^2+\frac{p+4}{6}z+\frac{1}{6z^2}\right)ln\frac{z^2-z+1}{\gamma_1^2-z\gamma_1+z^2}-$$
$$-\left(\frac{p+3}{2}z^2-\frac{p+4}{2}z-\frac{1}{2z^2}\right)\frac{2\sqrt{3}}{3}\left(bg\ tg\frac{2-z}{z\sqrt{3}}-\right.$$
$$\left.-bg\ tg\frac{2\gamma_1-z}{z\sqrt{3}}\right).$$

Dus is

$$p_{\gamma_1}=\frac{\varphi_0\sqrt{a_0}}{a_0}z^3\left\{\frac{p+3}{2}(1-\gamma_1^2)-(p+4)(1-\gamma_1)+\right.$$
$$+\left(\frac{p+3}{6}z^2+\frac{p+4}{6}z+\frac{1}{6z^2}\right)\left(2ln\frac{z+1}{\gamma_1+z}-\right.$$
$$\left.-ln\frac{z^2-z+1}{\gamma_1^2-z\gamma_1+z^2}\right)-\frac{2\sqrt{3}}{3}\left(\frac{p+3}{2}z^2-\frac{p+4}{2}z-\right.$$
$$\left.\left.-\frac{1}{2z^2}\right)\left(bg\ tg\frac{2-z}{z\sqrt{3}}-bg\ tg\frac{2\gamma_1-z}{z\sqrt{3}}\right)\right\}.$$

Schrijft men weer

$$p_{\gamma_1}=\frac{\varphi_0\sqrt{a_0}}{a_0}[pf_{11}(z,\gamma_1)+f_{12}(z,\gamma_1)],$$

dan ontstaat

$$f_{11}(z,\gamma_1)=z^3\left\{\frac{1-\gamma_1^2}{2}-(1-\gamma_1)+\right.$$
$$+\frac{1}{6}(z^2+z)\left(2ln\frac{z+1}{\gamma_1+z}-ln\frac{z^2-z+1}{\gamma_1^2-z\gamma_1+z^2}-\right.$$
$$\left.\left.-\frac{2\sqrt{3}}{6}(z^2-z)\left(bg\ tg\frac{2-z}{z\sqrt{3}}-bg\ tg\frac{2\gamma_1-z}{z\sqrt{3}}\right)\right\}\right.$$

en

$$f_{12}(z,\gamma_1)=z^3\left\{\frac{3(1-\gamma_1^2)}{2}-4(1-\gamma_1)+\right.$$
$$+\frac{1}{6}\left(3z^2+4z+\frac{1}{z^2}\right)\left(2ln\frac{z+1}{\gamma_1+z}-ln\frac{z^2-z+1}{\gamma_1^2-z\gamma_1+z^2}-\right.$$
$$\left.-\frac{2\sqrt{3}}{6}\left(3z^2-4z-\frac{1}{z^2}\right)\left(bg\ tg\frac{2-z}{z\sqrt{3}}-\right.\right.$$
$$\left.\left.\left.-bg\ tg\frac{2\gamma_1-z}{z\sqrt{3}}\right)\right\}\right.$$

09.6 *Berekening van de functies f_1 t/m f_{12}.*

De functies f_1 t/m f_7 en f_{11} en f_{12} zijn voor verschillende getallenwaarden van z en γ_1 berekend; deze berekeningen zijn wegens den omvang niet in dit rapport opgenomen, zij liggen echter bij het N.L.L. ter inzage. Bovendien zijn de functies f_8, f_9 en f_{10} (zie (67) en (68)) berekend.

De resultaten zijn weergegeven in de figuren 13 t/m 15 en wel:

de functies f_1 en f_2 (constanten) voor de waarden $\gamma=1$ en 0,5,

de functies f_3 t/m f_{10} voor de waarden $\gamma=1$ en $\gamma=0{,}5$ en voor een aantal z-waarden tusschen 1,2 en 2,5,

de functies f_{11} en f_{12} voor de waarden $\gamma=0$, 0,4 en 0,7 en voor z-waarden tusschen 1,2 en 2,5.

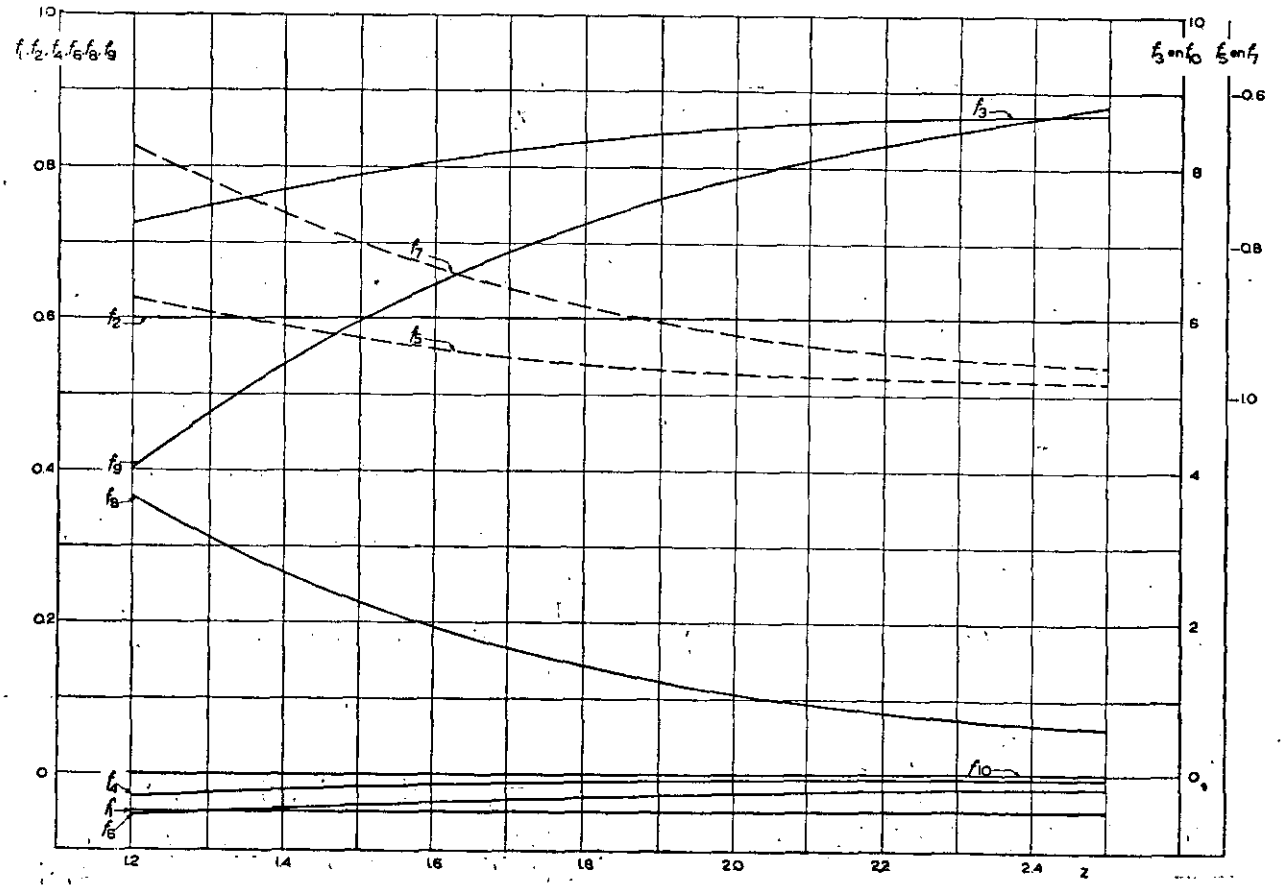

Fig. 13. De functies $f_1(z)$ t/m $f_{10}(z)$ voor $\gamma=1$.

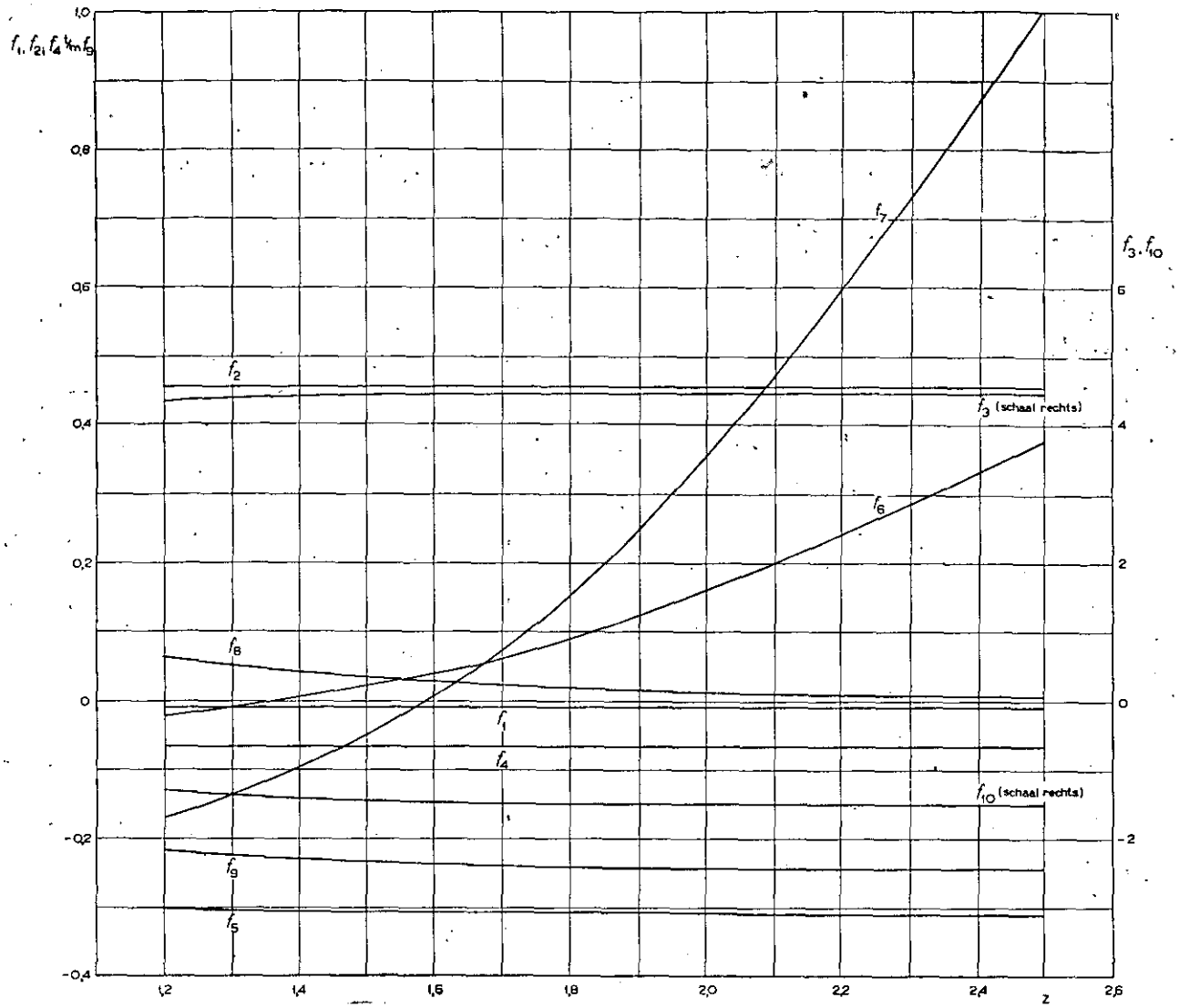

Fig. 14. De functies $f_1(z)$ t/m $f_{10}(\ )$ voor $\gamma = 0.5$.

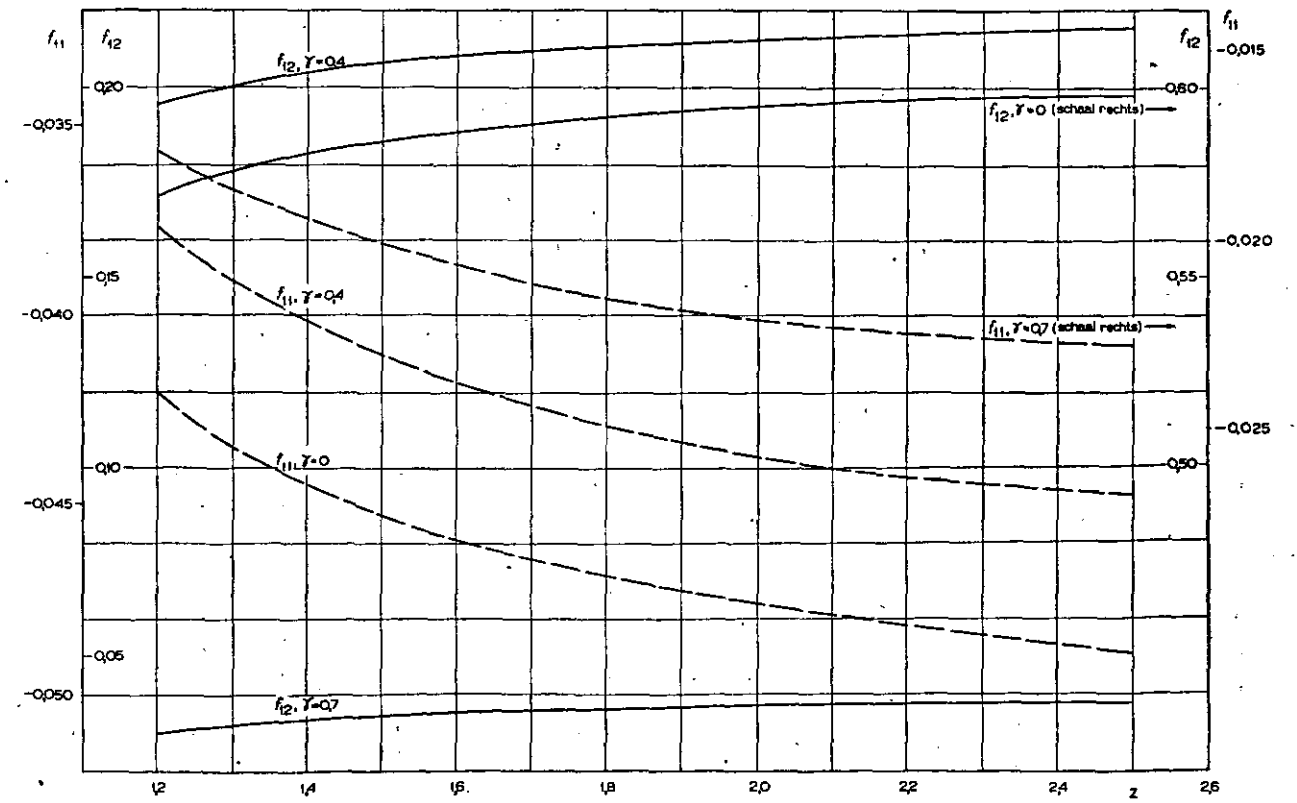

Fig. 15. De functies van $f_{11}(z)$ en $f_{12}(z)$ voor verschillende waarden van γ.

Bovengenoemde grafieken bieden de mogelijkheid de in dit rapport beschreven berekeningen aanmerkelijk te vereenvoudigen.

10. Notaties.

Symbolen.

B = traagheidsmoment om de dwarsas.

$c_1 = \frac{\partial c_n}{\partial \alpha_h}$.

$c_2 = \frac{\partial c_n}{\partial \beta}$.

c_a = draagkrachtcoëfficiënt.

$c_a' = \frac{d c_a}{d \alpha}$ van het door een lineaire functie benaderde verband $c_a - \alpha$ in het voor de landing in aanmerking komende gebied van invalshoeken (zie fig. 2).

c_m = momentencoëfficiënt van het vliegtuig zonder staartvlakken.

c_n = normaalkrachtcoëfficiënt van de horizontale staartvlakken.

c_w = weerstandscoëfficiënt.

$c_w' = \frac{d c_w}{d \alpha}$ van het door een lineaire functie benaderde verband $c_w - \alpha$ in het voor de landing in aanmerking komende gebied van invalshoeken (zie fig. 2).

c_{w_a} = door interpolatie van het lineaire verband $c_w - \alpha$ bepaalde waarde van c_w bij den invalshoek, waarbij de, door extra-polatie van het lineaire verband $c_a - \alpha$ bepaalde, waarde van c_a gelijk is aan 0 (zie fig. 2).

f = oppervlak horizontale staartvlakken.

F = vleugeloppervlak.

g = versnelling van de zwaartekracht.

G = totaalgewicht van het vliegtuig.

h = de hoogte van het vliegtuig boven den grond tijdens de afvangmanoeuvre.

k_β = hoogteroercoëfficiënt, zie onder 07.1.

l = afstand drukpunt horizontale staartvlakken tot zwaartepunt vliegtuig.

M = totaal moment van de luchtkrachten om de dwarsas.

M_{ds} = dempend moment van de staartvlakken bij rotatie om de dwarsas.

M_h = moment om de dwarsas van de luchtkrachten op de staartvlakken.

M_v = moment om de dwarsas van de luchtkrachten op het vliegtuig zonder staartvlakken.

M_{vs} = dempend moment van vleugel en romp bij rotatie om de dwarsas.

p = een parameter in het verband $\varphi - \gamma$.

t = tijd.

t_a = totale tijd voor het uitvoeren van de afvangmanoeuvre.

t_v = vleugelkoorde (grootste of gemiddelde).

v = snelheid van de ongestoorde lucht t.o.v. het vliegtuig.

v_h = snelheid van de gestoorde strooming t.p.v. de staartvlakken t.o.v. de staartvlakken.

x = afstand van het zwaartepunt tot den neus van de grootste of de gemiddelde vleugelkoorde.

Δx = verplaatsing van het zwaartepunt.

$z = \sqrt[3]{\frac{\sqrt{\alpha_0}}{\sqrt{\alpha_g} - \sqrt{\alpha_0}}}$ (zie ook onder „Indices").

α = invalshoek betrokken op de, door extrapolatie van het lineaire verband $c_a - \alpha$ bepaalde, draagkracht-nullijn (zie fig. 1).

α' = invalshoek betrokken op de vleugelkoorde.

$\bar{\alpha}$ = hoek tusschen draagkracht-nullijn en vleugelkoorde (zie fig. 1).

α_h = invalshoek van de strooming t.p.v. de horizontale staartvlakken.

β = hoek van het hoogteroer t.o.v. het stabilo.

β^x = hoek van het hoogteroer t.o.v. het stabilo in stationnaire zweefvlucht.

$\gamma = \frac{t}{t_a}$.

γ_1 = een bepaalde waarde van γ, overeenkomende met den tijd $t = t_1$.

δ = uitslag van de landingsklep, gemeten t.o.v. den stand bij ingetrokken klep.

ε = neerstroomingshoek.

$\eta = \frac{v_h}{v}$.

Θ = standhoek (betrokken op vleugelkoorde (zie fig. 1).

$\varkappa = 1 - \frac{d \varepsilon}{d \alpha}$, neerstroomfactor.

$\mu = \varrho g \frac{F}{G}$.

ϱ = luchtdichtheid.

σ = instelhoek van het stabilo, betrokken op de vleugelkoorde.

φ = baanhoek (t.o.v. de ongestoorde lucht).

Indices.

Indices a en b duiden aan, dat de grootheid betrekking heeft op de zwaartepuntsligging vastgelegd door x_a resp. x_b.

Index g duidt aan de waarde van de grootheid op het tijdstip $t = t_a$, dus op het oogenblik van aan den grond komen (zie fig. 3).

Index ^{x} duidt aan, dat bedoeld wordt de waarde van de grootheid in stationnaire vlucht bij dezelfde waarde van α als in de niet-stationnaire vlucht.

Index γ_1 duidt aan de waarde van de grootheid op het tijdstip $t_1 = \gamma_1 t_a$.

Index 0 duidt aan de waarde van de grootheid ten tijde $t = 0$, dus bij het begin van de afvangmanoeuvre (zie fig. 3).

11 Literatuuropgave.

1. Durand, W. F. Aerodynamic Theory IV en V, Springer, Berlijn, 1935.
2. Silverstein, A. en Katzoff, S. Design charts for predicting downwash angles and wake characteristics. N.A.C.A.-report No 648, 1939.
3. Ower, E. Warden, R. and Brown, W. S. An investigation of ground effect with a model of a mid-wing monoplane. Rep. and Mem. No 1847, 1938.
4. Tani, Itokawa Tarina and Simudu. The effect of ground on the aerodynamic characteristics of a monoplane wing. Reports of the Aeronautical Research Institute, Tokyo Imperial University, No 156 en No 158, 1937.
5. Miller, M. P. en Soulé, H. A. Moments of inertia of several airplanes, N.A.C.A. Tech-nical Note No 375, 1931.

REPORT V. 1286.

An approximative method for the determination of the elevator deflections required for landing an aeroplane and of the extreme forward position of the centre of gravity, which is admissible in view of the landing characteristics.

Summary.

It is presumed that the landing is made from a steady glide. The aerodynamic data on which the calculations have to be based are the curves of lift and drag against angle of incidence in the landing condition (flaps open, undercarriage extended, airscrews idling), the curve of elevator deflection against angle of incidence in steady flight for at least one position of the c.g., curves of lift-coefficient of the tail surfaces against angle of incidence at the tail and elevator deflection. Furthermore the weight, wing area, horizontal tail area, tail length, moment of inertia about the lateral axis, *etc. have to be known.*

Methods for the determination of the ground influence on lift, drag, downwash and pitching moment in steady conditions, either theoretical or experimental, are supposed to be known so that the abovementioned aerodynamic characteristics can be reduced in view of the ground effect, which is gradually becoming of importance while the landing manoeuvre is proceeding. The way in which this effect can be taken into account is explained in the report.

Under 02.1 the equations of motion are given by (1), (2) and (3) ,the last one, describing the *motions around the c.g., is elaborated further into* (16).

The damping provided by all parts of the airplane is supposed to be 1,2 times the damping provided by the horizontal tail surfaces alone. Furthermore the symbol β^x in this equation represents the elevator deflection necessary for equilibrium if the flight at each moment during the landing manoeuvre might be considered to be steady. As stated before these deflections are supposed to be known.

In 02.2 the equations for the motion of the c.g. (1) and (2) are reduced to formulae given by *(26) and (27). This is done by assuming that the* curves of lift and drag against incidence, between the angle of incidence of the steady approach glide α_0 and the angle of incidence α_g at the moment of touching the ground, which mostly will be chosen in connection with the attitude of the airplane when making a „three-point" landing, can be approximated by linear functions (17) and (18). This is illustrated in fig. 2 and 6. Ground *effect can be taken into account approximatively by* assuming that at the moment of initiating the landingmanoeuvre (incidence of the steady glide) there is no ground effect, while at the moment of touching the ground, (incidence α_g) ground effect can be calculated as the height above the ground is then known. The linear functions representing lift and drag as functions of incidence are determined by those two points. If desired a check on this approximation for intermediate values of the angle of incidence can be obtained by recalculating the lift and drag when the height above the ground is known by the method described hereafter. *If necessary a second approximation can thus* be made .

The reduction of the equations of motion (1) and (2) is further effected by some minor approximations which will be clear from the sequence of formulae (20) to (24).

Under **03** the method to obtain an approximate solution of the equations of motion is described. There are four equations (26), (27), (16) and (28) containing 5 variables. Normally one of these would be chosen as a function of time and the others evaluated by solving the equations. It is, however, impossible to choose a function, say $\alpha(t)$ or $\varphi(t)$, representing a normal landing, as the time t_a in which the landingmanoeuvre is performed is not known and has to be obtained from the solution of the problem. It would be possible to choose α or φ as functions of the relative time, that is the time expressed in units equal to the total time $t_a\left(\gamma=\frac{t}{t_a}\right)$, in such a way that a fair approximation of the change of these values during the landing is obtained.

When both $\alpha(\gamma)$ and $\varphi(\gamma)$ are fixed beforehand one variable too much is fixed and it is not possible to obtain an exact solution of the equations of motion. In this case it is, however, possible to obtain a first rough approximation of the problem by solving t_a in the following way. From equation (26) the value of the airspeed, expressed in t_a, can be calculated for the moment $\gamma=1$ (end of landing manoeuvre).

The same can be done by integration of (27) between $\gamma=0$ and $\gamma=1$. By equalling both results a relation is obtained from which t_a can be solved and a first rough approximative solution is found. It would only be an exact solution if an imaginary force K, varying with time, was introduced in equation (2). In consequence of the procedure followed by evaluating t_a from the problem, the variation of K with time is such that $\int_0 t_a K dt=0$, which means that the total momentum imparted to the aircraft by the force K during the

landing manoeuvre is zero. If the airspeed remained constant during this period it would also mean that the total work done by force K would be zero.

It is, however, possible to obtain a much better approximation of the motion by fixing α as a function of γ and φ as a function of γ and a parameter p, thus fixing the change of incidence and giving a bundle of curves for the change of φ, from which the one that gives the best approximation of the real change of angle of flightpath for the given change of angle of incidence, is chosen by solving p from the problem, together with t_a.

Then it is possible to solve both p and t_a by equating the values of v from (26) and (27) not only for the end of the manoeuvre but also for an arbitrarely chosen moment during the manoeuvre, say 0,5 t_a.

By this method the momentum imparted by the abovementioned imaginary force K is zero for the period 0 to 0,5 t_a and for the period 0.5 to 1,0 t_a As the variation of speed during each of these periods is relatively small, it means also that in rough approximation the total work done by this force is zero.

It is expected that in this way a rather good approximative solution of the problem is obtained.

Formulae (31) to (46) give the equations when the functions $\alpha(\gamma)$ and $\varphi(\gamma, p)$ are introduced. Equating both values for the airspeed v_{γ_1} at a certain moment γ_1 leads to the equations (48) and (50), the first for the time $\gamma = 1$ and the second forthe time $\gamma = 0{,}5$. The easiest way to get the values of p and t_a is to solve (48), obtaining t_a as a function of p.

The difference Δv between the speeds at time $\gamma = 0{,}5$ following from the first and second equation of motion can be plotted against t_a resp. p; the values of t_a and p, belonging to $\Delta v = 0$ can immediately be read. Formula (51) is used for this purpose.

To obtain a good approximation, much depends on the choice of $\alpha(\gamma)$ and $\varphi(\gamma, p)$, which is discussed under **04**. Assuming a smooth and gradual change of incidence, attitude, flight path, and elevator deflection for the transition from the steady approach-glide into the landing-manoeuvre and during the latter, certain conditions for $\alpha(\gamma)$ and $\varphi(\gamma, p)$ should be fulfilled, which are summed up under 04.1. Furthermore the functions have to be such that integration of (34) is possible. This leads to the functions (55) and (56) from which (57) to (60) are derived. With these functions the values of T, U, V and W which appear in the equations (48) and (51) become rather simple as is seen from (65), (66), (67) and (68). The functions f_1 to f_{10} are functions of z only; fixed by the chosen conditions for the incidences at the beginning and the end of the landing, see (54). They were evaluated once and for all for two values of γ i.e. 0,5 and 1,0 and are given in fig. 13 and 14. Thus no integrating of complicated functions is necessary anymore and the calculation of p and t_a is very simple.

If desired the height at any moment during the landing manoeuvre including the height at which the manoeuvre has to be initiated is easily found by equation (70a) and with a sufficient approximation by (70b) which can be simplified to (70). The functions f_{11} and f_{12} also are dependent of z only and are evaluated for the times $\gamma = 0$, 0,4 and 0,7 thus giving 4 points by which a good approximation of the change of height during the landing can be obtained.

Now that t_a is known it is possible by the sequence of formulae (71), (28), (58), (60), (57), (59), (72) and (73) under 05.3 to calculate the elevator deflection as a function of time.

As in most of the cases the maximum deflection occurring at the end of the landing is the most interesting, formula (78) can be used.

In this case it is necessary to take into account the groundeffect, Results of windtunnel experiments (R. and M. 1847) show that in formulae (71) or (78) only the value β^x (α) is seriously influenced. It is therefore desirable to calculate the elevator deflection β^x necessary for equilibrium in stationary flight taking the ground effect into account and making use of either theoretical or experimental data. It is possible to introduce this influence because by (70) the height above the ground at any moment is known.

As follows from (71), only β^x is affected by the c.g. position. It is therefore possible to calculate the most forward position of the c.g. for a given maximum possible elevator deflection β_{max} when the maximum required elevator deflection β_a for a normal landing with an arbitrarely chosen c.g. position is known. Formula (83) gives the maximum possible forward shift Δx with respect to a certain c.g.-position a.

Under **07** an example is given of the calculations for an aeroplane the characteristics of which are given in table 1 and fig. 6. Tables 2 to 4 give the calculations while in table 5 and 6 results are given. Calculations were made for the cases with and without flaps, each for three values of the speed in the steady approach condition.

Figures for the maximum elevator deflection are represented in fig. 10 (as a function of the approach speed), which also gives the height at which the landing manoeuvre has to be intiated and the value of $(\beta_g - \beta_g{}^x)$ which is called the „extra" elevator deflection, and is in a certain way responsible for the dynamic part of the motion during the landing manoeuvre. Attention is called to the fact that certain limitations for the approach speed are found. In the first place it is found that, when the approach speed is too low, the roots of equation (48), of which only the one with the negative sign given by (69) describes the real landing case, become complex. This means that a „normal" landing as defined by the curves $\alpha(\gamma)$ and $\varphi(\gamma, p)$ is impossible. In practice it is also known that a normal landing without vertical speed at the moment of contact with the ground is impossible when the approach speed is too low. On the other hand, when the approach speed is too high, positive values of p are found, which would mean that the aeroplane

is climbing at the moment the landing attitude is reached. When in practice a landing with too high an approach speed is attempted and the stick is gradually pulled back in the same way as for a normal landing the result is also a climb before the landing attitude and incidence are reached. Results show that normally speeds between 1,2 and 1,3 times the stalling speed are satisfactory for a normal landing.

Fig. 11 shows the change of the variables with time for one case. It is seen that the conditions for smooth and gradual change introduced in the problem are somewhat exaggerated compared with practice. The change of most of the variables is such that to reproduce such a landing in reality the pilot would initiate the manoeuvre at a moment between 0,3 and 0,4 γ. It is expected, however, that this will not have a serious influence on the latter part of the landing.

To conclude, some calculations were made concerning the effect of different flaps on the required „extra" elevator deflection. It is shown, that by enlarging the maximum liftcoefficient the required „extra" deflection is reduced, while by enlarging the dragcoefficient it is increased. The absolute elevator deflections required in those cases depend, however, also on the influence of the flaps on the pitching moment, so that in general nothing can be said about the influence of such devices on the landing characteristics.

To end, it is observed that it is necessary to check the results of his method by flight tests, which were impossible during the period of the occupation of the Netherlands.

Notations.

B = moment of inertia about the lateral axis.

$c_1 = \frac{\partial c_n}{\partial \alpha_h}$.

$c_2 = \frac{\partial c_n}{\partial \beta}$.

c_a = liftcoefficient.

c_a' = slope of the straight line, giving the best linear approximation for the relation between liftcoefficient and angle of incidence in the region of incidences occuring during the landing (see fig. 3).

c_m = dimensionless coefficient of moment M_v.

c_n = dimensionless coefficient of the normal force on the tail surfaces.

c_w = dragcoefficient.

c_w' = slope of the straight line giving the best linear approximation for the relation between dragcoefficient and angle of incidence in the region of incidences occurring during the landing.

c_{w_u} = value of dragcoefficient belonging to that angle of incidence, for which $c_a = 0$ (c_a and c_w extrapolated according to the linear approximation mentioned under c_a' and c_w').

f = area of the horizontal tail surfaces.

F = wing area.

g = acceleration of gravity.

G = total weight of the aeroplane.

h = height of the aeroplane above the ground during the landing manoeuvre.

k_β = elevator coefficient, see section 07.1.

l = distance of the centre of pressure of the tail surfaces from the centre of gravity of the aeroplane.

M = total moment of the air reactions about the lateral axis.

M_{d_s} = damping moment of the tail surfaces due to pitching.

M_h = moment of the air reactions on the tail surfaces about the lateral axis.

M_v = moment about the lateral axis of the air reactions on the aeroplane with the exception of the tail surfaces.

M_{v_s} = damping moment of wing and fuselage due to pitching.

p = parameter in $\varphi - \gamma$ relation.

t = time.

t_a = total time of the landingmanoeuvre.

t_v = wing chord.

v = velocity of the centre of gravity of the aeroplane with respect to the undisturbed air.

v_h = velocity of the disturbed flow at tail with respect to tail.

x = distance of the centre of gravity of the aeroplane from the leading edge of the wing.

Δx = shift of the centre of gravity of the aeroplane.

$z = \sqrt[3]{\frac{\sqrt{a_0}}{\sqrt{a_g} - \sqrt{a_0}}}$.

α = angle of incidence (with respect to line of zero lift; see fig. 1).

α' = angle of incidence (with respect to chord).

$\bar{\alpha} = \alpha - \alpha'$.

α_h = angle of incidence at tail.

β = elevator deflection.

β^x = elevator deflection in steady flight.

$\gamma = \frac{t}{t_a}$ (relative time).

γ_1 = value of γ according to time $t = t_1$.

δ = landing flap setting.

ε = angle of downwash at tail.

$\eta = \frac{v_h}{v}$.

Θ = inclination of chord to horizontal.

$\varkappa = 1 - \frac{d\varepsilon}{d\alpha}$, factor of downwash.

$\mu = \varrho g \frac{F}{G}$.

ϱ = density of the air.

σ = inclination of tail chord to wing chord.

φ = inclination of flight path to horizontal.

Suffices.

Suffix a and b indicate that the quantity relates to the c.g. position x_a and x_b respectively.

Suffix g indicates that the value of the quantity relates to time $t = t_a$ i.e. the moment of touching the ground.

Index * means, that that value of the quantity under consideration has to be taken, which corresponds to the stationary flight at the same angle of incidence as in the non-stationary flight.

Suffix o indicates, that the value of the quantity relates to time $t = 0$, i.e. the beginning of the landing manoeuvre.

TABEL 1. **Gegevens van het vliegtuig.**

$G = 1000$ kg.	$c_z = -0{,}79$/rad.	
$F = 19{,}4$ m².	$\frac{c_1}{c_2} = 2.$	
$t_v = 1{,}67$ m.	$\frac{d\varepsilon}{d\alpha} = 0{,}30.$	
$f = 3{,}19$ m².	$\varrho = 0{,}125$ kg sec²/m⁴.	
$l = 5{,}38$ m.	$\mu = 0{,}0238$/m.	
$g = 9{,}81$ m/sec.²		
$B = 350$ kg m sec².		

δ	0°	40°
c_a'	4,05	4,87
c_w'	0,485	0,573
c_{w_u}	− 0,018	0
η	0,80	0,70

TABEL 6. **Verkorte weergave van de berekening van $\beta(\dot\gamma)$.**

$\delta = 40°$; $v_0 = 96$ km/h $(1{,}2\ v_{min}) = 26{,}65$ m/sec; $\alpha_0 = 0{,}233$ rad; $\varphi_0 = -0{,}117$ rad; $\alpha_g = 0{,}332$ rad; $z = 1{:}727$; $t_a = 10{,}6$ sec (zie tabel 2); $p = -2{,}35$ (zie tabel 2).

Voor de overige gegevens wordt verwezen naar tabel 1.

γ	α	$\dot\alpha(\gamma)$	$\dot\varphi(\gamma)$	$\ddot\alpha(\gamma)$	$\ddot\varphi(\gamma)$	$\dot\Theta(\gamma)$	$\ddot\Theta(\gamma)$	$v(\gamma)$
Formule	(55)	(57)	(59)	(58)	(60)	(28)	(28)	(72)
0	0,2330	0	0	0	0	0	0	26,65
0,2	0,2340	0,00103	0,00194	0,00097	0,00173	0,00297	0,00270	26,67
0,4	0,2395	0,00415	0,00687	0,00198	0,00280	0,01100	0,00480	26,51
0,6	0,2538	0,00962	0,01335	0,00322	0,00324	0,02298	0,00646	26,01
0,8	0,2820	0,01805	0,02012	0,00483	0,00302	0,03820	0,00786	24,82
1	0,3328	0,03060	0,02575	0,00720	0,00216	0,05640	0,00937	22,97

γ	$-1{,}2\frac{c_1}{c_2}\frac{l}{v(\gamma)}\cdot\frac{d\varepsilon}{d\alpha}\dot\alpha(\gamma)$	$-1{,}2\frac{c_1}{c_2}\frac{l}{v(\gamma)}\frac{\dot\Theta(\gamma)}{\eta}$	$\frac{2B}{\varrho f l \eta^2 c_2}\frac{\ddot\Theta(\gamma)}{v(\gamma)^2}$	$\beta^{x}{}_{\alpha(\gamma)}$	$\beta(\gamma)$	$h(\gamma)$
Formule				fig. 6	(71)	(70)
0	0	0	0	+1,65	+1,65	23,1
0,2	− 0,00002	− 0,00206	− 0,00319	+1.62	+1,31	
0,4	− 0,00006	− 0,00765	− 0,00576	+1,48	+0,68	10,2
0,6	− 0,00014	− 0,01632	− 0,00802	+1,17	−0,31	
0,7						1,8
0,8	− 0,00028	− 0,02840	− 0,01072	+0,50	−1,90	
1	− 0,00052	− 0.04540	− 0,01558	−0,72	−4,51	0

TABEL 4. **Verkorte weergave van de berekening van β_g.**

δ		0°			40°		
V_0 in m/sec		30,0	31,1	32,5	26,1	26,6	28.9
z	(54)	1,76	1,63	1,52	1,803	1,727	1,510
$T_{\gamma=1}$	(65)	$-0{,}0475\,p-0{,}440$	$-0{,}0475\,p-0{,}420$	$-0{,}0481\,p-0{,}400$	$-0{,}0569\,p-0{,}442$	$-0{,}0571\,p-0{,}444$	$-0{,}0588\,p-0{,}435$
$U_{\gamma=1}$	(66)	$+0{,}0024\,p+0{,}284$	$+0{,}0032\,p+0{,}287$	$+0{,}0038\,p+0{,}295$	$+0{,}0046\,p+0{,}340$	$-0{,}0047\,p+0{,}348$	$+0{,}0074\,p+0{,}378$
$V_{\gamma=1}$	(67)	$-4{,}62$	$-5{,}91$	$-7{,}15$	$-3{,}78$	$-4{,}32$	$-6{,}45$
$W_{\gamma=1}$	(68)	$-3{,}13\,p$	$-3{,}13\,p$	$-3{,}18\,p$	$-2{,}99\,p$	$-3{,}01\,p$	$-3{,}11\,p$
t_a	(69)	*zie fig. 8*	id	id	fig. 9	id	id
$T_{\gamma=0{,}5}$	(65)	$-0{,}0086\,p-0{,}065$	$-0{,}0086-0{,}054$	$-0{,}0086\,p-0{,}040$	$-0{,}0103\,p-0{,}041$	$-0{,}0103\,p-0{,}044$	$-0{,}0106\,p-0{,}035$
$U_{\gamma=0{,}5}$	(66)	$+0{,}0266\,p+0{,}115$	$+0{,}0256\,p+0{,}113$	$+0{,}0250\,p+0{,}114$	$+0{,}0213\,p+0{,}110$	$+0{,}0226\,p+0{,}113$	$+0{,}0243\,p+0{,}125$
$V_{\gamma=0{,}5}$	(67)	$-0{,}600$	$-0{,}871$	$-1{,}105$	$-0{,}522$	$-0{,}610$	$-1{,}011$
$W_{\gamma=0{,}5}$	(68)	$+1{,}058\,p+6{,}22$	$+1{,}120\,p+6{,}678$	$+1{,}2615\,p+7{,}360$	$+0{,}991\,p+5{,}782$	$+1{,}024\,p+6{,}200$	$+1{,}194\,p+7{,}260$
δv	(51)	*zie fig. 9*	id	id	id	id	id
p	(fig. 9)	$-3{,}83$	$-2{,}25$	$-0{,}55$	$-2{,}70$	$-2{,}35$	$-0{,}45$
t_a in sec.	(fig. 9)	13,20	16,60	17,93	8,75	10,60	14,50
h_0 in m	(70)	29,5	34,7	34,9	19,1	23,1	30,6
α_g		0,320	0,320	0,320	0,332	0,332	0,332
v_g in m/sec	(77)	26,23	25,68	25,33	23,23	22,97	22,50
$\ddot{\Theta}_g$	(74)	0,0103	0,0039	0,0009	0,0156	0,0094	0,0052
$\dot{\Theta}_g$	(75)	0,0506	0,0347	0,0266	0,0686	0,0564	0,0346
$\dot{\alpha}_g$	(76)	0,0224	0,0216	0,0236	0,0328	0,0306	0,0309
$\beta(\alpha_g)^x$ in graden	(fig. 6)	$-3{,}32$	$-3{,}32$	$-3{,}32$	$-0{,}72$	$-0{,}72$	$-0{,}72$
β_g in graden	(71)	$-5{,}96$	$-4{,}98$	$-4{,}55$	$-5{,}56$	$-4{,}51$	-3.15
$\beta_g-\beta(\alpha_g)^x$ in graden		$-2{,}64$	$-1{,}66$	$-1{,}23$	$-4{,}84$	$-3{,}79$	$-2{,}43$

TABEL 4. Verkorte weergave van de berekening van β_g.

ϑ		0°			40°		
V_0 in m/sec		30.0	31.1	32.5	26.1	26.6	28.9
z	(54)	1.76	1.63	1.52	1.803	[illegible]	1.510
$T_{p=1}$	(55)	— 0.0475 p — 0.440	— 0.0475 p — 0.420	— 0.0481 p — 0.400	— 0.0569 p — 0.442	— 0.0571 p — 0.444	— 0.0588 p — 0.435
$U_{p=1}$	(66)	+ 0.0024 p + 0.284	+ 0.0032 p + 0.287	+ 0.0038 p + 0.295	+ 0.0046 p + 0.340	— 0.0247 p + 0.345	+ 0.0074 p + 0.378
$V_{p=1}$	(67)	— 4.62	— 5.91	— 7.15	— 3.78	— 4.32	— 6.45
$W_{p=1}$	(68)	— 3.13 p	— 3.13 p	— 3.18 p	— 2.99 p	— 3.01 p	— 3.11 p
t_a	(69)	zie fig. 8	id	id	fig. 9	id	id
$T_{p=0.5}$	(65)	— 0.0086 p — 0.065	— 0.0086 — 0.054	— 0.0086 p — 0.040	— 0.0103 p — 0.041	— 0.0103 p — 0.044	— 0.0106 p — 0.035
$U_{p=0.5}$	(66)	+ 0.0266 p + 0.115	+ 0.0256 p + 0.113	+ 0.0250 p + 0.114	+ 0.0213 p + 0.110	+ 0.0226 p + 0.113	+ 0.0243 p + 0.125
$V_{p=0.5}$	(67)	— 0.600	— 0.871	— 1.105	— 0.522	— 0.610	— 1.011
$W_{p=0.5}$	(68)	+ 1.058 p + 6.22	+ 1.120 p + 6.675	+ 1.261 p + 7.360	+ 0.991 p + 5.7[illegible]	+ 1.024 p + 6.200	+ 1.194 p + 7.260
δu	(51)	zie fig. 9	id	id	id	id	id
p	(fig. 9)	— 3.83	[illegible]	— 0.55	— 2.70	— 2.35	— 0.45
t_a in sec.	(fig. 9)	13.20	16.60	17.[illegible]3	8.75	10.60	14.50
h_0 in m	(70)	29.5	34.7	34.9	19.1	23.1	30.6
a_g		0.320	0.320	0.320	0.332	0.332	0.332
u_g in m/sec	(77)	26.23	25.68	25.33	23.23	22.97	22.50
$\ddot{\Theta}_g$	(74)	0.0103	0.0039	0.0009	0.0156	0.0094	0.0052
$\dot{\Theta}_g$	(75)	0.0506	0.0347	0.0266	0.0686	0.0564	0.0346
$\dot{u}_g$	(76)	0.0224	0.0216	0.0236	0.0328	0.0306	0.0309
$\beta(a_g)^*$ in graden (fig. 6)		— 3.32	— 3.32	— 3.32	— 0.72	— 0.72	— 0.72
δ_g in graden (71)		— 5.96	— 4.98	— 4.55	— 5.56	— 4.51	— 3.15
$\delta_g - \beta(a_g)^*$ in graden		— 2.64	— 1.66	— 1.23	— 4.84	— 3.79	— 2.43

REPORT V. 1380.

The Change in Flutter Speed due to Small Variations in Some Aileron Parameters

by

Ir. A. I. VAN DE VOOREN.

Summary.

In continuation of report V. 1297, this paper contains diagrams showing the change in flutter speed due to small variations in aileron static balance, in aileron moment of inertia, in the ratio of aileron chord to total chord and in the position of the aileron hinge axis. The principal conclusions are listed in section 4. The results are obtained by the method described in report V. 1366, of which the first approximation has been evaluated. The resulting changes in flutter speed are, hence, proportional to the applied variations.

Contents.

The notations are identical to those used in report V. 1297.

1 Introduction.

In report V. 1297 (ref. 1) diagrams have been published giving the flutter speed of wing-aileron systems of a certain standard type as a function of the stiffness ratio of the wing for various — systematically chosen — values of some of the structural parameters. The remaining parameters, among others including all aileron parameters (with the exception of the degree of aerodynamic balance, i.e. of the assumed value of the gap width between wing and aileron), had to be fixed as suitable mean values to keep the computations within reasonable limits.

In view of the important influence of the aileron parameters on the critical speed, additional calculations have been made to determine the change in flutter speed, connected with *small* variations of these parameters. Use was made of the perturbation method, described in report V. 1366 (ref. 2). The results represent first approximations only, which means that terms of second and higher degree in the variations have been neglected.

2 Range of investigation.

Successively, the influence of small variations in the following parameters was investigated:

(1) aileron static balance ($\mu_1\sigma_1$),
(2) aileron moment of inertia ($\mu_1\kappa_1^2$),
(3) ratio of aileron chord to total chord (η),
(4) position of the aileron hinge axis (ε_1).

They were varied with regard to the original values, attached to these parameters in report V. 1297, viz.

$$\mu_1\sigma_1 = 0, \quad \mu_1\kappa_1^2 = 0{,}05, \quad \eta = 0{,}25, \quad \varepsilon_1 = 0{,}10.$$

Other important parameter values, not mentioned in the diagrams, are

$$\kappa = 0{,}6, \qquad \eta_s = 7{,}881.10^{-3}.$$

The air density is always put equal to $\rho = {}^1/_8$ kg m^{-4} sec^2.

The results obtained in V. 1297 were used as zero-order approximations for the applied perturbation method. All calculations have been restricted to the cases of 62,4 % aileron aerodynamic balance and vanishing structural damping. Moreover, only two values of the reduced velocity have been considered, which made it possible to determine four points of every curve, relating the flutter speed to the stiffness ratio.

3 General method of calculation

3.1 *The fundamental equations.*

The starting point is formed by the equations of motion (compare with V. 1297):

$$\left.\begin{aligned} &m_{11}\ddot{z} + m_{12}\ddot{\varphi} + m_{13}\ddot{\gamma} + (B z'')'' = K,\\ &m_{21}\ddot{z} + m_{22}\ddot{\varphi} + m_{23}\ddot{\gamma} - (T\varphi')' = \\ &\qquad = M + elK - N - \varepsilon_1 lR,\\ &\int_{1/2\,b}^{b} m_{31}\ddot{z}dy + \int_{1/2\,b}^{b} m_{32}\ddot{\varphi}dy + \int_{1/2\,b}^{b} m_{33}\ddot{\gamma}dy = \\ &\qquad = \int_{1/2\,b}^{b} (N + \varepsilon_1 lR)dy, \end{aligned}\right\} \quad (1)$$

where

$$\left.\begin{aligned} m_{11} &= \mu f^2 \pi\rho l_i^2,\\ m_{12} = m_{21} &= -(\mu\sigma - \mu_1\sigma_1) f^3\pi\rho l_i^3,\\ m_{13} = m_{31} &= -\mu_1\sigma_1 f^3\pi\rho l_i^3,\\ m_{22} &= \{\mu(\kappa^2 + \sigma^2) - \mu_1(\kappa_1^2 + \sigma_1^2) - \\ &\qquad - 2\mu_1\sigma_1\zeta\} f^4\pi\rho l_i^4,\\ m_{23} = m_{32} &= \mu_1\sigma_1\zeta f^4\pi\rho l_i^4,\\ m_{33} &= \mu_1(\kappa_1^2 + \sigma_1^2) f^4\pi\rho l_i^4,\\ B &= B_0 f^3,\\ T &= T_0 f^3. \end{aligned}\right\} \quad (2)$$

In addition to the symbols of V. 1297, there appear also

$\sigma_1 l$ = distance of aileron inertia axis aft of hinge axis,

$\zeta\, l$ = distance of aileron hinge axis aft of flexural axis,

while $\kappa_1 l$ — in contrast to V. 1297 — is equal to the radius of gyration of the aileron about its inertia axis.

The aerodynamic forces and moments can be written in the following form

$$\left.\begin{aligned} K &= m_L\nu^2\{a_{11}z + 2a_{12}fl_i\varphi + 2a_{13}fl_i\gamma\},\\ M + elK - N - \varepsilon_1 lR &=\\ = m_L\nu^2\{2a_{21}fl_i z + 4a_{22}f^2 l_i^2\varphi + 4a_{23}f^2 l_i^2\gamma\},&\\ N + \varepsilon_1 lR &=\\ = m_L\nu^2\{2a_{31}fl_i z + 4a_{32}f^2 l_i^2\varphi + 4a_{33}f^2 l_i^2\gamma\},& \end{aligned}\right\} \quad (3)$$

with $m_L = \pi\rho f^2 l_i^2$.

The a_{ik} are dimensionless, complex coefficients of the aerodynamic forces, which depend on V_0, η, ε and ε_1. Their values can be taken from table 1 of report V. 1386 (ref. 3).

The method of solution of the eqs. (1) is explained in report V. 1297. Use is made of definite modes of displacement $z_1(y)$, $\varphi_1(y)$, 1 by the assumption

$$z = l_i q_1 e^{i\nu t} z_1(y), \quad \varphi = q_2 e^{i\nu t}\varphi_1(y), \quad \gamma = q_3 e^{i\nu t}, \quad (4)$$

where q_1, q_2 and q_3 are independent of y, and of weight functions, which are respectively

$$\frac{3w^2 - w^3}{6},\ w \text{ and } 1, \text{ where } w = \frac{y}{b}. \quad (5)$$

The algebraïc equations obtained have the form:

$$\sum_l q_l(\nu^2 A_{kl} - E_{kl}) = 0, \quad k, l = 1, 2, 3. \quad (6)$$

The solutions for the original system are calculated in V. 1297 and will be denoted by $\nu^2 = \nu_i^2$ and $q_l = (q_l)_i$ with $i = 1$ or 2.

For the slightly varied systems, investigated in this report, the coefficients A_{kl} and E_{kl} are subjected to small variations, denoted by α_{kl} resp. ε_{kl}. According to eq. (5.5) of report V. 1366 the corresponding change in the frequency ν_i is determined by

$$\Delta\nu_i^2 = \frac{\bar{\varepsilon}_{ii} - \nu_i^2\bar{\alpha}_{ii}}{\bar{A}_{ii}}, \quad (7)$$

with

$$\left.\begin{aligned} \bar{\alpha}_{ii} &= \sum_{k,l} (q_l)_i (Q_k)_i \alpha_{kl},\\ \bar{\varepsilon}_{ii} &= \sum_{k,l} (q_l)_i (Q_k)_i \varepsilon_{kl},\\ \bar{A}_{ii} &= \sum_{k,l} (q_l)_i (Q_k)_i A_{kl}, \end{aligned}\right\} \quad (8)$$

where $(Q_k)_i$ denote the amplitude ratios of the set

$$\sum_k Q_k(\nu^2 A_{kl} - E_{kl}) = 0,$$

which is adjoint to the set of equations (6) and therefore has the same characteristic values ν_i^2.

3.2 *Composition of diagrams.*

In report V. 1297 for each V_0-value two values of the ratio

$$\lambda = \left(\frac{\nu_A}{\nu_B}\right)^2 = \frac{E_{11}}{E_{22}} \cdot \frac{U_{22}}{U_{11}}$$ [1])

were calculated, to which belong real values of the frequency of the critical oscillation. In this way points were obtained all situated on the curve giving the relation between the flutter speed and the ratio λ. To obtain a similar curve for the varied system, the ratio λ must be altered for each value of V_0 in such a way that the frequency ν remains real, which means that $\Delta\nu_i^2$ must be real too.

The numbers at the horizontal axis of the diagrams in this report denote

$$\lambda = \frac{E_{11}}{E_{22}} \cdot \frac{U_{22}}{U_{11}}, \quad (9)$$

where $\frac{U_{22}}{U_{11}}$ refers for *all* curves to the *original*,

---

1) $\nu_A^2 = \frac{E_{11}}{U_{11}}$ and $\nu_B^2 = \frac{E_{22}}{U_{22}}$ determine the uncoupled flexural, resp. torsional resonance frequencies in still air ($U_{11} = \lim_{V_0 \to 0} A_{11}$, $U_{22} = \lim_{V_0 \to 0} A_{22}$).

non-varied system. This makes that for a varied system, λ is not equal to the square of the ratio of the uncoupled resonance frequencies of that system. The advantage of this method is that conditions with the *same stiffness ratio* $\left(\frac{E_{11}}{E_{22}}\right)$ are indicated by points on the same vertical line.

Since the dimensionless value of the flutter speed $\frac{v_{crit}}{v_B l_i}$ [2]) depends, for constant values of the parameters, upon the stiffness ratio $\frac{E_{11}}{E_{22}}$ only, but not upon E_{11} and E_{22} separately, a change of this ratio can be assumed to be due to a change in E_{11}, with E_{22} constant. Hence,

$$\lambda + \Delta\lambda = \frac{E_{11} + \varepsilon_{11}}{E_{22}} \cdot \frac{U_{22}}{U_{11}} \qquad (10)$$

From (9) and (10) it follows

$$\frac{\Delta\lambda}{\lambda} = \frac{\varepsilon_{11}}{E_{11}} \quad \text{or} \quad \varepsilon_{11} = E_{11}\frac{\Delta\lambda}{\lambda},$$

where λ again refers to the original system and hence is equal to $\left(\frac{v_A}{v_B}\right)^2$ of that system.

Since all ε_{kl} except ε_{11} vanish, the second of eqs. (8) becomes

$$\bar{\varepsilon}_{ii} = (q_1)_i\,(Q_1)_i\,\varepsilon_{11}$$

or, with the aid of footnote [1])

$$\frac{\bar{\varepsilon}_{ii}}{v_B{}^2} = (q_1)_i\,(Q_1)_i\,U_{11}\,\Delta\lambda. \qquad (11)$$

Substitution of eq. (11) in eq. (7) yields

$$\Delta\left(\frac{v}{v_B}\right)_i^2 = \frac{(q_1)_i(Q_1)_i U_{11}}{\bar{A}_{ii}}\Delta\lambda - \left(\frac{v}{v_B}\right)_i^2 \frac{\bar{\alpha}_{ii}}{\bar{A}_{ii}}. \qquad (12)$$

The requirement that $\Delta\left(\frac{v}{v_B}\right)_i^2$ must be real, gives the relation between $\Delta\lambda$ and the applied parameter variation, upon which $\bar{\alpha}_{ii}$ depends.

3.3 *Description of variations.*

When one of the parameters is varied, all other parameters are kept constant. This has the following consequences.

(1) The variation of aileron static balance $\mu_1\sigma_1$ in every case consists of a variation in σ_i (σ_1 originally vanishing), possibly accompanied by a variation in μ_1. The chordwise mass distribution of the system is changed in such a way that both μ, σ, κ and $\mu_1\kappa_1{}^2$ are fixed to the original values. The variation of $\mu_1\sigma_1{}^2$ can be neglected.

(2) The variation of the aileron moment of inertia $\mu_1\kappa_1{}^2$ again is performed in such a way, that the aileron remains statically balanced, while for instance μ and κ are also constant.

(3) A change in η alters the value of the aileron aerodynamic balance. The gap width, however, is kept constant. Likewise ε_1 and all other parameters are unchanged.

(4) The aileron aerodynamic balance is also influenced by a change in ε_1, but again the gap width is kept constant. The new aileron too is statically balanced, has the same chord and the same moment of inertia as the original one.

3.4 *Divergence speed.*

The divergence speed in dimensionless form depends upon the stationary aerodynamic forces only. Therefore, it is unaffected by the first two variations. For the two other variations, the divergence speed has been calculated by evaluating the stationary aerodynamic forces for a definite value of the variation considered and applying the usual formulae.

4 Results.

4.1 *General.*

The diagrams show the influence on flutter and on divergence speed resulting from the consecutive application of the following variations to the original wing-aileron system:

$$\Delta(\mu_1\sigma_1) = 0{,}01; \quad \Delta(\mu_1\kappa_1{}^2) = 0{,}01; \quad \Delta\eta = 0{,}01; \quad \Delta\varepsilon = -0{,}005.$$

Calculated points are specially marked. Since it is intended primarily to show the change in flutter speed, the values of V_0 corresponding to the calculated points have not been included. They can, however, be obtained by comparison with the diagrams of V. 1297, where the numbers near the dotted lines denote the reduced frequency at the wing root $\omega(=1/V_0)$.

In the first approximation, evaluated here, all changes are proportional to the variations applied.

4.2 *Variation of aileron static balance.*

Underbalancing of the aileron has apparently a very unfavourable influence on flutter speed; in all cases investigated the flutter speed decreases. Often the instability of a wing-aileron system vanishes again at a higher speed; by underbalancing this speed increases. Thus the range of speeds where the system is unstable, is extended to both sides. For overbalancing the opposite conclusions hold.

4.3 *Variation of aileron moment of inertia.*

In general, an increase of the aileron moment of inertia is unfavourable, though the reduction of flutter speed is far less serious than that, due to an underbalanced aileron. It is always unfavourable to increase the aileron moment of inertia if the flexural axis lies before the quarter chord axis. In the opposite case, an increase of the moment of inertia can, for small values of the stiff-

[2]) v_B always refers to the original system.

ness ratio, result in a, mostly very small, increase of the flutter speed. This last situation will in practice perhaps arise fairly often. The speed, where the instability again vanishes, is always raised by increasing the aileron moment of inertia.

4.4 *Variation of ratio of aileron chord to total chord.*

If the flexural axis lies before the quarter chord axis, an increase of aileron chord results in an increased flutter speed. In the more usual case of a flexural axis, located aft of the quarter chord axis, the flutter speed diminishes. The speed, at which some of the wing-aileron systems become stable again, shows a slight reduction if the chord ratio is increased. In general, this parameter has only a slight influence. There is a small increase in divergence speed, which is, however, too small to be visible in the diagrams.

4.5 *Variation of position of aileron hinge axis.*

This is a very important parameter. Shifting the hinge axis forward, leads to a lower flutter speed. Only, if both flexural axis and inertia axis have a very forward position, this general rule may fail. The speed, limiting the unstable range to the upper side, is decreased sometimes, but always substantially less than in consequence of an increased chord ratio. The divergence speed is again somewhat increased (not shown in the diagrams).

5 List of references.

1 Van de Vooren, A. I. and Greidanus, J. H.: "Diagrams of critical flutter speed for wings of a certain standard type", Report V. 1297.

2 van de Vooren, A. I.: "A method to determine the change in flutter speed due to small changes in the mechanical system". Report V. 1366.

3 van de Vooren, A. I.: "The treatment of a tab in flutter calculations including a complete account of the aerodynamic forces involved". Report V. 1386.

These three reports are published in "Reports and Transactions of the National Aeronautical Research Institute, Amsterdam", Vol. XIII (1946).

Completed: November 1946.

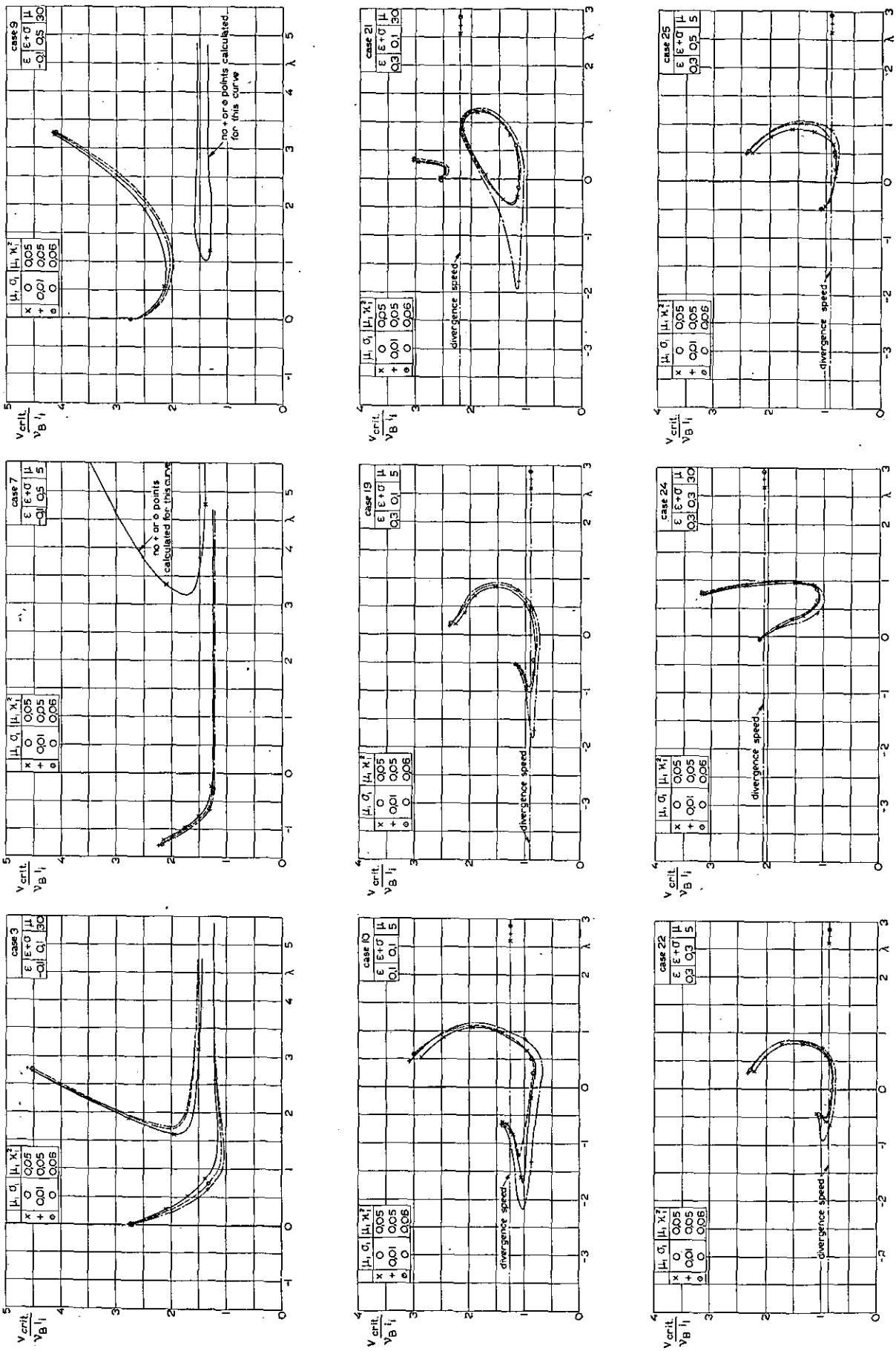

Fig. 1. Change of flutter speed due to variations in aileron static unbalance ($\mu_1\sigma_1$) and in aileron moment of inertia ($\mu_1\kappa_1^2$).

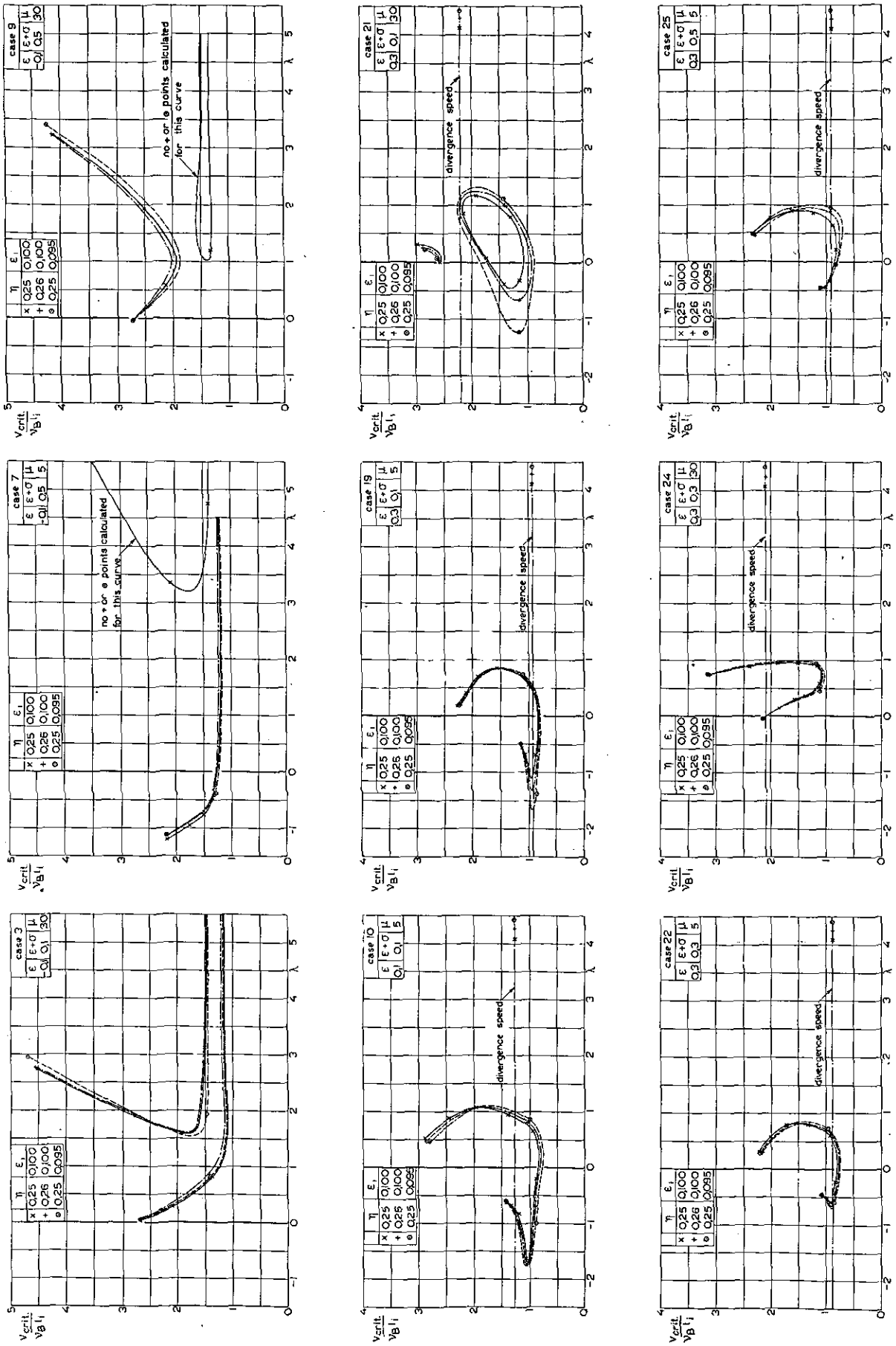

Fig. 2. Change of flutter speed due to variations in chord ratio (η) and in backward position of aileron hinge axis (ε_1).

REPORT V. 1397.

Diagrams of Flutter, Divergence and Aileron Reversal Speeds for Wings of a Certain Standard Type

by

Ir. A. I. VAN DE VOOREN.

Summary.

In this report diagrams are given in which the flutter speed, the divergence speed and the aileron reversal speed are plotted against the squared ratio of the uncoupled frequencies of aileron deflection (resulting from the stiffness of the control cables) to the wing torsion. These diagrams apply to several combinations of the following parameters: wing density, positions of flexural and inertia axes and aerodynamic aileron balance, permitting a reasonably complete survey of their influence. To simplify the calculations the flexural stiffness was neglected, which, especially for wings with a large density, results in a slightly unconservative value for the flutter speed.

It appeared that in almost all cases in which the aileron is completely mass-balanced, the aileron reversal speed is lower than the flutter speed. So, if the wing torsional stiffness is fixed by the requirement that the reversal speed exceeds the maximum attainable speed by a certain amount, the system will nearly always be free of flutter.

Other important conclusions reached are:

(i) Increasing wing density demands an increasing torsional stiffness (though the increase in stiffness need not be as large as to maintain the uncoupled frequency constant).

(ii) It is unfavourable to shift the flexural axis aft.

(iii) The most favourable position of the inertia axis is at about 45 % chord from the leading edge. More forward positions show a smaller aileron reversal speed and more aft positions a smaller flutter speed.

(iv) For constructions with small wing density, structural damping may have a very beneficial effect.

(v) If there is some damping, the most unfavourable situation is nearly always that, in which the ailerons can be deflected freely.

Contents.

1 Introduction.

This paper is to be considered as a continuation of the reports

(i) V. 1297 "Diagrams of critical flutter speed for wings of a certain standard type" (ref. 1), in which the flutter speed for wings of the same type as in this report is calculated, both for the case of wings without aileron and of wings with a freely deflected aileron (uncoupled aileron frequency equal to zero).

(ii) V. 1380 "The change in flutter speed due to small variations in some aileron parameters" (ref. 2).

The present report contains a series of diagrams in which the flutter, divergence and aileron reversal speeds are plotted against the squared ratio of the uncoupled frequencies of aileron deflection to wing torsion for several values of some structural wing parameters. The diagrams are obtained from calculations in which the flexural wing stiffness is neglected. No large differences are introduced by this approximation, since for most wings the natural frequencies of flexure and torsion have the ratio $^1/_3$ and it is already known (see also report V. 1297) that the flutter speed is not seriously altered if this ratio is changed from $^1/_3$ to zero (using the same modes of displacement in both cases). The results are checked by a small number of appropriate calculations in which the uncoupled frequencies again have the ratio $^1/_3$.

As in the previous reports, the modes of displacement of the wing are introduced as definite real functions i. e. not permitting any variations of phase along the span.

It is expected that the diagrams of the three reports together will give an even quantitatively useful picture of the variation of the flutter speed for many aeroplanes of simple construction. It will certainly often be possible to conclude in which sense the flutter speed (or aileron reversal speed) will change as the result of certain structural modifications.

Though fuselage mobility is always neglected, the diagrams will perhaps be a little more accurate for symmetric oscillations than for anti-symmetric ones, since the modes of displacement used in this report, resemble more symmetric than anti-symmetric modes.

2 The wing-aileron model.

2.1 *General shape.*

This was already described in report V. 1297 and thus may be omitted here except for the following points:

(I) Since no sweep-back effects have been considered, the flexural axis must be perpendicular to the wing root.

(II) The aileron is controlled in the section $y = {}^3/_4\, b$. It is statically balanced in such a way, that the centre of gravity of every section lies in the hinge axis.

2.2 *Elasticity assumptions.*

The elasticity of the control cables is represented by the symbol k_r. Assuming that the control stick is fixed (symmetric oscillations), the aileron is subject to a moment [1])

$$-k_r \{\gamma - \varphi\,({}^3/_4\, b)\}\,,$$

[1]) Moments are positive if they tend to move the trailing edge downwards.

while an equally large but opposite moment, also in the section $y = {}^3/_4\, b$, is acting on the wing.

The same assumptions as in report V. 1297 are introduced for flexural and torsional stiffnesses of wing and aileron, for the modes of displacement and for the structural damping.

2.3 *The neglect of the flexural stiffness of the wing.*

The neglect of the flexural stiffness signifies in fact, that terms containing a factor $\left(\frac{\nu_A}{\nu}\right)^2$ are omitted in the calculations. This will in general be permitted for wings with statically balanced ailerons if $\nu_A{}^2$ is small compared with $\nu_B{}^2$, since the critical frequency ν for such wings is of the same order as ν_B. The ratio $\frac{\nu_A}{\nu_B}$ is usually so small (about $^1/_3$) that the neglect mentioned has only little influence on the flutter speed. It is not necessary that $\nu_A{}^2$ is also small compared with $\nu_C{}^2$ since wing flexure-aileron oscillations never become unstable if the aileron is mass-balanced.

For three cases (13, 14, 15, see fig. 5) calculations were performed with $\nu_A = 0$ and with $\frac{\nu_A}{\nu_B} = {}^1/_3$. The results show only a slight difference, even when ν_C is small.

Since the introduced mode of deformation has the character of a fundamental, the flexure appearing at the critical oscillation must have the same character, as otherwise the calculation loses its justification. This means that in fact the flexural stiffness and also the ratio $\left(\frac{\nu_A}{\nu_B}\right)^2$ must be so large, that the uncoupled frequency of the first flexural overtone turns out to be sufficiently greater than ν_B.

For most aeroplanes the flexural stiffness satisfies these requirements. The neglect, producing a substantial reduction of the computational work without seriously influencing the results, may be justified sufficiently by the considerations given above.

2.4 *Aerodynamic assumptions.*

The aerodynamic forces are introduced in accordance with the theory of Küssner and Schwarz (ref. 3) for the limiting case of a sealed gap between wing and aileron. In this case a certain value must be assumed for the gap width. It was shown in report V. 1297 that there exists a relation between the gap width and the aerodynamic aileron balance at $\omega = 0$. The calculations are performed for two values of these parameters, viz.

$$\eta_s = 0{,}3048 \cdot 10^{-3},\ n = 80\ \%\ \text{ and }\ \eta_s = 7{,}881 \cdot 10^{-3},\ n = 62{,}4\ \%.$$

It is recommended by Theodorsen and Garrick (ref. 4) to choose for η_s values between $0{,}025\ \varepsilon_1$ and $0{,}20\ \varepsilon_1$. In the present investigation, where $\varepsilon_1 = 0{,}10$, this means that

$2{,}5.10^{-3} < \eta_s < 20.10^{-3}$ or $57{,}3\ \% < n < 68{,}6\ \%$,

which shows that the calculations with $n = 80\ \%$ will probably agree less with reality than those with $n = 62{,}4\ \%$.

When the calculations were begun, the work of Theodorsen and Garrick was not yet available in Holland. The results of V. 1297, however, did already point to a similar conclusion.

2.5 *Values of the parameters.*

These were chiefly the same as in report V. 1297, but may be repeated here for convenience sake

$$\begin{array}{rrrrr} \varepsilon = & -0{,}1 & 0{,}1 & 0{,}3 & \\ \varepsilon + \sigma = & 0{,}1 & 0{,}3 & 0{,}5 & \\ \mu = & 5 & 15 & 30 & \\ n = & 80 & 62{,}4\ \% & (\eta_s = 0{,}3048.10^{-3} & \text{resp.} \\ h = & 0 & 0{,}1 & 7{,}881.10^{-3}) & \end{array}$$

$x = 0{,}6 \quad \eta = 0{,}25 \quad \varepsilon_1 = 0{,}10 \quad \mu_1 \kappa_1^2 = 0{,}05.$

3 General method of solution.

3.1 *Flutter speed.*

The equations of motion for the wing are:

$$\left.\begin{aligned} m_{11}\ddot{z} + m_{12}\ddot{\varphi} + (Bz'')'' &= K, \\ m_{12}\ddot{z} + m_{22}\ddot{\varphi} - (T\varphi')' - k_r(\gamma - \varphi)\delta(y - {}^3/_4 b) &= \\ = M + \varepsilon l K - N - \varepsilon_1 l R, & \end{aligned}\right\} \quad (3.1)$$

where $\delta(y - y_1)$ is a singular function defined by

$$\delta(y - y_1) = 0 \text{ if } y \neq y_1 \text{ and}$$

$$\int_{y_1^-}^{y_1^+} \delta(y - y_1)\,dy = 1 \text{ if } y_1^- < y_1 < y_1^+ \quad (3.2)$$

The term $(Bz'')''$ vanishes in the calculations with zero flexural stiffness.

The equation of motion for the aileron, which is torsionally rigid, is

$$\ddot{\gamma} \int_{1/8\,b}^{b} m_{33}\,dy + k_r \{ \gamma - \varphi({}^3/_4 b) \} = \int_{1/8\,b}^{b} (N + \varepsilon_1 l R)\,dy. \quad (3.3)$$

The method of solution is essentially the same as that described in V. 1297. The first step is to substitute in the equations (3.1) and 3.3):

$$z = l_i q_1 e^{i\nu\tau} z_1(y)\,;\ \varphi = q_2 e^{i\nu\tau} \varphi_1(y)\,;\ \gamma = q_3 e^{i\nu\tau}, \quad (3.4)$$

where q_1, q_2 and q_3 are unknown coefficients, while $z_1(y)$ and $\varphi_1(y)$ are the assumed modes of displacements of the wing.

The problem is now reduced to the determination of approximate values of ν, q_1, q_2 and q_3. This is done by multiplying the two equations (3.1) with weight functions

$$\frac{3w^2 - w^3}{6} \text{ and } w, \text{ where } w = \frac{y}{b},$$

and integrating the result from $y = 0$ to $y = b$. Together with (3.3) three linear homogeneous equations are obtained, of which the determinant must vanish, if a non-trivial solution exists. The flutter speed follows from this condition as a function of the ratio $\left(\frac{v_C}{v_B}\right)^2$.

3.2 *Divergence speed.*

The divergence speed is calculated in quite the same way as already was described in report V. 1297.

3.3 *Aileron reversal speed.*

To calculate the wing torsion due to aileron deflection the condition of equilibrium for the moments about the flexural axis is considered. This is the second eq. (3.1), changing for a stationary state into

$$-(T\varphi')' - k_r \left(\gamma - \varphi - \frac{1}{n}\chi\right)\delta(y - {}^3/_4 b) = |M + \varepsilon l K - N - \varepsilon_1 l R|_{\text{stat.}}, \quad (3.5)$$

in which χ denotes the angle over which the control column is deflected and n a gear ratio. If the control cables showed no elasticity, n would be equal to $\frac{\chi}{\gamma - \varphi}$.

Like the flutter and divergence speed, the aileron reversal speed is only calculated in a first approximation. This means that the wing torsion is again assumed in agreement with the mode φ_1. The amount of torsion, given by q_2, is obtained by multiplication of (3.5) by the weight function w and successive integration over the span. The result is a relation between q_2 and q_3.

A second relation between q_2 and q_3 follows from the definition of the aileron reversal-speed, which says that at this speed the rolling moment due to aileron deflection vanishes. Both relations become lineair, homogeneous equations permitting calculations of the speed at which their determinant vanishes. This speed is identical with the aileron reversal speed.

4 Results.

4.1 *General.*

Flutter, divergence and aileron reversal speed, reduced to dimensionless form, are plotted in figs. 1—6 against the ratio $\left(\frac{v_C}{v_B}\right)^2$. The full lines on which calculated points are specially marked denote the flutter speed. Points referring to the same values of the reduced frequency are connected by dashed lines, the numbers near these lines denoting the reduced frequency at the wing root. The divergence and aileron reversal speeds are represented by dash-dot lines.

It appears that in most of the cases investigated, the admissible speed of the construction is determined by the speed at which the ailerons still function normally. In other words, the construction must be so torsionally rigid that no aileron

reversal occurs, which implies practically always freedom from flutter (for completely mass-balanced ailerons!).

4.2 *Influence of wing density.*

All calculated speeds rise if μ increases and the uncoupled frequencies are kept constant (fig. 7). If instead the stiffnesses remain constant, the effect is that all speeds decrease. This decrease is greater if μ_1 also increases and the elasticity of the cables remains constant (but $\mu_1\kappa_1^2$ remains at the value 0,05).

4.3 *Influence of position of flexural axis.*

The widespread opinion that it is favourable to shift the flexural axis aft, is not supported by these investigations. If this axis is shifted aft, it has already been shown in report V. 1297 that for a wing without aileron (or for a wing with an aileron of which the uncoupled frequency is infinitely large) the flutter speed decreases until the flexural axis closely approaches the inertia axis (i. e. to a distance of about 10 % of the chord) and only for still greater proximity of these axes again begins to increase. If, however, the aileron frequency falls, this last increase becomes less definite and ultimately vanishes (figs. 4—6).

The decrease in flutter speed due to shifting the flexural axis aft is particularly large if $\nu_C < \nu_B$. If the flexural axis lies in front of the quarter chord axis, divergence occurs only for very high speeds. Aileron reversal speed becomes smaller if the flexural axis is shifted aft.

4.4 *Influence of the position of the inertia axis.*

If the inertia axis is shifted aft, the flutter speed in general decreases. Only if $\nu_C < \nu_B$, the wing density is small and there is almost no damping, the opposite effect can occur. Divergence and aileron reversal speeds reach their minimum values (keeping ν_B constant) if inertia and flexural axes coincide while otherwise it is of no importance for these two speeds, which of these axes lies foremost. If instead of ν_B, the torsional stiffness is kept constant, divergence and aileron reversal speed become independent of the position of the inertia axis.

Combining these conclusions it can be said that there is a most favourable position for the inertia axis, namely at about 45 % chord from the leading edge. More aft positions decrease the flutter speed, while for more forward positions the aileron reversal speed decreases (ν_B constant).

4.5 *Influence of the aerodynamic aileron balance.*

For freely deflecting ailerons the flutter speed for $n = 80$ % is slightly above that for $n = 62{,}4$ %. For completely inelastic cables ($\nu_C = \infty$) the flutter speed becomes nearly independent of n. In most cases, however, from a certain, usually rather small, value of ν_C the flutter speed for $n = 80$ % is lower than that for $n = 62{,}4$ %. The differences are not large.

The divergence speed is, especially for negative values of ε, smaller for $n = 80$ %. The aileron reversal speed also is smaller for $n = 80$ %.

4.6 *Influence of flexural stiffness.*

The neglect of the flexural stiffness ($\nu_A = 0$) tends to give unconservative values for the flutter speed, especially if μ is large. The difference amounts to about 10 % if $\nu_A = {}^1/_3\,\nu_B$ and $\mu = 15$ or 30 (fig. 5). The two other speeds calculated are independent of the flexural stiffness.

4.7 *Influence of wing torsional stiffness.*

It is well-known that an increase in torsional stiffness is nearly always favourable to the prevention of aero-elastic difficulties. For constructions where the inertia axis coincides with the flexural axis or lies in front of it, an increase in torsional stiffness may lead to flutter, which, however, can be suppressed by a small amount of damping and which vanishes completely if the torsional stiffness is still further increased.

4.8 *Influence of the elasticity of control cables.*

The change in the speeds investigated can be read immediately from figs. 1—6. In the absence of damping there exists a minimum flutter speed at $\nu_C \sim \nu_B$ in the cases $n = 80$ % and at $\nu_C \sim 0{,}8\,\nu_B$ if $n = 62{,}4$ %. The minimum disappears if the inertia axis is far beyond the quarter chord axis. Consequently, only for damped constructions (though the damping need not be large) freely deflected ailerons form the most unfavourable condition. Divergence speed increases with ν_C^2, but aileron reversal speed is unaffected by ν_C^2.

4.9 *Influence of structural damping.*

Structural damping always increases the flutter speed. The influence of this parameter is most pronounced for large values of μ. Damping increases the flutter speed less if the inertia axis is shifted aft.

5 List of symbols.

The notations are the same as in report V. 1297, but the following symbols are added:

k_r elasticity of the aileron control cables
ν_C uncoupled aileron frequency
χ angle of deflection of control column.

6 List of references.

1 van de Vooren, A. I. and Greidanus, J. H.: "Diagrams of critical flutter speed for wings of a certain standard type". Report V. 1297. Vol. XIII of the Reports and Transactions of the National Aeronautical Research Institute (1946) Amsterdam.

2 van de Vooren, A. I.: "The change in flutter speed due to small variations in some aileron parameters". Report V. 1380. Vol. XIII, see ref. 1.

3 Küssner, H. G. and Schwarz, L.: "Der schwingende Flügel mit aerodynamisch ausgeglichenem Ruder", Luftfahrtforschung Vol. 17, 337 (1940).

4 Theodorsen, Th. and Garrick, I. E.: "Non stationary flow about a wing-aileron-tab combination including aerodynamic balance, N. A. C. A. report No. 736 (1942).

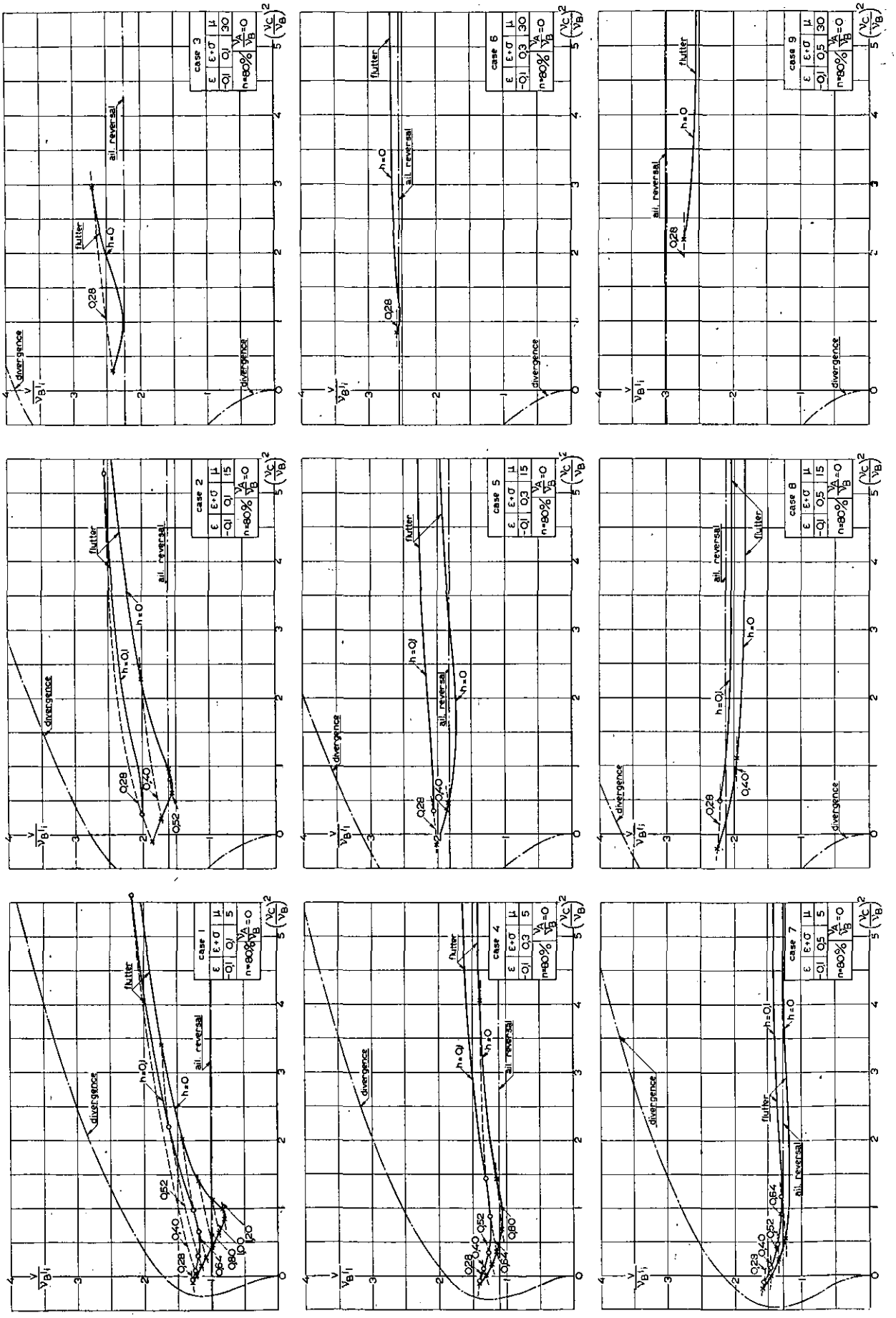
case 1
case 2
case 3
case 4
case 5
case 6
case 7
case 8
case 9
divergence
flutter
ail. reversal
h=0
h=0.1

Fig. 1.

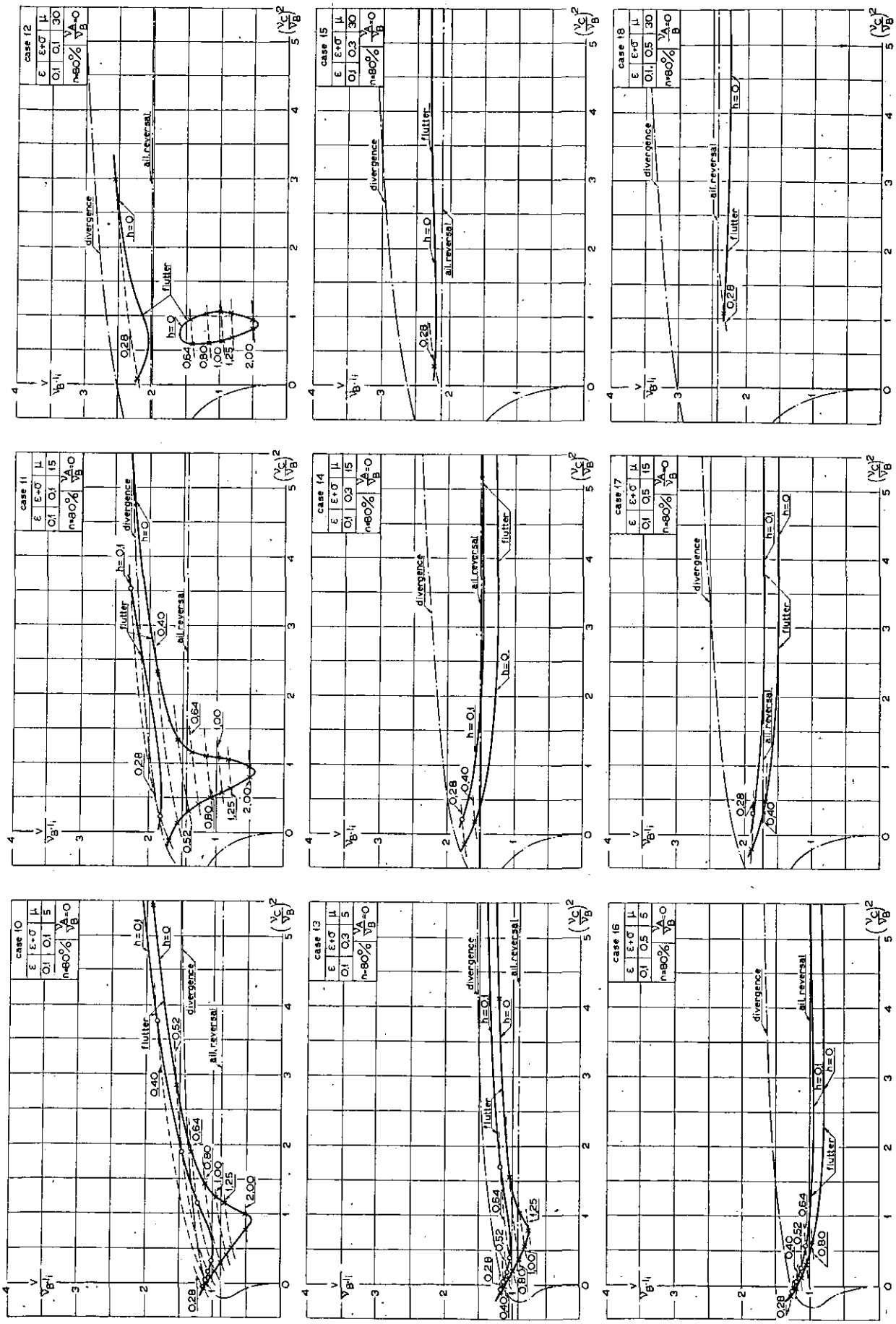
case 12
case 11
case 10
case 15
case 14
case 13
case 18
case 17
case 16
divergence
flutter
ail. reversal
h=0
h=0.1

Fig. 2.

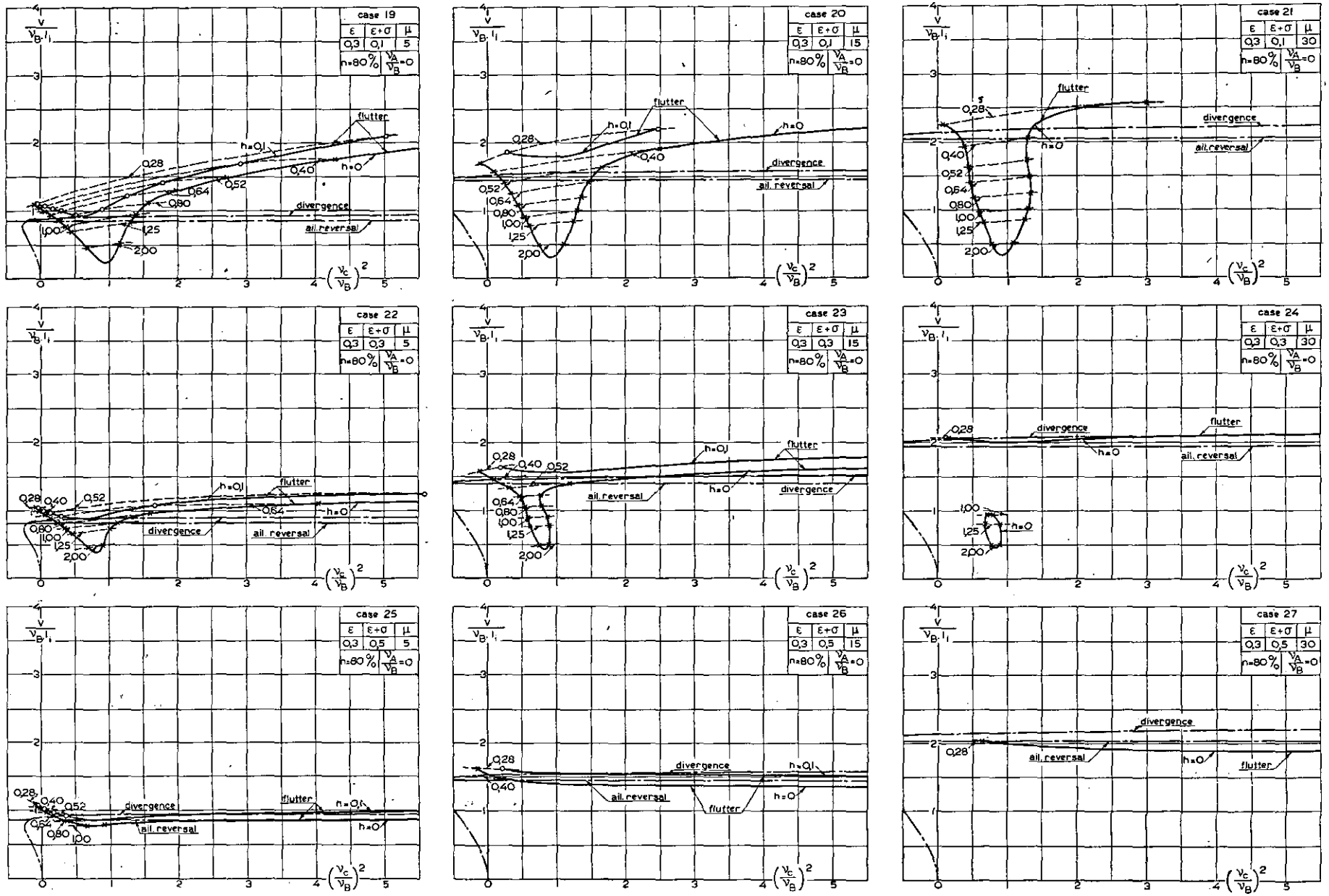
case 19
ε | ε+σ | μ
0,3 | 0,1 | 5
η=80% | $\frac{v_A}{v_B}$=0
case 20
ε | ε+σ | μ
0,3 | 0,1 | 15
η=80% | $\frac{v_A}{v_B}$=0
case 21
ε | ε+σ | μ
0,3 | 0,1 | 30
η=80% | $\frac{v_A}{v_B}$=0
case 22
ε | ε+σ | μ
0,3 | 0,3 | 5
η=80% | $\frac{v_A}{v_B}$=0
case 23
ε | ε+σ | μ
0,3 | 0,3 | 15
η=80% | $\frac{v_A}{v_B}$=0
case 24
ε | ε+σ | μ
0,3 | 0,3 | 30
η=80% | $\frac{v_A}{v_B}$=0
case 25
ε | ε+σ | μ
0,3 | 0,5 | 5
η=80% | $\frac{v_A}{v_B}$=0
case 26
ε | ε+σ | μ
0,3 | 0,5 | 15
η=80% | $\frac{v_A}{v_B}$=0
case 27
ε | ε+σ | μ
0,3 | 0,5 | 30
η=80% | $\frac{v_A}{v_B}$=0
$\frac{v}{v_B \cdot l_1}$
$\left(\frac{v_c}{v_B}\right)^2$
flutter
divergence
ail. reversal
h=0,1
h=0
0,28
0,40
0,52
0,64
0,80
1,00
1,25
2,00

Fig. 3.

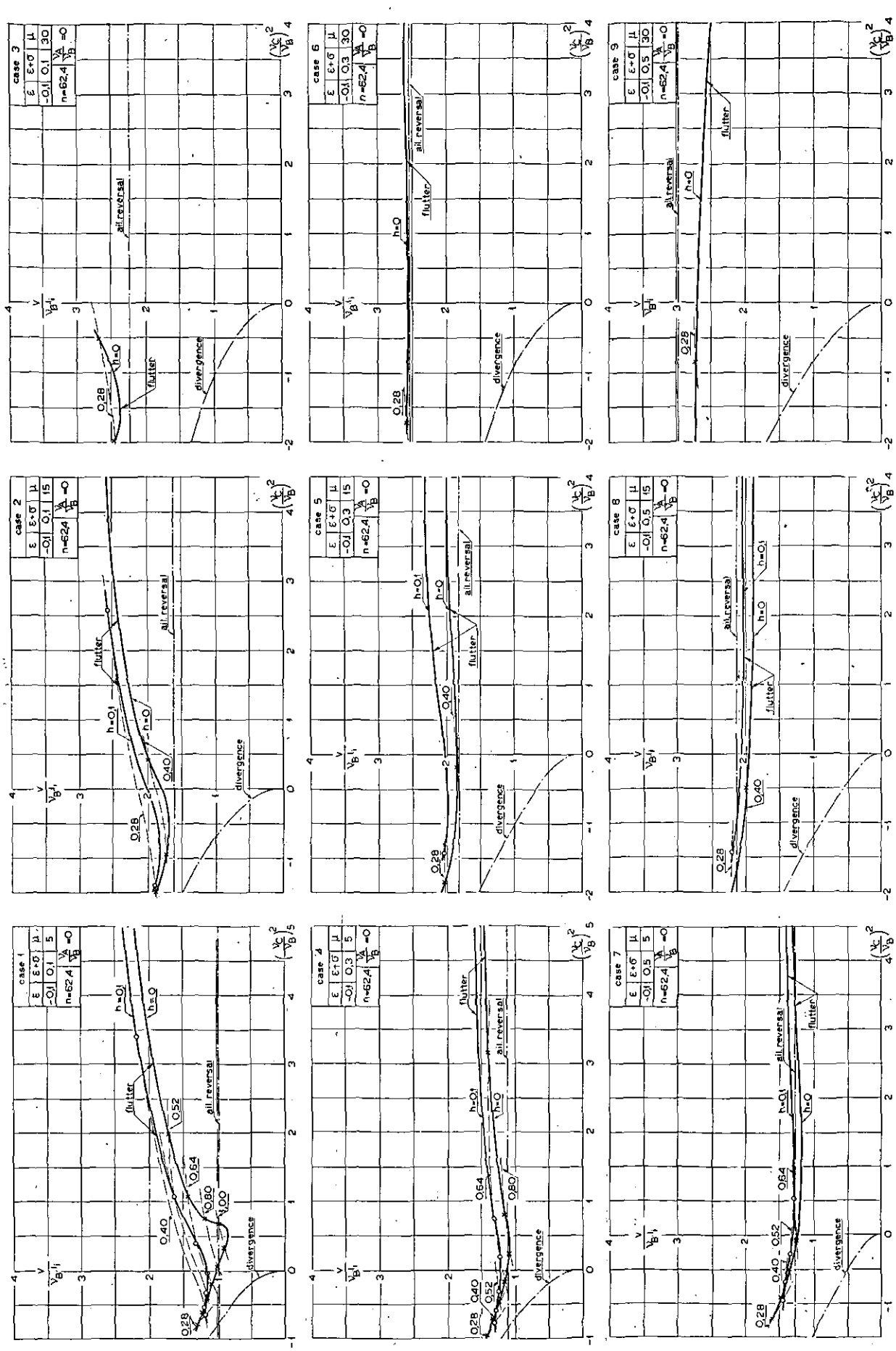
case 1
case 2
case 3
case 4
case 5
case 6
case 7
case 8
case 9
flutter
divergence
ail reversal
h=0
h=-0,1
0,28
0,40
0,52
0,64
0,80
1,00

Fig. 4.

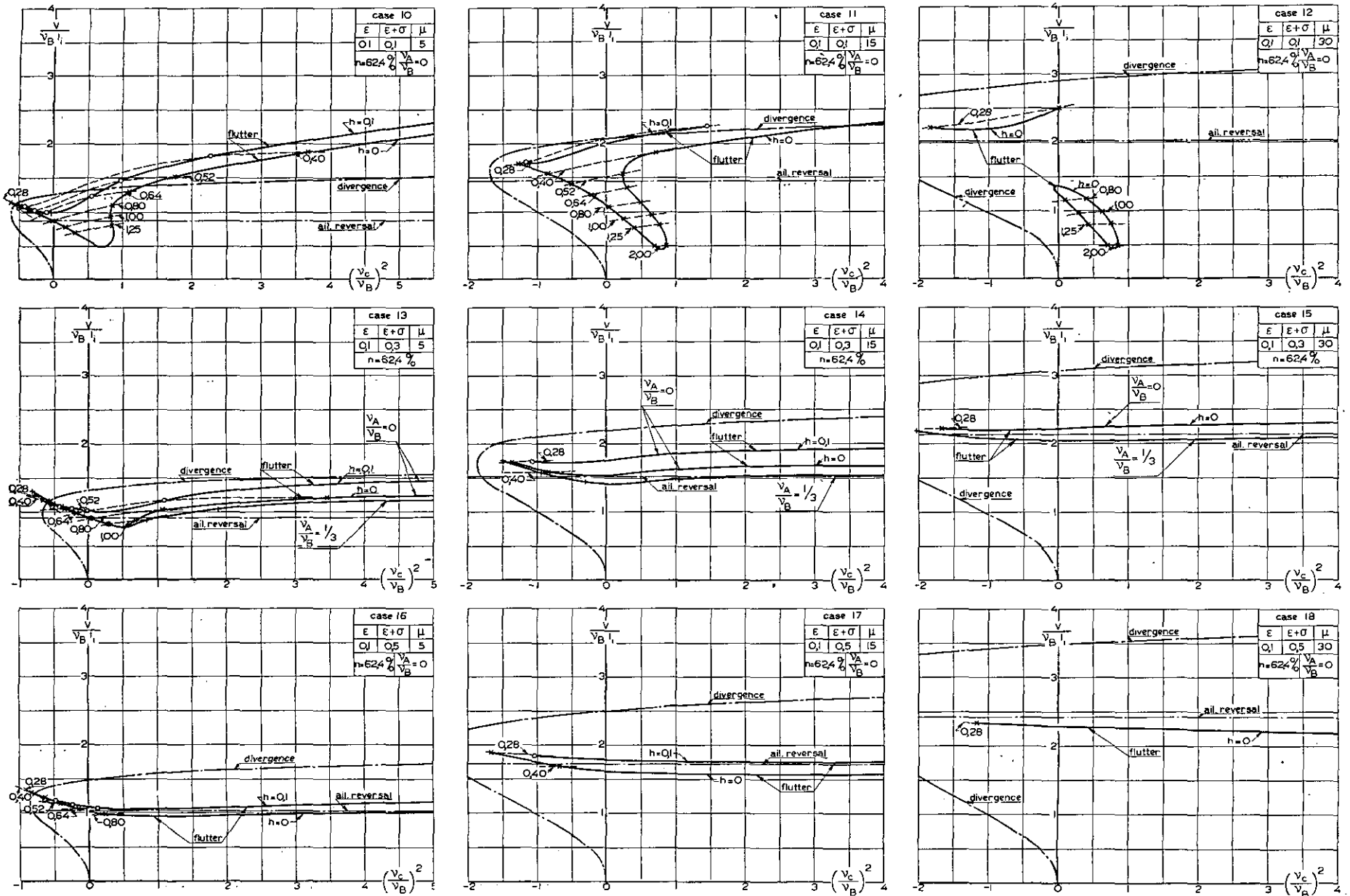
case 10
ε | ε+σ | μ
0,1 | 0,1 | 5
n=62,4 % νA/νB=0
case 11
ε | ε+σ | μ
0,1 | 0,1 | 15
n=62,4 % νA/νB=0
case 12
ε | ε+σ | μ
0,1 | 0,1 | 30
n=62,4 % νA/νB=0
case 13
ε | ε+σ | μ
0,1 | 0,3 | 5
n=62,4 %
case 14
ε | ε+σ | μ
0,1 | 0,3 | 15
n=62,4 %
case 15
ε | ε+σ | μ
0,1 | 0,3 | 30
n=62,4 %
case 16
ε | ε+σ | μ
0,1 | 0,5 | 5
n=62,4 % νA/νB=0
case 17
ε | ε+σ | μ
0,1 | 0,5 | 15
n=62,4 % νA/νB=0
case 18
ε | ε+σ | μ
0,1 | 0,5 | 30
n=62,4 % νA/νB=0
V/νB l1
(νc/νB)²
flutter
divergence
ail. reversal
h=0,1
h=0
νA/νB=0
νA/νB=1/3
0,28
0,40
0,52
0,64
0,80
1,00
1,25
2,00

Fig. 5.

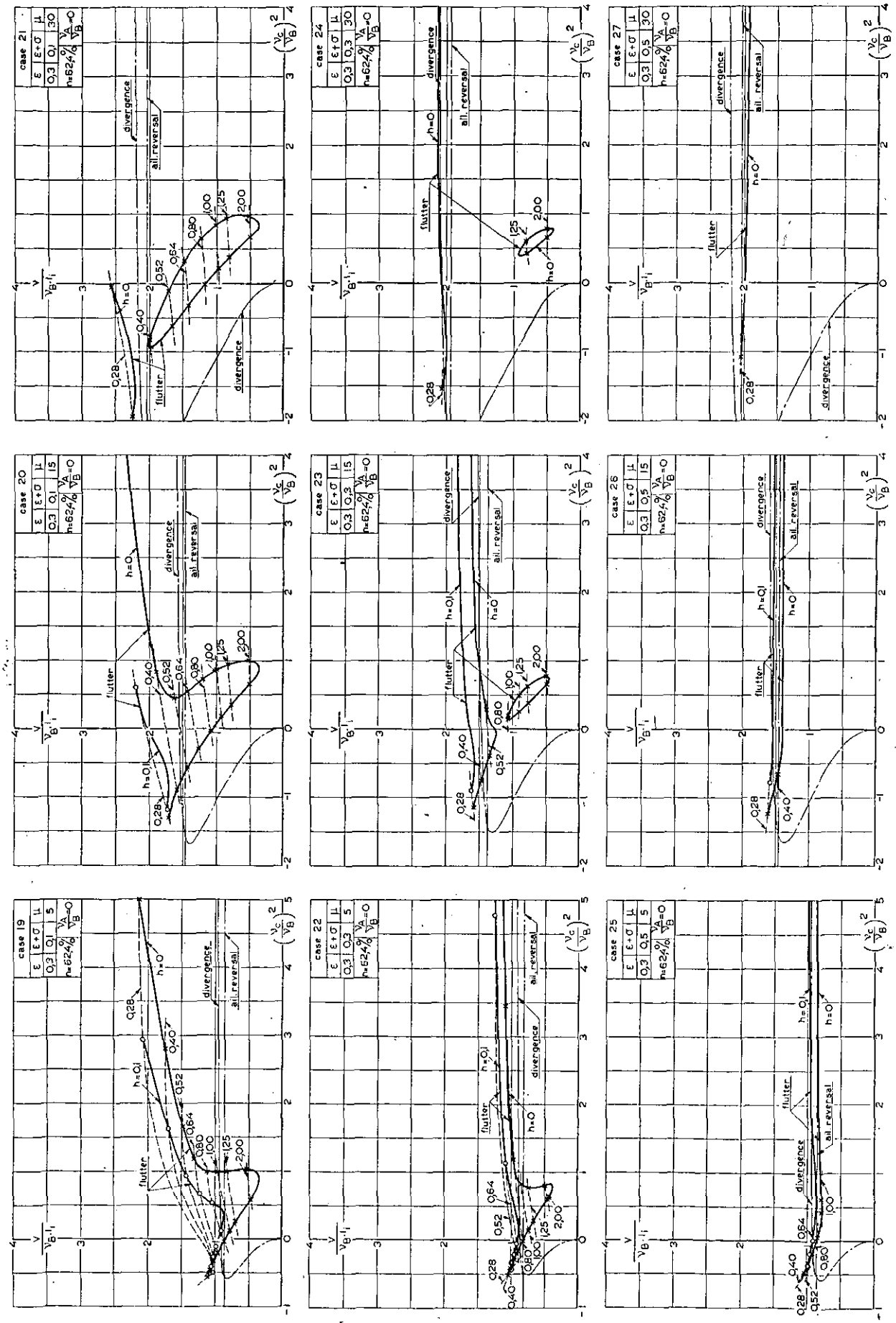
case 19
case 20
case 21
case 22
case 23
case 24
case 25
case 26
case 27
flutter
divergence
ail. reversal
h=0
h=0,1

Fig. 6.

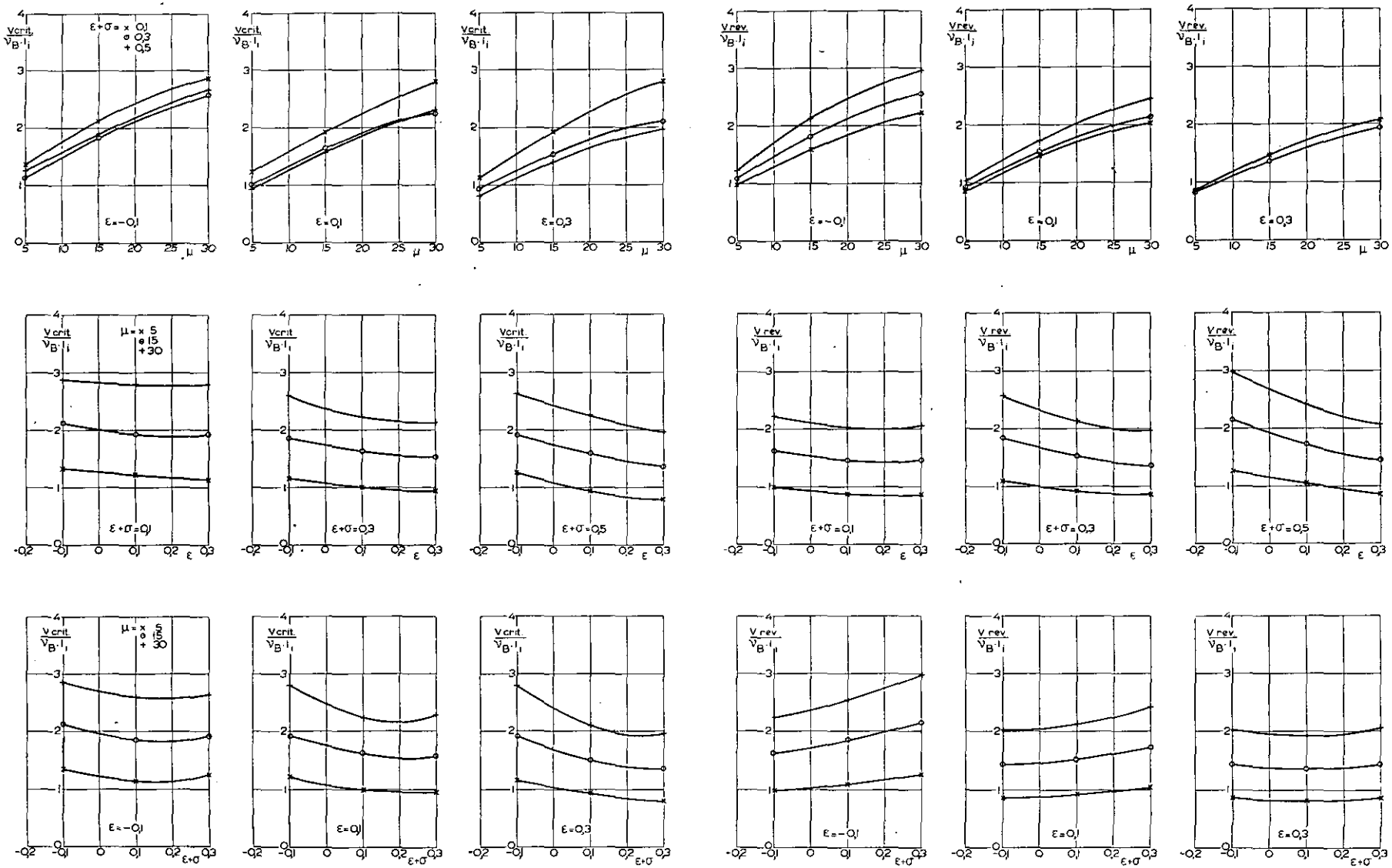

Fig. 7. Flutter speed and aileron reversal speed as functions of μ, ε and $\varepsilon + \sigma$ for $n = 62.4\ \%$, $\frac{v_A}{v_B} = 0$, $\frac{v_C}{v_B} = 1$.

REPORT V. 1366.

A Method to Determine the Change in Flutter Speed due to Small Changes in the Mechanical System

by

Ir. A. I. VAN DE VOOREN.

Summary.

In this paper a method is developed to evaluate the influence on flutter speed of small structural changes of the aeroplane, without performing another complete flutter calculation. Use is made of the results, obtained from the flutter calculation of the aeroplane in its original state.

Contents.

1 Introduction.

The flutter speed of an aeroplane depends in a very complicated way upon a large number of structural parameters. Its calculation requires, even for definite values of the complete set of *parameters, very laborious computations. This in*convenience is even more serious if large parts of the work must be repeated many times in order to establish the influence of changes in the aeroplane construction or to survey the possible consequences of *doubtful fundamental data. In view* of the common occurrence of such complications, a simplified method to evaluate corrections of a calculated flutter speed, representing the effect of small changes in the parameters, might be of considerable interest.

It appears possible to attain this object by the application of common perturbation methods to the system of linear, homogeneous, algebraic equations — containing definite modes of deformation — which may be assumed to represent the basis of the original flutter calculation (for the "imperturbed" state). Usually, it will be sufficient to take into account only the first order effects of the applied perturbations, but theoretically the procedure can be continued to higher approximations. Yet, these higher approximations imply computations, which rapidly regain an inconvenient extension and are, hence, of little interest.

A considerable part of the first order calculation appears to be independent of the applied variation. Consequently, the advantages of the perturbation method are the more sensible if the influence of several distinct variations has to be investigated.

2 The problem.

The set of linear, homogeneous, algebraic equations, determining the characteristic values of the *frequency ν, and constituting the basis of the per*turbation method, can be written in the following, general form

$$\begin{aligned}
&q_1(\nu^2 A_{11} - E_{11}) + q_2(\nu^2 A_{12} - E_{12}) + \ldots\ldots\ldots\ldots + q_n(\nu^2 A_{1n} - E_{1n}) = 0,\\
&q_1(\nu^2 A_{21} - E_{21}) + q_2(\nu^2 A_{22} - E_{22}) + \ldots\ldots\ldots\ldots + q_n(\nu^2 A_{2n} - E_{2n}) = 0,\\
&\qquad\vdots\qquad\qquad\qquad\vdots\qquad\qquad\qquad\qquad\qquad\vdots\\
&q_1(\nu^2 A_{n1} - E_{n1}) + q_2(\nu^2 A_{n2} - E_{n2}) + \ldots\ldots\ldots\ldots + q_n(\nu^2 A_{nn} - E_{nn}) = 0,
\end{aligned}$$

or, written in a shortened notation, which will be retained henceforward:

$$\sum_l q_l\,(\nu^2 A_{kl} - E_{kl}) = 0, \qquad k, l = 1 \ldots n. \quad (2,1)$$

The unknowns q_l determine the amplitude ratios between the assumed modes of deformation. The *generally complex elements A_{kl} depend among* others on the reduced velocity V_0 $(= \frac{v}{\nu c_0}$, where v.

denotes the speed and c_0 a reference chord).

Eqs. (2, 1) have, for a given value of V_0, n independent complex solutions

$$\nu^2 = \nu_i^2, \; q_l = (q_l)_i, \qquad i, l = 1 \dots n. \quad (2, 2)$$

Any slight change in the construction of the system will lead to small alterations of the values of one or more of the coefficients A_{kl}, E_{kl} of eqs. (2, 1). Hence, the basic equations of the varied system may be expressed by

$$\sum_l q_l \{ \nu^2 (A_{kl} + \alpha_{kl}) - (E_{kl} + \varepsilon_{kl}) \} = 0. \quad (2, 3)$$

The terms with factors α_{kl} or ε_{kl} will, in any equation, be small, compared with at least one of the other terms. It is just this property, which makes, that the results obtained with neglect of all terms, containing second or higher powers of α_{kl} or ε_{kl}, already have great practical value.

The problem shows some resemblance to a problem, dealt with by Courant and Hilbert (ref. 1).

3 Bi-orthogonality relation.

Since the determinant of the set of equations (2, 1) is not symmetric, no orthogonality relation exists. Considering, however, also the adjoint set,

$$\sum_k Q_k (\nu^2 A_{kl} - E_{kl}) = 0, \qquad k, l = 1 \dots n, \quad (3, 1)$$

it is possible to derive a bi-orthogonality relation.

The eqs. (2, 1) and (3, 1) have the same series of characteristic values, since their determinants are transformed into each other by interchange of rows and columns. The solution of eqs. (3, 1) can therefore be presented by

$$\nu^2 = \nu_i^2, \; Q_k = (Q_k)_i, \; i, k = 1 \dots n. \quad (3, 2)$$

When one of the solutions (2, 2) is substituted in the eqs. (2, 1), the following identities are obtained

$$\sum_l (q_l)_j (\nu_j^2 A_{kl} - E_{kl}) = 0. \quad (3, 3)$$

Multiplication of the k-th relation (3, 3) by $(Q_k)_i$ and subsequent summation over all n identities ($k = 1 \dots n$), yields the result

$$\nu_j^2 \sum_{k,l} (q)_j (Q_k)_i A_{kl} = \sum_{k,l} (q_l)_j (Q_k)_i E_{kl}. \quad (3, 4)$$

In a similar way, namely by multiplying the identities, arisen from the substitution of the characteristic values ν_i^2 and the amplitudes $(Q_k)_i$ in the set (3, 1), by $(q_l)_j$ and then summing over l, the relation is obtained

$$\nu_i^2 \sum_{k,l} (q_l)_j (Q_k)_i A_{kl} = \sum_{k,l} (q_l)_j (Q_k)_i E_{kl}. \quad (3, 5)$$

From (3, 4) and (3, 5) the following bi-orthogonality relation can be deduced

$$\sum_{k,l} (q_l)_j (Q_k)_i A_{kl} = 0 = \sum_{k,l} (q_l)_i (Q_k)_i E_{kl}, \text{ if } i \neq j, \quad (3, 6)$$

while for $i = j$ the relation holds

$$\nu_i^2 \sum_{k,l} (q_l)_i (Q_k)_i A_{kl} = \sum_{k,l} (q_l)_i (Q_k)_i E_{kl}. \quad (3, 7)$$

4 Transformation to normal coordinates.

The transformation of the set (2, 1) to the canonical form (i.e. with vanishing elements outside the main diagonal of its determinant) can be performed in the following way.

Introduce new variables p_j, connected with the original q_l by the linear relations

$$q_l = \sum_j (q_l)_j p_j, \quad (4, 1)$$

where $(q_l)_j$ denotes the amplitude ratios already defined by (2, 2). Substitution of (4, 1) into (2, 1) leads to

$$\sum_j p_j \{ \nu^2 \sum_l (q_l)_j A_{kl} - \sum_l (q_l)_j E_{kl} \} = 0. \quad (4, 2)$$

Next, multiply these equations by $(Q_k)_i$ and add them together. The result is

$$\sum_j p_j \{ \nu^2 \sum_{k,l} (q_l)_j (Q_k)_i A_{kl} - \sum_{k,l} (q_l)_j (Q_k)_i E_{kl} \} = 0, \quad (4, 3)$$

where i may have any value from 1 to n.

Introducing

$$\left. \begin{aligned} \overline{A}_{ij} &= \sum_{k,l} (q_l)_j (Q_k)_i A_{kl}, \\ \overline{E}_{ij} &= \sum_{k,l} (q_l)_j (Q_k)_i E_{kl}, \end{aligned} \right\} \quad (4, 4)$$

(4, 3) becomes

$$\sum_j p_j (\nu^2 \overline{A}_{ij} - \overline{E}_{ij}) = 0. \quad (4, 5)$$

From the relations (3, 6) and (3, 7) it is inferred that

$$\left. \begin{aligned} &\overline{A}_{ij} = \overline{E}_{ij} = 0 \text{ if } i \neq j, \\ &\nu_i^2 \overline{A}_{ii} = \overline{E}_{ii}. \end{aligned} \right\} \quad (4, 6)$$

Hence, eqs. (4, 3) reduce to the set

$$p_i (\nu^2 - \nu_i^2) \overline{A}_{ii} = 0, \; i = 1 \dots n, \quad (4, 7)$$

which possesses the canonical form.

Obviously the solutions of (4, 7) are

$$\nu^2 = \nu_i^2, \; p_j = (p_j)_i = \delta_{ij}, \quad (4, 8)$$

where δ_{ij} denotes Kronecker's symbol, viz.

$$\delta_{ij} = \begin{cases} 0 & \text{if } i \neq j. \\ 1 & \text{if } i = j. \end{cases} \quad (4, 9)$$

5 First approximation of the characteristic values of the varied system.

When the transformation of the preceding paragraph is applied to the basic equations (2, 3) of the varied system, there will remain perturbation terms outside the main diagonal of the determinant, leading to the result

$$\sum_j p_j \{ (\nu^2 - \nu_i^2)\overline{A}_{ij} + \nu^2\overline{\alpha}_{ij} - \overline{\varepsilon}_{ij} \} = 0, \quad (5,1)$$

with

$$\overline{\alpha}_{ij} = \sum_{k,l} (q_l)_j (Q_k)_i \alpha_{kl} \text{ and}$$
$$\overline{\varepsilon}_{ij} = \sum_{k,l} (q_l)_j (Q_k)_i \varepsilon_{kl}. \quad (5,2)$$

It will again be allowed to consider the perturbation terms $\overline{\alpha}_{ij}$ resp. $\overline{\varepsilon}_{ij}$ as small quantities. Consequently, the solution of (5, 1) may be expected to admit the representation

$$\left.\begin{aligned} &\nu^2 = \nu_i^2 + \Delta\nu_i^2 \text{ with } \frac{\Delta\nu_i^2}{\nu_i^2} << 1, \\ &p_j = \delta_i^j + \Delta(p_j)_i \text{ with } \Delta(p_j)_i << 1 \text{ if } i \neq j \\ &\qquad \text{and } \Delta(p_i)_i = 0. \end{aligned}\right\} (5,3)$$

The last relation fixes the normalization of the new solutions.

Substitution of the i-th solution (5, 3) in the i-th equation (5, 1) yields, if terms of second and higher order of smallness are neglected

$$\Delta\nu_i^2 . \overline{A}_{ii} + \nu_i^2\overline{\alpha}_{ii} - \overline{\varepsilon}_{ii} = 0. \quad (5,4)$$

Hence

$$\Delta\nu_i^2 = \frac{\overline{\varepsilon}_{ii} - \nu_i^2\overline{\alpha}_{ii}}{\overline{A}_{ii}}. \quad (5,5)$$

This relation yields the first order variation of the characteristic values.

It is seen that $\Delta\nu_i^2$ can easily be calculated if the numbers $\overline{A}_{ii}$, $\overline{\alpha}_{ii}$ and $\overline{\varepsilon}_{ii}$ are known. Now, the $\overline{A}_{ii}$ and the products $(q_l)_i(Q_k)_i$ appearing in the formulae (5, 2) are independent of the assumed variation. Hence, this part of the computation can be carried out once for all, irrespective of the kind of variation, which means that the labour involved in the calculation of $\Delta\nu_i^2$ for a second variation is much less extensive than that for the first variation.

6 First approximation of the amplitude values of the varied system.

When the i-th system (5, 3) is substituted in the h-th equation (5, 1), the amplitude ratios are obtained. With the aid of (4, 6) this substitution yields, after neglect of terms of second and higher order,

$$\nu_i^2\overline{\alpha}_{hi} - \overline{\varepsilon}_{hi} + \Delta(p_h)_i (\nu_i^2 - \nu_h^2)\overline{A}_{hh} = 0,$$

or

$$\Delta(p_h)_i = \frac{\overline{\varepsilon}_{hi} - \nu_i^2\overline{\alpha}_{hi}}{(\nu_i^2 - \nu_h^2)\overline{A}_{hh}}. \quad (6,1)$$

For $h = i$, the relation

$$\Delta(p_i)_i = 0$$

was already introduced (5, 3).

By means of eq. (4, 1) the changes in the amplitudes of the set (2, 3) with regard to the amplitudes of the set (2, 1) become

$$\Delta(q_l)_i = \sum_j (q_l)_j \Delta(p_j)_i. \quad (6,2)$$

The solution of the set of equations, adjoint to (5, 1) can be written in the form

$$\left.\begin{aligned} &\nu^2 = \nu_i^2 + \Delta\nu_i^2 \quad \text{and} \quad P_j = \delta_{ij} + \Delta(P_j)_i, \\ &\qquad \text{with} \quad \Delta(P_i)_i = 0. \end{aligned}\right\} (6,3)$$

In the same way as $\Delta(p_h)_i$ the first approximation of $\Delta(P_h)_i$ becomes equal to

$$\Delta(P_h)_i = \frac{\overline{\varepsilon}_{ih} - \nu_i^2\overline{\alpha}_{ih}}{(\nu_i^2 - \nu_h^2)\overline{A}_{hh}} \quad (6,4)$$

and similar to (6, 2)

$$\Delta(Q_l)_i = \sum_j (Q_l)_j \Delta(P_j)_i. \quad (6,5)$$

7 Higher approximations of characteristic values and amplitude ratios of the varied system.

Retaining perturbation terms of the first and second order when the i-th solution (5, 3) is substituted in the i-th equation (5, 1), the following relation is obtained

$$\sum_j \Delta(p_j)_i (\nu_i^2\overline{\alpha}_{ij} - \overline{\varepsilon}_{ij}) +$$
$$+ \{ \Delta\nu_i^2 . \overline{A}_{ii} + (\nu_i^2 + \Delta\nu_i^2)\overline{\alpha}_{ii} - \overline{\varepsilon}_{ii} \} = 0, \quad (7,1)$$

with $\Delta(p_j)_i$ in accordance with (6, 1) and (5, 3). It is allowed to substitute the result (5, 5) for $\Delta\nu_i^2$ in the term $\Delta\nu_i^2 . \overline{\alpha}_{ii}$, since $\overline{\alpha}_{ii}$ itself is small of the first order. Thereafter $\Delta\nu_i^2$ can be solved, which gives

$$\Delta\nu_i^2 = \frac{\overline{\varepsilon}_{ii} - \nu_i^2\overline{\alpha}_{ii}}{\overline{A}_{ii}} \left(1 - \frac{\overline{\alpha}_{ii}}{\overline{A}_{ii}}\right) +$$
$$+ \sum_{j \neq i} \frac{(\overline{\varepsilon}_{ji} - \nu_i^2\overline{\alpha}_{ji})(\overline{\varepsilon}_{ij} - \nu_i^2\overline{\alpha}_{ij})}{(\nu_i^2 - \nu_j^2)\overline{A}_{ii}\overline{A}_{jj}}, \quad (7,2)$$

being obviously the second approximation for the change in the characteristic value. The second approximation for the amplitude ratios can be obtained by neglecting terms of third and higher order after substitution of the i-th solution (5, 1) in the h-th equation (5, 3). In principle, this procedure can be continued to approximations of any order. Such continuations are, however, of little value in consequence of the rapidly growing extension of the formulae involved. Thus, there is not much reason to proceed beyond the results given above.

8 The change in the flutter speed.

In report V. 1384 (ref. 2) it is shown that it is possible to define by

$$h = -\frac{Im\ |\nu_i^2|}{Re\ |\nu_i^2|} \quad (8,1)$$

a structural damping (h denotes the phase lead of the elastic restoring force in regard to the displacement), to which corresponds the flutter speed

$$v_{crit} = V_0 c_0 \sqrt{Mod\,|\,\nu_i^2\,|}. \qquad (8,2)$$

Carrying out the calculation for several values of the reduced velocity V_0, a curve, connecting v_{crit} with h, may be obtained.

Substituting in the formulae (8,1) and (8,2) $\nu_i^2 + \Delta\nu_i^2$ instead of ν_i^2, again for a sequence of values of V_0, a similar curve is obtained, referring to the varied system. The change of the flutter speed at constant damping can immediately be deduced from the difference of both curves. Formula (8,2) alone, with $\nu_i^2 + \Delta\nu_i^2$ instead of ν_i^2, gives the change of the flutter speed at constant reduced velocity.

9 List of references.

1. Courant, R. and Hilbert, D.: "Methoden der mathematischen Physik", part I, chapter I, par. 6, Variierte Systeme, Springer, Berlin.
2. Greidanus, J. H.: "Mathematical methods of flutter analysis", Appendix II: Structural damping. Reports and Transactions of the National Aeronautical Research Institute. Vol. XIII (1946), Amsterdam.

REPORT V. 1384.

Mathematical Methods of Flutter Analysis

by

Dr J. H. GREIDANUS.

Contents.

1 Introduction.

A large part of the work on the flutter problem, carried out during the war by our Institute, was devoted to the theoretical methods of flutter analysis and their application, especially to wing-aileron systems. Many of the results have been published in two reports (ref. 1 and 2) written in Dutch and therefore accessible to a small circle of readers only. In order to promote the international exchange of technical knowledge and of results of

research we have decided to compile a detailed review in English language of our work, using the opportunity to present the results in an improved form, which continued investigation has made possible.

The present paper is the first part of this review. It must be said that the title promises something too much, for we have not tried to reach completeness. Remarking that the wing-aileron system is at the base of all discussions, the table of contents will give a good picture of the scope of the work.

Use is made of a simple formal representation of the aerodynamic forces, taking part in the dynamics of flutter. It depends upon widely used simplifying assumptions. No attention has been paid to the development of this representation of the aerodynamic forces, since a separate paper will treat the methods, used on this point in our flutter work.

Perhaps a third and last report will deal with the numerical application of the theoretical methods of flutter prediction.

2 Fundamental differential equations.

2.1 *Assumptions.*

In order to establish the equations, governing the oscillations of a (fuselage-) wing-aileron system, we assume that (y being a coordinate along a "reference axis" in the plane of the wing, and t the time)

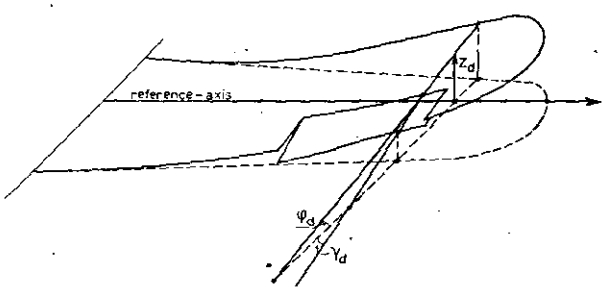

Fig. 1.

a. the most general *deformation* of the wing can be decomposed in accordance with fig. 1 into "flexure", defined by linear displacements (with respect to the plane of vanishing distortion) of the points of the reference axis, and "torsion", defined by angular displacements (with respect to the same plane) about the reference axis. The flexure is represented by the function $z_d(y, t)$ and the torsion by the function $\varphi_d(y, t)$.

b. the most general *deformation* of the aileron consists of "flexure", fitting exactly to the deformation of the wing at the place of the hinge axis, and "torsion" about the hinge axis[1]). Moreover, a "deflection" of the aileron may occur, to be defined by the angle between the aileron chord and the plane of (completely) vanishing distortion in the cross section, where the control mechanism acts on the aileron. (The complication, arising if this occurs in more than one section will not be considered). Deflection and torsion of the aileron will be concentrated into one single function $\gamma_d(y, t)$ (see fig. 1).

c. the elastic stiffness of wing and aileron may be represented with sufficient accuracy by continuous functions of the coordinate y with (as far as necessary) continuous derivatives.

d. the stiffness of the control mechanism of the aileron may be represented by a spring without mass, interconnecting wing and aileron in the cross section, where the control is applied to the aileron.

e. the fuselage and any appendages to the wing (e. g. the propulsion aggregate) can be treated as rigid bodies with (compared with the span) negligible dimensions in the direction of the reference axis and normal to the plane of the wing, and with a centre of gravity, falling in the plane of the wing.

f. no other deformations or *relative* displacements occur, than those specified under *a* and *b*.

g. no other parts than the wing and the aileron are subject to aerodynamic loadings.

h. the (varying part of the) aerodynamic forces on any narrow strip of the wing-aileron system between two neighbouring cross sections depends upon the total displacements in this strip only, the relation being linear.

i. there exists perfect symmetry with respect to the geometrical plane of symmetry of the aeroplane.

It is thought, that none of these assumptions will generally have a noticeable influence on the accuracy of the results. Nevertheless, it may incidentally be desirable to introduce certain modifications, e. g. to retain in the idealisation of the system an elastic support of motor masses or to admit elastic distortions of the fuselage. It is, however, easy to establish in cases like that the required modifications in the equations, making it unnecessary to incorporate them in the general investigation.

By way of exception it may be desirable to spend some particular attention to assumption *d*, which is obviously in disagreement with the facts, if the control mechanism is not irreversible. In this case the elastic component of the mechanism is actually located in the cables, interconnecting the port and starboard ailerons and containing the control column. The admissability of the assumption rests then upon the fact, that for symmetric vibrations the influence of the elasticity of the cables is equivalent to the effect of the assumed spring, while for antisymmetric oscillations the influence vanishes, a case which is equivalently obtained by reducing the constant of the assumed spring to zero.

For antisymmetric oscillations an error emerges, if the mass of the control column is not negligible. Some words about this point are to be found in appendix I.

[1]) Which is only for simplicity identified in fig. 1 with the leading edge of the aileron.

2.2 *Local displacements.*

It is easily seen that for small vibrations the motion of any point of the system may be considered to consist of "vertical" displacements $z_{loc}(x, y, t)$ only (x = distance to the reference axis in chordwise direction, to be counted positive backwards). If the function $z(y, t)$ gives the total displacement of the points of the reference axis, i. e.

$$z(y, t) = z_{loc}(0, y, t),$$

and if the function $\varphi(y, t)$ gives the total angular displacement of a chord about this axis, we clearly have for any point of the system not belonging to the aileron

$$z_{loc}(x, y, t) = z(y, t) - x\,\varphi(y, t).$$

If further the function $\gamma(y, t)$ gives the total angular displacements of the aileron chords out of the neutral position (of the complete system), we have for a point of the aileron (see fig. 2)

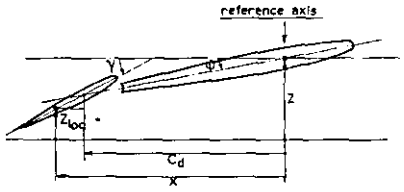

Fig. 2.

$$z_{loc}(x, y, t) = z(y, t) - c_d\,\varphi(y, t) - (x - c_d)\,\gamma(y, t),$$

c_d being the distance between the hinge axis and the reference axis.

It may be noted that the functions z, φ and γ are *not* identical with the triple z_d, φ_d, γ_d (see 2.1, a and b), the latter determining the *deformations* only and not the *total displacements* [1]).

2.3 *Equations, governing the balance of forces and of moments.*

Calculating the resulting inertia force on a strip of unit length (in spanwise direction) of the system we find, apart from contributions of concentrated loads (see 2.1, e),

$$-m_{11}'\ddot{z} - m_{12}'\ddot{\varphi} - m_{13}'\ddot{\gamma}$$

with

$$m_{11}' = m_v + m_r;\ m_{12}' = -m_v s_v - m_r c_d;\quad m_{13}' = -m_r s_r. \qquad (2.1)$$

(The significance of the parameters may be found in the List of Symbols).

We immediately make the substitution

$$z(y, t) = z_0(y)\,.\,e^{i\nu t};\ \varphi(y, t) = \varphi_0(y)\,.\,e^{i\nu t};\quad \gamma(y, t) = \gamma_0(y)\,e^{i\nu t} \qquad (2.2)$$

with complex amplitude functions z_0, φ_0, γ_0, thereby introducing the complex representation of harmonic variations, which will be used throughout.

The result is

$$\nu^2(m_{11}'z_0 + m_{12}'\varphi_0 + m_{13}'\gamma_0)\,.\,e^{i\nu t}. \qquad (2.3)$$

The resultant aerodynamic force may, according to 2.1, h, be put in the form

$$m_L\,\nu^2(a_{11}z_0 + a_{12}\,c\,\varphi_0 + a_{13}\,c\,\gamma_0)\,.\,e^{i\nu t} \qquad (2.4)$$

with

$$m_L = \tfrac{1}{4}\,\pi\,\rho\,c^2. \qquad (2.5)$$

The dimensionless coefficients a_{11} etc. depend upon certain geometrical parameters of the strip [1]) and upon the "reduced" velocity

$$V = \frac{v}{\nu\,c}, \qquad (2.6)$$

where v is the speed of flight. There is no dependence of the a_{11}, etc. upon v and ν separately. We shall give no further explanation about the structure of these coefficients, apart of the indication, that they have complex values.

The elastic restoring force can be most generally represented by an expression

$$(e_{11}z_0 + e_{12}\varphi_0 + e_{13}\gamma_0)\,.\,e^{i\nu t}. \qquad (2.7)$$

The coefficients $e_{11} \equiv e_{11}(y)$, etc. are differential operators. We may safely put

$$e_{11} = \frac{d^2}{dy^2}\left\{B_{11}(y)\,\frac{d^2}{dy^2}\right\}, \qquad (2.8)$$

$B_{11}(y)$ giving the flexural stiffness of the system. If the wing behaves elastically like a beam with definite elastic axis, the coefficient e_{12} may be assumed to vanish, provided that the reference axis is made to coïncide with this axis. But it is not true, that this is the general case. It is therefore desirable to retain the coefficient e_{12} in the expression. A possible formula for it will be

$$e_{12} = -\frac{d^2}{dy^2}\left\{B_{12}(y)\,\frac{d^2}{dy^2}\right\} \qquad (2.9)$$

depending upon an elastic "cross-stiffness" B_{12}.

The coefficient e_{13} represents the elastic coupling of aileron twist (or -deflection) with flexure of the wing. This coupling is always very small and will be neglected

$$e_{13} = 0. \qquad (2.10)$$

If there is no structural damping, the sum of (2.3) and (2.4) must balance the force (2.7). But the resulting equation will be valid only for the parts of the system *between* concentrated loads. This induces us to represent these (inertia) loads by the singular distribution

$$\nu^2(m_{11}^{(a)}z_0 + m_{12}^{(a)}\varphi_0 + m_{13}^{(a)}\gamma_0)\,\delta(y - b^{(a)})\,.\,e^{i\nu t};\quad a = 1, 2, \ldots\ldots, n_a, \qquad (2.11)$$

assuming that the number of loads is n_a and

[1]) The difference follows from the motions in the plane $y = 0$, i. e. from the motions of the fuselage. See eq. (3. 25).

[1]) The ratio of aileron chord to wing chord, the position of the quarter chord point, the aileron aerodynamic balance and possibly the gap between wing and aileron.

that they are located in sections with coordinates $y = b^{(a)}$. The function $\delta(y - y_1)$ (y_1: constant) is a singular one with the properties

$$\left.\begin{aligned} &\delta(y-y_1) = 0 \quad \text{if} \quad y \neq y_1, \\ &\int_{y_1-\varepsilon}^{y_1+\varepsilon} \delta(y-y_1)\,dy = 1; \quad \varepsilon > 0, \\ &\int_{y_1-\varepsilon}^{y_1} \delta(y-y_1)\,dy = \\ &= \int_{y_1}^{y_1+\varepsilon} \delta(y-y_1)\,dy = \tfrac{1}{2}; \quad \varepsilon > 0 \end{aligned}\right\} \qquad (2.12)$$

which serve for its definition.

No explanation will be needed about the determination of the constants $m_{11}^{(a)}$ etc.

With the addition of (2.11) the balance of forces leads to the equation

$$\begin{aligned} \nu^2 [(m_{11} + m_L a_{11}) z_0 + (m_{12} + m_L c\, a_{12}) \varphi_0 + \\ + (m_{13} + m_L c\, a_{13}) \gamma_0] - \\ - e_{11} z_0 - e_{12} \varphi_0 = 0, \ ^1) \end{aligned} \qquad (2.13)$$

containing the new abbreviations

$$\begin{aligned} m_{1k} = m_{1k}' + \sum_a m_{1k}^{(a)}\, \delta\,(y - b^{(a)}); \\ k = 1, 2, 3. \end{aligned} \qquad (2.14)$$

To prevent misunderstandings we state: *the range of the variable y extends from $y = -b$* (tip of the port wing) *to $y = +b$* (tip of the starboard wing). All coefficients are even functions of y (compare 2.1, *i*).

A second basic differential equation follows from the balance of moments on the wing alone about the reference axis. It can be written right down, if we keep in mind the fact, that in the sections $y = \pm b$, where the control mechanism is connected to the ailerons, a concentrated moment of magnitude

$$| k \{ \gamma(\pm b_r, t) - \varphi(\pm b_r, t) \} |$$

is exchanged between the wing and the aileron. With

$$\left.\begin{aligned} m_{21} = m_{21}' + \sum_a m_{21}^{(a)}\, \delta\,(y - b^{(a)}); \\ m_{21}' = m_{12}', \\ m_{22} = m_{22}' + \sum_a m_{22}^{(a)}\, \delta\,(y - b^{(a)}); \\ m_{22}' = I_v + m_v s_v^2 + m_r c_d^2, \\ m_{23} = m_{23}' + \sum_a m_{23}^{(a)}\, \delta\,(y - b^{(a)}); \\ m_{23}' = m_r s_r c_d, \end{aligned}\right\} \qquad (2.15)$$

and

$$\begin{aligned} e_{22} = (e_{22})_v + k\,\delta(y - b_r) + k\,\delta(y + b_r); \\ e_{23} = -k\,\delta(y - b_r) - k\,\delta(y + b_r) \end{aligned} \qquad (2.16)$$

we get without difficulty

$$\begin{aligned} \nu^2 [(m_{21} + m_L c\, a_{21}) z_0 + (m_{22} + m_L c^2 a_{22}) \varphi_0 + \\ + (m_{23} + m_L c^2 a_{23})\, \gamma_0] - \\ - e_{21} z_0 - e_{22} \varphi_0 - e_{23} \gamma_0 = 0. \end{aligned} \qquad (2.17)$$

It is

$$e_{21} = e_{12}. \qquad (2.18)$$

For $(e_{22})_v$ the simple formula

$$(e_{22})_v = -\frac{d}{dy}\left\{ T_v(y)\ \frac{d}{dy} \right\} \qquad (2.19a)$$

($T_v(y)$ = torsional stiffness of the wing) is generally accepted, but there is reason to believe, that it often may be more accurate (or even inevitable) to accept an expression like

$$\begin{aligned} (e_{22})_v = \frac{d^2}{dy^2}\left\{ B_{22}(y)\ \frac{d^2}{dy^2} \right\} - \\ - \frac{d}{dy}\left\{ T_v(y)\ \frac{d}{dy} \right\}. \end{aligned} \qquad (2.19b)$$

The third basic equation represents the balance of moments on the ailerons about the hinge axis. We easily find

$$\begin{aligned} \nu^2 [(m_{31} + m_L c\, a_{31}) z_0 + (m_{32} + m_L c^2 a_{32}) \varphi_0 + \\ + (m_{33} + m_L c^2 a_{33})\, \gamma_0 - \\ - e_{32} \varphi_0 - e_{33} \gamma_0 = 0, \end{aligned} \qquad (2.20)$$

with

$$\left.\begin{aligned} m_{31} = m_{31}' + \sum_a m_{31}^{(a)}\, \delta(y - b^{(a)}); \\ m_{31}' = m_{13}', \\ m_{32} = m_{32}' + \sum_a m_{32}^{(a)}\, \delta(y - b^{(a)}); \\ m_{32}' = m_{23}', \\ m_{33} = m_{33}' + \sum_a m_{33}^{(a)}\, \delta(y - b^{(a)}); \\ m_{33}' = I_r + m_r s_r^2 \end{aligned}\right\} \qquad (2.21)$$

and

$$\begin{aligned} e_{32} = e_{22}; \quad e_{33} = -\frac{d}{dy}\left\{ T_r(y)\ \frac{d}{dy} \right\} + \\ + k\,\delta(y - b_r) + k\,\delta(y + b_r). \end{aligned} \qquad (2.22)$$

($T_r(y)$ = torsional stiffness of the ailerons when twisted about the hinge axis).

---

[1]) This equation is, strictly speaking, the result of the elimination of the transverse force from the conditions of equilibrium of forces *and of moments* on the strip. That it does not contain the moment of inertia of the strip about its mid-chord (in reply to the rotations $\frac{dz_0}{dy}\, e^{i\nu t}$ of it about this chord) is a consequence of the fact, that this contribution is small of a high order if the deformation is supposed to be small of the first order. If, however, we don't want to neglect the influence of the non-vanishing moment of inertia *of the fuselage* about its longitudinal axis, we shall have to insert on the left side of (2.13) an according term, which obviously will again be singular, since the load is concentrated in the plane $y = 0$. It indeed assumes formally the remarkable form

$$-\nu^2 I \frac{d}{dy}\left\{ \delta(y) \frac{d}{dy} \right\} z_0$$

with I = moment of inertia of the fuselage about the longitudinal axis.

2.4 *Completing remarks.*

We may consider the triple (2.13), (2.17), (2.20) of basic equations as a system of three simultaneous differential equations for the functions z_0, φ_0 and γ_0 with ν as unknown parameter. The range of the variable y extends from $y = -b$ *to* $y = +b$ *for the equations* (2.13) *and* (2.17), while for (2.20) it falls apart in the intervals

$$-b_1 \leqq y \leqq -b_2 \; ; \quad b_2 \leqq y \leqq b_1 \qquad (2.23)$$

if the ends of the ailerons are in the sections $y = \pm b_1$, $y = \pm b_2$. The equation itself decomposes in fact into separate equations, each valid in one of the intervals (2.23). It will however be clear, that if desired there is no objection against adjudging the full range $-b \to +b$ likewise to equation (2.20), if only we agree to accept

$$m_{3k} = 0 \; ; \; m_{k3} = 0 \; ; \; a_{3k} = 0 \; ; \; a_{k3} = 0 \; ; \; k = 1, 2, 3.$$

for

$$-b \leqq y < -b_1 \; ; \; -b_2 < y < b_2 \; ; \; b_1 < y \leqq b.$$

We shall generally make use of this artifice.

Since

$$e_{hk} = e_{kh} \; ; \; m_{hk} = m_{kh} \; ; \; k, h = 1, 2, 3.$$

The system of basic equations would be self-adjoint if

$$a_{kh} = a_{hk} \, .$$

This is *not* true. We therefore see, that the equations, governing the oscillations *in still air* are self-adjoint, but that the equations, governing oscillations *in flight* are not. The boundary conditions (see 2.5) do not change these properties.

It may not be superfluous to repeat, that the functions z_0, φ_0, γ_0 are complex functions, just as the aerodynamic coefficients a_{hk}. All other quantities are real, perhaps with the exception of the frequency ν, whose nature may as yet remain unspecified.

2.5 *Boundary conditions.*

We must now add boundary conditions to our basic equations. Assuming that the operators e_{hk} ; $(h, k = 1, 2, 3)$ have the special forms (2.8), (2.9), (2.10), (2.16), (2.19), (2.22) we have

$$\left.\begin{aligned} &\text{for } y = \pm b: \\ &\quad z_0'' = 0, \;\; (B_{11} z_0'')' - (B_{12} \varphi_0'')' = 0, \\ &\quad \varphi_0'' = 0, \;\; \varphi_0' - \\ &\qquad - \frac{B_{11} B_{22} - B_{12}^2}{B_{11} T_v} \varphi_0''' = 0; \\ &\text{for } y = \pm b_1, \; \pm b_2: \\ &\qquad \gamma_0' = 0. \end{aligned}\right\} \qquad (2.24)$$

Apart of these boundary conditions we might establish special conditions for each value of y, specifying a section *where concentrated loads are exchanged or applied, that is* for $y = b^{(a)}$, $(a = 1 \ldots\ldots n_a)$ and for $y = \pm b_r$. We have, however, in fact inserted these additional conditions at least formally in the equations themselves by the use of the distribution function δ. There is indeed no difficulty in getting them out again. Each simple δ-symbol specifies a jump of a magnitude, determined by its factor, in the derivative agreeing with the first indefinite integral of the expression:

$$e_{k1} z_0 + e_{k2} \varphi_0 + e_{k3} \gamma_0, \quad k = 1, 2, 3.$$

The supplementary term to (2.13), mentioned in the accessory footnote is likewise seen to indicate a definite jump, this time in the derivative given by the second indefinite integral of the expression $e_{11} z_0 + e_{12} \varphi_0$, just as it obviously should be. Mathematically the δ-function is simply a tool, making it possible to collect a differential equation and given conditions of discontinuity at specified points of the interval into one single expression.

2.6 *First integrals.*

The basic equations are "equations of motion" of the mechanical system. Now this system may be regarded as a closed system with external forces acting upon it, agreeing with the aerodynamical loading. It must therefore be possible to establish "first integrals" of the equations, stating that the resulting external force equals the rate of change of the resulting impuls, and that the total momentum of all external forces equals the rate of change of the total moment of impulses. Now the resulting external force is

$$\nu^2 e^{i\nu t} \int_{-b}^{+b} m_L \, (a_{11} z_0 + a_{12} c \varphi_0 + a_{13} c \gamma_0) \, dy$$

and the rate of change of the total impuls

$$\nu^2 e^{i\nu t} \int_{-b}^{+b} (m_{11} z_0 + m_{12} \varphi_0 + m_{13} \gamma_0) \, dy \, .$$

These expressions must be equal. We indeed get the resulting equations by intervention of the boundary conditions if we integrate the first basic equation over the range $-b \leqq y \leqq +b$. We may give it the form

$$\int_{-b}^{+b} \{ \, (m_{11} + m_L a_{11}) \, z_0 + (m_{12} + m_L c \, a_{12}) \, \varphi_0 + \\ + (m_{13} + m_L c \, a_{13}) \, \gamma_0 \, \} \, dy = 0. \qquad (2.25)$$

It is evident, that there are no components of forces or impulses in other directions (than the vertical).

The first integrals, corresponding to the moment of impulses, are expressed by two equations, since we must consider moments about the reference axis and moments about the longitudinal axis of the system. The first equation is formed by integrating from $-b$ to $+b$ the *sum* of the second and third basic equation, since this sum is connected to the moments on the complete system about the axis of reference. The result clearly is

$$\int_{-b}^{+b} \{ \, (m_{21} + m_{31} + m_L c \, a_{21} + m_L c \, a_{31}) \, z_0 + \\ + (m_{22} + m_{32} + m_L c^2 a_{22} + m_L c^2 a_{32}) \, \varphi_0 + \\ + (m_{23} + m_{33} + m_L c^2 a_{23} + \\ + m_L c^2 a_{33}) \, \gamma_0 \, \} \, dy = 0. \qquad (2.26)$$

The last equation follows from the integral of the product of the first basic equation by y.

$$\int_{-b}^{+b} \{ (m_{11} + m_L a_{11}) z_0 + (m_{12} + m_L c a_{12}) \varphi_0 + (m_{13} + m_L c a_{13}) \gamma_0 \} y \, dy = 0. \text{ [1]} \quad (2.27)$$

Two other useful relations emerge by integration of (2.20). Summed up in one formula, they are

$$\nu^2 \int_{\pm b_2}^{\pm b_1} \{ (m_{31} + m_L c a_{31}) z_0 + (m_{32} + m_L c^2 a_{32}) \varphi_0 + (m_{33} + m_L c^2 a_{33}) \gamma_0 \} dy \mp \mp k \{ \gamma_0 (\pm b_r) - \varphi_0 (\pm b_r) \} = 0$$

(choose *all* signs upper or lower!). (2.28)

The equations are closely related to (2.26), they only refer to the ailerons alone and not to the complete system.

The triple (2.25), (2.26), (2.27) of integral relations, obtained above, permits a change-over from displacement-functions to deformation-functions by the introduction of separate variables, determining the motion in the plane $y = 0$ (motions of the fuselage).

Equation (2.28) permits a separation of deflection and twist in the aileron displacements.

Transformations like that have been used at the root of the calculations in our older work (loc. cit.). The crucial thing is, that it seems more easy to guess approximations to deformation functions than to displacements. We shall however make no use of them here, since it has appeared possible to reach the same benefits in a more satisfactory way.

3 The fundamental equations in integral form.

3.1 *Transformation of the differential equations into integral equations.*

We assume provisionally, that the wing has the simple elastic properties of a beam, i. e. we assume that

$$e_{12} = e_{21} = 0$$

and that for $(e_{22})_v$ the formula (2.19) holds.

Further, it will appear suitable to bring a slight change in the condition of the mechanical system. This change consists of the introduction of elastic restraints on displacements and rotations of the fuselage by spring connections to the ground. (Springs like that can actually be fitted in resonance tests). These springs will introduce a force $k_z z_0 (0)$, a moment about the reference axis $k_\varphi \varphi_0 (0)$ and a moment about the longitudinal axis $k_\vartheta z_0' (0)$, acting on the system in the plane of symmetry $(y = 0)$. The parameters k_z, k_φ, k_ϑ represent the spring constants.

It is easily seen, that these alterations may be represented in the basic equations by addition of the aggregate

$$-k_z \delta (y-0) z_0 + k_\vartheta \frac{d}{dy} \left\{ \delta (y-0) \frac{d}{dy} \right\} z_0 \text{ [1]}$$

to the left side of (2.13), and of the term

$$-k_\varphi \delta (y-0) \varphi_0$$

to the left side of (2.17), equation (2.20) remaining unchanged. We write the result in the form

$$e_{11} z_0 + k_z \delta (y-0) z_0 - k_\vartheta \frac{d}{dy} \left\{ \delta (y-0) \frac{d}{dy} \right\} z_0 = L_z, \quad (3.1)$$

$$e_{22} \varphi_0 + e_{23} \gamma_0 + k_\varphi \delta (y-0) \varphi_0 = L_\varphi, \quad (3.2)$$

$$e_{32} \varphi_0 + e_{33} \gamma_0 = L_\gamma, \quad (3.3)$$

L_z, L_φ and L_γ representing the load

$$\left.\begin{aligned} L_z &= \nu^2 \{ (m_{11} + m_L a_{11}) z_0 + (m_{12} + m_L c a_{12}) \varphi_0 + (m_{13} + m_L c a_{13}) \gamma_0 \}, \\ L_\varphi &= \nu^2 \{ (m_{21} + m_L c a_{21}) z_0 + (m_{22} + m_L c^2 a_{22}) \varphi_0 + (m_{23} + m_L c^2 a_{23}) \gamma_0 \}, \\ L_\gamma &= \nu^2 \{ (m_{31} + m_L c a_{31}) z_0 + (m_{32} + m_L c^2 a_{32}) \varphi_0 + (m_{33} + m_L c^2 a_{33}) \gamma_0 \}. \end{aligned}\right\} \quad (3.4)$$

Incidentically, it may be noted, that the effect of the alterations on the integral relations (2.25), (2.26), (2.27) consists merely of a replacement of the zeroes on the right side by $k_z z_0 (0)$, $k_\varphi \varphi_0 (0)$ and $k_\vartheta z_0' (0)$ consecutively.

Now, apply to (3.1) the operator

---

[1]) If we add to the left side of (2.13) the term, mentioned in the footnote to this equation, we must extend the left side of (2.27) with the term

$$-\int_{-b}^{+b} I y \frac{d}{dy} \left\{ \delta (y-0) \frac{dz_0}{dy} \right\} dy = -\left| I y \frac{dz_0}{dy} \delta (y-0) \right|_{y=-b}^{y=b} + \int_{-b}^{+b} I \frac{dz_0}{dy} \delta (y-0) \, dy = I \left(\frac{dz_0}{dy} \right)_{y=0},$$

representing the moment about the longitudinal axis of the inertia forces on the fuselage. Note that the formal procedure leads to the correct result.

[1]) The expression containing k_ϑ is similar to the addendum, mentioned in the footnote to eq. (2.13).

$$\frac{1}{k_z}\int_{-b}^{+b} dy + \frac{y}{k_\vartheta}\int_{-b}^{+b} dy\, y + \left\{\begin{array}{ll} \int_0^y\int_0^y \frac{1}{B_{11}(y)}\int_y^b\int_y^b (dy)^4 & \text{if } y>0. \\ \int_0^y\int_0^y \frac{1}{B_{11}(y)}\int_y^{-b}\int_y^{-b} (dy)^4 & \text{if } y<0. \end{array}\right\} \quad (3.5)$$

In view of (2.12) and the boundary conditions, imposed on the function z_0, we have

$$\frac{1}{k_z}\int_{-b}^{+b} dy\, e_{11}\, z_0 = 0\,; \qquad \frac{y}{k_\vartheta}\int_{-b}^{+b} dy\, y\, e_{11}\, z_0 = 0$$

$$\frac{1}{k_z}\int_{-b}^{+b} dy\, k_z\, \delta\,(y-0)\, z_0 = z_0\,(0)\,;$$

$$\frac{y}{k_\vartheta}\int_{-b}^{+b} dy\, y\, k_z\, \delta\,(y-0)\, z_0 = 0$$

$$\frac{1}{k_z}\int_{-b}^{+b} dy\, k_\vartheta \frac{d}{dy}\left\{\delta\,(y-0)\frac{d}{dy}\right\} z_0 = 0\,;$$

$$\frac{y}{k_\vartheta}\int_{-b}^{+b} dy\, y\, k_\vartheta \frac{d}{dy}\left\{\delta\,(y-0)\frac{d}{dy}\right\} z_0 = -\,y\, z_0'\,(0)$$

(compare the footnote to eq. (2.27))

Further the multiple integral part of the operator produces zero when applied to the second and third term on the left side of (3.1), while application to the first term gives, both for $y>0$ and for $y<0$ (in view of (2.8)),

$$z_0 - z_0\,(0) - y\, z_0'\,(0).$$

It follows that the complete result of the transformation of the left member of (3.1) is simply

$$z_0\,. \quad (3.6)$$

In order to give a suitable form to the right side result, we remark

$$\int_0^y dy \int_0^y dy \,\ldots\ldots = y\int_0^y dy \,\ldots\ldots - \int_0^y dy\, y \,\ldots\ldots \left\{\begin{array}{l} y>0 \\ y<0 \end{array}\right.,$$

$$\int_y^{\pm b} dy \int_y^{\pm b} dy \,\ldots\ldots = -\,y\int_y^{\pm b} dy \,\ldots\ldots + \int_y^{\pm b} dy\, y \,\ldots\ldots,$$

(*both* signs + or *both* −),

leading to the expression

$$\frac{1}{k_z}\int_{-b}^{+b} d\eta\, L_z(\eta) + \frac{y}{k_\vartheta}\int_{-b}^{+b} d\eta\, \eta\, L_z(\eta) + \left\{\begin{array}{ll} \int_0^y\int_{y_1}^b \frac{(y-y_1)\,(\eta-y_1)}{B_{11}(y_1)} L_z(\eta)\, d\eta\, dy_1\,; & y>0. \\ \int_0^y\int_{y_1}^{-b} \frac{(y-y_1)\,(\eta-y_1)}{B_{11}(y_1)} L_z(\eta)\, d\eta\, dy_1\,; & y<0. \end{array}\right. \quad (3.7)$$

Let now

$$\int_a^{<y,\eta} dy_1$$

define an integration over the range

$$\left.\begin{array}{ll} a \text{ to } y & \text{if } |y-a|<|\eta-a| \\ a \text{ to } \eta & \text{if } |y-a|>|\eta-a| \end{array}\right\} \quad -b \leqq a \leqq +b.$$

Then

$$\int_0^y\int_{y_1}^b \ldots\ldots d\eta\, dy_1 = \int_0^b\int_0^{<y,\eta} \ldots\ldots dy_1\, d\eta\,;$$

$$\int_0^y\int_{y_1}^{-b} \ldots\ldots d\eta\, dy_1 = \int_0^{-b}\int_0^{<y,\eta} \ldots\ldots dy_1\, d\eta\,, \quad (3.8)$$

formulae, that come down to an interchange of integrals, retaining the original area of integration in the η, y_1-plane.

These formulae permit a reduction of the multiple-integral part of (3.7) to

$$\int_0^b \left\{\int_0^{<y,\eta} \frac{(y-y_1)\,(\eta-y_1)}{B_{11}(y_1)}\, dy_1\right\} L_z(\eta)\, d\eta \quad \text{for } y>0,$$

$$\int_0^{-b} \left\{\int_0^{<y,\eta} \frac{(y-y_1)\,(\eta-y_1)}{B_{11}(y_1)}\, dy_1\right\} L_z(\eta)\, d\eta \quad \text{for } y<0.$$

So, if by definition

$$K_{11}(y,\eta) = \frac{1}{k_z} + \frac{y\,\eta}{k_\vartheta} + \left\{\begin{array}{ll} \int_0^{<y,\eta} \frac{(y-y_1)\,(\eta-y_1)}{B_{11}(y_1)}\, dy_1 & \text{for } y>0,\ \eta>0 \\ 0 & \text{for } y>0,\ \eta<0 \\ 0 & \text{for } y<0,\ \eta>0 \\ -\int_0^{<y,\eta} \frac{(y-y_1)\,(\eta-y_1)}{B_{11}(y_1)}\, dy_1 & \text{for } y<0,\ \eta<0 \end{array}\right. \quad (3.9)$$

the final result of the application of (3.5) to (3.1) clearly assumes the form

$$z_0(y) = \int_{-b}^{+b} K_{11}(y,\eta)\, L_z(\eta)\, d\eta\,. \quad (3.10)$$

A similar transformation of equation (3.2) can be obtained with the help of the operator

$$\frac{1}{k_\Phi}\int_{-b}^{+b} dy + \begin{cases} \int_0^y \frac{1}{T_v(y)} \int_y^b (dy)^2 & \text{for } y>0. \\ \int_0^y \frac{1}{T_v(y)} \int_y^{-b} (dy)^2 & \text{for } y<0. \end{cases} \tag{3.11}$$

We find, in view of (2.16) and (2.19) and the boundary-conditions for φ_0 and γ_0,

$$\frac{1}{k_\Phi}\int_{-b}^{+b} dy\,(e_{22}\varphi_0 + e_{23}\gamma_0 + k_\Phi \delta(y-0)\varphi_0) = $$
$$= -\frac{k}{k_\Phi}\{\gamma_0(b_r) + \gamma_0(-b_r) - $$
$$- \varphi_0(b_r) - \varphi_0(-b_r)\} + \varphi_0(0)$$

while the multiple-integral part of the operator, applied to the same expression, gives

$$\varphi_0 - \varphi_0(0) + \begin{cases} -k\{\gamma_0(b_r) - \varphi_0(b_r)\}\int_0^{<y,b_r} \frac{dy}{T_v(y)} & \text{for } y>0. \\ +k\{\gamma_0(-b_r) - \varphi_0(-b_r)\}\int_0^{<y,b_r} \frac{dy}{T_v(y)} & \text{for } y<0. \end{cases}$$

Adding the results and eliminating the differences $\gamma_0(\pm b_r) - \varphi_0(\pm b_r)$ with the help of (2.28), we obtain the expression

$$\varphi_0 - \frac{1}{k_\Phi}\int_{-b}^{+b} L_\gamma\, d\eta - \begin{cases} \int_0^b L_\gamma\, d\eta \cdot \int_0^{<y,b_r} \frac{dy}{T_v} & \text{for } y>0. \\ \int_0^{-b} L_\gamma\, d\eta \cdot \int_0^{<y,b_r} \frac{dy}{T_v} & \text{for } y<0. \end{cases}$$

Application of the operator to the right side of (3.2) gives, taking account of (3.8),

$$\frac{1}{k_\Phi}\int_{-b}^{+b} d\eta\, L_\Phi + \begin{cases} \int_0^b \int_0^{<y,\eta} \frac{dy_1}{T_v(y_1)} L_\Phi(\eta)\, d\eta\,; & y>0. \\ \int_0^b \int_0^{<y,\eta} \frac{dy_1}{T_v(y_1)} L_\Phi(\eta)\, d\eta\,; & y<0. \end{cases}$$

Consequently, if we define

$$K_{22}(y,\eta) = \frac{1}{k_\Phi} + \begin{cases} \int_0^{<y,\eta} \frac{dy_1}{T_v(y_1)} & \text{for } y>0,\ \eta>0 \\ 0 & \text{for } y>0,\ \eta<0 \\ 0 & \text{for } y<0,\ \eta>0 \\ -\int_0^{<y,\eta} \frac{dy_1}{T_v(y_1)} & \text{for } y<0,\ \eta<0 \end{cases} \tag{3.12}$$

and

$$K_{23}(y,\eta) = \frac{1}{k_\Phi} + \begin{cases} \int_0^{<y,b_r} \frac{dy_1}{T_v(y_1)} & \text{for } y>0,\ \eta>0 \\ 0 & \text{for } y>0,\ \eta<0 \end{cases} = K_{22}(y,b_r),\ \eta>0, $$
$$+ \begin{cases} 0 & \text{for } y<0,\ \eta>0 \\ -\int_0^{<y,-b_r} \frac{dy_1}{T_v(y_1)} & \text{for } y<0,\ \eta<0 \end{cases} = K_{22}(y,b_r),\ \eta<0, \tag{3.13}$$

the final result of the transformation appears to be

$$\varphi_0(y) = \int_{-b}^{+b} K_{22}(y,\eta)\, L_\Phi(\eta)\, d\eta + \int_{-b}^{+b} K_{23}(y,\eta)\, L_\gamma(\eta)\, d\eta. \tag{3.14}$$

Thirdly let us apply to (3.3), the operator

$$\begin{cases} \int_{b_r}^y \frac{1}{T_r(y)} \int_y^{b_1} (dy)^2 & \text{for } y>b_r. \\ \int_{b_r}^y \frac{1}{T_r(y)} \int_y^{b_2} (dy)^2 & \text{for } 0<y<b_r. \\ \int_{-b_r}^y \frac{1}{T_r(y)} \int_y^{-b_2} (dy)^2 & \text{for } -b_r<y<0. \\ \int_{-b_r}^y \frac{1}{T_r(y)} \int_y^{-b_1} (dy)^2 & \text{for } y<b_r. \end{cases} \tag{3.15}$$

The complete result is easily found to be (compare (3.8))

$$\gamma_0 - \gamma_0(b_r) = \begin{cases} \int_{b_r}^{b_1} \int_{b_r}^{<y,\eta} \frac{dy_1}{T_r(y_1)} L_\gamma(\eta)\, d\eta\,; & y > b_r. \\ \int_{b_r}^{b_2} \int_{b_r}^{<y,\eta} \frac{dy_1}{T_r(y_1)} L_\gamma(\eta)\, d\eta\,; & 0 < y < b_r. \end{cases} \tag{3.16}$$

$$\gamma_0 - \gamma_0(-b_r) = \begin{cases} \int_{-b_r}^{-b_2} \int_{-b_r}^{<y,\eta} \frac{dy_1}{T_r(y_1)} L_\gamma(\eta)\, d\eta\,; & -b_r < y < 0. \\ \int_{-b_r}^{-b_1} \int_{-b_r}^{<y,\eta} \frac{dy_1}{T_r(y_1)} L_\gamma(\eta)\, d\eta\,; & y < -b_r. \end{cases}$$

Now, equate in (3.14) y to $\pm b_r$ and add the resulting relation to (3.16). Then eliminate the emerging differences $\gamma_0(\pm b_r) - \varphi_0(\pm b_r)$ with the help of (2.28). This leads to

$$\gamma_0 - \frac{1}{k}\int_0^b L_\gamma\, d\eta = \int_{-b}^{+b} K_{22}(b_r,\eta)\, L_\Phi(\eta)\, d\eta + \int_{-b}^{+b} K_{23}(b_r,\eta)\, L_\gamma(\eta)\, d\eta + \text{right side of (3.16)};\ y > 0,$$

$$\gamma_0 - \frac{1}{k}\int_{-b}^0 L_\gamma d\eta = \int_{-b}^{+b} K_{22}(-b_r,\eta)\, L_\Phi(\eta)\, d\eta + \int_{-b}^{+b} K_{23}(-b_r,\eta)\, L_\gamma(\eta)\, d\eta + \text{right side of (3.16)};\ y < 0.$$

Careful consideration shows, that these relations may be expressed in the characteristic form

$$\gamma_0(y) = \int_{-b}^{+b} K_{32}(y,\eta)\, L_\Phi(\eta)\, d\eta + \int_{-b}^{+b} K_{33}(y,\eta)\, L_\gamma(\eta)\, d\eta, \tag{3.17}$$

if we define

$$K_{32}(y,\eta) = K_{23}(\eta, y) \tag{3.18}$$

and

$$K_{33}(y,\eta) = \frac{1}{k_\Phi} \begin{cases} +\frac{1}{k} + \int_0^{b_r} \frac{dy_1}{T_v(y_1)} \begin{cases} + \int_{b_r}^{<y,\eta} \frac{dy_1}{T_r(y_1)} & \text{for } y > b_r,\ \eta > b_r. \\ +0 & \text{for } y > b_r,\ 0 < \eta < b_r. \end{cases} \\ +0 \qquad +0 & \text{for } y > b_r,\ \eta < 0. \\ +\frac{1}{k} + \int_0^{b_r} \frac{dy_1}{T_v(y_1)} \begin{cases} - \int_{b_r}^{<y,\eta} \frac{dy_1}{T_r(y_1)} & \text{for } 0 < y < b_r,\ 0 < \eta < b_r. \\ +0 & \text{for } 0 < y < b_r,\ \eta > b_r. \end{cases} \\ +0 \qquad +0 & \text{for } 0 < y < b_r,\ \eta < 0. \\ +\frac{1}{k} - \int_0^{-b_r} \frac{dy_1}{T_v(y_1)} \begin{cases} + \int_{-b_r}^{<y,\eta} \frac{dy_1}{T_r(y_1)} & \text{for } -b_r < y < 0,\ -b_r < \eta < 0. \\ +0 & \text{for } -b_r < y < 0,\ \eta < -b_r. \end{cases} \\ +0 \qquad +0 & \text{for } -b_r < y < 0,\ \eta > 0. \\ +\frac{1}{k} - \int_0^{-b_r} \frac{dy_1}{T_v(y_1)} \begin{cases} - \int_{-b_r}^{<y,\eta} \frac{dy_1}{T_r(y_1)} & \text{for } y < -b_r,\ \eta < -b_r. \\ +0 & \text{for } y < -b_r,\ -b_r < \eta < 0. \end{cases} \\ +0 \qquad +0 & \text{for } y < -b_r,\ \eta > 0. \end{cases} \tag{3.19}$$

The transformation of the basic differential equations (with their boundary conditions) into completely equivalent integral-equations (without complementary conditions) is herewith finished [1]).

We may remark firstly, that it is immediately visible from (3.9), (3.12), (3.13) and (3.19) why it was desirable to introduce spring-contraints on motions in the $y = 0$-plane. If we remove them, the kernels of the integral-equations are no longer bounded. Secondly it will be accepted for certain, that equations (3.10), (3.14) and (3.17) may be considered as a simplification, related to the assumptions about the e_{ik}-operators, of a general set, containing K-functions with indices 12, 13, 21, 31 as well, and only submitted to the symmetry property

$$K_{hk}(y, \eta) = K_{kh}(\eta, y); \quad h, k = 1, 2, 3. \tag{3.20}$$

The way, in which the spring constants k_z, k_ϕ and k_ϑ enter in these general functions may be drawn from the special formulae (3.9), (3.12), (3.13) and (3.19) (though generally these special formulae will of course lose their validity if any of the simplifications is rejected).

3.2 *Elimination of spring constants k_z, k_ϕ, k_ϑ.*

It is of importance to trace the effect of a suppression of the parts in the operators $K_{hk}(y, \eta)$, depending upon the spring constants k_z, k_ϕ, k_ϑ. (This may be done by putting simply, $k_z = \infty$, $k_\phi = \infty$, $k_\vartheta = \infty$ in the formulae for the kernels). The following result will be found without much trouble

$$z_0(y) - z_0(0) - y\, z_0'(0) = \int_{-b}^{+b} \Xi_{11}(y, \eta)\, L_z(\eta)\, d\eta, \tag{3.21}$$

$$\varphi_0(y) - \varphi_0(0) = \int_{-b}^{+b} \Xi_{22}(y, \eta)\, L_\phi(\eta)\, d\eta + \int_{-b}^{+b} \Xi_{23}(y, \eta)\, L_\gamma(\eta)\, d\eta, \tag{3.22}$$

$$\gamma_0(y) - \varphi_0(0) = \int_{-b}^{+b} \Xi_{32}(y, \eta)\, L_\phi(\eta)\, d\eta + \int_{-b}^{+b} \Xi_{33}(y, \eta)\, L_\gamma(\eta)\, d\eta, \tag{3.23}$$

where a Ξ-symbol is used to represent the remaining parts of the K-kernels, i. e.

$$\Xi_{hk}(y, \eta) = \{ K_{hk}(y, \eta) \}_{k_z = \infty,\, k_\phi = \infty,\, k_\vartheta = \infty}. \tag{3.24}$$

[1]) Another method, making use of an identification of the $K_{ij}(y, \eta)$-functions with "influence functions", to establish the integral equations, has been followed in appendix I.

We must obviously come to the same kernels, if we *actually* give infinite stiffness to the "fuselage springs", that is: if we fix the fuselage rigidly to the ground. We indeed have under these circumstances

$$z_0(0) = 0, \quad z_0'(0) = 0, \quad \varphi_0(0) = 0$$

and (3.21) reduces to (3.10), (3.22) to (3.14) and (3.23) to (3.19) with Ξ on the place of K.

It is of importance to remark, that if *actually*

$$k_z \neq \infty, \quad k_\phi \neq \infty, \quad k_\vartheta \neq \infty$$

the triple (3.21), (3.22), (3.23) cannot be considered as a new integral-equivalent of the fundamental differential equations (with boundary-conditions), since this triple does not determine unambiguously the unknown functions z_0, φ_0, γ_0 and the parameter ν. Indeed, if we put

$$z_{d_0} = z_0 - z_0(0) - y\, z_0'(0), \quad \varphi_{d_0} = \varphi_0 - \varphi_0(0), \quad \gamma_{d_0} = \gamma_0 - \varphi_0(0), \tag{3.25}$$

a system of integral equations emerges, which may be considered as inhomogeneous, the right-side terms containing the parameters $z_0(0)$, $z_0'(0)$, $\varphi_0(0)$. The ambiguity disappears if we add as independent conditions the relations (2.25), (2.26) and (2.27) with the right side zeros replaced by $\frac{1}{\nu^2} k_z z_0(0)$, $\frac{1}{\nu^2} k_\phi \varphi_0(0)$, $\frac{1}{\nu^2} k_\vartheta z_0'(0)$ consecutively, for these equations join special values of $z_0(0)$, $\varphi_0(0)$, $z_0'(0)$ to given functions z_{d_0}, φ_{d_0}, γ_{d_0}. The extra equations can clearly be written in the form

$$\int_{-b}^{+b} L_z(\eta)\, d\eta = k_z z_0(0);$$

$$\int_{-b}^{+b} \{ L_\phi(\eta) + L_\gamma(\eta) \}\, d\eta = k_\phi \varphi_0(0);$$

$$\int_{-b}^{+b} \eta L_z(\eta)\, d\eta = k_\vartheta z_0'(0). \tag{3.26}$$

3.3 *Special forms for symmetrical oscillations.*

If the solution z_0, φ_0, γ_0 of the basic equations consists of even functions (symmetrical mode of vibration), the integral in (3.10) is equal to

$$2 \int_0^b \frac{K_{11}(y, \eta) + K_{11}(y, -\eta)}{2} L_z(\eta)\, d\eta$$

showing that we may write in this case

$$z_0(y) = \int_0^b K_{11}{}^S(y, \eta)\, L_z(\eta)\, d\eta \tag{3.27}$$

with

$$K_{11}{}^S(y, \eta) = \frac{2}{k_z} + \int_0^{<y, \eta} \frac{(y - y_1)(\eta - y_1)}{B_{11}(y_1)}\, dy_1 \tag{3.28}$$

Under the same restriction (3.14) and (3.17) may be replaced by

$$\varphi_0(y) = \int_0^b K_{22}^S(y,\eta)\, L_\Phi(\eta)\, d\eta + \int_0^b K_{23}^S(y,\eta)\, L_\gamma(\eta)\, d\eta, \tag{3.29}$$

$$\gamma_0(y) = \int_0^b K_{32}^S(y,\eta)\, L_\Phi(\eta)\, d\eta + \int_0^b K_{33}^S(y,\eta)\, L_\gamma(\eta)\, d\eta, \tag{3.30}$$

with

$$K_{22}^S(y,\eta) = \frac{2}{k_\Phi} + \int_0^{<y,\eta} \frac{dy_1}{T_v(y_1)}, \tag{3.31}$$

$$K_{23}^S(y,\eta) = \frac{2}{k_\Phi} + \int_0^{<y,b_r} \frac{dy_1}{T_v(y_1)} = K_{22}^S(y,b_r), \tag{3.32}$$

$$K_{32}^S(y,\eta) = \frac{2}{k_\Phi} + \int_0^{<b_r,\eta} \frac{dy_1}{T_v(y_1)} = K_{22}^S(b_r,\eta) = K_{23}^S(\eta,y), \tag{3.33}$$

$$K_{33}^S(y,\eta) = \frac{2}{k_\Phi} + \frac{1}{k} + \int_0^{b_r} \frac{dy_1}{T_v(y_1)} + \begin{cases} \int_{b_r}^{<y,\eta} \frac{dy_1}{T_r(y_1)}; & y > b_r,\ \eta > b_r. \\ 0 \qquad\qquad ; & y > b_r,\ \eta < b_r. \\ 0 \qquad\qquad ; & y < b_r,\ \eta > b_r. \\ -\int_0^{<y,\eta} \frac{dy_1}{T_r(y_1)}; & y < b_r,\ \eta < b_r. \end{cases} \tag{3.34}$$

Further, (3.21), (3.22) and (3.23) reduce to

$$z_0(y) - z_0(0) = \int_0^b \Xi_{11}^S(y,\eta)\, L_z(\eta)\, d\eta, \tag{3.35}$$

$$\varphi_0(y) - \varphi_0(0) = \int_0^b \Xi_{22}^S(y,\eta)\, L_\Phi(\eta)\, d\eta + \int_0^b \Xi_{23}^S(y,\eta)\, L_\gamma \eta)\, d\eta, \tag{3.36}$$

$$\gamma_0(y) - \varphi_0(0) = \int_0^b \Xi_{32}^S(y,\eta)\, L_\Phi(\eta)\, d\eta + \int_0^b \Xi_{33}^S(y,\eta)\, L_\gamma(\eta)\, d\eta. \tag{3.37}$$

Finally we have (see (3.26))

$$\int_0^b L_z(\eta)\, d\eta = \tfrac{1}{2} k_z z_0(0);$$

$$\int_0^b \{ L_\Phi(\eta) + L_\gamma(\eta) \}\, d\eta = \tfrac{1}{2} k_\Phi \varphi_0(0). \tag{3.38}$$

The third relation (3.26) is fulfilled automatically.

3.4 *Special forms for antisymmetrical oscillations.*

If on the contrary the solution z_0, φ_0, γ_0 consists of odd functions (antisymmetric mode of vibration), the integral in (3.10) is equal to

$$2\int_0^b \frac{K_{11}(y,\eta) - K_{11}(y,-\eta)}{2} L_z(\eta)\, d\eta,$$

showing that the equations may now be written in the form

$$z_0(y) = \int_0^b K_{11}^A(y,\eta)\, L_z(\eta)\, d\eta, \tag{3.39}$$

with

$$K_{11}^A(y,\eta) = 2\frac{y\,\eta}{k_\Phi} + \int_0^{<y,\eta} \frac{(y-y_1)(\eta-y_1)}{B_{11}(y_1)}\, dy_1. \tag{3.40}$$

Similarly we deduce for this case

$$\varphi_0(y) = \int_0^b K_{22}^A(y,\eta)\, L_\Phi(\eta)\, d\eta + \int_0^b K_{23}^A(y,\eta)\, L_\gamma(\eta)\, d\eta, \tag{3.41}$$

$$\gamma_0(y) = \int_0^b K_{32}^A(y,\eta)\, L_\Phi(\eta)\, d\eta + \int_0^b K_{33}^A(y,\eta)\, L_\gamma(\eta)\, d\eta, \tag{3.42}$$

with

$$K_{22}^A(y,\eta) = \int_0^{<y,\eta} \frac{dy_1}{T_v(y_1)}, \tag{3.43}$$

$$K_{23}^A(y,\eta) = \int_0^{<y,b_r} \frac{dy_1}{T_v(y_1)} = K_{22}^A(y,b_r), \tag{3.44}$$

$$K_{32}^A(y,\eta) = \int_0^{<b_r,\eta} \frac{dy_1}{T_v(y_1)} = K_{22}^A(b_r,\eta) = K_{23}^A(\eta,y) \tag{3.45}$$

$$K_{33}^A(y,\eta) = K_{33}^S(y,\eta) \quad (!) \tag{3.46}$$

We have further

$$z_0(y) - y z_0'(0) = \int_0^b \Xi_{11}^A(y,\eta)\, L_z(\eta)\, d\eta. \quad (3.47)$$

$$\varphi_0(y) = \int_0^b \Xi_{22}^A(y,\eta)\, L_\phi(\eta)\, d\eta + \int_0^b \Xi_{23}^A(y,\eta)\, L_\gamma(\eta)\, d\eta. \quad (3.48)$$

$$\gamma_0(y) = \int_0^b \Xi_{32}^A(y,\eta)\, L_\phi(\eta)\, d\eta + \int_0^b \Xi_{33}^A(y,\eta)\, L_\gamma(\eta)\, d\eta. \quad (3.49)$$

The Ξ^A-functions follow from the K^A-functions by putting $k_\delta = \infty$. They are in fact identical with the Ξ^S-functions, so that there is actually no reason to use the discrimitative indices S and A in connection with these functions. We shall indeed drop them in future.

It must be remarked, that for antisymmetrical vibrations an as yet unobserved complication may arise, which needs special treatment. It emerges from the fact, that in antisymmetrical distortion the spring constraint on the aileron may vanish, i.e.

$$k = 0$$

and consequently

$$K_{33}(y,\eta) = \infty.$$

Since it is inconvenient to interrupt the reasoning by considerations applying to this case only, we have shifted the treatment of it to appendix I.

4 Fundamental equations in matrix form.

4.1 *Differential equations in matrix form.*

We collect the displacement functions z_0, φ_0, γ_0 (whether even or odd) in a one-column or one-row matrix (a vector)

$$\mathbf{f}_0 = \begin{Vmatrix} z_0 \\ \varphi_0 \\ \gamma_0 \end{Vmatrix}; \quad \mathbf{f}_0^* = \| z_0 \ \varphi_0 \ \gamma_0 \| \quad (4.1)$$

(reserving the * sign, attached to the heavy-type symbols of matrices, to denote the *transposed* matrix).

Further, we compose an inertia-load : matrix (leaving out the factor ν^2!)

$$\mathbf{m} = \begin{Vmatrix} m_{11} & m_{12} & m_{13} \\ m_{21} & m_{22} & m_{23} \\ m_{31} & m_{32} & m_{33} \end{Vmatrix} \quad (4.2)$$

and an aerodynamic-load matrix (also without factor ν^2)

$$\mathbf{a} = m_L \begin{Vmatrix} a_{11} & a_{12}c & a_{13}c \\ a_{21}c & a_{22}c^2 & a_{23}c^2 \\ a_{31}c & a_{32}c^2 & a_{33}c^2 \end{Vmatrix}. \quad (4.3)$$

Introducing finally the operator-matrix

$$\mathbf{e} = \begin{Vmatrix} e_{11} & e_{12} & e_{13} \\ e_{21} & e_{22} & e_{23} \\ e_{31} & e_{32} & e_{33} \end{Vmatrix}, \quad (4.4)$$

depending upon the elastic properties of the system and generally containing nine non-vanishing elements, it appears possible to contract the set of basic differential equations into one single matrix-equation

$$\mathbf{e}\,\mathbf{f}_0 = \nu^2 (\mathbf{m} + \mathbf{a})\, \mathbf{f}_0 = \nu^2\, \mathbf{u}\, \mathbf{f}_0, \quad (4.5)$$

with

$$\mathbf{u} = \mathbf{m} + \mathbf{a}. \quad (4.6)$$

Indeed equations (2.13), (2.17), (2.20) are readily obtained if we develop (4.5) according to the well-known rules for the addition and the multiplication of matrices. An intermediate result is

$$\nu^2\, \mathbf{u}\, \mathbf{f}_0 = \mathbf{L} = \begin{Vmatrix} L_z \\ L_\phi \\ L_\gamma \end{Vmatrix}. \quad (4.7)$$

We have

$$\mathbf{m}^* \equiv \mathbf{m}, \quad (4.8)$$

$$\mathbf{e}^* \equiv \mathbf{e}, \quad (4.9)$$

but

$$\mathbf{a}^* \neq \mathbf{a}, \quad (4.10)$$

$$\mathbf{u}^* \neq \mathbf{u}. \quad (4.11)$$

The last inequality shows in connection with (4.9), that the set of differential equations is not self-adjoint.

To (4.5) belong boundary conditions, mentioned in par. 2.5.

We shall not trouble ourselves with matrix representations of these conditions.

4.2 *General integral equations in matrix form.*

Let

$$\mathbf{K}(y,\eta) = \begin{Vmatrix} K_{11}(y,\eta) & K_{12}(y,\eta) & K_{13}(y,\eta) \\ K_{21}(y,\eta) & K_{22}(y,\eta) & K_{23}(y,\eta) \\ K_{31}(y,\eta) & K_{32}(y,\eta) & K_{33}(y,\eta) \end{Vmatrix}. \quad (4.12)$$

Then the matrix-equation

$$\mathbf{f}_0(y) = \nu^2 \int_{-b}^{+b} \mathbf{K}(y,\eta)\, \mathbf{u}(\eta)\, \mathbf{f}_0(\eta)\, d\eta \quad (4.13)$$

will represent the integral equivalent (3.10), (3.14), (3.17) of fundamental equations (in a generalised form). We notice

$$\mathbf{K}^*(y,\eta) \equiv \mathbf{K}(\eta, y). \quad (4.14)$$

Similarly, with

$$\Xi(y,\eta) = \begin{Vmatrix} \Xi_{11}(y,\eta) & \Xi_{12}(y,\eta) & \Xi_{13}(y,\eta) \\ \Xi_{21}(y,\eta) & \Xi_{22}(y,\eta) & \Xi_{23}(y,\eta) \\ \Xi_{31}(y,\eta) & \Xi_{32}(y,\eta) & \Xi_{33}(y,\eta) \end{Vmatrix}, \quad (4.15)$$

we may represent the (generalised) set (3.21), (3.22), (3.23) by

$$\mathbf{f}_0 - \mathbf{c}_0 = \nu^2 \int_{-b}^{+b} \Xi(y, \eta)\, \mathbf{u}(\eta)\, \mathbf{f}_0(\eta)\, d\eta, \qquad (4.16)$$

with

$$\mathbf{c}_0^* = \| z_0(0) + y\, z_0'(0) \quad \varphi_0(0) \quad \varphi_0(0) \|. \qquad (4.17)$$

We remark again, that we must add to (4.16) the independent relations (3.26)

4.3 *Matrix equations for symmetrical oscillations.*

Denoting by $\mathbf{f}_{0,s}$ that the vector $\mathbf{f}_0$ is supposed to be composed of even functions, we infer from par. 3.3 that, for symmetrical oscillations only,

$$\mathbf{f}_{0,s}(y) = \nu^2 \int_0^b \mathbf{K}_S(y, \eta)\, \mathbf{u}(\eta)\, \mathbf{f}_{0,s}(\eta)\, d\eta, \qquad (4.18)$$

with

$$\mathbf{K}_S = \begin{Vmatrix} K_{11}S & K_{12}S & K_{13}S \\ K_{21}S & K_{22}S & K_{23}S \\ K_{31}S & K_{32}S & K_{33}S \end{Vmatrix}. \qquad (4.19)$$

Similarly we may contract the set (3.35), (3.36), (3.37) to [1])

$$\mathbf{f}_{0,s}(y) - \mathbf{c}_{0,s} = \nu^2 \int_0^b \Xi(y, \eta)\, \mathbf{u}(\eta)\, \mathbf{f}_{0,s}(\eta)\, d\eta, \qquad (4.20)$$

if

$$\mathbf{c}_{0,s}^* = \| z_0(0) \quad \varphi_0(0) \quad \varphi_0(0) \|. \qquad (4.21)$$

Let now

$$\mathbf{f}_{d_0,s}^* = \| z_{d_0} \quad \varphi_{d_0} \quad \gamma_{d_0} \quad Z_0 \quad \Phi_0 \|, \qquad (4.22)$$

with

$$z_{d_0} = z_0 - \dot{z}_0(0); \quad \varphi_{d_0} = \varphi_0 - \varphi_0(0); \quad \gamma_{d_0} = \gamma_0 - \varphi_0(0); \quad Z_0 = z_0(0); \quad \Phi_0 = \varphi_0(0), \qquad (4.23)$$

and

$$\mathbf{u}_{(d,s)} = \begin{Vmatrix} u_{11} & u_{12} & u_{13} & u_{11} & u_{12}+u_{13} \\ u_{21} & u_{22} & \cdots & \cdots & \cdots \\ u_{31} & u_{32} & \cdots & \cdots & \cdots \\ u_{11} & u_{12} & \cdots & \cdots & \cdots \\ u_{21}+u_{31} & u_{22}+u_{32} & \cdots & \cdots & u_{22}+u_{32}+u_{23}+u_{33} \end{Vmatrix}. \qquad (4.24)$$

Then

$$\nu^2\, \mathbf{u}_{(d,s)}\, \mathbf{f}_{d_0,s} = \begin{Vmatrix} L_z \\ L_\Phi \\ L_\gamma \\ L_z \\ L_\Phi + L_\gamma \end{Vmatrix}. \qquad (4.25)$$

So if we introduce the matrix

$$\mathbf{K}_{(d),s} = \begin{Vmatrix} & & & 0 & 0 \\ & \Xi & & 0 & 0 \\ & & & 0 & 0 \\ 0 & 0 & 0 & \frac{2}{k_z} & 0 \\ 0 & 0 & 0 & 0 & \frac{2}{k_\Phi} \end{Vmatrix}, \qquad (4.26)$$

the equation

$$\mathbf{f}_{d_0,s} = \nu^2 \int_0^b \mathbf{K}_{(d),s}\, \mathbf{u}_{(d,s)}\, \mathbf{f}_{d_0,s}\, d\eta \qquad (4.27)$$

easily appears to be equivalent to equation (4.20) *and* its independent addenda (3.38). It is therefore another complete equivalent of the basic equations, specialised to symmetric oscillations only.

4.4 *Matrix equations for antisymmetric oscillations.*

For antisymmetric vibrations only, we introduce the matrix

$$\mathbf{K}_A = \begin{Vmatrix} K_{11}A & K_{12}A & K_{13}A \\ K_{21}A & K_{22}A & K_{23}A \\ K_{31}A & K_{32}A & K_{33}A \end{Vmatrix} \qquad (4.28)$$

making it possible to contract the (generalized) set (3.39), (3.41), (3.42) to

$$\mathbf{f}_{0,A}(y) = \nu^2 \int_0^b \mathbf{K}_A(y, \eta)\, \mathbf{u}(\eta)\, \mathbf{f}_{0,A}(\eta)\, d\eta. \qquad (4.29)$$

Similarly,

$$\mathbf{f}_{0,A}(y) - \mathbf{c}_{0,A} = \nu^2 \int_0^b \Xi(y, \eta)\, \mathbf{u}(\eta)\, \mathbf{f}_{0,A}(\eta)\, d\eta, \qquad (4.30)$$

with

$$\mathbf{c}_{0,A}^* = \| y\, z_0'(0) \quad 0 \quad 0 \|. \qquad (4.31)$$

If

$$\mathbf{u}_{(d,A)} = \begin{Vmatrix} u_{11} & u_{12} & u_{13} & u_{11} \\ u_{21} & u_{22} & u_{23} & u_{21} \\ u_{31} & u_{32} & u_{33} & u_{31} \\ u_{11} & u_{12} & u_{13} & u_{11} \end{Vmatrix}, \qquad (4.32)$$

and

$$\mathbf{f}_{d_0,A}^* = \| z_{d_0} \quad \varphi_{d_0} \quad \gamma_{d_0} \quad y\, \theta_0 \|$$

with

$$\theta_0 = z_0'(0), \quad z_{d_0} = z_0 - y\, \theta_0; \quad \varphi_{d_0} = \varphi_0; \quad \gamma_{d_0} = \gamma_0, \qquad (4.33)$$

[1]) The discriminative appendices S and A to the Ξ-matrix have been dropped. See par. 3.4.

we easily find

$$\nu^2\,\mathbf{u}_{(d,\,A)}\,\mathbf{f}_{d_0,\,A} = \left\| \begin{array}{c} L_z \\ L_\varphi \\ L_\gamma \\ L_z \end{array} \right\| .$$

So a complete equivalent of (3.47), (3.48), (3.49) *and* the supplement

$$\int_0^b L_z\,(\eta)\;\eta\,d\eta = \tfrac{1}{2}\,k_\vartheta\,z_0'\,(0) = \tfrac{1}{2}\,k_\vartheta\,\theta_0$$

is given by

$$\mathbf{f}_{d_0,\,A}\,(y) = \\ = \nu^2 \int_0^b \mathbf{K}_{(d),\,A}\,(y,\eta)\;\mathbf{u}_{(d,\,A)}\,(\eta)\,\mathbf{f}_{d_0,\,A}\,(\eta)\,d\eta\,, \quad (4.34)$$

if

$$\mathbf{K}_{(d),\,A} = \left\| \begin{array}{cccc} & & & 0 \\ & \Xi & & 0 \\ & & & 0 \\ 0 & 0 & 0 & 2\,\dfrac{y\,\eta}{k_\vartheta} \end{array} \right\| . \quad (4.35)$$

4.5 *Numerical evaluation of integrals with the help of enlarged matrices.*

An integral being the limit of a sum, it is generally possible to approximate it by a finite sum. It is of interest to see, what comes out of the equations (4.18), (4.29) [1]), if we introduce such approximations for the integral.

We shall make use of the abbreviations

$$K_{hk}^{X}\,(\sigma,\tau) \equiv K_{hk}^{X}\,(y_\sigma,\,\eta_\tau), \text{ etc.} \quad (4.36)$$

The simplest method is to approximate the integral in accordance with the example (F: arbitrary function)

$$\int_0^b F\,(\eta)\,d\eta \approx \sum_1^n F\,(\sigma)\;(\eta_\sigma - \eta_{\sigma-1})$$

but a better accuracy may be reached by the use of some rule like Simpson's, based on quadratic interpolation. The integration-formula may in any case be represented by the general formula

$$\int_0^b F\,(\eta)\,d\eta = \sum_0^n a_\sigma\,F\,(\sigma),$$

the a_σ's being coefficients, following from the integration rule adopted. By the use of this formula the integral equation leads to a system of ordinary algebraïc equations, which again may be represented in the form of a single matrix equation. The fact, that the original equation is in the case under consideration a matrix equation of its own, does not imply essential difficulties. Omitting the simple intermediate calculations, we shall write the result right down. It is

$$\tilde{\mathbf{f}}_{0,\,X} = \nu^2\,\tilde{\mathbf{K}}_X\,\tilde{\mathbf{u}}\,\tilde{\mathbf{f}}_{0,\,X}\,; \quad X = S, A\,, \quad (4.34)$$

with (omitting the discrimination S, A)

$$\tilde{\mathbf{f}}_0^{\,*} = \| z_0\,(0) \quad z_0\,(1) \ldots z_0\,(n) \quad \varphi_0\,(0) \\ \varphi_0\,(1) \ldots \varphi_0\,(n) \quad \gamma_0\,(0) \quad \gamma_0\,(1) \ldots \gamma_0\,(n) \|\,, \quad (4.35)$$

$$\tilde{\mathbf{u}} = \left\| \begin{array}{cccccccccccc} a_0u_{11}(0) & 0 & \ldots & 0 & a_0u_{12}(0) & 0 & \ldots & 0 & a_0u_{13}(0) & 0 & \ldots & 0 \\ 0 & a_1u_{11}(1) & \ldots & 0 & 0 & a_1u_{12}(1) & \ldots & 0 & 0 & a_1u_{13}(1) & \ldots & 0 \\ \vdots & \vdots & & \vdots & \vdots & \vdots & & \vdots & \vdots & \vdots & & \vdots \\ 0 & 0 & \ldots & a_nu_{11}(n) & 0 & 0 & \ldots & a_nu_{12}(n) & 0 & 0 & \ldots & a_nu_{13}(n) \\ a_0u_{21}(0) & 0 & \ldots & 0 & a_0u_{22}(0) & 0 & \ldots & 0 & a_0u_{23}(0) & 0 & \ldots & 0 \\ 0 & a_1u_{21}(1) & \ldots & 0 & 0 & a_1u_{22}(1) & \ldots & 0 & 0 & a_1u_{23}(1) & \ldots & 0 \\ \vdots & \vdots & & \vdots & \vdots & \vdots & & \vdots & \vdots & \vdots & & \vdots \\ 0 & 0 & \ldots & a_nu_{21}(n) & 0 & 0 & \ldots & a_nu_{22}(n) & 0 & 0 & \ldots & a_nu_{23}(n) \\ a_0u_{31}(0) & 0 & \ldots & 0 & a_0u_{32}(0) & 0 & \ldots & 0 & a_0u_{33}(0) & 0 & \ldots & 0 \\ 0 & a_1u_{31}(1) & \ldots & 0 & 0 & a_1u_{32}(1) & \ldots & 0 & 0 & a_1u_{33}(1) & \ldots & 0 \\ \vdots & \vdots & & \vdots & \vdots & \vdots & & \vdots & \vdots & \vdots & & \vdots \\ 0 & 0 & \ldots & a_nu_{31}(n) & 0 & 0 & \ldots & a_nu_{32}(n) & 0 & 0 & \ldots & a_nu_{33}(n) \end{array} \right\| \quad (4.36)$$

We devide the interval $0 \leqq y \leqq b$ into n equal or unequal small parts by the points

$$y = y_1\,, \quad y = y_2\,, \quad \ldots\ldots\,, \quad y = y_{n-1}$$

and intend to operate with the numbers

$$K_{kh}^{X}\,(y_\sigma,\,\eta_\tau)\,;\; u_{hk}\,(\eta_\sigma)\,;\; z_0\,(\eta_\sigma)\,;\; \varphi_0\,(\eta_\sigma)\,;\; \gamma_0\,(\eta_\sigma)\,; \\ \sigma, \tau = 1, 2, \ldots\ldots\, n\,;\; X = S, A$$

only (y_0 being equal to zero and y_n to b).

and, in a more concise notation,

$$\tilde{\mathbf{K}}_X = \left\| \begin{array}{ccc} \mathbf{K}_{11}^{X}\,(\sigma,\tau) & \mathbf{K}_{12}^{X}\,(\sigma,\tau) & \mathbf{K}_{13}^{X}\,(\sigma,\tau) \\ \mathbf{K}_{21}^{X}\,(\sigma,\tau) & \mathbf{K}_{22}^{X}\,(\sigma,\tau) & \mathbf{K}_{23}^{X}\,(\sigma,\tau) \\ \mathbf{K}_{31}^{X}\,(\sigma,\tau) & \mathbf{K}_{32}^{X}\,(\sigma,\tau) & \mathbf{K}_{33}^{X}\,(\sigma,\tau) \end{array} \right\|, \quad 4.37)$$

with

$$\mathbf{K}_{hk}^{X} = \left\| \begin{array}{ccc} K_{hk}^{X}(0,0) & K_{hk}^{X}(0,1) \ldots & K_{hk}^{X}(0,n) \\ K_{hk}^{X}(1,0) & K_{hk}^{X}(1,1) \ldots & K_{hk}^{X}(1,n) \\ \vdots & \vdots & \vdots \\ K_{hk}^{X}(n,0) & K_{hk}^{X}(n,1) \ldots & K_{hk}^{X}(n,n) \end{array} \right\| \quad (4.38)$$

[1]) We take these equations instead of (4.13), since the halved range of integration implies some useful simplification of the resulting formulae.

It is obvious that other matrix-integral equations may be transformed by similar processes. We remark, that the results may be considered as *almost exact*, if we restrict the investigation to a small number of the "lowest" modes of natural vibration, and if the subdivision of the interval is not too rough.

5 General properties of the solutions.

5.1 *Biorthogonality and normalization.*

Let

$$\mathbf{g}_0^*(y) = \| w_0(y) \quad \psi_0(y) \quad \beta_0(y) \| \tag{5.1}$$

be any vector of complex functions, satisfying the boundary conditions imposed upon the functions z_0, φ_0, γ_0 of the vector $\mathbf{f}_0$. Then integration by parts shows immediately, that

$$\int_{-b}^{+b} \mathbf{g}_0^*(y)\,\mathbf{e}(y)\,\mathbf{f}_0(y)\,dy = \int_{-b}^{+b} \mathbf{f}_0^*(y)\,\mathbf{e}(y)\,\mathbf{g}_0(y)\,dy\,. \tag{5.2}$$

This is a *scalar* relation. The complete development of it is

$$\begin{aligned}\int_{-b}^{+b} \{\, & w_0(e_{11}z_0 + e_{12}\varphi_0 + e_{13}\gamma_0) + \\ & + \psi_0(e_{21}z_0 + e_{22}\varphi_0 + e_{23}\gamma_0) + \\ & + \beta_0(e_{31}z_0 + e_{32}\varphi_0 + e_{33}\gamma_0)\,\}\,dy = \\ = \int_{-b}^{+b} \{\, & z_0(e_{11}w_0 + e_{12}\psi_0 + e_{13}\beta_0) + \\ & + \varphi_0(e_{21}w_0 + \ldots) + \gamma_0(e_{31}w_0 + \ldots)\,\}\,dy\,. \end{aligned} \tag{5.3}$$

If we replace both $\mathbf{f}_0$ and $\mathbf{g}_0$ by the *same* vector *real* functions, satisfying the boundary conditions, the integrals (5.2), (5.3) give the potential energy, stored in the mechanical system when distorted in accordance with the chosen functions. The fact, that this energy is a homogeneous quadratic expression in z_0, φ_0, γ_0 and their derivatives secures the interchangeability of the $\mathbf{f}_0$ and $\mathbf{g}_0$ vectors. The symmetry ($\mathbf{e}^* \equiv \mathbf{e}$) of the **e**-matrix is another aspect of the same thing.

Since the **u**-matrix is *not* symmetrical, we have

$$\int_{-b}^{+b} \mathbf{g}_0^*\,\mathbf{u}\,\mathbf{f}_0\,dy \neq \int_{-b}^{+b} \mathbf{f}_0^*\,\mathbf{u}\,\mathbf{g}_0\,dy\,,$$

but

$$\int_{-b}^{+b} \mathbf{g}_0^*\,\mathbf{u}\,\mathbf{f}_0\,dy = \int_{-b}^{+b} \mathbf{f}_0^*\,\mathbf{u}^*\,\mathbf{g}_0\,dy\,. \tag{5.4}$$

Equations (5.2) and (5.4) are the base of many important theorems.

Assume that the solutions of our basic equation (5.4) with its homogeneous boundary conditions consist of an infinite set of "characteristic" vectors

$$\mathbf{f}_{0,1},\ \mathbf{f}_{0,2},\ \mathbf{f}_{0,3},\ \ldots\ldots \text{ ad inf.}$$

of complex functions, each belonging to a generally complex characteristic number ν_i^2 ($i = 1, 2, \ldots \infty$). We shall not trouble ourselves with a mathematical proof, that this well-known property of the real counterpart of our problem is preserved in the complex case.

Then, if $\mathbf{f}_{0,i}$ is the characteristic vector, belonging to the characteristic number ν_i^2,

$$\mathbf{e}\,\mathbf{f}_{0,i} = \nu_i^2\,\mathbf{u}\,\mathbf{f}_{0,i}\,. \tag{5.5}$$

Let now $\mathbf{g}_{0,j}$ be the characteristic function, belonging to the characteristic number μ_j^2, of the *adjoint* system; i. e. (compare (4.9) and (4.11))

$$\mathbf{e}\,\mathbf{g}_{0,j} = \mu_j^2\,\mathbf{u}^*\,\mathbf{g}_{0,j}\,. \tag{5.6}$$

(It may be remarked, that the adjoint boundary conditions are identical with the original ones). Then, from (5.5)

$$\int_{-b}^{+b} \mathbf{g}_{0,j}^*\,\mathbf{e}\,\mathbf{f}_{0,i}\,dy = \nu_i^2 \int_{-b}^{+b} \mathbf{g}_{0,j}^*\,\mathbf{u}\,\mathbf{f}_{0,i}\,dy\,. \tag{5.7}$$

The left side of this relation can, by virtue of (5.2), be changed into

$$\int_{-b}^{+b} \mathbf{f}_{0,i}^*\,\mathbf{e}\,\mathbf{g}_{0,j}\,dy\,,$$

and this is, by (5.6), equal to

$$\mu_j^2 \int_{-b}^{+b} \mathbf{f}_{0,i}^*\,\mathbf{u}^*\,\mathbf{g}_{0,j}\,dy\,.$$

We infer that, in view of (5.4),

$$(\nu_i^2 - \mu_j^2) \int_{-b}^{+b} \mathbf{g}_{0,j}^*\,\mathbf{u}\,\mathbf{f}_{0,i}\,dy = 0\,. \tag{5.8}$$

Now, imagine the antisymmetric part

$$\tfrac{1}{2}(\mathbf{u} - \mathbf{u}^*)$$

of the **u**-matrix to be gradually diminished in a suitable way. Then, in the end both **u** and $\mathbf{u}^*$ become equal to the matrix $\frac{1}{2}(\mathbf{u} + \mathbf{u}^*)$ of a self-adjoint system and the sets ν_i^2, $\mathbf{f}_{0,i}$; μ_j^2, $\mathbf{g}_{0,j}$; ($i, j = 1, 2 \ldots \infty$) consist of in-pairs-identical solutions. It is possible to arrange both sets in such a way, that for all values of i

$$\nu_i^2 = \mu_i^2\,;\quad \mathbf{f}_{0,i} \equiv \mathbf{g}_{0,i} \quad \text{for} \quad \mathbf{u} - \mathbf{u}^* = 0.$$

But in this limiting case the integral in (5.8) does not vanish for $i = j$. From this we may safely conclude, that it will not vanish generally (for $i = j$) at an arbitrary stage of the process. Hence, μ_i^2 must be equal to ν_i^2 in order to fulfil (5.8), i. e.: the original system and its adjoint companion have the same sets of characteristic numbers.

If $i \neq j$ we derive from (5.8) (since in the case

under consideration all characteristic numbers may safely be assumed to be distinct [1]))

$$\int_{-b}^{+b} \mathbf{g}_{0,j}^{*}\ \mathbf{u}\ \mathbf{f}_{0,i}\ dy = 0;\ i \neq j. \qquad (5.9)$$

This is the biorthogonality relation, holding for the functions of the sets $\mathbf{f}_{0,i}$; $\mathbf{g}_{0,j}$. It obviously reduces to common orthogonality if the system is self-adjoint.

To (5.9) we may add some suitable normalization of the function pairs $\mathbf{f}_{0,i}$; $\mathbf{g}_{0,j}$. We shall generally make use of the regulation

$$\nu_i^2 \int_{-b}^{+b} \mathbf{g}_{0,i}^{*}\ \mathbf{u}\ \mathbf{f}_{0,i}\ dy = 1, \qquad (5.10)$$

a regulation, which may be completed by some other one-fold condition, which by lack of interest may remain unspecified.

5.2 *Expansion of arbitrary function-vector.*

The properties (5.9), (5.10) are the base of the series development of an arbitrary function-vector $\mathbf{h}_0$, built upon the system of characteristic functions of one or the other of our systems of basic equations.

Indeed, assume

$$\mathbf{h}_0 = \sum_{1}^{\infty} a_i\ \mathbf{f}_{0,i}, \qquad (5.11)$$

then, by (5.9) and (5.10),

$$\int_{-b}^{+b} \mathbf{g}_{0,j}^{*}\ \mathbf{u}\ \mathbf{h}_0\ dy = \sum_{1}^{\infty} a_i \int_{-b}^{+b} \mathbf{g}_{0,j}^{*}\ \mathbf{u}\ \mathbf{f}_{0,i}\ dy = \frac{a_j}{\nu_j^2}. \qquad (5.12)$$

This formula determines the coefficients of the expansion. It is well-known, that the series (5.11), with (5.12), is convergent in all cases that may be met in problems of vibration analysis.

5.3 *Relations for the kernels of integral equations.*

Let

$$\mathbf{f}_0 = \nu^2 \int_{-b}^{+b} \mathbf{K}\ (y, \eta)\ \mathbf{u}\ (\eta)\ \mathbf{f}_0\ (\eta)\ d\eta$$

$$\mathbf{g}_0 = \nu^2 \int_{-b}^{+b} \mathbf{K}\ (y, \eta)\ \mathbf{u}^{*}\ (\eta)\ \mathbf{g}_0\ (\eta)\ d\eta \ \text{(adj. eq.)} \qquad (5.13)$$

(the adjoint equation containing — by virtue of (4.14) — the same kernel as the original one).

We then know from the theory of integral equations, that the kernel permits the development

$$\mathbf{K}\ (y, \eta) = \sum_i \mathbf{f}_{0,i}\ (y)\ \mathbf{g}_{0,i}^{*}\ (\eta) =$$
$$\mathbf{K}^{*}\ (\eta, y) = \sum_i \mathbf{g}_{0,i}\ (y)\ \mathbf{f}_{0,i}^{*}\ (\eta) \qquad (5.14)$$

if $\mathbf{f}_{0,i}$, $(i = 1 \ldots \infty)$, is the system of normalized (in accordance with (5.10)) -characteristic functions of the first equation of the pair (5.13), and $\mathbf{g}_{0,i}$, $i = 1 \ldots \infty$ the system of characteristic functions of the second one.

It is indeed easily seen (in view of (5.9) and (5.10)), that the equations

$$\mathbf{f}_0\ (y) = \nu^2 \int_{-b}^{+b} \{ \sum_i \mathbf{f}_{0,i}\ (y)\ \mathbf{g}_{0,i}^{*}(\eta) \}\, \mathbf{u}\ (\eta)\ \mathbf{f}_0\ (\eta)\ d\eta,$$

$$\mathbf{g}_0\ (y) = \nu^2 \int_{-b}^{+b} \{ \sum_i \mathbf{g}_{0,i}\ (y)\ \mathbf{f}_{0,i}^{*}(\eta) \}\, \mathbf{u}^{*}\ (\eta)\ \mathbf{g}_0\ (\eta)\ d\eta,$$

have the solutions

$$\nu^2 = \nu_j^2,\ \mathbf{f}_0 = \mathbf{f}_{0,j}\ ;\ \nu^2 = \nu_k^2,\ \mathbf{g}_0 = \mathbf{g}_{0,k}.$$

If we apply the development (5.14) to the kernel of equation (4.27) we get

$$\mathbf{K}_{(d),s}\ (y, \eta) = \sum_i \{ \mathbf{f}_{d_0,s}\ (y) \}_i\ \{ \mathbf{g}_{d_0,s}^{*}\ (\eta) \}_i. \qquad (5.15)$$

Since we may write in succession to (4.22)

$$(\mathbf{f}_{d_0,s}^{*})_i = \| (z_{d_0})_i\ (\Phi_{d_0})_i\ (\gamma_{d_0})_i\ Z_{0,i}\ \Phi_{0,i} \|$$
$$(\mathbf{g}_{d_0,s}^{*})_i = \| (w_{d_0})_i\ (\psi_{d_0})_i\ (\beta_{d_0})_i\ W_{0,i}\ \Psi_{0,i} \|$$

the right side of (5.15) produces the matrix

$$\left\| \begin{array}{ccccc} \Sigma \{ z_{d_0}(y) \}_i \{ w_{d_0}(\eta) \}_i & \Sigma \{ z_{d_0}(y) \}_i \{ \psi_{d_0}(\eta) \}_i & \Sigma \{ z_{d_0}(y) \}_i \{ \beta_{d_0}(\eta) \}_i & \Sigma \{ z_{d_0}(y) \}_i W_{0,i} & \Sigma \{ z_{d_0}(y) \}_i \Psi_{0,i} \\ \Sigma \{ \Phi_{d_0}(y) \}_i \{ w_{d_0}(\eta) \}_i & \Sigma \{ \Phi_{d_0}(y) \}_i \{ \psi_{d_0}(\eta) \}_i & \Sigma \{ \Phi_{d_0}(y) \}_i \{ \beta_{d_0}(\eta) \}_i & \Sigma \{ \Phi_{d_0}(y) \}_i W_{0,i} & \Sigma \{ \Phi_{d_0}(y) \}_i \Psi_{0,i} \\ \ldots & \ldots & \ldots & \ldots & \ldots \\ \ldots & \ldots & \ldots & \ldots & \ldots \\ \Sigma \Phi_{0,i} \{ w_{d_0}(\eta) \}_i & \Sigma \Phi_{0,i} \{ \psi_{d_0}(\eta) \}_i & \ldots & \ldots & \Sigma \Phi_{0,i} \Psi_{0,i} \end{array} \right\|$$

the functions implied being the even characteristic functions only. Comparing with (4.26) we conclude that

$$\Xi\ (y, \eta) = \sum_i \left\| \begin{array}{c} \{ z_{d_0}(y) \}_i \\ \{ \Phi_{d_0}(y) \}_i \\ \{ \gamma_{d_0}(y) \}_i \end{array} \right\| \left\| \{ w_{d_0}(\eta) \}_i \quad \{ \psi_{d_0}(\eta) \}_i \quad \{ \beta_{d_0}(\eta) \}_i \right\|, \qquad (5.16)$$

[1]) With the theoretical exception that by mere accident a natural frequency of some symmetric natural vibration would coincide exactly with the natural frequency of any of the antisymmetric vibrations.

or, making use of new abbreviations,

$$\Xi(y, \nu) = \sum_i \{ f_{d_0 S}(y) \}_i \{ g_{d_0 S^*}(\nu) \}_i . \quad (5.17)$$

Hence

$$\begin{aligned} 0 &= \sum_i \{ f_{d_0 S}(y) \}_i W_{0,i}, \\ 0 &= \sum_i \{ f_{d_0 S}(y) \}_i \Psi_{0,i}, \\ 0 &= \sum_i Z_{0,i} \{ g_{d_0 S^*}(\nu) \}_i, \\ 0 &= \sum_i \Phi_{0,i} \{ g_{d_0 S^*}(\nu) \}_i, \end{aligned} \quad (5.18)$$

$$\sum_i Z_{0,i} W_{0,i} = \frac{2}{k_z}; \quad \sum_i Z_{0,i} \Psi_{0,i} = 0;$$

$$\sum_i \Phi_{0,i} W_{0,i} = 0; \quad \sum_i \Phi_{0,i} \Psi_{0,i} = \frac{2}{k_\Phi}. \quad (5.19)$$

But from (4.18) we infer that

$$\mathbf{K}_S(y, \nu) = \sum_i \{ f_{0,S}(y) \}_i \{ g_{0,S^*}(\nu) \}_i$$

or

$$\mathbf{K}_S(y, \nu) = \sum_i [\{ f_{d_0 S}(y) \}_i + \left\| \begin{matrix} Z_{0,i} \\ \Phi_{0,i} \\ \Phi_{0,i} \end{matrix} \right\|] [\{ g_{d_0 S^*}(\nu) \}_i + \| W_{0,i} \Psi_{0,i} \Psi_{0,i} \|].$$

By (5.17), (5.18), (5.19) this is easily seen to be reducible to

$$\mathbf{K}_S(y, \nu) = \Xi(y, \nu) + \left\| \begin{matrix} \frac{2}{k_z} & 0 & 0 \\ 0 & \frac{2}{k_\Phi} & \frac{2}{k_\Phi} \\ 0 & \frac{2}{k_\Phi} & \frac{2}{k_\Phi} \end{matrix} \right\| \quad (5.20)$$

This formula presents the *general* relation between the $\mathbf{K}_S$ and the Ξ-matrices. It is easily seen to be confirmed by physical considerations (the interpretation of the elements of the **K**-matrix as influence functions, see appendix I). For the antisymmetrical group we must obviously find

$$\mathbf{K}_A(y, \nu) = \Xi(y, \nu) + \left\| \begin{matrix} \frac{y\nu}{k_\vartheta} & 0 & 0 \\ 0 & 0 & 0 \\ 0 & 0 & 0 \end{matrix} \right\|. \quad (5.21)$$

6 Approximation methods, employing series expressions for the solutions.

6.1 *Natural oscillations and solutions of the mathematical equations.*

Before we proceed to the discussion of procedures for solving the equations, it is desirable to pay some attention to the structure of the elements of the **a**-matrix (4.3), which makes part of the load-matrix **u**.

It has been stated already (par. 2.3), that the elements a_{hk} depend solely upon a number of *geometrical* parameters of the mechanical system, and upon a parameter V, the "reduced velocity", defined by (2.6), or, admitting also complex values of ν, in fact by

$$V = \frac{v}{c\, Re(\nu)}. \quad (6.1)$$

By the occurrence of the chord c and the other geometrical parameters the matrix **a** generally depends upon the coordinate y.

Now the first thing to remark is, that it is strictly speaking illegitimate to present the aerodynamic loading (assumption h of par. 2.1 being accepted!) in the form

$$\nu^2 \mathbf{a} \mathbf{f}_0 . e^{i\nu t} \quad (6.2)$$

(with (4.3)), unless the oscillation is sinusoïdal, that is, unless

$$Im(\nu) = 0.$$

If, however, this condition is *not* fulfilled, the convention (6.1) for the V-parameter, appearing in the a_{hk}-elements, valid strictly for sinusoïdal oscillations only, secures by (6.2) a sound approximation of the aerodynamic loading for *slightly* (exponentially) increasing or decreasing oscillations too. The approximation breaks down if $Im(\nu)$ reaches the same order of magnitude as $Re(\nu)$. But since the undamped (i.e. sinusoïdal) oscillation constitutes the transition between stability and instability, the range of ("exact or approximate") validity of our formulae fits exactly to the primary purposes of our calculations. This shows that there is effectively no objection against the formal acceptance of basic equations, containing aerodynamic loadings defined by (6.2), with (6.1). These equations define a definite mathematical problem. Having solved it, we have to restrict physical interpretation to solutions with

$$| Re(\nu) | \gg | Im(\nu) | ,$$

admitting that other solutions give only poor descriptions of actual — but from the point of view of change of stability: unimportant — modes of vibration.

Secondly we must reconsider the legality of treating ν^2 as the parameter of characteristic numbers, accepting for

$$V_0 = \frac{v}{c_0\, Re(\nu)}, \quad (c_0: \text{some reference chord}),$$

$$(V = V_0 \frac{c_0}{c} = V_0 \times \text{a known function of } y),$$

some *constant* value, in spite of the fact, that V_0 depends upon the frequency, that is upon the characteristic number itself (which really means, that ν enters in the equations in a highly complicated way). The admissability of the designed procedure clearly emerges from the fact, that V_0 depends also upon the parameter v, which may be supposed to assume any value within a wide range of variation. Indeed, we can clearly acquire any prescribed value of V_0 by combination of a frequency (that is: of a characteristic number belonging to *this* value of V_0) with a value of v (viz. the value $V_0 c_0 Re(\nu)$). This reveals that the solutions of our mathematical equations, valid for a prescribed value of V_0, describe (under restrictions mentioned before) actual natural vibrations of the mechanical system, but each exemplar becoming realised at its own speed.

Consequently, to find the natural vibrations, realised at a prescribed *speed* v, it is necessary to solve the basic equations for a series of suitable values of V_0, selecting from each set of solutions the appropriate exemplar. Hence the mathematical problem, explained in the preceding chapters, indeed constitutes the root of the flutter problem.

6.2 *Construction of the approximation basis.*

Nearly all customary methods to attain approximative solutions are built upon the assumption, that it will be possible to *guess* a *restricted* number of linearly independent functionvectors

$$\mathbf{F}_{0,1}(y),\ \mathbf{F}_{0,2}(y)\ \ldots\ldots\ \mathbf{F}_{0,N}(y), \qquad (6.3)$$

permitting by suitable choice of (sets of) the coefficients in the series

$$\sum_{1}^{N} q_H\ \mathbf{F}_{0,H}(y) \qquad (6.4)$$

a sufficiently close approximation to the required mode (or modes) $\mathbf{f}_{0,i}(y)$ of natural oscillation. It is the art

- *a* to guess vectors $\mathbf{F}_{0,H}(y)$, admitting a satisfactory result without *unavoidable* enlargement of the number N.
- *b* to determine (sets of) appropriate values

$$q_H = q_{H,K},\quad K = 1 \ldots N'$$

(N' = number of required modes) of the coefficients.

The necessity to keep the number N low is a consequence of the extremely rapid growth of the extent of the computations with increasing N. It really demands highest carefulness with the design of the functions $\mathbf{F}_{0,H}$. The best thing to do is to make use of all information available about the required solutions $\mathbf{f}_{0,i}$, especially to insert in the functions $\mathbf{F}_{0,H}$ all known properties of these functions. As such, we may refer to boundary conditions and to transition conditions in sections with concentrated loads, though it would truly be exaggerated to attach equal importance to all of these conditions.

Since the problem is, properly speaking, a common one in vibration-analysis, we may safely concentrate attention upon two typical complications, connected with the application to the flutter problem and hence generally falling outside the field of common experience.

The first arises from the absence of adequate knowledge to estimate suitable ratios between the constituents of the vectors $\mathbf{F}_{0,H}$.

It is generally solved by the use of vectors, each constructed from one constituent only. In this case it is highly recommendable to split off the motion of the fuselage (strictly the motion in the $y = 0$-plane). We thus arrive at a set of functions of the type

$$\left\| \begin{matrix} Z_0 \\ 0 \\ 0 \end{matrix} \right\|, \left\| \begin{matrix} z_{0,\mathrm{I}}(y) \\ 0 \\ 0 \end{matrix} \right\|, \left\| \begin{matrix} z_{0,\mathrm{II}}(y) \\ 0 \\ 0 \end{matrix} \right\|, \ldots\ldots, \left\| \begin{matrix} 0 \\ \Phi_0 \\ \Phi_0 \end{matrix} \right\|, \left\| \begin{matrix} 0 \\ \varphi_{0,\mathrm{I}}(y) \\ 0 \end{matrix} \right\|, \ldots\ldots, \left\| \begin{matrix} 0 \\ 0 \\ \gamma_{0,\mathrm{I}}(y) \end{matrix} \right\|, \ldots\ldots, \qquad (6.5)$$

with the important properties

$$0 = z_{0,\mathrm{I}}(0) = z_{0,\mathrm{I}}'(0),\ \text{etc.};\quad 0 = \varphi_{0,\mathrm{I}}(0),\ \text{etc.}$$

(If much aileron twist is to be expected, there is reason to split up moreover the aileron displacements into deflection and twist, e. g. by putting

$$\gamma_{0,\mathrm{I}} = \Gamma_0\ (\text{const.});\ \gamma_{0,K}(b_r) = 0,\ K = \mathrm{II}, \mathrm{III}, \ldots\ldots).$$

It is doubtlessly true, that the guess of suitable functions $z_{0,\mathrm{I}}, \ldots\ldots, \varphi_{0,\mathrm{I}}, \ldots\ldots, \gamma_{0,\mathrm{I}} \ldots\ldots$ is relatively easy, experience being a reliable guide. But theoretically a base like this may well be inferior to a base consisting of completely filled up function vectors, since it obviously offers no room to reproduce *any* property of mutual influence of the elementary deformations, which implies a tendency to rise the number N of functions, necessary to deal with the given number N' of required modes.

It may be remarked, that the difficulty explained above may be evaded partially or fully if modes of vibration are *known*, applying to "neighbouring circumstances", e. g.: if results of resonance tests in still air are available. It is then attractive to identify the vectors $\mathbf{F}_{0,H}$ with *measured* resonance modes, thus obtaining probably very effective functions. Yet, this possibility is seldom exploited. The factual reason is to be seen in the increase of the computations, bound to the use of complete vectors. It is thought to constitute an immoderate price for the presumed benefits.

The second, perhaps more serious, complication is linked to the *complex* constitution of even the *components* of the required vectors $\mathbf{f}_{0,i}(y)$. This property represents the *spanwise* phase shift, generally occurring in flutter oscillations (the *chordwise* phase shift leading to complex *ratios* of components only). These phase shifts are caused by the action of the aerodynamic forces. Little being known beforehand in this respect, adequate knowledge to lead a guess, pertinent to this point, fails. Theoretically it is possible to reproduce it with the help of complex coefficients q_H by vectors $\mathbf{F}_{0,H}$ with real components, but in this case a satisfactory result demands some minimum number of terms in (6.4), which is actually never used. Indeed, if we accept the (often used) only fivefold set (with separate representation of motions of the fuselage)

$$\left\| \begin{matrix} Z_0 \\ 0 \\ 0 \end{matrix} \right\|, \left\| \begin{matrix} z_{0,\mathrm{I}}(y) \\ 0 \\ 0 \end{matrix} \right\|, \left\| \begin{matrix} 0 \\ \Phi_0 \\ \Phi_0 \end{matrix} \right\|, \left\| \begin{matrix} 0 \\ \varphi_{0,\mathrm{I}}(y) \\ 0 \end{matrix} \right\|, \left\| \begin{matrix} 0 \\ 0 \\ \gamma_{0,\mathrm{I}}(y) \end{matrix} \right\|, \qquad (6.6)$$

belonging to the type (6.5), no useful reproduction of the spanwise phase shift remains possible if the functions $z_{0,\mathrm{I}}$, $\varphi_{0,\mathrm{I}}$ and $\gamma_{0,\mathrm{I}}$ are real.

It will appear in the next chapter, that the lacking knowledge about the complex nature of the components of the natural vibrations may be derived from preceding approximations, if we extend the calculation to a system of successive approximation. Practically this is the only way out, for the alternative: a raising of the number of vectors in the set (6.6), seems generally even more unprofitable.

Now the vast majority of all flutter calculations *ever made implies an approximation of the mode*, based on the set (6.6) containing real functions, or, in fact, even more simple representations (the smallest tolerable number of members in the set (6.3) being two, since otherwise any adequate representation of *chordwise* phase shifts is rendered impossible too, causing the grasp on the flutter phenomenon to break down completely). They all owe their sense to the fact, that the spanwise phase shift is generally small and that it seems to have no decisive effect on the stability of the vibration. It is actually *neglected*. Yet the availability of methods of successive approximation impells us to make no general use of simplifications, linked to a supposed absence of imaginary parts in the constituents of the vectors (6.3).

6.3 *Determination of coefficients and of approximations to natural frequencies.*

Let us introduce the approximation (6.4) into equation (4.5). Since it is just an approximation, we must expect that it will be impossible to assign such values to the coefficients q_H, that the equation is satisfied throughout. Hence, write

$$\sum_1^N q_H \{ -\mathbf{e}\,\mathbf{F}_{0,H} + \nu^2\,\mathbf{u}\,\mathbf{F}_{0,H} \} = \mathbf{d}, \quad (6.7)$$

$\mathbf{d} = \mathbf{d}(y)$ being the "error vector", depending upon the values of the coefficients q_H. Now, all common methods to find appropriate values of these coefficients come down to the reduction to zero of an N-fold series of linearly independent *mean values* of the error, each mean value being defined by a (generally complex) "weight vector" $\mathbf{G}_{0,J}^*(y)$ (the product $\mathbf{G}_{0,J}^*\mathbf{d}$ defining a *scalar*). In this way we get a system of N linear, mutually independent, equations for the N unknowns q_H

$$\sum_1^N q_H \int_{-b}^{+b} \{ -\mathbf{G}_{0,J}^*\,\mathbf{e}\,\mathbf{F}_{0,H} + \nu^2\,\mathbf{G}_{0,J}^*\,\mathbf{u}\,\mathbf{F}_{0,H} \}\, dy = 0,\ J = 1, 2, \ldots N. \quad (6.8)$$

It will be clear without detailed explanation that we may indeed get in a way like that justified approximations to the modes, actually accessible to approximative representation on the base (6.4), provided that the full set $\mathbf{G}_{0,J}$, $J = 1 \ldots N$, is *not* biorthogonal (or almost biorthogonal) to any required mode (which might provoke a mutilated result for such a mode).

The set (6.8) is soluble if its determinant vanishes, i. e. if

$$det \int_{-b}^{+b} \{ -\mathbf{G}_{0,J}^*\,\mathbf{e}\,\mathbf{F}_{0,H} + \nu^2\,\mathbf{G}_{0,J}^*\,\mathbf{u}\,\mathbf{F}_{0,H} \}\, dy = 0. \quad (6.9)$$

This condition, however, secures the solubility not only of the set (6.8), but also of the adjoint set

$$\sum_1^N r_J \int_{-b}^{+b} \{ -\mathbf{G}_{0,J}^*\,\mathbf{e}\,\mathbf{F}_{0,H} + \nu^2\,\mathbf{G}_{0,J}^*\,\mathbf{u}\,\mathbf{F}_{0,H} \}\, dy = 0,\ H = 1, 2, \ldots N. \quad (6.10)$$

The determinant of this set is equal to the transposed determinant of the original set.

Now, multiply the equations (6.8) by *arbitrary* (complex) numbers r_J $(J = 1, 2, \ldots N)$ and add the results

$$\int_{-b}^{+b} \{ \sum_1^N r_J\,\mathbf{G}_{0,J}^*\,\mathbf{e} \sum_1^N q_H\,\mathbf{F}_{0,H} - \nu^2 \sum_1^N r_J\,\mathbf{G}_{0,J}^*\,\mathbf{u} \sum_1^N q_H\,\mathbf{F}_{0,H} \}\, dy = 0. \quad (6.11)$$

If a solution

$$\nu^2 = \bar{\nu}_K^2\ ;\ q_H = q_{H,K},\ (H = 1 \ldots N) \quad (6.12)$$

of the set (6.8) actually constitutes a useful approximation to some mode of vibration, say the p^{th}, it is permissible to put

$$\sum_1^N q_{H,K}\,\mathbf{F}_{0,H} = \mathbf{f}_{0,p} + \sum_1^\infty \varepsilon_{pi}\,\mathbf{f}_{0,i} \quad (6.13)$$

with

$$|\varepsilon_{pi}| \ll 1, \quad (6.14)$$

provided that the solution is normalized in a suitable way. We shall in fact use the freedom, implied in the normalization, to make

$$\varepsilon_{pp} = 0. \quad (6.15)$$

Likewise it is allowed to put

$$\sum_1^N r_J\,\mathbf{G}_{0,J}^* = \sum_1^\infty g_j\,\mathbf{g}_{0,j}^*, \quad (6.16)$$

but it is not allowed to make any special assumption about the coefficients g_j of this development (apart of the effect of any normalization).

Inserting the expressions (6.12), (6.13) and (6.16) in (6.11), we get by virtue of (5.5), (5.9) and (5.10)

$$\sum_i g_i\,(\delta_{pi} + \varepsilon_{pi})\,\frac{\nu_i^2 - \bar{\nu}_K^2}{\nu_i^2} = 0.$$

Hence,

$$\frac{\bar{\nu}_K^2 - \nu_p^2}{\nu_p^2} = \sum_1^\infty \frac{g_i}{g_p}\,\varepsilon_{pi}\left(1 - \frac{\bar{\nu}_K^2}{\nu_i^2}\right). \quad (6.17)$$

This formula proves, that the root $\bar{\nu}_K^2$ of the determinantal equation (6.9) (which indeed is an algebraïc equation of degree N in ν^2) is *to first approximation* equal to ν_p^2, the square of the natural frequency of the p^{th} mode, provided that

a. the ratios $\frac{g_i}{g_p}$ $(i = 1 \dots \infty)$ are of unit order of magnitude,

b. the ratios $\frac{\bar{\nu}_K^2}{\nu_i^2}$ are not too large, that is: provided that the number p is not high [1]).

Since the first condition is fairly innocent (it leads to the restriction, mentioned in connection with eq. (6.8)), is appears that the equations (6.8), (6.9) furnish useful approximations to all modes of vibration *and* their accessory frequencies, accessible to satisfactory representation (as to the mode) on the base (6.4), and with small ordering number.

Up to now we have made no special assumption about the nature of the weight functions $\mathbf{G}_{0,J}$. It is natural to expect that some special choice may lead to particular profits. Indeed: assume that it has been possible to *guess* a set $\mathbf{G}_{0,J}$ $(J = 1, 2, \dots N)$, permitting by superpositions

$$\sum_1^N r_J \, \mathbf{G}_{0,J} \tag{6.18}$$

with appropriate coefficients, the construction of first approximations to the *adjoint* modes (i. e. to solutions of eq. $\mathbf{e}\,\mathbf{g}_0 - \nu^2 \mathbf{u}^* \mathbf{g}_0 = 0$), accompanying the original modes, accessible to approximation by (6.4). This means, that it is possible to choose numbers $r_{J,K}$ such that

$$\sum_1^N r_{J,K} \, \mathbf{G}_{0,J}{}^* = \mathbf{g}_{0,p}{}^* + \sum_1^\infty \gamma_{pi} \, \mathbf{g}_{0,i}{}^* \tag{6.19}$$

with

$$\gamma_{pi} \ll 1 \,;\; \gamma_{pp} = 0 \text{ (normalization)}. \tag{6.20}$$

Comparing with (6.16) we infer

$$g_j \to \delta_{pj} + \gamma_{pj}$$

and therefore (6.17) reduces to

$$\frac{\bar{\nu}_K^2 - \nu_p^2}{\nu_p^2} = \sum_1^\infty \gamma_{pi} \, \varepsilon_{pi} \left(1 - \frac{\bar{\nu}_K^2}{\nu_i^2} \right). \tag{6.21}$$

Hence, the error in the natural frequency comes down to *second* order of smallness. So if (and only if) we make use of weight functions, allowing the construction (by (6.18)) of a first approximation to the solution of the *adjoint* system, allied with a requested mode of vibration (itself accessible to approximative representation by (6.4)), one of the roots of eq. (6.9) will agree up to an error of second order of smallness with the accessory natural frequency. It will be clear, that this property is of high value, especially in flutter calculations, where the complex frequency-roots determine the stability of the oscillation.

[1]) The solutions ν_i^2, $\mathbf{f}_{0,i}$ are supposed to be ordered according to increasing *absolute* values of ν_i^2. If p is high, the real numbers $\left| \frac{\nu_p^2}{\nu_i^2} \right|$, with $i \ll p$ are generally very large.

6.4 *Construction of weight functions. The Galerkin/Lagrange-method.*

Let us look at the practical consequences of the results, achieved in the preceding paragraph.

The difference between the original system and its adjoint companion is known to be caused by the aerodynamic forces. Now it is just about the influence of these forces, that relatively little is known. So, if we look for a base to guess approximations to the solutions of the adjoint system, we shall generally come back to the same points of view, which have guided the construction of the functions, used to approximate the requested modes of vibration. In fact there will commonly be no reason at all to suppose some set of functions to be unsuitable for the approximation of solutions of the adjoint system, if it *is* considered satisfactory for the approximation of solutions of the *original* system. So it will in many cases be natural to put

$$\mathbf{G}_{0,J} \equiv \mathbf{F}_{0,J} \quad (J = 1 \dots N). \tag{6.22}$$

The way of treatment then reduces to a method, which, if applied to self-adjoint systems, is well-known and to which the name of Galerkin is connected. Indeed, the property of second-order errors in the calculated frequencies is a well-known feature of this method (when applied to self-adjoint systems). Moreover there is in this case equivalency with a method, based on a modified conception of the underlying mechanical system, viz. the conception, commonly characterised by the idea of "semi-rigidity". In this case we consider the mechanical system as a system of "restricted elasticity", assuming that in some way all distortions, *not* agreeing with the presupposed scheme (6.4), are "mechanically" made impossible. Indeed the Lagrangian set of equations of motion of a system like that appears to be reducible to (6.8) with (6.22) (Galerkin).

Though the identification (6.22) may be a natural expression of lacking knowledge, it is by no means the sole suitable proposal. It is perfectly permitted to guess again, with or without relation to the issue (6.3) of the "first guess", and there may be some reason to prefer this procedure to (6.22). Let for instance the guess be difficult. Then we must face the risk of relatively bad accuracy. A second guess gives another chance and may thereby limit the errors in the frequencies, though simultaneously increasing them *somewhat*, if the result of the first guess should happen to be *very* satisfactory.

It seems justified to summarize our conclusion as follows:

1°. there is one method to secure *second*-order errors in the frequencies, accompanying first-order errors in the modes. It employs weight functions, appropriate to the construction of first-order approximations to the accessory solutions of the adjoint system.

2°. if no special information (e.g. from preceding approximations in a sequence of successive approximations) is available, the Galerkin/

Lagrange-method may be used without disadvantage.

3°. the Galerkin/Lagrange-method is, however, theoretically a bad one to apply to non-self-adjoint systems.

4°. even for self-adjoint systems it may be advantageous to leave the Galerkin/Lagrange-method aside and to make use of an independent or related guess for the weight functions.

5°. it is generally dangerous to derive approximations to high modes from equations (6.8), (6.9), since the errors in the frequency will soon become excessive.

It seems wise to finish with the remark, that — the system $\mathbf{f}_{0,i}$ $(i=1 \dots \infty)$ being complete and hence suitable to represent (by a series) *any* function — the difference between the Galerkin/Lagrange method and the alternatives mentioned above may be supposed to vanish, if the number N is large and the number of requested lowest natural vibrations small. This is however a case, never met in flutter analysis!

6.5 *Approximation of a number of consecutive lowest modes and frequencies.*

We have already taken into account the possibility of approximating on a given base $\mathbf{F}_{0,H}$ *several* actual modes of vibration. The maximum number is obviously equal to the number of functions in the set $\mathbf{F}_{0,H}$, that is: to N.

Particularly attractive properties emerge, if the sets $\mathbf{F}_{0,H}$ *and* $\mathbf{G}_{0,J}$ permit approximative representations of every pair of solutions $\mathbf{f}_{0,p}$, $\mathbf{g}_{0,p}$ with $p \leqq N$. Since the solutions of equations (6.8) are invariant upon transformations of the type

$$(\mathbf{F}_{0,H})_{\text{new}} = \sum_{1}^{N} a_{HK}\, \mathbf{F}_{0,K}\,;$$

$$(\mathbf{G}_{0,J})_{\text{new}} = \sum_{1}^{N} b_{JK}\, \mathbf{G}_{0,K}\,; \quad H,J = 1 \dots N$$

in the basic sets $\mathbf{F}_{0,H}$, $\mathbf{G}_{0,J}$, we may in a case like that accept at once [1]) developments

$$\mathbf{F}_{0,H} = \sum_{i} (\delta_{Hi} + \varepsilon_{Hi})\, \mathbf{f}_{0,j}\,, \; H = 1 \dots N, \quad (6.23)$$

$$\mathbf{G}_{0,J} = \sum_{i} (\delta_{Ji} + \gamma_{Ji})\, \mathbf{g}_{0,i}\,, \; J = 1 \dots N, \quad (6,24)$$

with coefficients, satisfying the conditions

$$\varepsilon_{Hi} \ll 1\,, \; \varepsilon_{HH} = 0 \text{ (normalization)}\,;$$

$$H = 1 \dots N,\; i = 1 \dots \infty\,,$$

$$\gamma_{Ji} \ll 1\,. \; \gamma_{JJ} = 0 \text{ (normalization)}\,;$$

$$J = 1 \dots N,\; i = 1 \dots \infty\,.$$

Substituting these developments, we get from (6.8)

$$\sum_{H}\sum_{i} q_H\, (\delta_{Hi} + \varepsilon_{Hi})\, (\delta_{Ki} + \gamma_{Ki})\, \frac{\nu^2 - \nu_i^2}{\nu_i^2} = 0, K = 1 \dots N. \quad (6.25)$$

It is obvious, that the solutions must be of the type

$$q_K = \delta_{HP} + q_{HP}' \;\text{ with }\; q_{HP}' \ll 1,$$
$$\nu^2 \approx \nu_P^2,\; P = 1 \dots N \quad (6.26)$$

the latter approximation containing errors of the *second* order of smallness only. Inserting (6.26) into (6.25) and neglecting all terms of the second order, we easily get

$$q_{HP}'\, \frac{\nu_P^2 - \nu_H^2}{\nu_H^2} + \varepsilon_{PH}\, \frac{\nu_P^2 - \nu_H^2}{\nu_H^2} = 0,$$

or

$$q_{HP}' = -\varepsilon_{PH}\,,$$

a result, which may be considered to be valid to first approximation. Accordingly, again up to first approximation,

$$\sum q_H\, \mathbf{F}_{0,H} = \sum_{H}\sum_{i} (\delta_{HP} - \varepsilon_{PH})\, (\delta_{Hi} + \varepsilon_{Hi})\, \mathbf{f}_{0,i} \approx$$
$$\approx \sum_{i} (\delta_{Pi} + \varepsilon_{Pi})\, \mathbf{f}_{0,i} - \sum_{H} \varepsilon_{PH}\, \mathbf{f}_{0,H} =$$
$$= \mathbf{f}_{0,P} + \sum_{N+1}^{\infty} \varepsilon_{Pi}\, \mathbf{f}_{0,i}\,. \quad (6.27)$$

Hence all components with ordening number $\leqq N$ are — in the solutions — reduced to second order of smallness at least. This is apparently the typical feature of the approximations to the modes, produced in the present circumstances (weight functions in accordance with 1° par. 6.4; applicability of the base sets to N modes by the approximation procedure, embodied in the set (6.8)). It is a very useful feature, for we infer accordingly from (6.28), that the errors in the frequencies come out — at most with a failure of fourth order of smallness — at

$$\frac{\bar{\nu}_p^2 - \nu_p^2}{\nu_p^2} \approx \sum_{N+1}^{\infty} \gamma_{pi}\, \varepsilon_{pi} \left(1 - \frac{\bar{\nu}_p^2}{\nu_i^2}\right),$$
$$(p = 1 \dots N) \quad (6.28)$$

(writing $\bar{\nu}_p$ instead of $\bar{\nu}_K$, since we may now assume K to be equal to p). This formula contains *no* terms with large quantities $\frac{\bar{\nu}_p^2}{\nu_i^2}$, $i < p$, which justifies the expectation, that the approximations, found for the frequencies, may remain satisfactory even for modes of relatively high order.

This result is not valid, if we make use of weight functions, *not* permitting approximations to the adjoints of the requested low modes of vibration. This stresses again the value of a careful design of the weight functions.

6.6 *Superfluity of a seperation of fuselage displacements and distortions.*

It has been stated in par. (6.2), that we are often forced to accept a set like (6.5) for the functions $\mathbf{F}_{0,H}$. We infer that we shall commonly

[1]) as starting point for a theoretical discussion. The sets may actually permit these developments only after suitable transformation.

be obliged to use weight functions of a similar structure [1])

$$\left\| \begin{matrix} W_0 \\ 0 \\ 0 \end{matrix} \right\|, \quad \left\| \begin{matrix} w_{0,\mathrm{I}}(y) \\ 0 \\ 0 \end{matrix} \right\|, \ \ldots\ldots, \quad \left\| \begin{matrix} 0 \\ \Psi_0 \\ \Psi_0 \end{matrix} \right\|,$$

$$\left\| \begin{matrix} 0 \\ \psi_{0,\mathrm{I}}(y) \\ 0 \end{matrix} \right\|, \ \ldots\ldots, \quad \left\| \begin{matrix} 0 \\ 0 \\ \beta_{0,\mathrm{I}}(y) \end{matrix} \right\|, \ \ldots\ldots, \qquad (6.29)$$

$$w_{0,\mathrm{I}}(0) = w_{0,\mathrm{I}}'(0) = 0, \text{ etc. } \ldots .$$

It is then easy to verify, that the two equations of the set (6.8), following from the constant exemplars

$$\left\| \begin{matrix} W_0 \\ 0 \\ 0 \end{matrix} \right\| ; \quad \left\| \begin{matrix} 0 \\ \Psi_0 \\ \Psi_0 \end{matrix} \right\|$$

in this set of weight functions, become equivalent to the integral conditions (2.25), (2.26). Hence, any *independent* use of these conditions (e.g. combined with a separation of displacements of the fuselage and distortions in the basic equations, see par. 2.6, the end) is actually superfluous, since these conditions are automatically included in the scheme of calculation, if only we adopt identical points of view with respect to the construction of the sets $\mathbf{F}_{0,H}$ and $\mathbf{G}_{0,J}$.

6.7 *Approximation method based on the integral equations.*

The approximation methods of par. 6.3 to 6.6 are built upon the fundamental differential equations of the system. We might try to use the equivalent integral equation to the same purpose. Let us therefore introduce the assumption (6.4) in equation (4.13). It will again be necessary to introduce simultaneously some error-vector $\mathbf{d}$. Hence

$$\sum_H q_H \left\{ \mathbf{F}_{0,H}(y) - \right.$$

$$\left. - \nu^2 \int_{-b}^{+b} \mathbf{K}(y,\eta)\ \mathbf{u}(\eta)\ \mathbf{F}_{0,H}(\eta)\, d\eta \right\} = \mathbf{d}(y)$$

in perfect analogy with (6.7) (though the error vectors need not be identical). If now we equate again to zero a number of mean values of the error, it clearly appears to be natural to give to the weight functions the structure

$$\mathbf{G}_{0,J}^*(y)\ \mathbf{u}(y), \quad J = 1 \ldots N.$$

The result is

$$\sum_H q_H \left\{ \int_{-b}^{+b} \mathbf{G}_{0,J}^*\ \mathbf{u}\ \mathbf{F}_{0,H}\, dy - \nu^2 \int_{-b}^{+b} \int_{-b}^{+b} \mathbf{G}_{0,J}^*(y)\ \mathbf{u}(y)\ \mathbf{K}(y,\eta)\ \mathbf{u}(\eta)\ \mathbf{F}_{0,H}(\eta)\, d\eta\, dy \right\} =$$

$$= \int_{-b}^{+b} \mathbf{G}_{0,J}^*(y)\ \mathbf{u}(y)\ \mathbf{d}(y)\, dy = 0, \quad J = 1, \ldots, N. \qquad (6.30)$$

In order to find the properties of this set, put

$$\mathbf{K}(y,\eta) = \sum_i \mathbf{f}_{0,i}(y)\ \mathbf{g}_{0,i}^*(\eta)$$

and insert the developments

$$\mathbf{F}_{0,H} = \sum_k a_{Hk}\ \mathbf{f}_{0,k}; \quad \mathbf{G}_{0,J}^* = \sum_k b_{Jk}\ \mathbf{g}_{0,k}^*. \qquad (6.31)$$

Making use of the biorthogonality and the normalization of the functions $\mathbf{f}_{0,k}$, $\mathbf{g}_{0,k}^*$ we get without difficulty

$$\sum_H \sum_k q_H \left\{ a_{Hk}\, b_{Jk} \cdot \frac{1}{\nu_k^2} - \nu^2\, a_{Hk}\, b_{Jk} \cdot \frac{1}{\nu_k^4} \right\} = 0$$

or

$$\sum_H \sum_k q_H\ a_{Hk}\, b_{Jk}\, \frac{\nu^2 - \nu_k^2}{\nu_k^2} \cdot \frac{1}{\nu_k^2} = 0, \ J = 1 \ldots N. \qquad (6.32)$$

The same developments, substituted in the set (6.8), lead to

$$\sum_H \sum_k q_H\ a_{Hk}\, b_{Jk}\, \frac{\nu^2 - \nu_k^2}{\nu_k^2} = 0, \quad J = 1 \ldots N,$$

which reveals a high degree of similarity of both methods, the only difference being the additional factor $\frac{1}{\nu_k^2}$ in (6.32).

Making use of arbitrary coefficients r_J, we derive from (6.32)

$$\sum_J \sum_H \sum_k q_H\ a_{Hk}\, r_J\, b_{Jk}\, \frac{\nu^2 - \nu_k^2}{\nu_k^2} \cdot \frac{1}{\nu_k^2} = 0.$$

Specializing to a particular solution $q_{H,k}$, $\bar{\nu}_K^2$ and putting

$\sum_K q_{H,K}\ a_{Hk} = \delta_{pk} + \varepsilon_{pk}$ (assuming this solution to approximate the p^{th} mode of vibration),

$\sum_J u_J\, b_{Jk} = g_k$ (compare (6.16)),

the error in the frequency appears to be equal to

$$\frac{\bar{\nu}_K^2 - \nu_p^2}{\nu_p^2} = \sum_1^\infty \frac{g_i}{g_p}\ \varepsilon_{pi} \left(1 - \frac{\bar{\nu}_K^2}{\nu_i^2} \right)^{-1} \frac{\nu_p^2}{\nu_i^2}. \qquad (6.33)$$

This is again very similar to (6.17). Under the conditions, mentioned in connection with eq. (6.17) there is again first-order agreement between the appropriate $\bar{\nu}_K^2$ of the determinantal equation

[1]) the example refers to symmetrical vibrations.

$$det\left\{\int_{-b}^{+b} \mathbf{G}_{0,J}^{*}\ \mathbf{u}\ \mathbf{F}_{0,H}\,dy - \nu^2 \int_{-b}^{+b}\int_{-b}^{+b} \mathbf{G}_{0,J}^{*}(y)\ \mathbf{u}(y)\ \mathbf{K}(y,\eta)\ \mathbf{u}(\eta)\ \mathbf{F}_{0,H}(\eta)\,d\eta\,dy\right\}=0 \qquad (6.34)$$

and ν_p^2, improving to second-order agreement if the parts $\mathbf{G}_{0,J}$ of the weight functions $\mathbf{G}_{0,J}^{*}\mathbf{u}$ are tuned to the adjoints of the requested modes. If $p=1$, that is: if we try to find the first mode, the error in the frequency is, according to (6.33) (compared with (6.17), or, if $\frac{g_i}{g_p}=\gamma_{ip}$, with (6.21)), because of

$$\left|\frac{\nu_1^2}{\nu_i^2}\right|<1,\quad (i=2,3,\ldots\infty)$$

appreciably smaller than previously. If $p\neq 1$, the factors $\frac{\nu_p^2}{\nu_i^2}$ with $i<p$ will tend to increase the error, but this drawback will again lose its effect if the sets $\mathbf{F}_{0,H}$ and $\mathbf{G}_{0,J}$ permit approximation at least of *all* modes, resp. adjoint modes, with $i\leqq p$. Hence, we may consider the method (6.30) as *definitely better* than those of preceding paragraphs, at any rate if we restrict our attention to a small number of lowest modes, as it generally is. (For if p is high, the risk appears that the large factors $\frac{\nu_p^2}{\nu_i^2}$ with $i \ll p$ surmount the reduction to second order of smallness of components with $i<p$).

The method, embodied in eq. (6.30) has been initiated by Grammel (in its simplified form, referring to the calculation of fundamental frequencies of self-adjoint systems). In spite of its attractive accuracy for the frequency, the method is seldom used. The principal reason for this seems to be the increased extensiveness of the numerical computation. Yet it has perhaps attracted less attention than it deserves. In par. 7.6 we shall meet a different conception of the same procedure.

7 Methods of successive approximation.

7.1 *Iteration process for the fundamental mode.*

Let

$$\mathbf{f}_0^{[1]}$$

by any vector of functions, defined in the range $-b\leqq y\leqq +b$, accessible to a development

$$\mathbf{f}_0^{[1]}=\sum_1^{\infty} a_k^{[1]}\ \mathbf{f}_{0,k}. \qquad (7.1)$$

Submit this function to the transformation

$$\nu^2\int_{-b}^{+b}\mathbf{K}(y,\eta)\ \mathbf{u}(\eta)\ \mathbf{f}_0^{[1]}(\eta)\,d\eta=\mathbf{f}_0^{[2]}(y), \qquad (7.2)$$

the result being $\mathbf{f}_0^{[2]}$. The $\mathbf{K}$- and $\mathbf{u}$-matrices are those of chapter 4. Substituting (7.1) and (5.14) into (7.a) we get, in connection with (5.9) and (5.10),

$$\nu^2\int_{-b}^{+b}\mathbf{K}(y,\eta)\ \mathbf{u}(\eta)\ \mathbf{f}_0^{[1]}(\eta)\,d\eta=$$

$$=\nu^2\sum_i \mathbf{f}_{0,i}(y)\int_{-b}^{+b}\mathbf{g}_{0,i}^{*}(\eta)\ \mathbf{u}(\eta)\sum_k a_k^{[1]}\mathbf{f}_{0,k}(\eta)\,d\eta=$$

$$=\sum_i \mathbf{f}_{0,i}\,a_i^{[1]}\cdot\frac{\nu^2}{\nu_i^2}.$$

Writing

$$\mathbf{f}_0^{[2]}=\sum_1^{\infty} a_k^{[2]}\ \mathbf{f}_{0,k}$$

we infer

$$a_k^{[2]}=\frac{\nu^2}{\nu_k^2}\ a_k^{[1]}. \qquad (7.3)$$

Repeating the transformation $N-1$ times, we shall obviously get

$$a_k^{[N]}=\left(\frac{\nu^2}{\nu_k^2}\right)^{N-1} a_k^{[1]}. \qquad (7.4)$$

In view of the fact, that the sequence of natural oscillations is ordered according to increasing values of the moduli of the (complex) frequencies, we conclude that for $N\to\infty$ a finite result emerges, if we put $\nu=\nu_1$. Then [1])

$$\lim_{N=\infty} a_k^{[N]}=\begin{cases} a_1^{[1]} & \text{if } k=1\\ 0 & \text{if } k\neq 1\end{cases}.$$

Hence the procedure appears to lead, irrespective of the structure of the initial function, to the exact *fundamental* mode of vibration. Starting with some first approximation to this mode, the process will soon (that is for small values of N) produce a generally very effective improvement of it.

In the same way the transformation

$$\nu^2\int_{-b}^{+b}\mathbf{K}(y,\eta)\ \mathbf{u}^{*}(\eta)\ \mathbf{g}_0^{[i]}(\eta)\,d\eta=\mathbf{g}_0^{[i+1]}(y) \qquad (7.5)$$

will change, if repeated many times, any function $\mathbf{g}_0^{[1]}$ into an effective approximation of the fundamental mode of the adjoint system.

7.2 *Iterative approximation of higher modes.*

To acquire comparable results for other modes, biorthogonalisation processes must be added (as it is well-known from ordinary vibration analysis).

---

[1]) It will easily be seen, that it is actually not necessary to know the value of ν_1 in order to carry out the computation. The factor ν^2 in (7.2) effects the norming, but not the nature of the function, which in fact depends upon the ratios $\frac{a_k^{[N]}}{a_1^{[N]}}$ only.

Let

$$\sum_k (\delta_{jk} + \varepsilon_{1k}^{[1]})\ \mathbf{f}_{0,k}\ ;\ \sum_k (\delta_{2k} + \varepsilon_{2k}^{[1]})\ \mathbf{f}_{0,k},$$

$$\varepsilon_{1k}^{[1]} \ll 1,\ \varepsilon_{2k}^{[1]} \ll 1,\ \varepsilon_{11}^{[1]} = \varepsilon_{22}^{[1]} = 0;\ k = 1 \dots \infty$$

be any pair of initial (guessed) approximations to $\mathbf{f}_{0,1}$ and $\mathbf{f}_{0,2}$. Submit the first function to an N'-fold repetition of the operation (7.2) (assuming for simplicity $\nu = \nu_1$) and the second one to an N-fold repetition of the same transformation (with $\nu = \nu_2$). The resulting functions are

$$\sum_k \left\{ \delta_{1k} + \varepsilon_{1k}^{[1]} \left(\frac{\nu_1^2}{\nu_k^2} \right)^{N'} \right\} \mathbf{f}_{0,k}\ ;$$

$$\sum_k \left\{ \delta_{2k} + \varepsilon_{2k}^{[1]} \left(\frac{\nu_2^2}{\nu_k^2} \right)^{N} \right\} \mathbf{f}_{0,k}. \qquad (7.6)$$

Next assume

$$\mathbf{f}_{0,2}^{[N,N',N'']} = \sum_k \left\{ \delta_{2k} + \varepsilon_{2k}^{[1]} \left(\frac{\nu_2^2}{\nu_k^2} \right)^{N} \right\} \mathbf{f}_{0,k} +$$

$$+ \lambda \sum_k \left\{ \delta_{1k} + \varepsilon_{1k}^{[1]} \left(\frac{\nu_1^2}{\nu_k^2} \right)^{N'} \right\} \mathbf{f}_{0,k}^{0}, \qquad (7.7)$$

where λ is a constant determined by the condition, that (7.7) shall be biorthogonal to the N''-fold improved approximation

$$\mathbf{g}_{0,1}^{[N'']} = \sum_k \left\{ \delta_{1k} + \right.$$

$$\left. + \gamma_{1k}^{[1]} \left(\frac{\nu_1^2}{\nu_k^2} \right)^{N''} \right\} \mathbf{g}_{0,k},\quad \gamma_{1k} \ll 1,\quad \gamma_{11} = 0$$

of the fundamental of the adjoint system. The equation for λ is (see 5.9)

$$\int_{-b}^{+b} (\mathbf{g}_{0,1}^{[N'']})^* \ \mathbf{u}\ \mathbf{f}_{0,2}^{[N,N',N'']}\, dy = 0,$$

which by substitution of the developments is easily reduced to

$$\sum_k \frac{1}{\nu_k^2} \left\{ \delta_{1k} + \gamma_{1k}^{[1]} \left(\frac{\nu_1^2}{\nu_k^2} \right)^{N''} \right\} \left\{ \delta_{2k} + \varepsilon_{2k}^{[1]} \left(\frac{\nu_2^2}{\nu_k^2} \right)^{N} \right\} +$$

$$+ \lambda \sum_k \frac{1}{\nu_k^2} \left\{ \delta_{1k} + \gamma_{1k}^{[1]} \left(\frac{\nu_1^2}{\nu_k^2} \right)^{N''} \right\} \left\{ \delta_{1k} + \right.$$

$$\left. + \varepsilon_{1k}^{[1]} \left(\frac{\nu_1^2}{\nu_k^2} \right)^{N'} \right\} = 0.$$

The solution is

$$\lambda = -\varepsilon_{21}^{[1]} \left(\frac{\nu_2^2}{\nu_1^2} \right)^{N} - \gamma_{12}^{[1]} \left(\frac{\nu_1^2}{\nu_2^2} \right)^{N''+1} +$$

$$+ 2^{\text{nd}} \text{ order quantity}, \qquad (7.8)$$

the unspecified rest containing no factors $\frac{\nu_2^2}{\nu_1^2}$, which might become very large when raised to a high power.

Inserting (7.8) in (7.7) we get

$$\mathbf{f}_{0,2}^{[N,N',N'']} = \mathbf{f}_{0,2} - \gamma_{12}^{[1]} \left(\frac{\nu_1^2}{\nu_2^2} \right)^{N''+1} \mathbf{f}_{0,1} +$$

$$+ \sum_{k=3}^{\infty} \varepsilon_{2k}^{[1]} \left(\frac{\nu_2^2}{\nu_k^2} \right)^{N} \mathbf{f}_{0,k} -$$

$$- \varepsilon_{21}^{[1]} \left(\frac{\nu_2^2}{\nu_1^2} \right)^{N} \sum_{k=2}^{\infty} \varepsilon_{1k}^{[1]} \left(\frac{\nu_1^2}{\nu_k^2} \right)^{N'} \mathbf{f}_{0,k} +$$

$$+ \text{other second order quantities.}$$

The unspecified rest again contains no powers of $\frac{\nu_2^2}{\nu_1^2}$, as it is the case in the last but one term, which is formally also of second order of smallness. Neglecting the unspecified terms, we get further

$$\lim_{N,N''=\infty} \frac{\mathbf{f}_{0,2}^{[N,N',N'']}}{1 - \varepsilon_{21}^{[1]} \left(\frac{\nu_2^2}{\nu_1^2} \right)^{N} \varepsilon_{12}^{[1]} \left(\frac{\nu_1^2}{\nu_2^2} \right)^{N'}} = \mathbf{f}_{0,2} -$$

$$- \left\{ \frac{\varepsilon_{21}^{[1]} \left(\frac{\nu_2^2}{\nu_1^2} \right)^{N} \sum_{k=3}^{\infty} \varepsilon_{1k}^{[1]} \left(\frac{\nu_1^2}{\nu_k^2} \right)^{N'} \mathbf{f}_{0,k}}{1 - \varepsilon_{21}^{[1]} \left(\frac{\nu_2^2}{\nu_1^2} \right)^{N} \varepsilon_{12}^{[1]} \left(\frac{\nu_1^2}{\nu_2^2} \right)^{N'}} \right\}_{N=\infty}.$$

So if anyway $\left(\frac{\nu_2^2}{\nu_1^2} \right)^{N}$ is so large that the retained second-order term gets large too (compared with 1), we have yet

$$\lim_{N'=\infty} \lim_{N,N''=\infty} \frac{\mathbf{f}_{0,2}^{[N,N',N'']}}{1 - \varepsilon_{21}^{[1]} \left(\frac{\nu_2^2}{\nu_1^2} \right)^{N} \varepsilon_{12}^{[1]} \left(\frac{\nu_1^2}{\nu_2^2} \right)^{N'}} = \mathbf{f}_{0,2} +$$

$$+ \lim_{N'=\infty} \frac{\sum_{k=3}^{\infty} \varepsilon_{1k}^{[1]} \left(\frac{\nu_1^2}{\nu_2^2} \right)^{N'} \mathbf{f}_{0,k}}{\varepsilon_{12}^{[1]} \left(\frac{\nu_1^2}{\nu_k^2} \right)^{N'}} = \mathbf{f}_{0,2} +$$

$$+ \lim_{N'=\infty} \sum_{k=3}^{\infty} \frac{\varepsilon_{1k}^{[1]}}{\varepsilon_{12}^{[1]}} \left(\frac{\nu_2^2}{\nu_k^2} \right)^{N'} \mathbf{f}_{0,k} = \mathbf{f}_{0,2}, \qquad (7.9)$$

with the theoretical exception $\varepsilon_{12}^{[1]} = 0$.

We may safely conclude, that the explained procedure indeed converges to $\mathbf{f}_{0,2}$ and that it may be used with finite N, N', N'' to improve any initial approximation $\mathbf{f}_{0,2}^{[1,1,1]}$ to this function. It is remarkable, that the effective improvement depends primarily upon the numbers N and N'' and only by intervention of a second-order term upon N'. It is known, that generally even for $N = N' = N'' = 1$ the improvement is already substantial (the convergence commonly being rapid). We infer that under such circumstances it will not deteriorate very much if we reduce N' from 1 to zero.

It is easy to see, how the method should be generalized for modes of higher order than the second.

There is reason to point out, that it is in fact commonly desirable to repeat the biorthogonalisation acts *several times* in the course of an iterative improvement of an approximation to any mode, higher than the first, and not to put it at the end only. For if N is high, the second function (7.6) will (even if the initial error $\varepsilon_{21}^{[1]}$ is very small), in consequence of the very large factor $\left(\frac{\nu_2^2}{\nu_1^2} \right)^{N}$, have got so closely resemblant to the fundamental mode, that the numerical accuracy of the computation falls short to represent the difference satisfactorily.

7.3 *Simultaneous purification of approximations to a number of higher modes.*

The large number of biorthogonalisations, involved in the method of the preceding paragraph if a number of modes is to be determined, can be concentrated into one final "purification act", which evades the necessity to take into consideration the solutions of the adjoint system. This act consists of the solving of the set (6.8) of the preceding chapter, fitted up with the "simply iterated" (i.e. "unpurified") initial approximations of the desired (lowest) modes of vibration, that is: with the functions

$$\mathbf{F}_{0,H} = \sum_k (\delta_{Hk} + \varepsilon_{Hk}) \left(\frac{\nu_H^2}{\nu_k^2}\right)^{N_H} \mathbf{f}_{0,k}, \quad H = 1 \dots N.$$

found by N_H-fold application of the transformation (7.2) to the initial approximations

$$\mathbf{f}_{0,H}{}^{[1]} = \sum_k (\delta_{Hk} + \varepsilon_{Hk})\, \mathbf{f}_{0,k}.$$

The weight functions $\mathbf{G}_{0,J}$ may eventually be left arbitrary, but of course a close adaption to the solutions of the adjoint system is beneficial.

The proof is simple and falls back on the convergence of the standard-procedure of the preceding paragraphs. Since the solutions are invariant *upon recombination of the functions* $\mathbf{F}_{0,H}$, we may use a new set

$$\bar{\mathbf{F}}_{0,H} = \sum_{K=1}^{N} a_{HK}\, \mathbf{F}_{0,K} =$$

$$= \sum_{K=1}^{N} \sum_k a_{HK} (\delta_{Kk} + \varepsilon_{Kk}) \left(\frac{\nu_K^2}{\nu_k^2}\right)^{N_K} \mathbf{f}_{0,k}. \quad (7.10)$$

But it is known from the convergence of the standard procedure, that it is possible to adjust the coefficients a_{HK} to values, securing convergence (*for* $N_k = \infty$, $K = 1 \dots N$) *of the functions* $\bar{\mathbf{F}}_{0,H}$, $H = 1 \dots N$ to the solutions $\mathbf{f}_{0,H}$ ($H = 1 \dots N$). It is therefore allowed to assume, that the difference between any of the new functions $\bar{\mathbf{F}}_{0,H}$ and the accessory solution $\mathbf{f}_{0,H}$ is vanishingly small for very large values of N_J, $J = 1 \dots N$. Now, *the errors* in the solutions of the set (6.8) are continuous functions, vanishing for vanishing arguments, of the errors in the underlying system $\bar{\mathbf{F}}_{0,H}$ (to first approximation they are linear, with coefficients, not depending upon the numbers N_H). Hence in the limit the final errors in the solutions of (6.8) must vanish together with the errors, assumed to occur in the functions (7.10).

It will again be necessary to insert the "simultaneous purification" again and again after a small number of iteration steps, to prevent undue errors, caused by the restricted level of numerical accuracy.

It may be remarked, that equations (6.8) give (by 6.9)) also approximations to the frequencies. The accuracy of these approximations can of course be raised effectively by the use of approximations to accessory solutions of the adjoint system on the place of the weight functions. Obviously, a particularly satisfactory result will emerge if we submit these weight functions also to an iterative improvement by transformation. In this case separate purifications are again superfluous.

7.4 *Iteration process, using throughout function vectors with only one non-vanishing element.*

The execution of the attractive method of par. 7.3 in the case of flutter calculations is again troubled very much by the extensive growth of the labor involved. The principal source is to be seen in the necessity of the use of *complete* function vectors $\mathbf{F}_{0,H}$ in the equations (6.8), serving as simultaneous purification system *and* frequency computator. The same difficulties have once shared in with others in forcing us to simplify our basic function vectors to something like (6.5). It is very remarkable, that it seems *sometimes* allowed to submit *the purification, accompanying any iterative* analysis, to a similar simplification.

In the case of flutter calculations our main interest is generally devoted to only one of the modes of vibration: the one mode from which *at the lowest speed* instability develops. Let this mode be determined by an introductory calculation of the chapter 6-type and assume that the accuracy suffices to reach a definite conclusion *on this point,* so that no improvement of the calculation will ever compel us to admit, that actually another mode is the "most dangerous" one.

Suppose

$$\mathbf{f}_{0,i}{}^{[1]})^* = \| z_{0,i}{}^{[1]} \;\; \varphi_{0,i}{}^{[1]} \;\; \gamma_{0,i}{}^{[1]} \| \quad (7.11)$$

to be the approximation of the dangerous mode, derived by the introductory calculation.

Now submit (7.11) to one single application of the transformation (7.2), with the result

$$(\mathbf{f}_{0,i}{}^{[2]})^* = \| z_{0,i}{}^{[2]} \;\; \varphi_{0,i}{}^{[2]} \;\; \gamma_{0,i}{}^{[2]} \|.$$

Next split up this result in accordance with the scheme

$$\begin{aligned} (\mathbf{F}_{0,1}{}^{[2]})^* &= \| z_{0,i}{}^{[2]} \;\; 0 \;\; 0 \|; \\ (\mathbf{F}_{0,2}{}^{[2]})^* &= \| 0 \;\; \varphi_{0,i}{}^{[2]} \;\; 0 \|; \\ (\mathbf{F}_{0,3}{}^{[2]})^* &= \| 0 \;\; 0 \;\; \gamma_{0,i}{}^{[2]} \| \end{aligned} \quad (7.12)$$

and set-up with these functions a ternary representation of equations (6.8). The weight functions may be left arbitrary, though it is highly probable that the rapidity and the range of convergence will be much better, if we use here the result of a similar splitting-up of a singly-improved introductory solution (with the same index i) of the adjoint system.

Then it appears possible, that it will be allowed to consider the solution of this ternary set, accessory to the frequency root approximating ν_i^2, as an *improved approximation* to the required mode $\mathbf{f}_{0,i}$, an unlimited repetition of the process converging to the exact solution. It is clear, that the benefit of this method is lying in the many zeros, occurring in the functions (7.12).

As far as we know, the conditions of convergence have never been completely investigated. They will doubtlessly be complicated, for the method implies a mutilation of the invariance of

the equations upon changes in the representation of the displacements and distortions of the underlying mechanical system. The operation (7.12) indeed implies a dependence of the process e.g. upon the assumed position of the reference axis, and hence the convergence may depend also upon that choice. Yet, the chief properties may be revealed in the following way.

Let

$$\mathbf{f}_{0,i}{}^{[n]} = \sum_k (\delta_{ik} + \varepsilon_{ik}{}^{[n]})\, \mathbf{f}_{0,k} \qquad (7.13)$$

be the n^{th} result, and assume it to be actually an approximation, i.e.

$$\varepsilon_{ik}{}^{[n]} \ll 1.$$

Let further

$$\mathbf{g}_{0,i}{}^{[n]} = \sum_k (\delta_{ik} + \gamma_{ik}{}^{[n]})\, \mathbf{g}_{0,k};\ \gamma_{ik}{}^{[n]} \ll 1 \qquad (7.14)$$

be the n^{th} approximation to the accessory solution of the similarly treated adjoint system. Submit these functions to the transformations (7.2), (7.5) respectively. Let the result be represented by

$$\bar{\mathbf{f}}_{0,i}{}^{[n+1]} = \sum_k (\delta_{ik} + \bar{\varepsilon}_{ik}{}^{[n+1]})\, \mathbf{f}_{0,k};$$
$$\bar{\mathbf{g}}_{0,i}{}^{[n+1]} = \sum_k (\delta_{ik} + \bar{\gamma}_{ik}{}^{[n+1]})\, \mathbf{g}_{0,k}. \qquad (7.15)$$

The relation between $\bar{\varepsilon}_{ik}{}^{[n+1]}$ and $\varepsilon_{ik}{}^{[n]}$, etc., is known, but for the moment we shall make no use of it, intending to bring a slight change in the presentation of the problem, which will be explained later on.

Now, split up

$$\bar{\mathbf{f}}_{0,i}{}^{[n+1]} = (\bar{\mathbf{f}}_{0,i}{}^{[n+1]})_1 + (\bar{\mathbf{f}}_{0,i}{}^{[n+1]})_2 + (\bar{\mathbf{f}}_{0,i}{}^{[n+1]})_3, \qquad (7.16)$$

$$\bar{\mathbf{g}}_{0,i}{}^{[n+1]} = (\bar{\mathbf{g}}_{0,i}{}^{[n+1]})_1 + (\bar{\mathbf{g}}_{0,i}{}^{[n+1]})_2 + (\bar{\mathbf{g}}_{0,i}{}^{[n+1]})_3, \qquad (7.17)$$

with

$$(\bar{\mathbf{f}}_{0,i}{}^{[n+1]})_1{}^* = \| \bar{z}_{0,i}{}^{[n+1]}\ 0\ \ 0 \|;\quad (\bar{\mathbf{g}}_{0,i}{}^{[n+1]})_1{}^* = \| \bar{w}_{0,i}{}^{[n+1]}\ \ 0\ \ 0 \|,$$
$$(\bar{\mathbf{f}}_{0,i}{}^{[n+1]})_2{}^* = \| 0\ \ \varphi_{0,i}{}^{[n+1]}\ \ 0 \|;\quad (\bar{\mathbf{g}}_{0,i}{}^{[n+1]})_2{}^* = \| 0\ \ \psi_{0,i}{}^{[n+1]}\ \ 0 \|,$$
$$(\bar{\mathbf{f}}_{0,i}{}^{[n+1]})_3{}^* = \| 0\ \ 0\ \ \gamma_{0,i}{}^{[n+1]} \|;\quad (\bar{\mathbf{g}}_{0,i}{}^{[n+1]})_3{}^* = \| 0\ \ 0\ \ \beta_{0,i}{}^{[n+1]} \|.$$

Assume

$$(\bar{\mathbf{f}}_{0,i}{}^{[n+1]})_A = \sum_k \sigma_{A,ik}{}^{[n+1]}\ \mathbf{f}_{0,k};$$
$$(\bar{\mathbf{g}}_{0,i}{}^{[n+1]})_A{}^* = \sum_k \tau_{A,ik}{}^{[n+1]}\, \mathbf{g}_{0,k}{}^*;$$
$$A = 1, 2, 3, \qquad (7.18)$$

and insert these expressions in the "simplified purification set"

$$\sum_1^3 q_A{}^{[n+1]} \int_{-b}^{+b} (\bar{\mathbf{g}}_{0,i}{}^{[n+1]})_B{}^* (\mathbf{e} - \nu^2 \mathbf{u})\, (\bar{\mathbf{f}}_{0,i}{}^{[n+1]})_A\, dy = 0;\ B = 1, 2, 3,$$

which accordingly we assume to contain weight functions, derived from the $(n+1)^{\text{th}}$ approximation to the i^{th} solution of the adjoint system (diverging possibilities will not be considered).

The result is (compare (5.9), (5.10))

$$\sum_k \sum_A q_A{}^{[n+1]}\, \sigma_{A,ik}{}^{[n+1]}\, \tau_{B,ik}{}^{[n+1]} \left(1 - \frac{\nu^2}{\nu_k{}^2}\right) = 0,\quad B = 1, 2, 3. \qquad (7.19)$$

Similarly we get for the adjoint system

$$\sum_k \sum_A r_A{}^{[n+1]}\, \tau_{A,ik}{}^{[n+1]}\, \sigma_{B,ik}{}^{[n+1]} \left(1 - \frac{\nu^2}{\nu_k{}^2}\right) = 0,\quad B = 1, 2, 3. \qquad (7.20)$$

Let now

$$\left.\begin{aligned} \| z_{0,i}\ \ 0\ \ 0 \| &= \sum_k \sigma_{1,ik}\, \mathbf{f}_{0,k}{}^*; \\ \| w_{0,i}\ \ 0\ \ 0 \| &= \sum_k \tau_{1,ik}\, \mathbf{g}_{0,k}{}^*, \\ \| 0\ \ \varphi_{0,i}\ \ 0 \| &= \sum_k \sigma_{2,ik}\, \mathbf{f}_{0,k}{}^*; \\ \| 0\ \ \psi_{0,i}\ \ 0 \| &= \sum_k \tau_{2,ik}\, \mathbf{g}_{0,k}{}^*, \\ \| 0\ \ 0\ \ \gamma_{0,i} \| &= \sum_k \sigma_{3,ik}\, \mathbf{f}_{0,k}{}^*; \\ \| 0\ \ 0\ \ \beta_{0,i} \| &= \sum_k \tau_{3,ik}\, \mathbf{g}_{0,k}{}^*, \end{aligned}\right\} \qquad (7.21)$$

the sum of the left sides constituting the exact i^{th} solution. Then it is easy to prove that

$$\sigma_{A,ik}{}^{[n+1]} = \sum_j (\delta_{ij} + \bar{\varepsilon}_{ij}{}^{[n+1]})\, \sigma_{A,jk};$$
$$\tau_{A,ik}{}^{[n+1]} = \sum_j (\delta_{ij} + \bar{\gamma}_{ij}{}^{[n+1]})\, \tau_{A,jk}.$$

Substituting these relations into (7.19), (7.20) and taking account of the fact, that these equations (because of $\varepsilon_{ik}{}^{[n+1]} \ll 1$ and $\gamma_{ik}{}^{[n+1]} \ll 1$) must have a solution of the type

$$\left.\begin{aligned} &q_A{}^{[n+1]} = 1 + \delta q_A{}^{[n+1]};\ \ \delta q_A{}^{[n+1]} \ll 1, \\ &r_A{}^{[n+1]} = 1 + \delta r_A{}^{[n+1]};\ \ \delta r_A{}^{[n+1]} \ll 1, \\ &\nu^2 = \nu_i{}^2 + \text{error of } \textit{second} \text{ order of smallness}, \end{aligned}\right\} \qquad (7.22)$$

we readily find, if terms of second and higher orders of smallness are neglected

$$\sum_A \sum_k \left(1 - \frac{\nu_i{}^2}{\nu_k{}^2}\right) \delta q_A{}^{[n+1]}\, \sigma_{A,ik}\, \tau_{B,ik} + \sum_k \left(1 - \frac{\nu_i{}^2}{\nu_k{}^2}\right) \tau_{B,ik}\, \bar{\varepsilon}_{ik}{}^{[n+1]} = 0 \qquad (7.23)$$
$$B = 1, 2, 3,$$

and analogous equations for $\delta r_A{}^{[n+1]}$.

The set (7.23) is independent of the errors $\bar{\gamma}_{ik}{}^{[n+1]}$. Hence the values of $\delta q_A{}^{[n+1]}$ depend solely upon the errors $\bar{\varepsilon}_{ik}{}^{[n+1]}$ and similarly $\delta r_A{}^{[n+1]}$ will depend upon the $\bar{\gamma}_{ik}{}^{[n+1]}$ only. We infer from this, that it is sufficient to proceed with (7.23) only, the adjoint equation adding nothing new.

The equations (7.23), constituting the reduction of a homogeneous set, are not linearly independent. The existing relation may be found by summation over B, the result being zero by virtue of the properties

$$\sum_{B} \sigma_{B,ik} = \delta_{ik} \; ; \; \sum_{B} \tau_{B,ik} = \delta_{ik} \qquad (7.24)$$

of the σ- and τ-coefficients.

The explicite representation of the solution of (7.23) involving extensive formulae, we are invited here to accept a simplification. This consists of the assumption, that A and B shall have only *two* values (1 and 2), in other words: that the oscillations of the mechanical system are governed by *two* fundamental differential equations, e. g. by the absence of an aileron. We may well hope, that this assumption will not interfere too much with our main object: the problem of convergence of the iteration method for values of i, differing from 1.

If A and B are bound to the values 1 and 2, wet get from (7.23), putting $\delta q_2^{[n+1]} = 0$,

$$\delta q_1^{[n+1]} = -\frac{\sum_k \left(1 - \frac{\nu_i^2}{\nu_k^2}\right) \tau_{1,ik}\, \bar{\varepsilon}_{ik}^{[n+1]}}{\sum_k \left(1 - \frac{\nu_i^2}{\nu_k^2}\right) \sigma_{1,ik}\, \tau_{1,ik}}. \qquad (7.25)$$

With the help of this formula we are able to find the errors $\varepsilon_{ik}^{[n+1]}$ in the final $(n+1)^{\text{th}}$ approximation

$$\mathbf{f}_{0,i}^{[n+1]} = \sum_A q_A^{[n+1]} \left(\bar{\mathbf{f}}_{0,i}^{[n+1]}\right)_A =$$

$$= (1 + \delta q_1^{[n+1]}) \left(\bar{\mathbf{f}}_{0,i}^{[n+1]}\right)_1 + \left(\bar{\mathbf{f}}_{0,i}^{[n+1]}\right)_2 .$$

We get (compare (7.18))

$$\sum_k (\delta_{ik} + \varepsilon_{ik}^{[n+1]})\, \mathbf{f}_{0,k} =$$

$$= \left(\bar{\mathbf{f}}_{0,i}^{[n+1]}\right)_1 + \left(\bar{\mathbf{f}}_{0,i}^{[n+1]}\right)_2 + \delta q_1^{[n+1]} .$$

$$\sum_k \sigma_{1,ik}^{[n+1]}\, \mathbf{f}_{0,k} = \sum_k (\delta_{ik} + \bar{\varepsilon}_{ik}^{[n+1]})\, \mathbf{f}_{0,k} +$$

$$+ \delta q_1^{[n+1]} \sum_j \sum_k (\delta_{ij} + \varepsilon_{ij}^{[n+1]})\, \sigma_{1,jk}\, \mathbf{f}_{0,k} .$$

Comparing coefficients, we derive, if terms of the second order of smallness are neglected,

$$\varepsilon_{ik}^{[n+1]} = \bar{\varepsilon}_{ik}^{[n+1]} + \delta q_1^{[n+1]}\, \sigma_{1,ik} . \qquad (7.26)$$

Now we might take into account the first step of the process: the application of the transformation formula (7.2). But instead of that we may equally well consider the *next* step, which likewise consists of this transformation. For we may consider the sequence

(transf./purif./transf./purif. ..... ad inf.

equally well to be composed of groups (transf./purif.) as of groups (purif./transf.). Choosing the latter possibility, we must proceed with the formula

$$\bar{\mathbf{f}}_{0,i}^{[n+2]} = \nu_i^2 \int_{-b}^{+b} \mathbf{K}\mathbf{u}\, \mathbf{f}_{0,i}^{[n+1]}\, dy. \qquad (7.27)$$

But since $\delta q_1^{[n+1]}$ is known and the vector $\bar{\mathbf{f}}_{0,i}^{[n+2]}$ is really to be split up again, there is no objection against replacing the left side by

$$(1 + \delta q_1^{[n+1]}) \left(\bar{\mathbf{f}}_{0,i}^{[n+2]}\right)_1 + \left(\mathbf{f}_{0,i}^{[n+2]}\right)_2 \approx$$

$$\approx \sum_k (\delta_{ik} + \bar{\varepsilon}_{ik}^{[n+2]})\, \mathbf{f}_{0,k} + \delta q_1^{[n+1]} \sum_k \sigma_{1,ik}\, \mathbf{f}_{0,k} .$$

The right side of (7.27) being (by par. 07.1) equal to

$$\sum_k \frac{\nu_i^2}{\nu_k^2} (\delta_{ik} + \varepsilon_{ik}^{[n+1]})\, \mathbf{f}_{0,k} ,$$

we get by comparison of coefficients

$$\delta_{ik} + \bar{\varepsilon}_{ik}^{[n+2]} + \delta q_1^{[n+1]}\, \sigma_{1,ik} = \frac{\nu_i^2}{\nu_k^2} (\delta_{ik} + \varepsilon_{ik}^{[n+1]}).$$

Inserting (7.26), we get further (the terms with δ_{ik} cancelling out each other)

$$\bar{\varepsilon}_{ik}^{[n+2]} + \delta q_1^{[n+1]} \sigma_{1,ik} =$$

$$= \frac{\nu_i^2}{\nu_k^2} \left(\bar{\varepsilon}_{ik}^{[n+1]} + \delta q_1^{[n+1]}\, \sigma_{1,ik}\right)$$

or, substituting (7.25) for $\delta q_1^{[n+1]}$,

$$\bar{\varepsilon}_{ik}^{[n+2]} = \frac{\nu_i^2}{\nu_k^2}\, \bar{\varepsilon}_{ik}^{[n+1]} +$$

$$+ \sigma_{1,ik} \left(1 - \frac{\nu_i^2}{\nu_k^2}\right) \frac{\sum_h \left(1 - \frac{\nu_i^2}{\nu_h^2}\right) \tau_{1,ih}\, \bar{\varepsilon}_{ih}^{[n+1]}}{\sum_h \left(1 - \frac{\nu_i^2}{\nu_h^2}\right) \sigma_{1,ih}\, \tau_{1,ih}} . \qquad (7.28)$$

This formula presents the relation between the errors $\bar{\varepsilon}_{ik}^{[n+2]}$ and $\bar{\varepsilon}_{ik}^{[n+1]}$, or, of course, between $\bar{\varepsilon}_{ik}^{[n+1]}$ and $\bar{\varepsilon}_{ik}^{[n]}$. It is somewhat simpler than the formula, expressing $\varepsilon_{ik}^{[n+1]}$ in $\varepsilon_{ik}^{[n]}$, a formula, which would follow from (7.26) and the *preceding* transformation step.

The relation (7.28) can be written as follows

$$\bar{\varepsilon}_{ik}^{[n+1]} = \sum_h T_{i,kh}\, \bar{\varepsilon}_{ih}^{[n+1]} \qquad (7.29)$$

with

$$T_{i,kh} = \frac{\nu_i^2}{\nu_h^2}\, \delta_{kh} +$$

$$+ \frac{\left(1 - \frac{\nu_i^2}{\nu_k^2}\right) \sigma_{1,ik} \left(1 - \frac{\nu_i^2}{\nu_h^2}\right) \sigma_{1,ih}}{\sum_j \left(1 - \frac{\nu_i^2}{\nu_j^2}\right) \sigma_{1,ij}\, \tau_{1,ij}} . \qquad (7.30)$$

It is a linear transformation of the errors (and should strictly be considered as the first member of a Taylor development of some complete — non linear — function, connecting $\bar{\varepsilon}_{ik}^{[n+1]}$ with $\bar{\varepsilon}_{ik}^{[n]}$).

We may now proceed along lines, drawn from the theory of linear transformations. It then appears to be troublesome, that the infinite matrix $\mathbf{T}_i \equiv \| T_{i,hk} \|$, $(h, k = 1 \ldots\ldots \infty)$ is a complex, non-hermitian matrix. This induces us to leave aside the probably non-typical consequences of the complex, not-self-adjoint nature of our system and to restrict the continued investigation

to the case of a real, self-adjoint system. Our wing system gets these properties, if it is not exposed to an airstream. Hence the emerging results will anyhow be strictly applicable to a case like that. Actually it will appear easy to extend them to the more general original conception.

If the system is real and self-adjoint, the frequencies are real and there is no difference between the coefficients σ and τ. The matrix $\mathbf{T}_i$ becomes a real, symmetrical matrix. The iteration is convergent if

$$\lim_{n=\infty} \varepsilon_{ik}^{[n]} = 0 \quad \text{for all values of } k \text{ [1]}.$$

Now in matrix representation (employing infinite matrices and vectors)

$$\bar{\varepsilon}_i^{[n+1]} = \mathbf{T}_i \bar{\varepsilon}_i^{[n]} = \mathbf{T}_i \mathbf{T}_i \bar{\varepsilon}_i^{[n-1]} = \ldots\ldots = \mathbf{T}_i^n \bar{\varepsilon}_i^{[1]}$$

Hence there is convergence if

$$\lim_{n=\infty} \mathbf{T}_i^n = \text{null-matrix.}$$

The necessary and sufficient condition for this is, that the absolute values of all characteristic numbers of the matrix $\mathbf{T}_i$ are smaller than 1 (except one, which is by the property, mentioned in the foregoing footnote, just equal to 1). Hence, we come down to the equation

$$\det (\mathbf{T}_i - \lambda \mathbf{1}) = 0 \; ; \quad \mathbf{1} = \text{unit-matrix},$$

or

$$\det \left\{ \left(\frac{\nu_i^2}{\nu_h^2} - \lambda \right) \delta_{hk} + \right.$$

$$\left. + \frac{\left(1 - \frac{\nu_i^2}{\nu_h^2}\right)\left(1 - \frac{\nu_i^2}{\nu_k^2}\right) \sigma_{1,ik}\, \sigma_{1,ih}}{\sum_j \left(1 - \frac{\nu_i^2}{\nu_j^2}\right) \sigma_{1,ij}^2} \right\} = 0$$

(i constant). (7.31)

The determinant appears to be reducible. Omitting intermediate results, the final result is

$$\prod_k \frac{\frac{\nu_i^2}{\nu_k^2} - \lambda}{Q_{1,ik}^2} \cdot \left(1 + \sum_h \frac{Q_{1,ih}^2}{\frac{\nu_i^2}{\nu_h^2} - \lambda} \right);$$

$$Q_{1,ih}^2 = \frac{\left(1 - \frac{\nu_i^2}{\nu_h^2}\right) \sigma_{1,ih}^2}{\sum_j \left(1 - \frac{\nu_i^2}{\nu_j^2}\right) \sigma_{1,ij}^2}$$

Equating to zero, we see that the infinite product may be crossed. The remaining part is easily reduced to

$$(1 - \lambda) \sum_k \sigma_{1,ik}^2 \frac{\nu_k^2 - \nu_i^2}{\lambda\, \nu_k^2 - \nu_i^2} = 0. \qquad (7.32)$$

[1] We must add: for (07.29), with (07.30), leaves the normalization of the function $\bar{f}_{0,i}^{[n]}$ unaltered, transforming $\bar{\varepsilon}_{ii}^{[n]} = 0$ into $\bar{\varepsilon}_{ii}^{[n+1]} = 0$.

The factor $1 - \lambda$ delivers the solitary root $\lambda = 1$, announced before.

We may conclude from (7.32), that there can be no convergence for $i \geqq 3$ (and that there *is* convergence for $i = 1$, a trivial issue). For if $i = 3$, the function

$$f_i(\lambda) = \sum_k \sigma_{1,ik}^2 \frac{1 - \frac{\nu_i^2}{\nu_k^2}}{\lambda - \frac{\nu_i^2}{\nu_k^2}}$$

is negative if λ is a little bit larger than $\frac{\nu_3^2}{\nu_2^2}$ (> 1) and positive if λ is a little bit smaller than $\frac{\nu_3^2}{\nu_1^2}$ (> 1). The open interval

$$\frac{\nu_3^2}{\nu_2^2} < \lambda < \frac{\nu_3^2}{\nu_1^2}$$

containing no infinity of the function f_3, there must at least be one root within it. This root is larger than 1, consequently there is no convergence. The divergence for $i > 3$ may be demonstrated in a similar way. So it appears, that the only questionable case consists of $i = 2$, connected with the function

$$f_2(\lambda) = \sum_k \sigma_{1,2k}^2 \frac{1 - \frac{\nu_2^2}{\nu_k^2}}{\lambda - \frac{\nu_2^2}{\nu_k^2}}. \qquad (7.33)$$

Careful consideration shows, that the course of this function must correspond with the graph of fig. 3. The equation $f_2 = 0$ has accordingly single roots in every interval $\frac{\nu_2^2}{\nu_{k+1}^2} < \lambda < \frac{\nu_2^2}{\nu_k^2}$; $k \geqq 3$, *no* roots in the interval $\frac{\nu_2^2}{\nu_3^2} < \lambda < \frac{\nu_2^2}{\nu_1^2}$ and one and only one root, which

I) may fall in the interval $-1 < \lambda < 0$;

II) may be smaller than -1;

III) may be larger than $\frac{\nu_2^2}{\nu_1^2}$.

Case I is the only case of convergence. The necessary and sufficient condition is seen to be

$$f_2(-1) = \sum_k \sigma_{1,2k}^2 \frac{\nu_2^2 - \nu_k^2}{\nu_2^2 + \nu_k^2} > 0. \qquad (7.34)$$

This formula cannot be simplified anymore. Though it looks simple, it is really still very difficult to find its bearing. It has been carefully analysed elsewhere (ref. 3) and is shown to admit the following remarkable explanation:

The process of iteration converges for $i = 2$ only if the *components* $(z_{02}; \varphi_{02})$ of this mode have *both* a shape, which is common for flexural, resp. torsional *fundamentals*.

The realisation of this property demands:

If the elastic and inertia couplings, represented by the elements beyond the principal diagonal of the matrices **e** and **u** are gradually diminished, the mode $i = 2$ shall approach

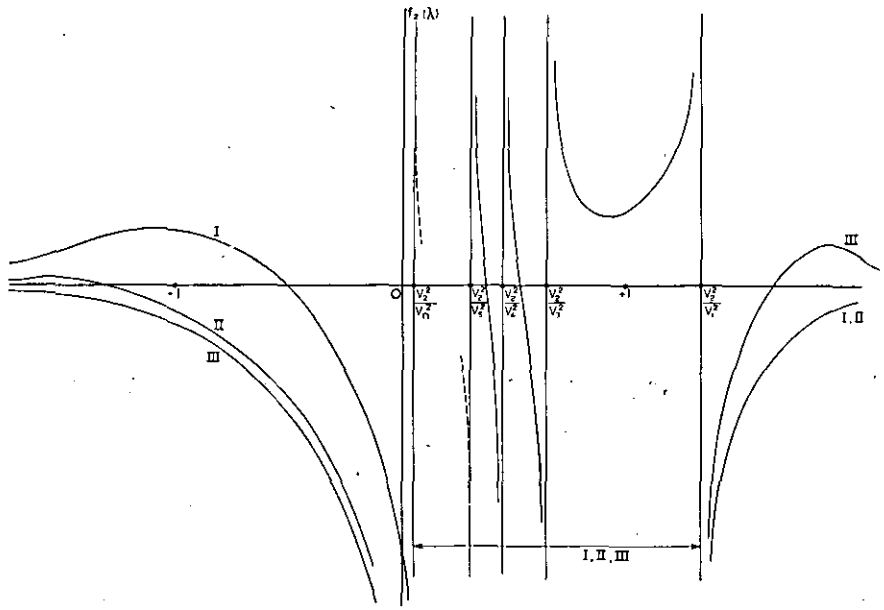

Fig. 3.

to the *fundamental* of one of the two mutually independent, completely uncoupled systems, defined by the principal-diagonal parts of these matrices (the mode $i=1$ becoming identical with the other fundamental). Moreover the difference between the frequency of this uncoupled fundamental and the (higher) frequency of the first overtone of the other uncoupled system shall not be very small, compared with the difference between the frequencies of the uncoupled fundamentals. (If this condition is not fulfilled, an "internal resonance" exists, forcing one of the components to "overtone shape"). Finally, there is a condition, referring to the distribution with y of the couplings, for it is possible to choose this in such a way, that the *effective* coupling between a fundamental-shaped component and an overtone-shaped accompanying component is very much larger than the effective coupling with a fundamental-shaped accompanying component. In this case the distribution of the coupling forces one component to overtone shape.

The generalization of these conditions to the case of systems, governed by equations with **e**- and **u**-matrices of higher order (3 for wing-aileron systems) is not difficult and needs no detailed explanation. It is clear, that the general, "summarizing", formulation (referring to the shape of the components) will remain valid.

Reviewing the situation it is seen, that the convergence is indeed bound to severe restrictions. Yet, it appears to be quite well possible, that all conditions are fulfilled in many flutter cases [1]. Therefore the method may really be a valuable tool of flutter research.

[1]) Particularly if the flutter mode is antisymmetrical, the first flexural overtone then falling commonly above the torsional fundamental, which may not be the case with the symmetrical vibrations.

7.5 *Biorthogonalisation to modes with vanishing frequency.*

We have seen (chapter 3), that the basic differential equations can be transformed into equivalent integral equations, provided that there are spring-restraints on the displacements in the $y=0$-plane. Suppose that these springs are weak. Then the iteration process based on the integral-equations, will converge primarily (if we do not insert biorthogonalisations) to a mode (the fundamental), which is largely influenced by the strength of these springs and which is of little importance, since there are actually no springs at all.

Let us assume therefore that the strength of the springs is (one for one) steadily decreased. Obviously if any of the constants k_z, k_φ, k_ϑ reaches zero, one of the natural frequencies gets zero too. But the limiting shape of the mode and of the accessory adjoint mode is also known. It indeed approaches for *both* to

$$\left\| \begin{matrix} z \text{ or } w_{01} \\ \varphi \text{ or } \psi_{01} \\ \gamma \text{ or } \beta_{01} \end{matrix} \right\| = \left\| \begin{matrix} \alpha_{01} \\ 0 \\ 0 \end{matrix} \right\| \text{ for } k_z = 0;$$

$$= \left\| \begin{matrix} 0 \\ \alpha_{02} \\ \alpha_{02} \end{matrix} \right\| \text{ for } k_\varphi = 0; = \left\| \begin{matrix} y\,\alpha_{03} \\ 0 \\ 0 \end{matrix} \right\| \text{ for } k_\vartheta = 0,$$

(α_{01}, α_{02}, α_{03} const.)

If $k_z = k_\varphi = k_\vartheta = 0$ we have to consider the right sides of these expressions as *coinciding independent modes*. Let us see what becomes of the biorthogonality conditions, which any higher mode must fulfil. We find

$$\left.\begin{aligned}
&\int_{-b}^{+b} \| \; a_{01} \quad 0 \quad 0 \; \| \; \mathbf{u}\, \mathbf{f}_{0,i} \; dy = 0 \\
&\int_{-b}^{+b} \| \; 0 \quad a_{02} \; a_{02} \; \| \; \mathbf{u}\, \mathbf{f}_{0,i} \; dy = 0 \\
&\int_{-b}^{+b} \| \; y\, a_{03} \; 0 \quad 0 \; \| \; \mathbf{u}\, \mathbf{f}_{0,i} \; dy = 0
\end{aligned}\right\} \; i \geqq 4.$$

But

$$\int_{-b}^{+b} \mathbf{K}\,(\eta, y)\; \mathbf{e}\,(y)\; \mathbf{F}_{0,H}\,(y)\; dy = \mathbf{F}_{0,H}\,(\eta)$$

for

$$\int_{-b}^{+b} dy\, \mathbf{K}\,(\eta, y) \quad \text{and} \quad \mathbf{e}$$

are reciprocal operators, their "product" being equal to the unit-matrix. Hence

$$\sum_H q_H \int_{-b}^{+b} \mathbf{G}_{0,J}^{*}\; \mathbf{u}\; \mathbf{F}_{0,H}\; dy - \nu^2 \sum_H q_H \int_{-b}^{+b} \int_{-b}^{+b} \mathbf{G}_{0,J}^{*}\,(\eta)\; \mathbf{u}\,(\eta)\; \mathbf{K}\,(\eta, y)\; \mathbf{u}\,(y)\, \mathbf{F}_{0,H}\,(y)\; dy\, d\eta = 0\,; \qquad (7.35)$$

$$J = 1 \ldots\ldots N.$$

The first equation is readily seen to be identical with (2.25), the second with (2.26) and the third with (2.27). Hence: if there are no spring restraints on displacements of the mechanical system as a whole, the integral-expression (4.16) instead of (4.13) may be used to approximate the solutions if eqs. (2.25), (2.26) and (2.27) are added to determine the matrix $\mathbf{c}_0$ between *every* step of a transformation sequence. To find higher modes, at the end biorthogonality to all lower modes with *non-vanishing* frequency should be demanded.

7.6 *Use of one-fold improved weight functions.*

It has been stated, that the approximations for the frequencies, delivered by the methods of par. 06.2 to par 06.6 incl. are generally particularly satisfactory, if the weight-functions permit close approximations to modes of the adjoint system. Now if

$$\sum_H r_{H,P}\; \mathbf{G}_{0,H}\,, \quad P = 1 \ldots\ldots N$$

represent these approximations (assuming that they are possible for all modes with order up to N), the transformations

$$\sum r_H \int_{-b}^{+b} \mathbf{K}\,(y, \eta)\; \mathbf{u}^{*}\,(\eta)\; \mathbf{G}_{0,H}\;(\eta)\; d\eta$$

and therefore the functions

$$\int_{-b}^{+b} \mathbf{K}\,(y, \eta)\; \mathbf{u}^{*}\,(\eta)\; \mathbf{G}_{0,H}\;(\eta)\; d\eta =$$

$$= \int_{-b}^{+b} \mathbf{G}_{0,H}^{*}\,(\eta)\; \mathbf{u}\,(\eta)\; \mathbf{K}^{*}\;(y, \eta)\; d\eta$$

will permit even more accurate representations. Let us use them as weight functions. Eqs. (6.8) then assume the form (compare (4.14))

$$\sum_H q_H \int_{-b}^{+b} \int_{-b}^{+b} \mathbf{G}_{0,J}^{*}\,(\eta)\; \mathbf{u}\,(\eta)\; \mathbf{K}\,(\eta, y)\,(\mathbf{e}\,(y) - - \nu^2\, \mathbf{u}\,(y)\,)\; \mathbf{F}_{0,H}\,(y)\; dy\, d\eta = 0,$$

$$J = 1 \ldots\ldots N.$$

These equations are seen to be identical with eq. (6.30). We obviously have discovered here an alternative conception of the Grammel-method. The new point of view reveals more clearly, why the Grammel-method gives approximations of improved accuracy for the frequencies. Moreover, we see that the method may — if desired — replace the set (6.8) everywhere, for instance to obtain a simultaneous purification of a number of modes, submitted to iterated transformation. Finally, we may conclude, that the Grammel-method is a most efficient one if we are mainly interested in frequencies and a one-fold improvement of *one* of the sets $\mathbf{F}_{0,H}$; $\mathbf{G}_{0,J}$ promises satisfactory accuracy.

7.7 *Pure matrix methods.*

The mathematics of our approximation methods involve many integrations, which commonly must be carried out numerically, and it may even be necessary (because of the matrix $\mathbf{e}$) to evaluate derivatives by numerical methods (this is generally superfluous if it is possible to use analytical basic sets $\mathbf{F}_{0,H}$, $\mathbf{G}_{0,J}$). The use of these numerical methods really comes down to a reduction of analytical processes to algebraical processes. This suggests that it might be possible to evade analytical operations right from the start and to treat the problem on a purely algebraical base. There exists indeed even a physical conception of the mechanical system, which suits this purpose: suppose the elasticity to be concentrated in springs without mass and suppose the mass to be concentrated into rigid elements, interconnected by the springs. In this way we may construct a model of the system, which reproduces the interesting features with an accuracy, which by refinement of the partition, can be made to meet any condition.

Yet this method is not so attractive as might seem. The analytical presentation is more concise and adaptable then the arithmetical one. It reveals directly the significance and bearing of any approximation. Making use of a spring-rigid mass system, the pursue of an optimal reduction of the computation desires a crude partition. The problem, how far to go in this respect and how to derive effective values for the spring constants and the elementary masses from their actually continuous distributions, is related to the problem,

how to evaluate integrals and differentials with arithmetical means on a base of large intervals in the range of the variables. The latter problem is a purely mathematical one. It has been carefully investigated and admits well-known solutions.

A closer investigation shows, that there is indeed little to be won (and more to be lost) by going straight back to a spring-mass reconstruction of the mechanical system, but that indeed part of the mathematics may assume — from the computational point of view — an attractive and appropriate form if the reduction from analysis to algebra is carried out explicitly.

The parts in question are connected with the matrices of par. 4.5. We assume the $\widetilde{\mathbf{K}}_X$- and $\widetilde{\mathbf{u}}$-matrices to be known (which for the $\widetilde{\mathbf{K}}_X$-matrix may imply a separate numerical evaluation of integrals).

Then the transformation formula (7.2) takes the form (compare 4.34),

$$\widetilde{\mathbf{f}}_{0,X}{}^{[n+1]} = \widetilde{\mathbf{K}}_X \, \widetilde{\mathbf{u}} \, \widetilde{\mathbf{f}}_{0,X}{}^{[n]}; \quad X = S, A. \tag{7.36}$$

without integral.

This formula can be used straight away for the successive approximation of the fundamental mode. The computational procedure appears to be very simple. Having once determined the matrix

$$\widetilde{\mathbf{R}}_X = \widetilde{\mathbf{K}}_X \, \widetilde{\mathbf{u}}$$

(algebraical process!), we must apparently execute repeatedly the algebraical operation

$$(\widetilde{\mathbf{f}}_{0,1}{}^{[i+1]})_X = \widetilde{\mathbf{R}}_X \, (\widetilde{\mathbf{f}}_{0,1}{}^{[i]})_X \tag{7.37}$$

until we reach satisfactory proportionality between consecutive $\widetilde{\mathbf{f}}$-approximations. Similarly, a repeated execution of the instruction

$$(\widetilde{\mathbf{g}}_{0,1}{}^{[i+1]})_X = \widetilde{\mathbf{R}}_X{}^* \, (\widetilde{\mathbf{g}}_{0,1}{}^{[i]})_X \tag{7.38}$$

will produce the first adjoint mode.

To find a higher mode, we must add biorthogonalisations to the transformations. These operations are again, if based on (4.34) of a purely algebraical type:

$$\widetilde{\mathbf{g}}_{0,J}{}^* \, \widetilde{\mathbf{u}} \, \widetilde{\mathbf{f}}_{0,k} = 0 \text{ if } j \neq k \text{ (index } X \text{ omitted)}. \tag{7.39}$$

To obtain a simultaneous purification of a number of modes, together with approximations to the frequencies, we need eqs. (6.8) or (7.35), of course preferably again in a purely algebraical formulation, employing matrices of $3n$-order. The set (6.30) can (starting with (4.34)) immediately be changed over to the desired form, the result obviously being (again with indices X omitted, a simplification to be continued in this paragraph)

$$\sum_H q_H \{ \widetilde{\mathbf{G}}_{0,J}{}^* \, \widetilde{\mathbf{u}} \, \widetilde{\mathbf{F}}_{0,H} - \nu^2 \, \widetilde{\mathbf{G}}_{0,J}{}^* \, \widetilde{\mathbf{u}} \, \widetilde{\mathbf{K}} \, \widetilde{\mathbf{u}} \, \widetilde{\mathbf{F}}_{0,H} \} = 0, \; j = 1 \ldots N. \tag{7.40}$$

If we want to make use of the set (06.8), we need a suitable $3n$-order representation $\widetilde{\mathbf{e}}$ of the $\mathbf{e}$-matrix. Now,

$$\mathbf{e} \text{ and } \int_0^b d\eta \; \mathbf{K}(y, \eta)$$

are reciprocal, so that

$$\widetilde{\mathbf{e}} = \widetilde{\mathbf{K}}^{-1}. \tag{7.41}$$

This is obviously a roundabout way to this matrix. The direct way will come down to a substitution of finite differences for the differentials in the exact representation of the $\mathbf{e}$-matrix.

With the help of the $\widetilde{\mathbf{e}}$-matrix we may represent the set (6.8) by

$$\sum_H q_H \{ \widetilde{\mathbf{G}}_{0,J}{}^* \, \widetilde{\mathbf{e}} \, \widetilde{\mathbf{F}}_{0,H} - \nu^2 \, \widetilde{\mathbf{G}}_{0,J}{}^* \, \widetilde{\mathbf{u}} \, \widetilde{\mathbf{F}}_{0,H} \} = 0, \; J = 1 \ldots N. \tag{7.42}$$

7.8 *Eliminating iteration method for higher modes.*

There exists a promising iteration method for natural vibrations higher than the fundamental, which is manifestly different from the "orthodox" iteration-biorthogonalisation procedures. It does not make the preliminary calculation of lower modes superfluous, but it avoids the necessity of repeatedly intervening biorthogonalisations. The idea is to suppress the reappearance of lower methods by eliminating them from the equations, placed at the basis of the iteration process. The method rests upon the development (5.14) for the kernels of the matrix integral equation.

Assume that the second original and adjoint modes are requested. Then, let the first modes be determined with high accuracy by the method of par. 7.1, with the result

$$\mathbf{F}_{0,1}, \quad \mathbf{G}_{0,1}$$

and the accessory frequency $\bar{\nu}_1$ (nearly equal to ν_1). These functions can accordingly be assumed to fulfil the normalization

$$\bar{\nu}_1{}^2 \int_{-b}^{+b} \mathbf{G}^*_{0,1} \, \mathbf{u} \, \mathbf{F}_{0,1} \, dy = 1.$$

Then, by (5.14),

$$\mathbf{K}(y, \eta) - \mathbf{F}_{0,1}(y) \, \mathbf{G}^*_{0,1}(\eta) \approx \approx \sum_{i=2}^{\infty} \mathbf{f}_{0,i}(y) \, \mathbf{g}^*_{0,i}(\eta) = \mathbf{K}_{(1)}(y, \eta)$$

and this new kernel will admit the approximation of $\mathbf{f}_{0,2}$, $\mathbf{g}_{0,2}$ by unaltered application of the simple procedure of par. 7.1. The result will of course show some error, caused by the inaccuracies left in the fundamentals, but yet the method converges to the requested modes in this sense, that these modes can be obtained with any prescribed exactitude. The proof is not difficult and may be omitted here. The generalisation to the calculation of 3rd, 4th, etc. modes is obvious and needs no explanation. It may be remarked that the degeneracy of the kernels $\mathbf{K}_{(1)}(y, \eta)$ etc., causes no trouble.

8 Perturbation methods. [1])

Supposing that the set $\mathbf{F}_{0,H}$ actually permits a satisfactory representation of the N lowest modes, let the vibration-problem be solved with the help of eq. (6.8), the solutions being

$$q_H = q_{H,K}\,,\ \nu^2 = \nu_K{}^2;\ H,K = 1 \ldots N. \qquad (8.1)$$

Now let any slight change be brought in the construction of the mechanical system. This change will cause small alterations in the matrices $\mathbf{e}$ and $\mathbf{u}$. Representing these alterations by $[\varepsilon]$ [2]) and $[\mu]$ we have

$$\mathbf{e} \to \mathbf{e} + [\varepsilon];\ [\varepsilon] \ll \mathbf{e},$$
$$\mathbf{u} \to \mathbf{u} + [\mu];\ [\mu] \ll \mathbf{u}. \qquad (8.2)$$

The amplified inequalities state, that homogolous elements in the matrices at both sides of the $\ll$ sign differ at least one order of magnitude.

Our objeet is to find a simplified method, permitting the calculation of the consequences of the alterations.

To start with, let the adjoint equations in their original version be solved also, with the result

$$r_J = r_{J,K}\,,\ (\nu^2 = \nu_K{}^2);\ J,K = 1 \ldots N. \qquad (8.3)$$

These solutions may or may not lead to approximations of the actual adjoint modes.

The solutions (8.1) and (8.3) fulfil a "biorthogonality-condition" of their own. Indeed, substituting any solution (8.1) in the original equations and any solution (8.3) in their adjoint companions, we get

$$\Sigma\ E_{JH}\, q_{H,K} = \nu_K{}^2\, U_{JH}\, q_{H,K}\ ;$$
$$\Sigma\ E_{JH}\, r_{J,L} = \nu_L{}^2\, U_{JH}\ r_{J,L} \qquad (8.4)$$

with the abbreviations

$$E_{J\,H} = \int_{-b}^{+b} \mathbf{G}_{0,J}{}^*\ \mathbf{e}\ \mathbf{F}_{0,H}\ dy\,;$$
$$U_{JH} = \int_{-b}^{+b} \mathbf{G}_{0,J}{}^*\ \mathbf{u}\ \mathbf{F}_{0,H}\ dy. \qquad (8.5)$$

Multiplying the first set (8.4) by $r_{J,L}$ and summing over J, and multiplying the second set by $q_{H,K}$ and summing over H, the left sides become identical and we infer by subtraction

$$\sum_J \sum_H r_{J,L}\, U_{JH}\, q_{H,K} = 0 \quad \text{if} \quad K \neq L. \qquad (8.6)$$

This is the biorthogonality-property. If

$$\sum_H q_{H,K}\, \mathbf{F}_{0,H} = \overline{\mathbf{f}}_{0,K};\ \Sigma\ r_{J,L}\, \mathbf{G}_{0,J} = \overline{\mathbf{g}}_{0,L} \qquad (8.7)$$

an equivalent version is

$$\int_{-b}^{+b} \overline{\mathbf{g}}_{0,L}{}^*\ \mathbf{u}\ \overline{\mathbf{f}}_{0,K}\ dy = 0;\ K \neq L. \qquad (8.8)$$

The relation is apparently identical with the biorthogonality-relation of the exact solutions. (This is at the same time a convincing proof of the purification properties of the set (6.8), formed with weight functions permitting satisfactory approximations to the adjoint modes).

Now set up, with the matrices (8.2), a new version of equations (8.4), using the functions (8.7) at the base [1]). We shall assume here (at variance with rules used hitherto) that these functions are normalized in accordance with

$$\int_{-b}^{+b} \overline{\mathbf{g}}_{0,K}{}^*\ \mathbf{u}\ \overline{\mathbf{f}}_{0,K}\ dy = 1. \qquad (8.9)$$

The result is (we now write $\overline{\nu^2}$ instead of ν^2)

$$\sum_H \overline{q}_H \int_{-b}^{+b} \overline{\mathbf{g}}_{0,J}{}^* \{\, \mathbf{e} - \overline{\nu^2}\, \mathbf{u} + [\varepsilon] - \overline{\nu^2}\, [\mu] \,\}\, \overline{\mathbf{f}}_{0,H}\, dy = 0,$$
$$J = 1 \ldots N.$$

But

$$\int_{-b}^{+b} \overline{\mathbf{g}}_{0,J}{}^*\ \mathbf{e}\ \mathbf{f}_{0,H}\ dy = \nu_H{}^2 \int_{-b}^{+b} \overline{\mathbf{g}}_{0,J}{}^*\ \mathbf{u}\ \overline{\mathbf{f}}_{0,H}\ dy = \nu_H{}^2\, \delta_{JH}\,.$$

Hence the equations reduce to

$$\sum_H q_H \left\{ (\nu_H{}^2 - \overline{\nu^2})\, \delta_{JH} + \right.$$
$$\left. + \int_{-b}^{+b} \overline{\mathbf{g}}_{0,J}{}^*\ ([\varepsilon] - \overline{\nu^2}\, [\mu])\, \overline{\mathbf{f}}_{0,H}\, dy \right\} = 0,$$
$$J = 1 \ldots N.$$

Putting

$$\int_{-b}^{+b} \overline{\mathbf{g}}_{0,J}{}^*\ [\varepsilon]\ \overline{\mathbf{f}}_{0,H}\, dy = \overline{\mathsf{E}}_{JH};$$
$$\int_{-b}^{+b} \overline{\mathbf{g}}_{0,J}{}^*\ [\mu]\ \overline{\mathbf{f}}_{0,H}\, dy = \overline{\mathsf{U}}_{JH} \qquad (8.10)$$

we may equivalently write

$$\sum_H \overline{q}_H \{\, (\nu_H{}^2 - \nu^2)\, \delta_{JH} + \overline{\mathsf{E}}_{JH} - \overline{\nu^2}\, \overline{\mathsf{U}}_{JH} \,\} = 0,$$
$$J = 1 \ldots N. \qquad (8.11)$$

It is clear that the solutions must be of the type

$$\overline{q}_H = \delta_{HK} + \overline{q}_{H,K'};\ |\overline{q}_{H,K'}| \ll 1;$$
$$\overline{\nu^2} = \nu_K{}^2 + \delta\, \overline{\nu}_K{}^2;\ \ \delta\, \overline{\nu}_K{}^2 \ll \nu_K{}^2$$
$$(= \text{"exact" } K\text{th frequency}).$$

---

[1]) A more complete description of these methods may be found in ref. 4. The basic idea is drawn from Courant-Hilbert: "Methoden der mathematischen Physik" (Berlin, Jul. Springer). See: Volume I, § 5 of Chapter I (2nd Ed.), Variierte Systeme.

[2]) We have already used the ε and $[\varepsilon]$-symbols for other purposes. Yet there will in this chapter be no ambiguity as to the meaning of the $[\varepsilon]$-symbol, employed here. *Greek* letters between square brackets represent vectors or matrices, like all heavy-type symbols.

[1]) It will be allowed to assume, that the small changes in the construction of the system will not stop the set (8.7), that is in fact: the set $\mathbf{F}_{0,H}$; $\mathbf{G}_{0,J}$, from being satisfactory.

Substituting these expressions, we get

$$\sum_H (\delta_{HK} + \bar{q}_{H,K'}) \{ (\nu_H^2 - \nu_K^2 - \delta \bar{\nu}_K^2) \delta_{JH} + \bar{E}_{JH} - (\nu_K^2 + \delta \bar{\nu}_K^2) \bar{U}_{JH} \} = 0, \; J = 1 \ldots N,$$

or

$$-\delta \bar{\nu}_K^2 . \delta_{JK} + \bar{E}_{JK} - (\nu_K^2 + \delta \nu_K^2) \bar{U}_{JK} + \bar{q}_{JK'} (\nu_J^2 - \nu_K^2 - \delta \nu_K^2) + \bar{q}_{H,K'} \{ \bar{E}_{JH} - (\nu_K^2 + \delta \bar{\nu}_K^2) \bar{U}_{JH} \} = 0, \quad J = 1 \ldots N. \tag{8.12}$$

Considering the coefficients $\bar{E}_{JH}$ and $\bar{U}_{JH}$ to be small of the first order, crossing of all terms of at least second order of smallness leaves behind:

$$\delta \bar{\nu}_K^2 \delta_{JK} + \bar{E}_{JK} - \nu_K^2 \bar{U}_{JK} + \bar{q}_{J,K'} (\nu_J^2 - \nu_K^2) = 0, \quad J = 1 \ldots N.$$

The solutions are

$$\delta \bar{\nu}_K^2 = \bar{E}_{KK} - \nu_K^2 \bar{U}_{KK}; \quad \bar{q}_{KK'} = 0 \; ^1); \quad \bar{q}_{J,K'} = \frac{\bar{E}_{JK} - \nu_K^2 \bar{U}_{JK}}{\nu_K^2 - \nu_J^2}, \; J \neq K. \tag{8.13}$$

They represent first approximations to the actual variations. Subsequent approximations may easily be determined by the restriction of neglections to quantities of the third, fourth, etc. order of smallness at least. A partial result is

$$(\delta \bar{\nu}_K^2)_2 = (1 - \bar{U}_{KK}) (\bar{E}_{KK} - \nu_K^2 \bar{U}_{KK}) + \sum_{H \neq K} \frac{(\bar{E}_{KH} - \nu_K^2 \bar{U}_{KH}) (\bar{E}_{HK} - \nu_K^2 \bar{U}_{HK})}{\nu_K^2 - \nu_H^2}, \quad K = 1 \ldots N. \tag{8.14}$$

The second approximation for $\bar{q}_{H,K'}$ is already complicated, and any higher approximations demand even more extensive formulae. This means that the benefits of the method are gradually going lost. The formulae, that have just been developed explicitly, constitute, however, a powerful tool of vibration analysis and especially of flutter analysis, for they permit the extension of a particular flutter calculation with well-founded estimates of the influence (particularly: on the critical speed, by intermediary of the formulae for the variation of the complex frequencies!) of small changes in the construction of the mechanical system. Without the use of perturbation-methods a similar result would demand terrible computation.

Another nice application of the perturbation procedure will be given in the next chapter.

9 Vibrations in still air.

9.1 *Introduction.*

If a wing oscillates in still air, the major part of the aerodynamic loading vanishes. The remaining parts constitute the well-known "aerodynamic additions" to the inertia of the system. It is indeed possible to include this effect in the mass distribution (par. 2.3). Assuming that the according corrections on these coefficients have been applied, we may cross the part **a** of the **u**-matrix (see par. 4.1) and write **m** instead of **u** everywhere. The equations are then self-adjoint, which leads to a substantial simplification of the theory. It is obviously unnecessary to add further explanation, nor will it be necessary to explain the application of the theory to the determination of resonance modes in still air (masses and stiffnesses being given).

The natural vibrations of the wing in still air are of the interest, since they are more or less narrowly related to the vibrations, encountered in flight. They constitute a most suitable source of information for the preparation of fluttercalculations. Typical data, preferably derived from resonance tests or from vibration calculations referring to still air, are modes, suiting the approximation by series development of the critical mode, and parameters representing the elastic properties of the system. For instance: if we build up a flutter calculation with the methods of par. 6.2 to 6.6 incl., making use of a base like (6.6), it often deserves recommendation to identify $z_{0,I}(y)$ with the measured or calculated flexural component of the "flexural fundamental", the function $\varphi_{0,I}(y)$ with the torsional component of the "torsional fundamental" and the function $\gamma_{0,I}(y)$ (if it is not reduced to a constant) with aileron deflection and twist in the "aileron fundamental" of the still-air modes.

9.2 *Vibrations of a fuselage-wing-aileron system with small couplings.*

For wings of simple construction we may attempt an interesting application of the perturbation method of the preceding chapter to the calculation of the resonance modes in still air. This application makes use of the assumption, that it shall be allowed to consider all elastic and intertia couplings to be small. This "condition" is actually seldom fulfilled in every respect. Yet it commonly holds for a good part and may lead to results, which give a very reasonable insight in the structure of the complicated "coupled" modes. The errors are indeed often no undue pay for the appreciable reduction of computation work.

In accordance with these indications the *unvaried* system is defined by the matrices

$$\mathbf{e} = \begin{Vmatrix} e_{11} & 0 & 0 \\ 0 & e_{22} & 0 \\ 0 & 0 & e_{33} \end{Vmatrix}; \quad \mathbf{m} = \begin{Vmatrix} m_{11} & 0 & 0 \\ 0 & m_{22} & 0 \\ 0 & 0 & m_{33} \end{Vmatrix}. \tag{9.1}$$

The variations are

$$[\varepsilon] = \begin{Vmatrix} 0 & 0 & 0 \\ 0 & 0 & e_{23} \\ 0 & e_{32} & 0 \end{Vmatrix}; \quad [\mu] = \begin{Vmatrix} 0 & m_{12} & m_{13} \\ m_{21} & 0 & m_{23} \\ m_{31} & m_{32} & 0 \end{Vmatrix}. \tag{9.2}$$

The basic equations

$$\mathbf{e}\, \mathbf{f}_0 = \nu^2 \mathbf{m}\, \mathbf{f}_0 \tag{9.3}$$

---

1) This particular value may be chosen to retain a suitable norming.

reduce to three mutually independent equations. A suitable series of lowest solutions may be supposed to be obtained with the help of the well-known, relatively simple methods for the calculation of flexural and torsional vibrations of rods. (Matrix methods of the par. 7.7-type are generally particularly efficient in a case like this).

Restricting the treatment to the sub-group of symmetrical vibrations only (the transfer to anti-symmetric vibrations encounters no difficulties), the (satisfactorily accurate) solutions may be represented by

$$\left.\begin{aligned}
&\nu = \nu_1 = 0 \quad ; \ \bar{\mathfrak{f}}_{0,1}{}^* = \| \, Z_0 \quad 0 \quad 0 \, \| \ ; \ Z_0 \text{: const.},\\
&\nu = \nu_2 = 0 \quad ; \ \bar{\mathfrak{f}}_{0,2}{}^* = \| \, 0 \quad \Phi_0 \quad 0 \, \| \ ; \ \Phi_0 \text{: const.},\\
&\nu = \nu_K = \nu_{z,K'} \ ; \ \bar{\mathfrak{f}}_{0,K}{}^* = \| \, z_{0,K'} \quad 0 \quad 0 \, \| \ ; \ K = 3, 4, \ldots, N_1 - 1; \ K' = 1, 2, \ldots, N_1 - 3 = N',\\
&\nu = \nu_K = \nu_{\Phi,K''} ; \ \bar{\mathfrak{f}}_{0,K}{}^* = \| \, 0 \quad \varphi_{0,K''} \quad 0 \, \| \ ; \ K = N_1, N_1 + 1, \ldots, N - 1; \ K'' = 1, 2, \ldots, N - N_1 = N'',\\
&\nu = \nu_N = \nu_\Gamma \quad ; \ \bar{\mathfrak{f}}_{0,H}{}^* = \| \, 0 \quad 0 \quad \Gamma_0 \, \| \ ; \ \Gamma_0 \text{ const.}
\end{aligned}\right\} \tag{9.4}$$

We evidently intend to neglect aileron twist. All functions are supposed to be normalized in accordance with (8.9). They have orthogonality properties of the type (8.8) (it is of course appropriate to replace $\bar{g}_{0,J}{}^*$ by $\bar{\mathfrak{f}}_{0,J}{}^*$ in these formulae):

We must now calculate the coefficients

$$\bar{U}_{JH} = \int_0^b \bar{\mathfrak{f}}_{0,J}{}^* \ [\mu] \ \bar{\mathfrak{f}}_{0,H} \ dy,$$

$$\bar{E}_{JH} = \int_0^b \bar{\mathfrak{f}}_{0,J}{}^* \ [\varepsilon] \ \bar{\mathfrak{f}}_{0,H} \ dy. \tag{9.5}$$

By development of the matrix-product we get without difficulty, making use of (9.2),

$\bar{U}_{11} = 0;$

$\bar{U}_{22} = 0,$

$$\bar{U}_{12} = \bar{U}_{21} = Z_0 \Phi_0 \int_0^b m_{12} dy = m_{12}{}^{00};$$

$$\bar{U}_{23} = \bar{U}_{32} = \Phi_0 \int_0^b m_{12} z_{0,1} dy = m_{12}{}^{10},$$

$\bar{U}_{13} = \bar{U}_{31} = 0;$

.....

.....;

$$\bar{U}_{2\,N_1-1} = \bar{U}_{N_1-1\,2} = \Phi_0 \int_0^b m_{12} z_{0,N'} dy = m_{12}{}^{N'0},$$

$\bar{U}_{1\,N_1-1} = \bar{U}_{N_1-1\,1} = 0;$

$\bar{U}_{2\,N_1} = \bar{U}_{N_1\,2} = 0,$

$$\bar{U}_{1\,N_1} = \bar{U}_{N_1\,1} = Z_0 \int_0^b m_{12} \varphi_{0,1} \, dy = m_{12}{}^{01};$$

.....

.....;

$\bar{U}_{2\,N-1} = \bar{U}_{N-1\,2} = 0,$

$$\bar{U}_{1\,N-1} = \bar{U}_{N-1\,1} = Z_0 \int_0^b m_{12} \varphi_{0,N'} dy = m_{12}{}^{0N'};$$

$$\bar{U}_{2\,N} = \bar{U}_{N2} = \Phi_0 \Gamma_0 \int_0^b m_{23} dy = m_{23}{}^{00},$$

$$\bar{U}_{1\,N} = \bar{U}_{N1} = Z_0 \Gamma_0 \int_0^b m_{13} dy = m_{13}{}^{00};$$

$\bar{U}_{JH} = 0; \ 3 \leqq J < N_1, \ 3 \leqq H < N_1;$

$\bar{U}_{JH} = 0; \ N_1 \leqq J < N, \ N_1 \leqq H < N,$

$\bar{U}_{NN} = 0,$

$$\bar{U}_{JH} = \bar{U}_{HJ} = \int_0^b z_{0,J'} \, m_{12} \, \varphi_{0,H''} \, dy = m_{12}{}^{J'H''};$$

$2 < J < N_1, \ N_1 \leqq H < N, \ J' = 1 \ldots N', \quad H'' = 1 \ldots N'',$

$$\bar{U}_{JN} = \bar{U}_{NJ} = \Gamma_0 \int_0^b z_{0,J'} \, m_{13} \, dy = m_{13}{}^{J'0};$$

$2 < J < N_1, \ J' = 1, 2, \ldots N',$

$$\bar{U}_{JN} = \bar{U}_{NJ} = \Gamma_0 \int_0^b \varphi_{0,J''} \, m_{23} dy = m_{23}{}^{J''0};$$

$N_1 \leqq J < N, \ J'' = 1, 2, \ldots N'',$

and, assuming (compare (2.16))

$$e_{23} = e_{32} = -k \, \delta \, (y - b_r),$$

$$\bar{E}_{2\,N} = \bar{E}_{N2} = -k \, \Phi_0 \Gamma_0 = e_{23}{}^{00}; \ \bar{E}_{JN} = \bar{E}_{NJ} = -k \, \varphi_{0,J''} \, (b_r) \, \Gamma_0 = e_{23}{}^{J''0};$$

$N_1 \leqq J < N, J'' = 1 \ldots N'',$

all other $\bar{E}_{JH}$'s vanishing.

Substituting the results in the formulae (8.13), the first one gives

$$(\delta \, \nu_K{}^2)_{1^{st} \text{ approx.}} = 0, \quad K = 1 \ldots N. \tag{9.6}$$

Hence the couplings do not change, to first approximation, the natural frequencies.

The second formula (8.13) constitutes the normalization

$$\bar{q}_{1,1}{}' = \bar{q}_{2,2}{}' = \ldots\ldots = \bar{q}_{N,N}{}' = 0.$$

The third formula demands some special care because of the vanishing of both ν_1 and ν_2. Yet, the following result is readily verified: *all* $\bar{q}_{J,K}{}'$ vanish with the exception of

$$\bar{q}_{1,N_1}' = m_{12}^{01}; \qquad \bar{q}_{2,3}' = -m_{12}^{10},$$

$$\ldots\ldots\ldots\ldots; \qquad \ldots\ldots\ldots\ldots,$$

$$\bar{q}_{1,N-1}' = m_{12}^{0N''}; \qquad \bar{q}_{2,N_1-1}' = -m_{12}^{N'0},$$

$$\bar{q}_{1,N}' = m_{13}^{00}; \qquad \bar{q}_{2N}' = \frac{e_{23}^{00} - \nu_\Gamma^2 m_{23}^{00}}{\nu_\Gamma^2},$$

$$\bar{q}_{3,N_1}' = \frac{-\nu_{\Phi,1}^2 m_{12}^{11}}{\nu_{\Phi,1}^2 - \nu_{z,1}^2}; \ \ldots\ldots\ldots; \ \bar{q}_{N_1-1,N_1}' = \frac{\nu_{\Phi,1}^2 m_{12}^{N'1}}{\nu_{\Phi,1}^2 - \nu_{z,N'}^2},$$

$$\ldots\ldots\ldots; \ \ldots\ldots\ldots; \ \ldots\ldots\ldots$$

$$\bar{q}_{3,N-1}' = \frac{-\nu_{\Phi,N''}^2 m_{12}^{1N''}}{\nu_{\Phi,N''}^2 - \nu_{z,1}^2}; \ \ldots\ldots\ldots; \ \bar{q}_{N_1-1,N-1}' = \frac{-\nu_{\Phi,N''}^2 m_{12}^{N'N''}}{\nu_{\Phi,N''}^2 - \nu_{z,N'}^2},$$

$$\bar{q}_{3,N}' = \frac{-\nu_\Gamma^2 m_{13}^{10}}{\nu_\Gamma^2 - \nu_{z,1}^2}; \ \ldots\ldots\ldots; \ \bar{q}_{N_1-1,N}' = \frac{-\nu_\Gamma^2 m_{13}^{N'0}}{\nu_\Gamma^2 - \nu_{z,N'}^2},$$

$$\bar{q}_{N_1,3}' = \frac{-\nu_{z,1}^2 m_{12}^{11}}{\nu_{z,1}^2 - \nu_{\Phi,1}^2}; \ \ldots\ldots\ldots; \ \bar{q}_{N-1,3}' = \frac{-\nu_{z,1}^2 m_{12}^{1N''}}{\nu_{z,1}^2 - \nu_{\Phi,N''}^2},$$

$$\ldots\ldots\ldots; \ \ldots\ldots\ldots; \ \ldots\ldots\ldots$$

$$\bar{q}_{N_1,N_1-1}' = \frac{-\nu_{z,N'}^2 m_{12}^{N'1}}{\nu_{z,N'}^2 - \nu_{\Phi,1}^2}; \ \ldots\ldots\ldots; \ \bar{q}_{N-1,N_1-1}' = \frac{-\nu_{z,N'}^2 m_{12}^{N'N''}}{\nu_{z,N'}^2 - \nu_{\Phi,N''}^2},$$

$$\bar{q}_{N_1,N}' = \frac{e_{23}^{10} - \nu_\Gamma^2 m_{23}^{10}}{\nu_\Gamma^2 - \nu_{\Phi,1}^2}; \ \ldots\ldots\ldots; \ \bar{q}_{N-1,N}' = \frac{e_{23}^{N''0} - \nu_\Gamma^2 m_{23}^{N''0}}{\nu_\Gamma^2 - \nu_{\Phi,N''}^2},$$

$$\bar{q}_{N,2}' = \frac{e_{23}^{00}}{\nu_\Gamma^2},$$

$$\bar{q}_{N,3}' = \frac{-\nu_{z,1}^2 m_{13}^{10}}{\nu_{z,1}^2 - \nu_\Gamma^2}; \qquad \bar{q}_{N,N_1}' = \frac{e_{23}^{10} - \nu_{\Phi,1}^2 m_{23}^{10}}{\nu_{\Phi,1}^2 - \nu_\Gamma^2},$$

$$\ldots\ldots\ldots \qquad \ldots\ldots\ldots$$

$$\bar{q}_{N,N_1-1}' = \frac{-\nu_{z,N'}^2 m_{13}^{N'0}}{\nu_{z,N'}^2 - \nu_\Gamma^2}; \qquad \bar{q}_{N,N-1}' = \frac{e_{23}^{N''0} - \nu_{\Phi,N''}^2 m_{23}^{N''0}}{\nu_{\Phi,N''}^2 - \nu_\Gamma^2}.$$

For the sake of clearness we summarize hereunder the non-vanishing terms of the "coupled" solutions (with non-vanishing frequencies).

$$(\bar{\mathbf{f}}_{0,3})_{\text{coupled}} = \bar{\mathbf{f}}_{0,3} + \bar{q}_{2,3}'\bar{\mathbf{f}}_{0,2} + \sum_{N_1}^{N-1} q_{H,3}'\bar{\mathbf{f}}_{0,H} + \bar{q}_{N,3}'\bar{\mathbf{f}}_{0,N},$$

$$\ldots\ldots\ldots\ldots\ldots\ldots\ldots\ldots$$

$$(\bar{\mathbf{f}}_{0,N_1-1})_{\text{coupled}} = \bar{\mathbf{f}}_{0,N_1-1} + \bar{q}_{2,N_1-1}'\bar{\mathbf{f}}_{0,2} + \sum_{N_1}^{N-1} \bar{q}_{H,N_1-1}'\bar{\mathbf{f}}_{0,H} + \bar{q}_{N,N_1-1}'\bar{\mathbf{f}}_{0,N},$$

$$(\bar{\mathbf{f}}_{0,N_1})_{\text{coupled}} = \bar{\mathbf{f}}_{0,N_1} + \bar{q}_{1,N_1}'\bar{\mathbf{f}}_{0,1} + \sum_{3}^{N_1-1} \bar{q}_{H,N_1}'\bar{\mathbf{f}}_{0,H} + \bar{q}_{N,N_1}'\bar{\mathbf{f}}_{0,N},$$

$$\ldots\ldots\ldots\ldots\ldots\ldots\ldots\ldots$$

$$(\bar{\mathbf{f}}_{0,N-1})_{\text{coupled}} = \bar{\mathbf{f}}_{0,N-1} + \bar{q}_{1,N-1}'\bar{\mathbf{f}}_{0,1} + \sum_{3}^{N_1-1} \bar{q}_{H,N-1}'\bar{\mathbf{f}}_{0,H} + \bar{q}_{N,N-1}'\bar{\mathbf{f}}_{0,N},$$

$$(\bar{\mathbf{f}}_{0,N})_{\text{coupled}} = \bar{\mathbf{f}}_{0,N} + \bar{q}_{1,N}'\bar{\mathbf{f}}_{0,1} + \bar{q}_{2,N}'\bar{\mathbf{f}}_{0,2} + \sum_{3}^{N_1-1} \bar{q}_{H,N}'\bar{\mathbf{f}}_{0,H} + \sum_{N_1}^{N-1} \bar{q}_{H,N}'\bar{\mathbf{f}}_{0,H}.$$

The typical item is apparently, that — to first approximation — the couplings *do not change* the original "major" component of any mode, and that "accompanying" components emerge with amplitudes, proportional to the particular coupling *integrals* $\bar{\mathsf{E}}_{JH}$, $\nu_H^2\,\bar{\mathsf{U}}_{JH}$ (defining couplings between pairs of originally uncoupled modes) and inversely proportional to the square-frequency differences $\nu_J^2 - \nu_H^2$. Hence, "internal resonances", that is: close neighboorhood of pairs of uncoupled natural frequencies, have a characteristic effect upon the form of the coupled modes, consisting of an uncommon increase of a generally small "accompanying component", moreover giving to this component the shape of the "resonating" uncoupled mode. It will be clear, that the accuracy of the formulae ceases to be satisfactory in such a case.

These results throw new light upon certain con-

clusions, connected with the convergence of the approximation method of par. 7.4.

Finally, the evaluation of the second-order variation of the frequencies given by (8.14) leads to the result

$$(\delta\,\nu_{z,K'})^2_{\text{2nd appr.}} = \nu_{z,K'}^2\,(m_{12}{}^{K'0})^2 + \\ + \sum_{H''=1}^{N''} \frac{\nu_{z,K'}^2\,(m_{12}{}^{K'H''})^2}{\nu_{z,K'}^2 - \nu_{\varphi,H''}^2} + \frac{\nu_{z,K'}^2\,(m_{13}{}^{K'0})^2}{\nu_{z,K'}^2 - \nu_\Gamma^2},$$

$$(\delta\,\nu_{\varphi,K''})^2_{\text{2nd appr.}} = \nu_{\varphi,K''}^2\,(m_{12}{}^{0K''})^2 + \\ + \sum_{H'=1}^{N'} \frac{\nu_{\varphi,K''}^2\,(m_{12}{}^{H'K''})^2}{\nu_{\varphi,K''}^2 - \nu_{z,H'}^2} + \\ + \frac{(k\,\varphi_{0,K''}(b_r)\Gamma_0 + \nu_{\varphi,K''}{}^2\,m_{23}{}^{K''0})^2}{\nu_{\varphi,K''}^2 - \nu_\Gamma^2},$$

$$(\delta\,\nu_\Gamma)^2_{\text{2nd appr.}} = \nu_\Gamma{}^2\,(m_{13}{}^{00})^2 + \nu_\Gamma{}^2\,(m_{23}{}^{00})^2 + \\ + \sum_{H'=1}^{N'} \frac{\nu_\Gamma{}^2\,(m_{13}{}^{H'0})^2}{\nu_\Gamma{}^2 - \nu_{z,H'}{}^2} + \\ + \frac{(k\,\varphi_{0,H''}(b_r)\,\Gamma_0 + \nu_\Gamma{}^2\,m_{23}{}^{H''0})^2}{\nu_\Gamma{}^2 - \nu_{\varphi,H''}{}^2}. \quad (9.8)$$

Let $\nu_{z,K'}$ and $\nu_{\varphi,H'}$ be any couple of nearly equal frequencies. Then the first and second equation obviously contain *one* relatively large term, which is easily seen to reduce the smaller frequency and to enlarge the larger one. Hence, the couplings tend to enlarge the gaps between neighbouring uncoupled frequencies. Since an incident like this again involves relatively large variations, the accuracy of the perturbation formulae must become less satisfactory.

9.3 *Derivation of integrals of elastic forces from resonance tests.*

If the establishment of equations (6.8), used a starting point of a flutter calculation, can be related with measurements of resonance tests with the aeroplane, it may be possible to deduce the "elastic parameters"

$$\int_{-b}^{+b} \mathbf{G}_{0,J}{}^* \,\mathbf{e}\, \mathbf{F}_{0,H}\, dy = E_{JH} \quad (9.9)$$

from the test data. This would be a good thing, for in this way we may not only escape from the partially intricate problem to analyse accurately the elastic properties of the system, but we may also avoid the necessity of using unpleasant numerical approximations for the derivatives, contained in the expression $\mathbf{e}\,\mathbf{F}_{0,H}$.

Obviously, the determination of the constants (9.9) encounters no difficulty if we employ a set $\mathbf{F}_{0,H}$, consisting of complete "measured" modes from the test, simultaneously putting

$$\mathbf{G}_{0,J} = \mathbf{F}_{0,J}$$

(that is: specializing to the Galerkin/Lagrange-method). Indeed, we then have

$$E_{JH} = (\nu_H^2)_{res}\,\delta_{JH} \quad (9.10)$$

if the norming of the functions agrees with

$$\int_{-b}^{+b} \mathbf{F}_{0,H}{}^* \,\mathbf{m}\, \mathbf{F}_{0,H}\, dy = 1. \quad (9.11)$$

The frequencies $(\nu_H)_{res}$ are the measured resonance frequencies. (Formula (9.10) rests upon the fact, that the aerodynamic forces do not change the **e**-matrix).

It is, however, known, that it is commonly impracticable to use functions $\mathbf{F}_{0,H}$ like that. Compare e. g. the frequently used assumption (6.5). In such a case there is only one suitable method to reach the desired result.

Again assuming that the Galerkin/Lagrange-method is used, start with eq. (6.8), applying to vibrations in still air

$$\sum E_{JH}\,q_H = \nu^2 \sum M_{JH}\,q_H;\; J = 1 \ldots N;$$

$$M_{JH} = \int_{-b}^{+b} \mathbf{F}_{0,J}{}^* \,\mathbf{m}\, \mathbf{F}_{0,H}\, dy. \quad (9.11)$$

Assuming that the functions $\mathbf{F}_{0,H}$ are still normed in accordance with (9.11) and that the solutions

$$q_H = q_{H,I}\,,\quad \nu^2 = \nu_I{}^2\,;\quad I = 1 \ldots N$$

are normed by the prescription

$$q_{H,H} = 1 \quad (9.12)$$

we have, in agreement with (8.6),

$$\sum_K \sum_L q_{K,J}\,M_{KL}\,q_{L,H} = \delta_{JH}\,.$$

Multiplying both sides by $\frac{q_{I,J}}{\nu_J{}^2}$ and summing over J we get

$$\sum_J \delta_{JH}\,\frac{q_{I,J}}{\nu_J{}^2} = \frac{q_{I,H}}{\nu_H{}^2} = \sum_J \sum_K \sum_L \frac{q_{I,J}\,q_{K,J}}{\nu_J{}^2} M_{KL}\,q_{L,H}\,. \quad (9.13)$$

But if we regard the right sides of (9.11) as *known* constants, we may solve [1])

$$q_I = \nu^2 \sum_K E_{IK}\dagger \sum_L M_{KL}\,q_L;$$

$$E_{IK}\dagger = \frac{\text{minor of } E_{IK} \text{ in det } E_{JH}}{\det E_{JH}}.$$

Inserting here the H^{th} solution, we find

$$\frac{q_{I,H}}{\nu_H{}^2} = \sum_K \sum_L E_{IK}\dagger M_{KL}\,q_{L,H}\,.$$

Comparing this formula with (9.13), we infer

$$E_{IK}\dagger = \sum_J \frac{q_{I,J}\,q_{K,J}}{\nu_J{}^2}, \quad (9.14)$$

a result, which is easily seen to be analogous to the development (5.14) of the kernel of an integral equation (the apparent difference emerging from the different normings employed).

---

[1]) Note that $E_{IK} = E_{KI}$; $E_{IK}\dagger = E_{KI}\dagger$.

Formula (9.14) makes the desired reduction possible. It indeed shows that

$$E_{JH} = \frac{\text{minor of } \sum_L \frac{q_{J,L}\, q_{H,L}}{\nu_L^2} \text{ in } \det \sum_L \frac{q_{I,L}\, q_{K,L}}{\nu_L^2}}{\det \sum_L \frac{q_{I,L}\, q_{K,L}}{\nu_L^2}} \qquad (9.15)$$

The result may be summarized as follows:

If the set $\mathbf{F}_{0,H}$ admits, by the Galerkin/Lagrange equations

$$\sum_H q_H \int_{-b}^{+b} \mathbf{F}_{0,J}^* \,(\mathbf{e} - \nu^2\, \mathbf{m})\, \mathbf{F}_{0,H}\, dy = 0,$$

the construction of *approximations* to modes of vibration in still air, *each* solution of this equation thus being linked to a particular resonance mode, the elastic constants

$$E_{JH} = \int_{-b}^{+b} \mathbf{F}_{0,J}^*\, \mathbf{e}\, \mathbf{F}_{0,H}\, dy$$

may be determined with the help of (9.15) from *prescribed* shapes of *these approximations* and *prescribed* resonance frequencies. The *same* constants may thereupon be used in the Galerkin/Lagrange set

$$\sum_H E_{JH}\, q_H = \nu^2 \sum_H q_H \int_{-b}^{+b} \mathbf{F}_{0,J}^*\, \mathbf{u}\, \mathbf{F}_{0,H}\, dy$$

appropriate to the analysis of flutter phenomena.

If we use weight functions, differing from the Galerkin/Lagrange adoption, a similar result can be reached if these weight-function equally permit the construction of approximations to the measured *resonance modes*. The necessary slight generalization of formula (9.15) need not be explained.

10 List of fundamental symbols.

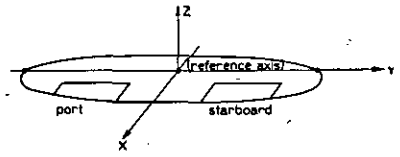

Fig. 4.

$x,\ y,\ z$	coordinates, defined by fig. 4
t	time
ν	frequency
$z_d(y,t) = z_{d_0}(y)\, e^{i\nu t}$ $\varphi_d(y,t) = \varphi_{d_0}(y)\, e^{i\nu t}$ $\gamma_d(y,t) = \gamma_{d_0}(y)\, e^{i\nu t}$	distortions, defined by fig. 1
$z(y,t) = z_0(y)\, e^{i\nu t}$ $\varphi(y,t) = \varphi_0(y)\, e^{i\nu t}$ $\gamma(y,t) = \gamma_0(y)\, e^{i\nu t}$	translational and angular displacements, out of the neutral position, of the reference axis, about this axis and about the aileron hinge axis (see fig. 2)
$Z = Z_0\, e^{i\nu t} = z_0(0)\, e^{i\nu t}$	
$\Phi = \Phi_0\, e^{i\nu t} = \varphi_0(0)\, e^{i\nu t}$	
$\theta = \theta_0\, e^{i\nu t} = \left(\frac{dz_0(y)}{dy}\right)_{y=0} e^{i\nu t}$	
$\chi = \chi_0\, e^{i\nu t}$	rotation, out of the neutral position, of the control column of the ailerons
b	semispan
$\pm b_1,\ \pm b_2$	outer and inner edges of the ailerons
$\pm b_r$	y-coordinate of the *section, containing the connection of controls* to the ailerons.
$b^{(a)}$	y-coordinate of sections containing point-loads
$c(y)$	chord of wing + aileron
c_0	reference chord
c_d	x-coordinate of the hinge axis (see fig. 2)
s_v	x-coordinate of the centre of gravity of the wing *without* aileron
s_r	distance behind the hinge axis of the centre of gravity of the aileron
$m_v(y)$	mass per unit of span of wing *without* aileron
$m_r(y)$	mass per unit of span of aileron
$I_v(y)$	moment of inertia, per unit of span, about spanwise axis through the local *centre of gravity, of the wing without* aileron
$I_r(y)$	moment of inertia per unit of span, of the aileron, about the hinge axis
$B_{11}(y),\ B_{12}(y),\ B_{22}(y),$ $T_v(y),\ T_r(y)$	stiffnesses
$k,\ k_z,\ k_\Phi,\ k_\varphi,\ k_z$	spring constants
$e_{ik}(y) = e_{ki}(y)$	operator-coefficients of the stiffness-distribution. See eqs. (2.8), (2.9), (2.10), (2.16), (2.19a and b), (2.22) and Appendix I, eqs. (3) and (5)

$m_{ik}'(y) = m_{ki}'(y)$; $m_{ik}^{(a)} = m_{ki}^{(a)}$; $m_{ik}(y) = m_{ki}(y)$	coefficients of mass-distribution. See eqs. (2.1), (2.14), (2.15), (2.21). The $m_{ik}^{(a)}$ define contributions of concentrated loads
$a_{ik}(y)$	coefficients of the aerodynamic loading
m_L	mass per unit of span of the surrounding cylinder of air
$K_{ik}(y, \eta)$	influence functions
$u_{ik}(y)$	coefficients of the distribution of the resulting loading (inertia loading + aerodynamic loading)
V	reduced velocity (eq. (6.1))
V_0	reduced velocity, adjoint to reference chord
A S	*indices*, referring to antisymmetrical, resp. symmetrical oscillations
$\mathbf{f}_0(y)$	vector of amplitude functions (Eq. 4.1)
$\mathbf{f}_{0,i}(y)$	modes of vibrations
$\mathbf{g}_{0,i}(y)$	characteristic functions of the adjoint equations
$\mathbf{m}(y)$	matrix of inertia-loads divided by ν^2 (eq. 4.2)
$\mathbf{a}(y)$	matrix of aerodynamic loads divided by ν^2 (eq. 4.3)
$\mathbf{u}(y)$	matrix of total load divided by ν^2 (eq. 4.6)
$\mathbf{e}(y)$	operator matrix of elastic forces (eq. 4.4)
$\mathbf{L}(y)$	load vector (eq. 4.7)
$\mathbf{K}(y, \eta)$	kernel matrix
$\mathbf{c}_0$	vector of amplitudes of the fuselage
$\tilde{\mathbf{f}}_0$, $\tilde{\mathbf{u}}$, $\tilde{\mathbf{K}}$	matrices of par. 4.5
$w_{0,i}(y)$, $\psi_{0,i}(y)$, $\beta_{0,i}(y)$	elements of the vector $\mathbf{g}_{0,i}(y)$
$\mathbf{F}_{0,H}$, $H = 1 \ldots N$	approximation base for a restricted number of modes of vibration
$\mathbf{G}_{0,J}$, $J = 1 \ldots N$	system of weight vectors
q_H	coefficients in the approximations of modes of vibration
r_J	coefficients in the approximations of adjoint modes.

11 References.

1. Greidanus, J. H., De berekening van de kritische snelheid voor onstabiele trillingen van vliegtuigvleugels. Rapport V 1252 van het Nationaal Luchtvaartlaboratorium, deel X van de Verslagen en Verhandelingen (1941).
2. Greidanus, J. H., De berekening van de kritische snelheid voor onstabiele trillingen van vliegtuigvleugels II. Rapport V 1304 van het Nationaal Luchtvaartlaboratorium, deel XII van de Verslagen en Handelingen (1943).
3. Greidanus, J. H., De nauwkeurigheid van benaderingsmethoden der berekening van vleugeltrillingen. Rapport V 1351 van het Nationaal Luchtvaartlaboratorium (1944).
4. Van de Vooren, A. I., A Method to Determine the Change in Flutter Speed Due to Small Changes in the Mechanical System. Report V 1366 of the National Aeronautical Research Institute, this Volume of the Reports and Transactions.

Completed: July 1946.

Appendix I. The accurate representation of the principal features of a reversible control mechanism of the ailerons.

We have already mentioned the fact that — at variance with assumption d of par. 2.1 — the mechanism of control of the ailerons actually constitutes an interconnection of the port and starboard aileron. If we want to take due account of this fact, we might assume this mechanism to be constructed of interconnecting elastic cables without mass and of a massive member, connected to these cables in the $y = 0$-plane and representing the control wheel. This conception obviously introduces another dependent variable in the equations, namely the rotation-angle χ of the control wheel. Simultaneously, the triple of basic equations will be extended with one equation.

It is easy to see that the concentrated moment, exchanged in the section $y = \pm b_r$ between wing and aileron and previously equal to

$$| k \{ \gamma (\pm b_r) - \varphi (\pm b_r) \} |$$

must now be changed into

$$| k \{ \gamma (\pm b_r) - \varphi (\pm b_r) \mp \chi \} | \ldots \quad (1)$$

Hence, the original fundamental (differential) equations become

$$\left.\begin{aligned} &\nu^2 (u_{11} z_0 + u_{12} \varphi_0 + u_{13} \gamma_0) - e_{11} z_0 - \\ &\quad - e_{12} \varphi_0 = 0, \\ &\nu^2 (u_{21} z_0 + u_{22} \varphi_0 + u_{23} \gamma_0) - e_{21} z_0 - \\ &\quad - e_{22} \varphi_0 - e_{23} \gamma_0 - e_{24} \chi_0 = 0, \\ &\nu^2 (u_{31} z_0 + u_{32} \varphi_0 + u_{33} \gamma_0) - \\ &\quad - e_{32} \varphi_0 - e_{33} \gamma_0 - e_{34} \chi_0 = 0, \end{aligned}\right\} \quad (2)$$

with

$$\begin{aligned} e_{24} &= k \{ \delta (y - b_r) - \delta (y + b_r) \}; \\ e_{34} &= - k \{ \delta (y - b_r) - \delta (y + b_r) \}, \end{aligned} \quad (3)$$

the original coefficients retaining their significance.

The completing (fourth) equation is effectively an ordinary algebraical one.

Making use of an appropriate inertia parameter I_χ, we may obviously write it in the form

$$-I_\chi \ddot{\chi} + k \{ -2\chi + \gamma(b_r) - \varphi(b_r) - \gamma(-b_r) + \varphi(-b_r) \} = 0$$

or

$$(I_\chi \nu^2 - 2k)\chi_0 + k \{ \gamma_0(b_r) - \gamma_0(-b_r) - \varphi_0(b_r) - \varphi_0(-b_r) \} = 0$$

or, again,

$$\int_{-b}^{+b} \{ \nu^2 m_{44} \chi_0 - e_{42}\varphi_0 - e_{43}\gamma_0 - e_{44}\chi_0 \} dy = 0, \quad (4)$$

with

$$e_{42} = e_{24}; \; e_{43} = e_{34}, \; m_{44} = I_\chi \delta(y-0); \; e_{44} = k \{ \delta(y-b_r) + \delta(y+b_r) \}. \quad (5)$$

The alternative (4) reveals the harmony with (2).

We might add here the remark, that the extension discussed above properly refers to a relatively simple case only. The construction of the control mechanism may give rise to several complications. Let for instance the control wheel be replaced by a control column or wheel with axis of rotation parallel to the longitudinal axis. Then the mass of it will, strictly, couple the control mechanism, with rotations $z_0'(0)$ of the fuselage, and indeed many other small couplings may arise from other particularities of the construction. Nobody will ever ponder about them, unless any such device has purposely been introduced to influence the vibration characteristics.

It is of course again possible to convert the differential-equations into pure integral equations. To determine the result, we again accept the simplifications, explained in par. 3.1. Instead of the analytical method, used in par. 3.1, we shall now employ a more physical one, based on the fact, that the integral-kernels are "influence" functions.

Applying a force of unit magnitude to the point $y = \eta \; (> 0)$ of the elastic axis, the displacements $z_0(y)$ of the points of this axis will — in the state of equilibrium — have grown to infinity, unless

a the displacements $z_0(0)$ and $z_0'(0)$ are given

b the displacements $z_0(0)$ and $z_0'(0)$ are reduced to finite values by virtue of spring-constraints $-k_z z_0(0) - k_\vartheta z_0'(0)$ in the plane $y = 0$.

In this case the displacement of the point $y \; (> 0)$ of the elastic axis amounts to

$$\begin{Bmatrix} z_0(0) + y z_0'(0) \\ \frac{1}{k_z} + \frac{y\eta}{k_\vartheta} \end{Bmatrix} + \int_0^{<y,\eta} \frac{(y-y_1)(\eta-y_1)}{B_{11}(y_1)} dy_1, \quad (6)$$

while the displacement, shifted to the port wing $(y < 0)$, is equal to

$$\begin{Bmatrix} z_0(0) + y z_0'(0) \\ \frac{1}{k_z} + \frac{y\eta}{k_\vartheta} \end{Bmatrix} \quad (7)$$

These formulae must be equivalent to the Ξ_{11} and K_{11}-influence functions, and indeed it is seen immediately that the result agrees with the corresponding formulae of chapter 3 [1]).

Since there is no elastic coupling between flexure and wing twist, aileron deflection or twist and control-wheel rotation, Ξ_{12}, Ξ_{13}, Ξ_{14}, K_{12}, K_{13} and K_{14} must vanish (again in agreement with chapter 3).

Applying a moment of unit magnitude about the elastic axis on the wing, in the cross section $y = \eta \; (> 0)$, there will emerge no flexure. Wing twist will grow to infinity, unless

a the displacement $\varphi_0(0)$ is given;

b the displacement $\varphi_0(0)$ is reduced to a finite value by a spring constraint $-k_\varphi \varphi_0(0)$.

In these cases, the unit moment will force an amount of twist, equal to

$$\varphi_0(y) = \begin{Bmatrix} \varphi_0(0) \\ \frac{1}{k_\varphi} \end{Bmatrix} + \int_0^{<y,\eta} \frac{dy_1}{T_v(y_1)}; \; (y > 0, \eta > 0), \quad (8)$$

while we shall find at the port wing

$$\varphi_0(y) = \begin{Bmatrix} \varphi_0(0) \\ \frac{1}{k_\varphi} \end{Bmatrix}; \; (y < 0, \; \eta > 0). \quad (9)$$

There will consequently emerge displacements $\varphi_0(b_r)$, $\varphi_0(-b_r)$ in the sections of the aileron control. They will, however, not lead to strains in the aileron springs if only

$$\gamma_0(b_r) = \varphi_0(b_r); \quad \gamma_0(-b_r) = \varphi_0(-b_r),$$

i. e. if

$$\gamma_0(y) = \begin{Bmatrix} \varphi_0(0) \\ \frac{1}{k_\varphi} \end{Bmatrix} + \int_0^{<b_r,\eta} \frac{dy_1}{T_v(y_1)}, \; (y > 0), \quad (10)$$

$$\gamma_0(y) = \begin{Bmatrix} \varphi_0(0) \\ \frac{1}{k_\varphi} \end{Bmatrix}, \; (y < 0). \quad (11)$$

Under these conditions there will be no displacement χ_0. We infer: formulae (8), (9) are aequivalent to $\Xi_{22}(y,\eta)$; $K_{22}(y,\eta)$, formulae (10) and (11) to $\Xi_{32}(y,\eta)$, $K_{32}(y,\eta)$ and Ξ_{42}, K_{42} vanish. The results for Ξ_{22}, K_{22}, Ξ_{32}, K_{32} will be seen to be in agreement with chapter 3.

Let, thirdly, the unit moment be applied in the section to the aileron. The conditions for finite displacements are then

a the displacements $\varphi_0(0)$ and χ_0 are given;

b the displacements $\varphi_0(0)$ and χ_0 are limited by means of springs k_φ and k_χ.

---

[1]) In case *a* the *load* causes displacements $z_0(y) - z_0(0) - y z_0'(0)$, hence the terms $z_0(0)$, $y z_0'(0)$ cannot make part of the kernel and have to be shifted to the left side. In case *b* the full displacement is immediately determined by the load, and $\frac{1}{k_z}$, $\frac{y\eta}{k_\vartheta}$ thus make part of the kernels.

The spring k_χ apparently constitutes a new element in the construction of the system. It tries to keep the control column in the plane of symmetry.

Assuming y and η to be larger than b_r, the amount of aileron torsion becomes equal to

$$\gamma_0(y) - \gamma_0(b_r) = \int_{b_r}^{<y,\eta} \frac{d\,y_1}{T_r(y_1)}.$$

The deflection $\gamma_0(b_r) - \varphi_0(b_r)$ obviously grows until

$$k\{\gamma_0(b_r) - \varphi_0(b_r)\} = 1,$$

whence

$$\gamma_0(b_r) = \varphi_0(b_r) + \chi_0 + \frac{1}{k}.$$

In case b we must add

$$\chi_0 = \frac{1}{k_\chi}.$$

The angular displacement $\varphi_0(b_r)$ is obviously equal to

$$\int_0^{b_r} \frac{dy_1}{T_v(y_1)} + \left\{\begin{matrix}\varphi_0(0)\\ \frac{1}{k_\varphi}\end{matrix}\right\}. \qquad (12)$$

We thus get, summarizing and completing,

Finally, applying a unit moment to the spring-constrained control column, we shall get

$$\chi_0 = \frac{1}{k_\chi};\quad \gamma_0 = \begin{cases} \frac{1}{k_\chi}\ ;\ y > 0, \\ -\frac{1}{k_\chi}\ ;\ y < 0, \end{cases} \qquad (16)$$

leading to K_{44} and K_{34}. The complete expressions for these elements obviously are

$$K_{44} = \frac{1}{k_\chi};\quad K_{34} = K_{43} =$$

$$= \begin{cases} \frac{1}{k_\chi};\ y > 0,\ \eta > 0 \\ -\frac{1}{k_\chi};\ y < 0,\ \eta > 0 \\ -\frac{1}{k_\chi};\ y > 0,\ \eta < 0 \\ \frac{1}{k_\chi};\ y < 0,\ \eta < 0 \end{cases} \qquad (17)$$

$$\gamma_0(y) = \left\{\begin{matrix} \left\{\begin{matrix}\varphi_0(0) + \chi_0\\ \frac{1}{k_\varphi} + \frac{1}{k_\chi}\end{matrix}\right\} + \frac{1}{k} + \int_0^{b_r} \frac{dy_1}{T_v(y_1)} + \int_0^{<y,\eta} \frac{dy_1}{T_r(y_1)} & ;\ y > 0, \\ \left\{\begin{matrix}\varphi_0(0) - \chi_0\\ \frac{1}{k_\varphi} - \frac{1}{k_\chi}\end{matrix}\right\} & ;\ y < 0, \end{matrix}\right\} \qquad (13)$$

$$\varphi_0(y) = \left\{\begin{matrix} \left\{\begin{matrix}\varphi_0(0)\\ \frac{1}{k_\varphi}\end{matrix}\right\} + \int_0^{<y,b_r} \frac{dy_1}{T_v(y_1)} & ;\ y > 0, \\ \left\{\begin{matrix}\varphi_0(0)\\ \frac{1}{k_\varphi}\end{matrix}\right\} & ;\ y < 0, \end{matrix}\right\} \qquad (14)$$

$$\chi_0 = \left\{\begin{matrix} \left\{\begin{matrix}\chi_0\\ \frac{1}{k_\chi}\end{matrix}\right\} & ;\ y > 0, \\ \left\{\begin{matrix}-\chi_0\\ -\frac{1}{k_\chi}\end{matrix}\right\} & ;\ y < 0. \end{matrix}\right\} \qquad (15)$$

Formula (12) is aequivalent to Ξ_{33}, K_{33}, formula (13) to Ξ_{23}, K_{23} and formula (14) to K_{43}, ($\Xi_{43} = 0$). Comparing with the results in chapter 3 we must first put $\chi_0 = 0$ or $k_\chi = 0$, which apparently leads to complete agreement.

It will be clear — but may be written out fully for the sake of clearness — that the integral equations, contracted to one matrix equation, have the form (without specification of independent variables)

$$\left\| \begin{matrix} z_0 \\ \varphi_0 \\ \gamma_0 \\ \chi_0 \end{matrix} \right\| = \int_{-b}^{+b} \left\| \begin{matrix} K_{11} & 0 & 0 & 0 \\ 0 & K_{22} & K_{23} & 0 \\ 0 & K_{32} & K_{33} & K_{34} \\ 0 & 0 & K_{43} & K_{44} \end{matrix} \right\| \cdot \left\| \begin{matrix} u_{11} & u_{12} & u_{13} & 0 \\ u_{21} & u_{22} & u_{23} & 0 \\ u_{31} & u_{32} & u_{33} & 0 \\ 0 & 0 & 0 & m_{44} \end{matrix} \right\| \cdot \left\| \begin{matrix} z_0 \\ \varphi_0 \\ \gamma_0 \\ \chi_0 \end{matrix} \right\| . d\eta .$$

All equations are now equally well applicable to antisymmetric and symmetric oscillations. There is no reason to make $k = 0$ in the first case. The aequivalent of $k = 0$ (chapter 3) is actually

$$m_{44} = 0, \quad k_\chi = 0, \quad k = \infty . \tag{18}$$

In this case the representation containing k_χ is no longer usable. The representation, containing χ_0 remains applicable. Yet, we must add some additional equation to determine the appropriate value of this parameter. This additional equation is actually given by equation (4); leading (for static equilibrium) by means of (18) to

$$\chi_0 = \tfrac{1}{2} \{ \gamma_0 (b_r) - \varphi_0 (b_r) - \gamma_0 (-b_r) + \varphi_0 (-b_r) \} . \tag{19}$$

This must be substituted into (13), i. e. in Ξ_{33} and K_{33}. The values of $\varphi_0 (b_r)$ and $\varphi_0 (-b_r)$ follow from (8). Thereupon $\gamma_0 (b_r)$ and $\gamma_0 (-b_r)$ may be solved *in advance* from (13) (by putting $y = \pm b_r$), leaving back this equation without unknown parameters and hence right down applicable for the calculation of the complete function $\gamma_0 (y)$.

Appendix II. Structural damping.

In this report we did not take any account of damping forces, having their origin in the structural parts of the mechanical system. It is well-known, that this omission can easily be made good. We might e. g. introduce velocity-proportional damping terms, or — and this is a more simple and not less accurate method — introduce complex stiffness parameters, giving to the negative elastic restoring forces a phase lead with respect to the distortion (hysteresis).

Actually, damping is often neglected in flutter calculations. There are, however, two important objections against this praxis. Firstly, damping may have (in certain cases) a very appreciable influence upon the stability, i. e. upon the critical velocity, and secondly we loose in this way a sound base to estimate the degree of danger, implied in any instability [1]).

Yet it is true, that reliable values for the structural damping are seldom available and that only exceptionally special damping-devices are used to suppress instabilities (which might lead to calculations, in which due account of these damping forces becomes of fundamental importance).

There is, however, a simple method to incorporate some damping in flutter calculations. Let

$$\det (E_{JH} - \nu^2 U_{JH}) = 0 \tag{1}$$

be the frequency equation, making part of any mathematical investigation of flutter. The constants E_{JH} depend upon the parameters, representing the stiffness. We assume *these* parameters to be originally *real* and thus to imply no structural damping. The constants U_{JH} depend upon the aerodynamic and inertia loading. For itself *both* E_{JH} and U_{JH} may be complex, the E_{JH} through complex representations of the modes. The constants U_{JH} are functions of the standard reduced velocity V_0. The roots of (1) will generally — i. e. for an arbitrary value of V_0 — be complex. Selecting the root which represents, or threatens to develop, the instability, we may write

$$\nu^2 = \nu_{fl}^2 \, e^{i a_\nu} \; ; \quad \nu = \nu_{fl} \, e^{\frac{1}{2} i a_\nu} ; \quad \nu_{fl} \text{ real and positive, } a \text{ real,} \tag{2}$$

for it. We assume

$$| a_\nu | \ll \pi \tag{3}$$

and infer accordingly that

$$\nu \approx \nu_{fl} (1 + \tfrac{1}{2} i a_\nu) . \tag{4}$$

Hence

$$e^{i\nu t} \approx e^{-\frac{a_\nu}{2} \nu_{fl} t} \, . \, e^{i \nu_{fl} t} \tag{5}$$

showing that the oscillation is unstable if $a_\nu < 0$.

Now (2) is a solution of (1), so

$$\det \{ E_{JH} - \nu_{fl}^2 \, e^{i a_\nu} U_{JH} \} = 0 .$$

Multiplying every element of the determinant by $e^{-i a_\nu}$ we get

$$\det \{ E_{JH} \, e^{-i a_\nu} - \nu_{fl}^2 \, U_{JH} \} = 0 .$$

Hence the equation

$$\det (E_{JH}' - \nu^2 U_{JH}) = 0 \tag{6}$$

with

$$E_{JH}' = E_{JH} \, . \, e^{-i a_\nu} \tag{7}$$

will have a *real* root

$$\nu^2 = \nu_{fl}^2$$

and will therefore represent formally a transition between stability and instability.

Now the transformation (7) is really aequivalent — provided that a_ν is negative — to the introduction of a special form of structural hysteresis damping, the particularity consisting of a similar affection of all elastic properties, occurring in the calculation (all elastic forces assuming the same angles of lead). This particularity, however, is not

[1]) It is often effectively possible, to distinguish cases of "relatively innocent" flutter and "acufely dangerous" flutter.

an unsatisfactory one, if no details about the actual damping are known, or at least, if there is no reason to compile the effect of such details.

These considerations lead to the following suggestion for the performance of flutter calculations:

Establish equations, governing the flutter oscillations, without explicit representation of structural damping. Don't use stability criteria, built upon the coefficients of the resulting frequency equation, but solve this equation completely for a sequence of values of V_0. Then each couple

$$V_0, \; \nu_{i,fl} = |\nu_i|$$

defines a critical velocity, i. e. a transition state between stability and instability (or conversely), accessory to the angle of lead

$$\alpha_i = -\alpha_{\nu,i} = -\arg \nu_i^2$$

due to generalized structural damping. These results permit the construction of a complete graph of v_{crit} against a (= generalized structural damping).

If α_i is *negative*, the generalized damping in facts converts to a physically infeasible form of generation of oscillations. Yet, even this part of the v_{crit}: a-plane is not completely useless, since it may bring to light seemingly stable (indeed *almost* unstable) states, which change over to instability if the system is slightly changed. Such changes may even fall within the range of accuracy of the parameters, which mathematically define the system.

REPORT V. 1386

The Treatment of a Tab in Flutter Calculations Including a Complete Account of Aerodynamic Coefficients

by

Ir. A. I. VAN DE VOOREN.

Summary.

In this paper the equations of motion for a wing-aileron-tab system, expressing the equilibrium of inertia, elastic and aerodynamic forces, are deduced. Explicit formulae permitting the immediate computation of these forces from the constructional data of the system are also given. The elastic forces of the control mechanism, which appear to depend upon the type of tab considered, are derived for all common tab designs (spring tab, trim tab, balance tab etc.). The aerodynamic forces are obtained by strip-theory from the results of the well-known aerodynamic theory of an oscillating airfoil in two-dimensional flow (ref. 2—7). All aerodynamic functions and coefficients are made suitable for immediate use in flutter calculations by the addition of extensive tables at the end of the paper. These tables include also the numerical material, necessary for the evaluation of Taylor-series (to the spanwise coordinate) of the aerodynamic coefficients, which series have been introduced in order to facilitate the computation of the aerodynamic integrals, appearing in the approximative solutions of the equations of motion. Throughout the whole report compressibility effects are neglected.

Contents.

1 Introduction [1]).

The main object of this paper is twofold. In the first place it is intended to extend the methods of calculation for the flutter speed of wing-aileron systems, given in previously published reports (ref. 1, 8, 9) to wing-aileron-tab systems. In view of the increasing application of tabs and, during the last few years, of spring tabs in particular, this extension seems very desirable. It is facilitated by the fact that the mathematical representation of the aerodynamic forces of a wing-aileron-tab system in a two-dimensional, incompressible flow has already been developed by the fundamental work both of Küssner and Schwarz, and of Theodorsen.

In the second place this report forms an indispensable supplement to ref. 1, since it contains a detailed description of the treatment of the aerodynamic forces in flutter calculations. This was intentionally omitted from that report, since it was preferred to deal with this subject when considering the more complete system of aerodynamic forces acting on a wing-aileron-tab combination.

---

[1]) This investigation has been performed by order of the "Rijksluchtvaartdienst".

2 The mechanical system.

2.1 *Representation of displacements.*

The most general deformation of the wing-aileron-tab system accounted for, consists of

(1) wing flexure, determined by the displacement z of the reference axis, which is usually chosen coïnciding with the flexural axis,

(2) wing torsion, determined by the rotation φ of the wing chord,

(3) aileron deflection + torsion, determined by the rotation γ of the aileron chord,

(4) tab deflection + torsion, determined by the rotation ε of the tab chord.

All displacements are defined relative to the neutral position of the system. Hence, the angle between aileron and wing is equal to

$$\gamma_r = \gamma - \varphi \tag{2.1}$$

and the angle between tab and aileron to

$$\varepsilon_r = \varepsilon - \gamma. \tag{2.2}$$

Though in general all displacements are functions of the spanwise coordinate y, it will nearly always be permitted to neglect torsion of the tab, thus assuming ε constant along the whole tab. The same approximation may often hold for the aileron, especially when antisymmetric oscillations are considered.

Aileron flexure is assumed to be determined by the deformation of the wing at the hinge axis, making a separate representation superfluous. In the same way the tab hinge axis is considered to move with the aileron, thus determining the flexure of the tab.

For the treatment of the aerodynamic forces it will appear convenient to introduce two more displacement functions, viz.

(1) the displacement ζ of the aileron leading edge relative to the wing trailing edge,

(2) the displacement χ of the tab leading edge relative to the aileron trailing edge.

They are connected with the displacements, previously introduced, by the relations

$$\zeta + c_{dr}\gamma_r = 0 \quad \text{and} \quad \chi + c_{es}\varepsilon_r = 0, \tag{2.3}$$

c_{dr} resp. c_{es} representing the distances of the aileron resp. tab hinge axis aft of the corresponding leading edge.

For harmonic oscillations — the only motion to be considered in this paper — the coordinates vary with time according to

$$z = z_0 e^{i\nu t} \text{ etc.}, \tag{2.4}$$

z_0 representing the amplitude of the oscillation (for wing flexure).

Finally it must be stated that all displacements and all forces are positive when directed upwards, while rotations and moments are positive when they are tailheavy,

2.2 *The equations of motion.*

These equations are obtained when the conditions of equilibrium, mentioned hereunder, are applied to an infinitely narrow strip of the system:

(1) the total of all forces perpendicular to the wing plane is zero,

(2) the total of all moments about the reference axis and acting on the wing (without aileron) is zero,

(3) the total of all moments about the aileron hinge axis and acting on the aileron (without tab) is zero,

(4) the total of all moments about the tab hinge axis and acting on the tab is zero.

The equations can be brought in the following well-known form, applying only to harmonic oscillations, i.e. using eq. (2.4),

$$\left.\begin{aligned}
&(\nu^2 m_{11} - e_{11})\, z + (\nu^2 m_{12} - e_{12})\, \varphi + \\
&(\nu^2 m_{13} - e_{13})\, \gamma + (\nu^2 m_{14} - e_{14})\, \varepsilon + K_L = 0, \\
&(\nu^2 m_{21} - e_{21})\, z + (\nu^2 m_{22} - e_{22})\, \varphi + \\
&(\nu^2 m_{23} - e_{23})\, \gamma + (\nu^2 m_{24} - e_{24})\, \varepsilon + M_L = 0, \\
&(\nu^2 m_{31} - e_{31})\, z + (\nu^2 m_{32} - e_{32})\, \varphi + \\
&(\nu^2 m_{33} - e_{33})\, \gamma + (\nu^2 m_{34} - e_{34})\, \varepsilon + N_L = 0, \\
&(\nu^2 m_{41} - e_{41})\, z + (\nu^2 m_{42} - e_{42})\, \varphi + \\
&(\nu^2 m_{43} - e_{43})\, \gamma + (\nu^2 m_{44} - e_{44})\, \varepsilon + Q_L = 0,
\end{aligned}\right\} \tag{2.5}$$

where u_{ik} determine the inertia, e_{ik} the elastic and K_L etc. the aerodynamic forces resp. moments of the system.

Using matrices, the equations take the following form

$$\mathbf{ef} = \nu^2 \mathbf{mf} + \mathbf{A}, \tag{2.6}$$

where

$$\mathbf{m} = \begin{Vmatrix} m_{11} & m_{12} & m_{13} & m_{14} \\ m_{21} & m_{22} & m_{23} & m_{24} \\ m_{31} & m_{32} & m_{33} & m_{34} \\ m_{41} & m_{42} & m_{43} & m_{44} \end{Vmatrix}, \quad \mathbf{e} = \begin{Vmatrix} e_{11} & e_{12} & e_{13} & e_{14} \\ e_{21} & e_{22} & e_{23} & e_{24} \\ e_{31} & e_{32} & e_{33} & e_{34} \\ e_{41} & e_{42} & e_{43} & e_{44} \end{Vmatrix},$$

$$\mathbf{f} = \begin{Vmatrix} z \\ \varphi \\ \gamma \\ \varepsilon \end{Vmatrix}, \quad \mathbf{A} = \begin{Vmatrix} K_L \\ M_L \\ N_L \\ Q_L \end{Vmatrix}. \tag{2.7}$$

2.3 *The inertia coefficients* m_{ik}.

It is convenient to arrange that the inertia forces and hence the coefficients m_{ik} shall include the part of the aerodynamic forces, constituting the well-known "aerodynamic inertias". The contribution due to this effect will be denoted in the formulae by certain coefficients $\alpha_{ik}^{(0)}$, the values of which will be given in table 2.1.

From simple considerations (ref. 1) it is found

$$\left.\begin{aligned}
m_{11} &= m + \sum_j m_{11}^{(j)}\,\delta(y-b^{(j)}) - I_L\frac{d}{dy}\left\{\delta(y-0)\frac{d}{dy}\right\} + m_L\alpha_{11}^{(0)},\\
m_{12} &= m_{21} = -ms + m_1 s_1 + \sum_j m_{12}^{(j)}\,\delta(y-b^{(j)}) + m_L c\,\alpha_{12}^{(0)},\\
m_{13} &= m_{31} = -m_1 s_1 + m_2 s_2 + \sum_j m_{13}^{(j)}\,\delta(y-b^{(j)}) + m_L c\,\alpha_{13}^{(0)},\\
m_{14} &= m_{41} = -m_2 s_2 + \sum_j m_{14}^{(j)}\,\delta(y-b^{(j)}) + m_L c\,\alpha_{14}^{(0)},\\
m_{22} &= I + ms^2 - I_1 - m_1 s_1^2 - 2\,m_1 s_1 c_d + \sum_j m_{22}^{(j)}\,\delta(y-b^{(j)}) + m_L c^2\,\alpha_{22}^{(0)},\\
m_{23} &= m_{32} = (m_1 s_1 - m_2 s_2)c_d + \sum_j m_{23}^{(j)}\,\delta(y-b^{(j)}) + m_L c^2\,\alpha_{23}^{(0)},\\
m_{24} &= m_{42} = m_2 s_2 c_d + \sum_j m_{24}^{(j)}\,\delta(y-b^{(j)}) + m_L c^2\,\alpha_{24}^{(0)},\\
m_{33} &= I_1 + m_1 s_1^2 - I_2 - m_2 s_2^2 - 2\,m_2 s_2 c_e + \sum_j m_{33}^{(j)}\,\delta(y-b^{(j)}) + m_L c^2\,\alpha_{33}^{(0)},\\
m_{34} &= m_{43} = m_2 s_2 c_e + \sum_j m_{34}^{(j)}\,\delta(y-b^{(j)}) + m_L c^2\,\alpha_{34}^{(0)},\\
m_{44} &= I_2 + m_2 s_2^2 + \sum_j m_{44}^{(j)}\,\delta(y-b^{(j)}) + m_L c^2\,\alpha_{44}^{(0)},
\end{aligned}\right\} \tag{2.8}$$

where

$$\left.\begin{aligned}
&m = m_v + m_r + m_s,\\
&s = \frac{m_v s_v + m_r(c_d + s_r) + m_s(c_d + c_e + s_s)}{m_v + m_r + m_s},\\
&m_1 = m_r + m_s,\quad s_1 = \frac{m_r s_r + m_s(c_e + s_s)}{m_r + m_s},\\
&m_2 = m_s,\qquad s_2 = \frac{m_s s_s}{m_s},\\
&I + ms^2 = I_v + m_v s_v^2 + I_r + m_r(c_d + s_r)^2 + \\
&\qquad + I_s + m_s(c_d + c_e + s_s)^2,\\
&I_1 + m_1 s_1^2 = I_r + m_r s_r^2 + I_s + m_s(c_e + s_s)^2,\\
&I_2 + m_2 s_2^2 = I_s + m_s s_s^2
\end{aligned}\right\} \tag{2.9}$$

and

$$m_L = {}^1/_4\,\pi\,\rho\,c^2 \quad (\rho = \text{air density}). \tag{2.10}$$

The distances are shown in fig. 2.1, where they possess positive values, like the displacements and the angles of rotation. For instance, c_v is positive when the reference axis lies before the quarter chord axis.

Other symbols are explained by the list of notations (section 5).

The terms with $m_{ik}^{(j)}\,\delta(y-b^{(j)})$ refer to concentrated masses, $\delta(y-b^{(j)})$ being a singular function, defined by:

$$\delta(y-b^{(j)}) = 0 \quad \text{for} \quad y \neq b^{(j)}$$

and $\int_{b^-}^{b^+} \delta(y-b^{(j)})\,dy = 1$ when $b^- < b^{(j)} < b^+$.

The coefficients $m_{ik}^{(j)}$ are formed in the same way as the corresponding coefficients of the continuous mass distribution. For instance, $m_{13}^{(j)}$ denotes the static moment about the aileron hinge axis of the concentrated masses, fixed at the section $y = b^{(j)}$ to aileron or tab, diminished with the static moment about the tab hinge axis of the masses fixed at the section $y = b^{(j)}$ to the tab.

2.4 *The elastic coefficients* e_{ik}.

The elastic forces in the system are due to the flexural stiffness of the wing (B), to the torsional stiffness of wing (T_v), aileron (T_r) and tab (T_s) and to the elasticity of the control mechanism. Those due to the flexural and torsional stiffnesses are, if the flexural axis of the wing is taken as reference axis [1]), determined by the following e_{ik}-operators

[1]) It is assumed here that a flexural axis is present. The complications, arising if it does not exist (e. g. appearance of an e_{12}-operator), are mentioned in ref. 1.

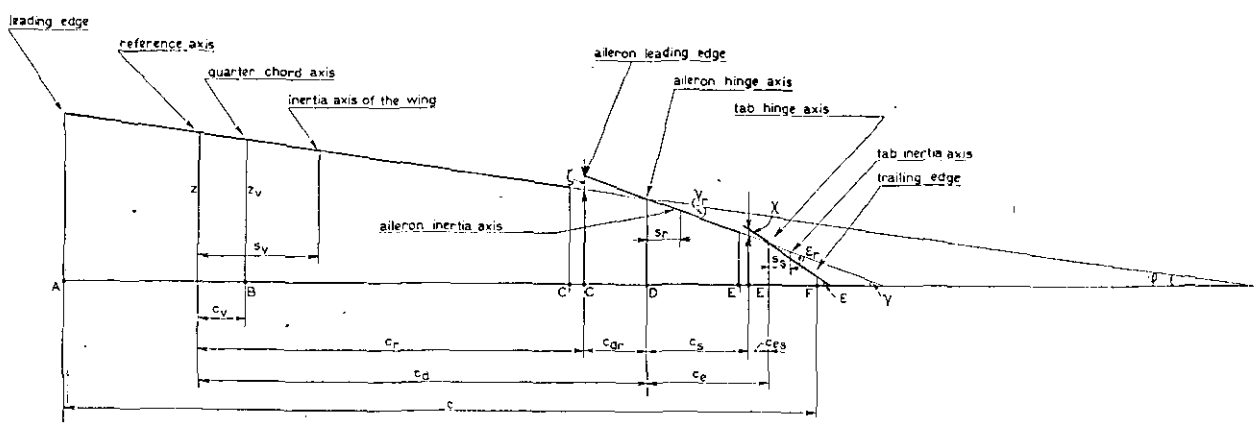

Fig. 2.1 General position of the wing-aileron-tab system.

$$(e_{11})_0 = \frac{d^2}{dy^2}\left(B\frac{d^2}{dy^2}\right);\quad (e_{22})_0 = -\frac{d}{dy}\left(T_v\frac{d}{dy}\right);$$
$$(e_{33})_0 = -\frac{d}{dy}\left(T_r\frac{d}{dy}\right);$$
$$(e_{44})_0 = -\frac{d}{dy}\left(T_s\frac{d}{dy}\right). \qquad (2.11)$$

When T_s or T_r are infinitely large, the terms $e_{33}\gamma$ and $e_{44}\varepsilon$ in the equations of motion (2.5) become indefinite. For practical use the equations containing these terms must at first be integrated along the whole span of the tab and aileron.

The elastic forces due to the elasticity of the control mechanism depend on its design, making it impossible to give formulae valuable for all sorts of tabs. At first the most complicated tab construction in use until now, i. e. the spring tab, will be discussed and from the results obtained for this tab, the elastic forces connected with more orthodox types will be deduced. Then the last step appears to be very simple indeed.

Fig. 2.2 shows the schematized construction of

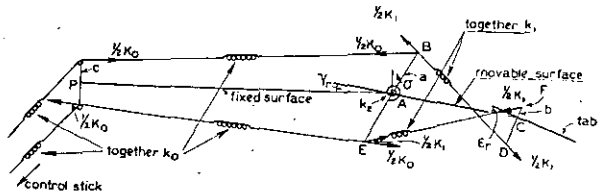

Fig. 2.2 Spring tab.

the spring tab. The mass of the control mechanism will be entirely neglected. The elasticity of the cables from the control stick to the arm BE is determined by k_0, where $^1/_2\ k_0$ denotes the force in each cable necessary for unit strain (positive in one and negative in the other cable). Likewise, $^1/_2\ k_1$ stands for the force producing unit strain in the cables BD and EF. The torsion spring at A has as strength k_2, indicating the moment required for a torsion of one radian.

When the control stick is not moved, as in the case of symmetric vibrations, the force in each of the cables from the stick to B or E, amounts to

$$^1/_2\ K_0 = {}^1/_2\ k_0 a\ (\gamma_r + \sigma),$$

while the force in the cables BD and EF is:

$$^1/_2\ K_1 = {}^1/_2\ k_1\ (b\varepsilon_r + a\sigma).$$

Both forces give moments about the point A, tending to rotate the lever BE against the action of the spring k_2. Since the mass of the lever is neglected, the elastic moments must balance each other, leading to the relation

$$(K_0 + K_1)\ a + k_2\sigma = 0,$$

whence

$$\sigma = -\frac{k_0 a^2\gamma_r + k_1 ab\varepsilon_r}{(k_0 + k_1)\ a^2 + k_2}. \qquad (2.12)$$

Successively the moments acting on the tab, the aileron and the wing will be examined.

(1) Tab. The forces K_1 cause an elastic moment

$$-K_1 b = k_1 b\frac{k_0 a^2\gamma_r - (k_0 a^2 + k_2)b\varepsilon_r}{(k_0 + k_1)\ a^2 + k_2} \qquad (2.13)$$

together with a resultant force at the hinge axis C equal to

$$-K_1 \cdot \frac{a+b}{AC} \qquad (2.14)$$

(2) Aileron. The aileron is subject to a moment

$$k_2\sigma = -(K_0 + K_1)a$$

and to a second moment due to the resultant force at C (2.14). This moment is

$$K_1(a+b),$$

making the total moment acting on the aileron equal to

$$-K_0 a + K_1 b = \frac{k_0 a^2\{k_1 a(a+b)+k_2\}\gamma_r - k_1 b\{k_0 a^2(a+b)+k_2 b\}\varepsilon_r}{(k_0+k_1)a^2+k_2} \qquad (2.15)$$

Besides this moment, there is again a resultant force at A amounting to

$$-K_0 \cdot \frac{a-c}{AP} \qquad (2.16)$$

(3) Wing. The forces K_0 cause a moment $+K_0 c$, while the vertical forces in the points A and P give a second moment $K_0\ (a-c)$. This makes the total moment independent of the distance c and equal to

$$K_0 a = k_0 a^2\ \frac{(k_1 a^2 + k_2)\ \gamma_r - k_1 ab\varepsilon_r}{(k_0+k_1)a^2+k_2}. \qquad (2.17)$$

From the obtained elastic moments, which are only present in the section $y = b_r$, where the control mechanism operates, the values for the e_{ik} coefficients can be deduced. Including the values of eq. (2.11) they become for a spring tab:

$$\left.\begin{aligned}
&e_{11} = \frac{d^2}{dy^2}\left(B\frac{d^2}{dy^2}\right),\\
&e_{12} = e_{13} = e_{14} = e_{21} = e_{31} = e_{41} = 0,\\
&e_{22} = -\frac{d}{dy}\left(T_v\frac{d}{dy}\right) + \\
&\qquad + k_0 a^2\frac{k_1 a^2 + k_2}{(k_0+k_1)a^2+k_2}\,\delta\,(y - b_r),\\
&e_{23} = e_{32} = -k_0 a^2\frac{k_1 a(a+b)+k_2}{(k_0+k_1)a^2+k_2}\,\delta\,(y-b_r),\\
&e_{24} = e_{42} = k_0 a^2\frac{k_1 ab}{(k_0+k_1)a^2+k_2}\,\delta\,(y-b_r),\\
&e_{33} = -\frac{d}{dy}\left(T_r\frac{d}{dy}\right) + \\
&+\frac{k_0 k_1 a^2(a+b)^2 + k_2(k_0 a^2 + k_1 b^2)}{(k_0+k_1)a^2+k_2}\,\delta\,(y-b_r),\\
&e_{34} = e_{43} = \\
&\qquad = -k_1 b\ \frac{k_0 a^2(a+b)+k_2 b}{(k_0+k_1)a^2+k_2}\,\delta\,(y-b_r),
\end{aligned}\right\} \qquad (2.18)$$

$$e_{44} = -\frac{d}{dy}\left(T_s \frac{d}{dy}\right) + + k_1 b^2 \frac{k_0 a^2 + k_2}{(k_0 + k_1) a^2 + k_2} \delta (y - b_r). \quad (2.18)$$

In general, k_1 will be very much larger than k_0. With the approximation $k_1 \to \infty$, (2.12) leads to

$$\sigma = -\frac{b}{a} \varepsilon_r ,$$

the same relation following from the condition that the force K_1 must remain finite. The elastic coefficients then become

$$\left.\begin{aligned}
e_{11} &= \frac{d^2}{dy^2}\left(B \frac{d^2}{dy^2}\right), \\
e_{12} &= e_{13} = e_{14} = e_{21} = e_{31} = e_{41} = 0, \\
e_{22} &= -\frac{d}{dy}\left(T_v \frac{d}{dy}\right) + k_0 a^2 \delta (y - b_r), \\
e_{23} &= e_{32} = -k_0 a (a + b) \delta (y - b_r), \\
e_{24} &= e_{42} = k_0 a b \delta (y - b_r), \\
e_{33} &= -\frac{d}{dy}\left(T_r \frac{d}{dy}\right) + \\
&\quad + \left\{ k_0 (a + b)^2 + k_2 \frac{b^2}{a^2} \right\} \delta (y - b_r), \\
e_{34} &= e_{43} = \\
&= -\left\{ k_0 (a + b) b + k_2 \frac{b^2}{a^2} \right\} \delta (y - b_r), \\
e_{44} &= -\frac{d}{dy}\left(T_s \frac{d}{dy}\right) + \\
&\quad + \left(k_0 b^2 + k_2 \frac{b^2}{a^2} \right) \delta (y - b_r).
\end{aligned}\right\} \quad (2.19)$$

For a servo tab (fig. 2.3) the lever DF is directly connected with the control stick. Hence, $k_2 = 0$

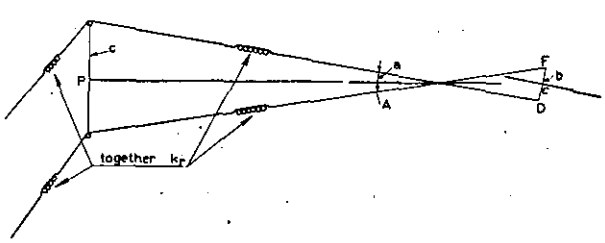

Fig. 2.3 Servo tab.

must be substituted in equations (2.18) to obtain the elastic coefficients for the servo tab. With the abbreviation $\frac{k_0 k_1}{k_0 + k_1} = k_r$, denoting the strength of the whole cable, it is found:

$$\left.\begin{aligned}
e_{11} &= \frac{d^2}{dy^2}\left(B \frac{d^2}{dy^2}\right), \\
e_{12} &= e_{13} = e_{14} = e_{21} = e_{31} = e_{41} = 0, \\
e_{22} &= -\frac{d}{dy}\left(T_v \frac{d}{dy}\right) + k_r a^2 \delta (y - b_r), \\
e_{23} &= e_{32} = -k_r a (a + b) \delta (y - b_r), \\
e_{24} &= e_{42} = k_r a b \delta (y - b_r), \\
e_{33} &= -\frac{d}{dy}\left(T_r \frac{d}{dy}\right) + \\
&\quad + k_r (a + b)^2 \delta (y - b_r), \\
e_{34} &= e_{43} = -k_r (a + b) b \delta (y - b_r), \\
e_{44} &= -\frac{d}{dy}\left(T_s \frac{d}{dy}\right) + k_r b^2 \delta (y - b_r).
\end{aligned}\right\} \quad (2.20)$$

In these formulae a denotes the distance of the aileron hinge axis to the cables in the neutral position.

For a balance tab (fig. 2.4) the lever CD is connected with a fixed point of the wing. This

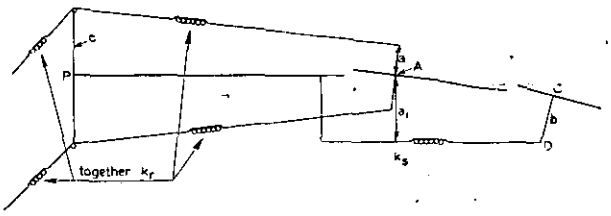

Fig. 2.4 Balance tab.

gives the same moments as if it were connected with the control stick. The total elastic forces are obtained from the superposition of the two following cases:

(1) the system of the servo tab, but b replaced by $-b$, since the cables do not cross each other, a replaced by a_1 and k_r by k_s,

(2) the system of common aileron control, obtained by taking in the spring tab construction $k_0 = k_r$, $k_1 = 0$ and $k_2 = \infty$.

Then it is found:

$$\left.\begin{aligned}
e_{11} &= \frac{d^2}{dy^2}\left(B \frac{d^2}{dy^2}\right), \\
e_{12} &= e_{13} = e_{14} = e_{21} = e_{31} = e_{41} = 0, \\
e_{22} &= -\frac{d}{dy}\left(T_v \frac{d}{dy}\right) + \\
&\quad + (k_s a_1^2 + k_r a^2) \delta (y - b_r), \\
e_{23} &= e_{32} = -\{k_s a_1 (a_1 - b) + k_r a^2\} \delta (y - b_r), \\
e_{24} &= e_{42} = -k_s a_1 b \delta (y - b_r), \\
e_{33} &= -\frac{d}{dy}\left(T_r \frac{d}{dy}\right) + \\
&\quad + \{k_s (a_1 - b)^2 + k_r a^2\} \delta (y - b_r), \\
e_{34} &= e_{43} = k_s (a_1 - b) b \delta (y - b_r), \\
e_{44} &= -\frac{d}{dy}\left(T_s \frac{d}{dy}\right) + k_s b^2 \delta (y - b_r).
\end{aligned}\right\} \quad (2.21)$$

For a rigid connection between wing and tab, i. e. $k_s = \infty$, it follows from the condition that the elastic forces must remain finite that

$$a_1 \gamma_r + b \varepsilon_r = 0. \quad (2.22)$$

When the tab is torsionnally rigid, it is possible to eliminate in flutter calculations the deformation ε.

A trim tab is a device (fig. 2.5) producing a constant angle between aileron and tab. The elastic forces are obtained by superposition of:

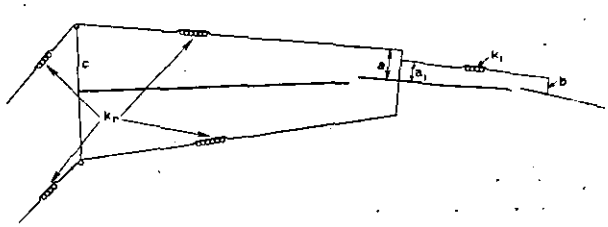

Fig. 2.5 Trim tab

(1) tab control, following from the formulae of the spring tab by taking $k_0 = 0$, $k_2 = \infty$ and $a = a_1$,

(2) aileron control, putting now $k_0 = k_r$, $k_1 = 0$ and $k_2 = \infty$.

In total

$$
\left.
\begin{aligned}
e_{11} &= \frac{d^2}{dy^2}\left(B\,\frac{d^2}{dy^2}\right),\\
e_{12} &= e_{13} = e_{14} = e_{21} = e_{31} = e_{41} = 0,\\
e_{22} &= -\frac{d}{dy}\left(T_v\,\frac{d}{dy}\right) + k_r a^2\,\delta\,(y - b_r),\\
e_{23} &= e_{32} = -k_r a^2\,\delta\,(y - b_r),\\
e_{24} &= e_{42} = 0,\\
e_{33} &= -\frac{d}{dy}\left(T_r\,\frac{d}{dy}\right) + \\
&\qquad + (k_r a^2 + k_1 b^2)\,\delta\,(y - b_r),\\
e_{34} &= -k_1 b^2\,\delta\,(y - b_r),\\
e_{44} &= -\frac{d}{dy}\left(T_s\,\frac{d}{dy}\right) + k_1 b^2\,\delta\,(y - b_r).
\end{aligned}
\right\} \qquad (2.23)
$$

For a rigid connection between aileron and tab, i. e. $k_1 = \infty$, the tab can not perform any oscillation relative to the aileron. If the tab itself is also rigid ($T_s = \infty$), it is again possible to eliminate ε in flutter calculations.

The foregoing holds when the control stick itself does not move. For anti-symmetric vibrations this does not apply. Neglecting the mass of the whole control mechanism including the control stick and also neglecting friction, no forces exist resisting a motion of the stick in phase with that of the ailerons. The result is that no strain arises in the cables leading to the control stick which leads to the following changes in the formulae: $k_0 = 0$ in (2.18) and (2.19); $k_r = 0$ in (2.20), (2.21) and (2.23). For the horizontal tail surfaces the same phenomenon occurs for symmetric vibrations.

3 The aerodynamic forces.

3.1 *General.*

The aerodynamic forces acting on a harmonically oscillating wing-aileron-tab system can be calculated to first approximation — which means that expressions depending to the second or higher degree upon the perturbation of the field of flow are neglected — under the following conditions:

(1) the air is an incompressible and inviscid fluid,

(2) the flow is two-dimensional,

(3) the wing thickness is negligible.

With the aid of these assumptions the aerodynamic forces are evaluated by Küssner (ref. 2 and 3), Cicala (ref. 4), Dietze (ref. 5) and Theodorsen (ref. 6 and 7).

For a finite wing the aerodynamic forces can be approximated by the "strip-theory". According to this theory the forces on an infinitely narrow, chordwise wing strip are identified with the forces, acting on it if the flow were two-dimensional. This signifies the complete neglect of the consequences of variations in strength of the spanwise vortices. It is indeed possible to take into account the influence of vortices parallel to the chord, but the theories in question are not fully satisfying and give rise to serious extensions of the computation. It is thought that at the moment the profits do not balance these objections. Hence, no such treatment has been given in this paper.

3.2 *Open and sealed gap.*

A special difficulty arises from the neglect of the wing thickness when the aileron is aerodynamically balanced. In this case a deflection of the aileron causes an airflow through the opening between wing and aileron. This flow, however, exists in reality only for an aileron, which has a vertical displacement in regard to the wing (as in the case of some Junkers constructions). Usually, the wing thickness prevents the flow through the opening almost entirely.

This choke-effect cannot be adequately represented in the mathematical theory. Therefore the assumption must be made that the flow through the gap ($C'C$ in fig. 2.1 and 3.1) is either completely unimpeded or completely barred, while in addition only the limiting case of a vanishing gap width (i. e. in the limit the point C' coincides with the aileron leading edge C) is considered. In the case of the free flow (fig. 3.1a), the simplified system,

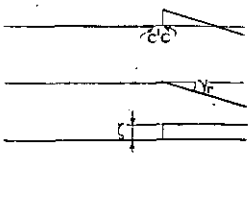

Fig. 3.1*a* Free flow through the gap.

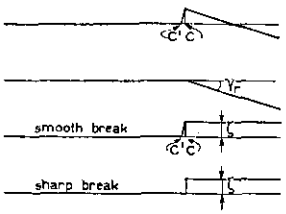

Fig. 3.1*b* No flow through the gap.

determining the pressure distribution and hence the forces and moments acting on the system, consists of one flat plate with a discontinuity at the point C. Only at the trailing edge of the whole system the condition of smooth flow has to be fulfilled (ref. 3).

The gap can be sealed by stretching a flat plate from the trailing edge of the aerofoil to the leading edge of the aileron. Accordingly this plate is placed under a very large angle of incidence (cf. fig. 3.1b, smooth break). The transition of vanishing gap width (fig. 3.1b, sharp break) involves no difficulties except in the expression for the aileron force, where a term $\log_e C'C$ appears, which tends to infinity for vanishing gap. Indeed, the theory is only valid for small angles of incidence and the transgression of this condition brings about the logarithmic singularity. To keep the aileron force finite, a certain gap width must be retained in the corresponding term (in all other terms the gap width is neglected). The fixing of this value will be discussed in section 34.

For an aerodynamically balanced tab the same question arises, but there being introduced no new aspects, this point can be left aside.

3.3 *The formulae for the aerodynamic forces and moments.*

Continuing the work of ref. 8 and 9 (cf. equation (269) of ref. 8) it is possible to write for the forces and moments, provided that the motion is harmonic and restricted to small amplitudes

$$\left.\begin{aligned}
K &= m_L v^2\ (k_z z_v + k_\varphi \varphi c + k_\zeta \zeta + k_\gamma \gamma_r c + \\
&\quad + k_\chi \chi + k_\varepsilon \varepsilon_r c),\\
M &= m_L v^2 c\ (m_z z_v + m_\varphi \varphi c + m_\zeta \zeta + \\
&\quad + m_\gamma \gamma_r c + m_\chi \chi + m_\varepsilon \varepsilon_r c),\\
R &= m_L v^2\ (r_z z_v + r_\varphi \varphi c + r_\zeta \zeta + r_\gamma \gamma_r c + \\
&\quad + r_\chi \chi + r_\varepsilon \varepsilon_r c),\\
N &= m_L v^2 c\ (n_z z_v + n_\varphi \varphi c + n_\zeta \zeta + n_\gamma \gamma_r c + \\
&\quad + n_\chi \chi + n_\varepsilon \varepsilon_r c),\\
P &= m_L v^2\ (p_z z_v + p_\varphi \varphi c + p_\zeta \zeta + p_\gamma \gamma_r c + \\
&\quad + p_\chi \chi + p_\varepsilon \varepsilon_r c),\\
Q &= m_L v^2 c\ (q_z z_v + q_\varphi \varphi c + q_\zeta \zeta + q_\gamma \gamma_r c + \\
&\quad + q_\chi \chi + q_\varepsilon \varepsilon_r c),
\end{aligned}\right\} \qquad (3.1)$$

with m_L given by eq. (2.10). The other symbols are explained in section 5.

Between the displacements z_v and z exists the simple relation

$$z = z_v + c_p \varphi \qquad (3.2)$$

The dimensionless coefficients $k_z \ldots q_\varepsilon$ are functions of the reduced velocity $V \left(= \frac{v}{vc}\right)$. They depend also on η and η', indicating resp. the ratios of aileron + tab chord to total chord and of the tab chord to the total chord. They are connected with the coefficients $k_a \ldots q_f$ used in ref. 3 by the following relations:

$$\left.\begin{aligned}
k_z &= -4V^2 k_a, \quad k_\varphi = 2V^2 k_b,\\
k_\zeta &= -4V^2 k_d, \quad k_\gamma = 2V^2 k_c,\\
k_\chi &= -4V^2 k_f, \quad k_\varepsilon = 2V^2 k_e,\\
m_z &= 2V^2 m_a, \quad m_\varphi = -V^2 m_b,\\
m_\zeta &= 2V^2 m_d, \quad m_\gamma = -V^2 m_c,\\
m_\chi &= 2V^2 m_f, \quad m_\varepsilon = -V^2 m_e,\\
r_z &= -4V^2 r_a, \quad r_\varphi = 2V^2 r_b,\\
r_\zeta &= -4V^2 r_d, \quad r_\gamma = 2V^2 r_c,\\
r_\chi &= -4V^2 r_f, \quad r_\varepsilon = 2V^2 r_e,\\
n_z &= 2V^2 n_a, \quad n_\varphi = -V^2 n_b,\\
n_\zeta &= 2V^2 n_d, \quad n_\gamma = -V^2 n_c,\\
n_\chi &= 2V^2 n_f, \quad n_\varepsilon = -V^2 n_e,\\
p_z &= -4V^2 p_a, \quad p_\varphi = 2V^2 p_b,\\
p_\zeta &= -4V^2 p_d, \quad p_\gamma = 2V^2 p_c,\\
p_\chi &= -4V^2 p_f, \quad p_\varepsilon = 2V^2 p_e,\\
q_z &= 2V^2 q_a, \quad q_\varphi = -V^2 q_b,\\
q_\zeta &= 2V^2 q_d, \quad q_\gamma = -V^2 q_c,\\
q_\chi &= 2V^2 q_f, \quad q_\varepsilon = -V^2 q_e.
\end{aligned}\right\} \qquad (3.3)$$

$k_z \ldots q_\varepsilon$ are obtained as functions of V, η and η' by substituting the values for $k_a \ldots q_f$, given in ref. 3 in the equations (3.3) and at the same time replacing $\frac{i}{2\omega}$ by V and $1 + T$ by $2P$. The two cases of open and sealed gap between wing and aileron or between aileron and tab have to be distinguished throughout. The open gap is denoted by the addition + and the sealed gap by —. With corresponding suffix ζ it refers to the gap between wing and aileron and with suffix χ to the gap between aileron and tab. It may happen, of course, that one gap has to be considered as open and the other as sealed.

The relations obtained are:

$$\left.\begin{aligned}
k_z &= 1 - 4iPV\\
k_\varphi &= -{}^1/_4 + 4PV^2 + 4iPV \,.\, {}^1/_2\\
\pi k_\zeta^+(\eta) &= \Phi_3(\eta) - 4iPV \,.\, \Phi_1(\eta)\\
\pi k_\zeta^-(\eta) &= \Phi_3(\eta) - 4PV^2 \,.\, 2\Phi_{13}(\eta) -\\
&\quad - 4iPV \,.\, \Phi_1(\eta) - iV \,.\, 2\Phi_{14}(\eta)\\
\pi k_\gamma(\eta) &= -{}^1/_4 \Phi_4(\eta) + 4PV^2 \,.\, \Phi_1(\eta) +\\
&\quad + 4iPV \,.\, {}^1/_4 \Phi_2(\eta) + iV \,.\, \Phi_3(\eta)\\
\pi k_\chi^+(\eta') &= \Phi_3(\eta') - 4iPV \,.\, \Phi_1(\eta')\\
\pi k_\chi^-(\eta') &= \Phi_3(\eta') - 4PV^2 \,.\, 2\Phi_{13}(\eta') -\\
&\quad - 4iPV \,.\, \Phi_1(\eta') - iV \,.\, 2\Phi_{14}(\eta')\\
\pi k_\varepsilon(\eta') &= -{}^1/_4 \Phi_4(\eta') + 4PV^2 \,.\, \Phi_1(\eta') +\\
&\quad + 4iPV \,.\, {}^1/_4 \Phi_2(\eta') + iV \,.\, \Phi_3(\eta')\\
m_z &= -{}^1/_4\\
m_\varphi &= {}^3/_{32} - iV \,.\, {}^1/_2\\
\pi m_\zeta^+(\eta) &= -{}^1/_8 \Phi_6(\eta) + iV \,.\, \Phi_5(\eta)\\
\pi m_\zeta^-(\eta) &= -{}^1/_8 \Phi_6(\eta) + V^2 \,.\, 2\Phi_{15}(\eta) +\\
&\quad + iV \,.\, 2\Phi_5(\eta)\\
\pi m_\gamma(\eta) &= {}^1/_{16} \Phi_7(\eta) - V^2 \,.\, \Phi_5(\eta) -\\
&\quad - iV \,.\, {}^1/_4 \Phi_6(\eta)\\
\pi m_\chi^+(\eta') &= -{}^1/_8 \Phi_6(\eta') + iV \,.\, \Phi_5(\eta')\\
\pi m_\chi^-(\eta') &= -{}^1/_8 \Phi_6(\eta') + V^2 \,.\, 2\Phi_{15}(\eta') +\\
&\quad + iV \,.\, 2\Phi_5(\eta')\\
\pi m_\varepsilon(\eta') &= {}^1/_{16} \Phi_7(\eta') - V^2 \,.\, \Phi_5(\eta') -\\
&\quad - iV \,.\, {}^1/_4 \Phi_6(\eta')\\
\pi r_z(\eta) &= \Phi_3(\eta) - 4iPV \,.\, \Phi_{31}(\eta)\\
\pi r_\varphi(\eta) &= -{}^1/_8 \Phi_6(\eta) + 4PV^2 \Phi_{31}(\eta) +\\
&\quad + 4iPV \,.\, {}^1/_2 \Phi_{31}(\eta) + iV \,.\, \Phi_{32}(\eta)\\
\pi^2 r_\zeta^+(\eta) &= \Phi_{17}(\eta) - 4iPV \,.\, \Phi_1(\eta)\, \Phi_{31}(\eta) -\\
&\quad - iV \,.\, 2\Phi_{35}(\eta)\\
\pi^2 r_\zeta^-(\eta) &= \Phi_{17}(\eta) -\\
&\quad - 4PV^2 \,.\, 2\Phi_{13}(\eta)\, \Phi_{31}(\eta) -\\
&\quad - 4iPV\, \Phi_1(\eta)\, \Phi_{31}(\eta) -\\
&\quad - V^2 \{ 4\Phi_{21}(\eta) + 8 \log_e \eta_s \} -\\
&\quad - iV \,.\, 2\Phi_{16}(\eta)\\
\pi^2 r_\gamma(\eta) &= -{}^1/_4 \Phi_{37}(\eta) +\\
&\quad 4PV^2 \,.\, \Phi_1(\eta)\, \Phi_{31}(\eta) +\\
&\quad 4iPV \,.\, {}^1/_4 \Phi_2(\eta)\, \Phi_{31}(\eta) +\\
&\quad + V^2 \,.\, 2\Phi_{35}(\eta) + iV \,.\, \Phi_{36}(\eta)\\
\pi^2 r_\chi^+(\eta, \eta') &= X_{14}(\eta', \eta) -\\
&\quad - 4iPV \,.\, X_1(\eta', \eta) - iV \,.\, 2X_3(\eta', \eta)\\
\pi^2 r_\chi^-(\eta, \eta') &= X_{14}(\eta', \eta) -\\
&\quad - 4PV^2 \,.\, 2X_{11}(\eta', \eta) -\\
&\quad - 4iPV \,.\, X_1(\eta', \eta) -\\
&\quad - V^2 \,.\, 4X_{12}(\eta', \eta) - iV \,.\, 2X_{13}(\eta', \eta)
\end{aligned}\right\} \qquad (3.4)$$

$$
\begin{aligned}
&\pi^2 r_\varepsilon(\eta,\eta') = -\tfrac{1}{2} X_5(\eta',\eta) + \\
&\quad + 4PV^2 . X_1(\eta',\eta) + \\
&\quad + 4iPV . \tfrac{1}{2} X_2(\eta',\eta) + \\
&\quad + V^2 . 2X_3(\eta',\eta) + \\
&\quad + iV . X_4(\eta',\eta) \\
&\pi n_z(\eta) = -\tfrac{1}{4}\Phi_4(\eta) + 4iPV . \tfrac{1}{4}\Phi_8(\eta) \\
&\pi n_\varphi(\eta) = \tfrac{1}{16}\Phi_7(\eta) - 4PV^2 . \tfrac{1}{4}\Phi_8(\eta) - \\
&\quad - 4iPV . \tfrac{1}{8}\Phi_8(\eta) - iV . \tfrac{1}{4}\Phi_9(\eta) \\
&\pi^2 n_\zeta{}^+(\eta) = -\tfrac{1}{4}\Phi_{37}(\eta) + \\
&\quad + 4iPV . \tfrac{1}{4}\Phi_1(\eta)\Phi_8(\eta) + \\
&\quad + iV . \Phi_{10}(\eta) \\
&\pi^2 n_\zeta{}^-(\eta) = -\tfrac{1}{4}\Phi_{37}(\eta) + \\
&\quad + 4PV^2 . \tfrac{1}{2}\Phi_8(\eta)\Phi_{13}(\eta) + \\
&\quad + 4iPV . \tfrac{1}{4}\Phi_1(\eta)\Phi_8(\eta) + \\
&\quad + V^2 . 2\Phi_{18}(\eta) + iV . \Phi_{19}(\eta) \\
&\pi^2 n_\gamma(\eta) = \tfrac{1}{16}\Phi_{12}(\eta) - \\
&\quad - 4PV^2 . \tfrac{1}{4}\Phi_1(\eta)\Phi_8(\eta) - \\
&\quad - 4iPV . \tfrac{1}{16}\Phi_2(\eta)\Phi_8(\eta) - \\
&\quad - V^2 . \Phi_{10}(\eta) - iV . \tfrac{1}{4}\Phi_{11}(\eta) \\
&\pi^2 n_\chi{}^+(\eta,\eta') = -\tfrac{1}{2} X_{18}(\eta',\eta) + \\
&\quad + 4iPV . \tfrac{1}{2} X_6(\eta',\eta) + iV . X_8(\eta',\eta) \\
&\pi^2 n_\chi{}^-(\eta,\eta') = -\tfrac{1}{2} X_{18}(\eta',\eta) + \\
&\quad + 4PV^2 . X_{15}(\eta',\eta) + \\
&\quad + 4iPV . \tfrac{1}{2} X_6(\eta',\eta) + \\
&\quad + V^2 . 2X_{16}(\eta',\eta) + iV . X_{17}(\eta',\eta) \\
&\pi^2 n(\eta,\eta') = \tfrac{1}{4} . X_{10}(\eta',\eta) - \\
&\quad - 4PV^2 . \tfrac{1}{2} X_6(\eta',\eta) - \\
&\quad - 4iPV . \tfrac{1}{4} X_7(\eta',\eta) - \\
&\quad - V^2 . X_8(\eta',\eta) - iV . \tfrac{1}{2} X_9(\eta',\eta) \\
&\pi p_z(\eta') = \Phi_3(\eta') - 4iPV . \Phi_{31}(\eta') \\
&\pi p_\varphi(\eta') = -\tfrac{1}{8}\Phi_6(\eta') + 4PV^2 . \Phi_{31}(\eta') + \\
&\quad + 4iPV . \tfrac{1}{2}\Phi_{31}(\eta') + iV . \Phi_{32}(\eta') \\
&\pi^2 p_\zeta{}^+(\eta,\eta') = X_{14}(\eta,\eta') - \\
&\quad - 4iPV . X_1(\eta,\eta') - iV . 2X_3(\eta,\eta') \\
&\pi^2 p_\zeta{}^-(\eta,\eta') = X_{14}(\eta,\eta') - \\
&\quad - 4PV^2 . 2X_{11}(\eta,\eta') - \\
&\quad - 4iPV . X_1(\eta,\eta') - V^2 . 4X_{12}(\eta,\eta') - \\
&\quad - iV . 2X_{13}(\eta,\eta') \\
&\pi^2 p_\gamma(\eta,\eta') = -\tfrac{1}{2} X_5(\eta,\eta') + \\
&\quad + 4PV^2 . X_1(\eta,\eta') + \\
&\quad + 4iPV . \tfrac{1}{2} X_2(\eta,\eta') + \\
&\quad + V^2 . 2X_3(\eta,\eta') + iV . X_4(\eta,\eta') \\
&\pi^2 p_\chi{}^+(\eta') = \Phi_{17}(\eta') - \\
&\quad - 4iPV . \Phi_1(\eta')\Phi_{31}(\eta') - iV . 2\Phi_{35}(\eta') \\
&\pi^2 p_\chi{}^-(\eta') = \Phi_{17}(\eta') - \\
&\quad - 4PV^2 . 2\Phi_{13}(\eta')\Phi_{31}(\eta') - \\
&\quad - 4iPV . \Phi_1(\eta')\Phi_{31}(\eta') - \\
&\quad - V^2\{4\Phi_{21}(\eta') + 8\log_e \eta'_s\} - \\
&\quad - iV . 2\Phi_{16}(\eta') \\
&\pi^2 p_\varepsilon(\eta') = -\tfrac{1}{4}\Phi_{37}(\eta') + \\
&\quad + 4PV^2 . \Phi_1(\eta')\Phi_{31}(\eta') + \\
&\quad + 4iPV . \tfrac{1}{4}\Phi_2(\eta')\Phi_{31}(\eta') + \\
&\quad + V^2 . 2\Phi_{35}(\eta') + iV . \Phi_{36}(\eta') \\
&\pi q_z(\eta') = -\tfrac{1}{4}\Phi_4(\eta') + 4iPV . \tfrac{1}{4}\Phi_8(\eta') \\
&\pi q_\varphi(\eta') = \tfrac{1}{16}\Phi_7(\eta') - \\
&\quad - 4PV^2 . \tfrac{1}{4}\Phi_8(\eta') - 4iPV . \tfrac{1}{8}\Phi_8(\eta') - \\
&\quad - iV . \tfrac{1}{4}\Phi_9(\eta') \\
&\pi^2 q_\zeta{}^+(\eta,\eta') = -\tfrac{1}{2} X_{18}(\eta,\eta') + \\
&\quad + 4iPV . \tfrac{1}{2} X_6(\eta,\eta') + iV . X_8(\eta,\eta') \\
&\pi^2 q_\zeta{}^-(\eta,\eta') = -\tfrac{1}{2} X_{18}(\eta,\eta') + \\
&\quad + 4PV^2 . X_{15}(\eta,\eta') + \\
&\quad + 4iPV . \tfrac{1}{2} X_6(\eta,\eta') + \\
&\quad + V^2 . 2X_{16}(\eta,\eta') + \\
&\quad + iV . X_{17}(\eta,\eta') \\
&\pi^2 q_\gamma(\eta,\eta') = \tfrac{1}{4} X_{10}(\eta,\eta') - \\
&\quad - 4PV^2 . \tfrac{1}{2} X_6(\eta,\eta') - \\
&\quad - 4iPV . \tfrac{1}{4} X_7(\eta,\eta') - \\
&\quad - V^2 . X_8(\eta,\eta') - iV . \tfrac{1}{2} X_9(\eta,\eta') \\
&\pi^2 q_\chi{}^+(\eta') = -\tfrac{1}{4}\Phi_{37}(\eta') + \\
&\quad + 4iPV . \tfrac{1}{4}\Phi_1(\eta')\Phi_8(\eta') + \\
&\quad + iV . \Phi_{10}(\eta') \\
&\pi^2 q_\chi{}^-(\eta') = -\tfrac{1}{4}\Phi_{37}(\eta') + \\
&\quad + 4PV^2 . \tfrac{1}{2}\Phi_8(\eta')\Phi_{13}(\eta') + \\
&\quad + 4iPV . \tfrac{1}{4}\Phi_1(\eta')\Phi_8(\eta') + \\
&\quad + V^2 . 2\Phi_{18}(\eta') + iV . \Phi_{19}(\eta') \\
&\pi^2 q_\varepsilon(\eta') = \tfrac{1}{16}\Phi_{12}(\eta') - \\
&\quad - 4PV^2 . \tfrac{1}{4}\Phi_1(\eta')\Phi_8(\eta') - \\
&\quad - 4iPV . \tfrac{1}{16}\Phi_2(\eta')\Phi_8(\eta') - \\
&\quad - V^2 . 2\Phi_{10}(\eta') - iV . \tfrac{1}{4}\Phi_{11}(\eta')
\end{aligned}
\qquad (3.4)
$$

η_s and η_s' denote the values, assigned to the gap width (wing-aileron, resp. aileron-tab) in the divergent logarithmic terms, divided by the total chord $\left(\text{cf. fig. 2.1 } \frac{CC'}{c} \text{ resp. } \frac{EE'}{c}\right)$.

3.4 *The aerodynamic coefficients* a_{ik}.

The aerodynamic forces and moments $K_L \dots Q_L$ appearing in the formulae (2.5) are given by

$$
\begin{aligned}
K_L &= K, \\
M_L &= M - c_v K - N - c_{dr} R, \\
N_L &= N + c_{dr} R - Q - c_{es} P, \\
Q_L &= Q + c_{es} P.
\end{aligned}
\qquad (3.5)
$$

Since in the formulae (2.5) the displacements z, φ, γ and ε are used, it is desirable to express the aerodynamic forces by the same displacements. This can be done by substituting for γ_r and ε_r the values given by (2.1) and (2.2) and by eliminating ζ and χ with the aid of the equations (2.3). The result can be brought in the form:

$$
\begin{aligned}
K_L &= m_L \nu^2 (a_{11} z + a_{12} c\varphi + a_{13} c\gamma + a_{14} c\varepsilon), \\
M_L &= m_L \nu^2 (a_{21} cz + a_{22} c^2\varphi + a_{23} c^2\gamma + a_{24} c^2\varepsilon), \\
N_L &= m_L \nu^2 (a_{31} cz + a_{32} c^2\varphi + a_{33} c^2\gamma + a_{34} c^2\varepsilon), \\
Q_L &= m_L \nu^2 (a_{41} cz + a_{42} c^2\varphi + a_{43} c^2\gamma + a_{44} c^2\varepsilon), \\
&\text{or} \quad \mathbf{A} = \nu^2 \mathbf{a} \mathbf{f},
\end{aligned}
\qquad (3.6)
$$

where $\mathbf{A}$ and $\mathbf{f}$ are given by (2.7), while $\mathbf{a}$ is equal to

$$\mathbf{a} = m_L \begin{Vmatrix} a_{11} & a_{12}c & a_{13}c & a_{14}c \\ a_{21}c & a_{22}c^2 & a_{23}c^2 & a_{24}c^2 \\ a_{31}c & a_{32}c^2 & a_{33}c^2 & a_{34}c^2 \\ a_{41}c & a_{42}c^2 & a_{43}c^2 & a_{44}c^2 \end{Vmatrix} \qquad (3.7)$$

After some calculations the following expressions are obtained for the coefficients a_{ik}.

$$\left.\begin{aligned}
a_{11} &= k_z, \\
a_{12} &= k_\varphi - c'_v k_z - k_\gamma - c'_{dr} k_\zeta, \\
a_{13} &= k_\gamma + c'_{dr} k_\zeta - k_\varepsilon - c'_{es} k_\chi, \\
a_{14} &= k_\varepsilon + c'_{es} k_\chi, \\
a_{21} &= m_z - c'_v k_z - n_z - c'_{dr} r_z, \\
a_{22} &= (m_\varphi - c'_v k_\varphi - n_\varphi - c'_{dr} r_\varphi) - \\
&\quad - c'_v (m_z - c'_v k_z - n_z - c'_{dr} r_z) - \\
&\quad - (m_\gamma - c'_v k_\gamma - n_\gamma - c'_{dr} r_\gamma) - \\
&\quad - c'_{dr} (m_\zeta - c'_v k_\zeta - n_\zeta - c'_{dr} r_\zeta), \\
a_{23} &= (m_\gamma - c'_v k_\gamma - n_\gamma - c'_{dr} r_\gamma) + \\
&\quad + c'_{dr} (m_\zeta - c'_v k_\zeta - n_\zeta - c'_{dr} r_\zeta) - \\
&\quad - (m_\varepsilon - c'_v k_\varepsilon - n_\varepsilon - c'_{dr} r_\varepsilon) - \\
&\quad - c'_{es} (m_\chi - c'_v k_\chi - n_\chi - c'_{dr} r_\chi), \\
a_{24} &= (m_\varepsilon - c'_v k_\varepsilon - n_\varepsilon - c'_{dr} r_\varepsilon) + \\
&\quad + c'_{es} (m_\chi - c'_v k_\chi - n_\chi - c'_{dr} r_\chi), \\
a_{31} &= n_z + c'_{dr} r_z - q_z - c'_{es} p_z, \\
a_{32} &= (n_\varphi + c'_{dr} r_\varphi - q_\varphi - c'_{es} p_\varphi) - \\
&\quad - c'_v (n_z + c'_{dr} r_z - q_z - c'_{es} p_z) - \\
&\quad - (n_\gamma + c'_{dr} r_\gamma - q_\gamma - c'_{es} p_\gamma) - \\
&\quad - c'_{dr} (n_\zeta + c'_{dr} r_\zeta - q_\zeta - c'_{es} p_\zeta), \\
a_{33} &= (n_\gamma + c'_{dr} r_\gamma - q_\gamma - c'_{es} p_\gamma) + \\
&\quad + c'_{dr} (n_\zeta + c'_{dr} r_\zeta - q_\zeta - c'_{es} p_\zeta) - \\
&\quad - (n_\varepsilon + c'_{dr} r_\varepsilon - q_\varepsilon - c'_{es} p_\varepsilon) - \\
&\quad - c'_{es} (n_\chi + c'_{dr} r_\chi - q_\chi - c'_{es} p_\chi), \\
a_{34} &= (n_\varepsilon + c'_{dr} r_\varepsilon - q_\varepsilon - c'_{es} p_\varepsilon) + \\
&\quad + c'_{es} (n_\chi + c'_{dr} r_\chi - q_\chi - c'_{es} p_\chi), \\
a_{41} &= q_z + c'_{es} p_z, \\
a_{42} &= (q_\varphi + c'_{es} p_\varphi) - c'_v (q_z + c'_{es} p_z) - \\
&\quad - (q_\gamma + c'_{es} p_\gamma) - c'_{dr} (q_\zeta + c'_{es} p_\zeta), \\
a_{43} &= (q_\gamma + c'_{es} p_\gamma) + c'_{dr} (q_\zeta + c'_{es} p_\zeta) - \\
&\quad - (q_\varepsilon + c'_{es} p_\varepsilon) - c'_{es} (q_\chi + c'_{es} p_\chi), \\
a_{44} &= (q_\varepsilon + c'_{es} p_\varepsilon) + c'_{es} (q_\chi + c'_{es} p_\chi),
\end{aligned}\right\} \qquad (3.8)$$

$$\text{with} \quad c'_v = \frac{c_v}{c}, \quad c'_{dr} = \frac{c_{dr}}{c}, \quad c'_{es} = \frac{c_{es}}{c}. \qquad (3.9)$$

When the expressions (3.4) are substituted in the formulae (3.8), the coefficients a_{ik} are obtained explicitly as functions of V, η and η'. It is easily seen that every coefficient assumes the form

$$a_{ik} = \alpha_{ik}^{(0)} + \alpha_{ik}^{(1)} 4\,iPV + \alpha_{ik}^{(2)} 4\,PV^2 + \\ + \alpha_{ik}^{(3)} V^2 + \alpha_{ik}^{(4)} iV \qquad (3.10)$$

where the a_{ik} appear in table 2.1, which contains the complete result.

Instead of the functions Φ and X used in formulae (3.4), new functions R and T have been introduced. Some of these are, like the a_{ik} and like $k_z \ldots q_\chi$, different for open and sealed gap. They are again distinguished by the signs +, resp. —. For the R-functions this sign is determined by the argument of the function, i. e. when the argument is η, the gap between wing and aileron fixes the sign and when the argument is η', the sign is given by the gap between aileron and tab. For the T-functions the sign is always determined by the first-mentioned variable. If, for instance, the gap between wing and aileron is sealed, but that between aileron and tab is open, the calculation should be performed with

$$R_i^-(\eta), \quad R_i^+(\eta'), \quad T_i^-(\eta, \eta') \quad \text{and} \quad T_i^+(\eta', \eta).$$

The functions R and T are derived from Φ and X as follows:

$$\left.\begin{aligned}
R_1 &= 1 - \frac{\Phi_1}{\pi} \\
R_2 &= {}^1\!/_2 - \frac{\Phi_2}{4\pi} \\
R_3 &= 1 - \frac{\Phi_3}{\pi} \\
R_4^+ &= 0 \\
R_4^- &= \frac{2\,\Phi_{13}}{\pi} \\
R_6^+ &= 0 \\
R_6^- &= \frac{2\,\Phi_{14}}{\pi} \\
R_7 &= \frac{\Phi_1}{\pi} \\
R_8 &= \frac{\Phi_2}{4\pi} \\
R_9 &= \frac{\Phi_3}{\pi} \\
R_{10} &= \frac{\Phi_8}{4\pi} \\
R_{11} &= \frac{\Phi_{31}}{\pi} \\
R_{12} &= \frac{\Phi_8}{4\pi} - \frac{\Phi_1 \Phi_8}{4\pi^2} \\
R_{13} &= \frac{\Phi_8}{8\pi} - \frac{\Phi_2 \Phi_8}{16\pi^2} \\
R_{14} &= \frac{\Phi_5}{\pi} - \frac{\Phi_{10}}{\pi^2} \\
R_{15} &= \frac{\Phi_9}{4\pi} + \frac{\Phi_6}{4\pi} - \frac{1}{2} - \frac{\Phi_{11}}{4\pi^2} \\
R_{16} &= \frac{1}{2} - \frac{\Phi_8}{4\pi} - \frac{\Phi_2}{4\pi} \\
R_{17}^+ &= \frac{\Phi_{31}}{\pi} - \frac{\Phi_1 \Phi_{31}}{\pi^2} \\
R_{17}^- &= \frac{\Phi_{31}}{\pi} - \frac{\Phi_1 \Phi_{31}}{\pi^2} - \frac{\Phi_8 \Phi_{13}}{2\pi^2} \\
R_{18}^+ &= \frac{\Phi_{31}}{2\pi} - \frac{\Phi_2 \Phi_{31}}{4\pi^2} - \frac{\Phi_1 \Phi_8}{4\pi^2} \\
R_{18}^- &= R_{18}^+ \\
R_{19}^+ &= -\frac{2\,\Phi_{35}}{\pi^2} \\
R_{19}^- &= \frac{2\,\Phi_{15}}{\pi} - \frac{2\,\Phi_{18}}{\pi^2} - \frac{2\,\Phi_{35}}{\pi^2}
\end{aligned}\right\} \qquad (3.11)$$

$$
\begin{aligned}
R_{20}{}^{+} &= \frac{\Phi_{32}}{\pi} - \frac{\Phi_{36}}{\pi^2} + \frac{\Phi_5}{\pi} - \frac{\Phi_{10}}{\pi^2} \\
R_{20}{}^{-} &= \frac{\Phi_{32}}{\pi} - \frac{\Phi_{36}}{\pi^2} + \frac{2\,\Phi_5}{\pi} - \frac{\Phi_{19}}{\pi^2} \\
R_{21}{}^{+} &= \frac{\Phi_{31}}{\pi} + \frac{\Phi_1}{\pi} \\
R_{21}{}^{-} &= R_{21}{}^{+} \\
R_{22}{}^{+} &= \frac{\Phi_1 \Phi_{31}}{\pi^2} \\
R_{22}{}^{-} &= R_{22}{}^{+} \\
R_{23}{}^{+} &= 0 \\
R_{23}{}^{-} &= \frac{2\,\Phi_{13}\Phi_{31}}{\pi^2} \\
R_{24}{}^{+} &= 0 \\
R_{24}{}^{-} &= \frac{4\,\Phi_{21}}{\pi^2} + \frac{8 \log_e \eta_8}{\pi^2} \\
R_{25}{}^{+} &= \frac{2\,\Phi_{35}}{\pi^2} \\
R_{25}{}^{-} &= \frac{2\,\Phi_{16}}{\pi^2} \\
R_{26} &= \frac{\Phi_1 \Phi_8}{4\,\pi^2} \\
R_{27} &= \frac{\Phi_2 \Phi_8}{16\,\pi^2} \\
R_{28} &= \frac{\Phi_{11}}{4\,\pi^2} - \frac{\Phi_6}{4\,\pi} \\
R_{29}{}^{+} &= \frac{\Phi_1 \Phi_{31}}{\pi^2} \\
R_{29}{}^{-} &= \frac{\Phi_1 \Phi_{31}}{\pi^2} + \frac{\Phi_8 \Phi_{13}}{2\,\pi^2} \\
R_{30}{}^{+} &= \frac{\Phi_2 \Phi_{31}}{4\,\pi^2} + \frac{\Phi_1 \Phi_8}{4\,\pi^2} \\
R_{30}{}^{-} &= R_{30}{}^{+} \\
R_{32}{}^{+} &= \frac{\Phi_{36}}{\pi^2} - \frac{\Phi_5}{\pi} + \frac{\Phi_{10}}{\pi^2} \\
R_{32}{}^{-} &= \frac{\Phi_{36}}{\pi^2} - \frac{2\,\Phi_5}{\pi} + \frac{\Phi_{19}}{\pi^2} \\
R_{33} &= \frac{\Phi_{10}}{\pi^2} \\
R_{34} &= \frac{\Phi_{11}}{4\,\pi^2} - \frac{\Phi_9}{4\,\pi} \\
R_{35}{}^{+} &= \frac{2\,\Phi_{35}}{\pi^2} \\
R_{35}{}^{-} &= \frac{2\,\Phi_{18}}{\pi^2} + \frac{2\,\Phi_{35}}{\pi^2} \\
R_{36}{}^{+} &= \frac{\Phi_{32}}{\pi} - \frac{\Phi_{36}}{\pi^2} - \frac{\Phi_{10}}{\pi^2} \\
R_{36}{}^{-} &= \frac{\Phi_{32}}{\pi} - \frac{\Phi_{36}}{\pi^2} - \frac{\Phi_{19}}{\pi^2} \\
R_{37}{}^{+} &= \frac{\Phi_{10}}{\pi^2} + \frac{\Phi_{36}}{\pi^2} \\
R_{37}{}^{-} &= \frac{\Phi_{19}}{\pi^2} + \frac{\Phi_{36}}{\pi^2} \\
R_{38} &= \frac{\Phi_{11}}{4\,\pi^2} \\
R_{39} &= \frac{1}{4} - \frac{\Phi_4}{4\,\pi} \\
R_{40} &= \frac{\Phi_4}{4\,\pi} \\
R_{41} &= \frac{3}{32} - \frac{\Phi_7}{8\,\pi} + \frac{\Phi_{12}}{16\,\pi^2} \\
R_{42} &= \frac{\Phi_6}{4\,\pi} - \frac{\Phi_{37}}{2\,\pi^2} \\
R_{43} &= \frac{\Phi_{17}}{\pi^2} \\
R_{44} &= \frac{\Phi_7}{16\,\pi} - \frac{\Phi_{12}}{16\,\pi^2} \\
R_{45} &= \frac{\Phi_{37}}{2\,\pi^2} - \frac{\Phi_6}{8\,\pi} \\
R_{46} &= \frac{\Phi_{12}}{16\,\pi^2} \\
R_{47} &= \frac{\Phi_{37}}{2\,\pi^2}
\end{aligned}
\qquad (3.11)
$$

$$
\begin{aligned}
T_1 \quad (\eta, \eta') &= \frac{2}{\pi^2} X_3 (\eta, \eta') \\
T_2 \quad (\eta, \eta') &= \frac{1}{\pi^2} X_4 (\eta, \eta') \\
T_3 \quad (\eta, \eta') &= \frac{1}{2\,\pi^2} X_5 (\eta, \eta') = \\
&= \frac{1}{2\,\pi^2} X_{18} (\eta', \eta) \\
T_4 \quad (\eta, \eta') &= \frac{1}{\pi^2} X_8 (\eta, \eta') \\
T_5 \quad (\eta, \eta') &= \frac{1}{2\,\pi^2} X_9 (\eta, \eta') \\
T_6 \quad (\eta, \eta') &= \frac{1}{4\,\pi^2} X_{10} (\eta, \eta') = T_6 (\eta', \eta) \\
T_7{}^{+} (\eta, \eta') &= 0 \\
T_7{}^{-} (\eta, \eta') &= \frac{4}{\pi^2} X_{12} (\eta, \eta') \\
T_8{}^{+} (\eta, \eta') &= T_1 (\eta, \eta') \\
T_8{}^{-} (\eta, \eta') &= \frac{2}{\pi^2} X_{13} (\eta, \eta') \\
T_9 \quad (\eta, \eta') &= \frac{1}{\pi^2} X_{14} (\eta, \eta') = T_9 (\eta', \eta) \\
T_{10}{}^{+} (\eta, \eta') &= 0 \\
T_{10}{}^{-} (\eta, \eta') &= \frac{2}{\pi^2} X_{16} (\eta, \eta') \\
T_{11}{}^{+} (\eta, \eta') &= T_4 (\eta, \eta') \\
T_{11}{}^{-} (\eta, \eta') &= \frac{1}{\pi^2} X_{17} (\eta, \eta')
\end{aligned}
\qquad (3.11)
$$

The R and T functions have been tabulated in tables 3.1 and 3.2. Only T_6 and T_9 are symmetric in the two variables η and η'.

Special attention has to be drawn to the fact, that not all R_i functions are equal to zero when $\eta = 0$. Some even become infinite, but these are, according to the a_{ik}-table, multiplied with c_{dr}. Since c_{dr} vanishes for $\eta \to 0$ they give products $0.\infty$, to which the value 0 must be credited. For those T-functions tending to infinity for $\eta_s \to 0$,

the same holds. The functions R_1, R_2, R_3, R_{15}, R_{16}, R_{39} and R_{41} are neither zero nor infinite for $\eta = 0$. As they appear without a factor c_{dr} in the a_{ik}-table, they give a non-vanishing contribution to the aerodynamic coefficients, which must not be overseen.

The part $\alpha_{ik}^{(0)}$ of a_{ik}, which is independent of the reduced velocity V, leads, when substituted in the equations (3.6) to forces and moments, which can be considered as due to the inertia of the surrounding air (aerodynamic inertia). This is allowed since the coefficients $\alpha_{ik}^{(0)}$ satisfy the relation

$$\alpha_{ik}^{(0)} = \alpha_{ki}^{(0)} \qquad (3.12)$$

making the matrix $[\alpha]^{(0)}$ just like the mass matrix **m** symmetric. The forces due to $\alpha_{ik}^{(0)}$ are usually accounted for by including them in the (mass) inertia forces and omitting them from the aerodynamic forces, in accordance with eq. (2.8).

3.5 *The divergence speed.*

Sometimes it is desirable to calculate the divergence speed, which makes it necessary to know the stationary forces too. These can be most easily derived from the instationary forces by the following limits

$$\nu \to 0,\ V \to \infty,\ \nu V \to \frac{v}{c},\ \nu^2 . 4\,iPV \to 0,$$
$$\nu^2 . 4\,PV^2 \to 4\frac{v^2}{c^2}. \qquad (3.13)$$

3.6 *The values of η_s and η_s'.*

It is still necessary to give some information concerning the value of the gap width as it appears in the terms $\log_e \eta_s$ and $\log_e \eta_s'$. These terms enter into the equations (2.5) in the combinations $N + c_{dr}R$ and $Q + c_{es}P$. Therefore the behaviour of $N + c_{dr}R$, when η_s is varied, will be examined considering for the moment an aileron without tab. Further the wing is assumed not to be subject to any deformations, i. e. $z = 0$ and $\varphi = 0$. For the steady case, that is with the limits (3.13), we obtain

$$N + c_{dr}R = \pi\,\rho v^2 c^2 \gamma \{ (-R_{26} + R_{29} - c'_{dr} - R_{23} - c'^2_{dr}) + \tfrac{1}{4}(-R_{33} + R_{35} - c'_{dr} - R_{24} - c'^2_{dr}) \} \qquad (3.14)$$

With $\eta = 0{,}25$, (3.14) is plotted in fig. 3.2 against c'_{dr} for some values of η_s. It is shown in this fig. that within the limits $\eta_s = 0{,}05\ c'_{dr}$ and $\eta_s = 0{,}40\ c'_{dr}$ the ordinate is fairly independent of η_s. It is therefore recommended in ref. 7 to accept $\eta_s = 0{,}25\ c'_{dr}$ as a presumably adequate average value.

For the combination $Q + c_{es}P$ similar reasoning holds, but now $z = 0$, $\varphi = 0$ and $\gamma = 0$ must be inserted. The same expression (3.14) appears, with γ replaced by ε and c'_{dr} by c'_{es}, while the R's are functions of η'. A similar figure could be drawn, taking for η' a smaller value than in fig. 3.2 for η.

Fig. 3.2 allows also the immediate estimation of the degree of the steady-state aerodynamic balance ($\omega = 0$). Aerodynamic balance n % means that the moment due to a stationary deflection of the aileron amounts to (100—n) % of the moment which would arise if the hinge axis of the aileron were shifted to the nose, while again it is assumed that the wing is not deformed. In fig. 3.2 the

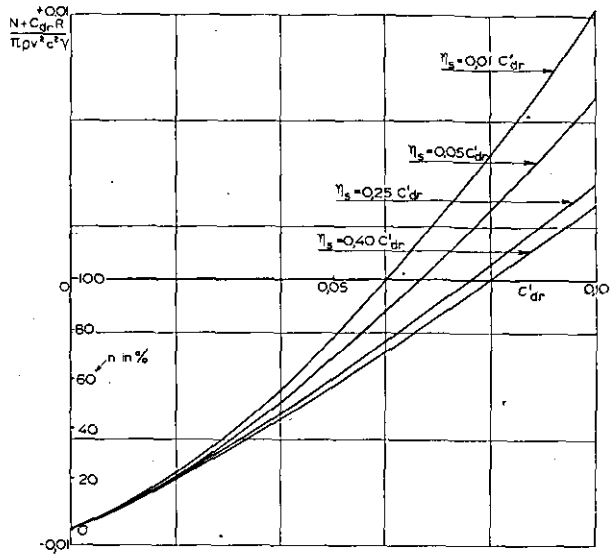

Fig. 3.2 Aerodynamic moment about aileron hinge axis.

ordinate for the existing configuration divided by the ordinate for $c_{dr} = 0$ is equal to $1 - \frac{n}{100}$, giving at once the value of n.

Conversely, the measured aerodynamic balance can theoretically be used to determine η_s.

4 Further treatment of the equations of motion.

4.1 *Method of solution.*

To obtain approximate solutions of the set of differential equations (2.6), which after elimination of **A** with the aid of (3.6) takes the form

$$\mathbf{e}\,\mathbf{f} = \nu^2\,(\mathbf{m} + \mathbf{a})\,\mathbf{f}, \qquad (4.1)$$

the deformation matrix **f** is usually supposed to admit with satisfactory accuracy a development

$$\mathbf{f} = \sum_1^N q_H\,\mathbf{F}_H \qquad (4.2)$$

into a finite (and actually very small) number of deformation matrices $\mathbf{F}_H$, constructed in advance. A good result will obviously be favoured by the insertion into the matrices $\mathbf{F}_H$ of all known properties of the required solution, e. g. by adaption to given boundary conditions. In this way the problem is reduced to the determination of approximate values of the frequencies ν and the coefficients q_H. Substitution of (4.2) in (4.1) gives

$$\sum_1^N q_H\,\{\mathbf{e}\,\mathbf{F}_H - \nu^2\,(\mathbf{m} + \mathbf{a})\,\mathbf{F}_H\} = [\varepsilon], \qquad (4.3)$$

where in the right side an error-vector $[\varepsilon]$ appears, due to the fact that for a finite number N, $\sum_1^N q_H\,\mathbf{F}_H$

in general can not exactly represent a true solution **f**.

Eq. (4.3) is now successively pre-multiplied by N suitably chosen "weighting vectors" $\mathbf{G}_J^*$ and integrated from $y = 0$ to $y = b$. The sign * denotes that the vector consists of one horizontal row. At the right side of each equation the mean value of the error $[\varepsilon]$ multiplied with the weighting vector $\mathbf{G}_J^*$ appears. The N resulting (scalar) mean values of the error are equated to zero, thus producing a set of N homogeneous, algebraic equations for the coefficients q_H with the frequency ν as parameter (susceptible of characteristic values).

It is proved in ref. 1 that it is recommendable to adapt the vectors $\mathbf{G}_J^*$ as much as possible to the adjoint companions of the required solutions, i. e. to solutions of eq. (4.1) with transposed matrices.

When the tab is supposed to be torsionally rigid, not only ε but also the corresponding solution of the adjoint system is independent of y. In building up $\int \mathbf{G}_J^* \varepsilon \, dy$, the horizontal row of (4.1) expressing the tab equation is being multiplied with a constant and then integrated. The formal difficulty due to the fact that the product $e_{44}\varepsilon$ in the equations of motion is indefinite if T_s is infinite, thus happens to vanish automatically.

4.2 *The integrals involving aerodynamic coefficients.*

The obtained algebraic equations contain the aerodynamic coefficients in the form of integrals of the type

$$\int_0^b m_L \, a_{ik} \, f_{Hk} g_{Ji} \, c^n \, dy; \quad H, J = 1 \ldots N, \tag{4.4}$$

where the exponent n is given by

$$\left.\begin{array}{ll} n = 0 & \text{when } i = 1,\ k = 1, \\ n = 1 & ,, \quad i \neq 1,\ k = 1 \text{ or } i = 1,\ k \neq 1, \\ n = 2 & ,, \quad i \neq 1 \text{ and } k \neq 1. \end{array}\right\} \tag{4.5}$$

f_{Hk} resp. g_{Ji} denotes the k^{th}, resp. the i^{th} element of the vectors $\mathbf{F}_H$ resp. $\mathbf{G}_J$.

Evaluation of these integrals at first encounters the inconvenience that the coefficients a_{ik} are, due to the expressions $4\,iPV$ etc. (see eq. (3.10)), functions of the reduced velocity, which itself is dependent upon the coordinate y. This makes that the computation generally demands unpleasant interpolations in the tables of the P-function. These inconveniences cancel if we replace the functions $4\,iPV$ and $4\,PV^2$ by Taylor-developments, referring to some basic value V_0 which is the reduced velocity at the reference chord c_0. In order that the successive terms of these developments decrease quickly, it is advantageous to choose for c_0 a chord somewhere at the middle of the aileron.

For the function $f(V)$ Taylor's development runs as follows:

$$f(V) = f(V_0) + (V - V_0) f'(V_0) + \tfrac{1}{2}(V - V_0)^2 f''(V_0) + \ldots \tag{4.6}$$

With

$$\xi(y) = \frac{c_0 - c(y)}{c(y)} = \frac{V(y) - V_0}{V_0} \tag{4.7}$$

this becomes

$$f(V) = f(V_0) + \xi V_0 f'(V_0) + \tfrac{1}{2}\xi^2 V_0^2 f''(V_0) + \ldots, \tag{4.8}$$

and applied to the functions $4\,iPV$ and $4\,PV^2$, it is obtained that

$$\left.\begin{aligned} 4\,iPV &= 4\,iP_0V_0 + \xi V_0 \left(\frac{d(4\,iPV)}{dV}\right)_{V=V_0} + \\ &\quad + \tfrac{1}{2}\xi^2 V_0^2 \left(\frac{d^2(4\,iPV)}{dV^2}\right)_{V=V_0} + \ldots, \\ 4\,PV^2 &= 4\,P_0V_0^2 + \xi V_0 \left(\frac{d(4\,PV^2)}{dV}\right)_{V=V_0} + \\ &\quad + \tfrac{1}{2}\xi^2 V_0^2 \left(\frac{d^2(4\,PV^2)}{dV^2}\right)_{V=V_0} + \ldots. \end{aligned}\right\} \tag{4.9}$$

It is usually not necessary to include terms of the third and higher order $\left(\frac{d^3}{dV^3}\right)$.

Writing for the complex P-function

$$P(V) = A(V) - iB(V) \tag{4.10}$$

where A and B are real and positive throughout, the equations (4.9) can be brought in the form

$$\left.\begin{aligned} 4\,iPV &= p_{10} + p_{11}\xi + p_{12}\xi^2 + \ldots + \\ &\quad + i\,(p'_{10} + p'_{11}\xi + p'_{12}\xi^2 + \ldots), \\ 4\,PV^2 &= p_{20} + p_{21}\xi + p_{22}\xi^2 + \ldots - \\ &\quad - i\,(p'_{20} + p'_{21}\xi + p'_{22}\xi^2 \ldots\ldots), \end{aligned}\right\} \tag{4.11}$$

with (omitting the suffix 0, attached to V_0):

$$\left.\begin{array}{ll} p_{10} = 4\,BV, & p'_{10} = 4\,AV, \\ p_{20} = 4\,AV^2, & p'_{20} = 4\,BV^2, \\ p_{11} = V\frac{dp_{10}}{dV}, & p'_{11} = V\frac{dp'_{10}}{dV}, \\ p_{21} = V\frac{dp_{20}}{dV}, & p'_{21} = V\frac{dp'_{20}}{dV}, \\ p_{12} = \tfrac{1}{2}V^2\frac{d^2p_{10}}{dV^2}, & p'_{12} = \tfrac{1}{2}V^2\frac{d^2p'_{10}}{dV^2}, \\ p_{22} = \tfrac{1}{2}V^2\frac{d^2p_{20}}{dV^2}, & p'_{22} = \tfrac{1}{2}V^2\frac{d^2p'_{20}}{dV^2}, \end{array}\right\} \tag{4.12}$$

With the aid of the differential equation of the P-function [1])

$$\frac{dP}{dV} = -\frac{P}{V}(P-1) - \frac{i}{2V^2}(2P-1), \tag{4.13}$$

it is possible to write the last 8 relations without differential-quotients.

---

[1]) In ref. 10 this equation is given as an equation for T, where $2P = 1 + T$.

It is easily derived that

$$\left.\begin{aligned}
p_{11} &= (2-4BV)(2A-1)+4BV,\\
p'_{11} &= B(4BV-4)-4AV(A-2),\\
p_{21} &= 12AV^2-4(A^2-B^2)V^2-4BV,\\
p'_{21} &= 12BV^2-8ABV^2+4AV-2V;\\
p_{12} &= p_{10}\{(A-1)^2-B^2\}+\\
&\quad +2p'_{10}(A-1)B+\\
&\quad +\frac{1}{V}\{{}^3/_2(p'_{11}-p'_{10})+4B-V\},\\
p'_{12} &= p'_{10}\{(A-1)^2-B^2\}-\\
&\quad -2p_{10}(A-1)B+\\
&\quad +\frac{1}{V}({}^3/_2 p_{10}-1)(2A-1),\\
p_{22} &= {}^1/_4 p_{11}(p_{10}-2)+\\
&\quad +p'_{11}V(1-A)+p_{20},\\
p'_{22} &= p_{11}V(1-A)-\\
&\quad -{}^1/_4 p'_{11}(p_{10}-2)+V(p_{10}-1).
\end{aligned}\right\}\quad(4.14)$$

The functions $p_{10}\ldots p'_{22}$ are tabulated with small intervals in table 4.1. Finally it is possible to replace the functions $V^2(y)$ and $V(y)$ themselves, appearing in (3.10) by (compare (4.7)):

$$V^2 = V_0^2(1+\xi)^2 \text{ and } V = V_0(1+\xi) \qquad (4.15)$$

Inserting the relation (3.10) in the integrals (4.4) (without the term $\alpha_{ik}^{(0)}$ being already included in the integrals containing m_{ik}), we obtain the following new integrals:

$$\left.\begin{aligned}
&(p_{10}\text{ or }p'_{10})\int_0^b m_L\alpha_{ik}^{(1)}f_{Hk}g_{Ji}c^n dy,\\
&(p_{11}\text{ or }p'_{11})\int_0^b m_L\alpha_{ik}^{(1)}f_{Hk}g_{Ji}c^n\xi dy,\\
&(p_{12}\text{ or }p'_{12})\int_0^b m_L\alpha_{ik}^{(1)}f_{Hk}g_{Ji}c^n\xi^2 dy,\\
&(p_{20}\text{ or }-p'_{20})\int_0^b m_L\alpha_{ik}^{(2)}f_{Hk}g_{Ji}c^n dy,\\
&(p_{21}\text{ or }-p'_{21})\int_0^b m_L\alpha_{ik}^{(2)}f_{Hk}g_{Ji}c^n\xi dy,\\
&(p_{22}\text{ or }-p'_{22})\int_0^b m_L\alpha_{ik}^{(2)}f_{Hk}g_{Ji}c^n\xi^2 dy,\\
&V_0^2\int_0^b m_L\alpha_{ik}^{(3)}f_{Hk}g_{Ji}c^n(1+\xi)^2 dy;\\
&V_0\int_0^b m_L\alpha_{ik}^{(4)}f_{Hk}g_{Ji}c^n(1+\xi)dy.
\end{aligned}\right\}\quad(4.16)$$

The integrals, which can be calculated by means of Simpson's rule, are independent of the reduced velocity V_0. This makes the evaluation, especially if it has to be carried our for a long sequence of values of V_0, comparatively concise, since the same integrals need then only to be multiplied with different factors.

5 Notations.

z	displacement of the reference axis
z_v	displacement of the quarter-chord axis
φ	rotation of the wing chord
γ	rotation of the aileron chord (with regard to the neutral position)
γ_r	rotation of the aileron chord relative to the wing chord
ε	rotation of the tab chord (with regard to the neutral position)
ε_r	rotation of the tab chord relative to the aileron chord
ζ	displacement of the aileron leading edge relative to the wing trailing edge
χ	displacement of the tab leading edge relative to the aileron trailing edge
$K = K_L$	aerodynamic force of wing + aileron + tab per unit span
M	aerodynamic moment of wing + aileron + tab per unit span about the quarter-chord axis
M_L	aerodynamic moment of wing per unit span about the reference axis
R	aerodynamic force of aileron + tab per unit span
N	aerodynamic moment of aileron + tab per unit span about the aileron leading edge
N_L	aerodynamic moment of aileron per unit span about the aileron hinge axis
P	aerodynamic force of tab per unit span
Q	aerodynamic moment of tab per unit span about the tab leading edge
Q_L	aerodynamic moment of tab per unit span about the tab hinge axis
c	total chord (wing + aileron + tab)
c_v	distance of quarter chord axis aft of reference axis $\left(c'_v = \frac{c_v}{c}\right)$
c_d	distance of aileron hinge axis aft of reference axis
c_r	distance of aileron leading edge aft of reference axis
c_{dr}	distance of aileron hinge axis aft of aileron leading edge $\left(c'_{dr} = \frac{c_{dr}}{c}\right)$
c_e	distance of tab hinge axis aft of aileron hinge axis
c_s	distance of tab leading edge aft of aileron hinge axis
c_{es}	distance of tab hinge axis aft of tab leading edge $\left(c'_{es} = \frac{c_{es}}{c}\right)$
s	distance of the centre of gravity of wing + aileron + tab aft of the reference axis
s'	distance of the centre of gravity of aileron + tab aft of the aileron hinge axis
$s'' = s_s$	distance of the centre of gravity of the tab aft of the tab hinge axis

s_r distance of the centre of gravity of the aileron aft of the aileron hinge axis

s_v distance of the centre of gravity of the wing aft of the reference axis

m mass of wing + aileron + tab per unit span

m' mass of aileron + tab per unit span

$m'' = m_s$ mass of tab per unit span

m_r mass of aileron per unit span

m_v mass of wing per unit span

m_L mass of air per unit span in the cylinder surrounding wing + aileron + tab (eq. (2.10))

I moment of inertia of wing + aileron + tab about the corresponding inertia axis per unit span

I' moment of inertia of aileron + tab about the corresponding inertia axis per unit span

$I'' = I_s$ moment of inertia of the tab about its inertia axis per unit span

I_r moment of inertia of the aileron about its inertia axis per unit span

I_v moment of inertia of the wing about its inertia axis per unit span

I_L moment of inertia of the fuselage about the longitudinal axis

B flexural stiffness of the wing

T_v torsional stiffness of the wing

T_r torsional stiffness of the aileron

T_s torsional stiffness of the tab

k_0 total spring constant of the cables connecting the aileron with the control stick in the case of a spring tab system

k_1 total spring constant of the cables or rods connecting the tab with the aileron (spring tab and trim tab)

k_2 constant of the torsion spring between the lever BE (fig. 2.2) and the aileron

k_r total spring constant of the cables connecting the control stick with the aileron (in the case of a balance or a trim tab) or with the tab (in the case of a servo tab)

k_s total spring constant of the cables or rods connecting the tab with the wing (balance tab)

σ angle of deformation of the torsion spring k_2, positive if it tends to increase γ_r

a distance of the aileron hinge axis to the control cables

b (1) distance of the tab hinge axis to the cables or rods controlling the tab

b (2) semispan

y spanwise coordinate

b_r y-coordinate of the section, where the control mechanism operates

$b^{(j)}$ y-coordinate of the section containing the concentrated mass $m_{11}{}^{(j)}$

m_{ik} inertia coefficients

e_{ik} elastic coefficients

a_{ik} aerodynamic coefficients

$\alpha_{ik}{}^{(0)}$ aerodynamic inertia coefficients

$\alpha_{ik}{}^{(j)}$, $j = 1 \ldots 4$ parts of the aerodynamic coefficienst defined by (3.10)

$\mathbf{m}$ mass matrix

$\mathbf{e}$ elastic matrix

$\mathbf{a}$ aerodynamic matrix

$\mathbf{A}$ column matrix of aerodynamic forces

$\mathbf{f}$ deformation matrix

$\mathbf{F}_H$ matrix consisting of special deformation functions f_{Hk}

$\mathbf{G}_J$ matrix consisting of weighting functions g_{Ji}

$[\varepsilon]$ error matrix

q_H coefficients appearing in the development of $\mathbf{f}$ to the matrices $\mathbf{F}_H$

ν frequency

ω reduced frequency $\left(= \frac{\nu c}{2 v}\right)$

V reduced velocity $\left(= \frac{v}{\nu c}\right)$

V_0 reduced velocity at reference chord

$P = A - iB$ fundamental function of instationary aerodynamic forces

v speed

t time

ρ air density

n degree of aerodynamic balance (cf. section 3.6)

η ratio of aileron chord to total chord

η' ratio of tab chord to total chord

η_s ratio of gap width between wing and aileron to total chord

η_s' ratio of gap width between aileron and tab to total chord

$\xi = \frac{c_0 - c}{c}$, where c_0 is the reference chord

Displacements and forces are positive if directed upwards, moments if they are tailheavy and rotations if they are due to a positive moment. The index 0 added to displacements or rotations denote their amplitude.

6 List of references.

1 Greidanus, J. H.: Mathematical methods of flutter analysis. Report V. 1384, Vol. XIII of the Reports and Transactions of the National Aeronautical Research Institute (1946), Amsterdam.

2 Küssner, H. G.: "Zusammenfassender Bericht über den instationären Auftrieb von Flügeln", Luftfahrtforschung Vol. 13 (1936), p. 410.

3 Küssner, H. G. und Schwarz, L.: "Der schwingende Flügel mit aerodynamisch ausgeglichenem Ruder", Luftfahrtforschung Vol. 17 (1940), p. 337.

4 Cicala, P.: "Le azioni aerodinamiche sul profilo oscillante", L'aerotecnica Vol. 16 (1936), p. 652.

5 Dietze, F.: "Die Luftkräfte der harmonisch schwingenden in sich verformbaren Platte (ebenes Problem)", Luftfahrtforschung Vol. 16 (1939), p. 84.

6 Theodorsen, Th.: "General theory of aerodynamic instability and the mechanism of flutter", NACA report No. 496 (1935).

7 Theodorsen, Th. and Garrick, J. E.: "Nonstationary flow about a wing-aileron-tab combination including aerodynamic balance". NACA report no. 736 (1942).

8 Greidanus, J. H.: "De berekening van de kritische snelheid voor onstabiele trillingen van vliegtuigvleugels, deel I" report V. 1252 Vol. X of the "Verslagen en Verhandelingen van het Nationaal Luchtvaartlaboratorium", Amsterdam (1941).

9 Like ref. 8, deel II, report V. 1304, Vol. XII (1943).

10 Schwarz: "Berechnung der Funktionen $U_1(s)$ und $U_2(s)$ für gröszere Werte von s". Luftfahrtforschung Vol. 17 (1940) p. 362.

η	R_1	R_2	R_3	R_4^+	R_4^-	R_6^+	R_6^-	R_7	R_8	R_9	R_{10}	R_{11}	R_{12}	R_{13}	R_{14}	R_{15}	R_{16}	R_{17}^+	R_{17}^-	$R_{18}^+=R_{18}^-$
0,60	0,124027	0,131031	0,373531	0	0,519800	0	1,247514	0,875973	0,368969	0,626469	0,055732	0,252216	0,006912	0,007303	0,186572	— 0,048940	0,075299	0,031281	0,002313	— 0,015771
0,55	0,151401	0,174158	0,436445	0	0,575840	0	1,266855	0,848599	0,325842	0,563555	0,044063	0,215171	0,006671	0,007674	0,223707	— 0,076007	0,130095	0,032577	0,007284	+ 0,000082
0,50	0,181689	0,215843	0,500000	0	0,636620	0	1,273240	0,818311	0,284157	0,500000	0,034155	0,181691	0,006206	0,007373	0,260476	— 0,107918	0,181688	0,033011	0,011267	0,011268
0,45	0,215168	0,255936	0,564556	0	0,703809	0	1,266855	0,784832	0,244064	0,436444	0,025841	0,151401	0,005560	0,006614	0,295641	— 0,144232	0,230095	0,032577	0,014389	0,018468
0,40	0,252217	0,294267	0,626470	0	0,779694	0	1,247514	0,747783	0,205733	0,373530	0,018967	0,124026	0,004784	0,005582	0,327839	— 0,184349	0,275300	0,031281	0,016494	0,022315
0,35	0,293339	0,330648	0,688082	0	0,867567	0	1,214595	0,706661	0,169352	0,311918	0,013392	0,099364	0,003928	0,004428	0,355520	— 0,227513	0,317256	0,029147	0,017529	0,023391
0,30	0,339255	0,364855	0,747685	0	0,972456	0	1,166944	0,660745	0,135145	0,252315	0,008987	0,077273	0,003049	0,003279	0,376868	— 0,272796	0,355868	0,026215	0,017476	0,022256
0,25	0,391003	0,396626	0,804500	0	1,102658	0	1,102658	0,608997	0,103374	0,195500	0,005624	0,057668	0,002199	0,002231	0,389651	— 0,319085	0,391002	0,022548	0,016347	0,019448
0,20	0,450183	0,425632	0,857620	0	1,273240	0	1,018592	0,549817	0,074368	0,142380	0,003179	0,040521	0,001431	0,001354	0,390928	— 0,365032	0,422453	0,018242	0,014194	0,015500
0,15	0,519498	0,451439	0,905939	0	1,515461	0	0,909278	0,480502	0,048561	0,094061	0,001530	0,025866	0,000795	0,000691	0,376446	— 0,408978	0,449909	0,013437	0,011118	0,010942
0,10	0,604182	0,473429	0,947956	0	1,909860	0	0,763944	0,395818	0,026571	0,052044	0,000549	0,013846	0,000332	0,000260	0,339015	— 0,448790	0,472880	0,008366	0,007317	0,006338
0,09	0,623837	0,477290	0,955421	0	2,024324	0	0,728758	0,376163	0,022710	0,044579	0,000421	0,011784	0,000263	0,000201	0,327676	— 0,456013	0,476869	0,007351	0,006499	0,005466
0,08	0,644734	0,480948	0,962522	0	2,158887	0	0,690841	0,355266	0,019052	0,037478	0,000313	0,009845	0,000202	0,000151	0,314659	— 0,462924	0,480635	0,006347	0,005671	0,004624
0,07	0,667105	0,484390	0,969229	0	2,320454	0	0,649728	0,332895	0,015610	0,030771	0,000224	0,008031	0,000149	0,000109	0,299697	— 0,469485	0,484166	0,005358	0,004838	0,003816
0,06	0,691268	0,487600	0,975503	0	2,519812	0	0,604757	0,308732	0,012400	0,024497	0,000152	0,006353	0,000105	0,000074	0,282429	— 0,475656	0,487448	0,004392	0,004009	0,003051
0,05	0,717684	0,490557	0,981306	0	2,774963	0	0,554993	0,282316	0,009443	0,018694	0,000096	0,004819	0,000069	0,000047	0,262350	— 0,481388	0,490461	0,003459	0,003193	0,002337
0,04	0,747061	0,493237	0,986583	0	3,118788	0	0,499008	0,252939	0,006763	0,013417	0,000055	0,003438	0,000041	0,000027	0,238697	— 0,486619	0,493182	0,002568	0,002396	0,001682
0,03	0,780576	0,495603	0,991259	0	3,619973	0	0,434398	0,219424	0,004397	0,008741	0,000026	0,002225	0,000020	0,000013	0,210211	— 0,491271	0,495577	0,001733	0,001639	0,001094
0,02	0,820540	0,497604	0,995229	0	4,456339	0	0,356507	0,179460	0,002396	0,004771	0,000010	0,001206	0,000008	0,000005	0,174479	— 0,495228	0,497594	0,000993	0,000951	0,000600
0,01	0,872889	0,499152	0,998310	0	6,334285	0	0,253375	0,127111	0,000848	0,001690	0,000002	0,000427	0,000002	0,000001	0,125366	— 0,498308	0,499150	0,000373	0,000360	0,000213
0,00	1,000000	0,500000	1,000000	0	∞	0	0,000000	0,000000	0,000000	0,000000	0,000000	0,000000	0,000000	0,000000	0,000000	— 0,500000	0,500000	0,000000	0,000000	0,000000

η	R_{19}^+	R_{19}^-	R_{20}^+	R_{20}^-	$R_{21}^+=R_{21}^-$	$R_{22}^+=R_{22}^-$	R_{23}^+	R_{23}^-	R_{24}^+	$R_{24}^- - \frac{8\log_e\eta_s}{\pi^2}$	R_{25}^+	R_{25}^-	R_{26}	R_{27}	R_{28}	R_{29}^+	R_{29}^-	$R_{30}^+=R_{30}^-$	R_{32}^+
0,60	— 0,389073	— 0,738716	0,373624	0,490670	1,128189	0,220934	0	0,131102	0	— 0,129027	0,389073	1,092791	0,048820	0,020563	— 0,181893	0,220934	0,249903	0,141880	0,627106
0,55	— 0,401231	— 0,742944	0,423111	0,590998	1,063770	0,182594	0	0,123903	0	— 0,072911	0,401231	1,075056	0,037392	0,014358	— 0,202667	0,182594	0,207967	0,107503	0,488831
0,50	— 0,405284	— 0,723594	0,466991	0,683980	1,000000	0,148680	0	0,115667	0	0,000000	0,405284	1,041906	0,027949	0,009705	— 0,214029	0,148680	0,170424	0,079577	0,351320
0,45	— 0,401231	— 0,678420	0,503631	0,766536	0,936233	0,118825	0	0,106557	0	0,089203	0,401231	0,994268	0,020281	0,006307	— 0,216220	0,118825	0,137012	0,057232	0,217857
0,40	— 0,389073	— 0,604334	0,531398	0,835575	0,871809	0,092745	0	0,096703	0	0,195200	0,389073	0,932871	0,014183	0,003902	— 0,209721	0,092745	0,107533	0,039699	+ 0,091637
0,35	— 0,368809	— 0,496951	0,548592	0,887844	0,806025	0,070217	0	0,086205	0	0,319615	0,368809	0,858305	0,009464	0,002268	— 0,195242	0,070217	0,081835	0,026291	— 0,024119
0,30	— 0,340439	— 0,349684	0,553412	0,919794	0,738018	0,051058	0	0,075145	0	0,465554	0,340439	0,771052	0,005938	0,001215	— 0,173745	0,051058	0,059797	0,016381	— 0,126055
0,25	— 0,303963	— 0,151981	0,543832	0,927282	0,666667	0,035120	0	0,063588	0	0,638469	0,303963	0,671516	0,003425	0,000581	— 0,146457	0,035120	0,041321	0,009386	— 0,210498
0,20	— 0,259382	+ 0,114638	0,517390	0,905079	0,590338	0,022279	0	0,051593	0	0,848086	0,259382	0,560036	0,001748	0,000236	— 0,114925	0,022279	0,026327	0,004761	— 0,273151
0,15	— 0,206695	0,487157	0,470732	0,845786	0,506368	0,012429	0	0,039199	0	1,113191	0,206695	0,436909	0,000735	0,000074	— 0,081106	0,012429	0,014748	0,001991	— 0,308477
0,10	— 0,145902	1,057098	0,398297	0,736892	0,409664	0,005480	0	0,026444	0	1,476573	0,145902	0,302383	0,000217	0,000015	— 0,047557	0,005480	0,006529	0,000585	— 0,308056
0,09	— 0,132771	1,213914	0,379850	0,707220	0,387947	0,004433	0	0,023855	0	1,569229	0,132771	0,274130	0,000158	0,000010	— 0,041172	0,004433	0,005285	0,000426	— 0,302478
0,08	— 0,119316	1,393928	0,359765	0,674210	0,365111	0,003498	0	0,021254	0	1,672053	0,119316	0,245432	0,000111	0,000006	— 0,034973	0,003498	0,004174	0,000299	— 0,294655
0,07	— 0,105536	1,604539	0,337823	0,637376	0,340926	0,002673	0	0,018636	0	1,787738	0,105536	0,216290	0,000075	0,000003	— 0,029005	0,002673	0,003193	0,000200	— 0,284309
0,06	— 0,091432	1,857178	0,313709	0,596047	0,315085	0,001961	0	0,016008	0	1,920229	0,091432	0,186706	0,000047	0,000002	— 0,023314	0,001961	0,002344	0,000126	— 0,271071
0,05	— 0,077004	2,170773	0,286992	0,549290	0,287125	0,001360	0	0,013373	0	2,075648	0,077004	0,156683	0,000027	0,000001	— 0,017957	0,001360	0,001626	0,000073	— 0,254426
0,04	— 0,062252	2,579650	0,257003	0,495672	0,256377	0,000870	0	0,010722	0	2,264252	0,062252	0,126218	0,000014	0,000000	— 0,013005	0,000870	0,001042	0,000037	— 0,233603
0,03	— 0,047175	3,154901	0,222592	0,432792	0,221649	0,000487	0	0,008036	0	2,505251	0,047175	0,095317	0,000006	0,000000	— 0,008545	0,000487	0,000581	0,000016	— 0,207332
0,02	— 0,031774	4,078999	0,181530	0,356005	0,180666	0,000217	0	0,005392	0	2,841804	0,031774	0,063980	0,000002	0,000000	— 0,004705	0,000217	0,000259	0,000005	— 0,173193
0,01	— 0,016049	6,070306	0,128003	0,253370	0,127538	0,000054	0	0,002705	0	3,411631	0,016049	0,032206	0,000000	0,000000	— 0,001680	0,000054	0,000067	0,000001	— 0,125043
0,00	0,000000	$-\infty$	0,000000	0,000000	0,000000	0,000000	0	0,000000	0	∞	0,000000	0,000000	0,000000	0,000000	0,000000	0,000000	0,000000	0,000000	0,000000

η	R_{32}^-	R_{33}	R_{34}	R_{35}^+	R_{35}^-	R_{36}^+	R_{36}^-	R_{37}^+	R_{37}^-	R_{38}	R_{39}	R_{40}	R_{41}	R_{42}	R_{43}	R_{44}	R_{45}	R_{46}	R_{47}
0,60	0,510060	0,062928	— 0,038021	0,389073	0,010996	0,124124	— 0,008330	0,876606	1,009060	0,231146	0,087551	0,162449	0,012338	0,146979	0,485841	0,019975	0,059540	0,041462	0,266060
0,55	0,320944	0,061333	— 0,037697	0,401231	0,051931	0,138071	+ 0,020918	0,773871	0,891024	0,183629	0,117305	0,132695	0,020508	0,177835	0,416899	0,021804	+ 0,015313	0,029634	0,208461
0,50	+ 0,134331	0,057834	— 0,035976	0,405284	0,086974	0,148681	0,047360	0,669630	0,770951	0,142077	0,143896	0,106104	0,029926	0,196951	0,351320	0,021673	— 0,018898	0,020478	0,159155
0,45	— 0,045048	0,052746	— 0,033028	0,401231	0,115370	0,155244	0,069762	0,566244	0,651726	0,106520	0,167306	0,082694	0,040017	0,204942	0,289788	0,020073	— 0,043572	0,013586	0,117798
0,40	— 0,212540	0,046417	— 0,029083	0,389073	0,136514	0,157142	0,087063	0,465893	0,535972	0,076847	0,187551	0,062449	0,050248	0,202637	0,232902	0,017465	— 0,059353	0,008573	0,083931
0,35	— 0,363371	0,039223	— 0,024421	0,368809	0,149923	0,153849	0,098358	0,370624	0,426115	0,052824	0,204681	0,045319	0,060127	0,191065	0,181198	0,014273	— 0,067032	0,005077	0,057001
0,30	— 0,492437	0,031562	— 0,019360	0,340439	0,155190	0,144982	0,102934	0,282375	0,324423	0,034099	0,218777	0,031223	0,069221	0,171477	0,135155	0,010881	— 0,067555	0,002768	0,036367
0,25	— 0,593948	0,023846	— 0,014248	0,303963	0,151981	0,130335	0,100288	0,202999	0,233046	0,020210	0,229959	0,020041	0,077166	0,145358	0,095213	0,007618	— 0,062025	0,001348	0,021309
0,20	— 0,660840	0,016509	— 0,009454	0,259382	0,140010	0,109953	0,090205	0,134286	0,154034	0,010589	0,238389	0,011611	0,083677	0,114473	0,061772	0,004758	— 0,051716	0,000557	0,011041
0,15	— 0,683531	0,009995	— 0,005348	0,206695	0,119026	0,084291	0,072904	0,077964	0,089351	0,004568	0,244277	0,005723	0,088569	0,080963	0,035201	0,002502	— 0,038126	0,000178	0,004711
0,10	— 0,646651	0,004760	— 0,002270	0,145902	0,088818	0,054522	0,049342	0,035719	0,040899	0,001383	0,247899	0,002101	0,091774	0,047529	0,015840	0,000971	— 0,023059	0,000035	0,001411
0,09	— 0,629848	0,003908	— 0,001803	0,132771	0,081652	0,048266	0,044052	0,029106	0,033320	0,001012	0,248382	0,001618	0,092217	0,041153	0,012862	0,000755	— 0,020061	0,000023	0,001031
0,08	— 0,609100	0,003129	— 0,001389	0,119316	0,074111	0,041977	0,038634	0,023133	0,026476	0,000714	0,248792	0,001208	0,092598	0,034961	0,010186	0,000569	— 0,017118	0,000015	0,000726
0,07	— 0,583862	0,002427	— 0,001030	0,105536	0,066187	0,035699	0,033128	0,017815	0,020386	0,000480	0,249133	0,000867	0,092918	0,028998	0,007817	0,000412	— 0,014256	0,000009	0,000487
0,06	— 0,553409	0,001806	— 0,000726	0,091432	0,057883	0,029474	0,027577	0,013164	0,015061	0,000304	0,249409	0,000591	0,093179	0,023310	0,005757	0,000283	— 0,011501	0,000005	0,000308
0,05	— 0,516724	0,001271	— 0,000478	0,077004	0,049193	0,023371	0,022048	0,009195	0,010518	0,000177	0,249624	0,000376	0,093384	0,017956	0,004007	0,000182	— 0,008889	0,000002	0,000178
0,04	— 0,472272	0,000823	— 0,000285	0,062252	0,040130	0,017483	0,016632	0,005917	0,006768	0,000091	0,249784	0,000216	0,093539	0,013004	0,002571	0,000105	— 0,006456	0,000001	0,000092
0,03	— 0,417532	0,000469	— 0,000145	0,047175	0,030675	0,011912	0,011432	0,003348	0,003828	0,000039	0,249895	0,000105	0,093646	0,008545	0,001449	0,000052	— 0,004253	0,000000	0,000039
0,02	— 0,347668	0,000211	— 0,000056	0,031774	0,020834	0,006840	0,006625	0,001497	0,001712	0,000011	0,249962	0,000038	0,093712	0,004704	0,000645	0,000019	— 0,002346	0,000000	0,000012
0,01	— 0,250410	0,000054	— 0,000010	0,016049	0,010612	0,002583	0,002530	0,000377	0,000430	0,000002	0,249993	0,000007	0,093743	0,001680	0,000162	0,000003	— 0,000839	0,000000	0,000002
0,00	0,000000	0,000000	0,000000	0,000000	0,000000	0,000000	0,000000	0,000000	0,000000	0,000000	0,250000	0,000000	0,093750	0,000000	0,000000	0,000000	0,000000	0,000000	0,000000

The functions $T\ (\eta,\ \eta')$ and $T\ (\eta',\ \eta)$.

$T_1\ (\eta,\ \eta')$

η' \ η	0,60	0,55	0,50	0,45	0,40	0,35	0,30	0,25	0,20	0,15	0,10
0,10	0,011946	0,014941	0,018432	0,022538	0,027426	0,033361	0,040778	0,050470	0,064079	0,086054	0,145902
0,09	0,010126	0,012659	0,015612	0,019075	0,023192	0,028179	0,034390	0,042456	0,053668	0,071328	0,110511
0,08	0,008426	0,010529	0,012979	0,015849	0,019253	0,023369	0,028477	0,035075	0,044160	0,058183	0,086654
0,07	0,006847	0,008556	0,010539	0,012862	0,015614	0,018933	0,023038	0,028315	0,035521	0,046450	0,067370
0,06	0,005396	0,006740	0,008298	0,010122	0,012280	0,014874	0,018076	0,022173	0,027723	0,036018	0,051216
0,05	0,004077	0,005090	0,006266	0,007638	0,009259	0,011206	0,013599	0,016651	0,020757	0,026812	0,037533
0,04	0,002898	0,003617	0,004450	0,005421	0,006568	0,007942	0,009628	0,011765	0,014627	0,018797	0,025979
0,03	0,001870	0,002332	0,002869	0,003494	0,004229	0,005111	0,006189	0,007550	0,009362	0,011976	0,016373
0,02	0,001011	0,001260	0,001550	0,001887	0,002284	0,002756	0,003333	0,004061	0,005023	0,006399	0,008671
0,01	0,000355	0,000444	0,000545	0,000663	0,000800	0,000967	0,001167	0,001421	0,001753	0,002223	0,002989
0,00	0,000000	0,000000	0,000000	0,000000	0,000000	0,000000	0,000000	0,000000	0,000000	0,000000	0,000000

$T_1\ (\eta',\ \eta)$

η' \ η	0,60	0,55	0,50	0,45	0,40	0,35	0,30	0,25	0,20	0,15	0,10
0,10	0,464569	0,468962	0,467908	0,461365	0,449089	0,430580	0,404960	0,370715	0,324993	0,261264	0,145902
0,09	0,444441	0,448953	0,448329	0,442540	0,431374	0,414391	0,390817	0,359327	0,317485	0,259992	0,167852
0,08	0,422492	0,427068	0,426825	0,421751	0,411663	0,396177	0,374610	0,345807	0,307684	0,255900	0,177229
0,07	0,398423	0,403000	0,403089	0,398692	0,389656	0,375644	0,356058	0,329897	0,295383	0,248940	0,180805
0,06	0,371824	0,376328	0,376699	0,372946	0,364940	0,352390	0,334781	0,311246	0,280276	0,238927	0,179784
0,05	0,342102	0,346457	0,347053	0,343910	0,336921	0,325838	0,310223	0,289332	0,261899	0,225508	0,174459
0,04	0,308360	0,312468	0,313228	0,310662	0,304690	0,295101	0,281529	0,263349	0,239515	0,208069	0,164626
0,03	0,269088	0,272827	0,273676	0,271666	0,266728	0,258697	0,247270	0,231944	0,211874	0,185517	0,149554
0,02	0,221362	0,224560	0,225409	0,223934	0,220089	0,213749	0,204677	0,192490	0,176544	0,155682	0,127504
0,01	0,157686	0,160049	0,160756	0,159830	0,157242	0,152906	0,146668	0,138271	0,127290	0,112969	0,093793
0,00	0,000000	0,000000	0,000000	0,000000	0,000000	0,000000	0,000000	0,000000	0,000000	0,000000	0,000000

T_2 $(\eta,\ \eta')$

η' \ η	0,60	0,55	0,50	0,45	0,40	0,35	0,30	0,25	0,20	0,15	0,10
0,10	0,081566	0,079355	0,076810	0,073888	0,070527	0,066644	0,062127	0,056802	0,050382	0,042313	0,030959
0,09	0,070001	0,068122	0,065964	0,063486	0,060637	0,057351	0,053532	0,049039	0,043642	0,036903	0,027679
0,08	0,058962	0,057396	0,055599	0,053536	0,051166	0,048435	0,045266	0,041545	0,037088	0,031554	0,024121
0,07	0,048501	0,047228	0,045766	0,044088	0,042163	0,039946	0,037376	0,034365	0,030767	0,026325	0,020442
0,06	0,038679	0,037674	0,036521	0,035199	0,033682	0,031937	0,029917	0,027552	0,024735	0.021274	0,016741
0,05	0,029570	0,028809	0,027936	0,026937	0,025791	0,024474	0,022951	0,021172	0,019056	0,016468	0,013111
0,04	0,021261	0,020719	0,020099	0,019388	0,018574	0,017639	0,016559	0,015298	0,013804	0,011982	0,009639
0,03	0,013876	0,013526	0,013125	0,012666	0,012141	0,011538	0,010843	0,010033	0,009073	0,007908	0,006421
0,02	0,007589	0,007399	0,007183	0,006934	0,006651	0,006324	0,005950	0,005513	0,004996	0,004372	0,003579
0,01	0,002696	0,002629	0,002553	0,002466	0,002366	0,002251	0,002120	0,001967	0,001786	0,001568	0,001294
0,00	0,000000	0,000000	0,000000	0,000000	0,000000	0,000000	0,000000	0,000000	0,000000	0,000000	0,000000

T_2 $(\eta',\ \eta)$

η' \ η	0,60	0,55	0,50	0,45	0,40	0,35	0,30	0,25	0,20	0,15	0,10
0,10	0,077115	0,075662	0,074278	0,072051	0,069244	0,065792	0,061599	0,056507	0,050245	0,042269	0,030959
0,09	0,066139	0,064916	0,063756	0,061880	0,059510	0,056597	0,053061	0,048773	0,043514	0,036859	0,027676
0,08	0,055676	0,054666	0,053711	0,052158	0,050195	0,047782	0,044854	0,041309	0,036971	0,031511	0,024114
0,07	0,045772	0,044956	0,044190	0,042934	0,041346	0,039394	0,037025	0,034160	0,030664	0,026285	0,020433
0,06	0,036482	0,035844	0,035247	0,034263	0,033016	0,031484	0,029627	0,027382	0,024648	0,021238	0,016733
0,05	0,027873	0,027395	0,026949	0,026210	0,025272	0,024119	0,022722	0,021035	0,018986	0,016437	0,013103
0,04	0,020030	0,019693	0,019380	0,018857	0,018194	0,017378	0,016390	0,015197	0,013749	0,011958	0,009632
0,03	0,013065	0,012850	0,012650	0,012315	0,011888	0,011364	0,010729	0,009964	0,009036	0,007892	0,006415
0,02	0,007142	0,007026	0,006919	0,006739	0,006510	0,006227	0,005886	0,005473	0,004975	0,004362	0,003576
0,01	0,002536	0,002496	0,002458	0,002395	0,002315	0,002216	0,002096	0,001952	0,001778	0,001565	0,001293
0,00	0,000000	0,000000	0,000000	0,000000	0,000000	0,000000	0,000000	0,000000	0,000000	0,000000	0,000000

T_s (η, η')

η' \ η	0,60	0,55	0,50	0,45	0,40	0,35	0,30	0,25	0,20	0,15	0,10
0,10	0,017720	0,015501	0,013364	0,011318	0,009371	0,007537	0,005828	0,004262	0,002861	0,001658	0,000706
0,09	0,015304	0,013401	0,011568	0,009811	0,008139	0,006563	0,005092	0,003742	0,002532	0,001487	0,000651
0,08	0,012972	0,011371	0,009827	0,008347	0,006938	0,005608	0,004366	0,003224	0,002198	0,001308	0,000589
0,07	0,010738	0,009422	0,008152	0,006934	0,005774	0,004679	0,003655	0,002712	0,001863	0,001123	0,000520
0,06	0,008618	0,007569	0,006557	0,005585	0,004659	0,003784	0,002966	0,002211	0,001529	0,000934	0,000444
0,05	0,006629	0,005828	0,005054	0,004312	0,003604	0,002933	0,002306	0,001727	0,001203	0,000744	0,000363
0,04	0,004797	0,004221	0,003664	0,003130	0,002621	0,002138	0,001687	0,001269	0,000890	0,000557	0,000279
0,03	0,003150	0,002774	0,002411	0,002063	0,001730	0,001415	0,001119	0,000846	0,000597	0,000377	0,000194
0,02	0,001734	0,001528	0,001330	0,001139	0,000957	0,000784	0,000622	0,000472	0,000335	0,000215	0,000112
0,01	0,000620	0,000547	0,000476	0,000408	0,000344	0,000282	0,000225	0,000171	0,000123	0,000079	0,000043
0,00	0,000000	0,000000	0,000000	0,000000	0,000000	0,000000	0,000000	0,000000	0,000000	0,000000	0,000000

T_s (η', η)

η' \ η	0,60	0,55	0,50	0,45	0,40	0,35	0,30	0,25	0,20	0,15	0,10
0,10	0,001827	0,001766	0,001699	0,001624	0,001541	0,001448	0,001344	0,001225	0,001087	0,000922	0,000706
0,09	0,001408	0,001362	0,001310	0,001253	0,001189	0,001118	0,001039	0,000948	0,000843	0,000717	0,000556
0,08	0,001052	0,001018	0,000979	0,000937	0,000890	0,000837	0,000778	0,000711	0,000634	0,000541	0,000423
0,07	0,000756	0,000731	0,000704	0,000673	0,000640	0,000602	0,000560	0,000513	0,000458	0,000392	0,000310
0,06	0,000516	0,000499	0,000480	0,000460	0,000437	0,000412	0,000384	0,000351	0,000314	0,000270	0,000215
0,05	0,000328	0,000317	0,000305	0,000293	0,000278	0,000262	0,000244	0,000224	0,000201	0,000173	0,000139
0,04	0,000188	0,000182	0,000175	0,000168	0,000160	0,000151	0,000141	0,000129	0,000116	0,000100	0,000081
0,03	0,000092	0,000089	0,000086	0,000082	0,000078	0,000074	0,000069	0,000063	0,000057	0,000049	0,000040
0,02	0,000033	0,000032	0,000031	0,000030	0,000028	0,000027	0,000025	0,000023	0,000021	0,000018	0,000015
0,01	0,000006	0,000006	0,000006	0,000005	0,000005	0,000005	0,000005	0,000004	0,000004	0,000003	0,000003
0,00	0,000000	0,000000	0,000000	0,000000	0,000000	0,000000	0,000000	0,000000	0,000000	0,000000	0,000000

T_4 (η, η')

η' \ η	0,60	0,55	0,50	0,45	0,40	0,35	0,30	0,25	0,20	0,15	0,10
0,10	0,000468	0,000586	0,000721	0,000879	0,001069	0,001296	0,001578	0,001940	0,002438	0,003200	0,004760
0,09	0,000358	0,000447	0,000551	0,000672	0,000816	0,000989	0,001203	0,001476	0,001850	0,002414	0,003499
0,08	0,000265	0,000331	0,000408	0,000497	0,000604	0,000732	0,000889	0,001089	0,001362	0,001768	0,002518
0,07	0,000189	0,000236	0,000291	0,000355	0,000430	0,000520	0,000631	0,000773	0,000964	0,001246	0,001751
0,06	0,000128	0,000160	0,000197	0,000239	0,000291	0,000352	0,000426	0,000521	0,000648	0,000835	0,001160
0,05	0,000081	0,000100	0,000124	0,000151	0,000183	0,000221	0,000267	0,000327	0,000406	0,000522	0,000718
0,04	0,000046	0,000058	0,000071	0,000086	0,000104	0,000126	0,000152	0,000185	0,000230	0,000295	0,000402
0,03	0,000022	0,000027	0,000034	0,000042	0,000051	0,000061	0,000074	0,000090	0,000111	0,000142	0,000191
0,02	0,000008	0,000010	0,000012	0,000015	0,000018	0,000022	0,000026	0,000032	0,000040	0,000051	0,000068
0,01	0,000001	0,000002	0,000002	0,000003	0,000003	0,000004	0,000005	0,000006	0,000007	0,000009	0,000012
0,00	0,000000	0,000000	0,000000	0,000000	0,000000	0,000000	0,000000	0,000000	0,000000	0,000000	0,000000

T_4 (η', η)

η' \ η	0,60	0,55	0,50	0,45	0,40	0,35	0,30	0,25	0,20	0,15	0,10
0,10	0,202848	0,179486	0,156041	0,132787	0,110001	0,087981	0,067061	0,047629	0,030179	0,015423	0,004760
0,09	0,196963	0,174606	0,152153	0,129859	0,107988	0,086819	0,066659	0,047868	0,030897	0,016377	0,005431
0,08	0,189998	0,168739	0,147372	0,126138	0,105281	0,085061	0,065763	0,047720	0,031338	0,017176	0,006172
0,07	0,181782	0,161728	0,141557	0,121493	0,101765	0,082610	0,064293	0,047114	0,031442	0,017772	0,006896
0,06	0,172081	0,153359	0,134517	0,115758	0,097292	0,079339	0,062138	0,045960	0,031136	0,018103	0,007531
0,05	0,160567	0,143338	0,125985	0,108694	0,091657	0,075071	0,059149	0,044136	0,030324	0,018094	0,008011
0,04	0,146752	0,131217	0,115561	0,099950	0,084551	0,069541	0,055107	0,041465	0,028866	0,017639	0,008256
0,03	0,129828	0,116267	0,102593	0,088948	0,075475	0,062326	0,049661	0,037664	0,026546	0,016580	0,008151
0,02	0,108254	0,097096	0,085837	0,074594	0,063484	0,052626	0,042154	0,032211	0,022967	0,014638	0,007519
0,01	0,078150	0,070199	0,062173	0,054151	0,046218	0,038456	0,030959	0,023826	0,017174	0,011151	0,005958
0,00	0,000000	0,000000	0,000000	0,000000	0,000000	0,000000	0,000000	0,000000	0,000000	0,000000	0,000000

$T_5\ (\eta,\ \eta')$

η' \ η	0,60	0,55	0,50	0,45	0,40	0,35	0,30	0,25	0,20	0,15	0,10
0,10	0,003310	0,003223	0,003123	0,003008	0,002877	0,002725	0,002549	0,002343	0,002096	0,001791	0,001383
0,09	0,002553	0,002486	0,002409	0,002322	0,002221	0,002105	0,001971	0,001814	0,001626	0,001395	0,001089
0,08	0,001908	0,001859	0,001802	0,001737	0,001662	0,001577	0,001477	0,001361	0,001223	0,001053	0,000830
0,07	0,001371	0,001336	0,001296	0,001249	0,001196	0,001135	0,001064	0,000982	0,000884	0,000763	0,000607
0,06	0,000936	0,000912	0,000885	0,000854	0,000818	0,000776	0,000729	0,000673	0,000606	0,000526	0,000421
0,05	0,000595	0,000581	0,000563	0,000543	0,000521	0,000494	0,000465	0,000430	0,000388	0,000337	0,000272
0,04	0,000342	0,000333	0,000324	0,000312	0,000299	0,000285	0,000267	0,000247	0,000224	0,000195	0,000159
0,03	0,000167	0,000163	0,000158	0,000153	0,000146	0,000139	0,000131	0,000122	0,000110	0,000096	0,000079
0,02	0,000061	0,000059	0,000058	0,000056	0,000053	0,000051	0,000048	0,000045	0,000040	0,000035	0,000029
0,01	0,000011	0,000011	0,000010	0,000010	0,000010	0,000009	0,000009	0,000008	0,000007	0,000006	0,000005
0,00	0,000000	0,000000	0,000000	0,000000	0,000000	0,000000	0,000000	0,000000	0,000000	0,000000	0,000000

$T_5\ (\eta',\ \eta)$

η' \ η	0,60	0,55	0,50	0,45	0,40	0,35	0,30	0,25	0,20	0,15	0,10
0,10	0,032539	0,028710	0,024951	0,021291	0,017756	0,014377	0,011189	0,008232	0,005558	0,003236	0,001383
0,09	0,028123	0,024838	0,021613	0,018470	0,015433	0,012528	0,009784	0,007234	0,004922	0,002906	0,001277
0,08	0,023855	0,021090	0,018374	0,015725	0,013164	0,010713	0,008395	0,006238	0,004277	0,002559	0,001157
0,07	0,019762	0,017488	0,015254	0,013074	0,010966	0,008945	0,007033	0,005251	0,003627	0,002199	0,001023
0,06	0,015871	0,014058	0,012276	0,010537	0,008854	0,007240	0,005711	0,004284	0,002981	0,001830	0,000875
0,05	0,012217	0,010832	0,009470	0,008140	0,006852	0,005616	0,004444	0,003349	0,002347	0,001459	0,000716
0,04	0,008845	0,007850	0,006871	0,005914	0,004987	0,004097	0,003252	0,002462	0,001737	0,001093	0,000550
0,03	0,005813	0,005163	0,004525	0,003900	0,003294	0,002713	0,002160	0,001642	0,001166	0,000742	0,000382
0,02	0,003201	0,002846	0,002497	0,002155	0,001823	0,001505	0,001202	0,000917	0,000656	0,000422	0,000222
0,01	0,001145	0,001019	0,000895	0,000773	0,000656	0,000542	0,000434	0,000333	0,000240	0,000156	0,000084
0,00	0,000000	0,000000	0,000000	0,000000	0,000000	0,000000	0,000000	0,000000	0,000000	0,000000	0,000000

$T_6\ (\eta,\ \eta') = T_6\ (\eta',\ \eta)$

η' \ η	0,60	0,55	0,50	0,45	0,40	0,35	0,30	0,25	0,20	0,15	0,10
0,10	0,000732	0,000642	0,000556	0,000473	0,000394	0,000319	0,000249	0,000185	0,000127	0,000076	0,000035
0,09	0,000567	0,000498	0,000431	0,000367	0,000306	0,000248	0,000194	0,000145	0,000100	0,000061	0,000029
0,08	0,000426	0,000374	0,000324	0,000276	0,000231	0,000187	0,000147	0,000110	0,000076	0,000047	0,000023
0,07	0,000308	0,000270	0,000235	0,000200	0,000167	0,000136	0,000107	0,000080	0,000056	0,000034	0,000017
0,06	0,000211	0,000185	0,000161	0,000138	0,000115	0,000094	0,000074	0,000055	0,000039	0,000024	0,000012
0,05	0,000135	0,000119	0,000103	0,000088	0,000074	0,000060	0,000048	0,000036	0,000025	0,000016	0,000008
0,04	0,000078	0,000068	0,000060	0,000051	0,000043	0,000035	0,000028	0,000021	0,000015	0,000009	0,000005
0,03	0,000038	0,000034	0,000029	0,000025	0,000021	0,000017	0,000014	0,000010	0,000007	0,000005	0,000003
0,02	0,000014	0,000012	0,000011	0,000009	0,000008	0,000006	0,000005	0,000004	0,000003	0,000002	0,000001
0,01	0,000003	0,000002	0,000002	0,000002	0,000001	0,000001	0,000001	0,000001	0,000001	0,000000	0,000000
0,00	0,000000	0,000000	0,000000	0,000000	0,000000	0,000000	0,000000	0,000000	0,000000	0,000000	0,000000

$T_7 - (\eta, \eta')$

η / η'	0,60	0,55	0,50	0,45	0,40	0,35	0,30	0,25	0,20	0,15	0,10
0,10	— 0,055528	— 0,064554	— 0,075501	— 0,089228	— 0,107133	— 0,131669	— 0,167557	— 0,225116	— 0,331880	— 0,594387	— ∞
0,09	— 0,046993	— 0,054584	— 0,063763	— 0,075241	— 0,090152	— 0,110473	— 0,139961	— 0,186658	— 0,271294	— 0,467812	— 1,475335
0,08	— 0,039041	— 0,045311	— 0,052869	— 0,062296	— 0,074495	— 0,091031	— 0,114854	— 0,152152	— 0,218404	— 0,365332	— 0,944950
0,07	— 0,031685	— 0,036739	— 0,042826	— 0,050389	— 0,060140	— 0,073304	— 0,092129	— 0,121306	— 0,172214	— 0,280931	— 0,649708
0,06	— 0,024933	— 0,028889	— 0,033639	— 0,039527	— 0,047094	— 0,057259	— 0,071707	— 0,093884	— 0,131981	— 0,210801	— 0,452116
0,05	— 0,018813	— 0,021780	— 0,025334	— 0,029732	— 0,035365	— 0,042895	— 0,053542	— 0,069737	— 0,097171	— 0,152420	— 0,309285
0,04	— 0,013350	— 0,015445	— 0,017950	— 0,021042	— 0,024986	— 0,030242	— 0,037627	— 0,048776	— 0,067423	— 0,104110	— 0,202367
0,03	— 0,008604	— 0,009946	— 0,011547	— 0,013520	— 0,016029	— 0,019360	— 0,024017	— 0,030996	— 0,042535	— 0,064781	— 0,121646
0,02	— 0,004645	— 0,005366	— 0,006225	— 0,007283	— 0,008620	— 0,010392	— 0,012856	— 0,016523	— 0,022522	— 0,033886	— 0,061838
0,01	— 0,001629	— 0,001881	— 0,002180	— 0,002549	— 0,003011	— 0,003623	— 0,004470	— 0,005727	— 0,007757	— 0,011543	— 0,020564
0,00	0,000000	0,000000	0,000000	0,000000	0,000000	0,000000	0,000000	0,000000	0,000000	0,000000	0,000000

$T_7 - (\eta', \eta)$

η / η'	0,60	0,55	0,50	0,45	0,40	0,35	0,30	0,25	0,20	0,15	0,10
0,10	1,929955	1,915053	1,869867	1,792624	1,679805	1,525262	1,318242	1,038437	0,640804	— 0,015522	— ∞
0,09	2,099575	2,090294	2,049741	1,976380	1,867014	1,716013	1,513630	1,241911	0,862783	+ 0,268453	— 1,320686
0,08	2,295101	2,291870	2,256100	2,186480	2,080097	1,931779	1,732630	1,466593	1,101005	0,550742	— 0,615097
0,07	2,525388	2,528804	2,498039	2,432010	2,328066	2,181422	1,983878	1,720933	1,364124	0,844367	— 0,117901
0,06	2,804224	2,815114	2,789690	2,727086	2,624885	2,478626	2,280676	2,017772	1,664684	1,163922	+ 0,317881
0,05	3,154511	3,174115	3,154540	3,095141	2,993719	2,846061	2,644979	2,378131	2,022745	1,529716	0,750673
0,04	3,618004	3,648266	3,635338	3,578817	3,476677	3,324897	3,116561	2,839950	2,473997	1,975505	1,227179
0,03	4,281573	4,325903	4,321003	4,266739	4,161243	4,000568	3,777856	3,481605	3,091652	2,568461	1,814173
0,02	5,369394	5,434888	5,440805	5,387352	5,272762	5,092953	4,840756	4,504192	4,062751	3,477880	2,661677
0,01	7,768791	7,876860	7,901586	7,843768	7,701558	7,470144	7,140895	6,699446	6,121696	5,364093	4,334572
0,00	∞	∞	∞	∞	∞	∞	∞	∞	∞	∞	∞

$T_s-(\eta, \eta')$

η' \ η	0,60	0,55	0,50	0,45	0,40	0,35	0,30	0,25	0,20	0,15	0,10
0,10	0,041167	0,047424	0,054497	0,062616	0,072124	0,083539	0,097716	0,116207	0,142265	0,184696	0,302382
0,09	0,034954	0,040249	0,046227	0,053078	0,061084	0,070671	0,082532	0,097906	0,119338	0,153370	0,230023
0,08	0,029132	0,033531	0,038490	0,044168	0,050788	0,058695	0,068442	0,081004	0,098346	0,125316	0,180828
0,07	0,023717	0,027286	0,031304	0,035900	0,041248	0,047621	0,055449	0,065486	0,079221	0,100202	0,140877
0,06	0,018720	0,021529	0,024688	0,028295	0,032486	0,037466	0,043566	0,051349	0,061917	0,077810	0,107285
0,05	0,014167	0,016284	0,018665	0,021379	0,024528	0,028262	0,032822	0,038613	0,046419	0,058004	0,078749
0,04	0,010083	0,011587	0,013275	0,015196	0,017423	0,020058	0,023265	0,027322	0,032755	0,040719	0,054584
0,03	0,006517	0,007486	0,008572	0,009808	0,011236	0,012925	0,014973	0,017555	0,020990	0,025975	0,034447
0,02	0,003530	0,004053	0,004638	0,005303	0,006073	0,006979	0,008077	0,009455	0,011279	0,013899	0,018264
0,01	0,001242	0,001425	0,001631	0,001864	0,002132	0,002448	0,002831	0,003309	0,003937	0,004835	0,006302
0,00	0,000000	0,000000	0,000000	0,000000	0,000000	0,000000	0,000000	0,000000	0,000000	0,000000	0,000000

$T_s-(\eta', \eta)$

η' \ η	0,60	0,55	0,50	0,45	0,40	0,35	0,30	0,25	0,20	0,15	0,10
0,10	1,121816	1,102302	1,074617	1,038392	0,992930	0,937067	0,868953	0,785485	0,680938	0,542286	0,302382
0,09	1,072683	1,054715	1,029065	0,995414	0,953135	0,901196	0,837949	0,760682	0,664498	0,538833	0,345798
0,08	1,019224	1,002786	0,979168	0,948095	0,909009	0,860997	0,802602	0,731453	0,643358	0,529670	0,364022
0,07	0,960716	0,945801	0,924226	0,895755	0,859897	0,815847	0,762323	0,697263	0,617091	0,514684	0,370610
0,06	0,896174	0,882784	0,863277	0,837453	0,804886	0,764872	0,716295	0,657369	0,585056	0,493496	0,367941
0,05	0,824181	0,812331	0,794942	0,771845	0,742677	0,706823	0,663330	0,610670	0,546284	0,465371	0,356599
0,04	0,742578	0,732306	0,717118	0,696876	0,671270	0,639787	0,601616	0,555476	0,499249	0,429046	0,336163
0,03	0,647737	0,639121	0,626277	0,609099	0,587334	0,560558	0,528107	0,488941	0,441350	0,382270	0,305122
0,02	0,532640	0,525830	0,515592	0,501845	0,484397	0,462921	0,436904	0,405541	0,367532	0,320584	0,259947
0,01	0,379277	0,374616	0,367548	0,358022	0,345908	0,330987	0,312916	0,291154	0,264843	0,232489	0,191093
0,00	0,000000	0,000000	0,000000	0,000000	0,000000	0,000000	0,000000	0,000000	0,000000	0,000000	0,000000

$T_s(\eta, \eta') = T_s(\eta', \eta)$

η' \ η	0,60	0,55	0,50	0,45	0,40	0,35	0,30	0,25	0,20	0,15	0,10
0,10	0,045120	0,043579	0,041867	0,039966	0,037849	0,035482	0,032810	0,029754	0,026177	0,021807	0,015840
0,09	0,038691	0,037381	0,035928	0,034314	0,032519	0,030513	0,028252	0,025672	0,022660	0,019006	0,014146
0,08	0,032565	0,031472	0,030261	0,028916	0,027422	0,025753	0,023875	0,021734	0,019245	0,016241	0,012317
0,07	0,026766	0,025877	0,024891	0,023796	0,022581	0,021226	0,019702	0,017967	0,015955	0,013541	0,010430
0,06	0,021330	0,020628	0,019849	0,018986	0,018028	0,016959	0,015759	0,014398	0,012820	0,010936	0,008536
0,05	0,016293	0,015763	0,015173	0,014519	0,013796	0,012988	0,012084	0,011057	0,009872	0,008460	0,006681
0,04	0,011707	0,011329	0,010908	0,010444	0,009929	0,009356	0,008713	0,007985	0,007147	0,006152	0,004909
0,03	0,007635	0,007390	0,007119	0,006819	0,006487	0,006117	0,005702	0,005234	0,004695	0,004059	0,003268
0,02	0,004172	0,004040	0,003893	0,003731	0,003551	0,003351	0,003127	0,002874	0,002585	0,002242	0,001821
0,01	0,001481	0,001435	0,001383	0,001325	0,001262	0,001193	0,001114	0,001025	0,000924	0,000804	0,000658
0,00	0,000000	0,000000	0,000000	0,000000	0,000000	0,000000	0,000000	0,000000	0,000000	0,000000	0,000000

$T_{10}^{-}(\eta, \eta')$

η' \ η	0,60	0,55	0,50	0,45	0,40	0,35	0,30	0,25	0,20	0,15	0,10
0,10	— 0,002168	— 0,002515	— 0,002932	— 0,003451	— 0,004120	— 0,005028	— 0,006326	— 0,008351	— 0,011919	— 0,019774	— 0,057084
0,09	— 0,001656	— 0,001919	— 0,002235	— 0,002628	— 0,003135	— 0,003818	— 0,004790	— 0,006296	— 0,008912	— 0,014485	— 0,034374
0,08	— 0,001226	— 0,001421	— 0,001654	— 0,001941	— 0,002314	— 0,002811	— 0,003520	— 0,004604	— 0,006468	— 0,010337	— 0,022597
0,07	— 0,000873	— 0,001011	— 0,001175	— 0,001380	— 0,001641	— 0,001992	— 0,002486	— 0,003240	— 0,004521	— 0,007119	— 0,014736
0,06	— 0,000590	— 0,000683	— 0,000794	— 0,000930	— 0,001106	— 0,001339	— 0,001670	— 0,002166	— 0,003005	— 0,004671	— 0,009285
0,05	— 0,000373	— 0,000430	— 0,000501	— 0,000586	— 0,000695	— 0,000841	— 0,001044	— 0,001352	— 0,001862	— 0,002863	— 0,005514
0,04	— 0,000211	— 0,000245	— 0,000284	— 0,000332	— 0,000395	— 0,000476	— 0,000590	— 0,000762	— 0,001044	— 0,001589	— 0,002981
0,03	— 0,000103	— 0,000118	— 0,000138	— 0,000160	— 0,000190	— 0,000229	— 0,000284	— 0,000365	— 0,000498	— 0,000752	— 0,001380
0,02	— 0,000036	— 0,000043	— 0,000049	— 0,000059	— 0,000069	— 0,000083	— 0,000101	— 0,000132	— 0,000178	— 0,000265	— 0,000478
0,01	— 0,000006	— 0,000008	— 0,000008	— 0,000010	— 0,000012	— 0,000014	— 0,000018	— 0,000022	— 0,000030	— 0,000047	— 0,000081
0,00	0,000000	0,000000	0,000000	0,000000	0,000000	0,000000	0,000000	0,000000	0,000000	0,000000	0,000000

$T_{10}^{-}(\eta', \eta)$

η' \ η	0,60	0,55	0,50	0,45	0,40	0,35	0,30	0,25	0,20	0,15	0,10
0,10	0,539220	0,442971	0,348220	0,256518	0,169549	0,089231	0,017893	— 0,041392	— 0,084023	— 0,101382	— 0,057084
0,09	0,639931	0,535056	0,431423	0,330629	0,234384	0,144620	0,063636	— 0,005597	— 0,058795	— 0,088433	— 0,072590
0,08	0,755741	0,640932	0,527096	0,415886	0,309059	0,208573	0,116726	+ 0,036417	— 0,028297	— 0,070704	— 0,074436
0,07	0,891398	0,764901	0,639086	0,515685	0,396518	0,283587	0,179221	0,086283	+ 0,008673	— 0,047483	— 0,069038
0,06	1,054233	0,913599	0,773326	0,635250	0,501278	0,373494	0,254275	0,146504	0,053986	— 0,017555	— 0,057017
0,05	1,256348	1,097967	0,939588	0,783177	0,630774	0,484576	0,347057	0,221170	0,110707	+ 0,021150	— 0,037722
0,04	1,519606	1,337770	1,155499	0,974961	0,798379	0,628121	0,466830	0,317599	0,184313	0,072378	— 0,009222
0,03	1,889152	1,673758	1,457381	1,242481	1,031561	0,827276	0,632537	0,450712	0,285930	0,143742	+ 0,032830
0,02	2,480478	2,210121	1,937983	1,667030	1,400266	1,140840	0,892176	0,658167	0,443496	0,254261	0,099483
0,01	3,746642	3,355150	2,960346	2,566368	2,177376	1,797698	1,431990	1,085474	0,764309	0,476282	0,232359
0,00	∞	∞	∞	∞	∞	∞	∞	∞	∞	∞	∞

$T_{11}-(\eta, \eta')$

η' \ η	0,60	0,55	0,50	0,45	0,40	0,35	0,30	0,25	0,20	0,15	0,10
0,10	0,001621	0,001865	0,002141	0,002455	0,002822	0,003258	0,003795	0,004486	0,005435	0,006898	0,009940
0,09	0,001241	0,001428	0,001637	0,001877	0,002156	0,002488	0,002896	0,003417	0,004128	0,005211	0,007318
0,08	0,000921	0,001059	0,001215	0,001391	0,001598	0,001842	0,002141	0,002523	0,003042	0,003820	0,005275
0,07	0,000658	0,000756	0,000866	0,000992	0,001138	0,001311	0,001523	0,001792	0,002155	0,002695	0,003672
0,06	0,000445	0,000512	0,000587	0,000672	0,000770	0,000887	0,001028	0,001209	0,001451	0,001807	0,002436
0,05	0,000282	0,000323	0,000370	0,000424	0,000485	0,000558	0,000647	0,000760	0,000911	0,001130	0,001510
0,04	0,000160	0,000184	0,000211	0,000241	0,000277	0,000318	0,000369	0,000432	0,000516	0,000638	0,000846
0,03	0,000078	0,000089	0,000102	0,000117	0,000134	0,000154	0,000178	0,000209	0,000249	0,000307	0,000404
0,02	0,000028	0,000032	0,000037	0,000043	0,000049	0,000056	0,000064	0,000075	0,000089	0,000110	0,000144
0,01	0,000005	0,000006	0,000006	0,000007	0,000008	0,000010	0,000011	0,000013	0,000015	0,000019	0,000025
0,00	0,000000	0,000000	0,000000	0,000000	0,000000	0,000000	0,000000	0,000000	0,000000	0,000000	0,000000

$T_{11}-(\eta', \eta)$

η' \ η	0,60	0,55	0,50	0,45	0,40	0,35	0,30	0,25	0,20	0,15	0,10
0,10	0,448270	0,392634	0,338176	0,285314	0,234490	0,186195	0,140987	0,099553	0,062787	0,032015	0,009940
0,09	0,434539	0,381324	0,329196	0,278550	0,229798	0,183397	0,139867	0,099835	0,064111	0,033868	0,011261
0,08	0,418498	0,367919	0,318339	0,270126	0,223663	0,179374	0,137736	0,099325	0,064871	0,035409	0,012725
0,07	0,399774	0,352083	0,305304	0,259776	0,215852	0,173923	0,134425	0,097881	0,064949	0,036538	0,014147
0,06	0,377865	0,333365	0,289688	0,247143	0,206056	0,166778	0,129710	0,095321	0,064195	0,037132	0,015395
0,05	0,352065	0,311129	0,270924	0,231730	0,193840	0,157573	0,123285	0,091393	0,062413	0,037037	0,016328
0,04	0,321314	0,284422	0,248166	0,212794	0,178567	0,145764	0,114699	0,085736	0,059319	0,036042	0,016785
0,03	0,283864	0,251675	0,220023	0,189120	0,159188	0,130469	0,103228	0,077770	0,054473	0,033825	0,016542
0,02	0,236377	0,209901	0,183851	0,158400	0,133729	0,110028	0,087511	0,066426	0,047068	0,029821	0,015234
0,01	0,170421	0,151564	0,132999	0,114849	0,097240	0,080306	0,064194	0,049076	0,035154	0,022691	0,012054
0,00	0,000000	0,000000	0,000000	0,000000	0,000000	0,000000	0,000000	0,000000	0,000000	0,000000	0,000000

Functions of the reduced velocity determining the aerodynamic forces of an oscillating wing.

V_o	$1:2\,V_o$	p_{10}	p'_{10}	p_{20}	p'_{20}	p_{11}	p'_{11}	p_{21}	p'_{21}	p_{12}	p'_{12}	p_{22}	p'_{22}
0,00000	∞	0,00000	0,00000	0,00000	0,00000	0,00000	0,00000	0,00000	0,00000	0,00000	0,00000	0,00000	0,00000
0,05000	10,00	0,00249	0,10012	0,00501	0,00012	0,00496	0,10036	0,01003	0,00037	0,00238	0,00036	0,00504	0,00037
0,10000	5,00	0,00984	0,20096	0,02010	0,00098	0,01938	0,20281	0,04038	0,00292	0,00911	0,00265	0,02055	0,00285
0,12500	4,00	0,01525	0,25184	0,03148	0,00191	0,02982	0,25532	0,06339	0,00564	0,01372	0,00487	0,03252	0,00544
0,16667	3,00	0,02667	0,33753	0,05626	0,00445	0,05145	0,34523	0,11380	0,01303	0,02252	0,01045	0,05928	0,01232
0,20000	2,50	0,03784	0,40700	0,08140	0,00757	0,07215	0,41954	0,16531	0,02200	0,03013	0,01659	0,08723	0,02046
0,25000	2,00	0,05769	0,51295	0,12824	0,01442	0,10802	0,53534	0,26208	0,04143	0,04203	0,02854	0,14097	0,03753
0,33333	1,50	0,09808	0,69468	0,23156	0,03269	0,17801	0,74038	0,47835	0,09203	0,06146	0,05500	0,26513	0,07982
0,41667	1,20	0,14618	0,88327	0,36803	0,06091	0,25725	0,96043	0,76821	0,16810	0,07813	0,08815	0,43691	0,13974
0,45455	1,10	0,17019	0,97129	0,44149	0,07736	0,29540	1,06521	0,92567	0,21163	0,08441	0,10494	0,53188	0,17264
0,50000	1,00	0,20055	1,07887	0,53943	0,10027	0,34247	1,19478	1,13682	0,27151	0,09078	0,12624	0,66050	0,21663
0,51020	0,98	0,20757	1,10330	0,56290	0,10590	0,35319	1,22440	1,18759	0,28610	0,09201	0,13116	0,69160	0,22714
0,53191	0,94	0,22276	1,15563	0,61469	0,11849	0,37615	1,28810	1,29984	0,31857	0,09441	0,14179	0,76057	0,25030
0,55556	0,90	0,23967	1,21318	0,67400	0,13315	0,40137	1,35850	1,42873	0,35614	0,09664	0,15359	0,84006	0,27669
0,58140	0,86	0,25854	1,27670	0,74227	0,15032	0,42912	1,43658	1,57750	0,39981	0,09870	0,16671	0,93215	0,30688
0,60976	0,82	0,27970	1,34717	0,82145	0,17055	0,45977	1,52362	1,75049	0,45090	0,10039	0,18133	1,03961	0,34156
0,62500	0,80	0,29126	1,38537	0,86585	0,18204	0,47630	1,57097	1,84770	0,47973	0,10108	0,18927	1,10014	0,36086
0,64103	0,78	0,30354	1,42578	0,91397	0,19458	0,49372	1,62117	1,95319	0,51107	0,10158	0,19768	1,16594	0,38162
0,65789	0,76	0,31659	1,46856	0,96615	0,20828	0,51206	1,67444	2,06775	0,54516	0,10197	0,20656	1,23749	0,40396
0,67568	0,74	0,33051	1,51399	1,02297	0,22332	0,53142	1,73115	2,19267	0,58239	0,10216	0,21599	1,31564	0,42810
0,69444	0,72	0,34535	1,56222	1,08487	0,23982	0,55186	1,79148	2,32894	0,62305	0,10213	0,22596	1,40099	0,45415
0,71429	0,70	0,36120	1,61361	1,15258	0,25800	0,57346	1,85590	2,47823	0,66761	0,10183	0,23655	1,49461	0,48236
0,73529	0,68	0,37815	1,66836	1,22674	0,27805	0,59629	1,92470	2,64196	0,71650	0,10122	0,24777	1,59740	0,51289
0,75758	0,66	0,39631	1,72695	1,30830	0,30024	0,62047	1,99843	2,82227	0,77030	0,10031	0,25970	1,71071	0,54605
0,78125	0,64	0,41580	1,78964	1,39816	0,32484	0,64610	2,07748	3,02119	0,82960	0,09897	0,27236	1,83582	0,58207
0,80645	0,62	0,43674	1,85694	1,49753	0,35221	0,67326	2,16250	3,24148	0,89516	0,09715	0,28582	1,97445	0,62130
0,83333	0,60	0,45928	1,92933	1,60777	0,38273	0,70210	2,25410	3,48618	0,96781	0,09478	0,30012	2,12852	0,66407
0,86207	0,58	0,48360	2,00742	1,73054	0,41690	0,73275	2,35306	3,75904	1,04858	0,09180	0,31535	2,30036	0,71082
0,89286	0,56	0,50989	2,09187	1,86774	0,45526	0,76536	2,46021	4,06436	1,13862	0,08807	0,33154	2,49264	0,76200
0,92593	0,54	0,53835	2,18344	2,02171	0,49848	0,80006	2,57652	4,40739	1,23928	0,08350	0,34877	2,70862	0,81812
0,96154	0,52	0,56924	2,28304	2,19523	0,54735	0,83705	2,70313	4,79440	1,35221	0,07793	0,36711	2,95215	0,87979
1,00000	0,50	0,60284	2,39174	2,39174	0,60284	0,87650	2,84139	5,23313	1,47934	0,07121	0,38662	3,22800	0,94771
1,04167	0,48	0,63948	2,51081	2,61543	0,66612	0,91864	2,99287	5,73302	1,62304	0,06316	0,40737	3,54193	1,02271
1,08696	0,46	0,67953	2,64170	2,87142	0,73862	0,96366	3,15938	6,30553	1,78608	0,05355	0,42943	3,90088	1,10566
1,13636	0,44	0,72343	2,78616	3,16608	0,82207	1,01183	3,34304	6,96498	1,97187	0,04211	0,45285	4,31350	1,19765
1,19048	0,42	0,77170	2,94639	3,50761	0,91869	1,06339	3,54657	7,72973	2,18463	0,02855	0,47770	4,79080	1,29993
1,25000	0,40	0,82492	3,12488	3,90610	1,03115	1,11863	3,77295	8,62228	2,42944	0,01251	0,50398	5,34615	1,41391
1,31579	0,38	0,88381	3,32483	4,37478	1,16291	1,17785	4,02602	9,67218	2,71271	— 0,00644	0,53173	5,99704	1,54133
1,38889	0,36	0,94921	3,55011	4,93072	1,31835	1,24137	4,31038	10,91736	3,04248	— 0,02878	0,56090	6,76568	1,68416
1,47059	0,34	1,02211	3,80557	5,59643	1,50310	1,30950	4,63171	12,40777	3,42884	— 0,05509	0,59141	7,68106	1,84473
1,56250	0,32	1,10371	4,09730	6,40204	1,72454	1,38258	4,99707	14,20997	3,88482	— 0,08606	0,62310	8,78153	2,02582
1,66667	0,30	1,19546	4,43315	7,38860	1,99244	1,46091	5,41548	16,41441	4,42729	— 0,12246	0,65571	10,11867	2,23076
1,78571	0,28	1,29914	4,82320	8,61283	2,31990	1,54479	5,89830	19,14549	5,07845	— 0,16524	0,68880	11,76265	2,46349
1,92308	0,26	1,41696	5,28087	10,15554	2,72492	1,63445	6,46055	22,57967	5,86810	— 0,21543	0,72174	13,81212	2,72888
2,08333	0,24	1,55161	5,82406	12,13343	3,23252	1,72997	7,12188	26,97065	6,83662	— 0,27424	0,75358	16,40716	3,03277
2,27273	0,22	1,70658	6,47747	14,72155	3,87859	1,83130	7,90908	32,69675	8,04064	— 0,34298	0,78298	19,75471	3,38254
2,50000	0,20	1,88624	7,27580	18,18950	4,71561	1,93802	8,85917	40,33742	9,56066	— 0,42304	0,80800	24,16791	3,78744
2,77778	0,18	2,09637	8,26953	22,97093	5,82324	2,04929	10,02524	50,81884	11,51572	— 0,51579	0,82595	30,14218	4,25975
3,12500	0,16	2,34457	9,53465	29,79578	7,32679	2,16348	11,48603	65,68963	14,08767	— 0,62230	0,83306	38,49722	4,81621
3,57143	0,14	2,64129	11,19103	39,96797	9,43319	2,27784	13,36411	87,69695	17,56834	— 0,74301	0,82421	50,67258	5,48149
4,16667	0,12	3,00121	13,43880	55,99504	12,50507	2,38781	15,86168	122,08541	22,45429	— 0,87700	0,79254	69,39257	6,29508
5,00000	0,10	3,44604	16,63848	83,19241	17,23022	2,48609	19,33956	179,89021	29,66067	— 1,02049	0,72918	100,34385	7,32797
6,25000	0,08	4,01005	21,51080	134,44247	25,06283	2,56108	24,51463	287,65891	41,06958	— 1,16461	0,62354	157,11362	8,72790
8,33333	0,06	4,75314	29,73464	247,78861	39,60952	2,59446	33,05218	523,22337	61,23001	— 1,29114	0,46506	279,31020	10,86104
12,50000	0,04	5,80007	46,33509	579,18863	72,50081	2,55708	49,94017	1203,44073	104,46431	— 1,36513	0,24978	627,37445	14,89958
25,00000	0,02	7,52079	96,37253	2409,31325	188,01975	2,40053	100,13323	4912,64410	248,03300	— 1,32078	0,00416	2503,43557	26,99204
∞	0,00	$0\times\infty$	∞	∞	$0\times\infty$								